Amr E. Abbas
Editor

Aortic Stenosis

Case-Based Diagnosis and Therapy

Springer

Aortic Stenosis

Amr E. Abbas
Editor

Aortic Stenosis

Case-Based Diagnosis and Therapy

Springer

Editor
Amr E. Abbas, MD, FACC, FSCAI, FSVM, FASE, RPVI
Interventional Cardiology Research
Beaumont Health System
Royal Oak
Michigan
USA

ISBN 978-1-4471-5241-5 ISBN 978-1-4471-5242-2 (eBook)
DOI 10.1007/978-1-4471-5242-2

Library of Congress Control Number: 2015942633

Springer London Heidelberg New York Dordrecht

Printed on acid-free paper

Springer-Verlag London Ltd. is part of Springer Science+Business Media (www.springer.com)

This book is dedicated to my parents who I owe everything to and then more, my wife who I love dearly, my children who are my life and then some, and my co-authors who without them, this book would not be possible.

Preface

Ever since the earliest description of aortic stenosis by Riverius in 1646, aortic stenosis has become known as a common cause of morbidity and mortality. However, it was not until the twentieth century that the management of these patients included diagnosis via echocardiography, CTA and MRI, cardiac catheterization, and treatment via valvulplasty and surgical aortic valve replacement. Moreover, during the earliest part of the twenty-first century, transcatheter approaches have been described providing options for patients who were previously deemed as nonsurgical candidates.

This book is designed to provide a case-based overview of aortic stenosis including pathophysiology, presentation, diagnosis with both invasive and multimodality noninvasive techniques, and the approach to management options in the multidisciplinary setting. This book will provide an assessment of cases that appear to be complex in terms of determining the true severity of aortic stenosis as patients with low flow, higher gradients with nonsevere valve areas, as well as patients with prosthetic valves. In addition, it will provide a review of current available treatment options such as valvuloplasty, transcatheter, and surgical valve replacement techniques.

We believe this book is essential for individuals in the structural heart disease world including cardiac surgeons, interventional and imaging cardiologists, as well as cardiology fellows who are interested, or in or involved in the management of patients with aortic stenosis. Imaging and interventional cardiologists, cardiac surgeons, and scientists, who are well renowned on the national and international level in managing patients with aortic stenosis, have all been involved in this book and to those individuals we are indebted for their time and expertise.

Royal Oak, MI, USA

Amr E. Abbas, MD, FACC, FSCAI, FSVM, FASE, RPVI

Contents

Contributors

Amr E. Abbas, MD, FACC, FSCAI, FSVM, FASE, RPVI Department of Cardiovascular Medicine, Beaumont Health, Oakland University/William Beaumont School of Medicine, Royal Oak, MI, USA

Aaron David Berman, MD, FACC Department of Cardiology, William Beaumont Hospital, Royal Oak, MI, USA

A. Neil Bilolikar, MD Department of Cardiovascular Medicine, Beaumont Health, Oakland University/William Beaumont School of Medicine, Royal Oak, MI, USA

Laura M. Franey, MD Department of Cardiovascular Medicine, Beaumont Health, Oakland University/William Beaumont School of Medicine, Royal Oak, MI, USA

Michael J. Gallagher, MD, FACC Department of Cardiovascular Medicine, Beaumont Health, Oakland University/William Beaumont School of Medicine, Royal Oak, MI, USA

James A. Goldstein, MD Department of Cardiovascular Medicine, Beaumont Health, Oakland University/William Beaumont School of Medicine, Royal Oak, MI, USA

Ivan Hanson, MD Department of Cardiovascular Medicine, Beaumont Health, Oakland University/William Beaumont School of Medicine, Royal Oak, MI, USA

George S. Hanzel, MD Department of Cardiovascular Medicine, Beaumont Health, Oakland University/William Beaumont School of Medicine, Royal Oak, MI, USA

Robert L. Johnson, PA-C, BS-Medicine Department of Cardiovascular Surgery, Beaumont Health, Royal Oak, MI, USA

Nathan Kerner, MD, FACC, FASE Department of Cardiovascular Medicine, Beaumont Health, Oakland University/William Beaumont School of Medicine, Royal Oak, MI, USA

Steven J. Lester, MD Department of Medicine, Mayo Clinic, Scottsdale, AZ, USA

Michael J. Mack, MD Department of Cardiovascular Disease, Baylor Scott & White Health, Plano, TX, USA

Philippe Pibarot, DVM, PhD, FAHA, FACC, FESC, FASE Department of Research, Quebec Heart and Lung Institute, Quebec City, QC, Canada

Mark C. Pica, BS, CCRP Department of Cardiology/Research Institute, Beaumont Health System, Royal Oak, MI, USA

Karl K.C. Poon, MBBS Cardiology Program, The Prince Charles Hospital, Chermside, QLD, Australia

Gilbert L. Raff, MD, FACC, FSCCT Department of Cardiovascular Medicine, Beaumont Health, Oakland University/William Beaumont School of Medicine, Royal Oak, MI, USA

Marc P. Sakwa Department of Cardiovascular Surgery, Beaumont Health, Oakland University School of Medicine, Royal Oak, MI, USA

Francis L. Shannon, MD Department of Cardiovascular Surgery, Beaumont Health, Oakland University School of Medicine, Royal Oak, MI, USA

Frances O. Wood, MD Department of Cardiovascular Medicine, Beaumont Health, Oakland University/William Beaumont School of Medicine, Royal Oak, MI, USA

Sibin K. Zacharias, MD Department of Cardiovascular Medicine, Beaumont Health, Oakland University/William Beaumont School of Medicine, Royal Oak, MI, USA

General Considerations and Etiologies of Aortic Stenosis

1

Frances O. Wood and Amr E. Abbas

Abstract

The ***earliest*** descriptions of aortic stenosis are credited to Riverius in 1646 where he provided a clear-cut description of the observed pathological findings of calcified aortic valve cusps in association with weak and diminished peripheral pulses. Aortic stenosis was described again by Bonet in 1679, however, John Baptist Morgagni, professor of anatomy in the University of Padua, referred to aortic stenosis in 1761 and is credited in providing a brilliant description of an autopsy specimen of calcified aortic valve cusps found in a patient and suggested the valve was both stenotic and incompetent. In his description, he quoted a similar case described by Georgius Greiselius and he clarified the anatomical and pathophysiological features of acquired aortic stenosis. In 1806, Corvisart provided another impressive correlation of clinical and autopsy findings and in 1854, William Stokes provided yet another vivid description of the disease. This chapter will provide a general overview of aortic stenosis as well as a review of the common etiologies of aortic stenosis.

Keywords

Aortic stenosis • Etiology of aortic stenosis • Left ventricular outflow tract (LVOT) • Valvular aortic stenosis • Supra-valvular aortic stenosis • Sub-valvular aortic stenosis • Epidemiology of aortic stenosis • Causes of aortic stenosis

Historical Perspective

The ***earliest*** descriptions of aortic stenosis are credited to Riverius in 1646 where he provided a clear-cut description of the observed pathological findings of calcified aortic valve cusps in association with weak and diminished peripheral pulses.

F.O. Wood, MD • A.E. Abbas, MD, FACC, FSCAI, FSVM, FASE, RPVI (✉)
Department of Cardiovascular Medicine, Beaumont Health, Oakland University/William Beaumont School of Medicine, Royal Oak, MI, USA
e-mail: aabbas@beaumont.edu

A.E. Abbas (ed.), *Aortic Stenosis: Case-Based Diagnosis and Therapy*,
DOI 10.1007/978-1-4471-5242-2_1

Aortic stenosis was described again by Bonet in 1679, however, John Baptist Morgagni, professor of anatomy in the University of Padua, referred to aortic stenosis in 1761 and is credited in providing a brilliant description of an autopsy specimen of calcified aortic valve cusps found in a patient and suggested the valve was both stenotic and incompetent. In his description, he quoted a similar case described by Georgius Greiselius and he clarified the anatomical and pathophysiological features of acquired aortic stenosis. In 1806, Corvisart provided another impressive correlation of clinical and autopsy findings and in 1854, William Stokes provided yet another vivid description of the disease [1–3].

Diagnosis of aortic stenosis has undergone several developments throughout history. Throughout the nineteenth century, physicians could identify the murmur even with the use of primitive stethoscopes. Hemodynamic assessment of aortic stenosis was initially limited due to the inherent belief that retrograde catheterization through a stenotic aortic valve was contraindicated. As such, transbronchial arteriotomy, transthoracic left ventricular puncture, and transseptal approaches were developed to assess the left ventricular pressure. In congruence with the realization of the feasibility of retrograde catheterization in these patients, Gorlin and Gorlin developed the formula to measure the aortic valve area in 1951. It wasn't until 1981 when non-invasive Doppler techniques were developed to measure gradient and valve area.

Management of aortic valve stenosis included early attempts of dilatation, concurrently; implantation of a ball-valve prosthesis in the descending aorta for aortic regurgitation was performed by Hugffnagel in 1952. In the following decade, and with the development of cardiopulmonary bypass by Gibbon in 1953, Harken et al. reported the first successful aortic valve replacement with a mechanical prosthesis in 1960. In 1962, Ross reported the use of an aortic valve homograft in the orthotropic position and in 1967, he reported the transfer of the pulmonic valve to the aortic position [4]. Finally, in the early part of this century, Crebier et al. described the percutaneous implantation of an aortic valve in a human subject. The rest, as they would say, is history.

This book will provide an overview of all aspects of aortic stenosis in a case-based format including anatomical, clinical, diagnostic, and therapeutic considerations.

Introduction

Obstruction of the blood flow from the left ventricular outflow tract (LVOT) may occur at various levels including that ***at*** the aortic valve level (valvular aortic stenosis), ***above*** (supra-valvular aortic stenosis), or ***beneath*** the semilunar valve (sub-valvular aortic stenosis). However, the clinical presentation may be similar with either shortness of breath, syncope, and/or chest pain. Patients may present with a systolic ejection murmur that may be constant or vary with certain maneuvers (as in the presence of hypertrophic obstructive cardiomyopathy) as well as with a variable intensity of the second heart sound depending on the severity of obstruction.

The diagnosis of the site and severity of aortic stenosis depends on the anatomical assessment via echocardiography (echo), cardiac computed tomography (CT), and cardiac magnetic resonance imaging (MRI) as well as the physiological assessment of area reduction and trans-valve gradient by cardiac catheterization, Doppler echocardiography, and more recently cardiac MRI.

Treatment of the various forms of severe aortic stenosis (AS) has been traditionally a surgical endeavor. However, with the advent of transcatheter aortic valve replacement (TAVR), alcohol septal ablation (ASA) for hypertrophic obstructive cardiomyopathy (HOCM), and balloon valvuloplasty of congenital aortic valve stenosis and sub-aortic membranes, interventional cardiology has gained an increasing role in management of these conditions.

This chapter will serve to provide an overview of the anatomy of the aortic valve (AV) as well as the epidemiology, etiology and general considerations regarding aortic stenosis.

Prior to discussing aortic stenosis, it will be essential to review the complex anatomy of the aortic root.

The Aortic Valve and Root Apparatus

The ***aortic root*** is an extension of the LVOT that involves the ventricular septum, aortic wall, sinuses of Valsalva formed by the three semi-lunar leaflets, fibrous continuity to the mitral valve, coronary arteries and the left bundle branch. The aortic root extends from the basal attachments of the semi-lunar valvular leaflets within the left ventricle to the sinutubular junction. The three valvular sinuses and their respective leaflets form the right, left, and non-coronary (or posterior) sinuses (Figs. 1.1 and 1.2). Normally, the left coronary

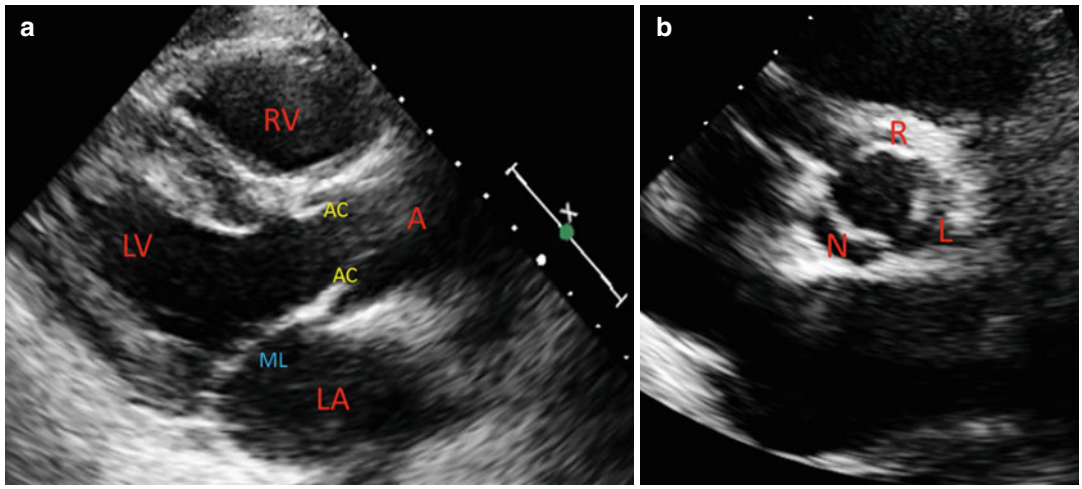

Fig. 1.1 Parasternal long (*left*, **a**) and short (*right*, **b**) axis transthoracic echocardiographic view of a normal aortic valve in systole. In the parasternal long axis, the leaflet closest to the right ventricle is the right leaflet while the leaflet closest to the mitral valve is either the left or non-coronary cusp depending on the angle. In the short axis view, the interatrial septum points to the non-leaflet and the right is closest to the right ventricle *RV* right ventricle, *LV* left ventricle, *AC* aortic valve cusp, *A* aorta, *ML* mitral valve leaflets, *LA* left atrium, *N* non-coronary cusp, *L* left coronary cusp, *R* right coronary cusp

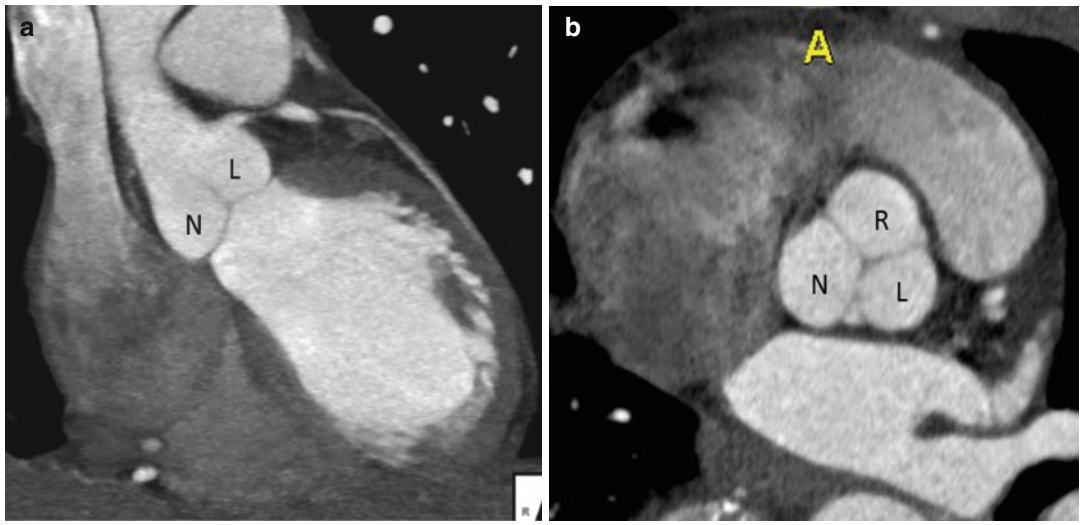

Fig. 1.2 Long (*left*, **a**) and short (*right*, **b**) axis cardiac CT angiographic view of the aortic valve in diastole. *N* non-coronary cusp, *L* left coronary cusp, *R* right coronary cusp

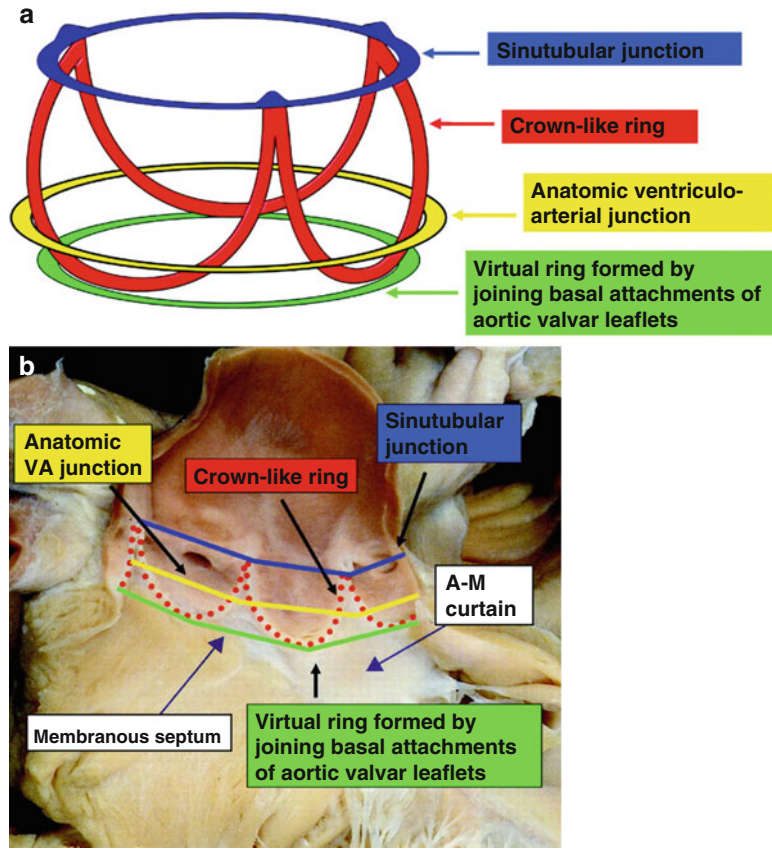

Fig. 1.3 (**a**, *top*). Anatomical specimen of the aortic root with leaflets removed showing location of three virtual rings relative to the crown-like hinges of the leaflets (From Piazza et al. [5] with permission). (**b**, *bottom*) reveals a diagram representing the three circular anatomic rings of aortic root (Modified from Piazza et al. [5] with permission)

artery arises from the left coronary sinus while the right coronary artery arises from the right coronary sinus. The left bundle branch courses through the right and non-coronary sinuses.

The nomenclature of the *aortic valve apparatus* includes three rings: basal, ventriculo-aortic junction, and sinotubular junction (Fig. 1.3a, b) [5].

(A) The ***basal ring*** comprises of the bottom of the sinuses formed by the semi-lunar leaflets and membranous septum.

(B) The ***ventriculo-aortic junction*** is an anatomic ring where the membranous septum connects to the aortic wall at the bases of the right and left coronary sinuses while the aortic wall connects to the fibrous continuity of the anterior leaflet of the mitral valve at the base of the non-coronary sinus. The interleaftlet trigones between the semilunar leaflets and the membranous ventricular attachment are made of fibrous tissue.

(C) The ***ring of the sinotubular junction*** is formed by the attachment of the sinuses to the ascending aorta.

Prevalance and Epidemiology of Aortic Stenosis

The Euro Heart study on valvular heart disease revealed that aortic stenosis was the most common valve disease in a population of 4,910 patients greater than 65 years of age (43.1 % of patients) and degenerative pathology accounted for almost 82 % of the cases [5].

In the US study of 1,797 patients older than 60 years, aortic stenosis was the second most common disease after mitral regurgitation. There appears to be a trend towards a higher prevalance of AS in men which becomes significant after adjusting for age [6]. Osnabrugge et al. pooled

data from seven studies of elderly (≥75 years) patients with severe aortic stenosis to determine the prevalence of aortic stenosis in Europe and North America and to estimate the potential surgical and transcatheter procedures [7]. The prevalence of mild to severe aortic stenosis was 2.4 % (2.7 million North Americans, 4.9 million Europeans) while severe aortic stenosis was 3.4 %. Three quarters of the patients with severe AS were symptomatic which corresponds to 540,000 North Americans and one million Europeans. The prevelance of AS, expectedly, increases with age and it is four times more common over the age of 65 (1.3 % vs 0.32 %) [6, 7].

In a survey of patients with severe AS at a single center, only half of patients with AS underwent AVR, 75 % of which were symptomatic despite a predicted mortality of <10 %, and fewer than one third were even referred to a surgeon [8].

Causes of Aortic Stenosis

As mentioned above, AS may occur at the level of, beneath, or above the level of the AV. The most common cause is ***valvular*** AS and its main causes are congenital, calcific, and rheumatic. ***Para-valvular*** obstruction (supra, and sub valvular aortic stenosis) can occur through membranes, muscular hypertrophy, or iatrogenically following surgical procedures.

Valvular Aortic Stenosis

Valvular aortic stenosis is by far the most common form of aortic stenosis and rheumatic heart disease remains the most common cause of valvular aortic stenosis worldwide especially in developing nations [9].

Calcific aortic stenosis is the most common form of valvular aortic stenosis in industrialized countries. It is primarily a disease of the elderly with increasing in prevalence with age. Superimposed calcification of congenital aortic stenosis is the second most common form of aortic stenosis in industrialized nations and commonly presents after the age of 50. Half of the adults with aortic stenosis have underlying bicuspid stenosis [10] and it is the most common cause of aortic stenosis before the age of 65. Other uncommon forms of aortic stenosis in the industrialized world is radiation and drug-induced aortic valve disease. Childhood aortic stenosis from either homozygous type II hyperlipoproteinemia, ochronosis with alkaptonuria, and Paget's disease [9] is exceedingly rare.

Calcific Aortic Valve Stenosis

The prevailing mechanism causing calcification is thought to be secondary to lipid accumulation, inflammation and proliferative cellular and extracellular changes (Fig. 1.4). Calcification leads to leaflet immobility and obstruction without commissure fusion (Fig. 1.5a, b). Atherosclerosis and calcific aortic stenosis share similar pathophysiologic features in that risk factors include hypertension, smoking, elevated LDL cholesterol [9]. However, various studies examining the role of statin therapy for delaying the progression of valvular aortic stenosis have been unsuccessful in documenting a preventative or therapeutic role for statin in patients with AS [11].

Congenital Aortic Valve Stenosis

Congenital aortic stenosis may be unicuspid or bicuspid (Fig. 1.6) with fusion of one or more commissures, and less commonly quadricuspid with a four leaflet aortic valve. Infants do not survive the severe obstruction caused from rare congenital unicuspid or quadricuspid valves unless surgically corrected. Bicuspid aortic valve disease is more common and occurs in 0.5–2 % of the population and in 66 % of all valves excised surgically for aortic stenosis with almost a double prevalence in males compared to women [9, 12]. However, only 1 in 50 children will develop significant obstruction by adolescence [13]. Patients may also present with aortic regurgitation with or without aortic stenosis [14, 15].

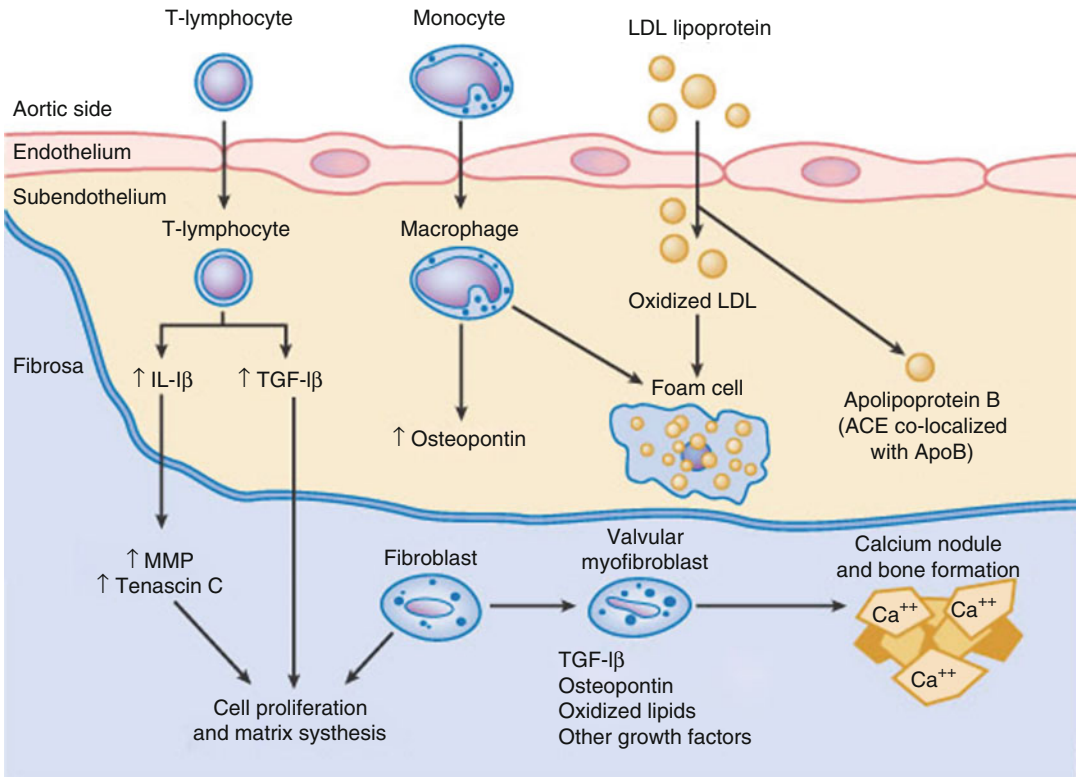

Fig. 1.4 Potential pathway depicting calcific valvular aortic stenosis pathophysiology. *1*. **T-lymphocytes and macrophages** infiltrate the endothelium and release cytokines, which act on valvular fibroblasts to promote cellular proliferations and extracellular matrix remodeling. *2*. A subset of **valvular fibroblasts** within the fibrosa layer differentiates into **myofibroblasts**, which possesses characteristics of smooth muscle cells. *3*. LDL particles taken into the subendothelial layer are oxidized an taken up by **macrophages** that become **foam cells**. *4*. ACE is co-localized with APoB and facilitates the conversion of angiotensin II, which acts on angiotensin 1 receptors, expressed on valve myofibroblasts. *5*. A subset of myofibroblast differentiates into an **osteoblast** phenotype that can promote calcium nodule and bone formation (From Libby et al. [10] with permission)

Bicuspid aortic valve (BAV) usually occurs from fusion of the right and left aortic cusps (70 %) and maybe associated with other forms of congenital heart disease including coarctation of the aorta (50–80 %), interruption of the aorta (36 %) and isolated ventricular septal defect (20 %) [16, 17]. Patients with either aortic coarctation or Turner syndrome should be screened for the presence of BAV as the incidence approaches 50 % and 10–12 %, respectively [18, 19]. Systolic doming of the aortic valve leaflets is demonstrated in the long axis of the AV on various imaging modalities as echocardiography and MRI. While a classic "fish mouth" appearance is noted in the short axis view during diastole, with the corresponding fused leaflets appearing as one as demonstrated in Fig. 1.6 [20]. Extensive hypertrophy and supernormal ejection performance are the rule with congenital aortic stenosis and systolic dysfunction is uncommon unless severe stenosis is present at birth. However, sudden cardiac death is more common in infants and children than in adults [8].

BAV maybe also associated with aortopathy and patients are at an increased risk of aortic dissection, dilatation and aneurysm formation due to medial tissue changings including loss of elastic fibers, altered smooth muscle cell alignment, and cystic medial necrosis [21]. Multiple studies have

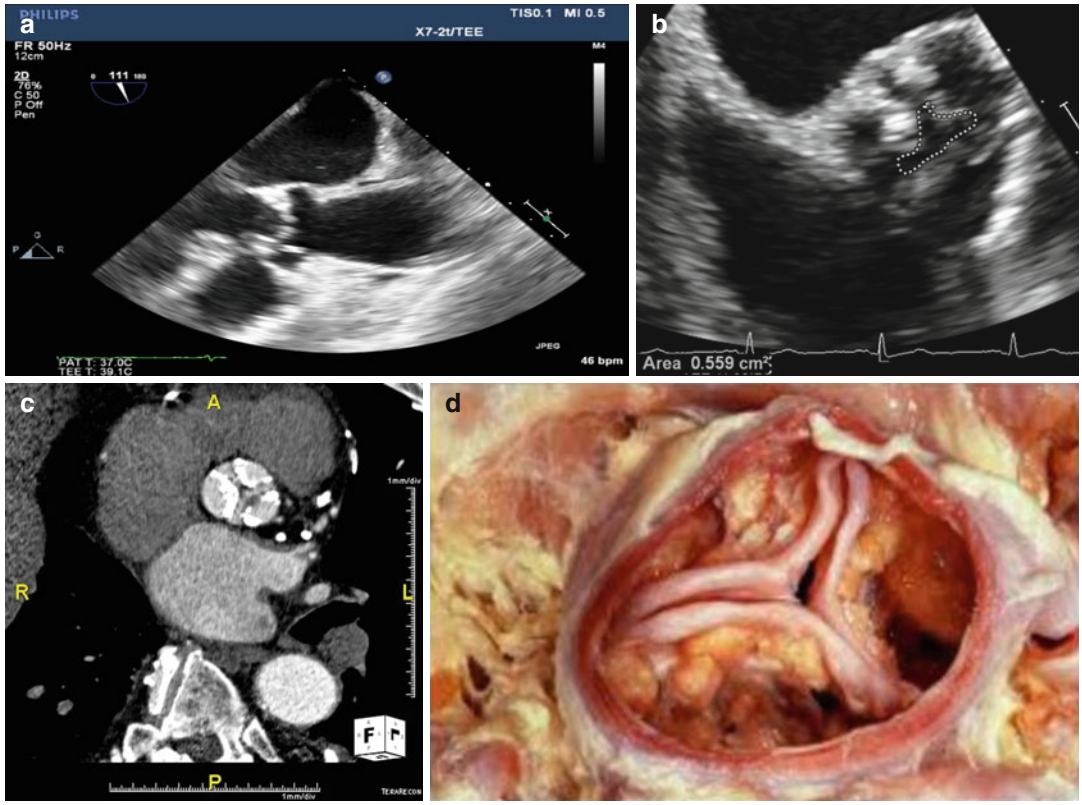

Fig. 1.5 Parasternal long (*top left*, **a**) and short (*top right*, **b**) axis transesophageal echocardiography showing reduced excursion aortic leaflets due to severe aortic stenosis. Cardiac CT angiography (*bottom left*, **c**) and surgical field (*bottom right*, **d**) demonstrating severe aortic stenosis

shown familial clustering but the exact genetic mechanisms are still under investigation. Inheritance is likely multifactorial and in some instances autosomal dominant inheritance with incomplete penetrance [9, 14, 22].

Rheumatic Aortic Valve Stenosis

Rheumatic aortic stenosis is rare due to the decline in rheumatic fever and is primarily associated with rheumatic mitral stenosis. Unlike calcific aortic stenosis, there is fusion of both the leaflets and commissures creating an immobile small triangular or round opening with eversion of leaflet tips. Calcific nodules can form on the leaflets and commissures creating a fixed opening that may lead to both aortic stenosis and aortic regurgitation (Fig. 1.7) [9, 15].

Para-valvular Aortic Stenosis

Supra Valvular Aortic Stenosis

Supra valvular aortic stenosis is exceedingly rare and may present either in isolation or as a part of congenital syndromes as autosomal dominant William's Syndrome or familial non-Williams supra valvular aortic stenosis. It may occur in the form of membranes, muscular ridges, or tunneling of the ascending aorta for variable distances (Fig. 1.8). The coronary arteries are proximal to the stenosis and are subjected to high systolic and limited diastolic flow and can have atretic ostia, ectasia, or aneurysms [23]. It has also been reported after arterial switch operation.

Associated features of patients with **William's Syndrome** include:

(a) Other cardiovascular abnormalities: aortic valve stenosis, pulmonary stenosis, renal

artery stenosis, and hypertension, sub valvular aortic stenosis, parachute mitral valve, bicuspid aortic valve, ventricular septal defect, and circle of Willis aneurysms.

(b) **Elfin features**: these include puffy eyes, star like pattern in the iris, short nose with broad nasal tip, full cheeks and lips, small chin, wide mouth, and small widely spaced teeth.

(c) Short stature, long neck, sloping shoulder, limited joint mobility, low muscle tone, and spine curvature, hyperacusis, strabismus, and poor growth

(d) Hypercalcemia, chronic ear infections, gastric reflux, and hernias

(e) Developmental delays, self mutilation, anxiety, phobias

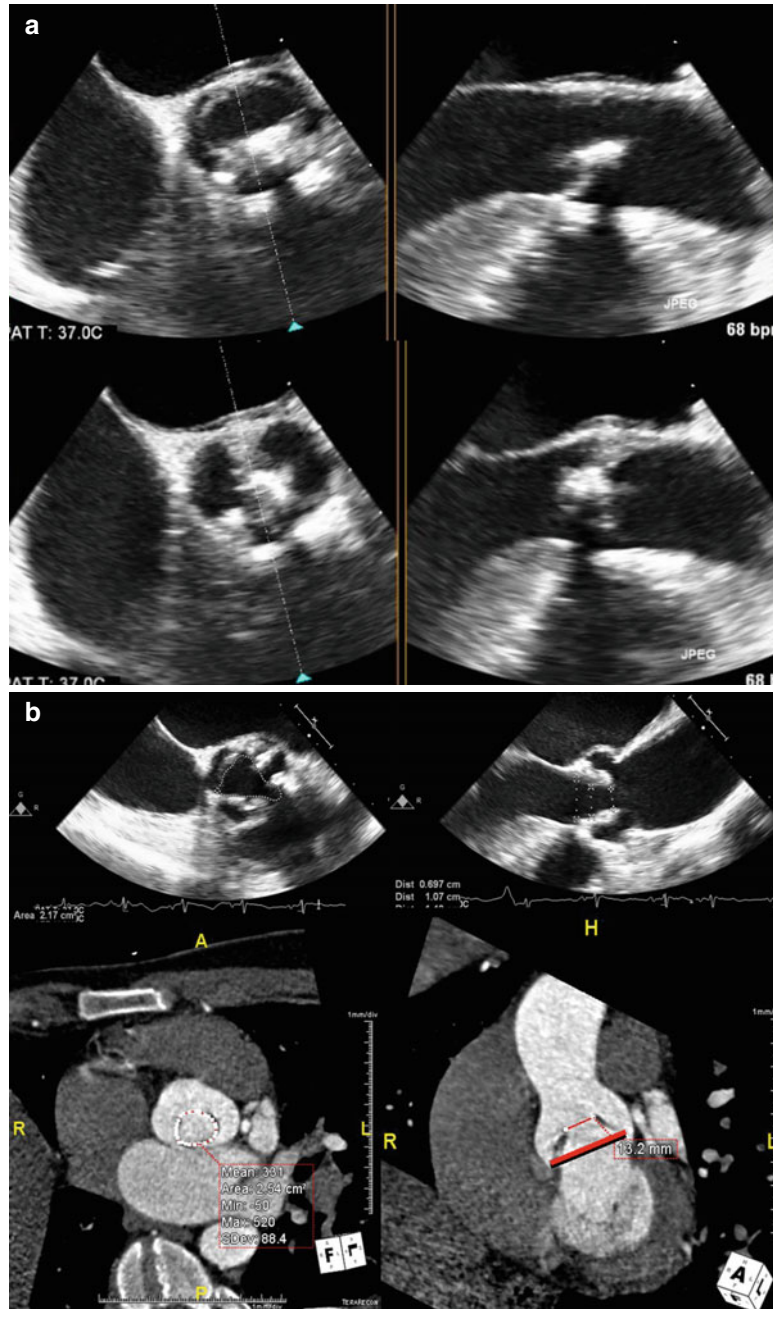

Fig. 1.6 Congenital unicuspid (**a**) and bicuspid valves (**b**) noted on echocardiography. The right cusp and non-coronary cusps are fused. (**c**) Demonstrates a calcified bicuspid aortic valve noted on CTA

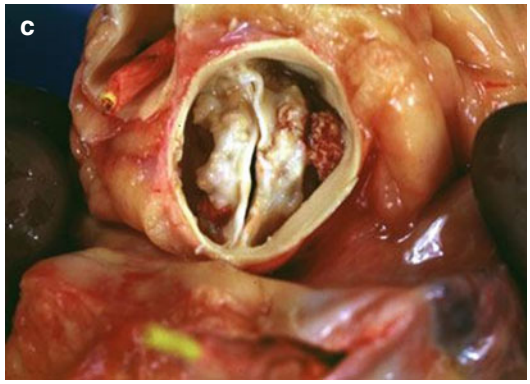

Fig. 1.6 (continued)

Surgical correction is indicated in patients with a mean Doppler gradient of 50 mmHg and/or a peak Doppler gradient of 70 mmHg, symptoms of angina, dyspnea, or syncope, in the presence of LVH, and in case of the desire of pregnancy or greater exercise [23].

It is performed by either a single patch through a single sinus incision (McGoon), inverted Y patch requiring double sinus incision (Doty), and the Brom and Myers techniques with either a three patch or direct three sinus incision, respectively. The latter is the most recent approach to surgical correction [23].

Sub Valvular Aortic Stenosis

Sub valvular aortic stenosis may occur due to a multitude of etiologies:

1. Fixed congenital: Fixed congenital sub valvular aortic stenosis is more common than the supra valvular form (Fig. 1.9). It may occur as a part of a familial syndrome as Shone's complex or occur in isolation with a 2:1 male predominance. Sub aortic membranes, muscular ridges, and tunnels can also account for the obstruction and can extend to the mitral valve anterior leaflet. It may occur with ventricular and atrioventricular septal defects and conotruncal abnormalities. Accessory mitral valve tissue or anomalous chords may also cause a fixed sub valvular obstruction [23]. Associated features of **Shone's complex** include: coarctation of the aorta, parachute mitral valve, supravalvar mitral membrane, bicuspid aortic valve, and valvular aortic stenosis.

Damage to the aortic valve from the eccentric high velocity jet may lead to aortic valve regurgitation further increasing the hemodynamic burden on the left ventricle and is present in 50 % of cases. Moreover, a dynamic element of obstruction may also co-exist from left ventricular hypertrophy, and in contrast to valvular aortic stenosis, no ejection click is noted.

Surgical intervention is indicated in patients with a peak Doppler gradient >50 mmHg, mean Doppler gradient >30 mmHg, or catheter peak-to-peak gradient >50 mmHg. Similar to patients with supravalvular obstruction, the presence of symptoms of angina, dyspnea, or syncope, or in the presence of LV systolic dysfunction or significant aortic valve regurgitation or the patient desires to become pregnant or to participate in active sports may be considered for surgery with lesser gradients. In patients with a lesser degree of obstruction, an exercise challenge may unmask higher gradients not noted on rest [23]. The presence of LV systolic dysfunction or a ventricular septal defect proximal to the subvalvular obstruction may result in underestimation of obstruction [23].

Surgical repair of the discrete membranous form usually involves circumferential resection of the fibrous ring and some degree of resection of the muscular base along the left septal surface. Injury to the aortic or mitral valves, complete heart block, or creation of a ventricular septal defect may occur as the result of surgery. Patients with associated aortic regurgitation often undergo valve repair at the time of subaortic resection. Fibromuscular or tunnel-type subvalvular obstruction is more difficult to palliate surgically and usually involves a more aggressive septal resection and sometimes mitral valve replacement. Patients with subvalvular obstruction due to severe long-segment LVOT obstruction may require a Konno procedure, which involves an extensive patch augmentation of the LV outflow area to the aortic annulus.

Postoperative complications may include infective endocarditis. Subvalvular obstruction may recur after surgical repair; repair of subvalvular obstruction in children does not necessarily

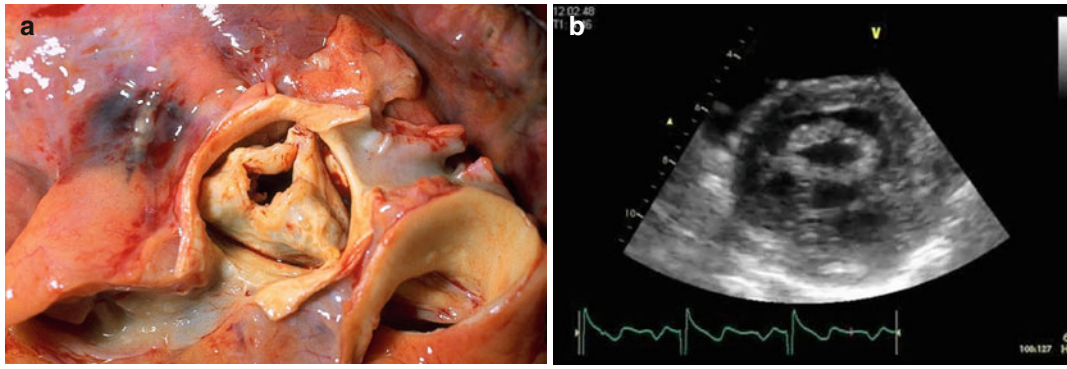

Fig. 1.7 Rheumatic aortic stenosis noted on a surgical specimen (*left*, **a**) and on echocardiography (*right*, **b**). Note the thickening and eversion of leaflet tips

prevent development of aortic regurgitation in adults [23]. The value of surgical resection for the sole purpose of preventing progressive aortic regurgitation in patients without other criteria for surgical intervention has not been determined and is an issue about which there is no clear consensus. However, data exist to suggest that surgical resection of fixed subvalvular before the development of a more than 40-mmHg LVOT gradient may prevent reoperation and secondary progressive aortic valve disease [23]. Although catheter palliation has been performed in some centers on an experimental basis, its efficacy has not been demonstrated [23].

2. Acquired Fixed: This can occur after ventricular septal defect patching or from a tilted mitral valve bioprosthesis into the LVOT. It occurs particularly in patients who with hypertrophic obstructive cardiomyopathy who undergo incomplete myomectomy and mitral valve bioprosthetic replacement (Fig. 1.10) [23].
3. Hypertrophic obstructive cardiomyopathy: Hypertrophic obstructive cardiomyopathy can also account for a dynamic obstruction of the left ventricular outflow and present in a similar fashion to that of other form of aortic stenosis in conjunction to other special features related to the cardiomyopathy (Fig. 1.11). Patient may suffer shortness of breath, chest pain, and/or syncope and management includes beta-blockers, calcium channel blockers, and adequate hydration. In patients with persistent symptoms, reduction of septal wall thickness either through surgical myomectomy or alcohol septal ablation (Fig. 1.12) may help alleviate symptoms. Identification of patients at risk for sudden cardiac death includes assessment of the presence of non-sustained ventricular tachycardia, septal wall thickness >3 cm, late Gadolinium enhancement on MRI, history of syncope, and family history of sudden cardiac death. Family members of patients with HOCM should undergo clinical and echocardiographic screening, while genetic screening of family members is indicated when an identifiable genetic mutation is discovered in the index patient [23].

Natural History of Aortic Valve Stenosis

In both calcific and bicuspid aortic stenosis, there is a long latent period of disease progression before symptoms develop. Onset of symptoms tends to occur between the ages of 50–70 years for patients with bicuspid valves and after age 70 for calcific trileaflet valves [24].

Angina, syncope and heart failure can develop with moderate or severe aortic stenosis and patients with severe or critical aortic stenosis can remain asymptomatic. Symptoms depend on left ventricular systolic function; stroke volume based on body surface area, preload, afterload and heart rate [25].

Risk factors for mortality in asymptomatic patients with moderate to severe aortic stenosis

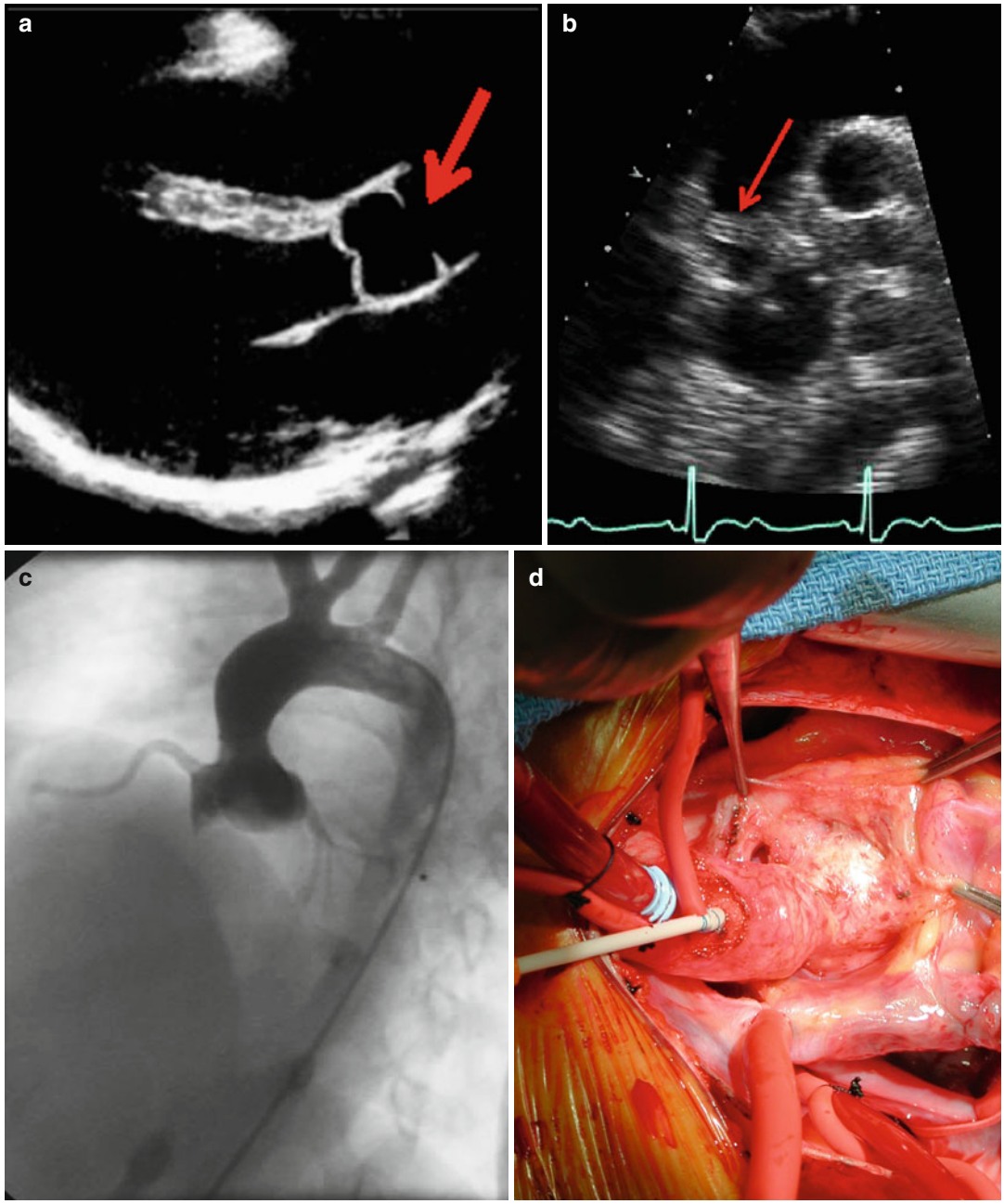

Fig. 1.8 Supravalvular obstruction noted on parasternal long (*top left*, **a**) and suprasternal (*top right*, **b**) echocardiographic images (*red arrows*). Also noted on angiography (*bottom left*, **c**) and surgical specimen (*bottom right*, **d**) (*black arrows*)

include elevated B-type natriuretic peptide (BNP), increase peak velocity across the aortic valve, female gender, and severity of ventricular remodeling [26]. Elevated BNP in asymptomatic or symptomatic patients independently predict symptoms and survival while N-terminal BNP predict post-operative morbidity and mortality after aortic valve placement [27, 28]. Women tend to have hypercontractile ventricles, poorer functional capacity, increased relative wall

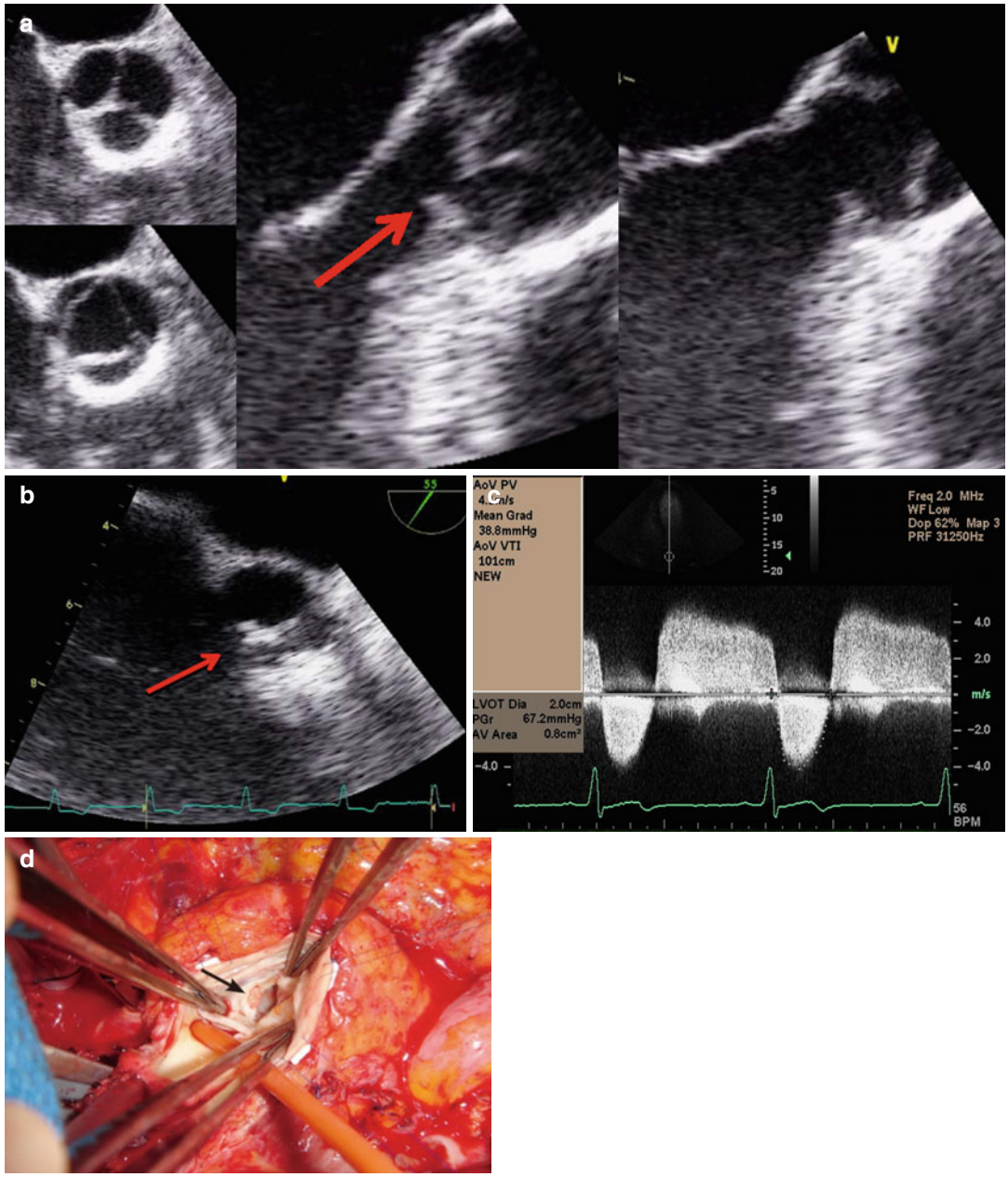

Fig. 1.9 Subaortic membrane: on TEE (*top left*, **a**) long axis, short axis (*top right*, **b**). Doppler across the LVOT revealing aortic stenosis and regurgitation (*bottom left*, **c**). *Bottom right* (**d**) image demonstrated surgical excision of a subaortic membrane

thickness, and more symptoms [29]. Patients with a depressed ejection fraction and low flow/low gradient severe aortic stenosis have worse outcomes, particularly in the absence of contractile reserve [9]. Normal left ventricular function with low flow/low gradient severe aortic stenosis occurs more frequently in women [30] and survival has also been reported as lower in these patients compared to those with normal flow and normal gradient aortic stenosis.

In severe aortic stenosis, ventricular remodeling including hypertrophy and altered geometry

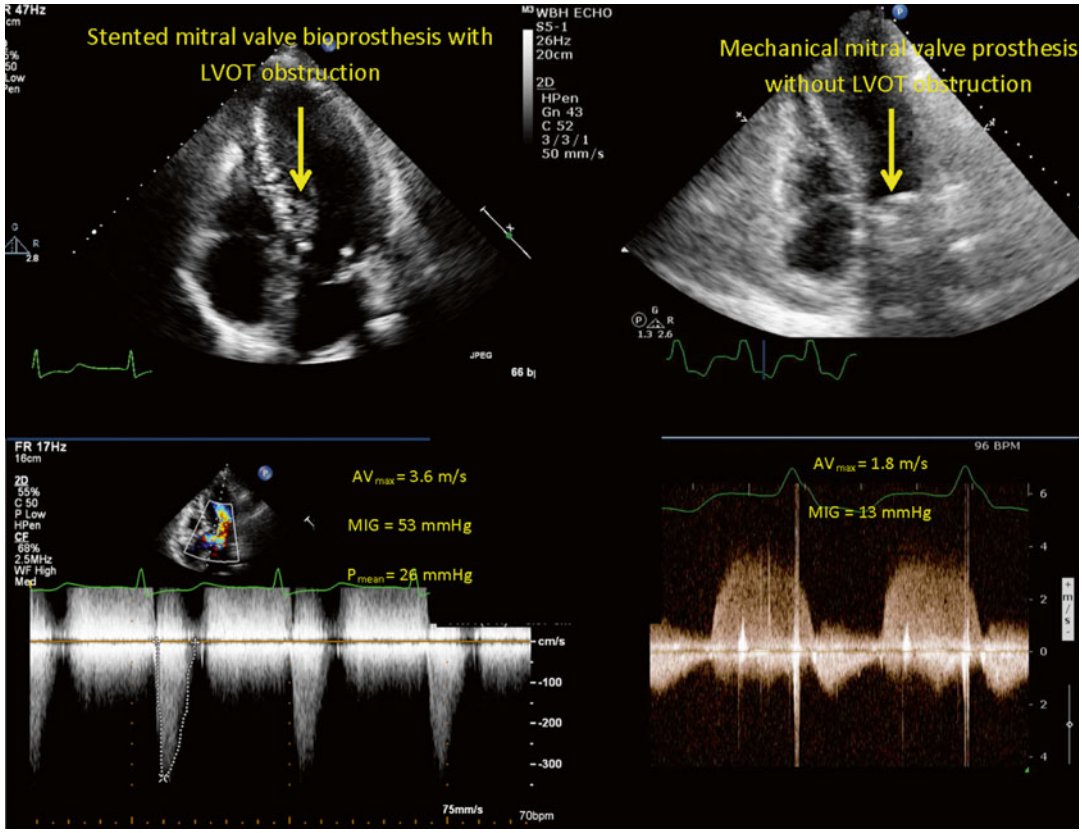

Fig. 1.10 Acquired fixed sub valvular obstruction secondary to a bioprosthetic mitral valve (*left*). Note the elevated gradient across the LVOT. After surgical redo with a lower profile mechanical valve leading to resolution of the trans outflow gradient (*right*)

from pressure overload is associated with increased mortality and adverse outcomes [31, 32]. There is continued debate about whether the increased left ventricular mass or relative wall thickness plays a more important role in effecting outcomes in patients who undergo aortic valve replacement [33–36].

Morbidity and Mortality

Multiple studies have shown that the presence of aortic sclerosis increased the risk of myocardial infarction and cardiovascular death by 50 % [37–39]. Once symptoms start, survival was 5 years for angina, 3 years for syncope and 2 years for heart failure [36]. Event free survival in asymptomatic patients with severe aortic stenosis ranges from 20 to 50 % at 2 years [37–40]. Rosenhek's prospective evaluation of 116 asymptomatic patients demonstrates decreased survival as peak aortic jet increases [41]. The risk of sudden cardiac death in truly asymptomatic patients is less than 1 % per year [41–44].

Despite guideline recommendations of surgical or transcatheter management of aortic stenosis for symptoms and reduced left ventricular function [15, 45, 46], multiple studies have reported that 30–40 % of patients with symptomatic severe aortic stenosis are not treated [8, 47–50]. Patients not referred for treatment tend to be older, high operative risk, reduced left ventricular function, have symptoms unrelated to aortic stenosis or refuse interventions [8, 51].

Mortality for all-comers with aortic stenosis who undergo isolated surgical aortic valve replacement is <2.5 % and is dependent on age (<1 % <60 years, 1.3 % <70 years, <3.5 % <80 years,

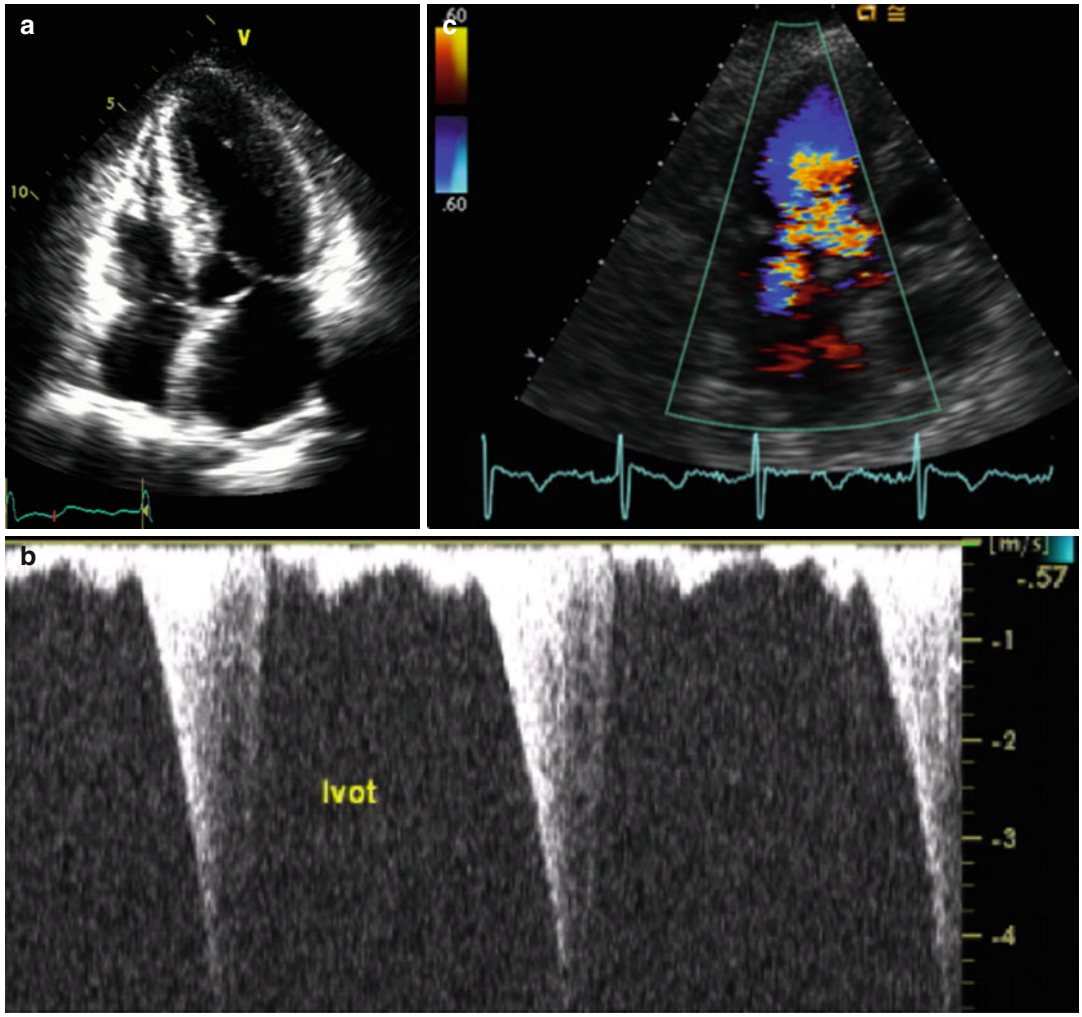

Fig. 1.11 Hypertrophic obstructive cardiomyopathy: On the *left* (**a**), systolic anterior motion (*SAM*) of the mitral valve is noted causing obstruction of the left ventricular outflow. A classic dragger shaped, late systolic peaking high velocity gradient is noted (*top right*, **b**). SAM causes distortion of mitral leaflet coaptation and mitral regurgitation with a characteristic inverted Y appearance with color Doppler (*bottom right*, **c**)

<5 % 85 years old) and co-morbidities [52]. Transcatheter aortic valve replacement (TAVR) has spurred the re-evaluation of "inoperable" patients and further investigation into different types of aortic stenosis including low flow low gradient aortic stenosis. Currently, there are two US FDA approved transcatheter valves: Edwards Sapien (Edwards Lifesciences, Irvine, California), a balloon expandable cobalt chromium frame with bovine pericardial leaflets and Medtronic CoreValve (Medtronic Inc., Minneapolis, Minnesota), nitinol self-expandable porcine pericardial tissue valve.

Inoperable patients who undergo TAVR survive longer, have reduced hospitalizations, reduced symptoms and better quality of life compared to medically treated patients [53–56]. High risk surgical and operable TAVR patients have similar survival but paravalvular regurgitation is higher in the TAVR group and associated with increased mortality [49–51]. The risk of stroke is initially higher in the TAVR group compared to the surgical AVR group but stroke incidence is no different at 2 years [49]. As patient screening, imaging, and equipment improve, TAVR will continue to be a viable option for sicker patients.

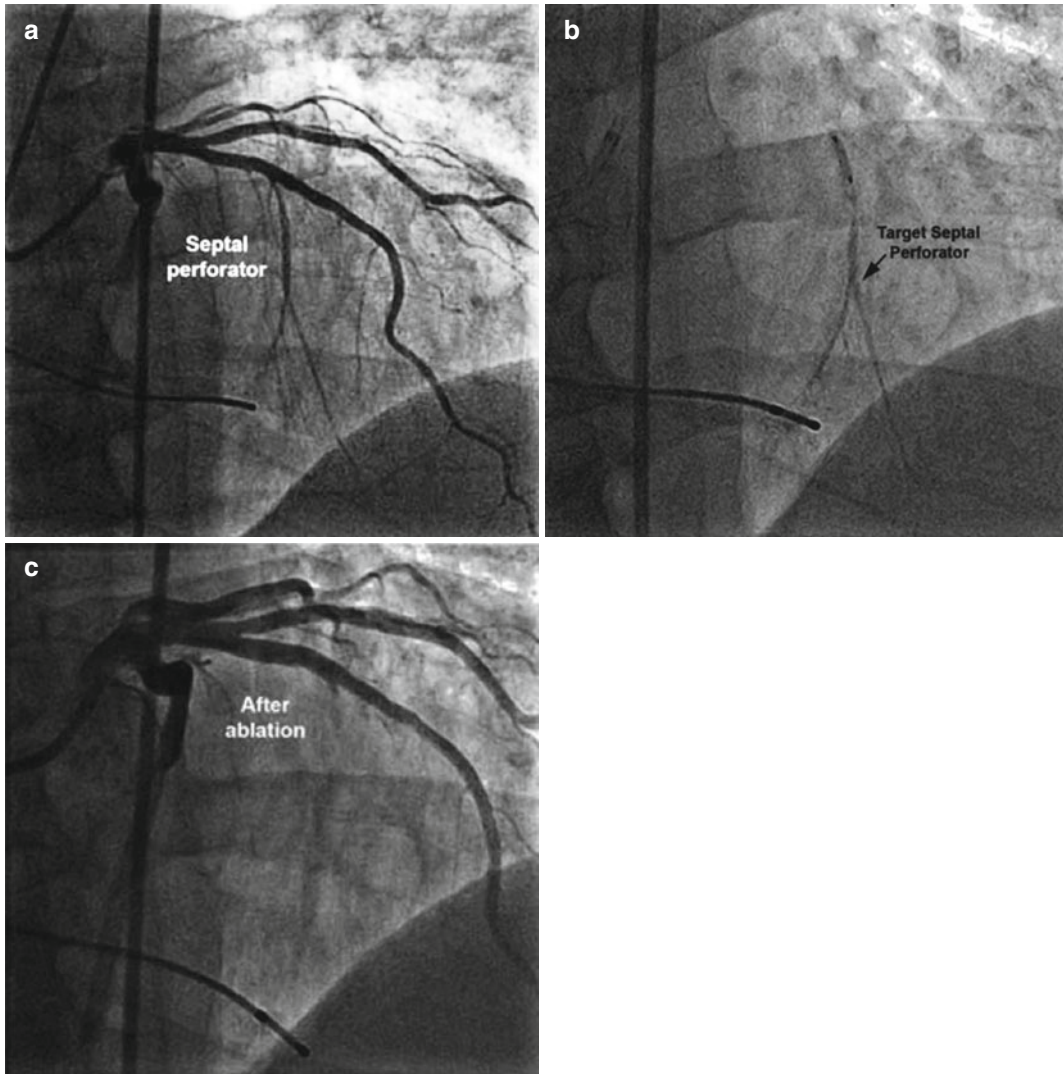

Fig. 1.12 Alcohol septal ablation. (**a**–**c**): Demonstrates the LAD and septal perforator (*top*, **a**), A balloon is introduced in the septal perforator over a wire and inflated during alcohol injection (*top*, **b**), after alcohol ablation, the septal perforator is ablated (*bottom*, **c**). (*top*, **d**): Reveals myocardial contrast injection of sepal perforator to determine the myocardial bed supplied prior to ethanol injection. An MRI following ablation denoting microvascular obstruction at the segment of the ablated septum (*bottom*, **e**). (**f**, **g**): The gradient across the LVOT before (*top*, **f**) and after (*bottom*, **e**) ablation

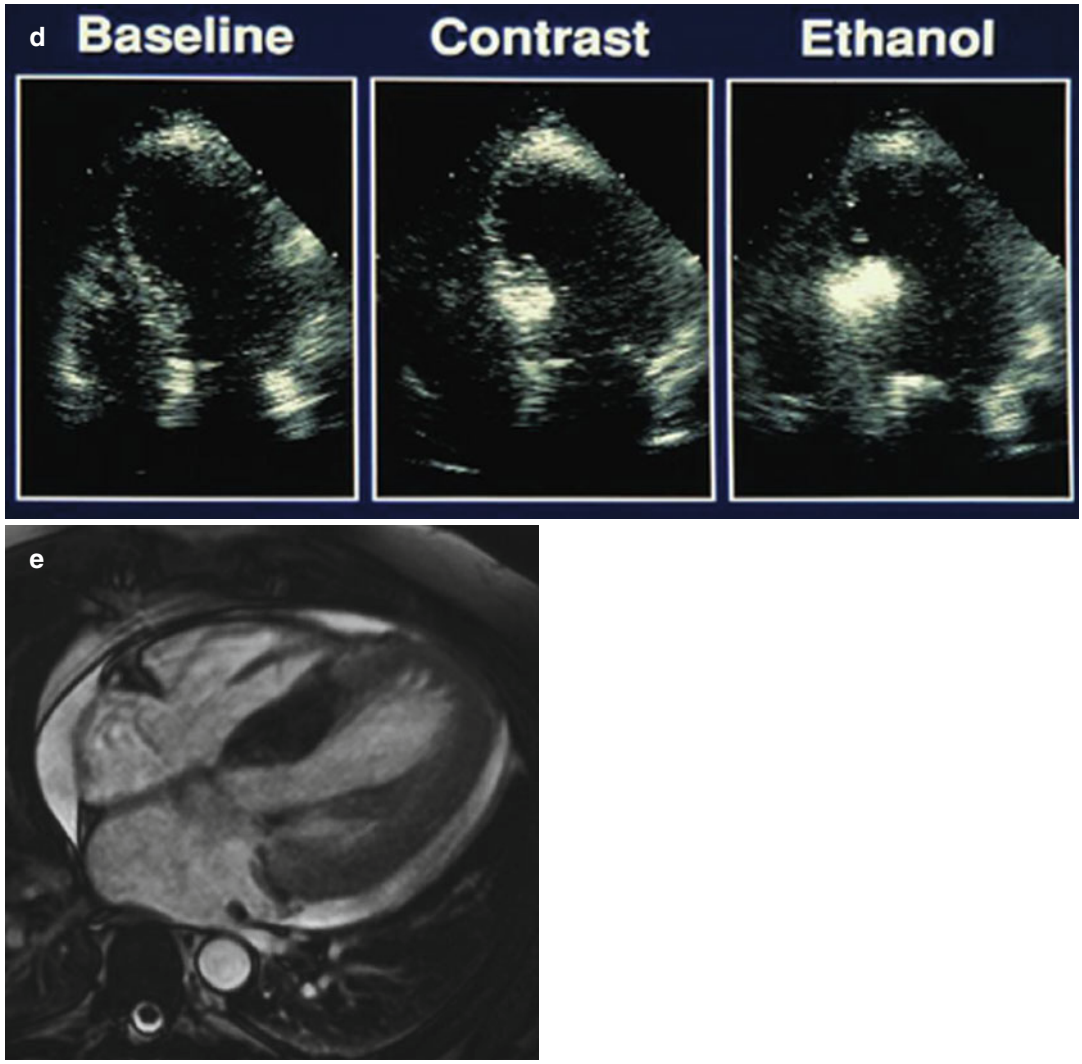

Fig. 1.12 (continued)

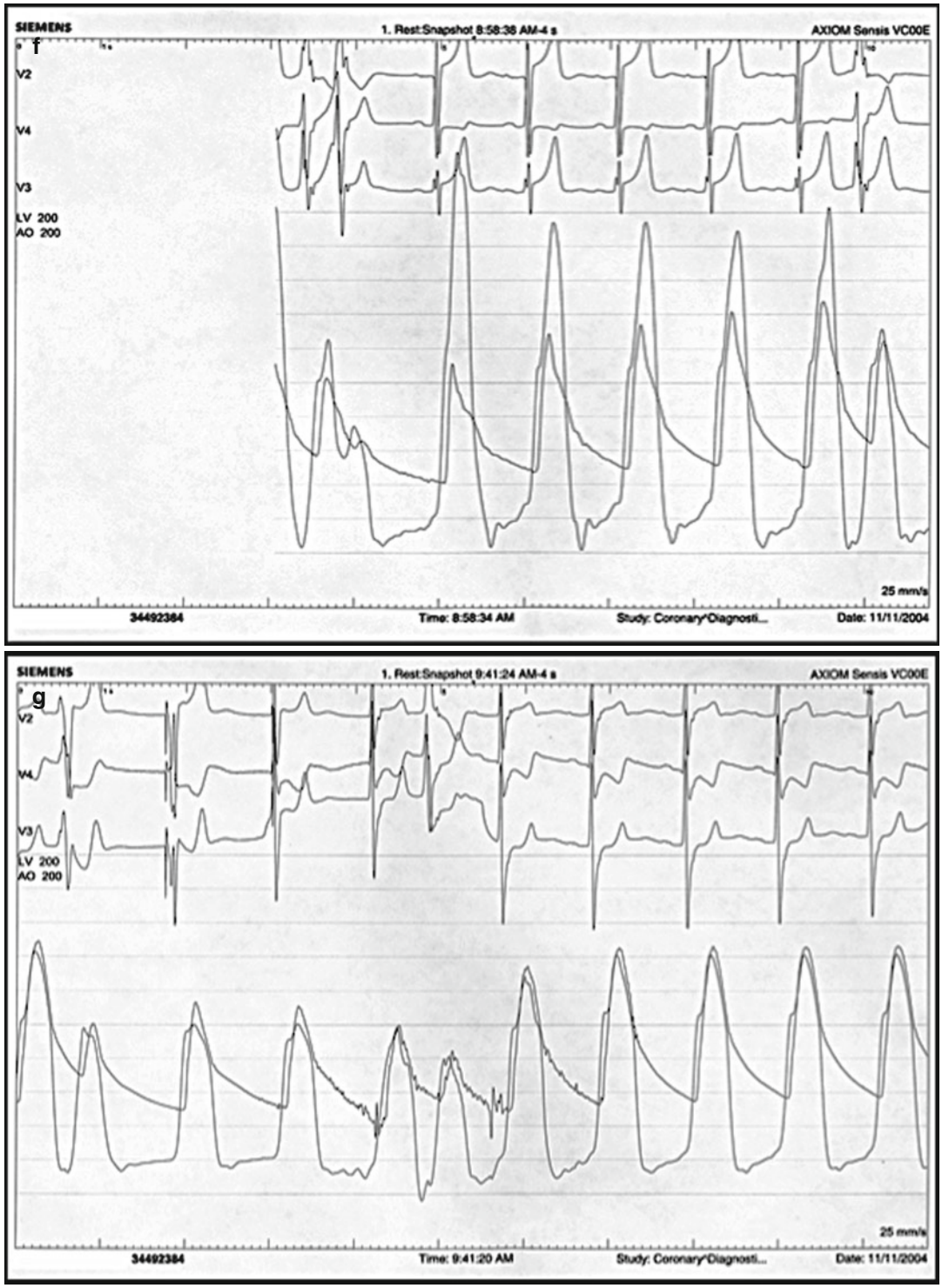

Fig. 1.12 (continued)

Conclusions

Aortic stenosis is a common disease with a guarded prognosis in the absence of aortic valve replacement. Both invasive and non-invasive methods are available to assess the severity of aortic stenosis. Novel technologies have extended therapeutic option to patients who are otherwise inoperable to high risk surgical candidates.

References

1. Willius FA, Dry TJ. A history of the heart and circulation. Philadelphia: W. B. Saunders Company; 1948. p. 456.
2. Mulcahy R. The early descriptions of aortic incompetence. Br Heart J. 1961;24:633–6.
3. Bailey C, Likoff W. Surgical management of aortic stenosis: an evolution of techniques and results. Arch Intern Med. 1957;99(6):859–87.
4. Carabelo BA, Stewat WJ, Crawford FA. Aortic valve disease. In: Topol EJ, editor. Text book of cardiovascular medicine. 2nd ed. Philadelphia: Lippincott-Raven; 2002. p. 509–28.
5. Piazza N, de Jaegere P, Becker AE, Serruys PW, Anderson RH. Anatomy of the aortic valvular complex and its implications for transcatheter implantation of the aortic valve. Circ Cardiovasc Interv. 2008;1:74–81.
6. Lung B, Baron G, Butchart EG, Delahaye F, Gohlke-Barwolf C, Levang OW, Tornos P, Vanoverschelde JL, Vermeer F, Bpersma E, Ravaud P, Vahanian A. A prospective survey of patients with valvular heart disease in Europe: the Euro heart survey on valvular heart disease. Eur Heart J. 2003;24(13):1231–43.
7. Nkomo VT, Gardin JM, Skelton TN, Gottdiener JS, Scott CG, Enriquez-Sarano M. Burden of valvular heart diseases: a population based study. Lancet. 2006;368:1005–11.
8. Osnabrugge RL, Mylotte D, Head SJ, Van Mieghem NM, Nkomo VT, LeReun CM, Bogers AJ, Piazza N, Kappetein AP. Aortic stenosis in the elderly disease prevalence and number of candidates for transcatheter aortic valve replacement: a meta-analysis and modeling study. J Am Coll Cardiol. 2013;62:1002–12.
9. Bach DS, Siao D, Girard SE, Duvernoy C, McCallister Jr BD, Gualano SK. Evaluation of patients with severe symptomatic aortic stenosis who do not undergo aortic valve replacement: the potential role of subjectively overestimated operative risk. Circ Cardiovasc Qual Outcomes. 2009;2:533–9.
10. Libby P, Bonow RO, Mann DL, Zipes DP. Braunwald's heart disease: a textbook of cardiovascular medicine. 8th ed. Philadelphia: Saunders/Elsevier; 2008.
11. Ward C. Clinical significance of the bicuspid aortic valve. Heart. 2000;83:81–5.
12. Rossebø AB M.D., Pedersen TR M.D., Ph.D., Boman K M.D., Ph.D., Brudi P M.D., Chambers JB M.D., Egstrup K M.D., Ph.D., Gerdts E M.D., Ph.D., Gohlke-Bärwolf C M.D., Holme I Ph.D., Kesäniemi AY M.D., Ph.D., Malbecq W Ph.D., Nienaber CA M.D., Ph.D., Ray S M.D., Skjærpe T M.D., Ph.D., Wachtell K M.D., Ph.D., Willenheimer R M.D., Ph.D. Intensive lipid lowering with simvastatin and ezetimibe in aortic stenosis. N Engl J Med. 2008;359:1343–56.
13. Roberts WC. The congenitally bicuspid aortic valve. A study of 85 autopsy cases. Am J Cardiol. 1970;26:72–83.
14. Steinberger J, Moller JH, Berry JM, Sinaiko AR. Echocardiographic diagnosis of heart disease in apparently healthy adolescents. Pediatrics. 2000;105:815–8.
15. Emanuel R, Withers R, O'Brien K, Ross P, Feizi O. Congenitally bicuspid aortic valves. Clinicogenetic study of 41 families. Br Heart J. 1978;40:1402–7.
16. Bonow RO, Carabello BA, Chatterjee K, de Leon AC, Faxon DP, Freed MD, Gaasch WH, Lytle BW, Nishimura RA, O'Gara PT, O'Rourke RA, Otto CM, Sha PM, Shanewise JS. ACC/AHA 2006 guidelines for the management of patients with valvular heart disease: a report of the American College of Cardiology/American Heart Association Task Force on Practice Guidelines (Writing Committee to Revise the 1998 Guidelines for the Management of Patients With Valvular Heart Disease) developed in collaboration with the Society of Cardiovascular Anesthesiologists endorsed by the Society for Cardiovascular Angiography and Interventions and the Society of Thoracic Surgeons. Circulation. 2006;114:e84–231.
17. Mack G, Silberbach M. Aortic and pulmonary stenosis. Pediatr Rev. 2000;21:79–85.
18. Duran AC, Frescura C, Sans-Coma V, Angelini A, Basso C, Thiene G. Bicuspid aortic valves in hearts with other congenital heart disease. J Heart Valve Dis. 1995;4:581–90.
19. Roose-Hesselink JW, Scholzel BE, Heijdra RJ, Spitaels SE, Meijboom FJ, Boersma E, Bogers AJ, Simoons ML. Aortic valve and aortic arch pathology after coarctation repair. Heart. 2003;89:1074–7.
20. Sybert VP. Cardiovascular malformations and complications in Turner syndrome. Pediatrics. 1998;101(1):E11.
21. Fernandes SM, Sanders SP, Khairy P, Jenkins KJ, Gauvreau K, Lang P, Simonds H, Colan SD. Morphology of bicuspid aortic valve in children and adolescents. J Am Coll Cardiol. 2004;44:1648–51.
22. Fedak PW, Verma S, David TE, Leask RL, Weisel RD, Butany J. Clinical and pathophysiological implications of a bicuspid aortic valve. Circulation. 2002;106:900–4.
23. Cripe L, Andelfinger G, Martin LJ, Shooner K, Benson DW. Bicuspid aortic valve is heritable. J Am Coll Cardiol. 2004;44:138–43.
24. Warnes CA, Williams RG, Bashore TM, Child JS, Connolly HM, Dearani JA, del Nido P, Fasules JW, Graham Jr TP, Hijazi ZM, Hunt SA, King ME, Landzberg MJ, Miner PD, Radford MJ, Walsh EP, Webb GD. ACC/AHA 2008 guidelines for the management of adults with congenital heart disease: a report of the American College of Cardiology/American Heart Association Task Force on Practice

Guidelines (Writing Committee to Develop Guidelines for the Management of Adults With Congenital Heart Disease). J Am Coll Cardiol. 2008;52:e143–263.
25. Roberts WC, Ko JM. Frequency by decades of unicuspid, bicuspid, and tricuspid aortic valves in adults having isolated aortic valve replacement for aortic stenosis, with or without associated aortic regurgitation. Circulation. 2005;111:920–5.
26. Park SJ, Enriquez-Sarano M, Choi JO, Lee SC, Park SW, Kim DK, Jeon ES, Oh JK, Chang SA. Hemodynamic patterns for symptomatic presentations of severe aortic stenosis. JACC: Card Imaging. 2013;6:137–46.
27. Monin JL, Lancellotti P, Monchi M, Lim P, Weiss E, Pierard L, Gueret P. Circulation. 2009;120:69–75.
28. Lim P, Monin JL, Monchi M, Garot J, Pasquet A, Hittinger L, Vanoverschelde JL, Carayon A, Gueret P. Predictors of outcome in patients with severe aortic stenosis and normal left ventricular function: role of B-type natriuretic peptide. Eur Heart J. 2004;25:2048–53.
29. Bergler-Klein J, Klaar U, Heger M, Rosenhek R, Mundigler G, Gabriel H, Binder T, Pacher R, Maurer G, Baumgartner H. Natriuretic peptides predict symptom-free survival and postoperative outcome in severe aortic stenosis. Circulation. 2004;109:2302–8.
30. Legget ME, Kuusisto J, Healy NL, Fujioka M, Schwaegler RG, Otto CM. Gender differences in left ventricular function at rest and with exercise in asymptomatic aortic stenosis. Am Heart J. 1996;131:94–100.
31. Hachicha Z, Dumesnil JG, Bogaty P, Pibarot P. Paradoxical low-flow, low-gradient severe aortic stenosis despite preserved ejection fraction is associated with higher afterload and reduced survival. Circulation. 2007;115:2856–64.
32. Cioffi G, Faggiano P, Vizzardi E, Tarantini L, Cramariuc D, Gerdts E, de Simone G. Prognostic value of inappropriately high left ventricular mass in asymptomatic severe aortic stenosis. Heart. 2011;97:301–7.
33. Duncan AI, Lowe BS, Garcia MJ, Xu M, Gillinov AM, Mihaljevic T, Koch CG. Influence of concentric left ventricular remodeling on early mortality after aortic valve replacement. Ann Thorac Surg. 2008;85:2030–9.
34. Orsinelli DA, Aurigemma GP, Battista S, Krendel S, Gaasch WH. Left ventricular hypertrophy and mortality after aortic valve replacement for aortic stenosis. J Am Coll Cardiol. 1993;22:1679–83.
35. Fuster RG, Argudo JA, Albarova OG, Sos FH, Lopez SC, Sorli MJ, Codoner MB, Minano JA. Left ventricular mass index in aortic valve surgery: a new index for early valve replacement? Eur J Cardiothorac Surg. 2003;23:696–702.
36. Mehta RH, Bruckman D, Das S, Tsai T, Russman P, Karavite D, Monaghan H, Sonnad S, Shea MJ, Eagle KA, Deeb GM. Implications of increased left ventricular mass index on in-hospital outcomes in patients undergoing aortic valve surgery. J Thorac Cardiovasc Surg. 2001;122:919–28.
37. Bech-Hanssen O, Wallentin I, Houltz E, Beckman Surrkula M, Larsson S, Caidahl K. Gender differences in patients with severe aortic stenosis: impact on preoperative left ventricular geometry and function, as well as early postoperative morbidity and mortality. Eur J Cardiothorac Surg. 1999;15:24–30.
38. Otto CM, Lind BK, Kitzman DW, Gersh BJ, Siscovick DS. Association of aortic-valve sclerosis with cardiovascular mortality and morbidity in the elderly. N Engl J Med. 1999;34:142–7.
39. Olsen MH, Wachtell K, Bella JN, Gerdts E, Palmieri V, Nieminen MS, Smith G, Ibsen H, Devereux RB, LIFE Substudy. Aortic valve sclerosis relates to cardiovascular events in patients with hypertension (a LIFE substudy). Am J Cardiol. 2005;95:132–6.
40. Taylor HA, Clark BL, Garrison RJ, Andrew ME, Han H, Fox ER, Arnett DK, Samdarshi T, Jones DW. Relation of aortic valve sclerosis to risk of coronary heart disease in African. Am J Cardiol. 2005;95(3):401–4.
41. Ross J, Braunwald E. Aortic stenosis. Circulation. 1968;38:V-61–7.
42. Otto CM, Burwash IG, Legget ME, Munt BI, Fujioka M, Healy NL, Kraft CD, Miyake-Hull CY, Schwaegler RG. Prospective study of asymptomatic valvular aortic stenosis clinical, echocardiographic and exercise predictors of outcome. Circulation. 1997;95:2262–70.
43. Rosenhek R, Binder T, Porenta G, Lang I, Christ G, Schemper M, Maurer G, Baumgartner H. Predictors of outcome in severe, asymptomatic aortic stenosis. N Engl J Med. 2000;343:611–7.
44. Pellikka PA, Sarano ME, Nishimura RA, Malouf JF, Bailey KR, Scott CG, Barnes ME, Tajik AJ. Outcome of 622 adults with asymptomatic, hemodynamically significant aortic stenosis during prolonged follow-up. Circulation. 2005;111:3290–5.
45. Rosenhek R, Zilberszac R, Schemper M, Czerny M, Mundigler G, Graf S, Bergler-Klein J, Grimm M, Gabriel H, Maurer G, Makkar RR, Fontana GP, Jilaihawi H, Kapadia S, Pichard AD, Douglas PS, Thourani VH, Babaliaros VC, Webb JG, Herrmann HC, Bavaria JE, Kodali S, Brown DL, Bowers B, Dewey TM, Svensson LG, Tuzcu M, Moses JW, Williams MR, Siegel RJ, Akin JJ, Anderson WN, Pocock S, Smith CR, Leon MB, PARTNER Trial Investigators. Transcatheter aortic-valve replacement for inoperable severe aortic stenosis. N Engl J Med. 2012;366:1696–704.
46. The Joint Task Force on the Management of Valvular Heart Disease of the European Society of Cardiology (ESC), The European Association for Cardio-Thoracic Surgery (EACTS). Guidelines on the management of valvular heart disease. Eur Heart J. 2012;33:2451–96.
47. Nishimura RA, Otto CM, Bonow RO, Carabello BA, Erwin JP, Guyton RA, O'Gara PT, Ruiz CE, Skubas NJ, Sorajja P, Sundt TM, Thomas JD. 2014 AHA/ACC guideline for the management of patients with valvular heart disease: executive summary: a report of the American College of Cardiology/American Heart Association Task Force on Practice Guidelines. Circulation. 2014;129(23):2440–92.
48. Ussia GP, Mule M, Barbanti M, Cammalleri V, Scarabelli M, Imme S, Capodanno D, Ciriminna S,

Tamburino C. Quality of life assessment after percutaneous aortic valve implantation. Eur Heart J. 2009;30: 1790–6.
49. Bouma BJ, van den Brink RBA, van der Meulen JHP, Verheul HA, Cheriex EC, Hamer HPM, Dekker E, Lie KI, Tijssen JGP. To operate or not on elderly patients with aortic stenosis: the decision and its consequences. Heart. 1999;82:143–8.
50. Iung B, Baron G, Butchart EG, Delahaye F, Gohlke-Ba¨rwolf C, Levang OW, Tornos P, Vanoverschelde JL, Vermeer F, Boersma E, Ravaud P, Vahanian A. A prospective survey of patients with valvular heart disease in Europe: the Euro Heart Survey on valvular heart disease. Eur Heart J. 2003;24:1231–43.
51. Varadarajan P, Kapoor N, Bansal RC, Pai RG. Clinical profile and natural; history of 453 nonsurgically managed patients with severe aortic stenosis. Ann Thorac Surg. 2006;82:2111–5.
52. Iung B, Cachier A, Baron G, Messika-Zeitoun D, Delahaye F, Tornos P, Gohlke-Bärwolf C, Boersma E, Ravaud P, Vahanian A. Decision-making in elderly patients with severe aortic stenosis: why are so many denied surgery? Eur Heart J. 2005;26:2714–20.
53. Brown JM, O'Brien SM, Wu C, Sikora JAH, Griffith BP, Gammie JS. Isolated aortic valve replacement in North America comprising 108,687 patients in 10 years: changes in risks, valve types, and outcomes in the Society of Thoracic Surgeons National Database. J Thorac Cardiovasc Surg. 2009;137:82–90.
54. Kodali SK, Williams MR, Smith CR, Svensson LG, Webb JG, Makkar RR, Fontana GP, Dewey TM, Thourani VH, Pichard AD, Fischbein M, Szeto WY, Lim S, Greason KL, Teirstein PS, Malaisrie SC, Doublas PS, Hahn RT, Whisenant B, Zajarias A, Wang D, Akin JJ, Anderson WN, Leon MB, PARNTER Trial Investigators. Two-year outcomes after transcatheter or surgical aortic-valve replacement. NEJM. 2012;366:1686–95.
55. Makker RR, Fontana GP, Jilaihawi H, Kapadia S, Pichard AD, Doublas PS, Thouruani VH, Babaliasros VC, Webb JC, Herrmann HC, Bavaria JE, Kodali S, Brown DL, Bowers B, Dewey TM, Svenssson LG, Tuzcu M, Moses JW, Williams MR, Siegel RJ, Akin JJ, Anderson WN, Pocock S, Smith CR, Leon MB, PARTNER Trial Investigators. Transcatheter aortic-valve replacement for inoperable severe aortic stenosis. NEJM. 2012;366:1697–704.
56. Adams DH, Popma JJ, Reardon MJ, Yakubov SJ, Coselli JS, Deeb GM, Gleason TG, Buchbinder M, Hermiller Jr J, Kleiman NS, Chetcuti S, Heiser J, Merhi W, Zorn G, Tadros P, Robinson N, Petrossian G, Hughes GC, Harrison JK, Conte J, Maini B, Mumtaz M, Chenoweth S, Oh JK, U. S. CoreValve Clinical Investigators. Transcatheter aortic-valve replacement with a self-expanding prosthesis. NEJM. 2014;370:1790–8.

Clinical Assessment of the Severity of Aortic Stenosis

2

Sibin K. Zacharias and James A. Goldstein

Abstract

Valvular aortic stenosis (AS) has three primary etiologies: age-related degenerative calcification, congenital bicuspid valve with superimposed calcification, and rheumatic disease. Despite the progressive histopathological changes that lead to anatomical alteration of the aortic valve apparatus, aortic stenosis has a long asymptomatic period. Eventually, AS results in predictable pathophysiologic alterations in cardiac pressures and blood flow that elicit the classic symptomatology and physical stigmata of this disease. The development of symptoms signals an abrupt worsening in prognosis. An appreciation of these pathophysiologic derangements is essential to the clinical assessment of aortic valve obstruction.

Keywords

Pathophysiology of aortic stenosis (AS) • Angina and aortic stenosis • Syncope and aortic stenosis • Dyspnea and aortic stenosis • Gastrointestinal (GI) bleeding and aortic stenosis • Physical exam for aortic stenosis • Low flow, low gradient aortic stenosis • Exercise and aortic stenosis

Introduction

Valvular aortic stenosis (AS) has three primary etiologies: age-related degenerative calcification, congenital bicuspid valve with superimposed calcification, and rheumatic disease. Despite the progressive histopathological changes that lead to anatomical alteration of the aortic valve apparatus, aortic stenosis has a long asymptomatic period [1]. Eventually, AS results in predictable pathophysiologic alterations in cardiac pressures and blood flow that elicit the classic symptomatology and physical stigmata of this disease. The development of symptoms signals an abrupt worsening in prognosis. An appreciation of these pathophysiologic derangements is essential to the clinical assessment of aortic valve obstruction.

S.K. Zacharias, MD • J.A. Goldstein, MD (✉)
Department of Cardiovascular Medicine,
Beaumont Health, Oakland University/William
Beaumont School of Medicine, Royal Oak, MI, USA
e-mail: jgoldstein@beaumont.edu

A.E. Abbas (ed.), *Aortic Stenosis: Case-Based Diagnosis and Therapy*,
DOI 10.1007/978-1-4471-5242-2_2

Pathophysiology

Aortic stenosis may result in both diastolic and systolic derangement of ventricular function with a resultant decline in ejection fraction, transvalvular flow and an increase in mean left atrial pressure. The key pathophysiologic components of and compensatory responses to AS include: (1) Obstruction to outflow which limits cardiac output (CO), first with exercise then later at rest; (2) Increased afterload leading to compensatory left ventricular hypertrophy (LVH), ultimately resulting in impaired LV compliance and filling; and (3) Prolongation of LV ejection time (LVET), which maintains stroke volume under conditions of fixed obstruction. All symptoms and physical signs of AS are a direct manifestation of these pathophysiologic mechanisms. Thus, these three pathophysiologic tenets form the basis for clinical assessment of the presence and severity of AS.

Outflow Obstruction: Effects on Cardiac Output

Progressive narrowing of the aortic valve area limits stroke volume (SV) and cardiac output (CO), which manifests symptomatically as exertional fatigue. With exercise, the rise in aortic jet velocity and pressure gradient between the LV and aorta increases with increased flow. This may result in an abnormal blood pressure response, either blunted or hypotensive. Further, in the setting of AS and a fixed SV, exercise-induced systemic arterial vasodilation may induce hypotension which manifests as syncope. This scenario is more likely if the patient is not well hydrated or has been administered vasodilating drugs.

Increased Afterload: Effects on LV Compliance and Contractility

AS imposes a fixed obstruction to LV outflow, a process that develops over several decades. As the primary compensatory mechanism to chronic pressure overload, the LV remodels by concentric hypertrophy (LVH), through parallel replication of the sarcomere, which is characterized by increased wall thickness but normal LV diastolic dimensions [2]. Increased wall thickness normalizes wall stress, thereby preserving LV contractility as outlined in the Laplace equation:

$$\text{Wall Stress} = \text{Pressure} \times \text{Radius} / 2 \times \text{Wall thickness}$$

Progressive LVH (which may be attended by fibrosis) leads to impaired LV compliance, resulting in diastolic dysfunction that eventually leads to elevated mean left atrial pressures. Moreover, as the disease progresses, the increase in wall thickness may be insufficient to offset the rise in pressure with afterload mismatch, resulting in a rise in wall stress and decline in left ventricular systolic function. True depression of myocardial contractility also occurs in the presence of aortic stenosis for unknown reasons, again leading to a decline in ventricular systolic function. A decline in LV systolic function also leads to elevated mean left atrial pressure and dyspnea. Over time, increased mean left atrial pressure induces left atrial dilation, which may result in atrial arrhythmias. Impaired filling also limits LV preload at rest and with exercise, thereby limiting stroke volume which compounds diminished cardiac output attributable to the obstruction itself.

Augmented atrial contractile function also plays an important compensatory role in AS. Under conditions of abnormal LV compliance, the atrial booster pump function disproportionately contributes to filling of the stiff LV chamber at a lower mean left atrial pressure, thereby allowing better functional capacity. Conversely, loss of this "atrial kick" due to atrial fibrillation may lead to clinical decompensation characterized by pulmonary congestive symptoms (dyspnea) and impaired output (fatigue).

Prolonged LV Ejection Time: Compensation and Insight into Severity of Obstruction

The second mechanism by which the heart compensates for AS is through prolongation of the

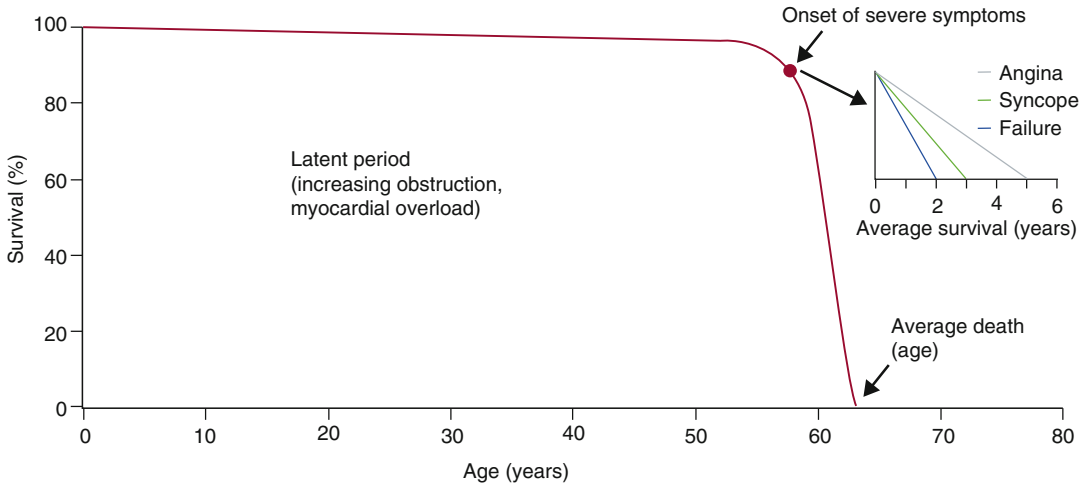

Fig. 2.1 Average survival and symptom onset in patients with aortic stenosis (From Ross and Braunwald [1] with permission)

LVET. In patients with normal valvular function, aortic valve flow peaks in mid-systole. Under conditions of outflow obstruction, the LVET prolongs in order for the LV to more fully empty and generate forward SV. This compensatory mechanism is detectable on physical exam by the pattern and timing of the peak of the systolic murmur, and the behavior of S2.

Historical Features of Aortic Stenosis

Survival in aortic stenosis is nearly normal until symptoms develop (Fig. 2.1). Symptoms typically develop only with at least moderate AS. Once symptoms occur, the prognosis varies according to the clinical presentation. Classic symptoms associated with AS include exertional dyspnea, angina, and syncope. Patients with known AS may also complain of progressive fatigue and decreased exercise tolerance. As the severity of aortic stenosis progresses, heart failure will progress and left ventricular function will eventually be compromised. Other associated findings with AS include gastrointestinal bleeding and infective endocarditis [2].

In an echocardiographic study of 498 patients with severe AS, Park et al. divided patients into four groups depending on the presentation; asymptomatic, syncope, dyspnea, and chest pain [3]. Despite similar valve area and gradient, symptomatic patients were older and had lower cardiac output, and a higher E/e' ratio (an echocardiographic correlate of left atrial pressure). Moreover, patients with syncope displayed smaller LV dimension, stroke volume, cardiac output, left atrial volume index, and E/e' ratio. Conversely, patient with dyspnea were found to have worst diastolic dysfunction with largest left atrial index and E/e' ratio.

Angina

Angina in the setting of aortic stenosis is multifactorial, and differs between those with and without coronary artery disease. As LV thickness increases as a compensatory mechanism secondary to chronic pressure overload, there is a reduction of oxygen delivery due to compression of the coronary vessels. Additionally, with increased ventricular end-diastolic pressure, and impaired relaxation, diminished diastolic coronary filling occurs leading to decreased coronary supply to the myocardium.

On the other hand, the hypertrophied myocardium has an increased oxygen requirement contributing to the mismatch between oxygen supply and demand and causing angina. An alternate mechanism may be seen in patients with CAD,

where coronary obstruction may lead to angina. In these patients, angina may be exacerbated by periods of decreased cardiac output as well as during exercise to the fixed obstruction of aortic stenosis again due to an imbalance between supply and demand, respectively.

Syncope

Syncope may be attributed to several etiologies. The predominant mechanism relates to reduced cerebral perfusion, usually occurring during exertion. In the presence of a fixed cardiac output, systemic arterial vasodilation results in reduced blood pressure. Malfunction of the baroreceptor mechanism and a vasodepressor response in the setting of severe AS can also lead to syncope. At rest, syncope may result from multiple transient mechanisms. Transient ventricular fibrillation may cause reduced perfusion. Atrial fibrillation may impair LV filling, leading to a reduced cardiac output and subsequent decrease in cardiac output. The extension of calcification into the conduction system may cause transient AV block leading to syncope.

Dyspnea

Exertional dyspnea may be caused by several factors. First, a rise in LV end-diastolic pressure may result from LV diastolic dysfunction, leading to pulmonary vascular congestion. Second, an inability to augment cardiac output in the setting of a fixed obstruction may lead to exertional symptoms. Patients may develop heart failure symptoms including orthopnea, paroxysmal nocturnal dyspnea, and pulmonary edema as the AS severity increases, leading to pulmonary venous hypertension.

Gastrointestinal Bleeding

Less commonly, GI bleeding develops with severe AS, and is related to AV malformations or angiodysplasia, a condition known as "Heyde's syndrome." Bleeding results from an acquired type IIA von Willebrand's syndrome, caused by a deficiency of high-molecular-weight multimers of von Willebrand factor. These abnormalities may be correctable with AVR.

Infective Endocarditis

Infective endocarditis is a complication of aortic stenosis, generally more prevalent in young rather than older individuals. These patients may develop cerebral emboli, TIAs, or loss of vision due to calcific embolic occlusion of the central retinal artery.

Frailty Assessment

Assessment of frailty has emerged as a tool to help guide the candidacy of patients for surgical versus transaortic valve replacement. This assessment includes dominant hand grip strength (in kg), 15-ft walk duration (seconds), Katz activities of daily living (which includes degree of independence in bathing, dressing, toileting, continence, and feeding), independence in ambulation and the serum albumin (g/dl).

Physical Exam

The physical signs of AS follow from the pathophysiologic mechanisms previously described. The cardinal features of the AS clinical examination include changes in the pulse waveform, precordial examination, and auscultation.

Pulse Waveform

AS inscribes a classic pulse wave abnormality which is palpable in the brachial arteries, but best appreciated in the carotid artery. As valve obstruction progresses from mild to severe, the carotid pulse demonstrates progressive alterations in upstroke, peak, and amplitude. In severe AS, the expected carotid waveform is characterized by a slow-rising, late peaking, low-amplitude

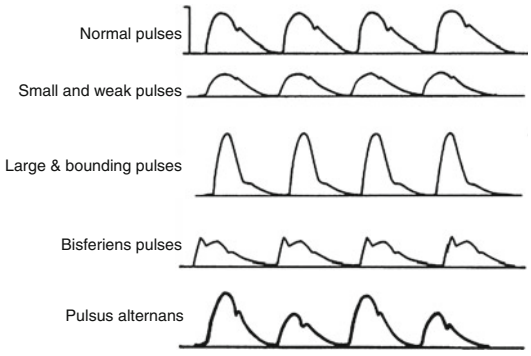

Fig. 2.2 Normal and various pathologic carotid waveforms

pulse (Fig. 2.2). In Latin, this is described as "pulsus parvus et tardus," which translates to "slow and late." Caution must be employed in ascribing a diminutive carotid pulse to AS alone, for severe depression of SV due to cardiomyopathy may mimic the pulse of AS (but not the murmur). Conversely, in those with very stiff arterial systems, which amplify pulses, severe AS may be present despite a seemingly normal carotid waveform. This should be kept in mind in elderly patients with symptoms and a systolic murmur consistent with AS. Such patients often have inelastic arterial vessels due to calcification, and may have normal or even increased carotid upstrokes due to increased reflected waves in the aorta. Similarly, patients with systemic hypertension or concurrent aortic insufficiency may also have a normal or increased carotid impulse. In the face of severe AS, echocardiography successfully adjudicates such cases.

Precordial Examination

Under conditions of significant AS, LVH is expected and severity should parallel the severity of valve obstruction. LVH is appreciated at the point of maximal impulse (PMI) as a progressively sustained impulse that may be displaced both inferiorly and laterally. The presence of a palpable thrill over the right neck, shoulder, or clavicle is indicative of more severe aortic stenosis, generally grade 4 intensity. If the patient is in sinus rhythm, a palpable S4 indicating augmented atrial contractile contribution to LV filling may be appreciated as an additional pre-systolic impulse.

Auscultation

Increasing severity of AS is associated with distinctive auscultatory findings characterized by a louder and later-peaking systolic ejection murmur, and abnormalities of the second heart sound [2, 4]. AS-induced turbulence through the narrowed valve always produces a systolic ejection murmur which is typically harsh, noisy, and impure. The murmur begins after the first heart sound, following isovolumetric contraction, when ventricular pressure exceeds the central aortic pressure. It rises in a crescendo pattern to a peak as flow proceeds through the LV outflow tract and across the aortic valve. It then declines in a decrescendo pattern as flow diminishes. The murmur ends just before the second heart sound. The murmur is best heard at the base of heart, in the right second intercostal space. The murmur may radiate to both carotid arteries due to the direction of the high velocity jet within the aortic root. It may have an early systolic peak and short duration, relatively late peak and prolonged duration, or any gradation in between [4, 5]. Regardless of the character, it generally always assumes a "diamond shape." As stenosis severity progresses, the murmur becomes louder, more harsh and later in its peak (Fig. 2.3).

Proper assessment of the murmur peak requires timing with the carotid upstroke and S2. The intensity of the murmur is related to the volume and velocity of transaortic flow, while the pitch is related to the transaortic pressure gradient and valve area. Both the intensity and pitch are related to sound conductivity through the pericardium, lungs, and chest wall. In general, a louder murmur with a higher pitch is associated with increased severity. However, in situations with decreased transaortic flow, with normal or decreased ejection fraction, or with COPD, obesity, or effusion, a low pitch murmur with low intensity may be auscultated in the presence of severe AS.

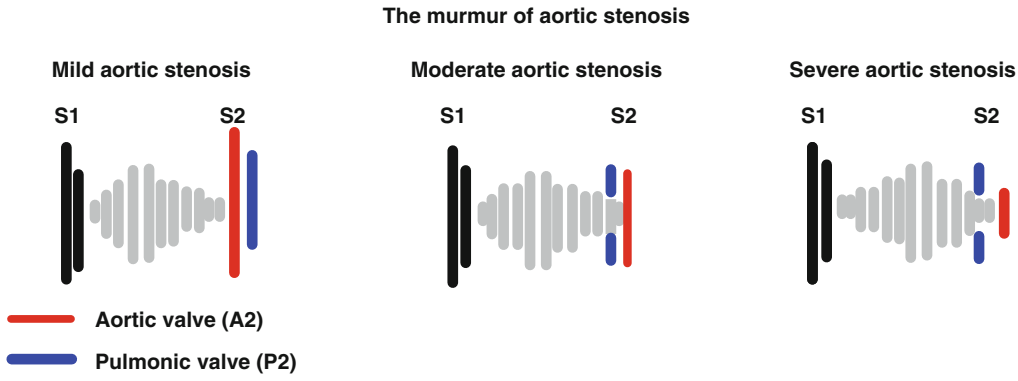

Fig. 2.3 The changing character of the murmur and second heart sound as the aortic stenosis severity progresses from mild to severe *left*, *center*, and *right*, accordingly

The murmur pitch and intensity also correlate well with echo-Doppler velocities. Munt et al. demonstrated that physical examination findings of systolic murmur intensity, time-to-peak murmur intensity, the presence of a single S2, and a delay or decrease in carotid upstroke statistically correlate with aortic stenosis severity as assessed by Doppler echocardiography [6].

In some patients, especially elderly patients with fibrocalcific aortic stenosis, a second murmur may be heard at the LV apex. This murmur differs in quality, and is often described as both pure and musical, caused by high frequency oscillations of the fibrocalcific cusps, which radiate to the apex. These two distinctive mid-systolic murmurs – the noisy right basal and the musical apical – have been termed the "Gallavardin dissociation." The pathophysiologic mechanism underlying this murmur has not been fully delineated. Its pattern and location suggest it may arise in part from acceleration of blood toward the LV outflow tract and beneath the valve itself [4].

One may also hear a soft diastolic decrescendo murmur indicative of concomitant aortic regurgitation (AR). When both systolic and diastolic aortic murmurs are present, the character of the pulse is helpful in grading mixed AS/AR, with bounding pulses indicating predominant AR and a more diminutive pulse consistent with more severe AS.

Analysis of the second heart sound is important when assessing the severity of AS. Under conditions of progressive AS, LVET prolongs to maintain SV. Therefore, the aortic component of S2 is delayed, which in severe AS may manifest as reversed splitting of S2, in which the timing of A2 follows P2. In fact, if normal splitting of S2 is present, AS is unlikely. Softening or absence of the second heart sound implies that the aortic valve leaflets are no longer pliable or flexible enough to create an audible closing sound (A2) and signifies severity. Severely calcified and immobile aortic valve leaflets are present in severe AS and will lead to a single S2. This may result from three factors: (1) A2 is inaudible, (2) P2 is buried in the prolonged aortic ejection murmur, or (3) A2 and P2 are superimposed on one another due a prolongation in LV systole. If the patient is in sinus rhythm, an audible S4 may be present as a low-pitched, late diastolic sound reflecting the atrial contraction into a LV with reduced compliance and increased end-diastolic pressure in patients with severe AS. Table 2.1 provides a summary of physical exam findings as the severity of AS increases.

Differentiating Aortic Stenosis from Other Murmurs

Aortic stenosis must be differentiated from other pathologies producing a systolic murmur, including mitral regurgitation (MR) and hypertrophic obstructive cardiomyopathy (HOCM).

Table 2.1 Classic physical examination findings according to the severity of aortic stenosis

	Mild	Moderate	Severe
Murmur peak	Early	Mid	Late
2nd heart sound	Normal	Soft	Absent
Carotid upstroke	Brisk	Delayed	Delayed, low volume
Pulse pressure	Normal	Normal	Narrow
PMI	Normal	Normal/lateral displacement	Lateral displacement
Precordium	Quiet	Quiet	LV heave

Murmur timing and dynamic auscultation are key factors differentiating these murmurs, as are their relationship to other physical signs, particularly the carotid pulse. One can differentiate AS from MR by timing the murmur precisely. A holosystolic murmur at the apex radiating to the axilla suggests MR. In primary MR, the carotid pulse is typically brisk with a smaller volume. Cessation of the murmur before A2 is indicative of AS, and is associated with the characteristic carotid waveform previously described. The intensity of the murmur may vary as diastolic filling varies, as when a pause is present after atrial fibrillation or a premature ventricular contraction. In this setting, the murmur intensity of aortic stenosis increases after a pause, whereas the murmur of mitral regurgitation remains essentially unchanged.

HOCM produces signs and symptoms identical to those observed in AS. Both conditions result in LVH, evident by precordial inspection of the apical impulse. HOCM induces a loud harsh systolic ejection murmur, but because the obstruction is dynamic, the initial carotid upstroke is intact, though the volume small. If resting obstruction is present, the result is a bifid or Bisfiriens carotid pulse indicating mid-systolic obstruction to flow.

Provocative maneuvers, such as squatting, increase the intensity of the murmur of AS due to increased preload. Standing and Valsalva, however, decrease preload and subsequently transvalvular flow, which decreases the AS murmur intensity. Maneuvers help differentiate murmurs of MR (intensifies with handgrip) and HOCM (worsens with Valsalva's maneuver) as well.

Specific Clinical Scenarios

Low Flow, Low Gradient AS

Patients with depressed left ventricular ejection fraction (EF) pose a particular diagnostic challenge to defining the severity of aortic stenosis. Depressed EF is generally caused by one of two factors, namely afterload mismatch or contractile dysfunction. Patients with a decline in ventricular systolic function from afterload mismatch are likely to restore function following aortic valve replacement compared to those who develop a true decline in contractility. When depressed EF is present, classic clinical findings associated with severe aortic stenosis, such as a loud, late peaking murmur, are usually not present due to lower cardiac output and decreased stroke volume. One is more likely to see features of LV failure with low output. In this setting, differentiating severe from pseudo-severe aortic stenosis may be accomplished by increasing cardiac output by increasing contractility using dobutamine or decreasing afterload with nitroprusside, respectively [7]. Cardiac output augmentation may bring forth the classic physical exam findings including a slow-rising arterial pulse and louder, late peaking murmur.

Exercise and AS

There is a quadratic relationship with transvalvular gradient and flow. Doubling the cardiac output, as may occur with exercise, would conceptually lead to a fourfold increase

in the transvalvular gradient while the systolic ejection time per minute remains unchanged. This may result in an abnormal blood pressure response and could manifest as syncope.

An increase in transvalvular gradient will also increase the LV systolic pressure to maintain systemic blood pressure, which will increase myocardial oxygen demand and limit the LV ejection performance. Accordingly, patients may exhibit ischemic chest pain and congestive heart failure symptoms. However, as the heart rate increases with exercise and the systolic ejection period shortens, increased venous return and vasodilation counteract this trend in an attempt to maintain or increase stroke volume. The net product of systolic ejection period and heart rate (systolic ejection time per minute) increases, offsetting the increase in cardiac output and diminishing the extent of gradient increase with exercise and thus the increase in LV systolic pressure. This increase in LV systolic pressure coupled with a decline in diastolic filling time during exercise, due to increased heart rate, will lead to a failure to increase preload and the LV reaches its preload reserve. Once preload reserve is reached, stroke volume now becomes only related to ventricular pressure (since preload is fixed) with an inability to augment cardiac output also leading to exertional dyspnea and fatigue.

In patients with severe AS who present with no or minimal symptoms and are being considered for surgery, a supervised treadmill exercise test may help to elicit symptoms, hypotension, and/or EKG changes suggesting the presence of severe symptomatic AS.

Summary

Assessing the clinical severity of aortic stenosis is paramount in the evaluation and management of this increasingly common valvular disease. Patients with severe AS often experience a long asymptomatic period. Classic physical findings in severe AS including a low volume carotid pulse; narrow pulse pressure; inferolaterally displaced cardiac impulse; loud, late-peaking, crescendo-decrescendo murmur; and soft or absent S2. In the setting of low cardiac output and stroke volume, these classic findings may be less prominent. Augmenting cardiac output by increasing contractility or decreasing afterload may be helpful in such cases. Non-invasive imaging with transthoracic and transesophageal echocardiogram assists in the confirmation of clinical suspicions developed from the history and physical examination.

References

1. Ross Jr J, Braunwald E. Aortic stenosis. Circulation. 1968;38(1 Suppl):61–7.
2. Libby P, Braunwald E. Braunwald's heart disease: a textbook of cardiovascular medicine. 8th ed. Philadelphia: Saunders/Elsevier; 2008.
3. Park SJ, et al. Hemodynamic patterns for symptomatic presentations of severe aortic stenosis. JACC Cardiovasc Imaging. 2013;6(2):137–46.
4. Perloff JK. Physical examination of the heart and circulation, vol. viii. 2nd ed. Philadelphia: Saunders; 1990. p. 292.
5. Harvey WP. Cardiac pearls. Newton: Laennec; 1993. p. 345.
6. Munt B, et al. Physical examination in valvular aortic stenosis: correlation with stenosis severity and prediction of clinical outcome. Am Heart J. 1999;137(2):298–306.
7. Carabello BA. Evaluation and management of patients with aortic stenosis. Circulation. 2002;105(15):1746–50.

3 Physiological Basis for Area and Gradient Assessment: Hemodynamic Principles of Aortic Stenosis

Amr E. Abbas and Philippe Pibarot

Abstract

The clinical syndrome of severe aortic stenosis (AS) is primarily diagnosed by a mean trans-valve pressure gradient (ΔP_{mean}) >40 mmHg, an aortic valve area (AVA) <1 cm^2, AVA indexed to BSA <0.6 cm^2/m^2, and/or a maximum transaortic velocity (AV_{Vel}) >4 m/s with or without symptoms. Surgical or transcatheter aortic valve replacement for symptomatic, severe AS results in significant improvement in survival and quality of life across a spectrum of surgical risk profiles. However, invasive treatments for non-severe AS have not demonstrated similar benefits, and may subject patients to unnecessary procedural risk. Therefore, precise quantification of AS severity is of paramount importance. Notwithstanding, it remains unclear whether area and gradient criteria have to present collectively or individually, or whether they must be obtained invasively or by Doppler.

In this chapter, we will review the physiological changes that occur as blood flow approaches the stenotic aortic valve with generation of a transvalvular ΔP, the relationship between AVA and ΔP, the determinants of transvalvular ΔP and AVA, and the role of Doppler and cardiac catheterization in assessing the severity of aortic stenosis.

Keywords

Transvalvular pressure gradient in aortic stenosis • Aortic valve area in aortic stenosis • Bernoulli equation and aortic stenosis • Assessment of aortic stenosis severity • Aortic valve gradient calculations • Measures of left ventricular hemodynamic burden

A.E. Abbas, MD, FACC, FSCAI, FSVM, FASE, RPVI (✉)
Department of Cardiovascular Medicine, Beaumont Health, Oakland University/William Beaumont School of Medicine, Royal Oak, MI, USA
e-mail: aabbas@beaumont.edu

P. Pibarot, DVM, PhD, FAHA, FACC, FESC, FASE
Department of Research, Quebec Heart and Lung Institute, Quebec City, QC, Canada

A.E. Abbas (ed.), *Aortic Stenosis: Case-Based Diagnosis and Therapy*,
DOI 10.1007/978-1-4471-5242-2_3

Introduction

The clinical syndrome of severe aortic stenosis (AS) is primarily diagnosed by a mean transvalve pressure gradient (ΔP_{mean}) >40 mmHg, an aortic valve area (AVA) <1 cm2, AVA indexed to BSA <0.6 cm^2/m^2, and/or a maximum transaortic velocity (AV_{Vel}) >4 m/s with or without symptoms [1, 2]. Surgical or transcatheter aortic valve replacement for symptomatic, severe AS results in significant improvement in survival and quality of life across a spectrum of surgical risk profiles [3–5]. However, invasive treatments for non-severe AS have not demonstrated similar benefits, and may subject patients to unnecessary procedural risk [1]. Therefore, precise quantification of AS severity is of paramount importance. Notwithstanding, it remains unclear whether area and gradient criteria have to present collectively or individually, or whether they must be obtained invasively or by Doppler [1, 6].

In this chapter, we will review the physiological changes that occur as blood flow approaches the stenotic aortic valve with generation of a transvalvular ΔP, the relationship between AVA and ΔP, the determinants of transvalvular ΔP and AVA, and the role of Doppler and cardiac catheterization in assessing the severity of aortic stenosis.

Physiological Considerations of Transvalvular Pressure Gradient (ΔP) and Aortic Valve Area (AVA) in Aortic Stenosis

The *geometric orifice area* (GOA) is the true anatomical measure of valve area is clinically obtained by planimetry utilizing different imaging techniques. As blood flows toward a narrowed orifice there is flow convergence beyond the GOA. The narrowest region of flow convergence is called the *vena contracta* and the cross sectional area of the vena contracta represents a measure of the *effective orifice area* (EOA).

The Doppler-obtained EOA (EOA_{Dop}) is a measure of the flow convergence area at the vena contracta, is smaller than the GOA, and is the smallest obtained measure of AVA.

The principle of conservation of energy states that the total amount of energy in a closed system remains constant. Energy can change form and location but is neither created nor destroyed. Accordingly, as flow approaches a narrowed orifice of the aortic valve, its kinetic energy increases as its pressure or potential energy decreases with partial energy dissipation through heat, vortex formation, flow acceleration, and viscous friction. The result is generation of a transvalvular pressure gradient (ΔP) that is dictated by the Bernoulli equation [7, 8].

Bernoulli Equation

$$\Delta P = \frac{1}{2}\rho\left(v_{max}^2 - v_{prox}^2\right) + \rho\, prox\int max\left(\frac{dv}{dt}\right)ds + R(v)$$

$$\Delta P = \text{Convective Acceleration} + \text{Flow Acceleration} + \text{Viscous loss}$$

Where ΔP = pressure gradient across the constricted area (or stenotic valve), v_{max} and v_{prox} are the velocity in and proximal to the stenosis, respectively, ρ = mass density of blood, *prox* ∫*max* (dv/dt)/ds is the varying velocity vector of the fluid element at each distance along the flow stream path, and R (*v*) is a constant describing the viscous losses.

Accordingly, the ΔP occurs due to energy loss as a result of:

- Convective acceleration: Conversion of pressure or potential energy to kinetic energy occurs with convection of fluid with normal flow velocity from one point in space to another point in space at the stenosis with

high velocity flow. This is the most energy-dissipating portion and distal to the narrowed orifice, kinetic energy is reconverted back to pressure or potential energy. However, some of the pressure energy is lost, in part because of dissipation of kinetic energy as heat, flow separation, as well as conversion of flow distal to the stenosis into turbulent non-laminar flow with vortex formation. These flow vortices develop circumferentially around the ejected jet distal to the AV and constrict the flow current at the vena contracta, thus constricting the EOA.

- Flow acceleration: additional acceleration occurs through changes in the blood flow velocity during systole to overcome inertial forces especially at the time of valve opening and closing. Flow acceleration occurs proportionately to the square of the distance. However, it is negligible at peak velocity and can be omitted.
- Viscous friction: This occurs between the laminar layers of fluid (viscous losses), specifically from friction between the fluid element and the neighboring fluid and depends on maximum velocity (v_{max}) and the whole velocity profile. However, the viscous losses are negligible for the fluid element with the v_{max} and can be omitted. Moreover, with turbulent flow as seen with aortic stenosis, the contribution of the viscous forces is minimal.

The Reynolds number describes the ratio of inertial or acceleration forces to viscous forces [9]:

$$Re = \rho VL / \nu$$

Where ρ = mass density of blood, V is velocity of flow, L is length, and v is viscosity.

Acceleration or inertial forces are more prevalent with turbulent flow (at high Reynolds number), while viscous forces are prevalent at laminar flow (at low Reynolds number) and become negligible. As such, with increase turbulent flow with severe AS, viscous forces are omitted in the gradient calculation.

Accordingly, the acceleration losses increase *exponentially* with flow, while viscous losses are negligible and are *linearly* related to flow [9].

Additionally, the flow vortices generated are highly dependent on flow. In the presence of high or normal flow, more kinetic energy develops that leads to destruction of these vortices, thus causing a larger EOA. In conditions of low flow across the aortic valve, whether the EF is preserved or not, there is a decrease in kinetic energy that leads to lesser destruction of flow vortices that develop on the sides of the aorta beyond the AV resulting in more "squeeze" on the ejection jet by the flow vortices and constricting the EOA [6] (Fig. 3.1).

The resultant ΔP generated is exponentially proportionate to baseline stenosis and translesion flow in a curvilinear fashion. The ΔP is thus directly proportionate to the square of Q and inversely proportionate to the square of AVA.

$$\Delta P = \frac{Q^2}{KxAVA^2} \left(\text{K is constant}\right).$$

As such, higher relative gradients are generated with a delta reduction in aortic valve area in the severe range as well as delta increase in flow in the higher range than with reduction in aortic valve area in the mild to moderate range and increase in flow in the mild to moderate range.

The pressure gradient at the vena contracta is measured by Doppler and is the highest gradient measured across the AV. Upstream from the vena contracta the vortices eventually break up and flow decelerates and diverges with reconversion of kinetic energy to potential energy. A portion of pressure loss is gradually recovered until a plateau is reached, a phenomenon known as *pressure recovery* (P_{rec}) [10] (Figs. 3.1 and 3.2). This leads to a lower ΔP at catheterization, than that determined at the vena contracta by Doppler. Since the *catheter-obtained EOA* (EOA_{cath}) is derived from the invasively obtained gradients, it is larger that the EOA_{Dop}, and closer in value to the GOA, a phenomenon known as area recovery (A_{rec}) [11, 12] (Figs. 3.1 and 3.2).

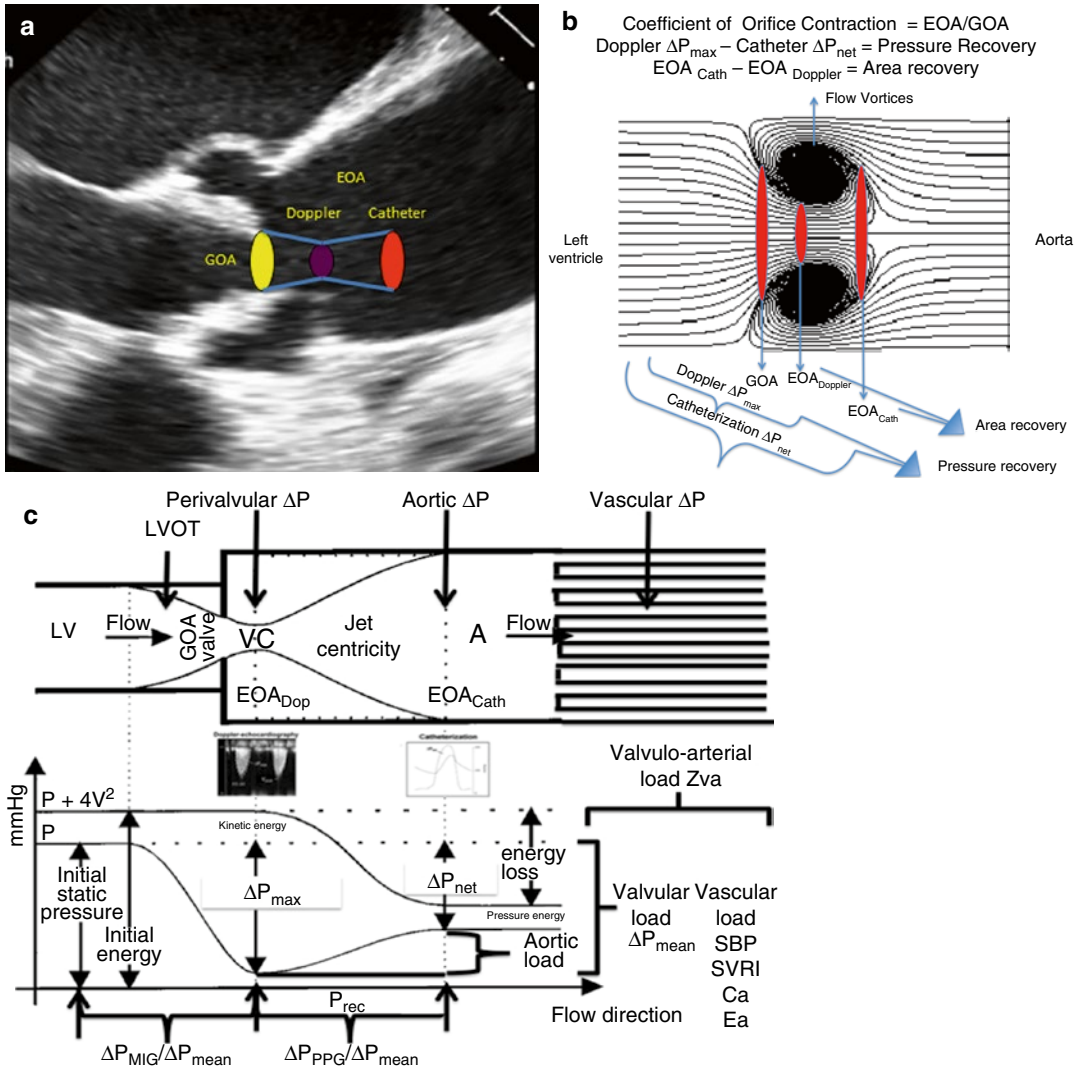

Fig. 3.1 (**a**, **b**) Illustrates the GOA, EOA by both catheter and Doppler, as well as pressure and area recovery. (**c**) Illustrates: (1) The initial pressure, kinetic, lost, and final pressure energy. (2) The various types of gradients (ΔP_{max}, ΔP_{net}, ΔP_{mean}, ΔP_{MIG}, ΔP_{PPG}, and P_{rec}) generated across the AV in the presence of a stenosis. (3) The pressure gradient determinants (perivalvular, aortic, and vascular). (4) The methods of gradient detection (Doppler and Catheterization). (5) The different types of area assessment (GOA, EOA_{cath}, and EOA_{Dop}). (*LV* left ventricle, *Valve* aortic valve, *A* aorta, *VC* vena contracta, remaining abbreviations as text) (From Garcia et al. [10] with permission)

Assessing the Severity of Aortic Stenosis

This section will include an overview of the physiological principles of invasive and echocardiographic measures that evaluate the severity of aortic stenosis:

1. Measures of trans-aortic pressure gradient
2. Measures of aortic valve area
3. Other measures to assess severity of aortic valve stenosis
4. Measures of left ventricular hemodynamic burden

Aortic Valve Gradient Calculations

As noted, the principle of conservation of energy states that the total amount of energy in a closed system remains constant. Energy can change its

location and form but can be neither created nor destroyed.

ΔP is mainly measured invasively or via Doppler echocardiography (and more recently MRI, Chap. 4). Depending on the level of ΔP determination, a different measure of gradient is obtained as outlined below.

Maximum Achievable Pressure Gradient (ΔP_{max})

At the vena contracta, the ΔP generated is the maximum achievable gradient (ΔP_{max}) (Fig. 3.1). ΔP_{max} is estimated by Doppler, which assumes that pressure is irretrievably lost across the AV and measures the gradient between the peak LV systolic pressure and the aortic pressure at a single and the same point in time [1] (Fig. 3.3).

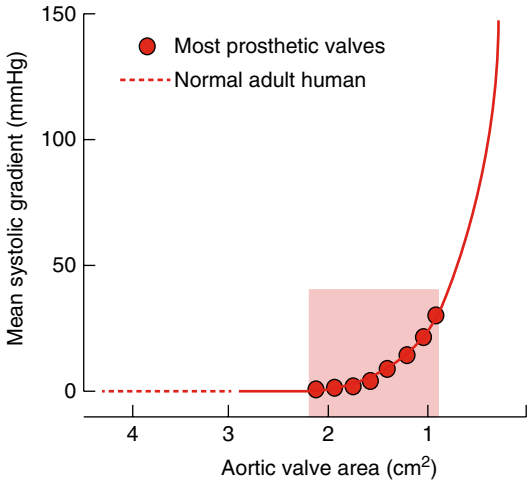

Fig. 3.2 The relationship between transvalvular ΔP and AVA in normal and $AV_{prosthesis}$. ΔP starts to increase at an AVA <1.5 cm^2, with a steeper increase <1 cm^2, and even a more marked increase with an AVA <0.8 cm^2 (From Deneshvar and Rahimtoola [30] with permission)

Noninvasively, ΔP_{max} is determined by Doppler on the principles of the Bernoulli equation as described above. The equation is further modified in clinical cardiology as:

$$\Delta P_{max} = 4V_2^2 - 4V_1^2.$$

V_2 represents the Doppler derived blood flow velocity distal to the valve and V_1 the proximal blood flow velocity. In the presence of severe AS, V_2 is usually significantly greater than V_1 and thus V_1 is omitted and the equation is further simplified into

$$\Delta P_{max} = 4\left(V_2^2\right).$$

When either $V_1 > 1.5$ and/or $V_2 < 3$ m/s, the modified Bernoulli equation, but not the simplified one, should be used, as the difference between V_1 and V_2 becomes non substantial and the proximal velocity (V_1) has to be included in the equation. However, because it is not possible to match each point on the ejection curve between the proximal and distal velocity profiles, it is not possible to "correct" the mean gradient when V_1 is significant, and in these circumstances, the measure of mean gradient should not be used to grade stenosis severity [1, 2]. Utilization of a derivative of the Bernoulli equation to noninvasively estimate transvalvular ΔP was initially

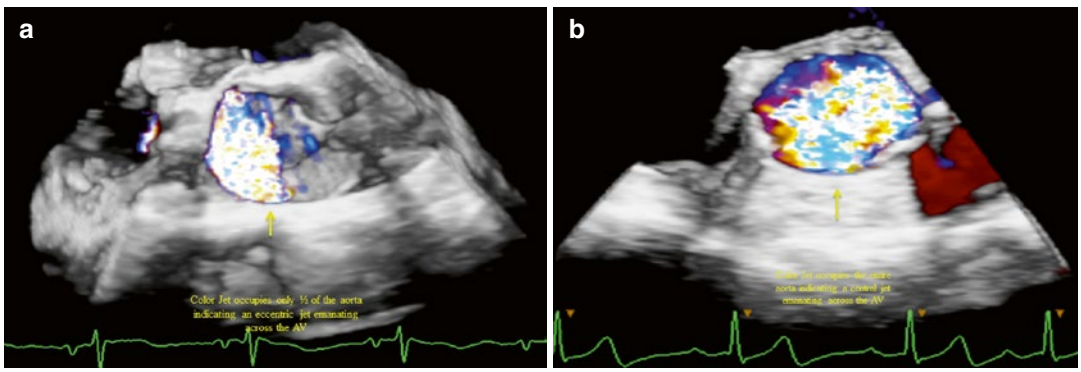

Fig. 3.3 Eccentric (**a**) and centric (**b**) jets across the aortic valve as viewed above the valve from the aorta as demonstrated on 3D color in two different patients with bicuspid (*left*) and tricuspid (*right*) severe aortic stenosis

proposed by Hatle et al. for mitral stenosis [7] and then further extrapolated to aortic stenosis in another study [8].

Doppler provides a maximum instantaneous gradient (ΔP_{MIG}), which is the highest achievable instantaneous gradient across the AV (Fig. 3.3), and a mean gradient (ΔP_{mean}) that is generated as an average of instantaneous gradients over ejection time and is the highest achievable ΔP_{mean}.

Net Pressure Gradient (ΔP_{net})

As noted above, the pressure lost is *not irretrievable* and the final resulting ΔP following complete P_{rec} is known as the net pressure gradient (ΔP_{net}) and is an overall lower ΔP than initially generated at the vena contracta [10] (Figs. 3.1 and 3.2).

Cardiac catheterization measures an invasive ΔP that progressively decreases as the site of the catheter placement in the aorta moves downstream from the vena contracta, where the pressure measured is partially recovered, until the extent of P_{rec} has reached its plateau, at which ΔP_{net} is achieved.

$$\Delta P_{net} = \Delta P_{max} - P_{rec}$$

Invasively, ΔP_{net} is obtained via a double lumen single catheter, dual catheters, or pull back of a single catheter across the AV. Utilizing a catheter placed in the LV and another placed in the femoral artery will lead to an overestimation of the true ΔP_{net} due to the delay that occurs in pressure transmission from the proximal aorta to the femoral artery and should not be used. Conversely, the practice of "aligning" the LV and peripheral tracing will lead to an underestimation of the true ΔP_{net} and should also not be used.

Catheterization provides the peak-to-peak gradient (ΔP_{PPG}), which is the difference between *peak LV pressure* and the *peak aortic pressure*, (which occur at two different points in time) and the mean gradient (ΔP_{mean}) (average peak to peak gradients over time) [1] (Fig. 3.3), both of which occur during or following P_{rec}. The ΔP_{PPG} has little physiological meaning as the two peaks of pressure gradient do not occur at the same time of the cardiac cycle as described above thus no "real" actually ΔP_{PPG} exists. Clinically, the "recovered pressure gradient or ΔP_{net}" obtained invasively is more representative of the actual hemodynamic burden placed on the left ventricle than the instantaneous gradient obtained by Doppler [13].

Pressure Recovery (P_{rec})

The *absolute degree* of P_{rec} is the absolute difference between ΔP_{max} and ΔP_{net} ($P_{rec} = \Delta P_{max} - \Delta P_{net}$), while the *relative degree* or extent of pressure recovery is the ratio between both (P_{rec}/P_{max}) and is more clinically relevant. A P_{rec}/P_{max} >20 % is considered clinically significant and manifests as discordance between Doppler and catheter-derived ΔP_{mean} [14].

Determinants of Transvalvular Gradients (ΔP) and P_{rec}

The generated trans aortic valve ΔP and degree of P_{rec} are dependent on perivalvular determinants (factors around the AV including the presence and type of a prosthesis); vascular determinants: including measures of afterload; and aortic determinants (aortic diameter and area). These determinants are illustrated in Table 3.1.

Para Valvular Determinants

The relationship between the AVA and the generated ΔP is highlighted in Fig. 3.2, with a steep increase in ΔP when the AVA <1 cm^2. Similarly, as transvalvular flow increases, the ΔP is increased in an exponential manner and the delta change of ΔP for the amount of Q is higher with severely stenotic valves (<1 cm^2) (Fig. 3.4).

High flow may occur with fever, severe anemia, pregnancy, thyrotoxicosis, arterio-venous fistulas, and thiamine deficiency [12]. In addition, aortic regurgitation may also increase transaortic flow leading to an increase in the AV_{vel} and thus the ΔP, particularly in the presence of combined valve stenosis and regurgitation.

Conversely, for gradients to remain low, the EOA must be proportionate to Q requirements that under resting conditions are related to BSA. As such, in patients with an AVprosthesis that has a fixed and too small of an area relative

Table 3.1 Factors determining the trans aortic valve gradient

Variable	ΔP_{max}	ΔP_{net}	Absolute P_{rec} (P_{max}- P_{net})	Relative P_{rec} (P_{rec}/P_{max})
Peri-valvular determinants				
Aortic valve area (AVA)	The smaller the AVA, the more severe the AS, the higher the ΔP_{max}	The smaller the AVA, the more severe the AS, the higher the ΔP_{net}	The smaller the AVA, the more severe the AS, the higher the absolute P_{rec}	The higher the AVA, the less severe the AS, the higher the relative P_{rec} (more with moderate AS)
Left ventricular outflow tract (LVOTD) diameter	Increased LVOTD increases the ΔP_{max} for the same AVA	Increased LVOTD increases ΔP_{net}	Increased LVOTD decreases the absolute P_{rec}	Increased LVOTD decreases the relative P_{rec}
Jet eccentricity	Increased jet eccentricity, increases ΔP_{max}	Increased jet eccentricity, increases ΔP_{net}	Increased jet eccentricity decreases absolute P_{rec}	Increased jet eccentricity decreases relative P_{rec}
Flow	Increased flow increases ΔP_{max}	Increased flow increases ΔP_{net}	Increased flow increases absolute P_{rec}	No effect
Bileaflet mechanical prosthetic valve	Increases ΔP_{max}	Decreases ΔP_{net}	Increases absolute P_{rec}	Increases relative P_{rec}
Aortic valve morphology	Variable	Variable	Variable	Variable
Aortic determinants				
Ascending aorta diameter (AoD)/ratio of AVA/AoD	No effect	Increased AoD increases ΔP_{net}	Increased AoD decreases absolute P_{rec}	Increased AoD decreases relative P_{rec}
Vascular determinants				
Systolic blood pressure (SBP)	Increased afterload via increased SBP, Ea, and SVRI, and/or decrease in Ca causes a decrease in trans AV flow leading to a decreases in ΔP_{max}	Increased afterload decreases ΔP_{net} due to decrease flow	Increased afterload decreases absolute P_{rec} due to decrease flow	Changes in flow do not affect the relative P_{rec}
Systemic vascular compliance (Ca)				
Effective arterial elastance (Ea)				
Systemic vascular resistance index (SVRI)				

to patients' BSA (and hence cardiac output, CO), a disproportionately higher ΔP is generated across the prosthesis, a condition that is referred to as prosthesis-patient mismatch (PPM).

Q is usually assessed by stroke volume indexed to BSA (SVI) via Doppler, where a low flow is considered at a SVI ≤35 ml/m^2 and a high flow at a SVI ≥58 ml/m^2. Invasively, CO and cardiac index (CI) are usually used to determine flow status. Q is dependent on preload, LV contractility, and afterload but not on ejection fraction (EF).

ΔP_{max} is also directly related to the LVOT diameter and eccentricity of the flow jet through the AV [10, 15] (Fig. 3.3). Increased LVOT diameter will lead to more initial drop of pressure as blood flow converges towards the AV. Thus, with larger LVOT diameters, there is an elevation in both Doppler ΔP_{max} and invasive ΔP_{net} that is disproportionate to the degree of area stenosis. However, Doppler and invasive gradients are close to each other [15–17] (Doppler-Catheter Concordance). Thus for a given AVA, a larger LVOT diameter yields a higher gradient, higher AV_{Vel}, and a smaller dimensionless index ($LVOT_{vel}/AV_{vel}$, DI). Moreover, the larger the LVOT size compared to that of the GOA, the lower the EOA [15]. Stated differently, with a more abrupt narrowing at the AV from a large

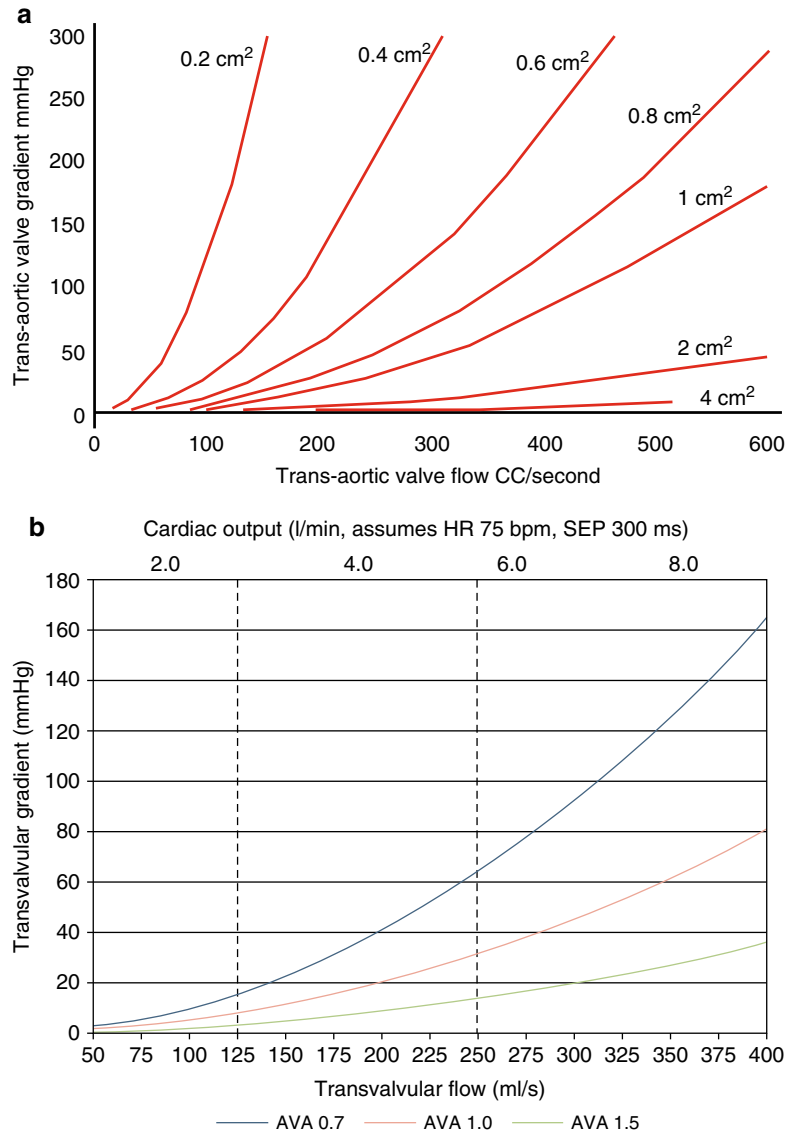

Fig. 3.4 The relationship between transvalvular ΔP and flow at variable EOA (**a**). Based on the Gorlin equation (**b**), at a flow of 125 ml/s, mild (AVA 1.5 cm^2), moderate (AVA 1.0 cm^2), and severe AS (AVA 0.7 cm^2) all have a ΔP<20 mmHg. However, at a flow of 250 ml/s, we are able to distinguish the severity based on ΔP and severe AS has a ΔP>40 mmHg (**a** data from Tandon and Grayburn [48] with permission)

LVOT to a stenotic AV, there is a sudden expansion in the lumen beyond the AS. This causes more energy loss and less energy is recovered as pressure distally. These effects cause an increase in both Doppler and catheter-derived gradients with less pressure recovery.

The impact of LVOT diameter on Doppler-derived P_{mean} was further elucidated in a recent Doppler study of about 10,000 patients. In this study, an AVA of 1 cm^2 corresponded to a P_{mean} of 42 mmHg, AV_{Vel} of 4.1 m/s, and a DI of 0.22 in patients with a large $LVOT_D$ (>2.3 cm). While it corresponded to a P_{mean} of 35 mmHg, AV_{Vel} 3.8 m/s, and a DI of 0.29 in patients with an average $LVOT_D$ (2–2.2 cm). Finally, it corresponded to a P_{mean} of 29 mmHg, AV_{Vel} 3.5 m/s, and a DI of 0.36 in patients was with a small $LVOT_D$ (1.7–1.9 cm) [17].

Similarly, in the presence an eccentric jet across the AV (as in cases of a bicuspid AV, non uniform calcification of cusps, and uneven restriction of AV leaflets), there is an increase in pressure loss as the eccentric jet collides with the ascending aortic wall with resultant energy

loss due to heat, flow separation, and vortex formation. In addition to increased pressure loss, there is a decrease in P_{rec}, and the ΔP derived from either Doppler or catheterization, will be disproportionately higher relative to the GOA (Doppler-Catheter Concordance). Similarly, the EOA is constricted between the vortices on one side and the aortic wall on the other, and being derived from gradients, will be disproportionately lower compared to the GOA. Based on computational models, this effect occurs to a higher degree in the presence of more severe AS [15, 18, 19]. However, no further significant effect on either Doppler or catheter-derived gradients or EOA is noted beyond an eccentricity angle of 30–35°.

Finally, ΔP_{max} also becomes higher in the presence of a bileaflet mechanical AVprosthesis. This occurs due to localized high velocity and pressure drop within the central orifice, causing an overestimation of ΔP_{max} by Doppler [13] and published reference values for expected gradients across mechanical valves are available.

Vascular Determinants

Afterload represents what will be referred to as the vascular determinants of ΔP_{max}. In addition to systolic blood pressure (SBP), it includes:

- **Systemic vascular compliance** (**Ca**), which reflects the pulsatile component of afterload.

$$\text{Compliance} = \text{Stroke volume index} / \text{pulse pressure}$$
$$\text{Ca} = \text{SVI} / \text{PP}.$$

- **Systemic vascular resistance index** (**SVRI**), which reflects the static component of afterload.

$$\text{Systemic vascular resistance index} = \text{Mean arterial pressure - right atrial pressure} / \text{cardiac index}.$$
$$\text{SVRI} = \text{MAP - RAP} / \text{CI}$$

- **Effective arterial elastance** (**Ea**), which is a lumped measure of arterial load that *combines* the effects of static and pulsatile afterload.

$$\text{Elastance} = \text{Left ventricular end systolic pressure} / \text{stroke volume index}.$$
$$\text{Ea} = \text{LVESP} / \text{SVI}$$

Increase in afterload via an increase in SBP, SVRI, and Ea or a decline in Ca indirectly decreases ΔP_{max} through decreasing Q rather than a direct effect on ΔP [20, 21], thus underestimating ΔP_{max} for the degree of AS, regardless of the presence of normal or low EF [22–25].

Valvulo-arterial impedance (Zva) is a global load that has been suggested to account non-invasively for both perivalvular and vascular (Ea) loads. Its increase has been correlated with poor prognosis in several studies [22–24, 26].

$$\text{Zva} = \text{SBP} + \Delta P_{max} / \text{SVI}$$

Normalized LV stroke work (LV stroke work/stroke volume) is a newly introduced non-invasive variable obtained from echocardiography and cardiac MRI to also assess global load and account for both perivalvular and valvular loads [25].

Aortic Determinants

The energy loss across the aortic valve and thus both absolute and relative P_{rec} are affected by the ratio of the AVA to the ascending aortic area (Aa) [10], which will be referred to as the *aortic determinant* of the ΔP. The smaller the aortic diameter/or the greater the ratio of the AVA/Aa, the less is the energy loss and the greater is the absolute and relative P_{rec} leading to a lower ΔP_{net}, and increased Doppler/catheter discordance [10, 27].

Conversely, with a progressive increase in aortic root diameter, the energy loss increases and the P_{rec} decreases until the root becomes ≥3 cm where no significant P_{rec} occurs.

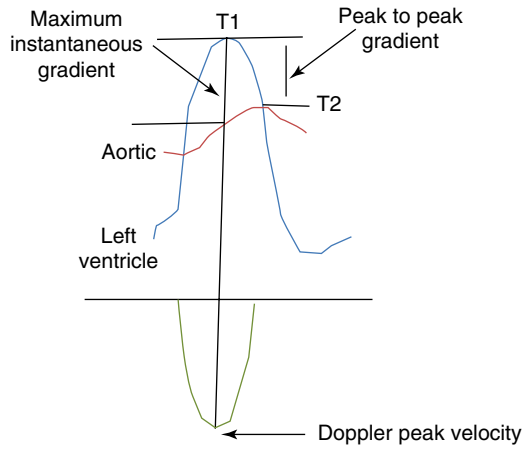

Fig. 3.5 Catheter ΔP_{PPG} versus Doppler ΔP_{MIG}: Note that the ΔP_{MIG} measures the gradient between the aortic and ventricular pressure at the same point in time (T_1, peak LV pressure), while the ΔP_{PPG} measures the gradient at two different points in time (T_1 and T_2, peak aortic pressure). As such, ΔP_{MIG} is always higher than ΔP_{PPG} regardless of P_{rec}. However, the ΔP_{mean} by either technique are comparable except in the presence of significant P_{rec}, where ΔP_{mean} by catheterization is less than that by Doppler

Determinants of Pressure Recovery and Concordance Between Doppler and Catheter Measures of Gradient

Doppler-derived ΔP_{MIG} is routinely higher than catheter-derived ΔP_{PPG} irrespective of Prec due to the inherent difference in the timing of measured data points (Fig. 3.5) [1, 28]. These gradients are not primarily used for diagnostic purposes of AS severity. Conversely, the ΔP_{mean} obtained by either method generally compare well in the absence of significant P_{rec} [1, 28] and are mostly used for diagnostic purposes. Accordingly, ΔP_{max} and ΔP_{net} will be used in this chapter to reflect ΔP_{mean} obtained by Doppler and catheterization, respectively.

Peri-valvular and vascular determinants of ΔP mentioned above determine the absolute value of both Doppler-derived ΔP_{max} and catheter-derived ΔP_{net}, while the aortic determinant affects the P_{rec}, and hence determines only the absolute value of catheter-derived ΔP_{net} and thus the *difference* between Doppler-derived ΔP_{max} and catheter-derived ΔP_{net}.

As the extent of P_{rec} increases, the discrepancy of Doppler and catheter derived measures of gradient increase (Doppler/catheter discordance) [27]. The greater and faster the pressure recovers, the greater the difference between Doppler- and catheter-derived gradients with the Doppler-derived gradients being higher.

The *larger the aortic root and/or the LVOT diameter*, the more is the energy loss and the less is the P_{rec} with Doppler/catheter concordance. However, the ΔP_{max} is not affected. Similarly, in the presence of *eccentric flow jets*, more energy is lost with less absolute and relative P_{rec} and a higher ΔP_{net}. However, due to the initial energy lost as explained above, the ΔP_{max} is also increased with elevated but concordant Doppler and catheter gradients [10, 27].

In the presence of an $AV_{prosthesis}$, localized high velocity and pressure drop within the central orifice leads to an increase in ΔP_{max} with immediate realignment of the central jet with flow from the lateral orifices and rapid recovery of pressure, and hence ΔP_{net} remains within normal levels [13]. There are published "expected" Doppler gradients for most prosthetic valves that account for this phenomenon.

In addition to the effect of the aortic and LVOT areas and jet eccentricity on pressure recovery, absolute P_{rec} increases with *increased Q and a smaller AVA*, while the relative P_{rec} is independent of Q and increases with increased AVA (more with moderate AS than severe AS).

Absolute P_{rec} maybe estimated directly as noted above, or non-invasively:

$$P_{rec} = \Delta P_{max}\left(4V^2\right) * 2\left(EOA / Aa\right) * \left(1 - \left[EOA / Aa\right]\right).$$

Or accounted for through assessing the energy loss coefficient (ELCo) and the energy loss index (ELI)

$$ELCo = \left(EOA * Aa\right) / \left(Aa - EOA\right).$$

$$ELI = ELCo / BSA$$

Both reflect the energy loss across the AV, and correct for distal recovered pressure in the aorta [7, 28]. An ELI <0.52–0.76 cm^2/m^2 has been correlated with severe AS and poor outcomes [7, 14]. However, accurate measurement of the ascending

aorta is imperative in either method, which may introduce variability and complexity [28].

In-vitro and in-vivo studies accounting for P_{rec} for variable (AVA/Aa) values using non-invasive methods have shown excellent comparisons of Doppler-derived ΔP_{max} and catheter-derived ΔP_{net}, except in the presence of eccentric jets and $AV_{prosthesis}$ [14]. A summary of how the various determinants affect ΔP_{max}, ΔP_{net}, and both absolute and relative P_{rec} is highlighted in Table 3.1.

The clinical impact of P_{rec} is highlighted in study of 1,563 patients with AS, 47.5 % initially classified as severe were reclassified as moderate when P_{rec} was accounted for [14]. A clinically relevant P_{rec} (>20 % of ΔP_{max}) was present in 16.8 % of patients [14]. Reclassification into moderate rather than severe AS was more often in those with a smaller ascending aorta (<3.0 cm) and lower transaortic velocities regardless of flow state. However, the absolute magnitude of P_{rec} was greater in the presence of higher trans-valve velocities (>3.33 m/s) [14].

Aortic Valve Area Calculations

Effective Versus Geometric Orifice Area

As mentioned above, the GOA describes the true anatomical area of the AV that is obtained at *peak systole*. It is derived by planimetry from echocardiography, CTA, or MRI images of either a native or bioprosthetic $AV_{prosthesis}$ and on assessment of occluder motion with fluoroscopy or cine CT for mechanical $AV_{prosthesis}$. The fundamental limitations to accurate and reproducible measurements of the GOA are image attenuation secondary to leaflet calcification and the spatial integration of images required to ensure planimetry of the minimal opening area at the leaflet tips (Fig. 3.1). It is for these reasons that this measurement is reserved clinically for those circumstances where Doppler and invasive measurements are unreliable and is doubt regarding the true degree of AS via Doppler or catheter estimates of the EOA.

The EOA, as described above, is a Q-dependent, gradient-derived, estimate of the AVA and obtained as the cross-sectional area at the vena contracta (echocardiography-derived continuity equation, EOA_{Dop}) or at the site of catheter placement (invasively-derived Gorlin Equation, EOA_{Cath}). The EOA, however, is less dependent on Q than pressure gradient [28] and is measured through the entire systole. As such, Doppler provides the "smallest" EOA and catheterization provides a "recovered" EOA.

An EOA indexed to BSA (iEOA) is best used to account for the variation of CO with BSA, especially in smaller patients where the absolute value of CO may be low but CI is relatively normal [28]. However, in obese patients with increased BSA, its use may yield markedly low values and hence overestimates the degree of AS [28].

Coefficient of Orifice Contraction and Its Determinants

The relationship between the GOA and both the ΔP and the EOA is complex. As noted above, due to the valvular and vascular determinants of transvalvular gradients, the ΔP, and hence the EOA, is not constant for a specific GOA.

The EOA, derived from either Doppler or catheterization, is almost always smaller than the GOA due to multiple factors.

First, since EOA_{Dop} is a measure of the area of the vena contracta where flow converges distal to the AV and hence by definition is smaller than the GOA. On the other hand, although the EOA_{Cath} was initially set up as a measure of the GOA, inherent errors in the Gorlin equation render the catheter-derived area more a reflection of the EOA rather than the GOA. However, the EOA_{Cath} is closer in value to the GOA than the EOA_{Dop} is, since it is measured upstream where flow has diverged (area recovery) and is derived from a lower transvalvular gradient that is obtained upstream from the Doppler-derived gradient (pressure recovery) (considered a recovered EOA).

Second, valve inertia may also explain why the EOA is smaller than the GOA, as some of the inflow pressure would be absorbed in moving the valve itself and the actual gradient producing flow would be less than the mean gradient measured, and hence the EOA would be less than the GOA [29].

Finally, The EOA_{cath} is usually measured via a retrograde placement of a catheter across the stenotic aortic valve (unless trans-septal catheter-

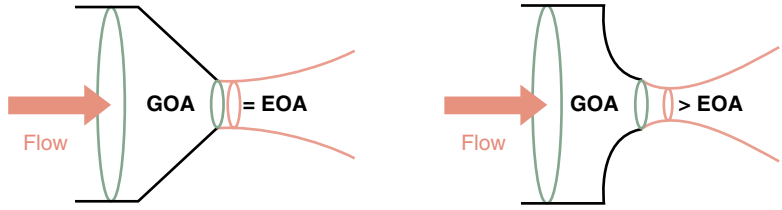

Fig. 3.6 The relationship between GOA, EOA, and the contraction coefficient (CC, EOA/GOA). With a more gradually narrowed GOA, the EOA is almost equal to the GOA and the CC is close to 1. However, with a more abrupt narrowing, the EOA is more distal and smaller than the GOA (From Tandon and Grayburn [48] with permission)

ization is performed) which may further reduce the AVA and/or cause aortic regurgitation that may also affect the gradient. Clinically, this does not affect the decision-making process, since it only occurs with severely and obviously stenotic valves. However, it may affect the exact gradient measurement and further account for discrepancy between the EOA_{cath} and the GOA [29].

The ratio EOA/GOA, in a native valve, is known as the coefficient of orifice contraction (COC) and is usually 0.6–0.9 depending on the LVOT geometry and AV morphology, but maybe as low as 0.38 in certain cases. The COC is almost 1 when the LVOT and GOA are similar in dimension and vice versa. On the other hand, a pliable domed AV with a gradually narrowed orifice will have an almost similar GOA and EOA leading to a higher contraction coefficient.

Conversely, a relatively flat AV with abrupt narrowing as seen with a degenerative or $AV_{prosthesis}$ will increase the disparity between the EOA and the GOA [13] (Fig. 3.6).

In situations with increased pressure loss, particularly with eccentric jets, there is a further disproportionately smaller EOA for a given GOA, thus markedly decreasing the COC (may be lower than 0.5) as seen with bicuspid aortic valves [27].

As noted, the EOA and hence the COC are both directly related to *transaortic flow* that influences the flow vortices that develop on both sides of the aortic jet at the EOA (and vena contracta) distal to the GOA [6] (Fig. 3.4a, b). In low flow states, the EOA, and hence the COC are both lower in value.

In the presence of an $AV_{prosthesis}$, the difference between the manufacture-provided projected or reference iEOA and both the actual $AV_{prosthesis}$ iEOA and GOA are parameters that have been proposed in evaluating patients with prosthesis mismatch (PPM), however, their value remains debated [30, 31]. $AV_{prosthesis}$ GOA is the internal area within the margins of the $AV_{prosthesis}$ and grossly overestimated the true EOA.

Effect of Flow on Aortic Valve Area

It is important to recognize that regardless of the method used, both invasive and Doppler techniques measure the EOA and not the GOA and thus values obtained are "flow-dependent". In addition, since they are all derived from the transvalvular pressure gradients, they are also "pressure dependent" [6]. There appear to be a *linear* relation between trans valvular flow (measured by both Doppler and transit flow rate) and both invasive and Doppler-derived AVA. In one study by Burwash et al. this linear relationship between AVA and flow appeared with both increase in Doppler and transit time flow rate, however, was less robust between Doppler-derived AVA and transit time flow rate. Doppler AVA tends to underestimate AVA at higher flow rates and overestimate them at lower flow rates [24]. The change in AVA with flow maybe related to various factors as delineated below.

First, a true change in the GOA with increased flow as has been demonstrated on video imaging of in vivo models [29, 32]. This maybe related to an increase in pressure against the valve with increased flow and actually opening it to a greater GOA [29].

Second, as noted above, the constant in the Gorlin equation (C) is itself dependent on flow and varies with the square root of the mean pressure gradient and thus will lead to increased values of EOA_{cath} with increased flow for a given GOA [32].

Finally, as described above, with increased flow, the flow vortices that develop upstream the

stenotic valve and constrict the vena contracts are destroyed with increased flow leading to an increase in EOA_{Dop} [19].

Measurements of Aortic Valve Area

Echocardiography

Echocardiography is the principle clinical tool used to calculate AVA. Doppler provides an estimate of the EOA based on the *continuity equation*, which assumes the principle of conservation of mass where flow across the left ventricular outflow tract is assumed equal to flow across the aortic valve [1].

$$\text{Area}_1 \times \text{Velocity}_1 = \text{Area}_2 \times \text{Velocity}_2$$

$$\text{Area}_2 = \text{Area}_1 \times \text{Velocity}_1 / \text{Velocity}_2$$

Where $Area_1$ = LVOT area, $velocity_1$ = LVOT velocity or Time velocity integral obtained by Pulse Wave Doppler, $Area_2$ = Aortic valve area, and $Velocity_2$ = Aortic valve velocity or TVI obtained by continuous wave Doppler. Assuming the circular nature of the LVOT, the LVOT area = $3.14 \times r^2$, or LVOT area = $0.785\ d^2$.

Thus, this equation can as such be rewritten as:

$$\text{AVA} = \frac{\pi r^2 \times \text{LVOT velocity}(\text{TVI})}{\text{AV velocity}(\text{TVI})}$$

$$\text{AVA} = \frac{3.14t^2 \times \text{LVOT velocity}(\text{TVI})}{\text{AV velocity}(\text{TVI})}$$

$$\text{AVA} = \frac{0.785d^2 \times \text{LVOT velocity}(\text{TVI})}{\text{AV velocity}(\text{TVI})}$$

The assumptions of the continuity equations are many and include, as noted, the circular nature of the LVOT (which is known to be not true based on 3D assessment of the LVOT area), flow in the LVOT and vena contracta are assumed to be laminar with flat velocity profiles and assumed to represent the mean spatial velocities, and finally a parallel Doppler/blood flow angle intercept angle is expected on all occasions.

Short axis views of the aortic valve using TTE, or more commonly TEE, may also allow direct planimetry of the GOA with the caveat of tracing the narrowest orifice in the correct plane despite the calcifications. Further detail on echocardiographic assessment of the AVA is highlighted in the following chapter. The application of the continuity equation to AVA measurement in patient with AS was initially described by Hatle et al. and correlated best with invasive measures when the LVOT diameter was measured from leading edge to leading edge and the AVA was compared to the Gorlin equation while using the Fick method to assess cardiac output [33].

Catheterization

Invasively derived estimates of valve area are reserved for cases where discrepancy between clinical and Doppler derived measures of stenosis severity exists. In the catheterization laboratory, the *Gorlin equation* is used to calculate AVA [1, 34–36].

$$\text{AVA} = \text{Cardiac output} / \text{C} \times 44.3 \times (\text{SEP}) \times (\text{HR}) \sqrt{\Delta P_{\text{mean}}}$$

(SEP = systolic ejection period, HR = heart rate, C = empiric constant assumed to be 1 in aortic stenosis, 44.3 = square root of twice the gravity acceleration factor ($2\sqrt{gh}$)

Gorlin and Gorlin first described this equation in a steady flow model through a fixed orifice in 11 subjects (6 autopsy and 5 operative subjects) and the equation was initially derived for the mitral valve. As such, the surprise was that the "equation worked at all" as Richard Gorlin stated in his editorial in the Journal of the American College of cardiology in 1987 and it has since undergone rigorous review and validation [37].

The Gorlin equation was initially created to provide an estimate of the GOA and as such, included a *constant for the COC* (*Cc*) that relates the jet stream area at the vena contracta (EOA) to the GOA. In addition to the COC, the Gorlin equation included a *velocity conversion factor or velocity coefficient* (*Cv*) to account for losses due to viscous friction (this is not needed in the continuity equation, as it directly measures velocity). It relates the space average velocity of the formed jet stream to its velocity profile. If there is a relatively flat velocity profile through

the stenosis, the maximal velocity measured = space average velocity and $C_v = 1$. The *discharge coefficient* (*Cd*) relates the ideal pressure difference where by all pressure energy is converted to velocity to the real pressure difference, which included pressure energy losses noted above. The Gorlin equation, also empirically incorporates the *conversion factor of mmHg to cm H2O* and the conversion factor for blood density. The final constant C was assumed to be 1 for estimation of the aortic valve area (and 0.85 for the mitral valve area) [38, 39].

In reality, the continuity equation and the Gorlin equation are based on similar hydrodynamic principles and as such should both provide a measure of the EOA and not the GOA. Historically, the Gorlin equation was set out to estimate the GOA by accounting for the COC. However, Dumesnil and Yoganthan described two small errors in the Gorlin equation that explain why the equation measures an estimate of the EOA rather than that of the GOA. The first error is the use of mean flow instead of square root of the mean flow squared (the square root of the average of the squared instantaneous flow) as the mean flow is slightly greater than the other value and thus leads to an inherent small underestimation of the AVA. The second is the use of the constant 44.3 instead of 50.4. These errors seem to compensate for one another, and the use of a C of 1.0 yields a result closer to the EOA rather than the GOA in practice [35]. It is to be noted, that Cannon et al. have demonstrated in a known and fixed orifice area in a hydraulic chamber model that the constant C is not in fact "constant" but rather changes with the square root of the mean pressure gradient and hence in itself is dependent on flow [35].

A more simplified form known as the **Hakki equation** is also utilized for invasive AVA measurement and described in 1981 by Hakki et al. [40].

$$\text{AVA} = \text{Cardiac output} / \sqrt{\Delta P_{PPG}} \left(\text{or } \sqrt{\Delta P_{mean}} \right)$$

The rationale described for this simplification is that the product of SEP × Heart rate × 44.3 appear to very close to a single value of 1×10^3 across a wide range of valve areas in their study. Moreover, there appeared to excellent correlation regardless of whether ΔP_{PPG} or ΔP_{mean} were used.

Doppler versus Catheter-Derived Measures of Aortic Valve Area

As a general rule, catheter-derived area calculations (EOA_{Cath}) will differ from, and tend to exceed those obtained by Doppler (EOA_{Dop}) due to multiple reasons excluding measurement errors.

First, since the EOA is derived from ΔP measurements both invasively and by Doppler (Fig. 3.1), Doppler calculations of EOA are a direct estimate of the vena contracta area where the Doppler gradient is derived, while the catheter measurements derive valve area from a catheter position in flow upstream from the vena contracta, where the flow stream has diverged (a recovered EOA) (Fig. 3.4) [6, 11, 12]. In one study, more than half of the patients with catheter-derived areas of 1.0–1.5 cm^2 had Doppler-derived areas of 0.5–1.0 cm^2 [41]. Moreover, the more upstream from the vena contracta the invasive measure is obtained, the greater the estimated valve area until a plateau is reached, the point where P_{rec} is complete. This was termed "area recovery" (A_{rec}) by Levine et al. [11] and was first described by Schobel et al. [12].

Second, both equations are conceptually different as the Gorlin equation that derives the EOA_{Cath} was initially set up as a measure of the GOA. However, inherent errors in the Gorlin equation render the catheter-derived area more a reflection of the EOA rather than the GOA. Accordingly, the EOA_{Cath} is closer in value to the GOA than the EOA_{Dop} is, since it is measured upstream where flow has diverged (area recovery) and is derived from a lower transvalvular gradient that is obtained upstream from the Doppler-derived gradient (pressure recovery) [11, 12, 35]. This explains to some degree the inherent difference between these methods.

Third, there are inherent limitations of both equations. The two components of the constant in the Gorlin equation (coefficient of velocity and orifice contraction) appear to be within themselves, dependent on flow and may change depending the hemodynamic status during which they were derived. Similarly, it is to be noted that the stroke volume measures derived from echo

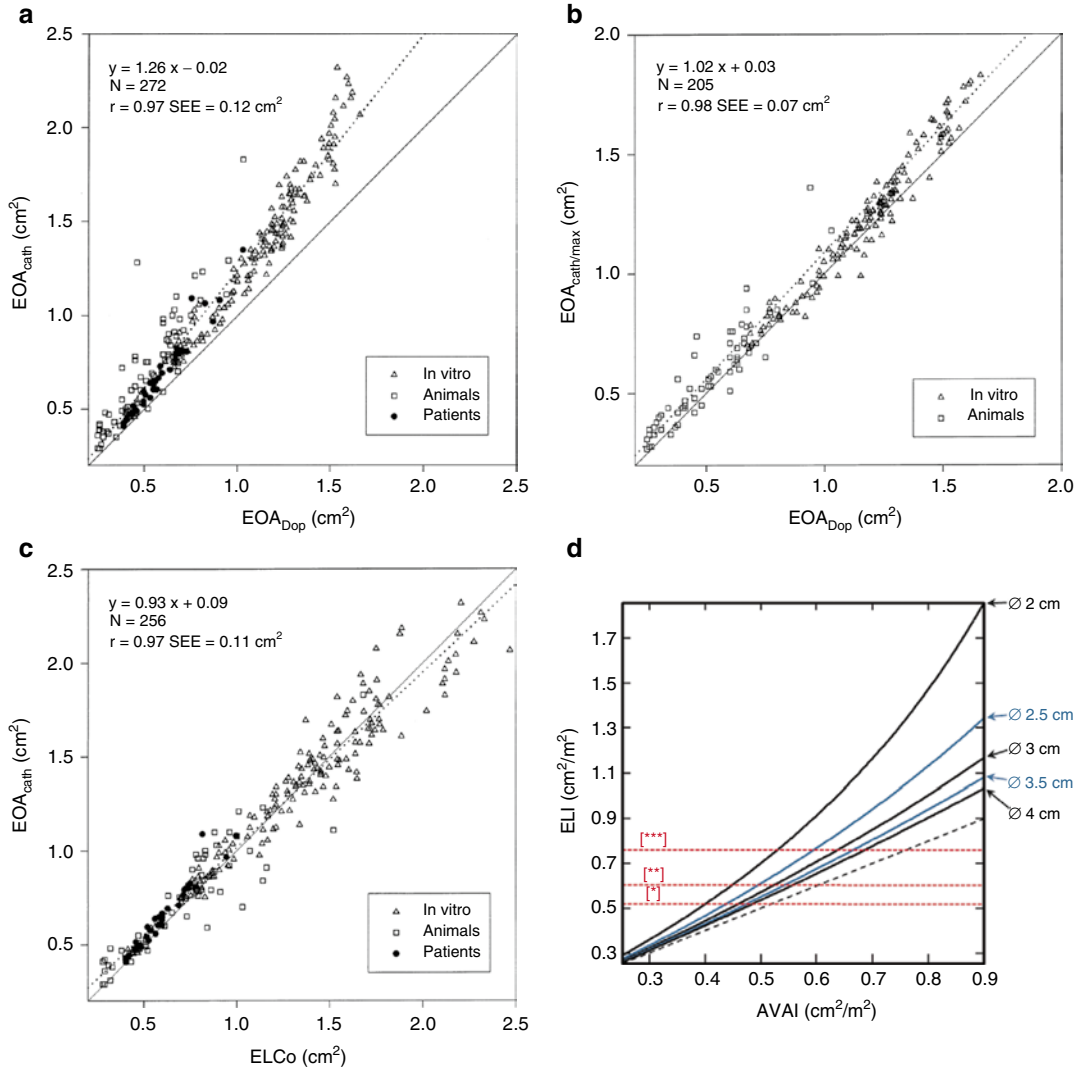

Fig. 3.7 EOA_{Dop} compared to EOA_{cath} by utilizing of both catheter-derived ΔP_{mean} (*top left*) and ΔP_{PPG} (*top right*). Both appear to be closer in value when using the ΔP_{PPG}. ELCo compared to EOA_{cath} (*bottom left*) and ELI compared to $iEOA_{Dop}$ at various aortic diameters (*bottom right*). Both ELCo and ELI account for pressure recovery, which in turn depends on aortic diameter and area. As such, ELCo compares well with EOA_{cath}, while ELI compares better with EOA_{Dop} at larger aortic diameters (>3 cm) when there is no significant pressure recovery (**a–c** from Garcia et al. [49] with permission. **d** from Pibarot et al. [50] with permission)

utilize the LVOT diameter. Echo measures inherently underestimate the LVOT diameter an area by 20 % as has been shown in recent studies compared to 3D modalities as CTA and 3D echocardiography. As such, The LVOT area, and hence stroke volume, utilized in the continuity equation is always underestimated, leading to an underestimation by Doppler of the AVA.

Finally, small differences in valve area measurements by either technique may affect the correlation coefficient significantly over the narrow range of stenotic valve areas studied leading to the statistically different findings between both methods [32].

The ELCo described above, compares more favorably with the invasive EOA_{Cath} rather than EOA_{Dop} since it accounts for P_{rec} (Fig. 3.7). Moreover, the relation between ELI and iEOA depends on the aortic diameter as demonstrated in Fig. 3.7.

Other Measures to Assess Aortic Stenosis Severity

In addition to the various methods to assess the different measures of aortic valve area and transvalvular gradient, other techniques have been proposed to help delineate the true severity of aortic stenosis. They are usually obtained by echocardiography except for aortic valve calcium score, which is obtained by CT and will be discussed in the following section.

Dimensionless Index

As discussed earlier, many assumptions are involved in the continuity equation, the most important of which are the accurate measurement of an LVOT diameter and the assumption of a circular configuration of the LVOT. Errors are common while obtaining the LVOT diameter and 3D studies as CTA and 3D echo have noted the noncircular nature of the LVOT and that 2D measurement underestimate the LVOT by approximately 20 %. The dimensionless index avoids errors caused by LVOT assumptions and is the ratio of the LVOT velocity (or TVI) to the AV velocity (or TVI). Traditionally, a value <0.25 has been considered to indicate severe AS, which essentially means that the AV area is a quarter of the LVOT area [1].

$$\text{Area}_1 \times \text{Velocity}_1 = \text{Area}_2 \times \text{Velocity}_2$$

Or

$$\text{Area}_2 / \text{Area}_1 = \text{Velocity}_1 (\text{or TVI}_1) / \text{Velocity}_2 (\text{or TVI}_2)$$

Recently a study of almost 10,000 patients by the Mayo clinic suggested that the limit for the diagnostic value for severe AS varies by the LVOT diameter. An AVA of 1 cm^2 corresponded to a DI of 0.22 in patients with a large $LVOT_D$ (>2.3 cm), corresponded to a DI of 0.29 in patients with an average $LVOT_D$ (2–2.2 cm), and finally, corresponded to a DI of 0.36 in patients was with a small $LVOT_D$ (1.7–1.9 cm) [17]. A similar value, the Doppler velocity index (DVI) is the ratio of LVOT velocity to aortic valve velocity that is used with increased gradients across the aortic valve prosthesis. A value >0.3 is considered normal and excluded prosthetic valve stenosis.

Energy Loss Coefficient and Index

As noted earlier, the severity of Doppler and catheter derived measures of area and gradient do not always correlate. In the absence of measurement errors, a large portion of these discrepancies may be due to the impact of pressure recovery. As mentioned, pressure recovery is highly dependent on the ascending aortic area. The assessment of the energy loss across the AV has been studied in vitro and in vivo model and has been shown to correlate better with the EOA_{cath} and has also been linked to poor outcomes.

Energy loss coefficient (ELCo) and the energy loss index (ELI) are noted below

$$\text{ELCo} = \left(\text{EOA}_{\text{Dop}} * \text{Aa}\right) / \left(\text{Aa} - \text{EOA}_{\text{Dop}}\right).$$

$$\text{ELI} = \text{ELCo} / \text{BSA}$$

Where Aa is the ascending aortic area obtained at the sinotubular junction and BSA is the body surface area. Both values reflect the energy loss across the AV, and correct for distal recovered pressure in the aorta [10]. An ELI <0.52–0.76 cm^2/m^2 has been correlated with severe AS and poor outcomes [10, 14, 42]. However, accurate measurement of the ascending aorta is imperative in either method, which may introduce variability and complexity [1, 28].

Aortic Valve Resistance

AV resistance has been proposed to provide more important information beyond area and gradient calculations. This is primarily due to its simplicity, lack of a constant as in Gorlin equation, suggested to be less flow dependent, and finally claimed to be able to differentiate between pseudo from true severe aortic stenosis in patients with low flow low gradient aortic stenosis with low ejection fraction.

It is calculated either invasively:

$$\text{AV resistance} = 1333 \times \Delta P_{mean} / Q_{mean} \left(SV \times SEP\right)$$

Or via echocardiography:

$$\text{AV resistance} = 4 \times \text{AV Velocity}^2 / \text{LVOT radius}^2 \times \text{LVOT TVI}$$

A value <1.5 WU was shown to suggest pseudo severe AS, while a value >2.25 WU correlated with true severe AS. Values in between are common and were considered indeterminate. However, AV resistance has been shown to be flow dependent and not superior to valve area calculations in assessing AS stenosis [28, 43].

Projected Aortic Valve Area

As noted above, the generated gradient has a quadratic relation to transvalvular flow, while the EOA has a linear relationship to flow. Moreover, due to the variability of flow augmentation during dobutamine infusion in patients with low flow low gradient AS with depressed ejection fraction, there remains patients with unclear degree of AS severity after dobutamine infusion. To overcome inter-individual variability in flow augmentation, the projected AVA (AVA_{proj}) (defined as the estimated AVA at a standard flow rate of 250 mL) has been proposed.

It is derived from the slope of regression when plotting AVA versus flow during dobutamine infusion.

$$AVA_{proj} = AVA_{rest} + VC \times \left(250 - Q_{rest}\right)$$
$$VC = \text{Valve Compliance} = AVA_{peak} - AVA_{rest} / Q_{peak} - Q_{rest}$$

AVA_{proj} >1.2 cm^2 denotes a good prognosis, together with a peak dobutamine EF >35 %, high Duke activity status index, and 6-min walk test [44, 45].

AV Calcification and AV Calcium Score

The presence of aortic valve calcification noted on both echocardiography and CTA also appears to correlate with severe AS. An echo score of 4/4 and a calcium score >1,650 AU indicates severe AS [46].

Measures of Left Ventricular Hemodynamic Burden

These are variables that assess the impact of the total increase in afterload on the left ventricle. The hemodynamic models can be obtained via catheterization and/or echocardiography, while the structural models are acquired through various imaging modalities, and BNP is a laboratory value.

Hemodynamic Models

These models include the following components:

Left Ventricular Stroke Work Loss

Left Ventricular Stroke Work loss is a measure of the percentage of LV work wasted during systole for flow across the AV. It is very easy to measure and has been linked to outcome in one study. However, it remains flow dependent and has limited prognostic data. A value >25 % indicates increase LV hemodynamic load [6]

$$\%\ \text{LV Stroke Work Loss} = DP_{mean} / DP_{mean} \times SBP \times 100$$

Stroke and Cardiac Work Index

These represent the cardiac trans-systemic workload per beat and per minute, respectively. An increase in these variables indicates increase LV hemodynamic load. They are also flow dependent [6].

$$\text{Stroke (Cardiac) Work Index} = (\text{Mean Arterial Pressure} - \text{Pulmonary Capillary Wedge pressure}) \times \text{SVI (CI)} \times 0.0136$$

Systemic Vascular Resistance, Systemic Arterial Compliance, Effective Arterial Elastance

Systemic vascular resistance index (SVRI): Reflects the static component of afterload.

Systemic vascular resistance index = Mean arterial pressure–right atrial pressure/cardiac index.

SVRI = MAP – RAP / CI

Systemic vascular compliance (Ca): Reflects the pulsatile component of afterload.

Compliance = Stroke volume index / pulse pressure

Ca = SVI / PP.

Effective arterial elastance (Ea): Is a lumped measure of arterial load that combines the effects of static and pulsatile afterload.

Elastance = Left ventricular end systolic pressure / stroke volume index.

Ea = LVESP / SVI

Increase in afterload via an increase in SBP, SVRI (>25 WU), and Ea or a decline in Ca (<0.6 ml/mmHg/m^{-2}) increases the hemodynamic burden on the LV [6, 17, 18]. This will lead to indirectly decreasing ΔP_{max} through decreasing Q rather than a direct effect on ΔP.

Valvulo-Arterial Impedance (Zva)

Valvulo-Arterial Impedance (Zva) is a global load that has been suggested to account non-invasively for both perivalvular and vascular (Ea) loads. It represents the cost in mmHg of each ml of blood ejected. Its increase (>4.5 mmHg/ml/m^2) has been correlated with poor prognosis in several studies. However, it only includes a measure of the static component of afterload (SVR) [19–21, 26].

$Zva = SBP + \Delta P_{mean} / SVI$

Normalized LV Stroke Work

Normalized LV Stroke Work (LV stroke work/stroke volume) is a newly introduced non-invasive variable obtained from echocardiography and cardiac MRI to also assess global load and account for both perivalvular and valvular loads [22].

Structural Models

These include geometric or structural changes in the myocardium and are usually assessed by various imaging modalities. They include the following:

Global Myocardial Longitudinal Strain (GMLS)

This can be obtained by speckle tracking echocardiography but can be also obtained by MRI. A decrease in GMLS indicates an early decline in contractility even before there is a change in the EF. A value less than 15 % decrease in GMLS indicates early intrinsic myocardial dysfunction [47].

Mitral Ring Displacement

This can be obtained from M-Mode and signals another way of compromised myocardial longitudinal function [6].

Myocardial Fibrosis

This is obtained by MRI and will be discussed in the next chapter. The presence of severe late gadolinium enhancement signals advance structural changes in the myocardium and has been shown to be present in patients with severe AS [6].

Brain Natriuretic Peptide (BNP)

BNP and other laboratory parameters of CHF indicate increased left atrial pressure as a result of increased LV hemodynamic burden. A value >500 pg/dl has been shown to correlate with severe AS in the patients with preserved LV EF [6].

Effect on the Right Ventricle

In an echocardiographic study, the incidence of right ventricular dysfunction in AS patients, as defined by tricuspid annular plane systolic excursion (TAPSE) < 17 mm, was present in 48/200 patients (24%) with severe AS Biventricualr failure emerged as the strongest predictor of poor prognosis (HR 4.08 95% CI 1.36–12.22) [51].

Conclusions

With progressive AS, a pressure gradient is generated across the AV that can be measured invasively or via echocardiography together with the estimated AV valve area. Several determinants impact these measures and thus other variables besides area and gradient have been proposed to help assess AS severity. The final hemodynamic burden on the LV can be assessed via hemodynamic, structural, and laboratory models.

References

1. Nishimura RA, Otto CM, Bonow RO, Carabello BA, Erwin JP, Guyton RRA, O'Gara PT, Ruiz CE, Skubas NJ, Sorajja P, Sundt TM, Thomas JM. ACC/AHA guideline for the management of patients with valvular heart disease. J Am Coll Cardiol. 2014. doi:10.1016/j.jacc.2014.02.536.
2. Vahanian A, Alfieri O, Andreotti F, et al. Guidelines for the management of valvular heart disease. Eur Heart J. 2012;33:2451–96.
3. Leon MB, Smith CR, Mack M, Miller DC, Moses JW, Svensson LG, Tuzcu EM, Webb JG, Fontana GP, Makkar RR, et al. Transcatheter aortic-valve implantation for aortic stenosis in patients who cannot undergo surgery. N Engl J Med. 2010;363(17):1597–607.
4. Smith CR, Leon MB, Mack MJ, Miller DC, Moses JW, Svensson LG, Tuzcu EM, Webb JG, Fontana GP, Makkar RR, et al. Transcatheter versus surgical aortic-valve replacement in high-risk patients. N Engl J Med. 2011;364(23):2187–98.
5. Kvidal P, Bergstrom R, Horte LG, Stahle E. Observed and relative survival after aortic valve replacement. J Am Coll Cardiol. 2000;35(3):747–56.
6. Abbas AE, Franey LM, Goldstein J, Lester S. Aortic valve stenosis: to the gradient and beyond-the mismatch between area and gradient severity. J Interv Cardiol. 2013;26(2):183–94.
7. Hatle L, Brubakk A, Tromsdal A. Noninvasive assessment of pressure drop in mitral stenosis by Doppler ultrasound. Br Heart J. 1978;40:131–40.
8. Hatle L, Angelsen BA, Tromsdal A. Noninvasive assessment of aortic stenosis by Doppler ultrasound. Br Heart J. 1980;43:284–92.
9. Adams JC, Jiamsripong P, Belohlavek M, McMahon EM, Marupakula V, Heys J, Chaliki HP. Potential role of Reynolds number in resolving Doppler- and catheter- based transvalvular gradient discrepancies in aortic stenosis. J Heart Valve Dis. 2011;20:159–64.
10. Garcia D, Pibarot P, Dumesnil JG, Sakr F, Durand LG. Assessment of aortic valve stenosis severity: a new index based on the energy loss concept. Circulation. 2000;101(7):765–71.
11. Levine RA, Schwammenthal E. Stenosis is in the eye of the observer: impact of pressure recovery on assessing aortic valve area. J Am Coll Cardiol. 2003; 41(3):443–5.
12. Schobel WA, Voelker W, Haase KK, Karsch KR. Extent, determinants and clinical importance of pressure recovery in patients with aortic valve stenosis. Eur Heart J. 1999;20(18):1355–63.
13. Bach D. Echo/Doppler evaluation of hemodynamics after aortic valve replacement: principles of interrogation and evaluation of high gradients. J Am Coll Cardiol Img. 2010;3:296–304.
14. Bahlmann E, Cramariuc D, Gerdts E, et al. Impact of pressure recovery on echocardiographic assessment of asymptomatic aortic stenosis. A SEAS substudy. JACC Cardiovasc Imaging. 2010;3:555–62.
15. Saikrishnan N, Kumar G, Sawaya FJ, Lerakis S, Yoganathan AP. Accurate assessment of aortic stenosis: a review of diagnostic moalities and hemodynamics. Circulation. 2014;129:244–53.
16. Ennezat PV, Marechaux S, Pibarot P. From excessive high-flow, high-gradient to paradoxical low-flow, low-gradient aortic valve stenosis: hemodialysis arteriovenous fistula model. Cardiology. 2010;116(1): 70–2.
17. Michelena HI, Margaryan E, Miller FA, Eleid M, Maalouf J, Suri R, Messika-Zeitoun D, Pellikka PA, Enriquez-Sarano M. Inconsistent, echocardiographic grading of aortic stenosis: is the left ventricular outflow tract important? Heart. 2013;99(13):921–31.
18. Donal E, Novaro GM, Deserrano D, Popovic ZB, Greenberg NL, Richards KE, Thomas JD, Garcia MJ. Planimetric assessment of anatomic valve area overestimates effective orifice area in bicuspid aortic stenosis. J Am Soc Echocardiogr. 2005;18(12):1392–8.
19. Richards KE, Deserranno D, Donal E, Greenberg NL, Thomas JD, Garcia MJ. Influence of structural geometry on the severity of bicuspid aortic stenosis. Am J Physiol Heart Circ Physiol. 2004;287(3):H1410–6.
20. Little SH, Chan KL, Burwash IG. Impact of blood pressure on the Doppler echocardiographic assessment of severity of aortic stenosis. Heart. 2007;93:848–55.
21. Change SA, Kim HK, Sohn DW. Impact of afterload on the assessment of severity of aortic stenosis. J Cardiovasc Ultrasound. 2012;20(2):79–84.
22. Hachicha Z, Dumesnil JG, Bogarty P, et al. Paradoxical low-flow, low-gradient severe aortic stenosis despite preserved ejection fraction is associated with higher afterload and reduced survival. Circulation. 2007;115: 2856–64.
23. Burwash IG. Low-flow, low-gradient aortic stenosis: from evaluation to treatment. Curr Opin Cardiol. 2007;22:84–91.
24. Pibarot P, Dumesnil JG, Clavel MA. Paradoxical low flow, low gradient aortic stenosis despite preserved ejection fraction. ACVD. 2008;101:595–6.

25. Keshavarz-Motamed Z, Garcia J, Gaillard E, Capoulade R, Le Ven F, et al. Non-invasive determination of left ventricular workload in patients with aortic stenosis using magnetic resonance imaging and Doppler echocardiography. PLoS ONE. 2014;9(1): e86793. doi:10.1371/journal.pone.0086793.
26. Dumesnil JG, Pibarot P, Carabello B. Paradoxical low flow and/or low gradient severe aortic stenosis despite preserved left ventricular ejection fraction: implications for diagnosis and treatment. Eur Heart J. 2010;31: 281–9.
27. VanAuker MD, Chandra M, Shirani J, Strom JA. Jet eccentricity: a misleading source of agreement between Doppler/catheter pressure gradients in aortic stenosis. J Am Soc Echocardiogr. 2001;14(9):853–62.
28. Baumgartner H, Hung J, Bermejo J, et al. Echocardiographic assessment of valve stenosis: EAE/ASE recommendations for clinical practice. J Am Soc Echocardiogr. 2009;22(1):1–23.
29. Carabello BA. Advances in the hemodynamic assessment of stenotic cardiac valves. J Am Coll Cardiol. 1987;10:912–9.
30. Daneshvar SA, Rahimtoola SH. Valve prosthesis-patient mismatch. A long term perspective. J Am Coll Cardiol Img. 2012;60:1123–35.
31. Pibarot P, Dumesnil JG. Valve prosthesis–patient mismatch, 1978 to 2011. From original concept to compelling evidence. J Am Coll Cardiol Img. 2012;60:1136–9.
32. Burwash JG, Thomas DD, Sadahiro M, Pearlman AS, Verrier ED, Thomas R, Kraft CD, Otto CM. Dependence of Gorlin formula and continuity equation valve areas on transvalvular volume flow rate in valvular aortic stenosis. Circulation. 1994;89:827–35.
33. Skjaerpe T, Hegrenaes L, Hatle L. Noninvasive estimation of valve area in patients with aortic stenosis by Doppler ultrasound and two-dimensional echocardiography. Circulation. 1986;72:810–8.
34. Carabello BA, Grossman W. Grossman's cardiac catheteization, angiography, and intervention. 6th ed. Philadelphia: Lippincott Williams & Wilkins; 2000.
35. Dumesnil JG, Yoanathan AP. Theoretical and practical differences between te Gorlin equation and the continuity equation for calculating aortic and mitral valve areas. Am J Cardiol. 1991;67:1268–72.
36. Gorlin R, Gorlin SG. Hydraulic formula for calculation of the area of the stenotic mitral valve. other cardiac valves, and central circulatory shunts. Am Heart J. 1951;41:1–29.
37. Gorlin R. Calculations of cardiac valve stenosis: restoring an old concept for advanced applications. J Am Coll Cardiol. 1987;10(4):920–2.
38. Segal J, Lerner D, Miller DC, Mitchell RS, Alderman EA. When should Doppler-determined valve area be better than the Gorlin formula? variation in hydraulic constants in low flow states. JACC. 1987;9(6):1294–305.
39. Canon SR, Richards KL, Crawford M. Hydraulic estimation of stenotic orifice area: a correction of the Gorlin equation. Circulation. 1985;71:110–78.
40. Hakki AH, Iskandrian AS, Bemis CE, Kimbiris D, Mintz GS, Segal BL, Brice C. A simplified valve formula for the calculation of stenotic cardiac valve areas. Circulation. 1981;63:1050–5.
41. Oh JK, Taliercio CP, Holmes Jr DR, et al. Prediction of the severity of aortic stenosis by Doppler aortic valve area determination: prospective Doppler-catheterization correlation in 100 patients. J Am Coll Cardiol. 1988;11:1227–34.
42. Bahlmann E, Gerdts E, Cramariuc D, Gohlke-Baerwolf C, Nienaber CA, Wachtell K, Seifert R, Chambers JB, Kuck KH, Ray S. Prognostic value of energy loss index in asymptomatic aortic stenosis. Circulation. 2013;127:1149–56.
43. Mascherbauer J, Schima H, Rosenhek R, et al. Value and limitations of aortic valve resistance with particular consideration of low flow – low gradient aortic stenosis: an in vitro study. Eur Heart J. 2004;25: 787–93.
44. Clavel MA, Ennezat PV, Maréchaux S M.D†., Dumesnil JG M.D*., Capoulade R M.S., Zeineb Hachicha Z, Mathieu P, Annaïk Bellouin A, Bergeron S, Meimoun P, Arsenault M, Le Tourneau T, Pasquet A, Couture C M.D., Pibarot P. Stress echocardiography to assess stenosis severity and predict outcome in patients with paradoxical low-flow, low-gradient aortic stenosis and preserved LVEF. J Am Coll Cardiol Imaging. 2013;6:175–83.
45. Blais C, Burwash IG, Mundigler G, et al. Projected valve area at normal flow rate improves the assessment of stenosis severity in patients with low-flow, low-gradient aortic stenosis. Circulation. 2006;113:711–21.
46. Cueff C, Serfaty JM, Cimadevilla C, Laissy JP, Himbert D, Tubach F, Duval X, Iung B, Enriquez-Sarano M, Vahanian A, Messika-Zeitoun D. Measurement of aortic valve calcification using multislice computed tomography: correlation with haemodynamic severity of aortic stenosis and clinical implication for patients with low ejection fraction. Heart. 2011;97(9):721–6.
47. Lindman BR. Left ventricular mechanics in aortic stenosis: fancy tool or clinically useful. J Am Soc Echocardiogr Off Publ Am Soc Echocardiogr (Impact Factor: 298) 08/2014. 2014;27(8):826–8. doi:10.1016/j.echo.2014.06.003.
48. Tandon A, Grayburn PA. Imaging of low-gradient severe aortic stenosis. JACC Cardiovasc Imaging. 2013;6(2):184–95.
49. Garcia D, Dumesnil JG, Durand LG, et al. Discrepancies between catheter and Doppler estimates of valve effective orifice area can be predicted from the pressure recovery phenomenon: practical implications with regard to quantification of aortic stenosis severity. J Am Coll Cardiol. 2003;41(3):435–42.
50. Pibarot P, Garcia D, Dumesnil JG. Energy loss index in aortic stenosis: from fluid mechanic concept to clinical application. Circulation. 2013;127(10):1101–4.
51. Galli E, Guirette Y, Feneon D, Daudin M, Fournet M, Leguerrier A, Flecher E, Mabo P, Donal E. Prevalence and prognostic value of right ventricular dysfunction in severe aortic stenosis. Eur Heart J Cardiovasc Imaging. 2015;16(5):531–8.

Different Classifications of Aortic Stenosis

4

Amr E. Abbas

Abstract

Different classification systems for aortic stenosis (AS) exist depending on the underlying pathology and native versus prosthetic AS, stages of progression, severity of AS, ejection fraction (EF) and flow, and the presence of area/gradient concordance.

Keywords

Aortic stenosis classifications • Stages of aortic stenosis • Severity of aortic stenosis • Ejection fraction and flow • Area/gradient match or concordance

Different classification systems for aortic stenosis (AS) exist depending on the underlying pathology and native versus prosthetic AS, stages of progression, severity of AS, ejection fraction (EF) and flow, and the presence of area/gradient concordance.

Underlying Pathology

Valvular

These will be further discussed in Chaps. 1 and 10 [1].

- Calcific AS: Most common form.
- Rheumatic AS: Common in developing countries.
- Congenital AS: Usually related to abnormal cusps.
- Prosthetic AS: Bioprosthetic or mechanical.

A.E. Abbas, MD, FACC, FSCAI, FSVM, FASE, RPVI
Department of Cardiovascular Medicine, Beaumont Health, Oakland University/William Beaumont School of Medicine, Royal Oak, MI, USA
e-mail: aabbas@beaumont.edu

A.E. Abbas (ed.), *Aortic Stenosis: Case-Based Diagnosis and Therapy*,
DOI 10.1007/978-1-4471-5242-2_4

Paravalvular AS

These will be further discussed in Chap. 9

- Subaortic fixed obstruction: may be related to membranes, muscular ridges, or tunnels. May also occur in isolation or as a part of Shone's complex
- Supra-aortic obstruction: Also be related to membranes, muscular ridges, or tunnels. May also occur in isolation or as a part of William's syndrome
- Hypertrophic obstructive cardiomyopathy
- Mitral valve prosthesis: Usually large profile bioprosthetic valves obstructing the left ventricular (LV) outflow

Stages of Aortic Stenosis

Nishimura et al. [2] have proposed a novel classification for the stages of progression of valvular heart disease inclusive of AS in the most recent guidelines for valvular heart disease (Table 4.1).

Stage A, at Risk

Stage A, at risk includes patients at risk for development of AS.

Stage B, Progressive

Stage B, progressive includes patients with mild to moderate AS and are asymptomatic.

1. Mild AS: Maximum trans-aortic velocity $\left(V_{max}\right) = 2.0 - 2.9\,m/s$, (mean trans-aortic gradient $\left(\Delta P_{mean}\right) < 20\,mmHg$
2. Moderate AS:
   $V_{max}\ 3.0 - 3.9\,m/s, \Delta P_{mean}\ 20 - 39\,mmHg$

Stage C, Asymptomatic Severe Aortic Stenosis

Stage C, asymptomatic severe aortic stenosis includes patients with severe AS who remain asymptomatic. These are further divided into two categories:

C1: Patients with severe AS and LV compensation.
C2: Patients with severe AS and LV dysfunction.

Stage D, Symptomatic Severe AS

Stage D, symptomatic severe AS includes patients with symptoms as a result of severe AS.

1. D1 with high gradient:

   $V_{max} > 4\,m/s, DP_{mean} < 40\,mmHg,$
   aortic valve area $AVA < 1\,cm^2,$

   indexed aortic valve area
   $\left(AVAi\right) < 0.6\,cm^2/m^2$
2. D2 with low flow/low gradient and reduced (left ventricular ejection fraction (LVEF):

   $V_{max} < 4\,m/s, \Delta P_{mean} < 40\,mmHg, AVA < 1\,cm^2,$
   $AVAi < 0.6\,cm^2/m^2, EF < 50\%,$

   dobutamine stress echocardiography (DSE) with $AVA\left\langle 1\,cm^2 \text{ with } V_{max}\right\rangle 4\,m/s$ at any flow rate.
3. D3 with low gradient and normal LVEF, paradoxically low flow:

   $V_{max} < 4\,m/s, \Delta P_{mean} < 40\,mmHg, AVA < 1\,cm^2,$
   $AVAi < 0.6\,cm^2/m^2, EF > 50\%,$

   stroke volume index (SVI) <35 ml/m^2,
   systolic blood pressure (SBP) <140 mmHg.

Severity of AS

This is based on the severity of aortic stenosis regardless of symptoms, in the new guidelines [2], there is no area cutoff for mild or moderate AS

Table 4.1 Stages of valvular AS

Stage	Definition	Valve anatomy	Valve hemodynamics	Hemodynamic consequence	Symptoms
A	At risk AS	Bicuspid/unicuspid/ quadricuspid aortic valve Aortic valve sclerosis	V_{max} <2 m/s	None	None
B	Progressive	Mild to Moderate leaflet calcification with some reduction in systolic motion Rheumatic valve changes with commissural fusion	Mild AS V_{max} 2–2.9 m/s, or ΔP_{mean} <20 mmHg Moderate AS: V_{max} 3–3.9 m/s, or ΔP_{mean} 20–39 mmHg	Early LV diastolic dysfunction may be present Normal LVEF	None
C: Asymptomatic severe AS					
C1	Preserved LVEF	Severe leaflet calcification or congenital stenosis with severely leaflet opening	V_{max} ≥4 m/s, or ΔP_{mean} ≥40 mmHg AVA ≤1 cm^2, or AVAi ≤0.6 cm^2/m^2 Very severe V_{max} ≥5 m/s or ΔP_{mean} ≥60 mmHg	LV diastolic dysfunction Mild LVH Normal LVEF	None Exercise testing may confirm symptom status
C2	Reduced LVEF	Severe leaflet calcification or congenital stenosis with severely leaflet opening	V_{max} ≥4 m/s, or ΔP_{mean} ≥40 mmHg AVA ≤1 cm^2, or AVAi ≤0.6 cm^2/m^2	LVEF <50 %	None
D: Symptomatic severe AS					
D1	High gradient	Severe leaflet calcification or congenital stenosis with severely leaflet opening	V_{max} ≥4 m/s, or ΔP_{mean} ≥40 mmHg AVA ≤1 cm^2, or AVAi ≤0.6 cm^2/m^2, or larger with mixed AS/AR	LV diastolic dysfunction LVH Pulmonary hypertension	Exertional dyspnea/angina/ syncope/presyncope or reduced exercise tolerance
D2	Low flow/low gradient with reduced EF	Severe leaflet calcification with severely leaflet opening	V_{max} ≤4 m/s, or ΔP_{mean} ≤40 mmHg with AVA ≤1 cm^2. DSE shows AVA ≤1 cm^2 with V_{max} ≥4 m/s at any flow rate	LV diastolic dysfunction LVH LVEF ≤50 %	HF/angina syncope/or presyncope
D3	Low gradient with normal LVEF or paradoxical low-flow severe AS	Severe leaflet calcification with severely leaflet opening	V_{max} ≤4 m/s, or ΔP_{mean} ≤40 mmHg with AVA ≤1 cm^2 AVAi ≤0.6 cm^2/m^2 &SVI <35 mL/m^2. Measured at SBP <140 mmHg	Increased LV RWT Small LV chamber with low SV Restrictive diastolic filling. LVEF ≥50 %	HF/angina syncope/or presyncope

Modified from Nishimura et al. [2] with permission

and there is a very severe form of AS that was added.

1. **Mild AS**:
   $V_{max}\ 2.0-2.9 m/s, \Delta P_{mean} < 20 mmHg$.
2. **Moderate AS**:
   $V_{max}\ 3.0-3.9 m/s, \Delta P_{mean}\ 20-39 mmHg$.
3. **Severe AS**:
   (a) High gradient:

   $$V_{max} > 4 m/s, \Delta P_{mean} > 40 mmHg,$$
   $$AVA < 1 cm^2, AVAi < 0.6 cm^2/m^2$$

   (b) Low flow/low gradient and reduced LVEF:

   $$V_{max} < 4 m/s, \Delta P_{mean} < 40 mmHg,$$
   $$AVA < 1 cm^2, AVAi < 0.6 cm^2/m^2,$$
   $$EF < 50\%,$$

   DSE with $AVA \langle 1 cm^2 \text{ with } V_{max} \rangle 4 m/s$ at any flow rate.

   (c) Low gradient and normal LVEF, paradoxically low flow:

   $$V_{max} < 4 m/s, \Delta P_{mean} < 40 mmHg,$$
   $$AVA < 1 cm^2, AVAi < 0.6 cm^2/m^2,$$
   $$EF > 50\%, SVI < 35 ml/m^2,$$
   $$SBP < 140 mmHg.$$

4. **Very Severe AS**:
   $V_{max} > 5 m/s, \Delta P_{mean} > 60 mmHg$

Ejection Fraction and Flow

Low Ejection Fraction, Low Flow/Low Gradient Severe Aortic Stenosis

These patients have an $LVEF < 35-40\%, a \Delta P_{mean} < 40 mmHg$, and an AVA <1 cm^2 at rest. The gradient is assumed to be low secondary to the decrease in trans-aortic flow. Based on the change in stroke volume, mean gradient, and aortic valve area during dobutamine infusion invasively or via Doppler [3, 4], this group is further divided into

- True severe AS: These patients have contractile reserve as defined by a 20 % increase in stroke volume (SV) with dobutamine infusion. In addition, the AVA does not change, with an increase in ΔP_{mean}. A projected aortic valve area (AVA_{proj}) ≤1.2 cm^2 is also noted in this group [5].
- Pseudo severe AS: These patients have contractile reserve as defined by a 20 % increase in SV with dobutamine infusion. There is an increase in the AVA, while there is no change or a mild increase in the ΔP_{mean}. An AVA_{proj} <1.2 cm^2 is also noted in this group.
- Indeterminate AS: These patients have no contractile reserve without a significant increase in the SV with dobutamine infusion. No assessment of the actual severity of AS can be determined

Normal Ejection Fraction Severe Aortic Stenosis

This classification has been recently introduced in an echocardiographic model and each group had distinct diagnostic and prognostic data [6]. All patients have an AVA <1 cm^2 and an LVEF >50 %. This group is further divided according to echocardiography-derived SVI and ΔP_{mean} into:

- Normal flow/high gradient severe AS:
  $SVI > 35 ml/m^2 \text{ and a } \Delta P_{mean} > 40 mmHg$.
- Normal flow/low gradient severe AS:
  $SVI > 35 ml/m^2 \text{ and a } \Delta P_{mean} > 40 mmHg$.
- Low flow/high gradient severe AS:
  $SVI > 35 ml/m^2 \text{ and a } \Delta P_{mean} > 40 mmHg$.
- Low flow/low gradient severe AS (AKA, paradoxically severe low flow/low gradient severe AS with preserved LVEF:
  $SVI > 35 ml/m^2 \text{ and a } \Delta P_{mean} > 40 mmHg$.

Area/Gradient Match or Concordance

This classification is based on whether or not there is a match or concordance in the area and gradient estimates of severity [7]. It also displays whether or not there is Doppler and catheter concordance of AS severity.

Area/Gradient Match or Concordance

This occurs regardless of the presence of normal or depressed LVEF, and presence or absence of normal or low SVI. Clinical decision-making is relatively straightforward and there is no confusion regarding the true nature of severity. In these cases, the measures of geometric orifice area (GOA), effective orifice area (EOA), and ΔP_{mean} all point to the severity of AS, and in the absence of measurement errors, no further diagnostic workup is required beyond echocardiography. It includes

- Normal flow/high gradient severe AS with preserved LVEF:
- Low flow/high gradient severe AS with preserved LVEF:
- Low LVEF severe AS, and a high gradient:

Area/Gradient Mismatch or Discordance

In these cases, the patient has severe AS by area measurements; however, the gradient remains in the non-severe form and it will be discussed in Chap. 8 in more detail. It occurs due to errors of measurement, errors of assumption, and the presence of low flow with or without reduced LVEF. It includes:

- Normal flow/low gradient severe AS with preserved LVEF:
- Low flow/low gradient severe AS with preserved LVEF:
- Low flow/low gradient severe AS with reduced LVEF:

Reverse Area/Gradient Mismatch or Discordance

In these cases, the patient has severe AS by gradient measurements; however, the area remains in the non-severe form and it will be discussed in more detail in Chap. 9. Usually, there is discordance between the GOA and the ΔP_{mean}; however, less likely there will be a mismatch between the EOA and the estimated ΔP_{mean}.

It occurs due to errors of measurement, the presence of an eccentric jet (with Doppler and catheter concordance), and in the presence of a small ascending aorta due to significant pressure recovery (with Doppler and catheter discordance). It also occurs in prosthetic valves with acceleration of the central jet in bileaflet mechanical valves (with Doppler catheter discordance), and in patients with prosthesis/patient mismatch. In these cases, there is no true prosthetic stenosis; however, there is an elevated ΔP_{mean} despite fluoroscopic or echocardiographic suggestion of normal prosthetic leaflet mobility (Chap. 10).

In the presence of increased systemic and/or local flow (as with severe aortic regurgitation), reverse area/gradient mismatch may also occur with Doppler catheter concordance. In patients with an arterio-venous fistula for hemodialysis and mild to moderate AS, an elevated gradient (sometimes in the severe range) will occur due to an increased flow and is noted on both Doppler and catheterization. In addition, a high cardiac output may be noted on cardiac catheterization leading to an increase in the estimated catheter-derived AVA by the Gorlin equation, even up to only mild or moderate degree of AS. However, the increase in flow may only be minimally reflected in the LVOT TVI causing the echo-derived AVA to remain in the severe range. This leads to a reverse area/gradient mismatch noted only on cardiac catheterization. Finally, paravalvular obstruction also accounts for the discrepant area and gradient measures across the LVOT, aortic valve, and aortic root. The GOA appears to be non-stenotic; however, there is an elevated gradient due to associated membranes or hypertrophied muscle (Chap. 9).

Both types of mismatch likely require further modalities to adjudicate the true degree of aortic stenosis. Visualization of the aortic valve and planimetry may also provide useful as well as fluoroscopy, CTA, or TEE visualization of aortic valve prosthesis.

References

1. Libby P, Bonow RO, Mann DL, Zipes DP. Braunwald's heart disease: a textbook of cardiovascular medicine. 8th ed. Philadelphia: Saunders/Elsevier; 2008.
2. Nishimura RA, Otto CM, Bonow RO, Carabello BA, Erwin JP, Guyton RRA, O'Gara PT, Ruiz CE, Skubas NJ, Sorajja P, Sundt TM, Thomas JM. ACC/AHA guideline for the management of patients with valvular heart disease. J Am Coll Cardiol. 2014. doi:10.1016/j.jacc.2014.02.536.
3. de Filippi CR, Willett DL, Brickner ME, et al. Usefulness of dobutamine echocardiography in distinguishing severe from nonsevere valvular aortic stenosis in patients with depressed left ventricular function and low transvalvular gradients. Am J Cardiol. 1995;75:191–4.
4. Nishimura RA, Grantham A, Connolly HM, et al. Low-output, low-gradient aortic stenosis in patients with depressed left ventricular systolic function: the clinical utility of the dobutamine challenge in the catheterization laboratory. Circulation. 2002;106:809–13.
5. Clavel MA, Fuchs C, Burwash IG, et al. Predictors of outcomes in low-flow, low-gradient aortic stenosis: results of the multicenter TOPAS study. Circulation. 2008;118:S234–42.
6. Lancellotti P, Magne J, Donal E, Davin L, O'Connor K, Rosca M, Szymanski C, Cosyns B, Pierard LA. Clinical outcome in asymptomatic severe aortic stenosis: insights from the new proposed aortic stenosis grading classification. J Am Coll Cardiol. 2012;59(3):235–43.
7. Abbas AE, Franey LM, Goldstein J, Lester S. Aortic valve stenosis: to the gradient and beyond-the mismatch between area and gradient severity. J Interv Cardiol. 2013;26(2):183–94.

Invasive Evaluation of Aortic Stenosis

5

Amr E. Abbas, Ivan Hanson, and Mark C. Pica

Abstract

In the current valvular guidelines, Doppler Echocardiography is considered the mainstay of diagnosis aortic valve stenosis. Invasive assessment of aortic valve stenosis is reserved in those cases with inconclusive non-invasive studies, discrepant clinical and Doppler findings, and for research purposes prior to TAVR.

In this chapter we will review the different methods of invasive assessment of aortic valve stenosis by both gradient and area measures, the indications, the advantages, and the pitfalls. We will also briefly review the invasive hemodynamics of hypertrophic obstructive cardiomyopathy.

Keywords

Invasive assessment of aortic valve stenosis • Doppler echocardiography and aortic valve stenosis • Hypertrophic obstructive cardiomyopathy • Invasive pressure gradient assessment • Gorlin equation • Hakki equation

Introduction

In the current valvular guidelines, Doppler Echocardiography is considered the mainstay of diagnosis aortic valve stenosis. Invasive assessment of aortic valve stenosis is reserved in those cases with inconclusive non-invasive studies, discrepant clinical and Doppler findings, and for research purposes prior to TAVR [1, 2].

In this chapter we will review the different methods of invasive assessment of aortic valve stenosis by both gradient and area measures, the

A.E. Abbas, MD, FACC, FSCAI, FSVM, FASE, RPVI (✉) • I. Hanson, MD
Department of Cardiovascular Medicine, Beaumont Health, Oakland University/William Beaumont School of Medicine, Royal Oak, MI, USA
e-mail: aabbas@beaumont.edu

M.C. Pica, BS, CCRP
Department of Cardiology/Research Institute, Beaumont Health System, Royal Oak, MI, USA

A.E. Abbas (ed.), *Aortic Stenosis: Case-Based Diagnosis and Therapy*,
DOI 10.1007/978-1-4471-5242-2_5

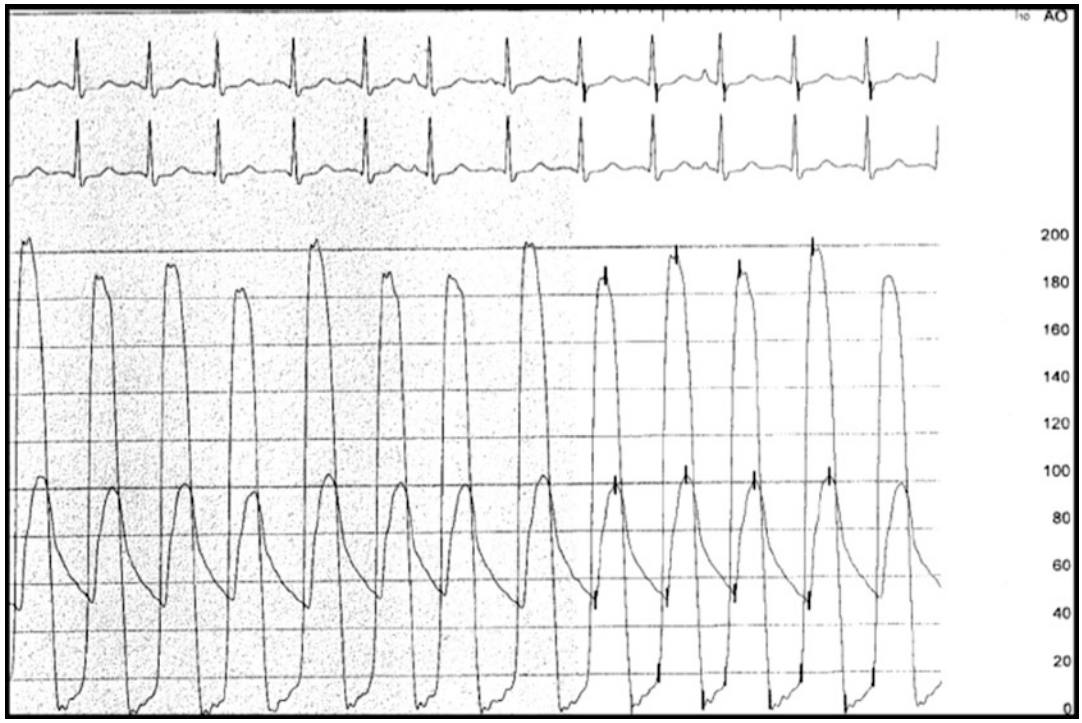

Fig. 5.1 Simultaneous left ventricular and aortic pressure using a dual lumen Langston catheter revealing severe aortic stenosis: Peak Gradient: 89 mmHg, Mean Gradient: 70 mmHg, Cardiac Output: 6.3 l/min, Aortic valve area: 0.65 cm^2

indications, the advantages, and the pitfalls. We will also briefly review the invasive hemodynamics of hypertrophic obstructive cardiomyopathy.

Invasive Measures of Trans-aortic Valve Gradients

As previously noted, invasive measures of aortic valve gradient provides the **peak-to-peak transvalvular gradients** (ΔP_{PPG}) as well as a **mean transvalvular gradient** (ΔP_{mean}). The ΔP_{PPG} is the difference between the highest aortic and highest ventricular pressure and occurs at two separate points on time and is considered of no physiological significance. However, ΔP_{mean} is more reflective of the true hemodynamic burden on the left ventricle and measures the trans-valve gradient after pressure recovery, also known as the net pressure gradient (ΔP_{net}) (Chap. 3). It is measured by planimetry of the area separating the left ventricular and aortic pressure curves. It can also be estimated by the equation [3]:

$$\Delta P_{mean} = 0.71 \times \Delta P_{PPG} + 17 \text{mmHg}$$

Two points of measurement are required; one in the left ventricle and one in the aorta.

The ventricular and aortic pressures can be measured as follows:

1. A catheter placed **retrograde** into the ventricle. This may be either:
   (a) A ***dual lumen*** Langston catheter with one "pigtail" in the left ventricle and the other "pigtail" in the aorta (Fig. 5.1).
   (b) Single catheter in the ventricle that is **pulled back** into the aorta (Fig. 5.2).
   (c) Catheter or pressure wire in the ventricle and
      (i) A side arm of the arterial sheath in the ***common femoral/iliac artery***.
      (ii) A side arm of the arterial sheath placed in the ***descending aorta***.
      (iii) A catheter placed in into ***another access site*** and positioned in the aorta.
   (d) Micro ***manometer*** catheter in the ventricle and one in the aorta

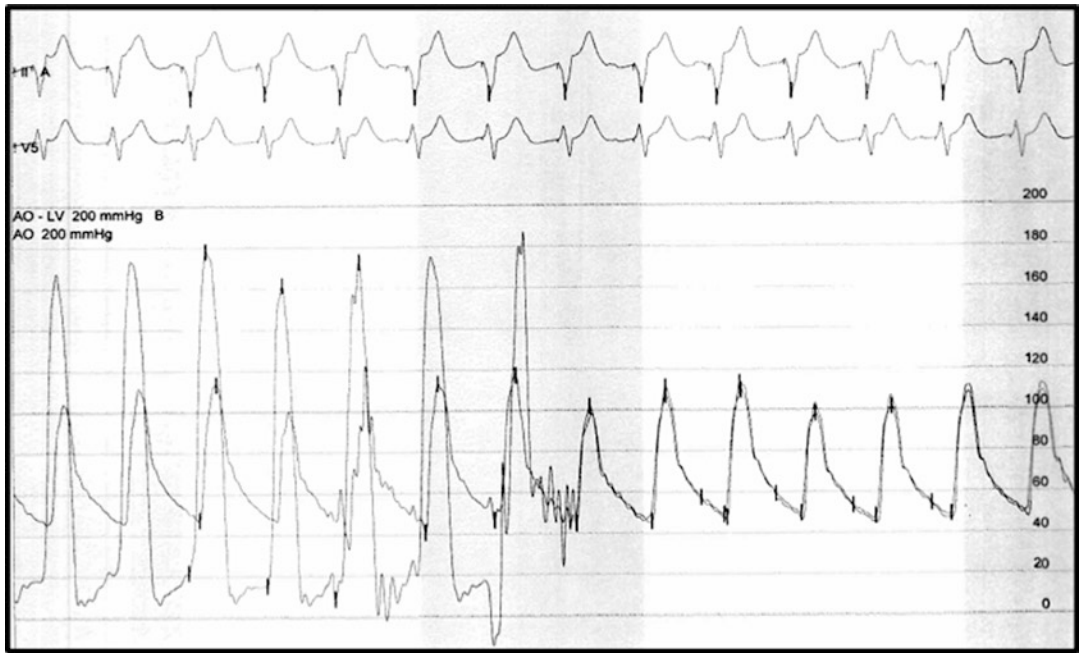

Fig. 5.2 Simultaneous left ventricular and aortic pressure using a dual lumen Langston catheter followed by a pull back gradient revealing severe aortic stenosis

2. A catheter placed via **direct apical puncture** and a catheter in the aorta.
3. A catheter placed via **trans-septal puncture** in the left ventricle and a catheter in the aorta.

General Considerations in Invasive Pressure Gradient Assessment

Certain physiological phenomena and measurement errors may lead to over- or under- estimation of the invasively measured gradient.

1. Utilizing the peripheral circulation (iliac arteries), as compared to the central aortic pressure, in the presence of ***peripheral arterial disease*** as distal aortic or iliac artery ***stenosis***, will lead to an **overestimation** of the aortic valve gradient.
2. Utilizing the peripheral circulation (iliac arteries), as compared to the central aortic pressure leads to a ***time delay*** of 80–120 ms compared to the peak aortic pressure waveform. In a classic study by Folland et al. in 26 patients, utilizing the ventricular and femoral artery pressure lead to an **overestimation** of the ventricular-aortic pressure gradient by 9 mmHg. On the other hand, ***phase-shift*** of the femoral arterial pressure tracing to **align** with the ventricular pressure lead to an **underestimation** of the ventricular-aortic pressure gradient by an average of 10 mmHg. Averaging of the unaligned and aligned ventricular-arterial pressure gradient may be used as a closer value to the true trans-aortic gradient [4] (Fig. 5.3).
3. Additionally, the peak arterial pressure obtained using the femoral artery may be higher than the aortic pressure due to **amplification**. This is pressure amplification occurs mainly in elderly patients with calcified blood vessels and results from pressure wave form moving into small diameter conduits with faster velocity and decrease arterial compliance. Amplification leads to an **underestimation** of the pressure gradient (Fig. 5.4) [3].
4. In severely stenotic aortic valves, the mere presence of a catheter across the aortic valve may decrease the peripheral arterial pressure

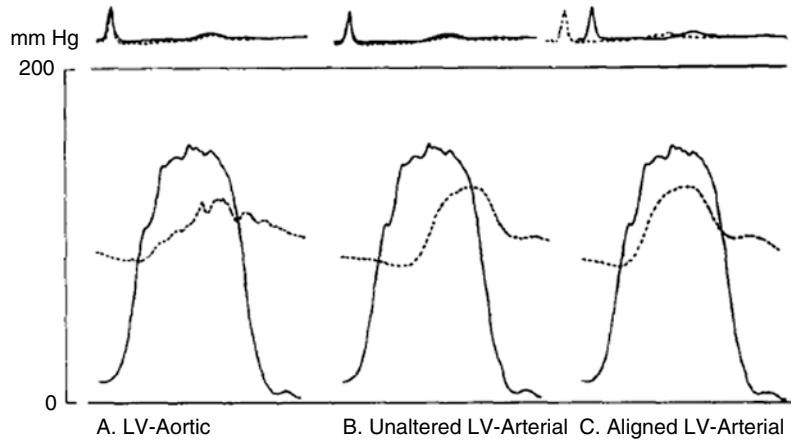

Fig. 5.3 A case from the study by Folland et al. demonstrating a mean LV-aortic gradient in a patient of 31 mmHg (A), an unaligned with time delay LV-arterial mean gradient of 37 mmHg (B), an aligned LV-arterial mean gradient of 22 mmHg (C)

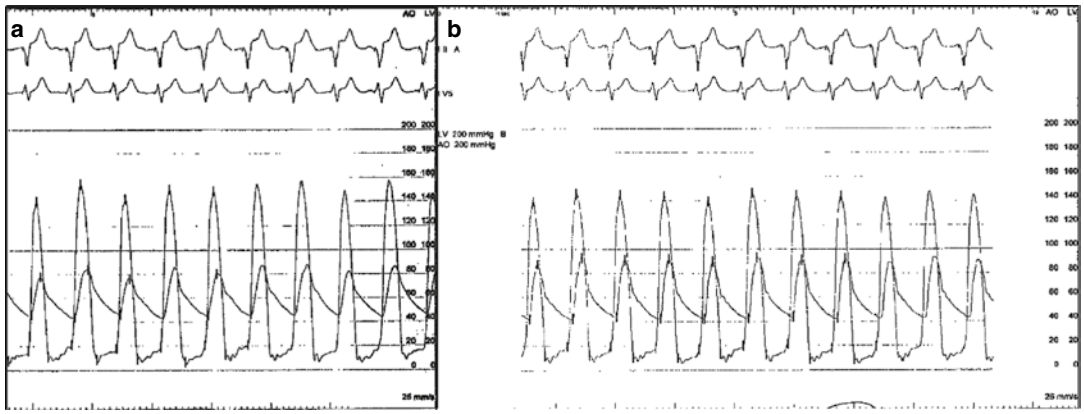

Fig. 5.4 The pressure gradient in the same patient using the ventricular-aortic pressure waveform (ΔP_{PPG} 68 mmHg & ΔP_{mean} 43 mmHg) (Panel **a**) is higher than the pressure gradient obtained using the ventricular arterial pressure waveform (ΔP_{PPG} 53 mmHg & ΔP_{mean} 34 mmHg) (Panel **b**). This occurs due to amplification noted in the peripheral circulation leading to underestimation of the pressure gradient

by 10 mmHg that is recovered after the catheter is withdrawn from the ventricle (***Carabello's sign***). This **overestimates** the severity of aortic valve stenosis, but is highly specific for the presence of severe artic valve stenosis. Carabello noticed an increase in peripheral arterial pressure of 10 mmHg when the catheter was withdrawn from the left ventricle across a severely stenotic aortic valve (<0.6 cm^2). This was shown to be 75 % sensitive and 100 % specific for severe aortic stenosis in one study [3]

5. ***Pull back gradients*** may be affected by catheter whip, bounce effects, ectopic beats, and respiratory variations
6. ***Catheter site-placement*** in either the ventricular cavity or the ascending aorta can alter the measured pressure gradients. As such, placing the ventricular catheter in the ventricular outflow tract as opposed to the LV apex may **underestimate** the gradient by as much as 30 mmHg. Conversely, placing the aortic catheter too close to the aortic valve may **overestimate** the aortic valve gradient, while placing it more distally (after pressure recovery) provides a lower gradient that is more reflective of the true hemodynamic burden (ΔP_{net}) [3].
7. Proper ***transducer calibration***, ensuring the absence of bubbles within the system, and utilizing dual catheters or a dual lumen catheter

placed in the ventricle and ascending aorta provide the most accurate assessment of trans aortic valve gradients.

8. Common artifacts in pressure gradient may include
   (a) An underestimated gradient may occur when one or more of the side holes of the pigtail is in the aorta and the others are in the ventricle
   (b) When two catheters are used and with pull back there is disparity of diastolic pressures, sheath damping is suggested
   (c) Ringing refers to artifacts from the transducer chambers, catheters, pressure tubing, or manifolds that confound waveform analysis and appear as an overshoot of the pressure waveform and also know as under-damping. Over-damping may occur when pressure waveforms are obtained after the pigtail is filled with contrast [3]
   (d) Utilizing the side arm of a sheath with the same caliber of the catheter (six french catheter in a six french sheath) placed in the iliac arteries or abdominal aorta will lead to a **dampened pressure waveform**.

Invasive Measures of Aortic Valve Areas

In their original article in 1951, Richard Gorlin (a cardiologist) and his father, an engineer, published an equation to invasively derive the mitral valve area. This equation has been extended to derive areas of other cardiac valves (including the aortic valve area) as well as cardiac shunts [5].

Since its inception, the equation has undergone rigorous review and critique and suggested modifications and/or simplifications, the most famous of which is the simplified equation proposed by Hakki et al. in 1981 [6].

Gorlin Equation

The Gorlin equation was derived from the "rounded edge" orifice or short tube hydraulic system model. This model was selected since it approximates flow across stenotic orifices where kinetic energy losses are very high with pressure losses are mainly and rapidly dissipated in conversion to velocity as opposed to pressure losses that occur mainly due to friction forces (as occurs with the large wetted perimeter hydraulic model). As such, the Gorlins deducted that resistance calculated by Poiseuille's law would not be an accurate gauge of stenosis severity [5].

Two equations were the basis of the derived Gorlin equation; the first was the relationship of flow to area and velocity; **Torricelli's law** and the second was the **conservation of energy law** where in a closed circuit, the kinetic energy equals the pressure or potential energy.

These equations are highlighted as follows:

1. **Torricelli's law**:

$$F = C_O \times A \times V$$

Where F = Flow, A = Area, V = Velocity, C_O = coefficient of orifice contraction dictating the ratio of the stream contraction area to that of the orifice area.

2. **Law of Conservation of Energy**:
   Since energy can only be transferred from one form to the other, kinetic energy = potential energy. Hence,

$$\tfrac{1}{2}\, mV^2 = mgh, \text{ since m is similar}$$
$$\text{Hence, } V^2 = C_V \times 2gh,$$
$$\text{Hence, } V = C_V \sqrt{2gh}$$

m = mass

C_V = coefficient of velocity (only a portion of pressure is converted to velocity and the rest is lost as friction and turbulence).

g = gravitational acceleration constant = 980 cm/s/s.

h = pressure in height of a given fluid above orifice.

If we rearrange the equations, we come up with the equation

3. $A = F / C_O \times C_V \sqrt{2gh}$ or $F / C \times 44.5 \times \sqrt{P_1 - P_2}$

A = Area

F = blood flow rate through the orifice when it is open.

C is an empirical constant (discharge coefficient) that accounts for both C_O and C_V and also incorporates the conversion of pressure from mmHg to cm of H_2O (and a correction for the equation used to calculate the diastolic filling period in the mitral valve cases).

h = P_1–P_2 = pressure gradient across the orifice.

The **Gorlin equation** for calculating the aortic valve area is:

$$CO / C \times HR \times SEP \times 44.3 \times \sqrt{P_1 - P_2}$$

CO = Cardiac Output.

C = Empirical constant (discharge coefficient) and has a **value of 1** in calculating aortic valve area

HR = Heart rate

SEP = systolic ejection period

P_1–P_2 = mean pressure gradient across the aortic valve

The Gorlin equation was initially created to provide an estimate of the GOA and as such, included a ***constant for the coefficient of contraction*** (*Co*) that relates the jet stream area at the vena contracta (EOA) to the GOA. In addition to the *Co*, the Gorlin equation included a *velocity conversion factor or* ***coefficient of velocity*** *(Cv)* whereby only a certain fraction of pressure is converted to velocity and the rest is dissipated as losses due to viscous friction losses, turbulence, and so forth. It relates the space average velocity of the formed jet stream to its velocity profile.

If there is a relatively flat velocity profile through the stenosis, the maximal velocity measured = space average velocity and $C_v = 1$. C_0 and C_v are both included in the empiric constant C (***discharge coefficient***) that also empirically incorporates the ***conversion factor of pressure units from mmHg to cm H2O***, the ***conversion factor for blood density***. The final constant C was estimated at 0.7 and later adjusted to 0.85 for the mitral valve area calculation (it also included a ***correction*** for the method used to estimate the diastolic filling period for patients with mitral stenosis). The empiric constant C was further assumed to have a value of 1 for aortic valve area calculation [7, 8].

In reality, the continuity equation and the Gorlin equation are based on similar hydrodynamic principles and as such should both provide a measure of the EOA and not the GOA. Although the EOA_{Cath} was initially set up as a measure of the GOA, inherent errors in the Gorlin equation render the catheter-derived area more a **reflection of the EOA** rather than the GOA. Dumesnil and Yoganthan described two small errors in the Gorlin equation that explain why the equation measures an estimate of the EOA rather than that of the GOA.

1. The first error is the use of *mean flow* instead of *square root of the mean flow squared* (the square root of the average of the squared instantaneous flow) as the mean flow is slightly greater than the other value and thus leads to an inherent small underestimation of the AVA.
2. The second is the use of the constant 44.3 instead of 50.4. These errors seem to compensate for one another, and the use of a C of 1.0 yields a result closer to the EOA rather then the GOA in practice [9].

It should be noted that Gorlin and his father elegantly stated that, concerning the derived valvular orifice area, the *"values, of course, may not be the-actual size, but they will differ from the actual size in each case only by the C factor; hence, values in a group of patients will have interpretative usefulness if considered in relation to one another. Once the coefficient is settled upon, all answers may be corrected to give the true orifice area"* [5].

The equation was evaluated from a mere **11 patients** with mitral stenosis; 6 on autopsy (by standard gross techniques) and 5 operative specimens (by intra-cardiac digital palpation by Dwight E Harken, MD). Repeated calculations from different sets of data checked well and changes in valve area were detected in two

patients who underwent fracture finger valvuloplasty [5].

In an insightful comment about the equation he helped develop, Richard Gorlin in an editorial published in 1987 stated, "*In our original presentation we pointed out that blood is a nonlinear, non-Newtonian fluid, which traverses cardiac valves in an intermittent, pulsatile, rather than steady flow. Considering that the equations were derived from systems of steady flow through fixed orifices, the surprise was that the equations worked at all!*" [10].

The Hakki Equation

Hakki et al. [6] described another simplified method to estimate aortic valve area. This equation is highlighted below

$$A = CO / \sqrt{P_1 - P_2}$$

A = Area
CO = Cardiac Output
P_1–P_2 = pressure gradient across the aortic valve (either mean or peak to peak)

The rationale described for this simplification is that the product of SEP × Heart rate × 44.3 appear to very close to a single value of 1×10^3 across a wide range of valve areas in their study. Moreover, there appeared to excellent correlation regardless of whether ΔP_{PPG} or ΔP_{mean} were used.

In a patient with aortic stenosis and an average cardiac output of 5 l/min, and mean gradient of 40 mmHg would have an aortic valve area of 0.79 cm^2 by Hakki and an area of 0.73 cm^2 by Gorlin. It is unclear whether in patients with extreme heart rates, especially in tachycardic or bradycardic patients; that the Hakki equation would be viable [3].

Aortic Valve Resistance

Resistance is the ratio of the pressure gradient to flow. Determining the aortic valve resistance has been proposed as an alternative or supplementary measure to assess aortic valve stenosis. The aortic valve resistance does not have a discharge coefficient and can be measured as

$$\sqrt{P_1 - P_2} \times SEP \times HR \times 1.33 / CO$$

Resistance was initially believed to be less flow-dependent and was used to differentiate patients with low flow low gradient severe AS from pseudo-severe AS. However, this has come into question and hemodynamic challenges using dobutamine and nitroprusside in patients with low flow aortic vale stenosis have been employed for further risk stratification [11].

General Considerations in Invasive Aortic Valve Area Assessment

1. **Valve inertia** may explain why the measured AVA is smaller than the GOA, as some of the inflow pressure would be absorbed in moving the valve itself and the actual gradient producing flow would be less than the mean gradient measured, and hence the EOA would be less than the GOA [12].
2. There appears to be a **linear** relation between trans valvular flow (measured by both Doppler and transit flow rate) and both invasive and Doppler-derived AVA. In one study by Burwash et al. this linear relationship between AVA and flow appeared with both increase in Doppler and transit time flow rate [13]. Moreover, a true change in the GOA with increased flow has been demonstrated on video imaging of in vivo models [12, 13]. This maybe related to an increase in pressure against the AV with increased flow and actually physically opening it to a greater GOA [12].
3. The two **components of the discharge coefficient constant (C) in the Gorlin equation** (coefficient of velocity C_v and orifice contraction C_O) **appear to be within themselves, dependent on flow** and may change depending the hemodynamic status during which they were derived. Cannon et al. have demonstrated

that in a known and fixed orifice area in a hydraulic chamber model that the constant C is not in fact "constant" but rather changes with the **square root of the mean pressure gradient** and hence in itself is dependent on flow. This will lead to increased values of EOA_{cath} with increased flow for a given GOA [9, 12].

4. As a general rule, catheter-derived area calculations (EOA_{Cath}) will differ from, and tend to exceed those obtained by Doppler (EOA_{Dop}) due to multiple reasons excluding measurement errors. Doppler calculations of EOA are a direct estimate of the vena contracta area where the Doppler gradient is derived, while the catheter measurements derive valve area from a catheter position in flow **upstream** from the vena contracta, where the flow stream has diverged [14–16]. In one study, more than half of the patients with catheter-derived areas of 1.0–1.5 cm^2 had Doppler-derived areas of 0.5–1.0 cm^2 [17]. Moreover, the more upstream from the vena contracta the invasive measure is obtained, the greater the estimated valve area until a plateau is reached, the point where P_{rec} is complete. This was termed "**area recovery**" (A_{rec}) by Levine et al. [15] and was first described by Schobel et al. [16]. Thus, the EOA_{Cath} is closer in value to the GOA (albeit not the same) than the EOA_{Dop}
5. The application of the continuity equation by Doppler to AVA measurement in patients with AS was initially described by Hatle et al. and correlated best with invasive measures when the AVA by Doppler was compared to the Gorlin equation while **using the Fick method to assess cardiac output** [18].
6. The EOA_{cath} is usually measured via a **retrograde placement** of a catheter across the stenotic aortic valve (unless trans-septal or apical catheterization is performed) which may further reduce the AVA and/or cause aortic regurgitation that may also affect the gradient. Clinically, this does not affect the decision-making process, since it only occurs with severely and obviously stenotic valves. However, it may affect the exact gradient measurement and further account for discrepancy between the EOA_{cath} and the GOA [13].
7. The ELCo described in earlier chapters, compares more favorably with the invasive EOA_{Cath} rather than EOA_{Dop} since it accounts for P_{rec} [19].

Invasive Pharmacological Challenges for Assessment and Stratification of Severe Aortic Stenosis

Dobutamine

Patients with low flow/low gradient severe aortic stenosis with low ejection fraction constitute a diagnostic dilemma. The determination of patients who may benefit from surgical or trans aortic valve replacement has been suggested by the use of dobutamine echocardiography. The goal is to enhance ventricular contractility with a resultant increase in stroke volume and transaortic flow. This was based on the realization that both the GOA as well as the EOA is dependent on flow.

Similarly, dobutamine has been utilized in the cardiac catheterization in a similar fashion to enhance contractility and hence stroke volume and transaortic flow. In a study by Nishimura et al. [20] of 32 patients who met criteria of an AVA <1 cm^2, mean gradient <40 mmHg, and an EF <40 %. Dobutamine infusion was started at 5 μg·kg_1·min_1 and was increased with increments of 3–10 μg·kg_1·min_1 every 5 min. The predetermined end points were a maximal dose of 40 μg·kg_1·min_1, mean gradient of 40 mmHg, 50 % increase in the cardiac output, heart rate of 140 beats per minute, or intolerable symptoms or side effects. Contractile reserve was defined as a 20 % increase in stroke volume. In patients who had a contractile reserve and encountered an increase in calculated aortic valve area with no major change in gradient were classified as pseudo-severe AS, while those who had a contractile reserve and encountered no

change in the calculated aortic valve area with an increase in gradient were classified as truly severe AS.

In this study, true fixed aortic stenosis was suggested in:

1. Patients with a mean gradient >30 mmHg at rest or with dobutamine infusion
2. Patients with an AVA <1.2 cm^2 with dobutamine infusion.

Additionally,

1. The presence of contractile reserve was noted to be of a prognostic significance in patients undergoing aortic valve surgery.
2. Aortic valve resistance as not helpful in discriminating patients with severe and pseudo aortic valve stenosis.

The projected aortic valve area (AVA_{proj}) [21] as well as the use of dobutamine in patients with low flow low gradient AS with preserved EF has been discussed elsewhere and has been proposed with echocardiography [22].

Nitroprusside

Another pharmacological agent that has been utilized in patients with severe aortic stenosis is nitroprusside. Nitroprusside decreases all invasive measures of afterload (reduces effective arterial elastance and systemic vascular resistance, and increases total arterial compliance) with a resultant increase in stroke volume and trans aortic flow. Nitroprusside should be used with extreme caution as it may cause precipitous hypotension. Nitroprusside has been used in:

1. Patients with **low flow/low gradient severe aortic stenosis and preserved ejection fraction** [23]. In addition to the afterload changes, there is an increase in stroke volume, aortic valve area, and mean aortic valve gradient (mean dose 1.0 ± 0.5 mcg/kg/min)
2. Patients with **critically ill patients with left ventricular dysfunction and aortic stenosis** [24]. There was almost a 58 % increase in cardiac index, 58 % increase in stroke volume, and surprisingly no change in aortic valve area with an increase in mean and peak gradients. Nitroprusside was started at a mean dose of 14 ± 10 μg per minute, and the dose was increased to a mean of 103 ± 67 μg per minute at 6 h and 128 ± 96 μg per minute at 24 h. This increase in cardiac index was noted in both patients with low and high gradients.
3. The use of nitroprusside has also been suggested in differentiating true versus pseudo severe AS in patients with **low flow/low gradient severe AS and depressed EF**. This has been suggested in a similar fashion as the use of dobutamine [25].

Invasive Evaluation of Dynamic Outflow Tract Obstruction

In contrast to patients with valvular AS and subaortic membranes, patients with HOCM develop a ***dynamic*** rather than a ***fixed*** obstruction of the left ventricular outflow tract (LVOT) related to basal septal hypertrophy as well as systolic anterior motion (SAM) of the anterior mitral leaflet further obstructing the LVOT. The cause of the SAM of the mitral valve is not clearly defined but may be related to the generation of Venturi forces pulling the anterior mitral valve towards the septum. SAM also leads to mitral regurgitation of various degrees due to malcoaptation of the mitral valve leaflets. Certain hemodynamic factors lead to the specific invasive tracings that are noted in patients with HOCM as noted below.

General Considerations in Patients with HOCM

1. The classic aortic pressure waveform is characterized by a rapid upstroke ***(spike)***

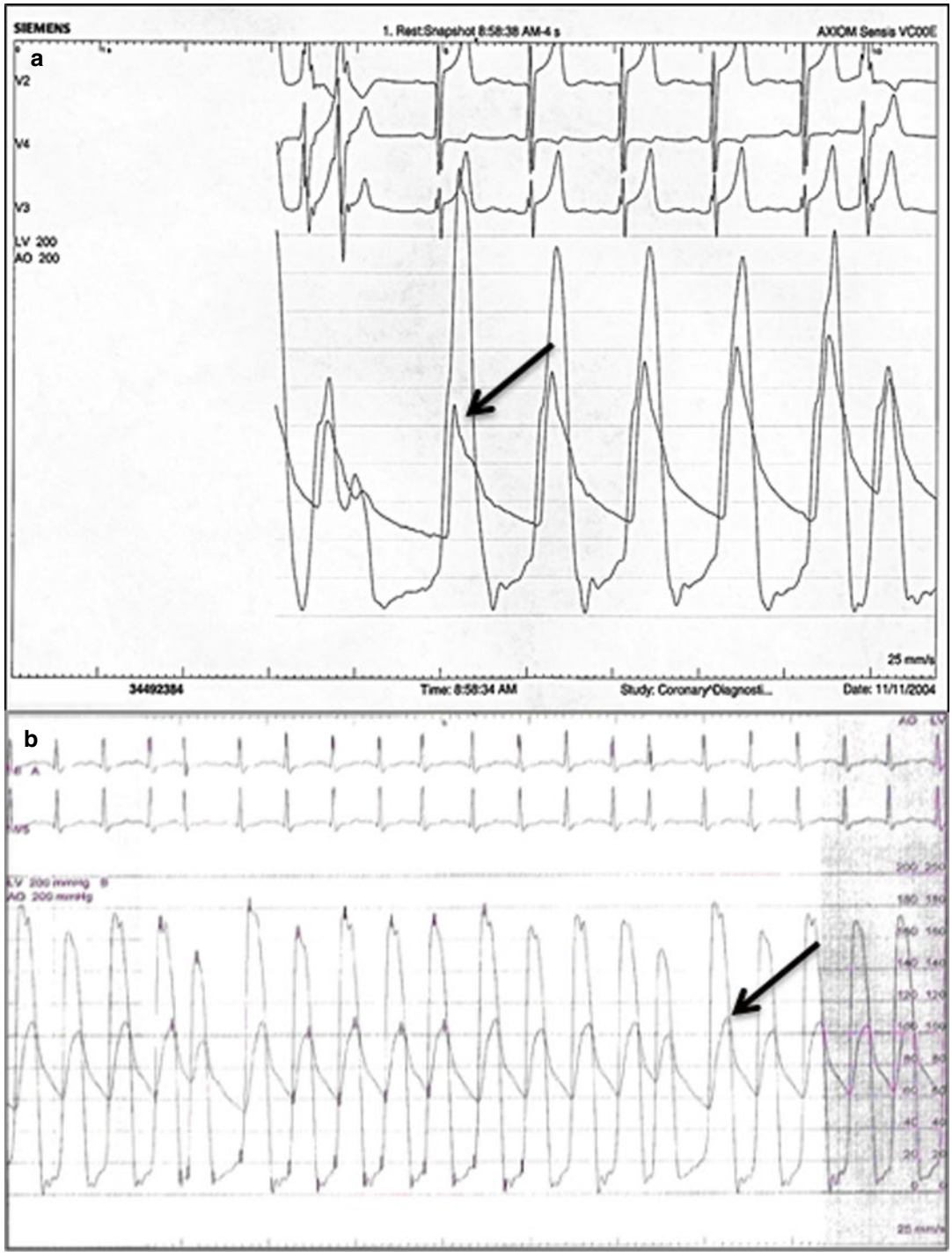

Fig. 5.5 Panel (**a**) Demonstrates a patient with hypertrophic obstructive cardiomyopathy characterized by an increased gradient and a rapid aortic pressure upstroke. A post-extra-systolic beat (*dark arrow*) reveals a decrease in the aortic pulse and peak systolic pressures and an increase in the left ventricular systolic pressure and the outflow tract gradient. The aortic pressure reveals a sharp rise (spike) followed by delayed pressure (dome) especially in the second beat. Panel (**b**) Demonstrates a patient with severe aortic valve stenosis characterized by an increased gradient and a delayed aortic pressure upstroke. A post-extra-systolic beat reveals an increase in the ventriculo-aortic pressure gradient, wider aortic pulse pressure, and a persistently delayed aortic pressure upstroke suggesting a fixed valvular obstruction

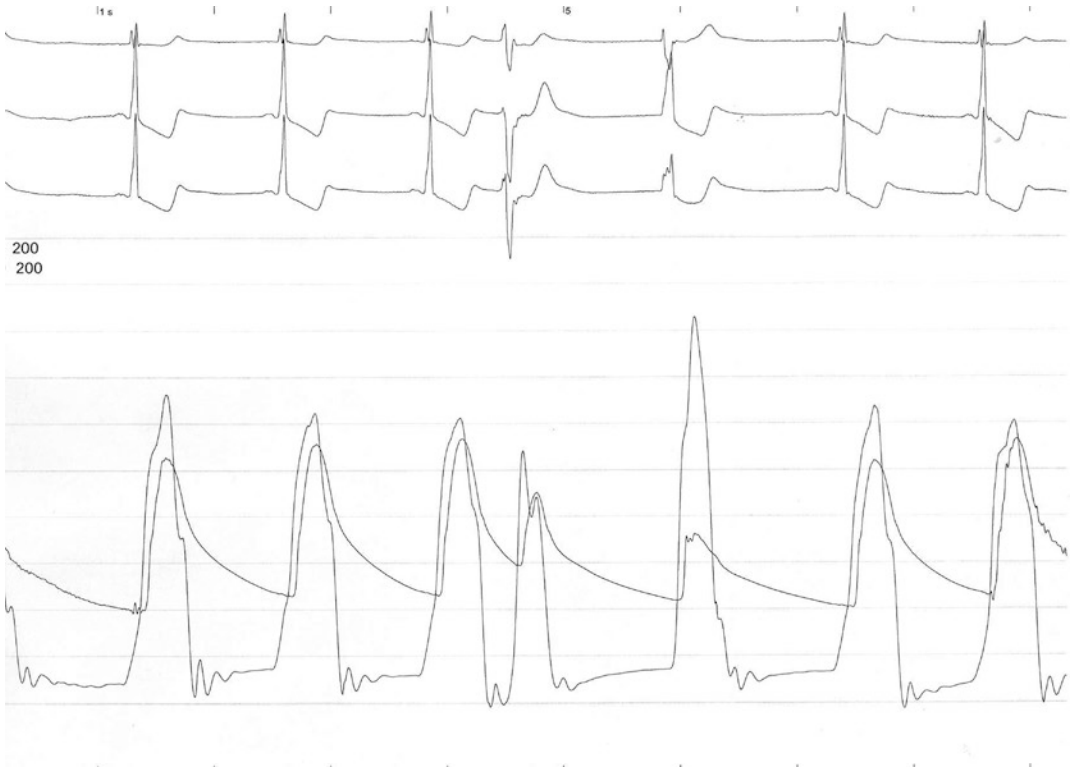

Fig. 5.6 A patient with HOCM demonstrating a negligible gradient at rest. However, following a PVC, a significant gradient is noted consistent with a dynamic outflow obstruction

from rapid onset contraction of the hypertrophied left ventricle. This is followed by a delayed drop and plateau ***(dome)*** related to dynamic outflow obstruction in mid to late systole.

2. In the beat following a PVC, the LV has augmented contractility (due to calcium overload of the myocytes following the post PVC pause) with failure of the pulse pressure to increase, or an actual ***decrease in the aortic pulse pressure***, due to the LVOT obstruction. This is accompanied by an increase in LV systolic pressure and is known as the Brockenbrough-Braunwald-Morrow sign. It was described in 1961 and contrasts to fixed valvular and subvalvular AS where a PVC is followed by also an increase in LV systolic pressure with an ***increase in aortic pulse pressure*** [3] (Fig. 5.5).
3. The resting or basal gradient can be minimal or even absent (Fig. 5.6); many techniques have been proposed to provoke and increase the outflow gradient.
   (a) Valsalva (through decreasing preload)
   (b) Amyl nitrate/nitroglycerin (these decrease the gradient in patients with valvular AS)
   (c) Induction of a PVC with post extra-systolic potentiation
   (d) Exercise induced
   (e) Isoproterenol infusion
4. Physiological mechanism to increase the outflow gradient include
   (a) Decreasing preload and LV EDV, left atrial filling, and shorter diastole
   (b) Increasing LV contractility both in force and duration
   (c) Decreasing afterload and peripheral resistance

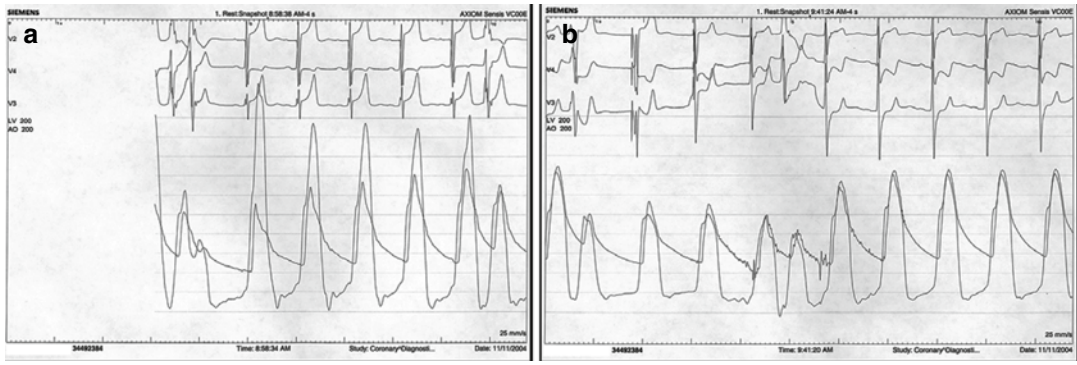

Fig. 5.7 Pre – (**a**) and post – (**b**) alcohol septal ablation waveforms demonstrating resolution of the outflow gradient both at rest and after PVC

5. Diastolic dysfunction in patients with HOCM may manifest as either a relaxation abnormality with a decline in diastolic pressure, as a large A wave suggesting increased LV end-diastolic pressure and decreased compliance, and/or prolongation of Tau.
6. The effects of alcohol septal ablation on patients with HOCM are a decline in outflow gradient (Fig. 5.7), left ventricular hypertrophy, and improvement in symptoms.

Combined Aortic Stenosis and Aortic Regurgitation

The presence of valvular or para-valvular AS together with aortic regurgitation (AR) can occur in various clinical scenarios. Moreover, the mere presence of significant AR can also increase the transaortic valve gradient. The presence of a high aortic/LV systolic gradient together with a low aortic/LV diastolic gradient (approximation of LV and aortic diastolic pressures) [3] denotes the presence of severe combined aortic disease (Fig. 5.8). Examples of combined aortic stenosis and regurgitation are noted below:

1. In patients with calcified or rheumatic valvular AS with combined valvular regurgitation due to **valve pathology**. This is more likely to be chronic in nature.
2. Patients with **bicuspid aortic valve disease** can develop a combined valvular pathology at an earlier age. The peak transvalvular velocity has been shown to be a prognostic marker in patients with bicuspid aortic valve disease regardless of the predominating pathology
3. Patients with a **sub-aortic membrane** can develop valve injury from the eccentric high jet beneath the AV leading to AR with a high gradient from the sub-aortic membrane
4. **Post percutaneous balloon aortic valvuloplasty** (**PBAV**) can develop AR on top of the existing and residual degree of AS
5. Patients **post TAVR** may develop various degrees of paravalvular and valvular regurgitation. The aortic regurgitation index (ARI) is calculated as

$$\text{ARI} = \left(\text{Diastolic blood pressure}\left(\text{DBP}\right) - \text{LV end diastolic pressure}\left(\text{LVEDP}\right) / \text{systolic blood pressure}\left(\text{SBP}\right)\right) \times 100$$

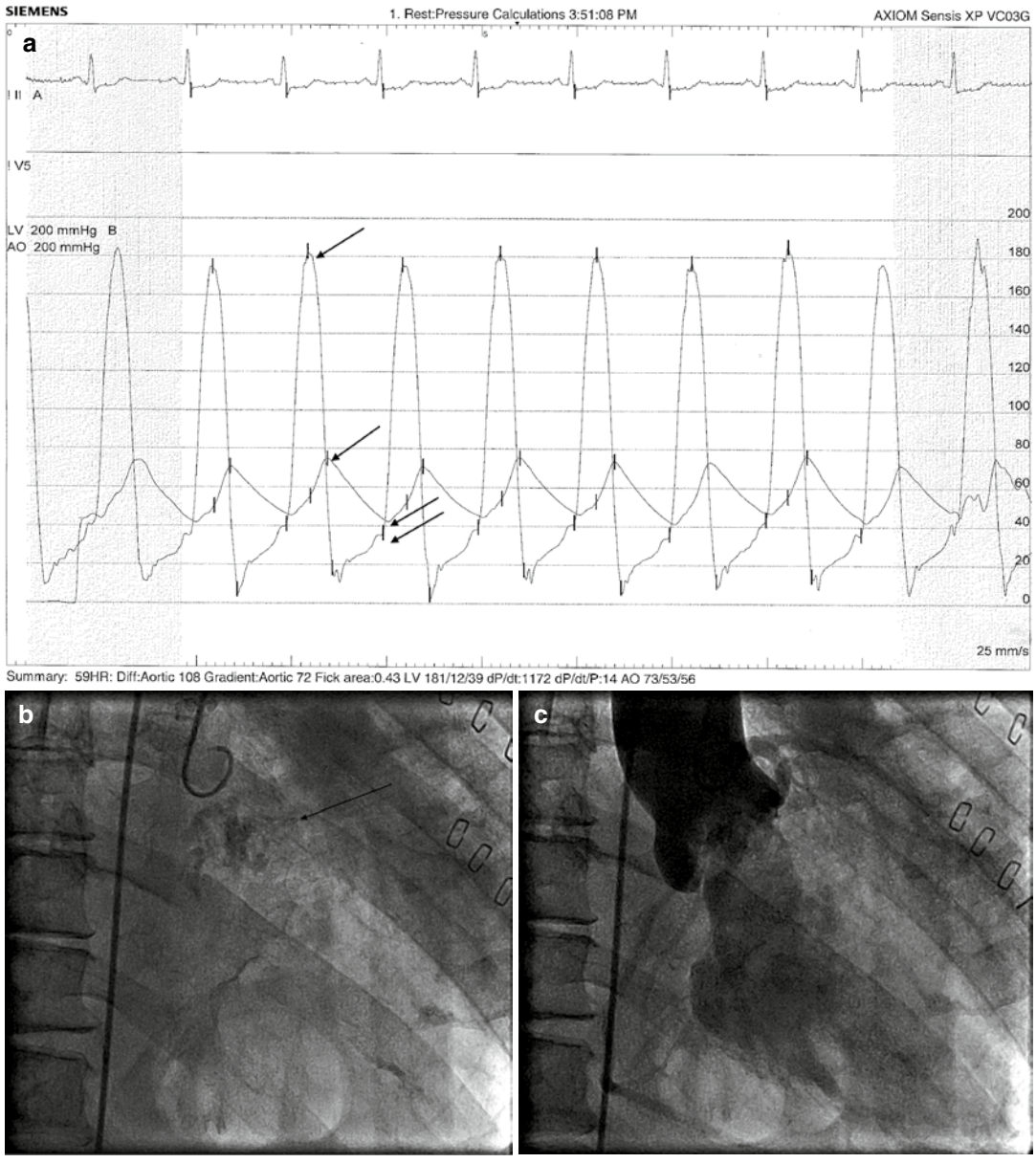

Fig. 5.8 (Panel **a**) Hemodynamic tracing of combined severe aortic stenosis and regurgitation. Note the systolic gradient between the LV and aorta (*black arrows* in third beat) and almost equalization of the LV and aortic diastolic pressures (*black arrows* in fourth beat). (Panel **b**) Fluoroscopy revealing a heavy calcified aortic valve in the same patient (*black arrow*). (Panel **c**) Aortography revealing severe aortic regurgitation in the same patient

A value <25 was shown to have increased 1 year morality compared to those with a value >25 [26]. Patients post both PBAV and TAVR suffer acute onset AR.

6. Patients with either a **mechanical or bioprosthetic AV** can develop a picture of prosthesis stenosis together with a paravalvular leak from **valve dehiscence**. In addition, patients with a **degenerated bioprosthetic or a mechanical valve with leaflet malfunction** can develop a mixed picture of AS and AR secondary to various pathologies as a thrombus, vegetation, or pannus.

Conclusions

Invasive assessment of aortic stenosis is reserved to cases when the non-invasive studies are inconclusive. Similar to non-invasive techniques, assessment of valve area and gradient are also subject to errors of measurement and assumptions. Invasive assessment of a dynamic outflow obstruction and combined aortic stenosis and regurgitation differs from that of isolated aortic valvular stenosis.

References

1. Nishimura RA, Otto CM, Bonow RO, Carabello BA, Erwin JP, Guyton RRA, O'Gara PT, Ruiz CE, Skubas NJ, Sorajja P, Sundt TM, Thomas JM. ACC/AHA guideline for the management of patients with valvular heart disease. J Am Coll Cardiol. 2014. doi:10.1016/j.jacc.2014.02.536.
2. Vahanian A, Alfieri O, Andreotti F, et al. Guidelines for the management of valvular heart disease. Eur Heart J. 2012;33:2451–96.
3. Kern MJ, Lim M, Goldstein JA. Hemodynamic rounds: interpretation of cardiac pathophysiology from pressure waveform analysis. 3rd ed. New York: Wiley- Blackwell; 2009.
4. Folland ED, Parisi AF, Carborne C. Is peripheral arterial pressure a satisfactory substitute for ascending aortic pressure when measuring aortic valve gradients? J Am Coll Cardiol. 1984;4(6):1207–12.
5. Gorlin R, Gorlin SG. Hydraulic formula for calculation of the area of the stenotic mitral valve. other cardiac valves, and central circulatory shunts. Am Heart J. 1951;41:1–29.
6. Hakki AH, Iskandrian AS, Bemis CE, Kimbiris D, Mintz GS, Segal BL, Brice C. A simplified valve formula for the calculation of stenotic cardiac valve areas. Circulation. 1981;63:1050–5.
7. Segal J, Lerner D, Miller DC, Mitchell RS, Alderman EA. When should Doppler-determined valve area be better than the Gorlin formula? Variation in hydraulic constants in low flow states. J Am Coll Cardiol. 1987;9(6):1294–305.
8. Canon SR, Richards KL, Crawford M. Hydraulic estimation of stenotic orifice area: a correction of the Gorlin equation. Circulation. 1985;71:110–78.
9. Dumesnil JG, Yoanathan AP. Theoretical and practical differences between te Gorlin equation and the continuity equation for calculating aortic and mitral valve areas. Am J Cardiol. 1991;67:1268–72.
10. Gorlin R. Calculations of cardiac valve stenosis: restoring an old concept for advanced applications. J Am Coll Cardiol. 1987;10(4):920–2.
11. Carabello BA, Grossman W. Grossman's cardiac catheteization, angiography, and intervention, 6th ed. Lippincott Williams & Wilkins; 2000.
12. Carabello BA. Advances in the hemodynamic assessment of stenotic cardiacvalves. J Am Coll Cardiol. 1987;10:912–9.
13. Burwash JG, Thomas DD, Sadahiro M, Pearlman AS, Verrier ED, Thomas R, Kraft CD, Otto CM. Dependence of gorlin formula and continuity equation valve areas on transvalvular volume flow rate in valvular aortic stenosis. Circulation. 1994;89:827–35.
14. Abbas AE, Franey LM, Goldstein J, Lester S. Aortic valve stenosis: to the gradient and beyond-the mismatch between area and gradient severity. J Interv Cardiol. 2013;26(2):183–94.
15. Levine RA, Schwammenthal E. Stenosis is in the eye of the observer: impact of pressure recovery on assessing aortic valve area. J Am Coll Cardiol. 2003;41(3):443–5.
16. Schobel WA, Voelker W, Haase KK, Karsch KR. Extent, determinants and clinical importance of pressure recovery in patients with aortic valve stenosis. Eur Heart J. 1999;20(18):1355–63.
17. Oh JK, Taliercio CP, Holmes Jr DR, et al. Prediction of the severity of aortic stenosis by Doppler aortic valve area determination: prospective Doppler-catheterization correlation in 100 patients. J Am Coll Cardiol. 1988;11:1227–34.
18. Skjaerpe T, Hegrenaes L, Hatle L. Noninvasive estimation of valve area in patients with aortic stenosis by Doppler ultrasound and two-dimesnional echocardiography. Circulation. 1986;72:810–8.
19. Garcia D, Pibarot P, Dumesnil JG, Sakr F, Durand LG. Assessment of aortic valve stenosis severity: a new index based on the energy loss concept. Circulation. 2000;101(7):765–71.
20. Nishimura RA, Grantham A, Connolly HM, et al. Low-output, low-gradient aortic stenosis in patients with depressed left ventricular systolic function: the clinical utility of the dobutamine challenge in the catheterization laboratory. Circulation. 2002;106:809–13.

21. Blais C, Burwash IG, Mundigler G, et al. Projected valve area at normal flow rate improves the assessment of stenosis severity in patients with low-flow, low-gradient aortic stenosis. Circulation. 2006;113:711–21.
22. Clavel MA, Ennezat PV, Sylvestre M M.D.,†., Dumesnil JG M.D*., Romain C, Zeineb Hachicha Z, Mathieu P, Annaïk Bellouin A, Bergeron S, Meimoun P, Arsenault M, Le Tourneau T, Pasquet A, Couture C, Pibarot P. Stress echocardiography to assess stenosis severity and predict outcome in patients with paradoxical low-flow, low-gradient aortic stenosis and preserved LVEF. J Am Coll Cardiol. 2013;6:175–83.
23. Eleid M, Nishimura R, Borlaug B, Sorajja P. Acute hemodynamic effects of sodium nitroprusside in low gradient severe aortic stenosis with preserved ejection fraction. J Am Coll Cardiol. 2013;61(10_S). doi:10.1016/S0735-1097(13)62114-2
24. Khot UN, Novaro GM, Popović ZB, Mills RM, Thomas JD, Murat Tuzcu E, Hammer D, Nissen SE, Francis GS. Nitroprusside in critically ill patients with left ventricular dysfunction and aortic stenosis. N Engl J Med. 2003;348:1756–63.
25. Carabello BA, Ballard WL, Gazes PC. Patient 65, cardiology pearls. Philadelphia: Hanley and Belfus; 1994. p. 142.
26. Sinning JM, Hammerstingl C, Vasa-Nicotera M, Adenauer V, lema Cachiguango SJ, Scheer AC, Hausen S, Sedaghat A, Ghanem A, Muller C, Grube E, Nickening G, Werner N. Aortic regurgitation index defines severity of peri-prosthetic regurgitation and predicts outcomes in patients after transcatheter aortic valve implantation. J Am Coll Cardiol. 2012;59(13):1134–41.

Echocardiographic Evaluation of Aortic Valve Stenosis

6

Nathan Kerner

Abstract

Echocardiography has become the mainstay of diagnosis of patients with valvular heart disease. Its non-invasive nature, absence of side effects, and portability have rendered it a valuable tool in the diagnosis, follow up, intraoperative, post-operative evaluation of patients with severe aortic stenosis.

In this chapter we will review the comprehensive role of echocardiography in the assessment of these patients.

Keywords

Echocardiography • Normal flow, high gradient • Doppler • Continuity equation

Introduction

Echocardiography has become the mainstay of diagnosis of patients with valvular heart disease. Its non-invasive nature, absence of side effects, and portability have rendered it a valuable tool in the diagnosis, follow up, intraoperative, post-operative evaluation of patients with severe aortic stenosis.

In this chapter we will review the comprehensive role of echocardiography in the assessment of these patients.

N. Kerner, MD, FACC, FASE
Department of Cardiovascular Medicine,
Beaumont Health, Oakland University/William
Beaumont School of Medicine, Royal Oak, MI, USA
e-mail: nkerner@beaumont.edu

Case Presentation

D.M. is an 80-year-old female brought in by her family after a fall and presumed syncope. She lives alone and called her family after losing consciousness without warning and after awakening on the floor. The patient denies shortness of breath, chest pain, pressure or tightness. She does not recall palpitations or dizziness leading up to her syncopal event. Past medical history is positive for history of myocardial infarction and hypertension.

The patient's examination demonstrates her to be alert and oriented and in no acute distress with a bruise in her periorbital area. Her vitals are unremarkable and she has no jugular venous distention. Carotid pulse shows delayed upstroke

A.E. Abbas (ed.), *Aortic Stenosis: Case-Based Diagnosis and Therapy*,
DOI 10.1007/978-1-4471-5242-2_6

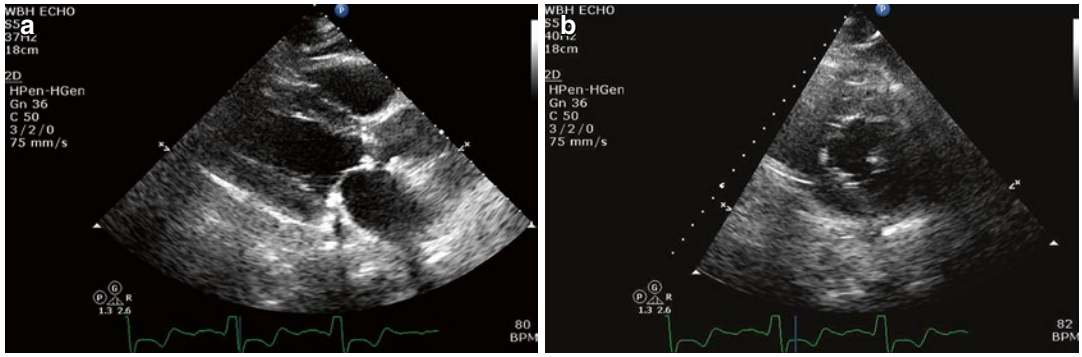

Fig. 6.1 Parasternal long (**a**) and parasternal short-axis (**a**) views of the left ventricle (*LV*) demonstrating increased wall thickness and normal chamber size. The aortic valve is calcified. The left atrium (*LA*) appears mildly dilated

and auscultation demonstrates a transmitted murmur. The cardiac examination shows regular rate and rhythm. The PMI is not displaced although is somewhat sustained. S1 is normal with single S2 and there is an S4 at the apex with no S3. ***There is a grade 3/6 late peaking, low pitched, harsh ejection murmur heard over the entire precordium and radiating to the lower cervical region with no palpable thrills.*** The lungs are clear to auscultation and percussion and her extremities show no edema.

EKG

The electrocardiogram demonstrates sinus rhythm with right bundle branch block pattern with no ischemic ST segment shifts and her laboratory evaluation is unremarkable.

Transthoracic Echocardiography (TTE)

Reveals normal left ventricular chamber size with moderate concentric hypertrophy (Fig. 6.1a, b). The ejection fraction is calculated at 69 % by the method of discs. The left atrium is moderately dilated. The right atrium and right ventricle are normal in size. There is no pericardial effusion. The aortic valve is thickened and heavily calcified. The systolic excursion of all three leaflets is reduced (Fig. 6.2). **Doppler assessment shows evidence of severe aortic stenosis with a peak**

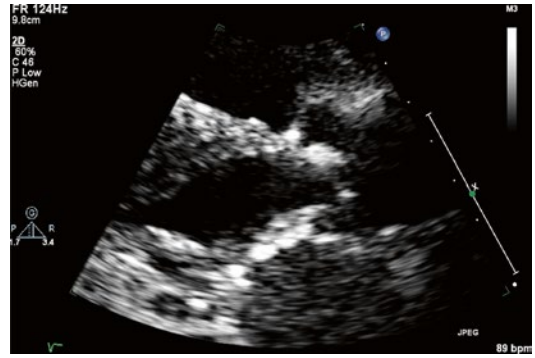

Fig. 6.2 Parasternal long axis view of the left ventricle (*LV*), left ventricular outflow tract (*LVOT*) and aortic valve (*AV*). The aortic leaflets are thickened, appear moderately calcified and demonstrate decreased excursion during this mid-systolic frame

gradient of 80 mmHg and a mean gradient of 50 mmHg. The aortic valve area by the continuity equation using the aortic and left ventricular outflow tract (LVOT) velocity time integral (VTI) is 0.65 cm^2 (Fig. 6.3a, b). There is mild mitral insufficiency. There is mild tricuspid insufficiency. The right ventricular systolic pressure is calculated at 31 mm mercury.

The patient was referred to a cardiothoracic surgeon for consideration of aortic valve replacement.

Patient Summary

This patient has a clinical presentation and echocardiographic findings of severe aortic stenosis.

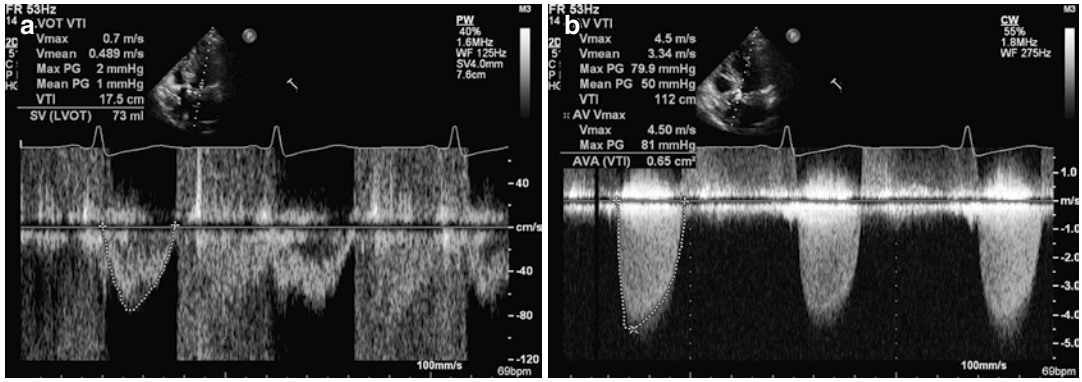

Fig. 6.3 Doppler tracings from the patient. The pulsed wave recording (**a**) shows normal velocity profile with predominantly laminar flow and a peak velocity of 0.9 m/s. The aortic continuous wave recording (**b**) shows a peak gradient of 80 mmHg and a mean gradient of 50 mmHg. The calculate aortic valve area using Doppler measurements is 0.65 cm^2. These findings are consistent with severe aortic stenosis

Each individual will behave differently in terms of his or her clinical response to the gradually progressing aortic valve obstruction [1, 2]. Despite the spectrum of disease entities and although the pathology and accompanying comorbidities may differ in terms of the response to valvular obstruction, there remain common denominators which allow for the documentation of the presence and severity of aortic stenosis.

Pathophysiology of Aortic Stenosis and Echocardiography

As the aortic valve becomes fibrotic and/or calcified, in the early stages there may be no significant change in terms of terms of hemodynamic consequences to the patient and the disease may be entirely asymptomatic [1, 3]. On occasion, the only indication that there is aortic valve pathology may be a prominent murmur detected on physical examination. As the valvular obstruction progresses, however, the afterload on the left ventricle gradually increases and the ventricle begins to adapt with concentric hypertrophy as a response to this increased resistance to outflow. During the early phases of this compensation, the systolic and diastolic function may remain preserved. However, diastolic function gradually becomes abnormal due to the added muscle mass and impaired relaxation of the hypertrophied ventricle and eventually left atrial enlargement will also ensue [4–7]. Once compensatory mechanisms have been overrun, left ventricular systolic function will become impaired. Chronic left ventricular diastolic and systolic dysfunction eventually may lead to in varying degrees of mitral insufficiency and pulmonary hypertension [8–11].

The above-described sequence of events allows us to define a collection of findings that will guide in the assessment of aortic stenosis by two-dimensional, Doppler as well as three-dimensional echocardiography.

Echocardiography and the Normal Aortic Valve

A normal aortic valve is a trileaflet structure with three thin, pliable leaflets, each having similar dimension (Fig. 6.4a, b). As valvular pathology and fibrosis progresses, the leaflets become thicker, with restricted motion and eventually demonstrate significant calcification as in (Fig. 6.5a, b).

In the normal pliable aortic the valve leaflets open with the onset of ventricular asystole once the left ventricular systolic pressure exceeds the central aortic pressure with only a minimal differential necessary to achieve valve opening. The valve remains open throughout left ventricular ejection until diastolic relaxation has allowed left

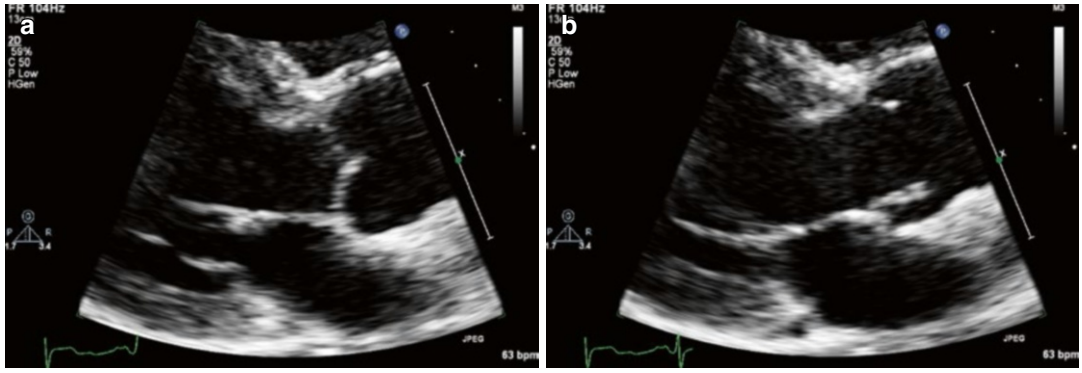

Fig. 6.4 This echocardiographic image of a normal aortic valve is taken from the parasternal long axis during diastole (**a**) and systole (**b**). Note the thin, symmetric leaflets with a central coaptation point during diastole. As the valve opens during systole, the pliable leaflet open to their maximum excursion and are flattened against the sinuses to allow minimal obstruction to the ejection of left ventricular outflow

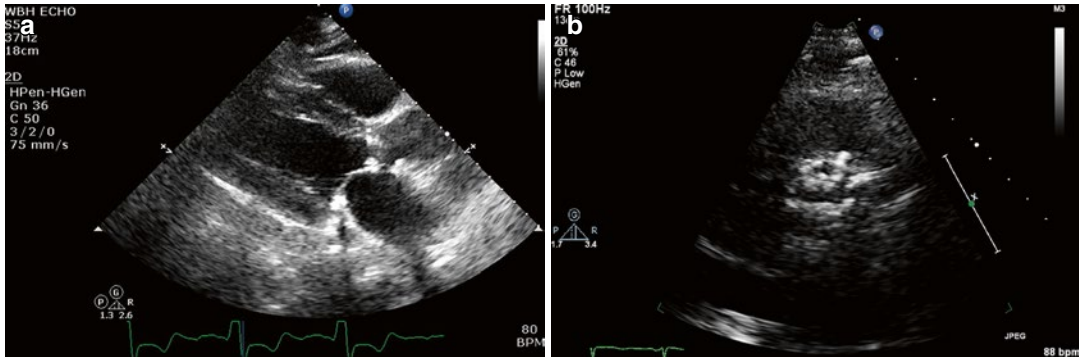

Fig. 6.5 Parasternal long axis (**a**) and short axis (**b**) taken during ventricular systole. As opposed to normal, thin pliable leaflets, the aortic valve depicted here is thickened with increased echodensity of the leaftlets, consistent with fibrosis and/or calcium infiltration. The excursion of the leaflets is significant restricted

ventricular pressure to decrease below that of the central aorta. Therefore, at any given time there will be a negligible pressure gradient between the left ventricle and the central aorta during systole.

Echocardiography and the Stenotic Aortic Valve

As opposed to the normal valve (with no significant gradient between the left ventricle and the aorta during systole) (Fig. 6.6a), a stenotic aortic valve will, by definition, create a pressure differential or gradient between the left ventricle and aorta in order to achieve valve opening (Fig. 6.6b). The gradient between the left ventricle and aorta during systole will depend predominantly on the degree of the aortic valvular obstruction to flow. Other factors, however, including left ventricular systolic function, aortic valve orifice geometry, (including whether the stenotic orifice is more centrally located or eccentric), and the geometry of the ascending aorta itself will also affect the magnitude and timing of occurrence of the peak gradient.

As shown in Fig. 6.6 the peak pressure differential between the left ventricle and aorta does not necessarily occur in conjunction with the peak left ventricular systolic pressure and there may be a poor correlation with the peak gradient measured with Doppler interrogation and the peak-to-peak gradient between the left ventricle

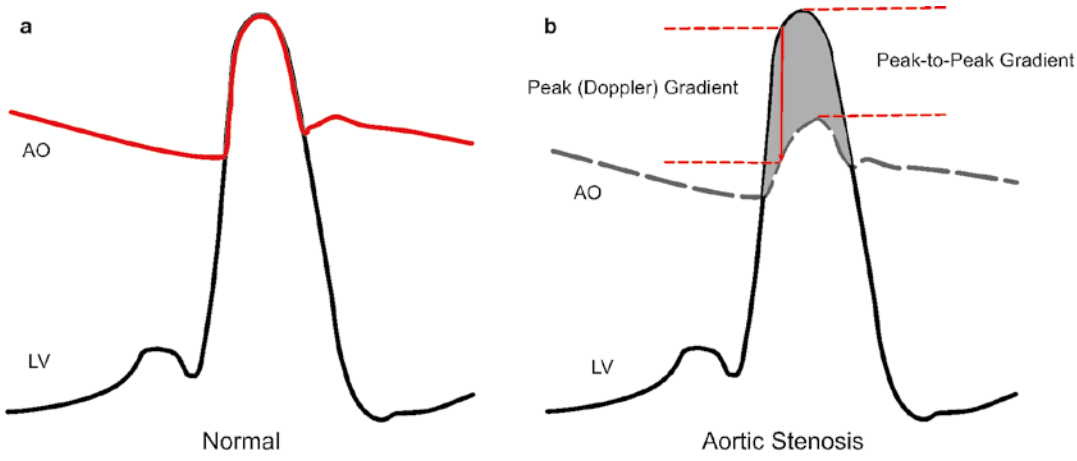

Fig. 6.6 Graphic depiction of simultaneous pressure recordings as would be recorded in the catheterization laboratory from the left ventricle and aorta in the normal state (**a**) and in the case of aortic stenosis (**b**). Note the different values that would be recorded for the peak-to-peak gradient typically measured during catheterization (labeled "Peak-to-Peak Gradient") and the peak instantaneous gradient ("Peak (Doppler) gradient")

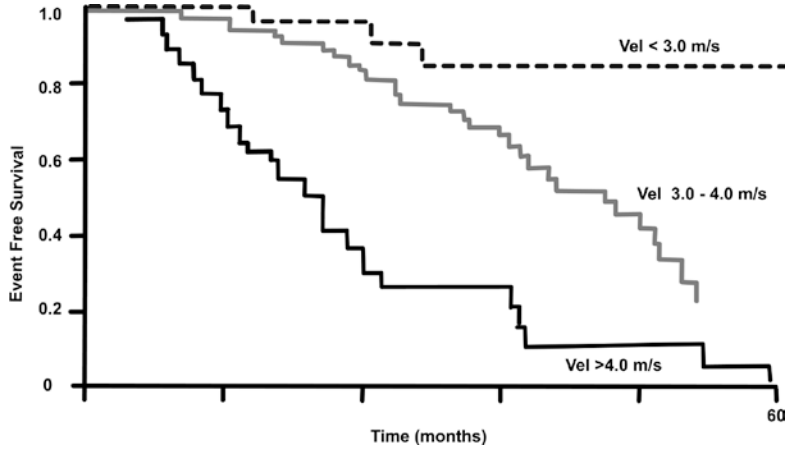

Fig. 6.7 Kaplan-Meier event free survival in asymptomatic individuals according to peak velocity of aortic stenotic jet ($p<0.0001$). Note the markedly decreased survival when aortic stenotic velocity progressed from a peak of less than 3.0 m/s (*dashed line*) to a velocity between 3.0 and 4.0 m/s (*gray line*) and the higher mortality with velocity of greater than 4.0 m/s (*Black line*) (Adapted from Otto et al. [31], with permission)

and central aorta as measured during cardiac catheterization. When comparing noninvasive echocardiographic measures of aortic stenosis with invasive measurements during catheterization, this potential discrepancy must be kept in mind.

It is well known that the presence of significant valvular obstruction due to aortic stenosis when combined with symptoms will predict long-term prognosis [12]. It has also been shown by Vahanian and Otto et al. that survival is significantly lower even in those asymptomatic individuals with high gradients (Fig. 6.7) [13]. It is important to remember nonetheless that symptoms such as dyspnea, chest pain or syncope from aortic stenosis may manifestations of other diseases and therefore it is important to distinguish whether individual symptoms are truly related to aortic stenosis.

Echocardiography has risen to the forefront and has become the "gold standard" in most institutions to screen for and assess the severity of aortic valve stenosis. Unfortunately, there are pitfalls that may be encountered along the way during these measurements. The accepted techniques and standards used in the determination of the

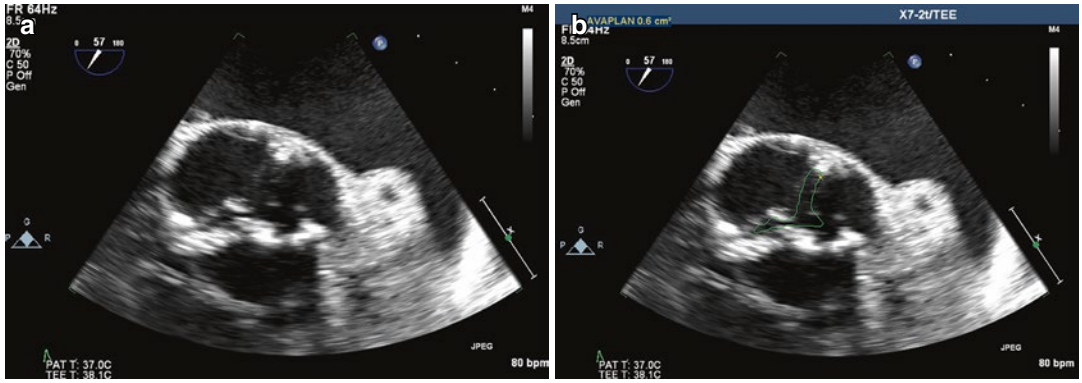

Fig. 6.8 Parasternal short axis of a severely stenotic aortic valve with mid-systolic frame without (**a**), and with planimetry of the estimated orifice area (**b**). Note that there are not always clearly defined borders to trace due to acoustic shadowing from calcification (*arrows*)

presence of aortic stenosis as well as the potential pitfalls in this assessment will be the focus of the rest of this chapter.

Two-Dimensional Echocardiographic Evaluation of Aortic Stenosis

Aortic Valve

Two-dimensional assessment of the aortic valve should include an assessment of the valve itself as well as surrounding structures. The number and symmetry of the leaflets, the thickness as well as the mobility of each individual leaflet, the presence or absence of fused commissures and the location of any calcium deposition should be described. This will help point to an understanding of the underlying valvular pathology (i.e. bicuspid versus trileaflet valve, rheumatic vs. degenerative, etc.). The distribution of calcium and/or fibrosis generally will be asymmetric and irregular in terms of distribution within the valve and the perivalvular tissues (annulus, sinuses, sinotubular junction and mitral annulus). The degree of calcification and the location has clinical relevance when considering valve replacement and especially percutaneous valve replacement [14].

In addition to the qualitative measures noted above, the aortic valve cross-sectional area can be measured in the parasternal short axis (Fig. 6.8a, b) [15]. As is the case with measurements by planimetry used in assessing the mitral valve, often extensive fibrosis and calcification that is present in aortic stenosis will make planimetry technically challenging, however [16]. For this reason, if the visual qualitative estimation of aortic valve stenosis severity does not correlate with the Doppler measurements, the measured valve area by planimetry alone may not mitigate this discrepancy. The evaluation of concomitant aortic regurgitation is also essential. Recent data suggest that the peak trans aortic velocity is the primary prognostic determinant in patients with combined valve disease.

Left Ventricular Outflow Tract

The accurate two-dimensional measurement of left ventricular outflow tract (LVOT) is of paramount importance during the assessment of aortic stenosis, as this is the greatest potential source of error in the calculation of aortic valve area by the continuity equation (see below). This LVOT measurement itself is squared within the continuity equation and therefore small errors in LVOT measurement are magnified in the calculation. According to EAE/ASE guidelines [17], the left ventricular outflow tract should be imaged from the parasternal long axis view in a zoomed

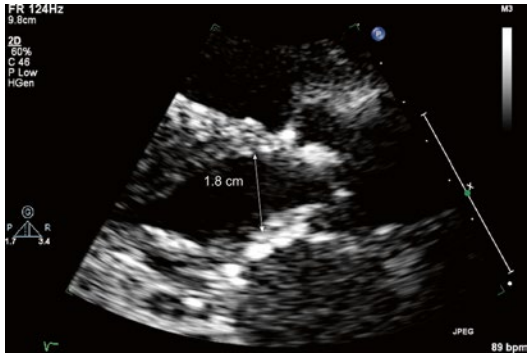

Fig. 6.9 Zoomed parasternal long axis view of the left ventricular outflow tract (*LVOT*) demonstrating method of measurement of the LVOT diameter, which in turn is used to calculate LVOT area used in the continuity equation

projection. A diameter measurement of the LVOT should be taken from inner edge to inner edge from the most basal aspect of the interventricular septum endocardium to the base of the anterior mitral valve leaflet during the mid-portion of systole (Fig. 6.9). The diameter of the aortic annulus, the adjoining aortic sinuses, proximal aorta and sinotubular junction should also be measured. The presence and extent of calcification in these areas may be important as well if future interventions, either surgical or percutaneous are undertaken.

Left Ventricle

As previously discussed, the increased afterload on the left ventricle during systole due to the aortic valve obstruction will cause the left equal to compensate with resulting hypertrophy of the myocardium. In general, however, the pattern and degree of left ventricular hypertrophy does not correlate well with the severity of aortic stenosis [18]. Whether surgery or percutaneous intervention is anticipated, a significant degree of left ventricular hypertrophy, especially involving the proximal interventricular septum may have implications for treatment. The wall thickness and pattern of hypertrophy should be characterized during the echocardiographic examination for aortic stenosis. Left ventricular systolic and diastolic function should be assessed in the standard manner as these parameters of left ventricular function are often abnormal with hemodynamically significant aortic stenosis, even if the patient is asymptomatic [5].

Left Atrium

As left ventricular diastolic pressures increase, there will be inevitably be a concomitant increase left atrial pressure and eventually in left atrial size. Left atrial enlargement when present is an independent indicator of prognosis in the aortic stenosis [7].

Mitral Insufficiency

Individuals with significant degenerative aortic valve stenosis may also show similar degenerative changes involving the mitral valve including mitral annular calcification and mitral leaflet thickening. Due to changes in left ventricular geometry and hemodynamics, as well as left atrial pressures, it is not uncommon for varying degrees of mitral insufficiency to be present [8, 9]. However, unless the underlying aortic valve pathology is rheumatic in origin, a primary mitral valvulopathy involving the leaflets themselves, which can be visualized on two-dimensional imaging is not often present. Patients with a more than moderate degree of mitral regurgitation and/or a structural problem with the mitral valve are unlikely to note improvement in mitral valve function following aortic valve replacement and as such require a double valve surgery.

Doppler Assessment of Aortic Stenosis

Hatle et al. [18] initially described the means of identifying and quantifying the severity of aortic stenosis by Doppler echocardiography. Since then, the use of Doppler echocardiography has been widely validated as an accurate modality to assess for the presence and severity of this entity. In the vast majority of individuals, the standard Doppler

study aimed at recording the parameters of the aortic systolic velocity spectrum will determine the presence or absence of significant valvular obstruction and yield an accurate assessment of the stenosis severity. As with any other technique, Doppler echocardiography may yield conflicting data in certain situations when normal physiology is disturbed. The remainder of this chapter will focus on that situation which is most commonly encountered, i.e. that of normal flow, high gradient aortic stenosis.

As noted above, by definition with aortic stenosis, a gradient exists during systole between the left ventricle and the aorta. The modified Bernoulli (Eq. 6.1) yields an estimation of the pressure differential between two chambers separate by a stenotic valve and can be calculated using the velocity of blood flow (in this case across the aortic valve). It is important to understand the strengths and limitations of the Bernoulli equation in assessing aortic valve gradients in order to use this measurement properly.

$$\Delta P\left(\text{mmHg}\right) = 4\left(v_1^{\,2} - v_2^{\,2}\right) \tag{6.1}$$

Bernoulli's theorem and resulting equation was initially derived to quantitate a pressure differential across a graduated narrowing in a smooth, rigid tube and is thus a model that is very different from that which represents the left ventricular outflow tract, aortic valve and proximal aorta. Even in the best of circumstances, this type of model could be expected to only partially translate to that of the intact human heart.

The modified Bernoulli equation itself and a more simplified version (Eq. 6.2), also involve assumptions that may or may not be proper in an individual patient. The modified Bernoulli equation itself arbitrarily eliminates the factors involved with viscosity and potential energy that are usually (although not always) relatively small as compared to the velocity factor in the equation. As may be seen with instances of significant pressure recovery, (covered in a subsequent chapter) elimination of factors that may impact on the calculation of gradients and create a significant error in the estimation of the true pressure gradient when using velocities across the valve.

$$\Delta P = 4v^2_{\,\text{max}} \tag{6.2}$$

In addition to the above considerations, changes in flow that are present as a result of normal variations in physiology in the individual heart will yield differences in the calculation of valve gradients using the Bernoulli equation. Increases in flow across the aortic valve as seen in high output states including anemia, hyperthyroidism and in other entities that increase flow such as significant aortic regurgitation may falsely overestimate the severity of aortic stenosis. Likewise, significant pathology that decreases flow rate such as intravascular volume depletion and mitral insufficiency will have the opposite effect. This is the case where there is left ventricular dysfunction from any cause resulting in decreased forward stroke-volume and therefore decreased flow across the aortic valve. In these situations one must resort to the use of other modalities such as dobutamine echocardiography to help in the assessment of the aortic valve gradient for this assessment. Dobutamine stress echocardiography is discussed subsequently in this text in the assessment of low flow, low gradient aortic stenosis.

Despite the above limitations and potential errors, the assessment of aortic stenosis severity by Doppler echocardiography remains the mainstay of noninvasive assessment in this disease entity [19, 20]. Subsequent discussion will discuss standard techniques for Doppler echocardiography in aortic stenosis.

Proper Doppler Flow Measurement

As described in previous chapters, generation of a tans-aortic valve gradient depends on the law of conservation of energy. The primary modality used in the assessment for the presence of, and quantification of aortic stenosis severity remains the continuous wave Doppler recording of the peak and mean gradients ΔP_{peak} and ΔP_{mean} across the aortic valve during systole. Multiple windows are used to record the highest velocities from aortic outflow during systole. The velocities recorded are then used to calculate the peak instantaneous gradient (using the peak velocity) and the mean instantaneous gradient (using the mean velocity) in the simplified Bernoulli equation where v equals the maximum jet velocity (in m/s). The assump-

tions inherent in this simplified Bernoulli formula are several, including the assumption that the velocity prior to flow through a narrowing is much less than the velocity in the narrowing (stenosis) itself and thus the velocity proximal to the stenosis is negligible. In certain situations of high flow the velocity proximal to the stenosis is not negligible, and one must estimate the pressure drop across the aortic valve using the non-simplified version (Eq. 6.1) where v_{max} equals the maximal aortic jet velocity and v_{prox} equals the peak velocity of the LVOT jet just proximal to the aortic valve. This equation is appropriate in those conditions with increased stroke volume such as in moderate to severe aortic insufficiency, high cardiac output states due to sepsis, thyrotoxicosis and anemia, or when there is a subvalvular gradient.

Depending on valvular anatomy and anatomy of the thorax, the systolic jet of aortic stenosis may be oriented in any of a number of different three-dimensional orientations. As is well known, Doppler assessment of the aortic valve gradient is dependent upon achieving a Doppler insonation angle as close to the true get orientation is possible. If the angle of insonation increases above 20 or 30° beyond the true jet orientation, the discrepancy between the true velocity and the measured velocity increases dramatically. Although the apical window will yield the maximum jet velocities in aortic stenosis most of the time, all windows including the apical, right parasternal, suprasternal and atypical windows should be imaged in the continuous wave (CW) mode and using a dedicated Doppler (Pedoff) transducer. Vmax is located outside the apical window in > 60 % of patients, and neglecting the nonapical windows results in the misclassification of AS severity in > 20 % of patients. The left ventricular to aortic root angle as measured in the parasternal long window influences the location of Vmax modestly, being far less likely in the apical window (< 20 %) if the angle is acute. The less standard left parasternal or subcostal windows may be necessary in certain individuals. Despite the best intentions and meticulous technique, angulation of the jet may lead to an underestimation of the velocity of the aortic stenotic jet and therefore in a normal rhythm, one should always use the highest measured jet (Fig. 6.10).

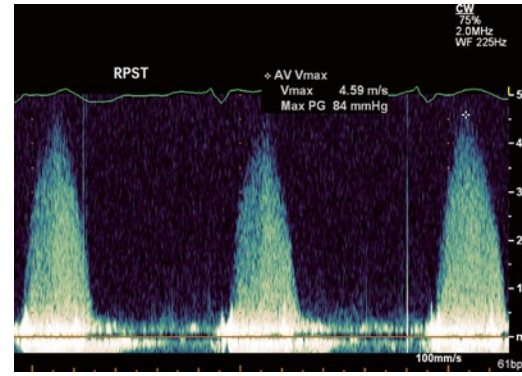

Fig. 6.10 Dedicated Doppler transducer recording from the right parasternal border (*RPST*) demonstrating peak velocity of 4.59 m/s giving a peak gradient of 84 mmHg. The recording from the apex in this same patient showed peak velocity of the aortic jet of 4.0 m/s and an estimated peak gradient of 64 mmHg, and would therefore have significantly underestimated the severity of aortic stenosis in this individual

Dysrhythmias may also be particularly problematic in determining the appropriate measurements to be used in quantitating aortic stenosis severity. With atrial fibrillation, where stroke-volume will very occasionally significantly from beat to beat, a minimum of five consecutive beats should be measured and averaged to obtain peak and mean velocities in gradients (Fig. 6.11).

The aortic stenosis spectral flow pattern is a systolic ejection flow and occurs upon opening of the aortic valve, progresses to a peak at some point during systole and ceases at the closure of the aortic valve. As this flow occurs during left ventricular ejection only, it will not be present during isovolumic ventricular contraction time (IVCT) or isovolumic ventricular relaxation time (IVRT). This fact helps differentiate the aortic stenosis flow pattern from the holosystolic flow of mitral insufficiency or tricuspid insufficiency. These latter two flow patterns, although occasionally confused with aortic stenosis due to their occurrence during systole, are holosystolic in nature. These regurgitant jets therefore begin immediately upon cessation of diastolic inflow velocities through the AV valves and continue throughout systole until, and sometimes into the next diastolic flow pattern. Careful examination of the timing of the turbulent systolic jet low pattern is necessary to avoid confusion and mistaking these jets for an aortic stenotic flow pattern (Fig. 6.12).

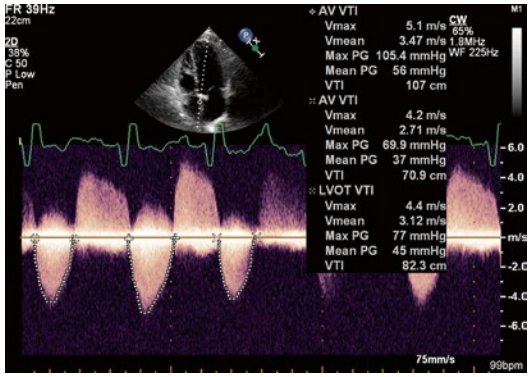

Fig. 6.11 Continuous wave Doppler recording of aortic flow as sampled from the left ventricular apical window in a patient with atrial fibrillation. Peak gradients in these three beats show a range of values from 70 to 105 mmHg with mean gradients varying from 37 to 56 mmHg. Sampling only one beat in this situation could lead to significant inaccuracies in determining the severity of stenosis in this patient

Systolic turbulence due to left ventricular outflow tract obstruction may be noted from the same windows used to interrogate the aortic valve. The continuous wave flow pattern in this pathologic entity differ from aortic stenosis in that the peak velocity of the jet tends to be in a much later part of systole and tends to be maximal in the late phase of systole and the velocity is usually negligible or very low in the early to mid-portion of systole (Fig. 6.12).

Once one is confident of the recording of an appropriate aortic stenosis spectrum via continuous wave interrogation, the peak and mean velocities should be measured. Clinical guidelines in terms of valve replacement depend heavily on the jet measurements including mean velocity, peak velocity and the calculation of valve area derived from these velocities as well as the left ventricular outflow tract velocity [17].

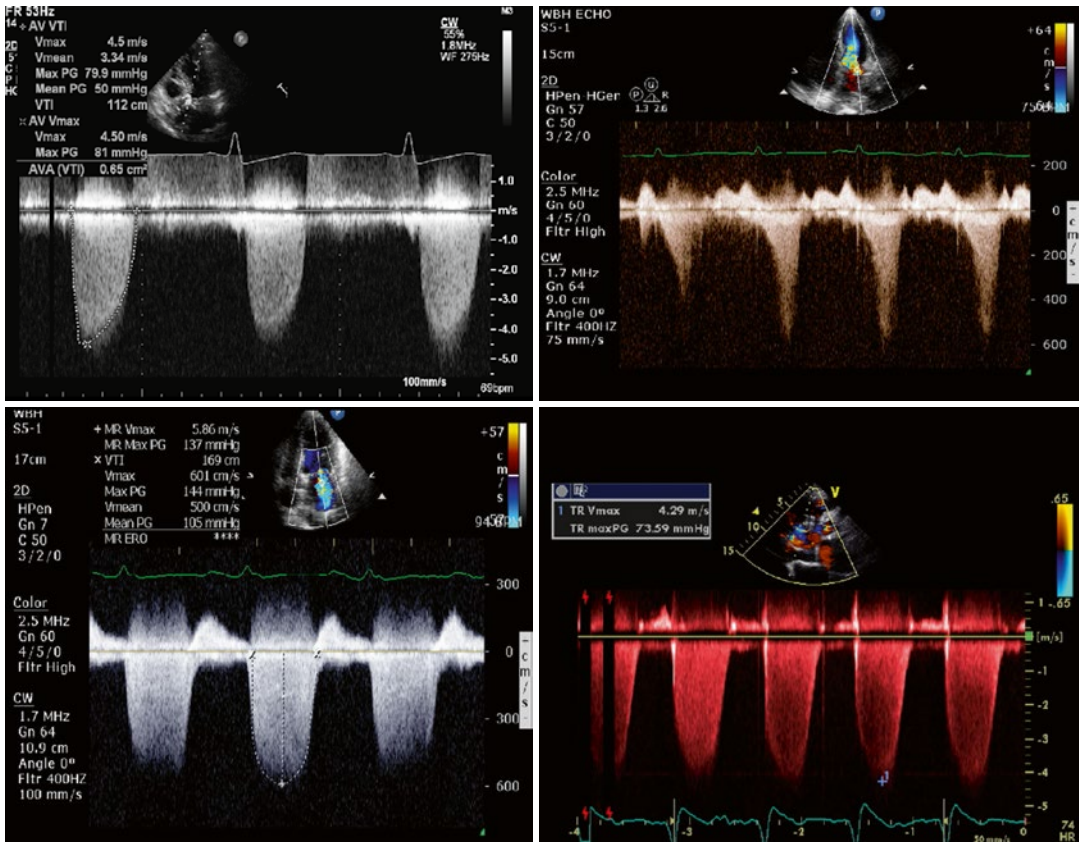

Fig. 6.12 Continuous wave Doppler recordings of aortic stenosis (*AS*) (*top left*), mitral regurgitation (*MR*) (*bottom left*), tricuspid regurgitation (*TR*) (*bottom right*) and hypertrophic cardiomyopathy with LVOT obstruction (*HOCM*) (*top right*). Note that even though the ranges of peak velocity are similar, the timing of the flow pattern can facilitate differentiation of the various flow patterns (see text)

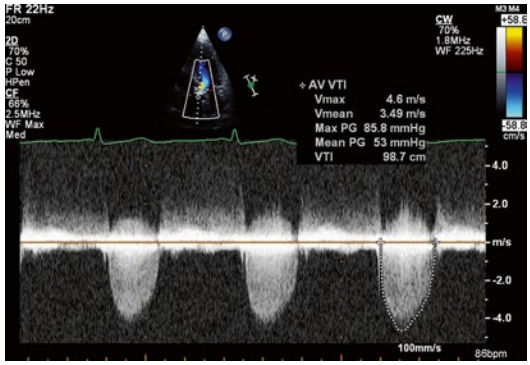

Fig. 6.13 Continuous wave Doppler spectral recording from the left ventricular apex demonstrating method of measurement in order to obtain peak and mean velocities. The spectral envelope should be traced at the clearly defined edges and without including any low intensity signals, if present

The tracing of the aortic stenosis spectrum should be taken along the outer edge of the clearly defined spectral border. Occasional ill-defined Doppler signals may be present, although not consistent with the true velocity of the jet and should not be included in the tracing as this will effect peak and mean velocity measurements (Fig. 6.13).

Continuity Equation and Effective Orifice Area

In addition to peak and mean velocities, an actual calculation of the aortic valve orifice area can be undertaken using the continuity equation. This equation is based on the principle of conservation of mass and assumes that without shunting at the level of the left ventricular outflow tract (LVOT), flow in the LVOT is equal to flow through the aortic valve. Flow in each region can be calculated by multiplying the area through which the flow is occurring by the time velocity integral (TVI), which is the distance that the flow travels during one cardiac cycle (Eq. 6.3).

$$\text{Area}_{AV} \times \text{TVI}_{AV} = \text{Area}_{LVOT} \times \text{TVI}_{LVOT} \quad (6.3)$$

The left ventricular outflow tract area, Area_{LVOT} is calculated utilizing (Eq. 6.5), where Diam_{LVOT} is the diameter of the LVOT obtained by two-dimensional imaging as described above.

$$\text{Area}_{LVOT} = \pi \left(\frac{\text{Diam}_{LVOT}}{2} \right)^2 \quad (6.4)$$

Obtaining the optimal recording of flow in the left ventricular outflow tract proximal to the AV requires meticulous technique using pulsed wave interrogation and should be measured in the apical 5 chamber view and according to EAE/ASE guidelines. This spectral recording should be taken by sampling at the same distance below the aortic valve as the recording of the left ventricular outflow tract diameter as measured in the parasternal long axis view. To avoid overestimation of left ventricular outflow tract velocities, which will underestimate the severity of aortic stenosis, one must take care to measure below the valve. This can be achieved by starting the pulsed-wave interrogation at the valve level where there is clear turbulence and moving the area of interest apically until a clear spectrum consistent with left ventricular outflow tract velocities (i.e. predominantly laminar flow) is identified. The measurement of the left ventricular outflow tract time velocity integral (TVI) should be performed by tracing within the dense portion of the spectral recording. This will give the best estimation of the true mean velocity of red blood cells in this region during systole. The peak velocity, mean velocity and the TVI are all pertinent to the quantification of aortic stenosis severity (Fig. 6.14).

Once the LVOT area is calculated, and the LVOT diameter and TVI is obtained, these values can be used in Eq. 6.5 to solve for the aortic valve area. A sample calculation with all three components of the continuity equation calculation is shown in Fig. 6.15.

$$\text{Area}_{AV} = \text{Area}_{LVOT} \frac{\text{TVI}_{LVOT}}{\text{TVI}_{AV}} \quad (6.5)$$

The measurements noted above, including the peak aortic valve velocity obtained by CW measurement, the mean gradient from the AV velocity, and the aortic valve area as calculated from the continuity equation are the measures that have been most correlated with

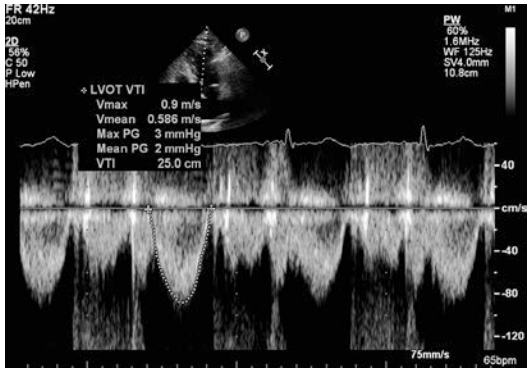

Fig. 6.14 Pulsed wave Doppler recording from the apical 5-chamber view with sample volume placed just below the turbulent flow as it accelerates to become transaortic flow. Tracing of this spectral recording is shown with measurement of velocities obtained by tracing along the dense portion of the LVOT velocity envelope and excluding the low intensity signals on the outer edges of the spectrum

clinical outcomes. These measurements are therefore most commonly used in making decisions regarding timing of valve replacement.

Pulmonary Hypertension

With long-standing aortic stenosis and with the changes in left ventricular function noted above, it is not uncommon for individuals with AS to develop significant pulmonary hypertension [10, 11]. Secondary findings of pulmonary hypertension involving right ventricular hypertrophy and/or enlargement or a dilated right atrium may therefore be noted in these individual patients.

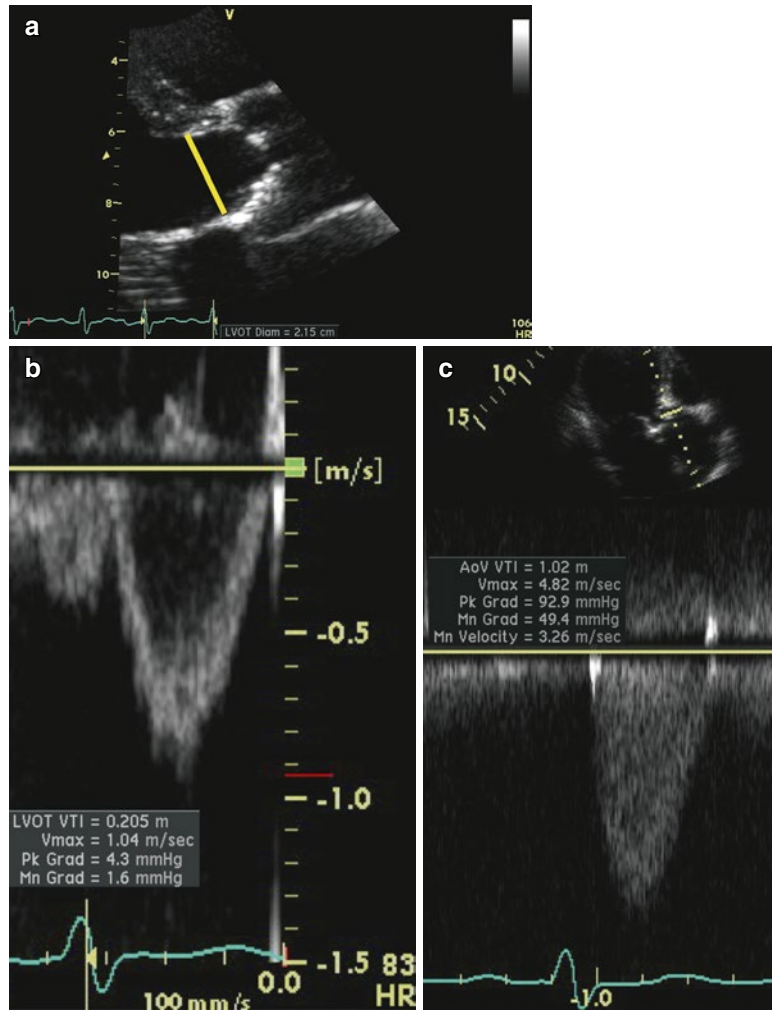

Fig. 6.15 Echocardiographic information used in the calculation of aortic valve area (*AVA*) using the continuity equation. Panel (**a**) is the recording of the LVOT diameter and panel (**b**) the LVOT Doppler flow pattern with measurement of velocities. Panel (**c**) shows the aortic stenosis jet velocity by CW and the tracing of the spectrum. The calculated AVA is seen to be 0.73 cm^2 once all required measurements are completed

Additional Echocardiographic Measurements of Aortic Stenosis Severity

Aortic valve resistance: The calculation of aortic valve resistance derives from Ohm's law and is represented by (Eq. 6.6). In this equation, ΔP_{mean} is the mean pressure across the aortic valve as assessed by Doppler interrogation of the aortic valve and $Flow_{mean}$ is the mean flow during systole. Aortic valve resistance has been documented to have prognostic value and is an independent factor in quantitating the severity of outflow obstruction [21, 22]. This value may not be necessarily additive beyond the above-mentioned standard measurements of aortic valve flow in the average individual.

$$\text{Resistance}_{AV} = \left(\frac{\Delta P_{mean}}{Flow_{mean}} \right) \times 1333 \quad (6.6)$$

Valvuloarterial impedance: Abbreviated as Z_{va}, is a measurement used to estimate global afterload experienced by the left ventricle which may help predict subsequent left ventricular dysfunction [23]. Conceptually, this is similar to the aortic valve resistance calculation noted above, however this calculation also takes into account left ventricular afterload that occurs as a result of systemic resistance (Eq. 6.7). In situations of relatively normal blood pressure and vascular resistance, this measurement will correlate well with the severity of aortic valve obstruction, despite variations in flow. This objective measurement may be particularly useful in suspected paradoxical low-flow, low gradient aortic stenosis. However, the data is controversial.

$$Z_{VA} = \frac{LVSP}{SVI} = \frac{SAP + AVGrad_{mean}}{SVI} \quad (6.7)$$

Energy loss index: The measurement of energy loss index may be helpful in patients who are not symptomatic from aortic stenosis, particularly in the situation where gradients are suspected to be overestimated due to pressure recovery. Bahlman et al. reviewed a large group of patients from the Simvastatin and Eztimibe in Aortic Stenosis (SEAS) study and found benefit for using this measurement of energy loss across a stenotic aortic valve [24]. The measurement is as noted in the Eq. 6.8. A value less than 0.6 cm^2/m^2 is considered consistent with severe aortic stenosis. The individuals with more significant energy loss index in this study experienced higher rates of hospitalization for heart failure and total mortality, however this measurement still needs to be evaluated as an independent predictor of events separate from the more accepted measurements of mean gradient and aortic valve area as previously documented. This measurement however may be particularly useful in patients with small aortic roots were the gradient is suspected to be overestimated due to pressure recovery [25].

$$ELI = \left(AVA \times A_a\right) / \left(A_a - AVA\right) / BSA \quad (6.8)$$

Where A_a is the area of the aorta at the sinotubular junction and AVA is the calculated aortic valve area by the continuity equation.

Other measurements including stroke work loss index and projected valve area at a normal flow rate can be used in situations of suspected low-flow, low gradient aortic stenosis [26, 27]. The calculations derived from these methods will be more thoroughly covered in subsequent chapters.

Though additional measurements in the assessment of aortic stenosis may be useful in selected circumstances, as noted in the recommendations of the European Association of echocardiography (EAE), and the American Society of echocardiography (ASE), the aortic stenosis jet velocity, the mean gradient and the aortic valve area calculated by the continuity equation remain the most reliable measurements in the vast majority of patients (see Table 6.1).

Three-Dimensional Imaging and Aortic Stenosis

Three-dimensional (3D) imaging has become an important adjunct both in the assessment of cardiac function including right and left ventricular, as well as valvular function, particularly the mitral valve. The aortic valve area can be measured using three-dimensional imaging as well as

Table 6.1 Measures of aortic stenosis severity

Measure	Formula	Cut off for severe	Advantages	Disadvantages
AS jet velocity [1]	Direct measure	4.0 m/s	Direct measurement Strongest predictor of clinical outcome	Requires parallel alignment of ultrasound beam Flow dependent
Mean gradient [1]	$\overline{\Delta P} = \sum 4v^2 / N$	40 or 50 mmHG	Mean gradient is averaged from the velocity curve Units comparable to invasive measurements	Accurate pressure gradients depend on accurate velocity data Flow dependant
Continuity equation for aortic valve area [1]	$\text{Area}_{AV} = \text{Area}_{LVOT} \frac{\text{TVI}_{LVOT}}{\text{TVI}_{AV}}$	1.0 cm^2	Measures effective orifice area Feasible in nearly all patients Relatively flow independent	Requires LVOT diameter and flow velocity data, along with aortic velocity. Measurement error more likely
Velocity ratio [2]	$VR = \frac{V_{LVOT}}{V_{AV}}$	0.25	Doppler-only method. No need to measure LVOT diameter Less variability than continuity equation	Limited longitudinal data. Ignores LVOT size and variability beyond patient size variability
Planimetry of anatomic valve area [2]	TTE, TEE, 3D echo	1.0 cm^2	Useful if Doppler measurements are unavailable	Difficult with severe valve calcification Contraction coefficient (anatomic/effective valve area) may be variable
Energy loss index [3]	$ELI = (AVA \times A_a) / A_a - (AVA / BSA)$	0.5 cm^2/m^2	Most exact measurement of AS in terms of flow dynamics Increased prognostic value in some studies	Introduces complexity and variability related to the measurement of the ascending aorta No advantage over standard methods

Valvulo-arterial impedance [3]	$Z_{VA} = \frac{SAP + AVGrad_{mean}}{SVI}$	>5.0 mmHG/ml/m^2	Integrates information on arterial load to the hemodynamic burden of AS	Only takes into account the static (mean) component of impedance. Longitudinal prospective data is lacking
Aortic valve resistance [3]	$Resistance_{AV} = \left(\frac{DP_{mean}}{Flow_{mean}} \right) \times 1333$	280 dyn/s/cm^{-5}	Less flow dependant than standard measurements though not entirely independent	Limited prognostic value Unrealistic mathematic modeling of flow-dynamics of AS

Recommendations for clinical application: (1) appropriate in all patients with AS (non-shaded); (2) reasonable when additional information is needed in selected patients (light shade areas), and (3) not recommended for routine clinical use (darker shaded areas) (Adapted from Baumgartner et al. [17] with permission)

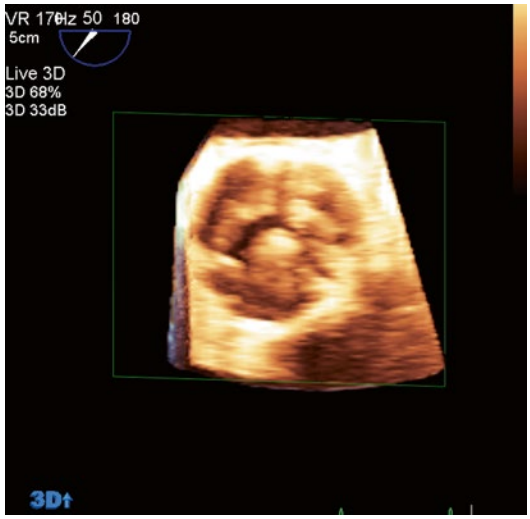

Fig. 6.16 Three-dimensional image of a stenotic aortic valve as seen from the aortic side of the valve during mid-systole. The valve orifice can be clearly identified and a planimetry measurement could feasibly be obtained from this type of image. The thickening of the leaflets can be appreciated

two-dimensional imaging as noted above, however the limitations are similar (i.e. valve calcification and the resultant artifacts) Nonetheless, aortic valve area measurement by planimetry can be obtained in selected individuals (Fig. 6.16).

With the advent of percutaneous transvalvular aortic valve replacement (TAVR), the assessment of the aortic valve annulus size has become a crucial measurement. This measurement is often times performed using CT angiography, however studies have shown a close correlation using three-dimensional echocardiographic measurement, with the ability to avoid increased radiation and contrast exposure.

The methodology to measure the aortic valve annulus by three-dimensional imaging involves obtaining a data set that includes the entire annulus as well as surrounding structures to allow for appropriate orientation of the image and to make sure that the entire annulus has been captured in the data sent.

Once the above data set is obtained it is manipulated to obtain a plane that is parallel to the aortic annulus. The plane is then adjusted either apically or toward the aorta to a plane that completely intersects the aortic annulus. This will most commonly generate an ovoid annulus, which can then be traced using off-label application of the current software. During this analysis, the presence, extent and distribution of calcium in the leaflets and annulus can be identified and should be noted. Extensive calcification, particularly if asymmetric and at the leaflet bases and annulus (i.e. the "landing zone" for transcutaneous aortic valve replacement (TAVR), may correlate with the presence of paravalvular leak following percutaneous TAVR procedures and also has clinical relevance to the surgeon performing aortic valve replacement whether by sternotomy or minimally invasive valve technique [28].

The above described technique used in annulus measurement by three-dimensional echo is similar to that reported by Jilaihawi et al. (Fig. 6.17) utilizes concepts similar to that use with computed tomography (CT) angiography, in that a plane perpendicular to the left ventricular outflow tract and in the same plane as the aortic annulus is adjusted using offline software to obtain a plane through the annulus itself. The annulus is then traced to obtain maximum and minimum diameters, circumference and annular area [29]. This technique yields results that correlate well with the measurements obtained by CT.

A second method that utilizes the same methods for collecting three-dimensional data, employs a different application of software originally designed to measure the mitral annulus and arrives at the same endpoints in terms of measurements of aortic annular area, circumference, minimum and maximum annular diameter (Fig. 6.18) [30]. In this situation, one again uses a three-dimensional dataset and with the referenced software. By rotating through the annulus, points along the aortic annulus are marked and the computer then constructs a three-dimensional model of the annulus complete with major and minor axes, circumference and area.

It is important to note that the techniques described above are, as mentioned, not standard measurements designed specifically for aortic annulus measurements. Once such applications are available these three dimensional measurements should become more straightforward.

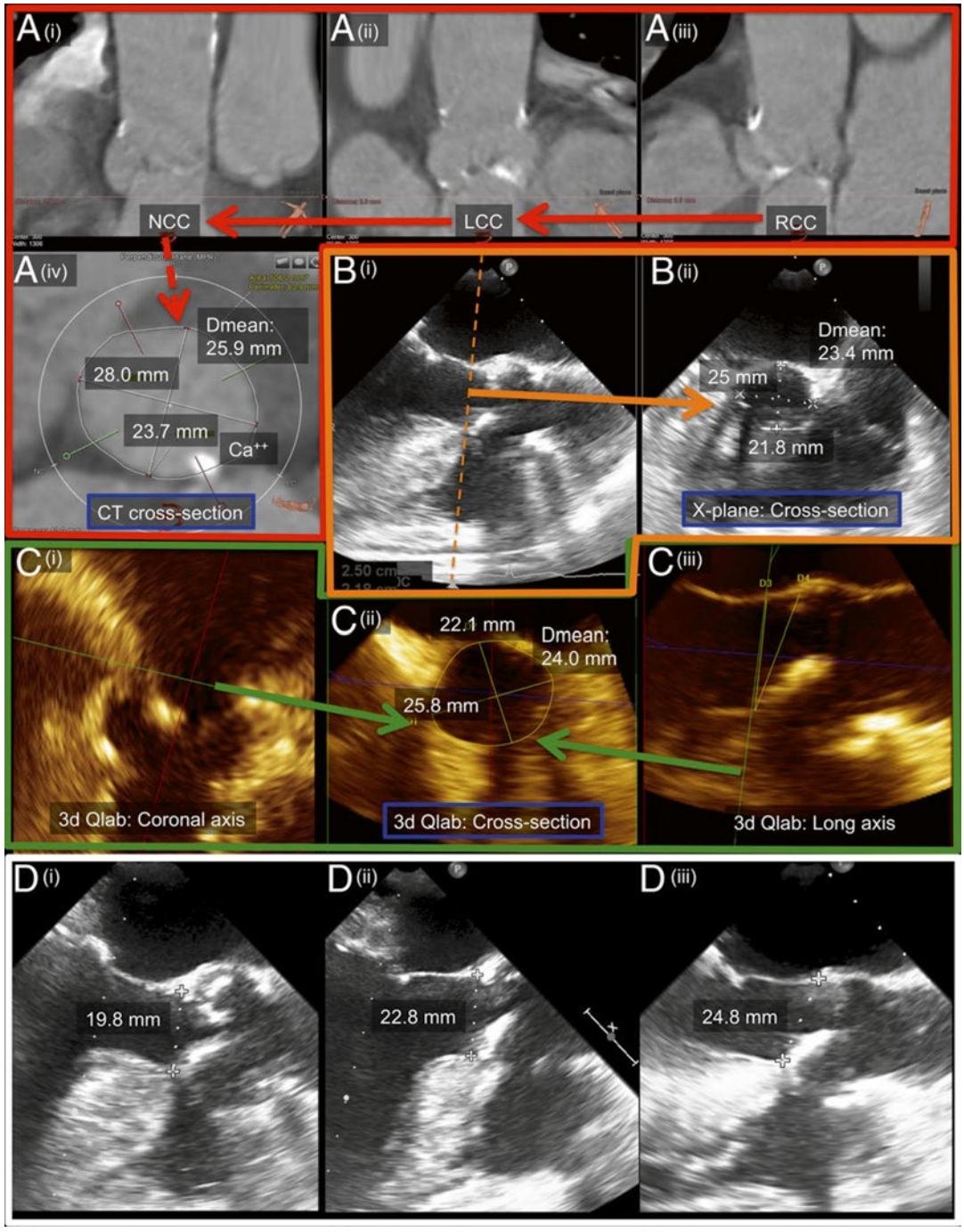

Fig. 6.17 Technique for measuring aortic annulus using cross sectional imaging. Measurements by (**a**) computed tomography (*CT*), (**b**) X-Plane transesophageal echocardiography, (**c**) QLab (Philips Ultrasound, Bothell, Washington), and (**d**) demonstrating variability of measurements by conventional hinge-point to hinge-point two-dimensional transesophageal echocardiography (From Jilaihawi et al. [29] with permission)

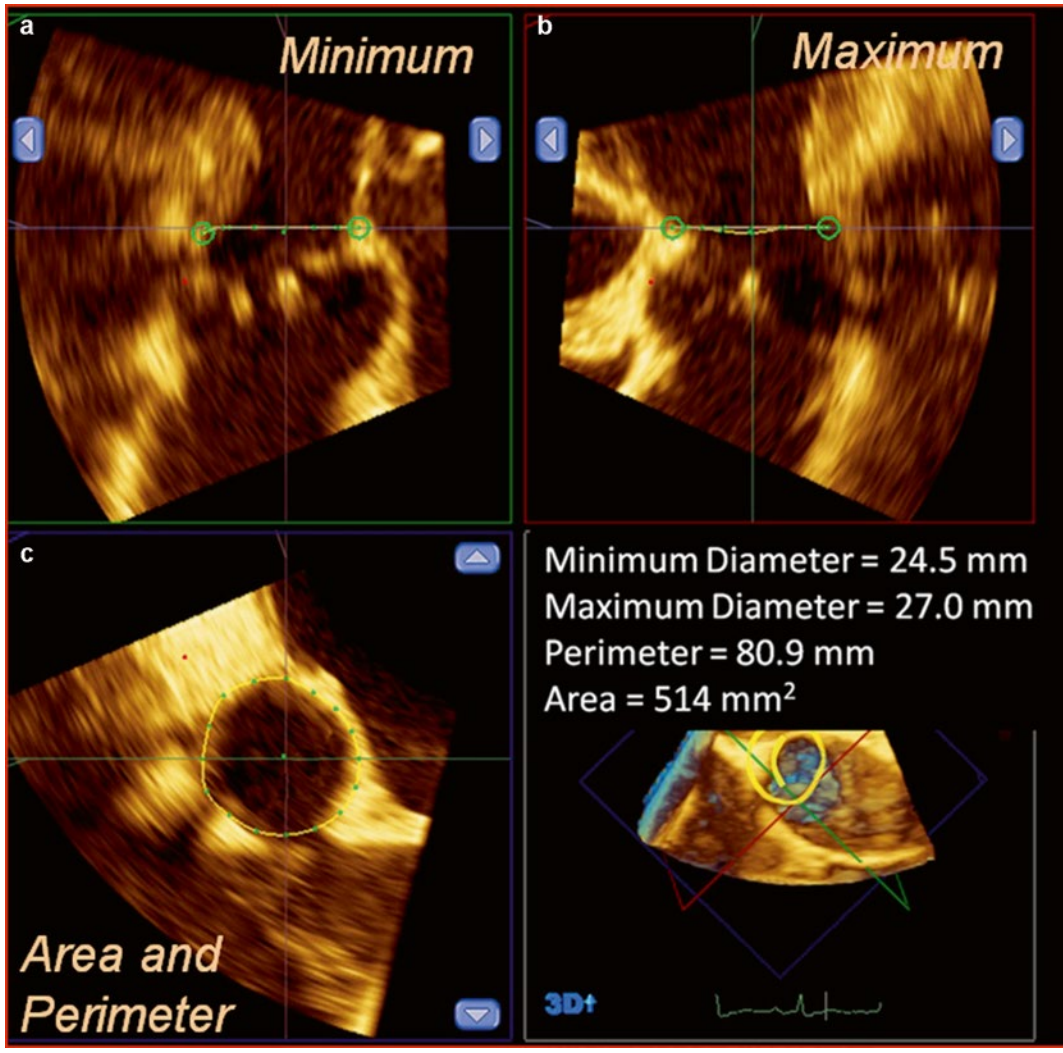

Fig. 6.18 Multiplanar reconstruction of the aortic annulus using off-label vendor specific analysis package. (See text for details) (From Hahn et al. [28] with permission). (**a**) Reveals minimum annular dimension, (**b**) reveals maximum annular dimension, and (**c**) reveals annular area and perimeter

Conclusions

Aortic stenosis is a common clinical entity, especially in an aging population. This valvular disease behaves in a progressive manner. Although occasionally predictable with time in terms of progression, the time course varies greatly from individual to individual. In the majority of individuals gradients can be accurately and reproducibly measured by catheterization, although the preferred method remains noninvasive assessment and quantitation by echocardiography. This noninvasive measurement requires meticulous attention to technique, which in turn requires time, patience and adherence to measurement guidelines. An experienced sonographer and astute echocardiographer will incorporate all clinical and echocardiographic data to create an accurate, reproducible and meaningful result for each individual patient.

References

1. Manning W. Asymptomatic aortic stenosis in the elderly: a clinical review. JAMA. 2013;310(14):1490–7.
2. Bahler R, Desser D, Finkelhor R, Brener S, Youssefi M. Factors leading to progression of valvular aortic stenosis. Am J Cardiol. 1999;84(9):1044–8.
3. Bhattacharyya S, Hayward C, Pepper J, Senior R. Risk stratification in asymptomatic severe aortic stenosis: a critical appraisal. Eur Heart J. 2012;33(19):2377–87.
4. Seiler C, Jenni R. Severe aortic stenosis without left ventricular hypertrophy: prevalence, predictors, and short-term follow up after aortic valve replacement. Heart. 1996;76(3):250–5.
5. Stewart R, Kerr A. Left ventricular systolic and diastolic function assessed by tissue Doppler imaging and outcomes in asymptomatic aortic stenosis. Eur Heart J. 2010;31:2216–22.
6. Dalsgaard M, Egstrup K, Wachtell K, Gerdts E, Cramariuc D, Kjaergaard J, Hassager C. Left atrial volume in patients with asymptomatic aortic valve stenosis (the Simvastatin and Ezetimibe in Aortic Stenosis study). Am J Cardiol. 2008;101(7): 1030–4.
7. Casaclang-Verzosa G, Malouf J, Scott C, Juracan E, Nishimura R, Pellikka P. Does left atrial size predict mortality in asymptomatic patients with severe aortic stenosis? Echocardiography. 2010;27(2):105–9.
8. Caballero-Borrego J, G'Omez-Doblas J, Cabrera-Bueno F, Garc'Ia-Pinilla J, Melero J, Porras C, Olalla E, Galv'An E. Incidence, associated factors and evolution of non-severe functional mitral regurgitation in patients with severe aortic stenosis undergoing aortic valve replacement. Eur J Cardiothorac Surg. 2008;34(1):62–6.
9. Toggweiler S, Boone R, Rod'Es-Cabau J, Humphries K, Lee M, Nombela-Franco L, Bagur R, Willson A, Binder R, Gurvitch R, et al. Transcatheter aortic valve replacement: outcomes of patients with moderate or severe mitral regurgitation. J Am Coll Cardiol. 2012;59(23): 2068–74.
10. Kapoor N, Varadarajan P, Pai R. Echocardiographic predictors of pulmonary hypertension in patients with severe aortic stenosis. Eur J Echocardiogr. 2008;9(1): 31–3.
11. Malouf J, Enriquez-Sarano M, Pellikka P, Oh J, Bailey K, Chrasekaran K, Mullany C, Tajik A. Severe pulmonary hypertension in patients with severe aortic valve stenosis: clinical profile and prognostic implications. J Am Coll Cardiol. 2002;40(4):789–95.
12. Ross Jr J, Braunwald E. Aortic stenosis. Circulation. 1968;38(1S5):V61–7.
13. Vahanian A, Otto C. Risk stratification of patients with aortic stenosis. Eur Heart J. 2010;31(4):416–23.
14. John D, Buellesfeld L, Yuecel S, Mueller R, Latsios G, Beucher H, Gerckens U, Grube E. Correlation of device landing zone calcification and acute procedural success in patients undergoing transcatheter aortic valve implantations with the self-expanding CoreValve prosthesis. JACC Cardiovasc Interv. 2010;3(2):233–43.
15. Okura H, Yoshida K, Hozumi T, Akasaka T, Yoshikawa J. Planimetry and transthoracic two-dimensional echocardiography in noninvasive assessment of aortic valve area in patients with valvular aortic stenosis. J Am Coll Cardiol. 1997;30(3):753–9.
16. Bernard Y, Meneveau N, Vuillemenot A, Magnin D, Anguenot T, Schiele F, Bass. Planimetry of aortic valve area using multiplane transoesophageal echocardiography is not a reliable method for assessing severity of aortic stenosis. Heart. 1997;78(1):68–73.
17. Baumgartner H, Hung J, Bermejo J, Chambers J, Evangelista A, Griffin B, Iung B, Otto C, Pellikka P, Qui~Nones M. Echocardiographic assessment of valve stenosis: EAE/ASE recommendations for clinical practice. Eur J Echocardiogr. 2009;10(1):1–25.
18. Hatle L, Angelsen B, Tromsdal A. Non-invasive assessment of aortic stenosis by Doppler ultrasound. Br Heart J. 1980;43(3):284–92.
19. Hegrenaes L, Hatle L. Aortic stenosis in adults. Noninvasive estimation of pressure differences by continuous wave Doppler echocardiography. Br Heart J. 1985;54(4):396–404.
20. Popovic A, Stewart W. Echocardiographic evaluation of valvular stenosis: the gold standard for the next millennium? Echocardiography. 2001;18(1):59–63.
21. Ford L, Feldman T, Chiu YC, Carroll JD. Hemodynamic resistance as a measure of functional impairment in aortic valvular stenosis. Circ Res. 1990;66(1):1–7.
22. Mascherbauer J, Schima H, Rosenhek R, Czerny M, et al. Value and limitations of aortic valve resistance with particular consideration of low flow– low gradient aortic stenosis: an in vitro study. Eur Heart J. 2004;25(9):787–93.
23. Hachicha Z, Dumesnil J, Pibarot P. Usefulness of the valvuloarterial impedance to predict adverse outcome in asymptomatic aortic stenosis. J Am Coll Cardiol. 2009;54(11):1003–11.
24. Bahlmann E, Gerdts E, Cramariuc D, Gohlke-Baerwolf C, Nienaber C, Wachtell K, Seifert R, Chambers J, Kuck K, Ray S. Prognostic value of energy loss index in asymptomatic aortic stenosis clinical perspective. Circulation. 2013;127(10):1149–56.
25. Garcia D, Pibarot P, Dumesnil J, Sakr F, Dur. Assessment of aortic valve stenosis severity a new index based on the energy loss concept. Circulation. 2000;101(7):765–71.
26. Sprigings D, Chambers J, Cochrane T, Allen J, Jackson G. Ventricular stroke work loss: validation of a method of quantifying the severity of aortic stenosis and derivation of an orifice formula. J Am Coll Cardiol. 1990;16(7):1608–14.
27. Blais C, Burwash IG, Mundigler G, Dumesinil JG, Loho N, Rader F, et al. Projected valve area at normal flow rate improves the assessment of stenosis severity in patients with low-flow, low-gradient aortic stenosis: the multicenter TOPAS (truly or pseudo-severe aortic stenosis) study. Circulation. 2006;113:711–21.
28. Hahn R, Khalique O, Williams M, Koss E, Paradis J, Daneault B, Kirtane A, George I, Leon M, Kodali S. Predicting paravalvular regurgitation following

transcatheter valve replacement: utility of a novel method for three-dimensional echocardiographic measurements of the aortic annulus. J Am Soc Echocardiogr. 2013;26(9):1043–52.
29. Jilaihawi H, Doctor N, Kashif M, Chakravarty T, Rafique A, Makar M, Furugen A, Nakamura M, Mirocha J, Gheorghiu M, et al. Aortic annular sizing for transcatheter aortic valve replacement using cross-sectional 3-dimensional transesophageal echocardiography. J Am Coll Cardiol. 2013;61(9):908–16.
30. Muraru D, Badano L, Vannan M, Iliceto S. Assessment of aortic valve complex by three-dimensional echocardiography: a framework for its effective application in clinical practice. Eur Heart J Cardiovasc Imaging. 2012;13(7):541–55.
31. Otto CM, Burwash IG, Legget ME, et al. Prospective study of asymptomatic valvular aortic stenosis: clinical, echocardiographical, and exercise predictors of outcome. Circulation. 1997;95: 2262–70.

Complimentary Role of CT/MRI in the Assessment of Aortic Stenosis

7

A. Neil Bilolikar and Gilbert L. Raff

Abstract

Cardiac magnetic resonance imaging (CMR) and cardiac computed tomography (CT) have specific advantages and disadvantages that supplement, but do not supplant echocardiography as the major imaging modality used for management of patients with aortic stenosis (AS). In general, CMR provides more complete physiologic information than CT, but CT angiography has broader general applicability, as it is now frequently used for coronary angiography and is a main tool in pre-procedural planning and valve sizing for transcutaneous aortic valve replacement (TAVR).

One major impediment to more pervasive use of these tests is the lack available equipment and expertise in many centers. In addition, there are application-specific intrinsic limitations, which we will delineate, that allow echocardiography to remain the mainstay of diagnosis of severe AS. However, specific advantages may make these techniques uniquely advantageous in select patients with inconclusive diagnosis. In this chapter we will review the incremental role of cardiac MRI and CTA in patients with aortic stenosis.

Keywords

Cardiac magnetic resonance imaging (CMR) and aortic stenosis • Cardiac computed tomography (CT) and aortic stenosis • CMR angiography • Transcutaneous aortic valve replacement (TAVR) • Multimodality imaging for aortic stenosis

Introduction

Cardiac magnetic resonance imaging (CMR) and cardiac computed tomography (CT) have specific advantages and disadvantages that supplement, but do not supplant echocardiography as the major imaging modality used for management of

A.N. Bilolikar, MD (✉) • G.L. Raff, MD, FACC, FSCCT
Department of Cardiovascular Medicine,
Beaumont Health, Oakland University/William
Beaumont School of Medicine, Royal Oak, MI, USA
e-mail: abhay.bilolikar@beaumont.edu

A.E. Abbas (ed.), *Aortic Stenosis: Case-Based Diagnosis and Therapy*,
DOI 10.1007/978-1-4471-5242-2_7

patients with aortic stenosis (AS). In general, CMR provides more complete physiologic information than CT, but CT angiography has broader general applicability, as it is now frequently used for coronary angiography and is a main tool in pre-procedural planning and valve sizing for transcutaneous aortic valve replacement (TAVR).

One major impediment to more pervasive use of these tests is the lack available equipment and expertise in many centers. In addition, there are application-specific intrinsic limitations, which we will delineate, that allow echocardiography to remain the mainstay of diagnosis of severe AS. However, specific advantages may make these techniques uniquely advantageous in select patients with inconclusive diagnosis. In this chapter we will review the incremental role of cardiac MRI and CTA in patients with aortic stenosis.

Cardiac Magnetic Resonance Imaging in Aortic Stenosis

Cardiac MRI at experienced centers potentially can provide complete diagnostic information for management of patients with AS including virtually all data routinely acquired by echocardiography.

MRI Modalities Utilized in Patients with Aortic Stenosis (Tables 7.1a and 7.1b)

- CMR angiography
- Cine MRI
- Tissue characterization protocols: Delayed contrast enhancement and tissue T1/T2 mapping
- Velocity encoded flow measures

Certain facets of CMR examinations are robust and routine, such as *valve planimetry*, *ventricular functional analysis,* and *measurement of aortic flow* [1–4] (Tables 7.1a and 7.1b). Nevertheless, while in general the data obtained is more complete, the process of acquisition is more technically demanding and time consuming. Thus, echocardiography remains the diagnostic mainstay except in particular circumstances, for example, when poor echocardiographic windows impede adequate visualization,

Table 7.1a Applications of cardiac MRI in aortic stenosis

1. **CMR angiography:** Aortic root morphology including ectasia, aneurysm, coarctation, and potentially planning access for transaortic TAVR
2. **Cine MRI**
(a) **Planimetry of aortic valve geometric area**
(b) Native valve morphology
(i) Leaflet/cusp anatomy
(ii) Endocarditis
1. Vegetations
2. Septic aneurysms
(c) Prosthetic valve morphology
(d) Visualization of stenotic outflow jet direction and pattern
(e) Visualization of associated regurgitation flow pattern and volume
(f) Chamber function and morphology
(i) Stroke volume/stroke volume index
(ii) Ejection fraction
(iii) Global/regional wall motion
(iv) Myocardial hypertrophy
(v) Myocardial mass
(vi) True LVOT area assessment
(g) Chamber morphology
(i) Hypertrophic patterns
(ii) Septic aneurysms; other acquired disorders
(h) Congenital anomalies
(i) Associated chamber/vascular anomalies
3. **Tissue characterization**
(a) Delayed contrast enhancement
(i) Infarction
(ii) Focal fibrosis
(b) Tissue T1/T2 mapping
(i) Diffuse fibrosis
(ii) Myocardial edema
4. **Velocity encoded flow**
(a) Aorta/pulmonary artery
(i) Stroke volume
(ii) Shunt flow
(iii) Aortic regurgitant volume
(iv) Mitral regurgitant volume
(b) **Trans-aortic valvular gradient**
(c) Congenital anomalies
(d) **Assessment of an effective orifice area (application of the continuity equation)**

Table 7.1b Limitations of cardiac MRI in aortic stenosis

1. Nephrogenic systemic fibrosis: in patients with renal insufficiency
2. Claustrophobia
3. **Cine MRI**
(a) Native valve morphology
(i) Low spatial/temporal resolution of vegetations, calcification
(b) Prosthetic valve morphology
(i) Metal artifacts
4. **Tissue characterization**
(e) Delayed contrast enhancement
(i) Artifacts due to patient noncooperation
(ii) Difficulty in diffuse fibrosis
(f) Tissue T1/T2 mapping
(i) Technically demanding
5. **Velocity encoded flow**
(a) Technically demanding for gradient measurement

when there is discrepant invasive and non-invasive data, or when there is area/gradient mismatch or discordance.

Indications

Aortic Morphology

The most common indication for referral of patients with severe AS to CMR after echocardiography is to define aortic morphology and to exclude aortic aneurysms in patients with bicuspid aortic valves. This is generally done by CMR angiography, but can be done with non-contrast cine CMR if renal dysfunction is significant. A related indication is the exclusion of additional pathology such as coarctation or aneurysm of the aorta or other vascular pathology, which is easily accomplished using CMR as it provides detailed imaging of all intrathoracic contents. Body habitus and the presence of intercurrent pathology such as chronic obstructive pulmonary disease do not degrade imaging as long as patients can cooperate with breath-holding instructions. A further requirement for cine MRI, is that patients have a stable cardiac rhythm with no frequent ectopy or rapid atrial fibrillation as this degrades image quality; however, this is not essential for aortic evaluation by CMR angiography.

Discrepant Diagnostic Data on Severity of Aortic Stenosis and Morphology of the Aortic Valve

The next most common indication is the broad category of discrepant diagnostic information from echocardiography, physical examination and/or cardiac catheterization. In particular, direct planimetry of aortic valve area (AVA), and complete morphologic visualization of aortic valve geometry in multiple oblique planes can resolve many clinical issues. In this context, CMR has become the gold standard for quantitative evaluation of chamber morphology and myocardial function, allowing very accurate assessment of stroke volume as long as mitral regurgitation is not a significant coincident problem [5–10]. Even in such cases, velocity encoded CMR (VENC) imaging, which provides analogous information to Doppler echocardiography and cardiac catheterization [11], can provide estimates of aortic or mitral regurgitant volume when needed to help determine the net forward cardiac output. Evaluation of the relatively laminar flow in the aorta and left ventricular outflow tract is very reliable in quantifying stroke volume and regurgitant volume [7–9]. However, determination of valve gradients is generally extremely technically demanding in comparison to echocardiography, for two reasons. First, very small changes in the direction of evaluation are easily accomplished by an experienced echocardiographer with a hand held probe, while each change in VENC imaging requires a separate breath-hold imaging sequence which can be very time consuming, on the order of 1–2 min of additional time per sequence acquisition [2, 3]. In addition, turbulent flow induces magnetic currents that change the velocity encoded flow rate. Thus, CMR gradient measurements are generally not robust enough to be decisive. Additional valuable information about the direction and pattern of high velocity outflow into the aorta downstream from the valve can be defined from cine CMR and velocity encoded imaging. Recent publications have confirmed the influence of angulated jets in affecting the degree of pressure recovery [12–14]. Based on in-vitro experiments and a limited number of patient studies, recent publications explain the discrepancy

between relatively large geometric valve area and high gradients frequently seen in bicuspid aortic valves (reverse area gradient mismatch), and have provided quantitative formulas to calculate pressure recovery from aortic size and flow angulation in the proximal aorta [12–16].

Assessment of Ventricular Function

Further relevant information from chamber morphology and function is often useful in patients with area/gradient mismatch as low-flow low-gradient physiology with normal or reduced ejection fraction (EF). The volume of the left ventricle and stroke volume is vital in assessing the hemodynamics of these patients and recent studies affirm the valuable accuracy CMR can provide in such cases. Further evidence that may be helpful in decision-making includes the degree of hypertrophy, fibrosis and elevated left ventricle mass that may confirm evidence of elevated left ventricular hemodynamic load, and chronic severe resistance to left ventricular outflow which portends a worse prognosis longer term for such patients [17–19]. Specific techniques such as delayed gadolinium contrast enhancement may reveal prior infarction or focal myocardial fibrosis that may mediate previously confusing symptomatology. In some cases the new technique of T1 or T2 quantitative mapping provide evidence of diffuse fibrosis that is not clearly revealed by traditional delayed enhancement. At this point a limited number of specialized centers have access to such technology but this is rapidly becoming a routine method. In LF/LG and NF/LG patients, MRI demonstrates larger AVA, less LVH, and similar focal fibrosis to LF/HG AS. This challenges the notion of the more advanced disease of the LF/LG AS patients.

Assessment of Paravalvular Obstruction, Associated Aortic Regurgitation, and Congenital Anomalies

Secondary causes of elevated left ventricular pressure such as intra-ventricular gradients from hypertrophic cardiomyopathy or subvalvular membranes that were missed on echocardiography may be revealed by CMR. In certain cases associated congenital anomalies that are occult or difficult to diagnose without access to thoracic angiography also may be revealed. MRI has become an integral part of evaluation of patients with HOCM for diagnostic, prognostic, and therapeutic considerations. It also can provide quantitative methods for assessment of concomitant aortic valve regurgitation as regurgitant volumes and ratios.

Cardiac Computed Tomography in Aortic Stenosis

CT coronary angiography is the most commonly used advanced imaging technique in patients with chest pain presenting to the emergency room. It has also become an integral part of standard pre-operative and pre-trans catheter valve replacement evaluation.

Indications

Assessment of Coronary Anatomy and Coronary Artery Disease

In native aortic stenosis, it frequently may obviate the need for preoperative invasive coronary angiography, particularly in younger patients with the congenital form of valvular aortic stenosis, bicuspid or unicuspid aortic valves, and subvalvular membrane. However, patients over 65 years old with calcific aortic stenosis or patients who have known prior infarction, and prior coronary bypass grafting or intracoronary stenting are unlikely to benefit from coronary CTA and will require invasive coronary angiography.

Pre SAVR and Pre-TAVR Evaluation by CT Aortography

CT is the state-of-art test for pre surgical and pre transcutaneous evaluation for aortic valve replacement. End-systolic measurement of the aortic annulus dimension and determination of calcification in the aortic valve, aortic root, LVOT, and ascending aorta calcification is also standard for potential TAVR patients, as is measurement of coronary height above the annulus. For potential trans-femoral TAVR patients, analysis of the distal aorto-iliac system and common femoral arteries is a required for size, tortuosity, and calcification. Lastly, assessment of the chest

wall morphology, rib site access for transaortic and trans-apical TAVR patients and prior to minimally invasive SAVR is also possible by CT. This will be discussed later in a separate chapter in more detail.

Aortic Morphology

Similar to MRI and MRA, CT and CTA can provide further assessment of the ascending aorta morphology for coarctation, aneurysm, and other vascular pathologies. Septic aneurysm visualization is equally accurate compared with CMR and trans-esophageal echocardiography and superior to TTE.

Discrepant Diagnostic Data on Severity of Aortic Stenosis and Aortic Valve Morphology

Evaluation of aortic valve leaflet and cusp morphology is very accurate with CT; however, detection of vegetations is much less sensitive than with trans-esophageal echocardiography. Interestingly, CTA may have clinical utility in patients with prosthetic heart valves in aiding to detect valvular vegetations when transthoracic echocardiography (TTE) and transesophageal echocardiography (TEE) were unsuccessful [20].

Planimetry of aortic valve area at mid-systole can provide confirmation of geometric valve area (GOA) [21–23]. By contrast, CT does not provide effective orifice valve area, as velocity measurements are not possible with current CT methods. Direct measurement of the LVOT area by CT scan and substituting that into the Doppler continuity equation has been proposed and provides a "hybrid" EOA with a cutoff of 1.2 cm^2 as severe.

A specifically acquired non-contrast CT can generate an aortic valve calcium score (AVCS), which has gained traction for in use for asymptomatic patients with aortic stenosis. In a study by Utsunomiya et al. [24], the aortic valve calcium score among patients with severe asymptomatic AS was found to be an independent predictor of aortic valve events and long term mortality, specifically when a threshold median value of 723 Agatston Units (AU) was used. Thus obtaining a baseline aortic calcium score in this patient and following serially may aid in decision-making and be used as a marker for serial follow up. In patients with low flow/low gradient AS, the use of AVCS may assist with differentiating patient with severe AS versus moderate AS. An AVCS >1,650 was shown to correlate with severe AS. Measurements of the ascending aorta from CT aortography in cases with discordant echocardiographic and catheterization data also allows for calculation of pressure recovery.

Assessment of Paravalvular Obstruction and Congenital Anomalies

CT angiography also provides detailed coincident data on chamber size and configuration, which can exclude coexisting pathology such as hypertrophic cardiomyopathy, subvalvar membranes, supravalvular stenosis, or other congenital anomalies.

Assessment of Ventricular Function

Cine CT reliably provides access to regional and global wall motion, although it should be restricted to selected cases as it generally doubles radiation exposure [25]. Calculation of ejection fraction (EF) and estimates of stroke volume is also possible without cine CT if static left ventricular images are acquired at both end-diastolic and end-systolic cardiac phases [26]. Additionally, to some extent, CT may reveal the presence of prior infarction by wall thinning, myocardial hypo-enhancement and/or delayed hyper-enhancement.

Multimodality Imaging for Aortic Stenosis: Clinical Application and Case Examples

Though these advanced imaging techniques are novel and exciting, the use of multi-modality imaging is not necessary for every patient with aortic stenosis, except in patients referred to TAVR. Multimodality imaging must be considered on a case-by-case basis, and used only in cases where the added testing provides truly incremental information about the patient's AS. The next section will highlight cases of aortic stenosis where traditional echocardiography may have reached its limits, and where CT and CMR can be useful adjuncts to help fully diagnose the patient and help drive decision-making. Pre-TAVR procedure planning is discussed elsewhere in the book.

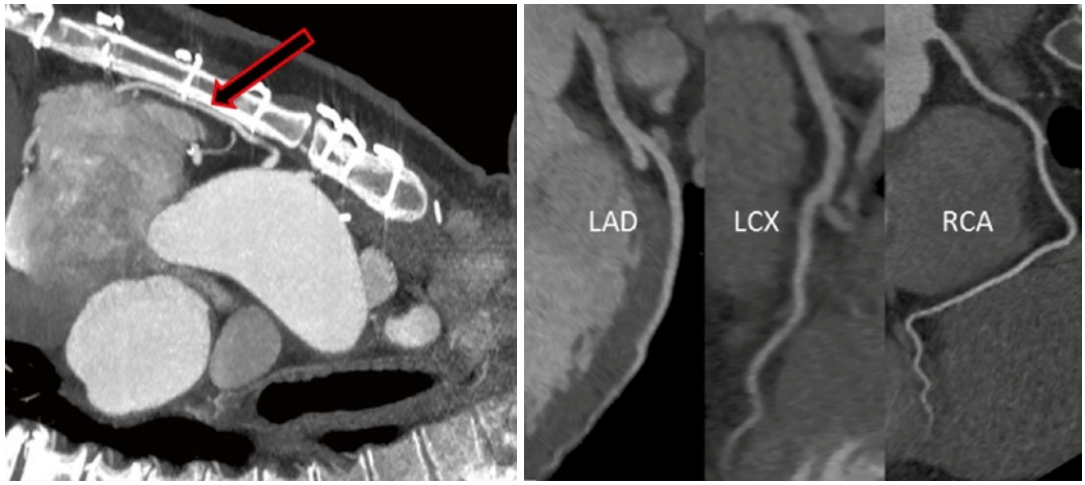

Fig. 7.1 CTA applications: (*Left*) CTA of patient with previous CABG showing course of the saphenous vein graft to the right coronary (*arrow*) as it sits just posterior to the sternum. (*Right*) CTA showing normal left anterior descending (*left*), Left circumflex (*center*) and right coronary artery(*right*) in a curved planar reconstruction

Normal Flow-High Gradient (NF/HG) Severe AS, Normal Ejection Fraction Symptomatic Severe AS

In cases where the severity of aortic stenosis is not in question and patients are symptomatic, echocardiography may be the only diagnostic tool needed to proceed to the operating room directly [27].

However, other important questions must be asked prior to surgery. Is coronary artery disease present and if so, what is the severity? Is there a concomitant aortopathy in need of repair at the time of aortic valve replacement? In the past, such questions would inevitably lead to a cardiac catheterization for coronary evaluation prior to surgery, and then lead to a static CT angiogram (CTA) of the chest or possibly a chest magnetic resonance angiogram to evaluate aortic size. Today, surgeons are more likely to accept a CTA for coronary evaluation (Fig. 7.1), and at the same time use that data to gather information about the ascending and descending thoracic aorta, as well as view the entire chest for potential 'pitfalls' when proceeding with possible sternotomy. It is now possible to get such accurate imaging of the chest to know if prior chest surgery would even allow for a repeat sternotomy, or when a minimally invasive mini-thoracotomy would be the preferred option. In cases of previous bypass, a CTA can clearly show the left internal mammary artery graft adhesion to the chest wall, or saphenous vein grafts which have become adherent to the chest or sternum, typically the graft to the right coronary artery (RCA) as it runs anterior to the heart and sits behind the sternum (Fig. 7.1). In this case, an MRI/MRA of the heart and chest would be less helpful as coronary and graft anatomy would not be well visualized. However, for patients who are unable to tolerate iodinated contrast, MRA can provide excellent imaging of aortic dimensions and pathology. With the chest and coronary anatomy in hand, the patient can be taken to the OR with a detailed surgical plan in place.

However, other valuable information can be gleaned from the CT or CMR. Information such as left ventricular outflow tract and aortic annular sizing as is done now for trans-catheter aortic valve replacement (TAVR) cases (see Chap. 9), as well as accurate valve planimetry for CT [21–24] and CMR [28–34] when compared to both TTE, and CMR. Lastly, CMR and cine CT will allow for a very accurate and reproducible left ventricular (LV) volume and EF [6–9, 26, 35]. Such information may be available from echocardiography, however in cases where echocardiograms may prove difficult to interpret due to patient body habitus or valvular calcification, CMR or cine CT can be helpful (Fig. 7.2). An overview of these and more applications and limitations of both CMR and CT can be found in Tables 7.1a, 7.1b, 7.2a, and 7.2b.

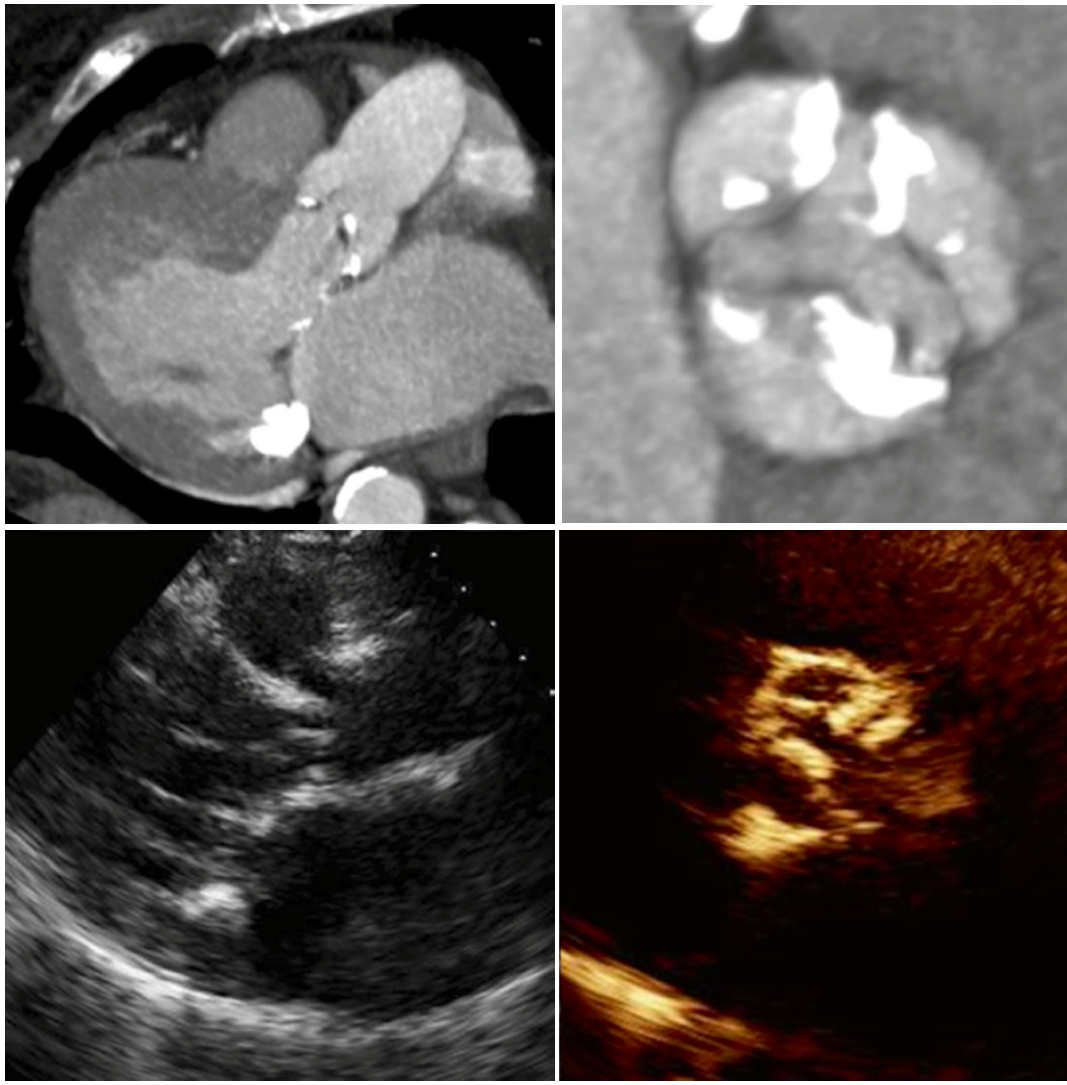

Fig. 7.2 (*Above*) Double oblique image of left ventricle by CTA (*left*) and short axis (*right*) showing the calcified aortic valve. The short axis valve area in systole can be accurately planimetered. (*Below*) Transthoracic echo images from the same patient in long axis (*left*) and short axis (*right*). CTA images are less affected by calcium than TTE in this case, resulting in greater ease of planimetry

Area/Gradient Mismatch: Low Flow/ Low Gradient Severe Aortic Stenosis with Reduced Ejection Fraction

A 71-year-old male with H/O CAD and prior myocardial infarctions presents with shortness of breath and fatigue. On auscultation, a single second heart sound, and a loud, harsh, III/VI mid to late peaking systolic ejection murmur which is mid to late peaking at the right upper sternal border.

His echocardiogram reveals a calcified AV with a peak velocity of 3.1 m/s, a mean gradient of 32 mmHg, an AVA of 0.6 cm^2, a calculated stroke volume index of 37 ml/m^2, and an EF of 38 %.

A dobutamine stress echo shows that the patient's EF rises to 50 %, the stroke volume rises by 25 %–51 ml/m^2, the mean gradient increases to 44 mmHg, and the AVA remains at 0.6 cm^2. The patient has a projected AVA of 1.0 cm^2. All signs in this case point to a low-flow, low gradient severe aortic stenosis with contractile reserve, which

Table 7.2a Applications of cardiac CTA in aortic stenosis

1. Coronary angiography
(a) Native vessels
(b) Coronary bypass grafts
(c) Stents
2. Aortic valve morphology
(a) Leaflet/cusp anatomy
(b) Valve area planimetry
(c) Valve calcification
3. Aortic morphology
(a) Sizing/aneurysm/atheroma
(b) Calcification
(c) Configuration
4. Myocardial morphology
(a) Hypertrophy
(b) Chamber sizing/configuration
(c) Annular sizing/calcification
(d) Myocardial perfusion pattern
(e) Delayed hyper-enhancement
5. Cine CT functional analysis
(a) Stroke volume/stroke volume index
(b) Ejection fraction
(c) Regional wall motion
(d) True LVOT area assessment
6. Trans aortic valve replacement (TAVR)
(a) Annulus size dimensions for sizing of TAVR prosthetic size
(b) Iliac artery dimension to determine candidacy for trans-femoral TAVR
(c) Ascending aortic CTA to determine candidacy for trans-aortic TAVR

Table 7.2b Limitations of cardiac CT in aortic stenosis

1. Radiation exposure
2. Contrast nephropathy
3. Coronary angiography
(a) Coronary/graft calcification
(b) Stent inaccuracy
(c) Moderate/severe lesions require ICA
4. Aortic valve morphology
(a) No effective orifice size
5. Myocardial morphology
(a) Myocardial perfusion difficult
(b) Delayed hyperenhancement difficult
6. Cine CT functional analysis
(a) Marked increase in radiation exposure

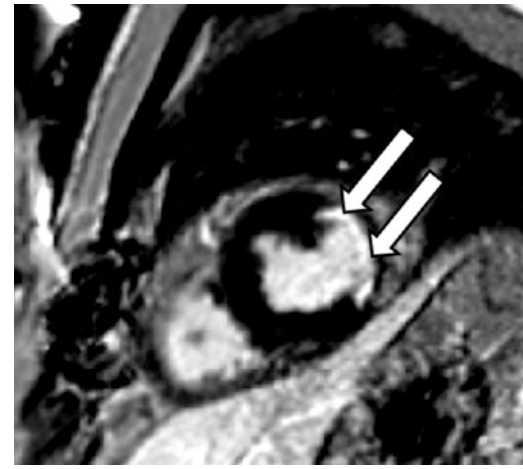

Fig. 7.3 Late gadolinium enhancement pattern seen in the patient from Case 1 with low flow, low gradient AS. This patient has had a prior MI in the lateral wall depicted by the white, delayed enhancement areas (*white arrows*), and thinned, darker appearing myocardium. Presence of infarction is an independent risk factor for death and poor long term prognosis, and the presence of any fibrosis is associated with decreased functional recovery post aortic valve replacement

would portend a favorable prognosis [36–40] (see Chap. 5). The patient undergoes a cardiac MRI for additional risk stratification prior to aortic valve surgery. This confirms his low ejection fraction of 34.75 %, however notable was a previous infarct in the lateral wall seen on delayed enhancement images (Fig. 7.3). His AVA planimetry reveals confirming the presence of severe AS as well as a low SVI confirming the low flow state. Though patients with poor contractile reserve have a higher mortality than those with reserve, their comparative mortality is much lower with surgery than with medical management [40–43]. Independent variables which predict poor surgical outcomes also include patients with previous myocardial infarction, any concomitant CAD (>50 % lesion stenosis) and those with immediate need for circulatory support following surgery (i.e. IABP or inotropes) [44].

In this setting, CMR is helpful to define the etiology of myocardial dysfunction. In addition to its ability to give accurate and reproducible ejection fraction and LV volumes pre and post operatively in this low flow group [45] the use of

delayed hyper-enhancement imaging can describe in detail if a patient has suffered a previous myocardial infarction, another independent preoperative risk factor [17–19] or additional etiologies such as inter-current amyloid heart disease. Other prospective studies in patients with LFLG aortic stenosis have shown that cardiac fibrosis in general is an independent risk factor for decreased functional class post aortic valve replacement [45]. Thus, an assessment of myocardial fibrosis with CMR pre-operatively among patients with depressed ejection fraction and confirmed severe aortic stenosis may prove beneficial to understand the level to which a patient's symptoms may improve.

Another means by which CMR can be helpful in this case would be calculation of valvulo-arterial impedance (Z_{va}), which is calculated as follows:

$$Zva = \frac{SAP + MPG}{SVI}$$

SAP=systolic arterial pressure in mmHg, MPG= mean pressure gradient in mmHg, and SVI is the stroke volume index in ml/m^2.

Z_{va} has also been validated among symptomatic patients with paradoxical LFLG AS to determine prognosis, with values >4.5 mmHg/ml/m^2 portending a much poorer prognosis and higher mortality [46–48]. Though TTE is fully capable of calculating this value, CMR has robust capabilities in measuring left ventricular volumes and stroke volume, and via flow mapping, calculation of the MPG can be made [2], or alternatively can be taken from echocardiographic findings. This positions CMR as an alternate method to accurately calculate the Z_{va}. Taking the SAP from the patient's physical exam, and MPG obtained from the time velocity integral of the trans-aortic flow by echocardiography, the patient's Z_{va} can be calculated readily. In this patient, we calculate $Z_{va}: 148\text{mmHg} + 32\text{mmHg} / (78\text{ml}) / 2.1\text{m}^2) = \boldsymbol{4.6\,mmHg/ml}/\text{m}^2$. This would place the patient in a severe range of >4.5 mmHg/ml/m^2. This would portend a poor prognosis for this patient, and valve surgery would be recommended [47–49].

Indeterminate Severity Aortic Stenosis, Preserved Ejection Fraction

Several times practitioners will face patients who clearly suffer from aortic stenosis with conflicting evidence about disease severity. The difficulties generally arise when there are conflicting test findings or when the patient's symptoms may be due to intercurrent non-cardiac disease as demonstrated below.

Clinical

A 74-year-old male presents with a recently discovered murmur and shortness of breath on minimal exertion with minimal exertion. He has a previous heavy smoking history with documented moderate range COPD. A grade III/VI mid to late peaking systolic ejection murmur with a single S2 is noted.

TTE

An echocardiogram shows an EF of 55 %, a peak aortic valve velocity of 3.6 m/s, a mean aortic valve gradient of 25 mmHg, and an aortic valve area of 0.82 cm^2, with a dimensionless index of 0.29. In addition, there is mild aortic regurgitation and no evidence of pulmonary hypertension.

Catheterization

Despite adequate medical treatment, the patient continues to experience shortness of breath with exertion and a right and left heart catheterization is performed. The right heart catheterization showed a mean right atrial pressure of 10 mmHg, PA pressure of 39/15 mmHg, and a mean PA pressure of 26 mmHg. The pulmonary capillary wedge pressure showed a mean of 17 mmHg without evidence of large V waves. A saturation run showed no evidence of 'step up' and the Fick cardiac output was calculated to be 4.7 L/min at rest, with a cardiac index of 2.2 L/min/m^2. Simultaneous measure of the central aortic pressure and LV pressure showed a central aortic pressure of 136/97 mmHg and an LV pressure of 167/18 mmHg, with a peak to peak gradient of 31 mmHg, and a calculated mean gradient of 23 mmHg. The calculated aortic valve area was

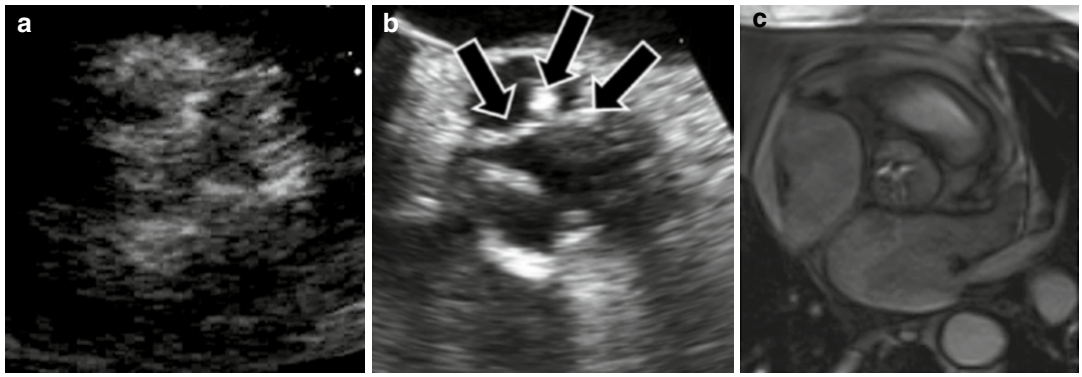

Fig. 7.4 Short axis images on (**a**) TTE, (**b**) TEE and (**c**) CMR for patient with moderate to severe aortic stenosis. (*Left*) The TTE aortic valve short axis image is of poor quality, and the valve opening is barely discernable. (*Center*) The TEE short axis shows a calcified valve (*dark arrows*) with at least partial opening, however due to shadowing, the valve cannot be accurately planimetered. (*Right*) The CMR shows a much more visible valve orifice which can be more easily planimetered

1.0 cm^2. This was felt to represent moderate to severe aortic stenosis. Coronary angiography showed a mid-LAD 40–50 % stenosis. The RCA showed a 90 % proximal segment lesion extending to mid vessel lesion. This was felt to be the lesion causing the patient's symptoms and was fixed with placement of overlapping drug eluting stents with post high pressure inflation.

The patient is seen in office post coronary stenting, and disappointingly he continues to experience the same level of exertional dyspnea. Though by exam his COPD is not active, the idea that his lung disease is contributing to or causing his symptoms is beginning to register with you. However, his moderate to severe aortic stenosis is still an impediment to your being able to fully place blame on another organ system, which does not outwardly appear to be causing much issue. For that reason, you have him undergo a TEE to assess the valve area by planimetry (Fig. 7.4).

TEE

The TEE is performed which confirms a GOA by planimetry of 1.22 cm^2, an EF of 55–60 %, and an aortic valve area by TVI of 1.0 cm^2. At this time, his valve is downgraded to a moderate level of stenosis. It is felt his continued exertional dyspnea is largely pulmonary in etiology, and he is referred to a pulmonologist for treatment.

Mr. L sees his pulmonologist, who performs spirometry and agrees that he has moderate COPD, but it is not active, and unlikely to be contributing to his symptoms. He places him on respiratory inhalers and he returns in 2 weeks to see you. After this consultation and intervention, the patient is still quite hampered with being able to only walk 25–50 ft before becoming dyspneic, and notes no change with the addition of the inhalers. For this reason, you have him undergo a cardiac MRI for better delineation of his aortic valve disease, to determine if the valve is of moderate, moderate to severe or in fact severe range disease.

MRI

The CMR images are also seen in Fig. 7.5. The valve itself is heavily calcified, and when planimetered, the valve area is 1.4 cm^2. The myocardial mass derived from the LV wall contours is 1.3× normal at 160 g. The velocity-encoded images show an aortic valve velocity of 350 cm/s (3.5 m/s). There was also noted to be an EF of 46 % calculated from the end diastolic volume of 205.88 ml and end systolic volume of 109.97 ml at a heart rate of 71 beats per minute. Also of note was the presence of at least mild aortic regurgitation. The consensus from the MRI was that the aortic valve was of moderate level of stenosis. However, as the EF was now felt to be mildly

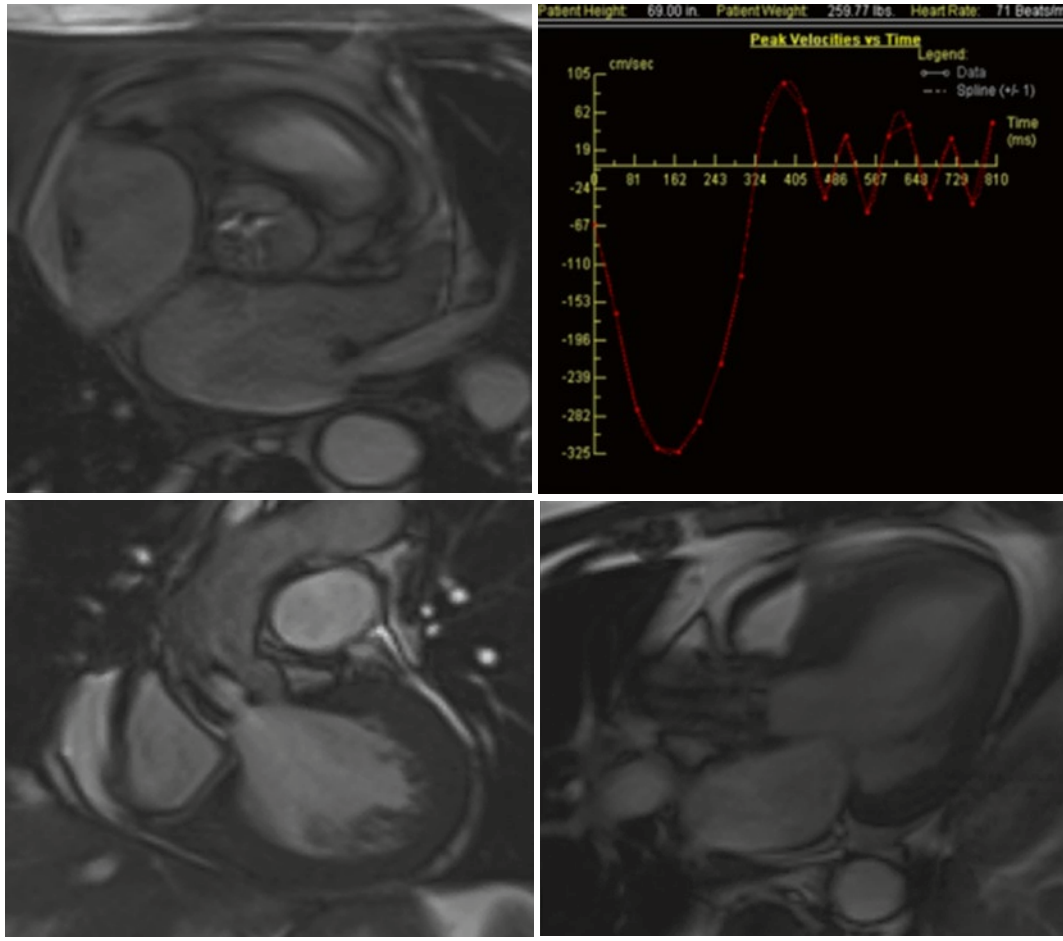

Fig. 7.5 CMR data from Case 2 patient with moderate to severe aortic stenosis. (*Top left*) The short axis view of the valve used for planimetry gives a planimetered valve area of 1.41 cm^2. (*Top right*) Velocity flow mapping data shows the peak aortic valve velocity to be 325 cm/s. (*Bottom left*) The LVOT view and the three chamber view (*bottom right*) shows significant turbulence at the level of the aortic valve

depressed for the first time, a dobutamine stress echocardiogram was recommended to help detect for low flow, low gradient severe AS.

Dobutamine Stress Echo

This dobutamine stress echocardiogram was performed, which confirmed a low EF of 45 %, and with peak dobutamine infusion to 40 mcg/kg/min, the patient's EF improved to 55 % and the mean gradient remained at 25 mmHg. This was consistent with moderate aortic stenosis.

In this case, the initial echo data suggested that the aortic valve had moderate to severe stenosis, however the exam evidence did not suggest severe stenosis. The subsequent cardiac catheterization demonstrated a moderate to severe level of disease, however the following TEE showed moderate disease, which was confirmed by CMR and subsequent dobutamine stress echocardiogram. So which one is correct?

CMR confirmed that the valve was of moderate range stenosis both by VENC measurements and planimetry, which was re-confirmed by TEE and dobutamine stress echocardiography. There is a wealth of data supporting the accuracy of CMR, CT and TEE aortic valve planimetry as compared to TTE derived Doppler gradients and catheterization gradients [21–23, 28–35, 50]. In

general with CMR, there is not felt to be a need to use the continuity equation with the LVOT and aortic valve velocities as those calculations can introduce error into the system [51, 52] (see Chap. 5). While it is true that CMR and TEE planimetry will tend to slightly overestimate valve area compared to TTE derived calculations and catheterization gradients [29, 30, 33], the overestimation in this case was similar by both, and well above the cutoff of 1.0 cm^2. The true difficulty in this case was whether the valvular stenosis valve was causing the patient's continued symptoms and volume overload. He had exam evidence of mild heart failure; however, his COPD was a confounding factor, possibly contributing to his right heart failure, his pulmonary hypertension and thus his dyspnea. His aortic stenosis has presumably always been in the moderate range, however mildly variable hemodynamic circumstances of volume expansion led in turn to relatively higher LVEDP and central aortic pressures, and thus higher estimated gradients by TTE and catheterization. The patient was likely more volume contracted from his diuretics by the time he underwent TEE and CMR, thus pushing him slightly toward a moderate range AS. Given that the planimetry valve area was never <1.0 cm^2, additional testing in this case offered insight and confirmation that the valvular stenosis was not in the severe range.

Energy Loss Index (ELI)

What else could have been done to help adjudicate this case? Further calculations may have been helpful in this case which may have helped reclassify the patient's disease. One such calculation would have been the energy loss index or ELI. ELI takes into account pressure recovery in the aorta, which may lead to valve severity overestimation [53]. ELI is calculated as:

$$ELI\left(\frac{cm^2}{m^2}\right) = \frac{AVA\left(cm^2\right) \times Aa\left(cm^2\right)}{\frac{\left(Aa\left(cm^2\right) - AVA\left(cm^2\right)\right)}{BSA\left(m^2\right)}}$$

(ELI=energy loss index, m^2=meters squared, cm^2=centimeters squared, AVA= effective orifice area derived from continuity equation, Aa is aortic area at the level of the sinotubular junction, BSA is body surface area)

In a study by Bahlmann et al. [54], use of the energy loss index (ELI) among asymptomatic patients was shown to accurately predict long-term outcomes. Their analysis of the SEAS (Simvastatin Ezetimibe in Aortic Stenosis) study data showed that systematically, patients with severe aortic stenosis were overclassified by traditional measures of AS, and when pressure recovery was accounted for in this group by calculating ELI, that the AVA index was generally larger, and overall 47.5 % of patients were reclassified from severe AS to non-severe AS. Further studies from the same group [55] showed that ELI is a powerful prognostic tool for patients with asymptomatic AS. ELI can be easily calculated from CMR with the use of VENC data and measurement of the aorta at the level of the sinotubular junction. The accuracy of such a measurement is well validated in echocardiography and MRI may obtain similar measures with proper imaging angles.

Calculating ELI by CMR in this case, the Aortic Area at the ST junction area is measured directly at 8 cm^2 (Fig. 7.6). The aortic valve area is measured by planimetry from the CMR, at 1.4 cm^2. And thus, the ELI calculates to the following: $\left(8cm^2 \times 1.4cm^2\right) / \left(8cm^2 - 1.4cm^2\right) / 2.1m^2 = 0.808cm^2 / m^2$. This value of 0.808 is above the cutoff of 0.52 cm^2/m^2 for severe aortic stenosis. Values below this level are considered to represent truly severe aortic stenosis. If we used echo parameters to calculate the same value, we would get a slightly different value. The ST junction measured from echo was 2.8 cm, thus the radius of that space is 1.4 cm, and the area (πr^2) at the ST junction is calculated at 6.15 cm^2. The AVA by echo (TVI) was 1.0 cm^2. Thus the ELI now calculates to: $\left(6.15cm^2 \times 1cm^2\right) / \left(6.15cm^2 - 1cm^2\right) / 2.1m^2 = 0.60cm^2 / m^2$. This value is still above the 'severe' cutoff, but much closer to it by the echocardiographic measurement. As the area calculation of the aorta is the most critical to the ELI, CMR's ability to generate this value quickly and accurately must be considered, as the echo

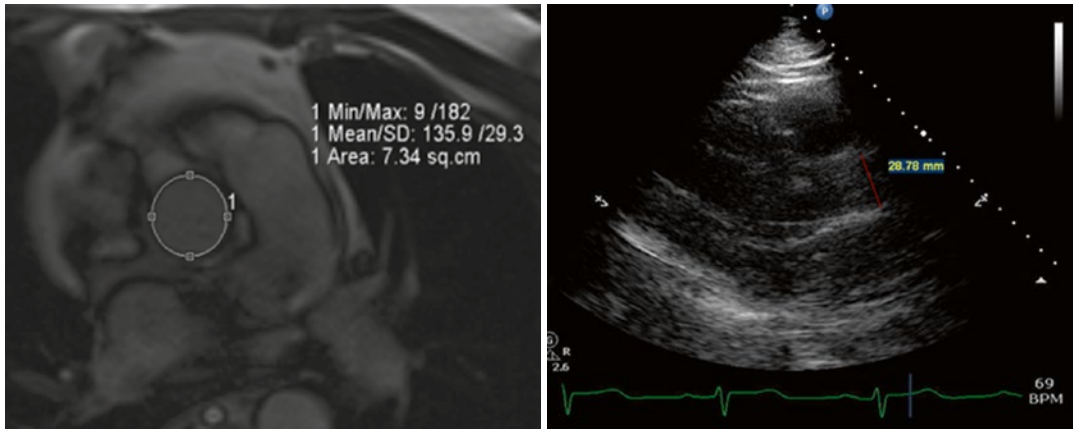

Fig. 7.6 Measurement of the aorta at the level of the sinotubular junction on CMR for calculation of ELI (*left*). TTE images (*right*) from the same patient place the aortic area at the ST junction at 6.15 cm^2, whereas direct measure of the area reveals an area of 7.34 cm^2. Echo measurements of aortic area are notoriously fraught with error for a variety of reasons, such as poor image quality as was the case in this patient

measure of the aortic area may be fraught with potential significant error [52, 56–59].

Other Data

There has also been some consideration to utilizing CMR to produce catheterization like data by using the Hakki equation for aortic valve area [60, 61]. The Hakki equation, which is a simplified version of the Gorlin equation [62, 63], uses parameters, which can easily be determined by CMR. The Hakki equation is:

$$AVA\left(cm^2\right) = \frac{cardiac\ \ output\left(liters / min\right)}{\sqrt{peak\ \ pressure\ \ gradient}\left(mmHg\right)}$$

From MRI, we generate a cardiac output from the stroke volume (calculated from the end diastolic volume-end systolic volume) multiplied by the average heart rate. The peak pressure gradient is obtained from the peak velocity squared, multiplied by 4 (the modified Bernoulli equation). The peak pressure gradient is thus known if detailed flow dynamics are obtained for each case of aortic stenosis. Taking our patient into consideration, and reviewing his hemodynamics and his volumes, we can calculate his valve area by the Hakki equation. His cardiac output at 71 beats per minute is equal to $\left(71*\left(205.88-109.97\right)\right)=6.81$ liters per minute. The peak pressure gradient is calculated as $4\left(3.25\ \mathrm{m/s}*3.25\mathrm{m/s}\right)=42.25$. The square root of this is 6.25. Thus, the AVA calculated by Hakki is 6.81/6.25 = 1.09 cm^2. This is still technically in the moderate range of stenosis, and correlates closely with this patient's cardiac catheterization AVA calculated by the Gorlin method.

For this case, CTA was not a testing modality, which was utilized. However the specific reasons CTA may have utility would be longitudinal management of this patient who clearly has calcific aortic valve disease. Generally, coronary calcium scores are elevated among patients with aortic stenosis, as the process, which causes calcification in the arteries, is implicated in the degeneration of the aortic leaflets as well [24, 64, 65]. As mentioned earlier, recent studies of aortic valve calcium scoring, a non-contrast scoring done solely on the aortic valve, show that monitoring such values can be used to track patients with aortic stenosis who are at risk for disease progression. This scoring is independent of their individual coronary calcium score, and suggests that among patients with high valve calcium scores, disease progression is much more rapid. The aortic valve score in Agatston Units of greater than 723 AU in patients with normal flow and ejection fraction [24] correlates closely to

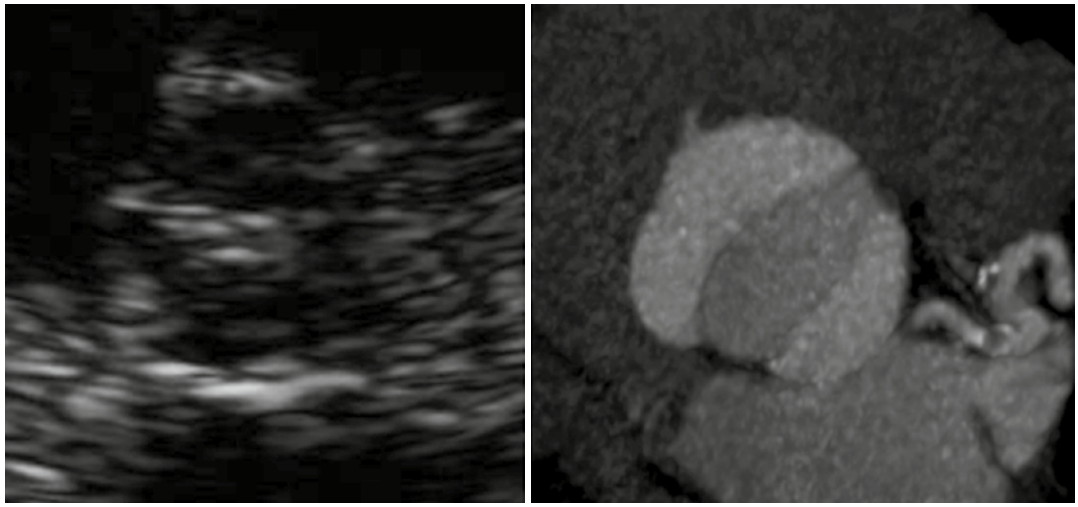

Fig. 7.7 Mid-systolic phase short axis aortic valve image from TTE (*left*) and corresponding CTA (*right*) from the same patient with a bicuspid aortic valve. Due poor acoustic windows, the aortic valve was difficult to visualize, and the echo images are non-diagnostic. The cine CT image clearly defines the two leaflets accurately diagnosing the bicuspid valve

severe AS and a score greater than 1,650 AU among indeterminate cases of LFLG severe AS [64]. In a study done by Cueff et al. [64], a non-contrast CT of the chest was done among indeterminate cases of Low Flow Low Gradient AS for total aortic valvular calcium scoring. Among 49 patients in the test group, those with a calcium score of >1,651 AU, 46 were confirmed to have severe aortic stenosis. Thus, among those with low ejection fraction and possibly low flow, low gradient AS, a non-contrast CT may be a cost effective tool to help determine the true severity of the aortic valvular disease. If values are lower than these thresholds, patients could be followed closely in cases of indeterminate stenosis.

An example of a patient with an indeterminate degree of aortic stenosis where calcium score of the aortic valve was helpful in adjudicating the degree of AS is presented below. An 88-year-old female, presented with two episodes of syncope and mild SOB. An echocardiogram demonstrated a preserved ejection fraction with a calcified and restricted aortic valve with a peak velocity of 3.5 m/s and a mean gradient of 34 mmHg. Her calculated aortic valve area was 0.8 cm^2. Her SVI was noted to be decreased at 28 ml/m^2 consistent with possible low flow low gradient severe AS with preserved ejection fraction of paradoxically low flow low gradient severe AS versus moderate AS.

Given the patients age, she was considered for TAVR and as a part of the work up received a cardiac CTA. Her aortic valve calcium score was calculated at 1,850 AU, well above the cutoff for severe AS. The patients underwent trans femoral TAVR with excellent outcome.

Reverse Area Gradient Mismatch and the Bicuspid Aortic Valve

Patients with a bicuspid aortic valve have a spectrum of diseases, which make them unique. In addition to being a valvulopathy, it is commonly accompanied by a mild to severe aortopathy [15, 66], which can add to the diagnostic burden. The natural history of bicuspid aortic valve disease is very different from tricuspid aortic valve disease [13–15, 66], thus confirming its presence is critical to management. A bicuspid aortic valve may be difficult to visualize by TTE due to commissural fusion or patient imaging issues previously discussed (Fig. 7.7), prompting further evaluation. The following case outlines some of the

more complex pitfalls in evaluating a patient with bicuspid aortic stenosis.

Clinical

Mrs. V is a 57-year-old female with a history of progressive dyspnea. She was referred to the office for a murmur. She has no medical history, but recalls being told in her teens that she should see a cardiologist 'every once in a while'. She has a blood pressure of 124/60 mmHg and heart rate of 90 beats per minute and her BSA is 1.7 m^2. Her cardiovascular exam reveals normal S1, a single S2 and a late peaking grade II/VI systolic murmur with a soft decrescendo diastolic murmur as well. There are brisk carotid upstrokes, which are full volume and moderately delayed. You hear the systolic cardiac murmur radiate to her right, but not left carotid. Her precordial exam reveals a normal PMI with no RV heaves. Her jugular venous pressure is not elevated, nor is there evidence of lower extremity swelling. She notes that her dyspnea had been stable for some time, but has now become worse over the past 6 months to where she is a now dyspneic with walking >50 ft. She undergoes an echocardiogram at your request (Fig. 7.8).

TTE

She was noted by TTE to have severe aortic stenosis, with a peak aortic velocity of 4.2 m/s, aortic valve TVI of 92 cm, LVOT TVI of 33 cm (Dimensionless index of 0.35), and a mean gradient of 43 mmHg and a calculated EOA of 1.1 m^2. Her ejection fraction was calculated at 63 %. She was also noted to have mild aortic insufficiency. Her valve was difficult to visualize by echocardiography.

TEE

Given the discrepancy of her stenosis severity and difficult to visualize valve, she was referred for a trans-esophageal echocardiogram which showed a clearly bicuspid valve, a peak aortic velocity of 4.1 m/s and a mean gradient of 44 mmHg, with a GOA by planimetry of 1.3 cm^2, all consistent with moderate to severe aortic stenosis. However, there was noted to angulation of the jet at the level of the aortic valve by color flow (Fig. 7.8).

MRI

As there was some conflict between the TEE and TTE, she underwent CMR to help resolve the differences between the two previous studies. Further, determining the angle of flow of the aortic jet could help to re-grade he stenosis severity. The aortic valve was interrogated and showed a GOA by planimetry of 1.34 cm^2, and her CMR showed that she clearly had a bicuspid aortic valve (Fig. 7.9), and VENC imaging revealed a peak velocity of 400 cm/s, and a myocardial mass of 145 g, 1.25× the upper limit of normal. CMR also demonstrated an acute angle of flow measured at 30° (Fig. 7.10), which was seen on TEE, much less so on TTE but not able to be measured accurately by either modality. Further, on delayed enhancement imaging, the patient was noted to have patchy, diffuse mid-myocardial fibrosis.

Determining the level of severity in bicuspid valve aortic stenosis is complex due to the many factors that accompany this valvulopathy. Traditional echo Doppler will be able to estimate peak valve flow velocities, and thus via the modified Bernoulli equation will yield a pressure gradient; however, in bicuspid aortic stenosis the angle of flow is not always perpendicular to the valve plane and traditional imaging angles will be inaccurate [13, 58]. As each case of bicuspid disease is unique, the angle of flow many be angled in any direction, which changes the velocity which is collected by continuous wave Doppler, causing even more confusion when traversing from patient to patient. This angulation produces more valvular and post valvular turbulence and causes pressure to convert from potential energy to kinetic energy and dissipate as heat, resulting in an irreversible pressure loss which cannot be recovered downstream, and thus aortic velocities will be overestimated [58, 67]; a situation which would not have occurred in a patient with central AS. The planimetered geometric orifice area in bicuspid valves is generally larger than that of a patient with tricuspid valve AS (Fig. 7.11), however the calculated effective orifice area will be smaller than a similar patient with tricuspid valve AS for the same reasons as outline above regarding overestimates of velocity. Another influential factor in the bicuspid

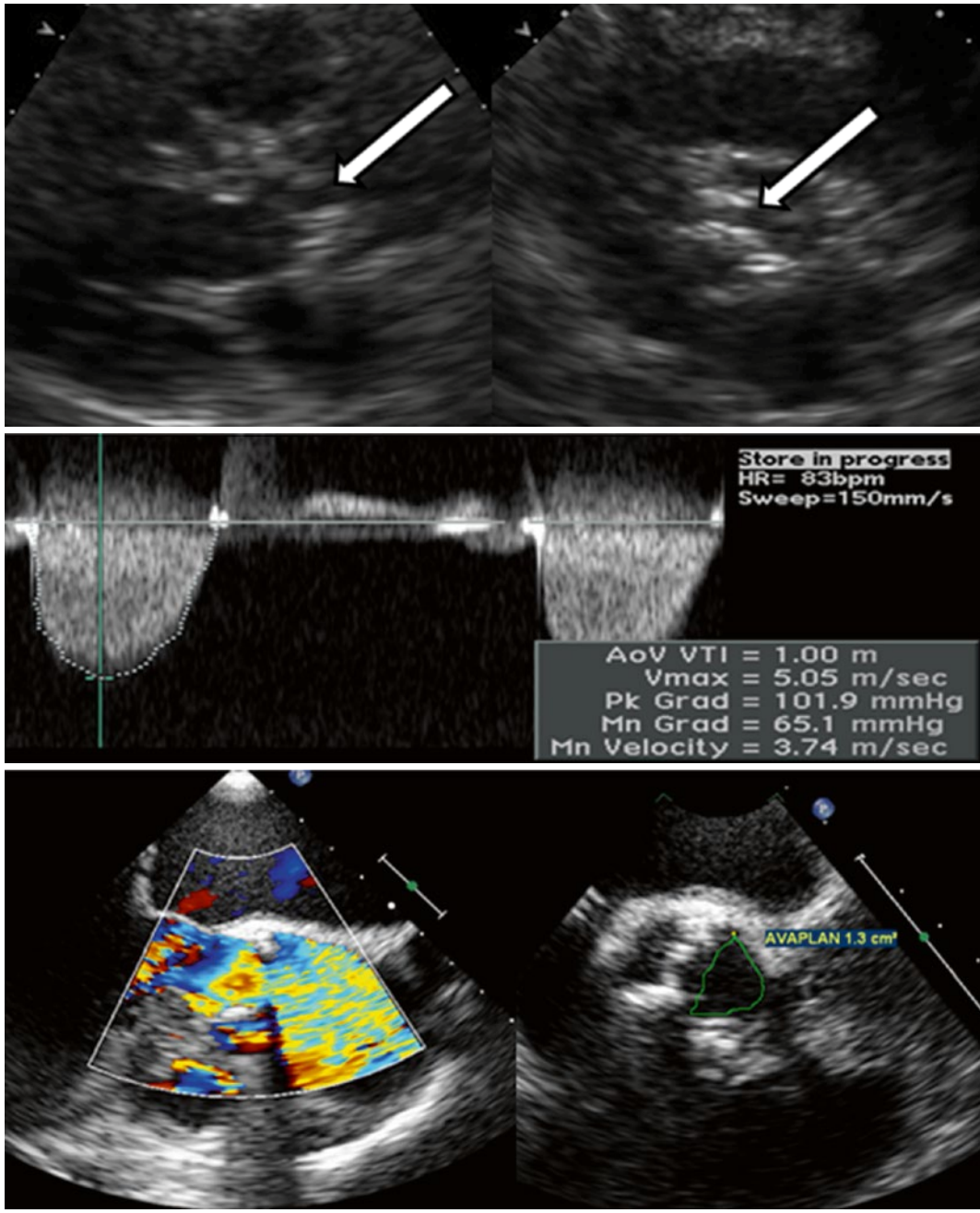

Fig. 7.8 Transthoracic and Transesophageal echo images from Case 4 patient with bicuspid aortic valve stenosis. (*Top left*) TTE long axis systolic frame, showing valve opening (*arrow*) (*Top right*) TTE short axis showing calcified valve opening (*arrow*). (*Center*) Spectral doppler of the aortic valve showing peak velocity of 5.05 m/s and mean gradient of 65.1 mmHg. (*Bottom left*) TEE color doppler image showing flow out of the LVOT through the aortic valve, slightly eccentric. (*Bottom right*) TEE short axis showing planimetered valve area 1.3 cm^2

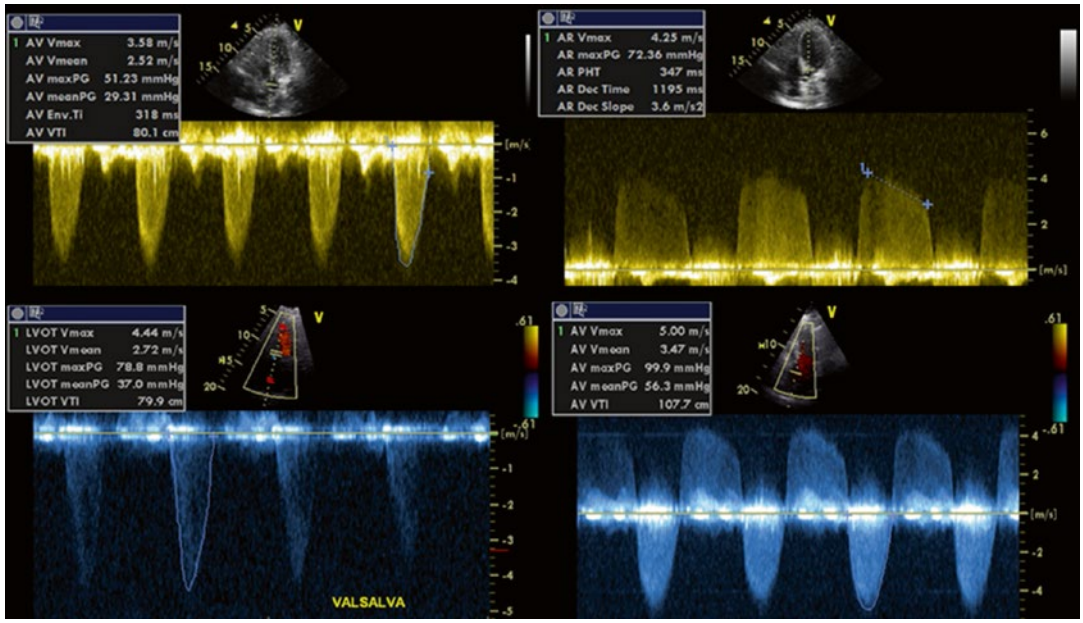

Fig. 7.9 Case 4 patient with presumed aortic stenosis. (*Top left*) TTE continuous wave spectral Doppler of the aortic valve showing peak velocity 3.58 m/s and mean gradient 29 mmHg, and peak gradient of 51 mmHg at rest. (*Top right*) Aortic insufficiency by continuous wave Doppler, pressure half-time of 347, moderate range insufficiency. (*Bottom left*) HPRF pulse wave Doppler of the LVOT with Valsalva Maneuver, showing a peak velocity of 4.4 m/s. (*Bottom right*) Continuous wave Doppler of the aortic valve with Valsalva maneuver (*bottom right*) showing peak velocity of 5 m/s and mean gradient of 56 mmHg, peak gradient of 99.9 mmHg. All findings are consistent with a dynamic outflow obstruction, and moderate aortic insufficiency

patient is that of the aortic size. There is a relationship with bicuspid aortic stenosis and aortopathy, which is related to an issue with collagen matrix deposition with in the aortic wall itself [15, 66]. However, the degree to which the proximal aorta is dilated can affect the severity of the valvular stenosis itself through the concept of energy loss as previously described. This difference in aortic size has a direct effect on pressure recovery, as a dilated aorta will tend to recover pressure to a lesser degree than a narrower one [3, 12, 13, 49, 58]. As such, the aortic size must be accounted for by calculating ELI. Thus, as CT and CMR imaging offer a far superior view of the ascending aorta at the level of the sinotubular junction, with a more proper calculation of the area at that level, their use in such patients with bicuspid valve disease may become critical.

In addition, combining these two concepts, the angle of the bicuspid jet directly affects the pressure drop seen across the valve and can affect pressure recovery in the aorta as well (Fig. 7.12). For example, if a given jet has an angle of ~4° off center, this may impact the resultant flow only slightly, causing an overestimation of the flow velocity and thus an underestimation of the effective orifice area. If one looks at an angle of 24° off center, this impacts the flow and the pressure recovery even more, causing a much sharper drop in pressure and even less pressure recovery, which will even further underestimate the effective orifice area. We can see from Fig. 7.12 that the more steep the angle, the worse the estimation of the effective orifice area, and thus we are more likely to estimate *smaller* valve sizes for these extremely angulated bicuspid valves.

Catheterization

For Mrs. V, following her two echocardiograms and CMR, her valve was felt to be in a moderate to severe range of stenosis, thus as she was still symptomatic, she underwent a right and left heart

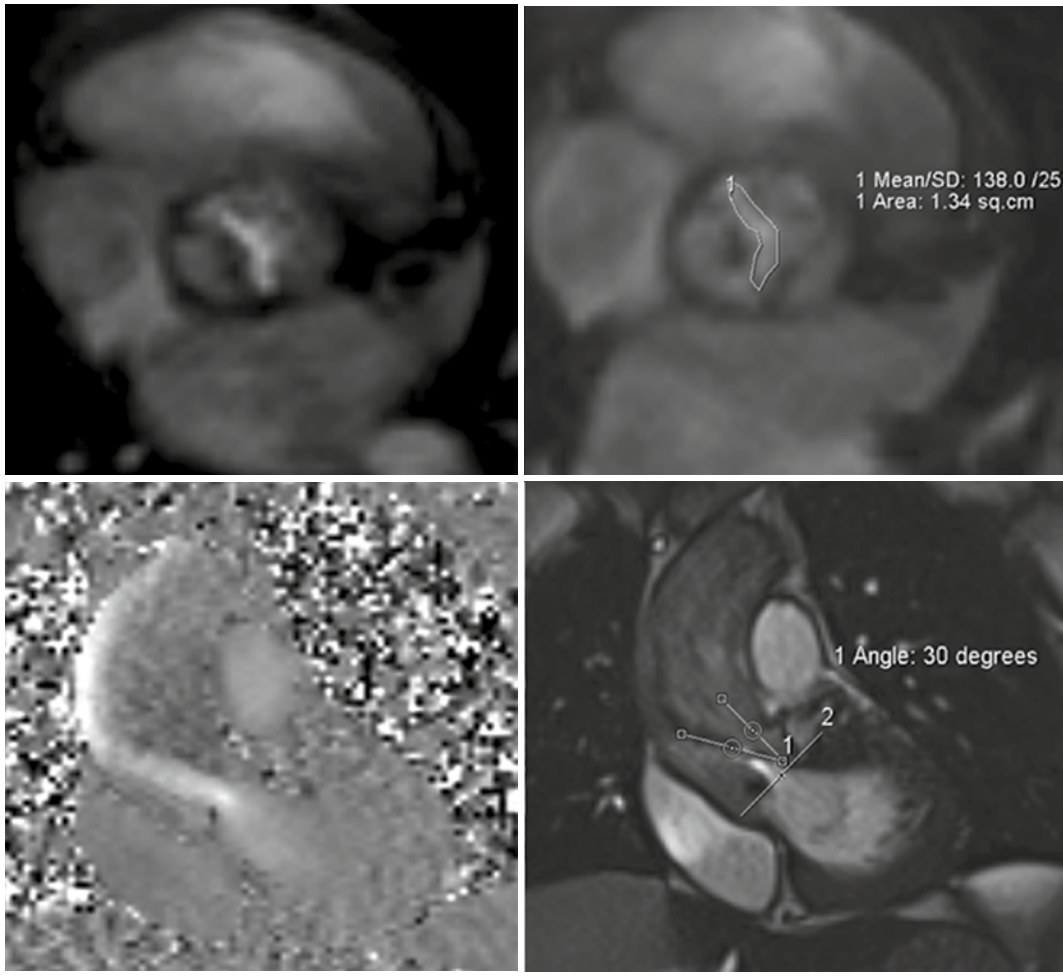

Fig. 7.10 CMR images of Case 4 patient with bicuspid aortic valve. (*Top left*) Short axis FLASH image of the aortic valve. (*Top right*) Valve planimetry from short axis, systolic CINE image. (*Bottom left*) In plane phase contrast image showing eccentric flow from aortic valve directed toward the outer aortic wall. (*Bottom right*) Calculation of angle of flow from the CINE LVOT view a centerline through the aortic valve plane, a 30° angulation

catheterization to help add data to her clinical scenario. The following right heart catheterization data was obtained: mean right atrial pressure 11 mmHg, PA pressure 33/16 mmHg and mean 24 mmHg, and a PCWP of 18 mmHg. The Fick cardiac output was calculated at 5.3 L/min. Simultaneous LV and central aortic pressure readings showed pressures of 201/30 mmHg and 125/75 mmHg respectively, with a peak-to-peak gradient of 76 mmHg, and a calculated mean gradient of 56 mmHg. The Gorlin calculated aortic valve area was 0.8 cm^2. Her valve was considered to be severely stenotic, and she was referred for surgical AVR.

In this case, multimodality imaging was of critical importance. CMR imaging showed the extent of the angulation of her aortic jet, which as has been shown, will affect pressure recovery due to the abnormally arranged flow vortices surrounding the valve. Such an angle of flow would cause a precipitous drop in pressure with much less pressure recovery, which would imply a larger pressure gradient than was seen or calculated from Doppler and the continuity equation. This will generally underestimate valvular stenosis in the patients with a bicuspid aortic valve. Further, her CMR shows patchy myocardial fibrosis, an independent risk

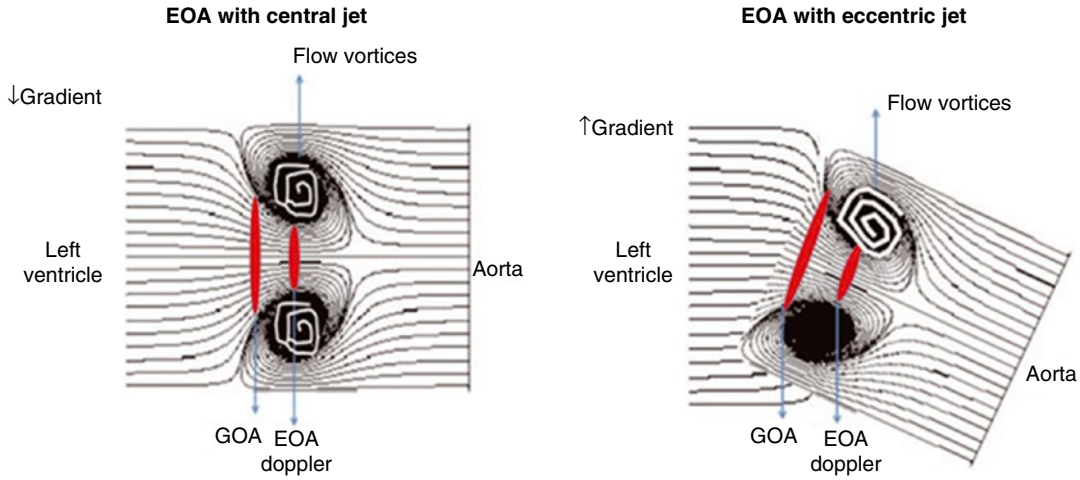

Fig. 7.11 Geometric orifice area and effective orifice area as it differs between a centrally stenotic aortic valve and a bicuspid valve with an eccentric jet. The angulated aortic valve will have a calculated effective orifice area which is similar to patient with central AS patient with a more narrow geometric orifice area (From Abbas et al. [58] with permission)

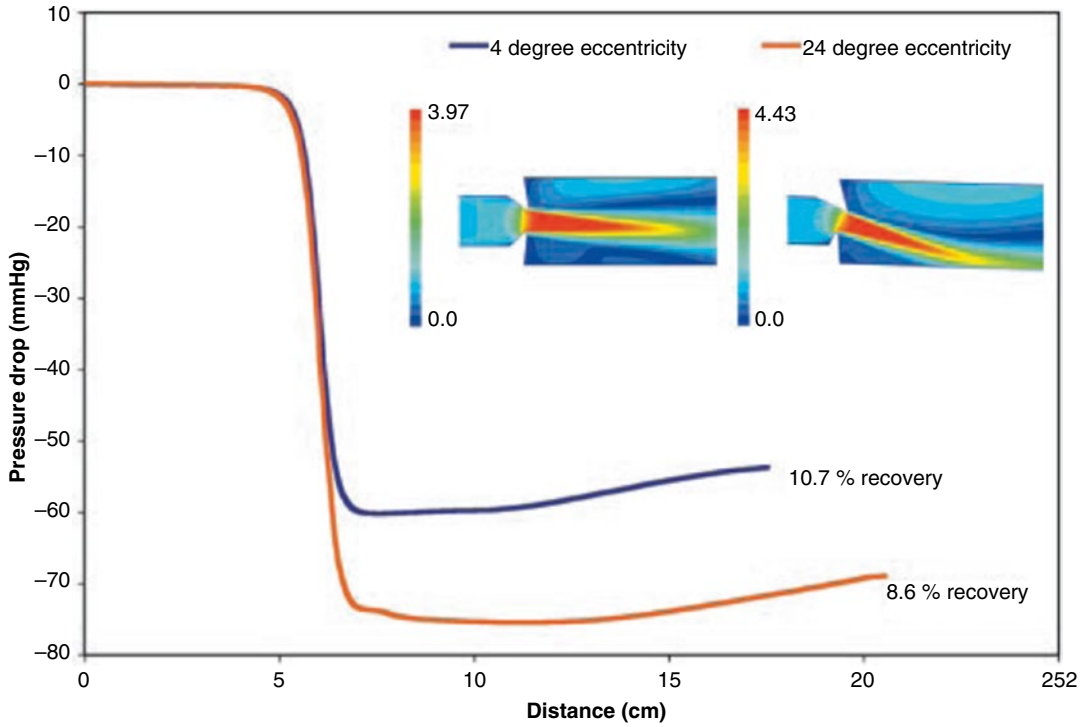

Fig. 7.12 Pressure recovery in bicuspid aortic valves at varying outflow angles. The degree of eccentricity affects the pressure drop across the valve, and subsequently the ability to 'recover' pressure (From Richards et al. [13] with permission)

factor for all-cause mortality [18, 19, 45]. This would suggest a larger hemodynamic load on the patient, and would prompt sooner valve surgery, as even further fibrosis would be likely with surgical delay. Interestingly, in cases where there is myocardial fibrosis seen, after the aortic valve has been replaced the fibrosis has been shown by CMR to regress over time [68, 69].

As previously discussed, CMR is also of great importance in cases of bicuspid disease for its ability to detect extra cardiac pathology from a surgical standpoint. The association of proximal aortic dilatation as well as coarctation of the aorta with bicuspid aortic valve places the full aortic evaluation at high importance for the patient, and this patient did receive a thorough aortic evaluation.

Further, specifically in cases of bicuspid valve disease, for a given valve geometric orifice area, while the planimetered valve area by TEE disease will tend to overestimate the valve area compared to the calculated gradient, the hemodynamic load 'felt' by the bicuspid valve is much more than a similar gradient may have on a tricuspid aortic stenosis [16]. Meaning, for a given valve size seen, a bicuspid patient will feel the hemodynamic affects sooner, and may start to accumulate MF at a faster rate than their tricuspid counterparts portending a poorer prognosis if not followed closely and replaced at an appropriate time interval. As such, the TEE planimetry showing the valve area of 1.6 cm^2 may in fact be underestimating the actual hemodynamic load on that valve. Another way of calculating the hemodynamic load on the patient would be to calculate the Z_{va}. Though such a calculation has not been validated among patients with bicuspid valve disease, its clinical implications would seem evident.

Overall, in imaging bicuspid valve disease a reasonable rule is to measure the valve in more than one modality and take into consideration all issues of valve jet angulation, aortic size and presence of aortopathy, as well as pressure recovery via calculation of ELI [12–16]. But know for certain that the planimetry from TEE, MRI and TTE will generally overestimate the valve size, and of equal importance will underestimate the hemodynamic load on the bicuspid as opposed to a similarly stenotic tricuspid valve [16].

Paravalvular Obstruction: Sub-aortic Stenosis

Clinical

Mrs. S is a 46-year-old female whom you are seeing in the emergency department initially for symptomatic shortness of breath. On taking her history you note that she has had progressive dyspnea on exertion over the previous 3–4 years. She finally presented to the emergency room as she could not walk up her steps today at all, and had to sit for 15 min to catch her breath on attempting this. She has no known cardiac history, and no medical history to speak of. There is no history of smoking.

In the ER, her blood pressure is 126/75 mmHg, her heart rate is 94 beats per minute, and she is well saturated on room air. On cardiac exam, she has a normal S1 and S2, with a loud, late peaking systolic murmur at the right sternal border which is IV/VI in intensity radiating to the carotid arteries, and a loud decrescendo murmur which is holodiastolic. Pulmonary exam reveals no rales, wheezing or rhonchi. She has no evidence of elevated jugular pressure, and no lower extremity swelling.

TTE

Mrs. S undergoes a TTE as part of her workup which was interpreted as showing moderate aortic stenosis based upon difficult to view images and elevated Doppler velocities, and mild to moderate aortic insufficiency. The spectral Doppler is seen in Fig. 7.9. The peak velocity of flow out of the area of the left ventricular outflow tract is 3.6 m/s, with a mean gradient of 29 mmHg, and peak gradient of 65 mHg. The aortic regurgitation pressure half time was 379 ms with a poor spectral envelope placing it in the mild to moderate range. There is noted to be sub-aortic septal hypertrophy as well, which was felt to be the culprit. On performing the Valsalva maneuver, the peak outflow gradient increased from 65 mHg to 100 mmHg (Fig. 7.9). From the echo images (Fig. 7.13), there is clear obstruction in the outflow tract, which is felt to represent hypertrophic obstructive cardiomyopathy.

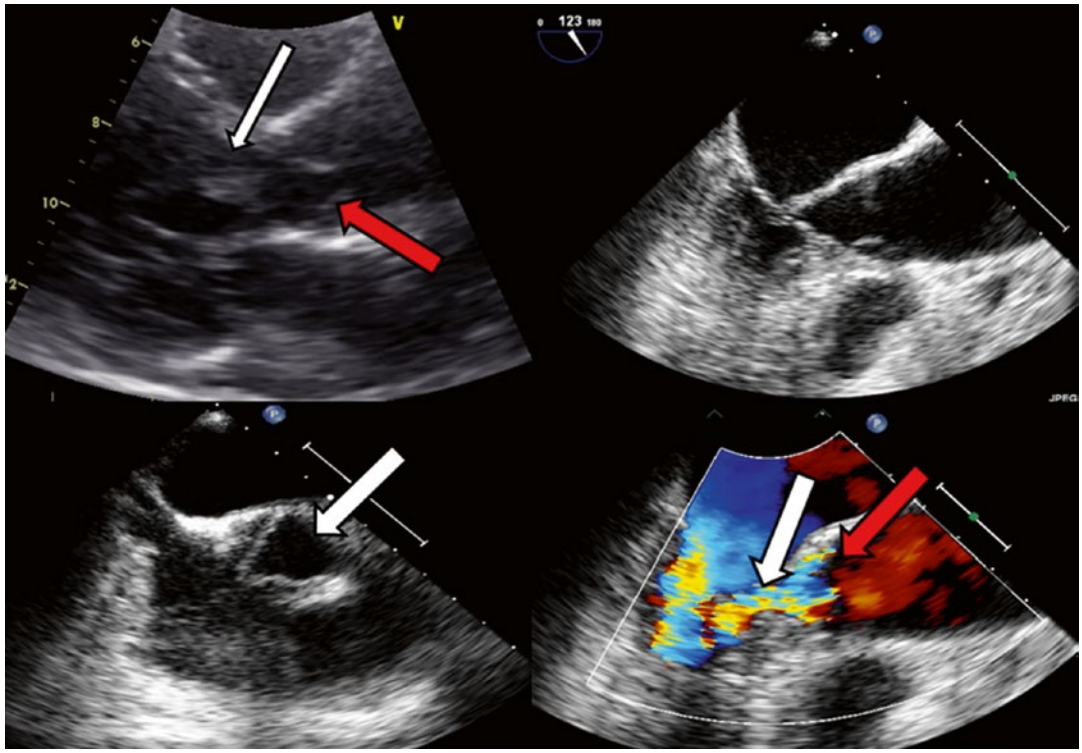

Fig. 7.13 Case 4 patient TTE and TEE images. (*Top left*) TTE parasternal long axis showing aortic valve (*red arrow*) and LVOT obstruction. The *white arrow* shows the location of flow. (*Top right*) TEE LVOT view, showing aortic valve (*red arrow*) and again outflow obstruction (*white arrow*). (*Bottom left*) TEE short axis aortic valve showing the open leaflets (*arrow*) and lack of aortic *valvular* stenosis. (*Bottom right*) TEE color Doppler showing LVOT obstruction (*white arrow*) below the level of the valve (*red arrow*)

TEE

For further evaluation, the patient undergoes a TEE (Fig. 7.13). The TEE shows turbulence in the left ventricular outflow tract (LVOT) again with a hypertrophied septum. The patient is being considered for alcohol septal ablation versus surgical myomectomy. As part of pre-operative planning, the patient undergoes a CMR to help define the anatomy further (Fig. 7.14). As is seen on the CMR images, there is a 'pinhole' flow acceleration seen just below the aortic valve, with abnormal tissue surrounding the 'pinhole', which does not have the same attenuation as myocardium. This was felt to be consistent with a subaortic membrane. There is concomitant septal hypertrophy, which is seen in up to 75 % of such cases [70], as a response to the pressure overload state. The high pressure aortic jet damages the aortic annulus and leaflets into a state of valvular regurgitation slowly over time. Thus, the patient has both a fixed and a dynamic LVOT obstruction, with concomitant aortic insufficiency.

The patient was referred to surgery for definitive repair of this complex lesion. Results from the operation confirmed that the patient had both a discrete sub-aortic membrane and septal hypertrophy. She underwent surgery for resection of the membrane, septal myomectomy and aortic valve repair. Post operatively, there was no gradient seen across the LVOT or aortic valve, and no evidence of aortic regurgitation.

In this case, the CMR was critical to help diagnose the patient correctly. The spatial resolution of CMR in this case outperformed that of TEE. Though the TEE images suggested an obstruction, the study did not reveal the subvalvar membrane. While a surgical intervention for myomectomy would have revealed the subvalvar

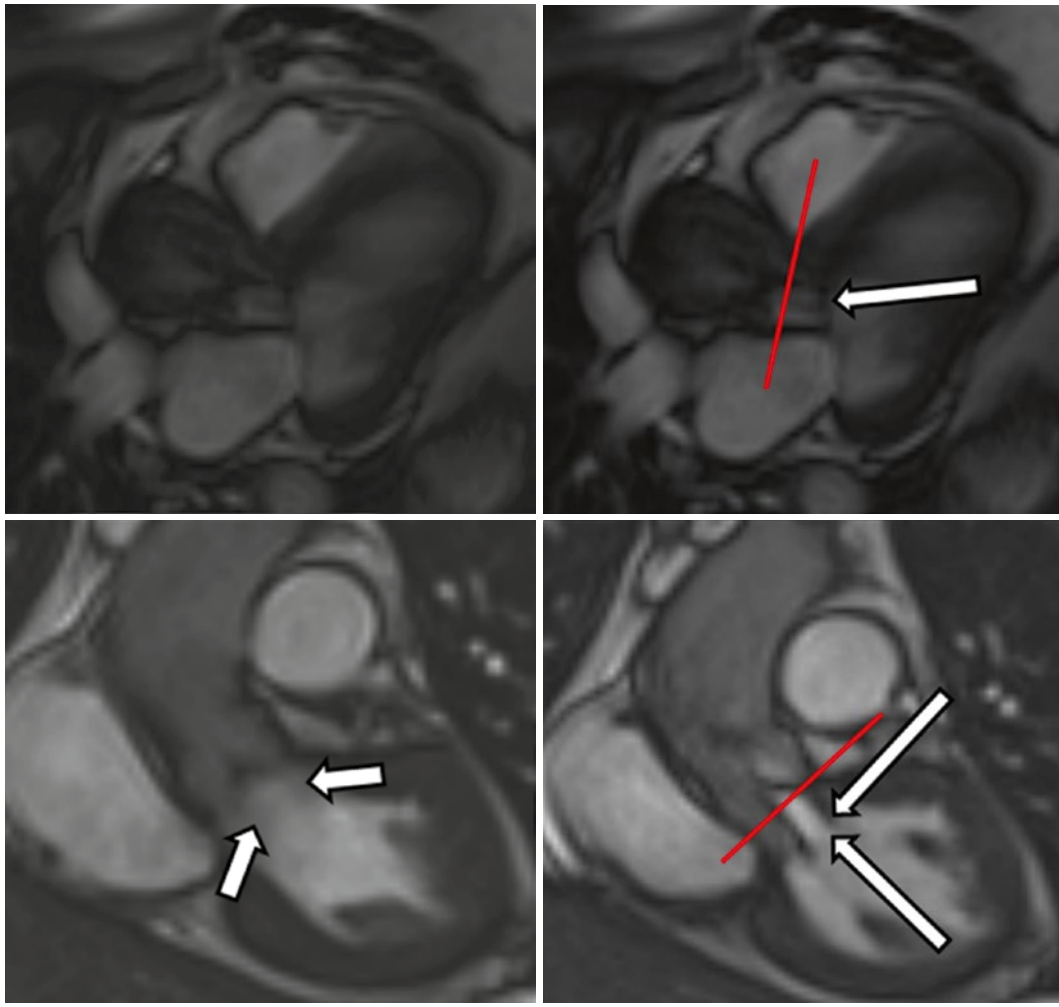

Fig. 7.14 Case 4 CMR images for suspected subvalvar stenosis. (*Top left*) systolic three chamber view showing outflow tract turbulence and in the *top right*, the *white arrow* shows the pinhole flow seen below the plane of the aortic valve (*red line*). (*Bottom left*) LVOT diastolic frame showing the aortic valve and abnormal tissue below (*white arrows*) (*Bottom right*) LVOT systolic frame showing the jet of flow acceleration (*white arrows*) just below the plane of the aortic valve (*red line*). This location and type of flow is consistent with a subvalvar membrane

membrane, alcohol ablation would have been ineffective.

Sub-aortic stenosis may be due either to a discrete sub-aortic membrane, abnormal or malformation of the mitral valve apparatus, sub-aortic hypertrophy which may or may not eventually result in obstruction of the LV outflow tract, or all of the above [70–74]. Though at least a portion of the membrane or outflow obstruction is present from birth, its hemodynamic effects may take years to be realized, and thus it is considered to be an acquired lesion, growing in size over time as progressive scar and fibrosis affect the surrounding myocardium [72]. The physical exam findings in response to the Valsalva maneuver in a patient with a discrete subvalvar membrane are similar to that of a patient with valvular aortic stenosis; the systolic murmur auscultated will decrease with Valsalva in both cases [73]. In addition, there will be an increased pulse pressure following a premature ventricular beat, the Brockenbrough-Braunwald-Morrow sign, in both valvular aortic

stenosis and a discrete subvalvar membrane. However, the pathophysiology that accompanies the discrete membrane *can* change over time and the pressure related effects of the membrane cause a slow scarring and fibrosis of surrounding myocardium over time, thus making the outflow tract narrower, and worsening the severity of the stenosis (note: the hemodynamic changes with a discrete subvalvar membrane may not change over time, or may change very slowly, as was determined by natural history studies [72–74]). The LVOT will narrow as septal hypertrophy proximal to the membrane occurs as a result of the pressure changes, leading to changes in the physical examination over time. If more septal hypertrophy occurs, the response to Valsalva will change and physical exam will become similar to hypertrophic cardiomyopathy: there will be an increased murmur with Valsalva later in the disease process. This patient had both a discrete membrane and septal hypertrophy causing the Valsalva gradients seen by echocardiography seen in Fig. 7.9. This patient's findings were similar to that of a patient with hypertrophic obstructive cardiomyopathy, with the Valsalva maneuver eliciting high transaortic gradients; however, the patient had a concomitant diastolic murmur. When a patient presents with both a systolic and diastolic murmur consistent with aortic stenosis and regurgitation, bicuspid valve disease and subvalvar aortic stenosis must be effectively excluded. Thus, the patient who has no history of heart murmur or any valvular symptoms in early life would be among the first in whom you would suspect such a lesion.

Conclusion

In summary, the use of multi-modality imaging to help assess the severity of aortic stenosis, or to aid with the peri-operative or peri-TAVR procedural planning has now been well established. Its use in a selected case by case basis should be considered when either additional information is needed for a specific case, conflicting data is received from standard thoracic or trans-esophageal echo imaging, or when discrepant information is obtained from previous evaluations and further information is needed. There is a wealth of prognostic information, which can be gathered through use of such modalities, when applied correctly to the correct patient. Both CT and CMR have unique advantages and disadvantages (Tables 7.1a, 7.1b, 7.2a, and 7.2b), which must be understood fully, and each modality must be used in the proper context to maximally assist in guiding decision making in these complex patients.

References

1. Kramer CM, Barkhausen J, Flamm SD, Kim RJ, Nagel E. Standardized cardiovascular magnetic resonance (CMR) protocols 2013 update. J Cardiovasc Magn Reson. 2013;15:91.
2. Cawley PJ, Maki JH, Otto CM. Cardiovascular magnetic resonance imaging for valvular heart disease: technique and validation. Circulation. 2009;119:468–78.
3. Pibarot P, Larose É, Dumesnil J. Imaging of valvular heart disease. Can J Cardiol. 2013;29(3):337–49.
4. Hendel RC, Patel MR, Kramer CM, Poon M, et al. ACCF/ACR/SCCT/SCMR/ASNC/NASCI/SCAI/SIR 2006 appropriateness criteria for cardiac computed tomography and cardiac magnetic resonance imaging. A report of the American College of Cardiology Foundation Quality Strategic Directions Committee Appropriateness Criteria Working Group, American College of Radiology, Society of Cardiovascular Computed Tomography, Society for Cardiovascular Magnetic Resonance, American Society of Nuclear Cardiology, North American Society for Cardiac Imaging, Society for Cardiovascular Angiography and Interventions, and Society of Interventional Radiology. J Am Coll Cardiol. 2006;48(7):1475–97.
5. Pennel DJ, Sechtem UP, Higgins CB, et al. Clinical indications for cardiovascular magnetic resonance (CMR): consensus panel report. J Cardiovasc Magn Reson. 2004;6:727–65.
6. Myerson SG. Heart valve disease: investigation by cardiovascular magnetic resonance. J Cardiovasc Magn Reson. 2012;14:7.
7. Longmore DB, Klipstein RH, Underwood SR, Firmin DN, Hounsfield GN, Watanabe M, Bland C, Fox K, Poole-Wilson PA, Rees RS. Dimensional accuracy of magnetic resonance in studies of the heart. Lancet. 1985;1:1360–2.
8. Rehr RB, Malloy CR, Filipchuk NG, Peshock RM. Left ventricular volumes measured by MR imaging. Radiology. 1985;156:717–9.
9. Sechtem U, Pflugfelder PW, Gould RG, Cassidy MM, Higgins CB. Measurement of right and left ventricular volumes in healthy individuals with cine MR imaging. Radiology. 1987;163:697–702.

10. Jauhiainen T, Jarvinen VM, Hekali PE, Poutanen VP, Penttila A, Kupari M. MR gradient echo volumetric analysis of human cardiac casts: focus on the right ventricle. J Comput Assist Tomogr. 1998;22: 899–903.
11. Eichenberger AC, Jenni R, von Schulthess GK. Aortic valve pressure gradients in patients with aortic valve stenosis: quantification with velocity-encoded cine MR imaging. AJR Am J Roentgenol. 1993;160:971–7.
12. Niederberger J, Schima H, Maurer G, Baumgartner H. Importance of pressure recovery for the assessment of aortic stenosis by doppler ultrasound: role of aortic size, aortic valve area, and direction of the stenotic jet in vitro. Circulation. 1996;94:1934–40.
13. Richards KE, Deserranno D, Donal E, Greenberg NL, Thomas JD, Garcia MJ. Influence of structural geometry on the severity of bicuspid aortic stenosis. Am J Physiol Heart Circ Physiol. 2004;287(3):H1410–6.
14. Joziasse IC, Vink A, Cramer MJ, van Oosterhout MF, et al. Bicuspid stenotic aortic valves: clinical characteristics and morphological assessment using MRI and echocardiography. Neth Heart J. 2011;19(3): 119–25.
15. Kari FA, Fazel SS, Mitchell RS, Fishbein MP, Miller DC. Bicuspid aortic valve configuration and aortopathy pattern might represent different pathophysiologic substrates. J Thorac Cardiovasc Surg. 2012;144(2): 516–7.
16. Donal E, Novaro GM, Deserrano D, Popovic ZB, Greenberg NL, Richards KE, Thomas JD, Garcia MJ. Planimetric assessment of anatomic valve area overestimates effective orifice area in bicuspid aortic stenosis. J Am Soc Echocardiogr. 2005;18:1392–8.
17. Dweck MR, Joshi S, Murigu T, Alpendurada F, Jabbour A, Melina G, Banya W, Gulati A, Roussin I, Raza S, Prasad NA, Wage R, Quarto C, Angeloni E, Refice S, Sheppard M, Cook SA, Kilner PJ, Pennell DJ, Newby DE, Mohiaddin RH, Pepper J, Prasad SK. Midwall fibrosis is an independent predictor of mortality in patients with aortic stenosis. J Am Coll Cardiol. 2011;58(12):1271–9.
18. Weidemann F, Herrmann S, Stork S, Niemann M, Frantz S, Lange V, Beer M, Gattenlohner S, Voelker W, Ertl G, Strotmann JM. Impact of myocardial fibrosis in patients with symptomatic severe aortic stenosis. Circulation. 2009;120(7):577–84.
19. Nigri M, Azevedo CF, Rochitte CE, Schraibman V, Tarasoutchi F, Pommerantzeff PM, Brandão CM, Sampaio RO, Parga JR, Avila LF, Spina GS, Grinberg M. Contrast-enhanced magnetic resonance imaging identifies focal regions of intramyocardial fibrosis in patients with severe aortic valve disease: correlation with quantitative histopathology. Am Heart J. 2009; 157(2):361–8.
20. Habets J, Tanis W, van Herwerden LA, van den Brink RB, Mali WP, de Mol BA, Chamuleau SA, Budde RP. Cardiac computed tomography angiography results in diagnostic and therapeutic change in prosthetic heart valve endocarditis. Int J Cardiovasc Imaging. 2014;30(2):377–87.
21. Piers LH, Dikkers R, Tio RA, van den Berg MP, Willems TP, Zijlstra F, Oudkerk M. A comparison of echocardiographic and electron beam computed tomographic assessment of aortic valve area in patients with valvular aortic stenosis. Int J Cardiovasc Imaging. 2007;23(6):781–8.
22. Westermann Y, Geigenmüller A, Elgeti T, Wagner M, Dushe S, Borges AC, Dohmen PM, Hein PA, Lembcke A. Planimetry of the aortic valve orifice area: comparison of multislice spiral computed tomography and magnetic resonance imaging. Eur J Radiol. 2011;77(3):426–35.
23. Chun EJ, Choi SI, Lim C, Park KH, Chang HJ, Choi DJ, Kim DH, Lee W, Park JH. Aortic stenosis: evaluation with multidetector CT angiography and MR imaging. Korean J Radiol. 2008;9(5):439–48.
24. Utsunomiya H, Yamamoto H, Kitagawa T, Kunita E, Urabe Y, Tsushiuma H, Hidaka T, Awai K, Kihara Y. Incremental prognostic value of cardiac computed tomography in asymptomatic aortic stenosis: significance of aortic valve calcium score. Int J Cardiol. 2013;168(6):5205–11.
25. Pflederer T, Jakstat J, Marwan M, Schepis T, Bachmann S, Kuettner A, Anders K, Lell M, Muschiol G, Ropers D, Daniel WG, Achenbach S. Radiation exposure and image quality in staged low-dose protocols for coronary dual-source CT angiography: a randomized comparison. Eur Radiol. 2010;20(5):1197–206.
26. Greupner J, Zimmermann E, Grohmann A, et al. Head-to-head comparison of left ventricular function assessment with 64-row computed tomography, biplane left cineventriculography, and both 2-and 3-dimensional transthoracic echocardiography: comparison with magnetic resonance imaging as the reference standard. J Am Coll Cardiol. 2012;59(21):1897–907.
27. Bonow RO, Carabello BA, Chatterjee K, et al. 2008 focused update incorporated into the ACC/AHA 2006 guidelines for the management of patients with valvular heart disease: a report of the American College of Cardiology/American Heart Association Task Force on Practice Guidelines (Writing Committee to revise the 1998 guidelines for the management of patients with valvular heart disease). Endorsed by the Society of Cardiovascular Anesthesiologists, Society for Cardiovascular Angiography and Interventions, and Society of Thoracic Surgeons. J Am Coll Cardiol. 2008;52(13):e1–142.
28. Kupfahl C, Honold M, Meinhardt G, Vogelsberg H, Wagner A, Mahrholdt H, Sechtem U. Evaluation of aortic stenosis by cardiovascular magnetic resonance imaging: comparison with established routine clinical techniques. Heart. 2004;90:893–901.
29. Van Pul C, de Jong NMCM, van Beek LM, Pasmans HLM, Wijn PFF, Visser RF. MRI for diagnosing aortic valve stenosis: a comparison study of MRI and ultrasound. Neth Heart J. 2005;13:11.
30. Garcia J, Kadem L, Larose E, Clavel MA, Pibarot P. Comparison between cardiovascular magnetic resonance and transthoracic Doppler echocardiography for the estimation of effective orifice area in aortic stenosis. J Cardiovasc Magn Reson. 2011;13:25.

31. Friedrich MG, Schulz-Menger J, et al. Quantification of valvular aortic stenosis by magnetic resonance imaging. Am Heart J. 2002;144(2):329–34.
32. John AS, Dill T, Brandt RR, Rau M, Ricken W, Bachmann G, Hamm CW. Magnetic resonance to assess the aortic valve area in aortic stenosis: how does it compare to current diagnostic standards? J Am Coll Cardiol. 2003;42(3):519–26.
33. Debl K, Djavidani B, Seitz J, Nitz W, Schmid FX, Muders F, Buchner S, Feuerbach S, Riegger G, Luchner A. Planimetry of aortic valve area in aortic stenosis by magnetic resonance imaging. Invest Radiol. 2005;40(10):631–6.
34. Malyar NM, Schlosser T, Barkhausen J, Gutersohn A, Buck T, Bartel T, Erbel R. Assessment of aortic valve area in aortic stenosis using cardiac magnetic resonance tomography: comparison with echocardiography. Cardiology. 2008;109(2):126–34.
35. Krishnam MS, Tomasian A, Iv M, Ruehm SG, Saleh R, Panknin C, Goldin JG. Left ventricular ejection fraction using 64-slice CT coronary angiography and new evaluation software: initial experience. Br J Radiol. 2008;81(966):450–5.
36. de Filippi CR, Willett DL, Brickner ME. Usefulness of dobutamine echocardiography in distinguishing severe from nonsevere valvular aortic stenosis in patients with depressed left ventricular function and low transvalvular gradients. Am J Cardiol. 1995;75:191–4.
37. Lange RA, Hillis LD. Dobutamine stress echocardiography in patients with low-gradient aortic stenosis. Circulation. 2006;113(14):1718–20.
38. Pereira JJ, Lauer MS, Bashir M, Afridi I, Blackstone EH, Stewart WJ, McCarthy PM, Thomas JD, Asher CR. Survival after aortic valve replacement for severe aortic stenosis with low transvalvular gradients and severe left ventricular dysfunction. J Am Coll Cardiol. 2002;39(8):1356–63.
39. Nishimura RA, Grantham JA, Connolly HM, Schaff HV, Higano ST, Holmes Jr DR. Low-output, low-gradient aortic stenosis in patients with depressed left ventricular systolic function: the clinical utility of the dobutamine challenge in the catheterization laboratory. Circulation. 2002;106(7):809–13.
40. Blais C, Burwash IG, Mundigler G, Dumesnil JG, Loho N, Rader F, Baumgartner H, Beanlands RS, Chayer B, Kadem L, Garcia D, Durand LG, Pibarot P. Projected valve area at normal flow rate improves the assessment of stenosis severity in patients with low-flow, low-gradient aortic stenosis: the multicenter TOPAS (Truly or Pseudo-Severe Aortic Stenosis) study. Circulation. 2006;113(5):711–21.
41. Tribouilloy C, Levy F, Rusinaru D, Gueret P, Petit-Eisenmann H, Baleynaud S, Jobic Y, Adams C, Lelong B, Pasquet A, Chauvel C, Metz D, Quere JP, Monin JL. Outcome after aortic valve replacement for low-flow/low-gradient aortic stenosis without contractile reserve on dobutamine stress echocardiography. J Am Coll Cardiol. 2009;53(20):1865–73.
42. Levy F, Laurent M, Monin JL, Maillet JM, Pasquet A, Le Tourneau T, Petit-Eisenmann H, Gori M, Jobic Y, Bauer F, Chauvel C, Leguerrier A, Tribouilloy C. Aortic valve replacement for low-flow/low-gradient aortic stenosis operative risk stratification and long-term outcome: a European multicenter study. J Am Coll Cardiol. 2008;51(15):1466–72.
43. Ozkan A, Hachamovitch R, Kapadia SR, Tuzcu EM, Marwick TH. Impact of aortic valve replacement on outcome of symptomatic patients with severe aortic stenosis with low gradient and preserved left ventricular ejection fraction. Circulation. 2013;128(6):622–31.
44. Connolly HM, Oh JK, Orszulak TA, Osborn SL, Roger VL, Hodge DO, Bailey KR, Seward JB, Tajik AJ. Aortic valve replacement for aortic stenosis with severe left ventricular dysfunction. Prognostic indicators. Circulation. 1997;95(10):2395–400.
45. Barone-Rochette G, Pierard S, Seldrum S, de Meester Ravenstein C, Melchior J, Maes F, Pouleur AC, Vancraeynest D, Pasquet A, Vanoverschelde JL, Gerber BL. Aortic valve area, stroke volume, left ventricular hypertrophy, remodeling, and fibrosis in aortic stenosis assessed by cardiac magnetic resonance imaging: comparison between high and low gradient and normal and low flow aortic stenosis. Circ Cardiovasc Imaging. 2013;6(6):1009–17.
46. Cramariuc D, Cioffi G, Rieck AE, Devereux RB, Staal EM, Ray S, Wachtell K, Gerdts E. Low-flow aortic stenosis in asymptomatic patients: valvular-arterial impedance and systolic function from the SEAS substudy. JACC Cardiovasc Imaging. 2009;2(4):390–9.
47. Lancellotti P, Donal E, Magne J, Moonen M, O'Connor K, Daubert JC, Pierard LA. Risk stratification in asymptomatic moderate to severe aortic stenosis: the importance of the valvular, arterial and ventricular interplay. Heart. 2010;96(17):1364–71.
48. Hachicha Z, Dumesnil JG, Pibarot P. Usefulness of the valvuloarterial impedance to predict adverse outcome in asymptomatic aortic stenosis. J Am Coll Cardiol. 2009;54(11):1003–11.
49. Pibarot P, Dumesnil JG. Improving assessment of aortic stenosis. J Am Coll Cardiol. 2012;60(3):169–80.
50. Thomas B, Freitas A, Ferreira R, Tavares NJ. The complementary role of cardiac magnetic resonance imaging in the evaluation of patients with aortic stenosis. Rev Port Cardiol. 2005;24(9):1117–21.
51. Dimitriou P, Kahari A, Emilsson K, Thunberg P. Cardiovascular magnetic resonance imaging and transthoracic echocardiography in the assessment of stenotic aortic valve area: a comparative study. Acta Radiol. 2012;53(9):995–1003.
52. Michelena HI, Margaryan E, Miller FA, Eleid M, Maalouf J, Suri R, Messika-Zeitoun D, Pellikka PA, Enriquez-Sarano M. Inconsistent echocardiographic grading of aortic stenosis: is the left ventricular outflow tract important? Heart. 2013;99(13):921–31.
53. Garcia D, Pibarot P, Dumesnil JG, Sakr F, Durand LG. Assessment of aortic valve stenosis severity: a new index based on the energy loss concept. Circulation. 2000;101(7):765–71.
54. Bahlmann E, Cramariuc D, Gerdts E, Gohlke-Baerwolf C, Nienaber CA, Eriksen E, Wachtell K,

Chambers J, Kuck KH, Ray S. Impact of pressure recovery on echocardiographic assessment of asymptomatic aortic stenosis: a SEAS substudy. JACC Cardiovasc Imaging. 2010;3(6):555–62.
55. Bahlmann E, Gerdts E, Cramariuc D, Gohlke-Baerwolf C, Nienaber CA, Wachtell K, Seifert R, Chambers JB, Kuck KH, Ray S. Prognostic value of energy loss index in asymptomatic aortic stenosis. Circulation. 2013;127(10):1149–56.
56. Van der Linde D, Rossi A, Yap SC, McGhie JS, van den Bosch AE, Kirschbaum SW, Russo B, van Dijk AP, Moelker A, Krestin GP, van Geuns RJ, Roos-Hesselink JW. Ascending aortic diameters in congenital aortic stenosis: cardiac magnetic resonance versus transthoracic echocardiography. Echocardiography. 2013;30(5):497–504.
57. Leong DP, Joseph MX, Selvanayagam JB. The evolving role of multimodality imaging in valvular heart disease. Heart. 2014;100(4):336–46.
58. Abbas AE, Franey LM, Goldstein J, Lester S. Aortic valve stenosis: to the gradient and beyond-the mismatch between area and gradient severity. J Interv Cardiol. 2013;26(2):183–94.
59. Masci PG, Dymarkowski S, Bogaert J. Valvular heart disease: what does cardiovascular MRI add? Eur Radiol. 2008;18(2):197–208.
60. Puymirat E, Chassaing S, Trinquart L, Barbey C, Chaudeurge A, Bar O, Blanchard D. Hakki's formula for measurement of aortic valve area by magnetic resonance imaging. Am J Cardiol. 2010;106(2): 249–54.
61. Haghi D, Kaden JJ, Suselbeck T, Fluechter S, Breithardt OA, Poerner T, Kalmar G, Borggrefe M, Papavassiliu T. Validation of the peak to mean pressure decrease ratio as a new method of assessing aortic stenosis using the Gorlin formula and the cardiovascular magnetic resonance-based hybrid method. Echocardiography. 2007;24(4):335–9.
62. Gorlin R, Gorlin SG. Hydraulic formula for calculation of the area of the stenotic mitral valve, other cardiac valves, and central circulatory shunts. Am Heart J. 1951;41:1–29.
63. Hakki AH, Iskandrian AS, Bemis CE, Kimbiris D, Mintz GS, Segal BL, Brice C. A simplified valve formula for the calculation of stenotic cardiac valve areas. Circulation. 1981;63:1050–5.
64. Cueff C, Serfaty JM, Cimadevilla C, Laissy JP, Himbert D, Tubach F, Duval X, Iung B, Enriquez-Sarano M, Vahanian A, Messika-Zeitoun D. Measurement of aortic valve calcification using multislice computed tomography: correlation with haemodynamic severity of aortic stenosis and clinical implication for patients with low ejection fraction. Heart. 2011;97(9):721–6.
65. Utsunomiya H, Yamamoto H, Kunita E, Kitagawa T, Ohashi N, Oka T, Yamazato R, Horiguchi J, Kihara Y. Combined presence of aortic valve calcification and mitral annular calcification as a marker of the extent and vulnerable characteristics of coronary artery plaque assessed by 64-multidetector computed tomography. Atherosclerosis. 2010;213(1):166–72.
66. Warnes CA. Bicuspid aortic valve and coarctation: two villains part of a diffuse problem. Heart. 2003; 89:965–6.
67. Dyverfeldt P, Hope MD, Tseng EE, Saloner D. Magnetic resonance measurement of turbulent kinetic energy for the estimation of irreversible pressure loss in aortic stenosis. JACC Cardiovasc Imaging. 2013;6(1):64–71.
68. Biederman RW, Doyle M, Yamrozik J, Williams RB, Rathi VK, Vido D, Caruppannan K, Osman N, Bress V, Rayarao G, Biederman CM, Mankad S, Magovern JA, Reichek N. Physiologic compensation is supranormal in compensated aortic stenosis: does it return to normal after aortic valve replacement or is it blunted by coexistent coronary artery disease? An intramyocardial magnetic resonance imaging study. Circulation. 2005;112(9 Suppl):I429–36.
69. Biederman RW, Magovern JA, Grant SB, Williams RB, Yamrozik JA, Vido DA, Rathi VK, Rayarao G, Caruppannan K, Doyle M. LV reverse remodeling imparted by aortic valve replacement for severe aortic stenosis; is it durable? A cardiovascular MRI study sponsored by the American Heart Association. J Cardiothorac Surg. 2011;6:53.
70. Hoffman JIE. The natural and unnatural history of congenital heart disease. Chichester/Hoboken: Wiley-Blackwell; 2009.
71. Aboulhosn J, Child JS. Left ventricular outflow obstruction: subaortic stenosis, bicuspid aortic valve, supravalvar aortic stenosis, and coarctation of the aorta. Circulation. 2006;114:2412–22.
72. van der Linde D, Takkenberg JJ, Rizopoulos D, et al. Natural history of discrete subaortic stenosis is adults: a multicenter study. Eur Heart J. 2013;34(21):1548–56.
73. Leichter DA, Sullivan I, Gersony WN. Acquired discrete subvalvular aortic stenosis: natural history and hemodynamics. J Am Coll Cardiol. 1989;14: 1539–44.
74. Trinchero R, Demarie D, Orzan F, Presbitero P, Defilippi G, Brusca A, Ottino G, Morea M. Fixed subaortic stenosis: natural history of patients with mild obstruction and follow-up of operated patients. G Ital Cardiol. 1988;18:738–44.

8 Area and Gradient Mismatch: The Discordance of a Small Valve Area and Low Gradients

Laura M. Franey, Steven J. Lester, Frances O. Wood, and Amr E. Abbas

Abstract

While the clinical severity of aortic stenosis (AS) is based largely on symptoms, indications for surgical aortic valve replacement (SAVR) and/or transcutaneous (TAVR) rely upon calculated estimates of the hemodynamic significance and degree of valvular stenosis. Severe AS is defined as an aortic valve area (AVA) <1.0 cm^2 or indexed AVA <0.6 cm^2/m^2, mean transvalvular pressure gradient (ΔP) >40 mmHg, and/or peak trans-aortic velocity >4 m/s by Doppler echocardiography. Whether the above conditions must be met individually or collectively remains unclear. As noted, "area/gradient match" occurs when both the AVA and ΔP fall within the severe range. This may occur regardless of the presence of normal or abnormal ejection fraction and regardless of the presence or absence of low flow (defined as a stroke volume index on echocardiography <35 ml/m^2). However, the AVA may be in the severe range, while the gradient may be in the non-severe range. This has been referred to as area/gradient mismatch and will be discussed further in this chapter.

Keywords

Aortic stenosis severity • Surgical aortic valve replacement (SAVR) • Transcutaneous aortic valve replacement (TAVR) • Area/gradient match • Low flow area-gradient mismatch

L.M. Franey, MD (✉) • F.O. Wood, MD
A.E. Abbas, MD, FACC, FSCAI, FSVM, FASE, RPVI (✉)
Department of Cardiovascular Medicine, Beaumont Health, Oakland University/William Beaumont School of Medicine, Royal Oak, MI, USA
e-mail: laura.goodman@beaumont.edu; aabbas@beaumont.edu

S.J. Lester, MD
Department of Medicine, Mayo Clinic, Scottsdale, AZ, USA

A.E. Abbas (ed.), *Aortic Stenosis: Case-Based Diagnosis and Therapy*,
DOI 10.1007/978-1-4471-5242-2_8

Introduction

While the clinical severity of aortic stenosis (AS) is based largely on symptoms, indications for surgical aortic valve replacement (SAVR) and/or transcutaneous (TAVR) rely upon calculated estimates of the hemodynamic significance and degree of valvular stenosis. Severe AS is defined as an aortic valve area (AVA) <1.0 cm^2 or indexed AVA <0.6 cm^2/m^2, mean trans-valvular pressure gradient (ΔP) >40 mmHg, and/or peak trans-aortic velocity >4 m/s by Doppler echocardiography [1, 2]. Whether the above conditions must be met individually or collectively remains unclear [3]. As noted, "area/gradient match" occurs when both the AVA and ΔP fall within the severe range. This may occur regardless of the presence of normal or abnormal ejection fraction and regardless of the presence or absence of low flow (defined as a stroke volume index on echocardiography ≤35 ml/m^2) [4].

In the presence of measurement or assumption errors, discordance of area and gradient measures of AS severity may occur. Additionally, this discordance may occur with a decrease in transvalvular flow that causes a decline in the trans aortic valve ΔP for a given AVA. This is due to the fact that the ΔP is more dependent, than the AVA, on trans-valvular flow [3, 5, 6]. As such, in the presence of low flow states, clinical scenarios may arise where the AVA suggests severe AS while the ΔP falls within the non-severe range. We previously proposed the term "area-gradient mismatch" to describe such a clinical entity of discordant area and gradient measures of AS severity [7]. This chapter will summarize common etiologies and examples of area-gradient mismatch including errors of measurement and/or assumption, and low flow states with and without preserved left ventricular ejection fraction (LVEF). The clinical approach to patients presenting with area-gradient mismatch as well as the prognosis for individual subgroups will also be reviewed.

Errors of Measurement

The continuity equation, based on the principle conservation of mass (that flow across the left ventricular outflow tract (LVOT) is equal to flow across the aortic valve), is most commonly used to estimate the aortic valve area by Doppler echocardiography [8]. The continuity equation assumes the LVOT is circular with area equal to πr^2. As such, any error in measurement of the LVOT diameter is magnified exponentially [7]. Even with accurate measurement of the LVOT diameter with echocardiography, studies have shown that 2D echo-derived LVOT area underestimates the true LVOT area, as assessed by CTA or 3D echocardiography by about 17 % ± 16 %.

Moreover, velocities obtained by Doppler must have parallel intercept angles with the direction of trans-valvular flow, limiting underestimation of amplitude parameters as noted in the Doppler frequency shift equation [8]. Finally, beat-to-beat variation of the Doppler waveform in atrial fibrillation may also be a source of measurement error and is resolved by averaging several beats [9].

With catheter-based techniques, measurement errors in cardiac output and ΔP may lead to errors in AVA calculations by the Gorlin formula. ΔP is obtained via a double lumen single catheter, dual catheters, or pull back of a single catheter across the AV. Poor balancing, air bubbles in transducers, or the positioning of the transducer either too high or too low in relation to the patient may account for errors. Moreover, utilizing the pressure difference between the left ventricular catheter and the femoral line rather than the ascending aorta as a surrogate for trans-aortic gradient may overestimate ΔP in the presence of descending aortic or iliac stenosis. Inherent errors in estimating the cardiac output may also account for errors of area measurement as may occur with utilizing an erroneous constant, utilizing estimated rather than measured O_2 consumption with Fick method, or using the thermodilution method with severe tricuspid regurgitation, atrial fibrillation, or low cardiac output. Finally, reports of the flow dependency of the constant in the Gorlin equation may also explain potential measurement errors with flow variations.

Errors of Assumption

After verification of correct hemodynamic calculations, approximately 30 % of patients with a measured of AVA <1.0 cm^2 will still have

ΔP_{mean} <40 mmHg by Doppler echocardiography [3]. Current clinical guidelines do not state whether an AVA <1.0 cm^2 is sufficient to determine severe stenosis, or whether a ΔP_{mean} >40 mmHg is also required. Moreover, there is no differentiation between invasive and noninvasive measurements [7]. After excluding erroneous echocardiographic data and low flow conditions, one catheterization study of AS patients confirmed the above scenario to be present in 48 % of area-gradient mismatch patients and in 12 % of the entire AS cohort, suggesting errors of assumption and inconsistent grading by current society recommendations [10]. By example, according to the Gorlin formula, an AVA of <0.81 cm^2 results in an expected ΔP_{mean} of 40 mmHg, however with an AVA of 1 cm^2, the expected ΔP_{mean} is only 28 mmHg [2, 3]. Thus, despite a calculated AVA ≤1 cm^2 under normal flow conditions, the ΔP_{mean} may remain lower than the assumed 40 mmHg (normal flow/low-gradient or NF/LG AS). Normal flow/low gradient AS is considered an early form of the disease with the best clinical prognosis and a 3-year cardiac event-free survival of 66 % [4]. Nevertheless, in clinical practice ΔP_{mean} >40 mmHg are often generated in patients with an AVA between 0.8 and 1.0 cm^2 [2, 3].

Low Flow Area-Gradient Mismatch

Low flow conditions, defined as a stroke volume index (SVI) <35 mL/m^2, may contribute to clinical cases of area-gradient mismatch. Such scenarios may occur with either a depressed or preserved LVEF and render lower than expected pressure gradients in the setting of an AVA <1 cm^2 [3].

Low Flow/Low Gradient AS with Depressed LVEF (Low LVEF Area-Gradient Mismatch)

The subset of patients with an AVA <0.7–1.2 cm^2, ΔP_{mean} <30–40 mmHg, and an LVEF <30–40 %, is classified as low flow/low gradient (LF/LG) AS with depressed LVEF, representing 5–10 % of the severe AS population [11]. The reduced LVEF in such patients may be related to intrinsic myocardial disease or failure of compensatory LV hypertrophy to normalize wall stress causing an afterload mismatch with subsequent decreased LV function [7]. The ensuing clinical dilemma results from determining whether the AVA is truly severe or rather a reflection of the inability of the LV to provide enough inertial force to open the valve and generate a significant ΔP. Additionally, as previously noted, the constant in the Gorlin equation appears to be flow-dependent, potentially underestimating the AVA in low flow conditions [5, 12].

In an effort to help resolve such clinical discrepancies, contemporary protocols attempt to increase flow across the AV using dobutamine infusion during catheterization or echocardiography, classifying patients into three categories [13]:

- **True-severe AS** where dobutamine induces a >20 % increase in SV with an associated increase in ΔP_{mean} and no change in AVA (Fig. 8.1, Table 8.1)
- **Pseudo-severe AS** where dobutamine induces a >20 % increase in SV with an associated increase in AVA and no change in ΔP_{mean} (Fig. 8.2, Table 8.2), and
- **Indeterminate AS** without contractile reserve where dobutamine infusion fails to increase SV (Fig. 8.3, Table 8.3)

Whether dobutamine truly distinguishes between different types of LF/LG AS with depressed LV EF or merely assesses flow-related changes to the effective orifice area (EOA) has come to question. Nevertheless, dobutamine infusion remains routine in clinical practice to help evaluate individual surgical risk and prognosis [2]. Previous studies have shown that patients with a ΔP_{mean} >30 mmHg at baseline or following dobutamine infusion likely have true or fixed AS with a better prognosis and improved LV function following AVR [5, 11, 14]. In general, AS patients with depressed LVEF have worse outcomes following surgery than those with preserved LVEF. However, regardless of the subtype as determined by dobutamine, all patients

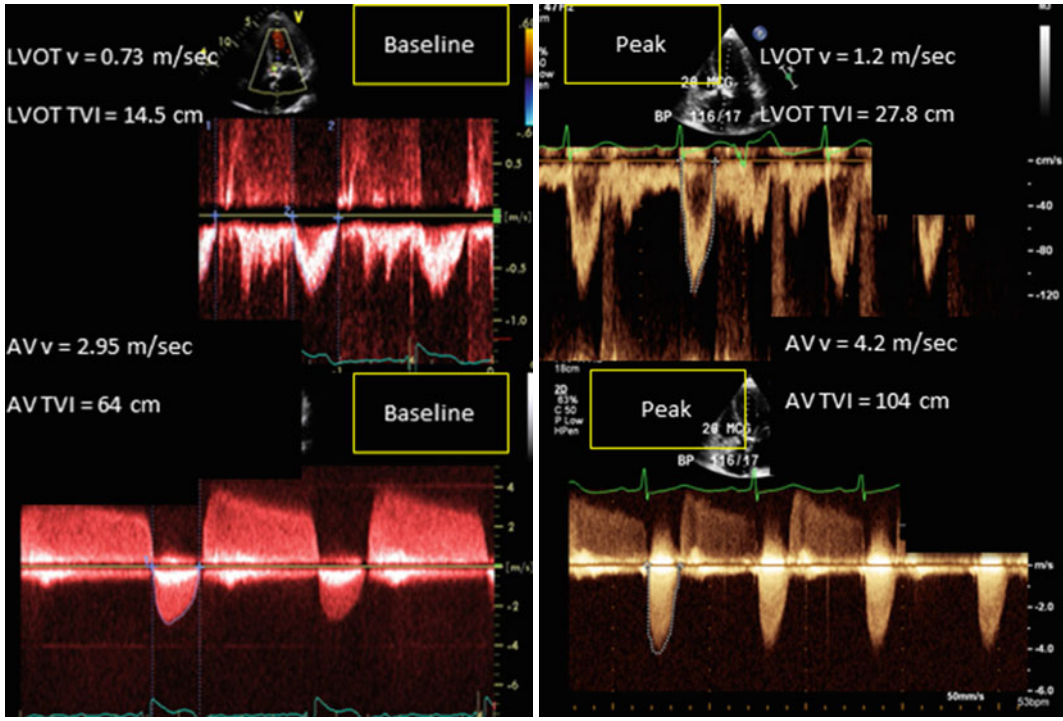

Fig. 8.1 True-severe low flow/low gradient severe AS with depressed EF and contractile reserve. 85 year-old female with class III heart failure, EF 40 %, coronary artery disease, chronic kidney disease, chronic obstructive lung disease on O_2, atrial fibrillation, and known aortic stenosis: She underwent Dobutamine echocardiography (see Table 8.1)

Table 8.1 True-severe low flow/low gradient severe AS with depressed EF and contractile reserve

Variable	Baseline	Peak dobutamine
LVOT Vmax (m/s)	0.73	1.2
LVOT TVI (cm)	14.5	27.8
LVOT Diameter (cm)	2	2
SVI (ml/m^2)	27	48.5
AVA (cm^2)	0.8	0.84
AV Vmax (m/s)	2.95	4.2
AV TVI (cm)	64	104
ΔP_{mean} (mmHg)	20.5	43
ΔP_{MIG} (mmHg)	34.75	70.3
DI	0.24	0.26

with low flow/low gradient with depressed ejection fraction and severe AS have a higher mortality in the absence of surgery [5, 12].

As there may be significant patient-to-patient variability in the peak trans-valvular flow rates achieved with dobutamine infusion, other parameters have been studied to improve the diagnostic accuracy of this test in the evaluation of LF/LG AS [15]. The projected AVA (AVAproj) defined as the expected AVA at a standardized flow rate of 250 mL/s is derived from the regression slope of AVA versus flow during dobutamine infusion and accounts for individual variations in flow augmentation in response to dobutamine [5, 11, 15] (Fig. 8.4, Table 8.4). An $AVA_{proj} \geq 1.2\ cm^2$, together with a peak dobutamine EF >35 %, and high Duke activity status index, denote a good prognosis [5, 11, 15].

$$AVA_{proj} = AVA_{rest} + (AVA_{peak} - AVA_{rest}/Q_{peak} - Q_{rest})\ (250 - Q_{rest})$$

Where AVA = aortic valve area, AVA_{rest} = aortic valve area at rest, AVA_{peak} = aortic valve area at peak dobutamine, Q = stroke volume/LV ejection time, Q_{rest} = Q at rest, Q_{peak} = Q at peak dobutamine.

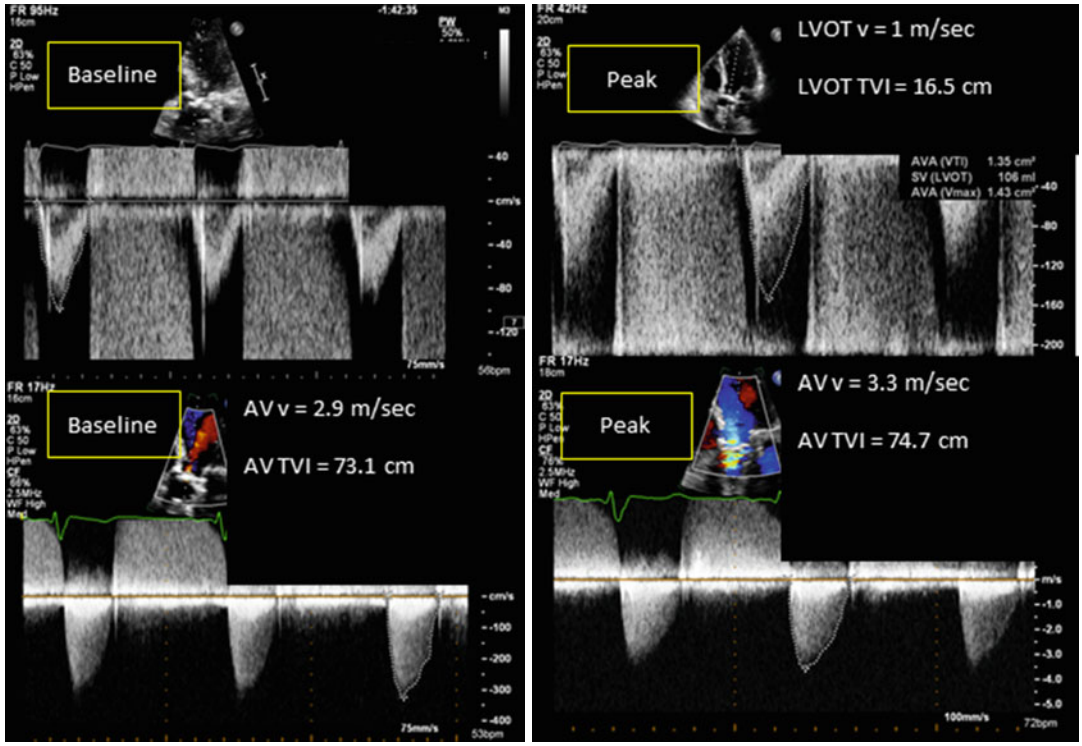

Fig. 8.2 Pseudo-severe low flow/low gradient AS with depressed EF and contractile reserve 81 year-old male with class III heart failure, EF 30 %, CAD, pulmonary hypertension, and known aortic stenosis: She underwent Dobutamine echocardiography (see Table 8.2)

Table 8.2 Pseudo-severe low flow/low gradient AS with depressed EF and contractile reserve

Variable	Baseline	Peak dobutamine
LVOT Vmax (m/s)	1	1.5
LVOT TVI (cm)	16.5	28.7
LVOT diameter (cm)	2.3	2.3
SVI (ml/m^2)	34	59
AVA (cm^2)	0.9	1.5
AV Vmax (m/s)	2.9	3.3
AV TVI (cm)	73.1	74.7
ΔP_{mean} (mmHg)	19	23
ΔP_{MIG} (mmHg)	33.6	43.5
DI	0.22	0.38

Other useful parameters in the assessment of LF/LG AS include the dimensionless index (DI) and AV resistance (Table 8.5). While AV resistance may be less flow dependent than other variables, its usefulness in this patient population remains controversial [9]. In one study, an AV resistance value <1.5 WU identified pseudo-severe AS while a value >2.25 WU identified true, severe AS. Values between 1.5 and 2.25 WU were considered indeterminate [16].

Low Flow/Low Gradient AS with Preserved LVEF (Normal LVEF Area-Gradient Mismatch)

The subset of patients with an indexed AVA <0.6 cm/m^2, ΔP_{mean} <40 mmHg, LVEF >50 %, and SVI <35 mL/m^2 is classified as low flow/low gradient AS with preserved LVEF, or paradoxical low flow/low gradient AS (PLF/LG AS) (Fig. 8.5, Table 8.6) [2, 9]. The low flow state in such patients may be explained by three components

- ***Diastolic or valve component*** limiting adequate ventricular filling or preload in thicker, smaller ventricles, manifested by lower LVOT

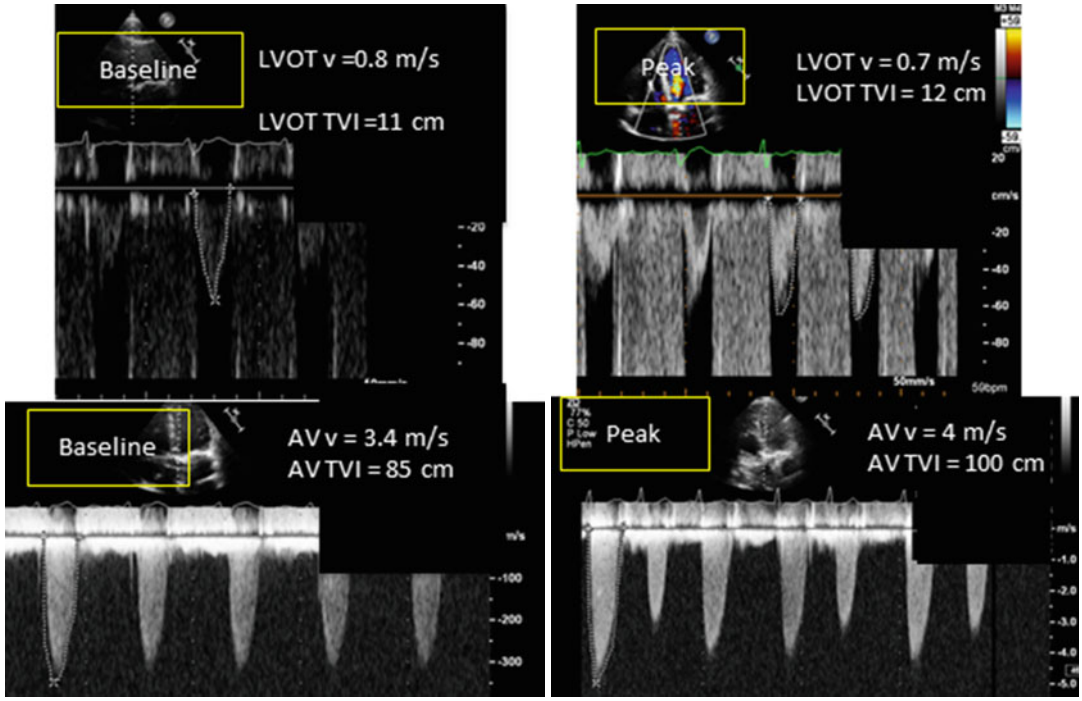

Fig. 8.3 Indeterminate flow/Low gradient AS with depressed EF and no contractile reserve. 85 year-old male with class III heart failure, EF 35 %, coronary artery disease, chronic kidney disease, chronic obstructive lung disease, bilateral carotid end arterectomy, atrial fibrillation, and known aortic stenosis: She underwent Dobutamine echocardiography (see Table 8.3)

Table 8.3 Indeterminate flow/Low gradient AS with depressed EF and no contractile reserve

Variable	Baseline (average beats)	Peak dobutamine (average beats)
LVOT Vmax (m/s)	0.8	0.7
LVOT TVI (cm)	11.3	12.2
LVOT diameter (cm)	1.8	1.8
SVI (ml/m^2)	14.6	15.6
AVA (cm^2)	0.3	0.24
AV Vmax (m/s)	3.4	4
AV TVI (cm)	85.5	100
ΔP_{mean} (mmHg)	31	42
ΔP_{MIG} (mmHg)	46.2	64
DI	0.13	0.12

and LV end diastolic diameters and increased relative wall thickness [2, 16]

- ***Myocardial component*** characterized by decreased contractility and intrinsic myocardial dysfunction with decreased global longitudinal strain and a relatively normal LVEF, yet lower than anticipated for the degree of LV hypertrophy [3, 17], and
- ***Vascular component*** with an increased hemodynamic burden or afterload on the LV through decreased systemic arterial compliance, increased blood pressure, and increased systemic vascular resistance causing higher vascular impedance [3, 17].

Evaluating the global LV hemodynamic burden in AS patients is essential to the complete understanding of individual trans-valvular flow

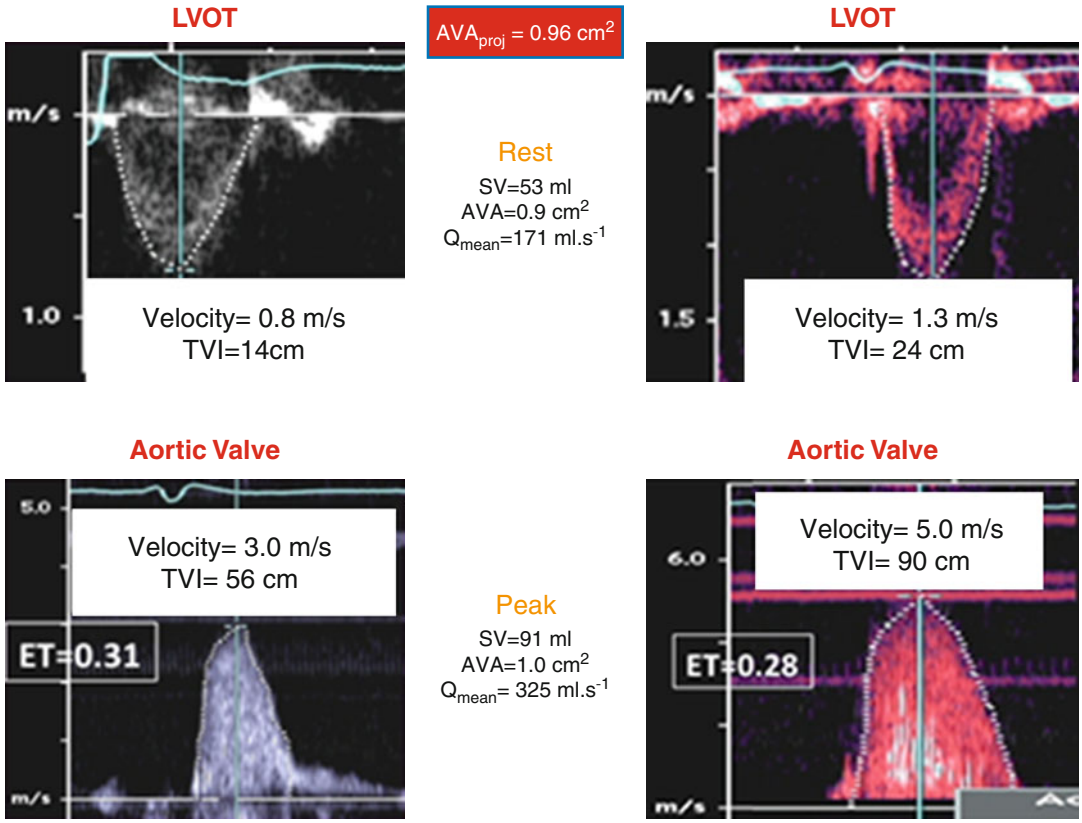

Fig. 8.4 Projected aortic valve area (AVA_{proj}) calculation. 75 year-old female with class III heart failure, EF 30 %, coronary artery disease, chronic kidney disease, DM, and known aortic stenosis: She underwent Dobutamine echocardiography (see Table 8.4)

Table 8.4 Projected aortic valve area (AVA_{proj}) calculation

Variable	Baseline	Peak dobutamine
LVOT Vmax (m/s)	0.8	1.3
LVOT TVI (cm)	14	24
Ejection time (s)	0.31	0.28
SV (ml)	*53*	91
Q_{mean} (ml.s^{-1})	171 (53/0.31)	325 (91/0.28)
SVI (ml/m^2)	26	40
AVA (cm^2)	0.9	1.0
AV Vmax (m/s)	3	5
AV TVI (cm)	56	90
ΔP_{mean} (mmHg)	26	52
ΔP_{MIG} (mmHg)	36	100

$AVA_{proj} = AVA_{rest} + (AVA_{peak} - AVA_{rest}/Q_{peak} - Q_{rest})\ (250 - Q_{rest})$

$AVA_{proj} = 0.9 + (1 - 0.9/325 - 171)(250 - 171) = 0.96\ cm^2$

dynamics and may be assessed by several methods [3, 17–19] (Table 8.7). One such approach is determining the valvulo-arterial impedance (Z_{va}), which is equal to the systolic blood pressure plus the mean ΔP divided by the stroke volume index [3, 17]. As demonstrated by the above calculation, the Z_{va} accounts for the valvular and post-valvular afterload burden imposed on the LV. Under normal circumstances, the Z_{va} is <5.5 mmHg/mL/m^2. In patients with PLF/LG AS higher values are associated with worse prognosis [3, 17]. Normalized LV stroke work (LV stroke work/stroke volume) is a newly introduced non-invasive variable obtained from echocardiography and cardiac MRI to also assess global load and account for both perivalvular and valvular loads [18].

Table 8.5 Alternative methods to assess AS severity in patients with area/gradient mismatch

Method	Assessment	Calculation	Critical value/use
Dimensionless index (DI) (All AS)	Echocardiography	LVOT TVI or V/aortic valve TVI or V	< 0.25
AV resistance (AVΩ) (LF/LG AS)	Echocardiography invasive	$1{,}333 \times \Delta$Pmean/Q (SV/LV ESP) $1{,}333 \times 4\ V^2/r^2_{LVOT} x\ v_{LVOT}$	<2.75 WU
Projected valve area at normal flow rate (AVA_{proj}) (LF/LG AS)	Dobutamine (echocardiography or catheterization)	$AVA_{rest} + AVA_{comp} \times (250–Q_{rest})$	≤1.2 cm^2
Energy loss index (ELI) (accounts for PR)	Echocardiography	AVA × Aa/Aa-AVA/BSA	<0.52 cm^2/m^2
AV calcification (All AS)	CT scan Echocardiography	Extent of AV calcification	>1,650 AU
			4/4
iEOA (native and $AVA_{prosthesis}$)	Doppler, invasive, and MRI	Effective orifice Area/BSA	<0.6 cm/m^2 native
			<0.65 cm/m^2 PPM

Aa ascending aorta diameter, *BSA* body surface area, *WU* wood units, P_{distal} pressure in the ascending aorta distal to the vena contracta, P_{vc} pressure at the vena contracta, *r* LVOT radius, *v* LVOT velocity, AVA_{comp} valve compliance derived as the slope of regression line fitted to the AVA versus Q plot, *PPM* prosthesis patient mismatch

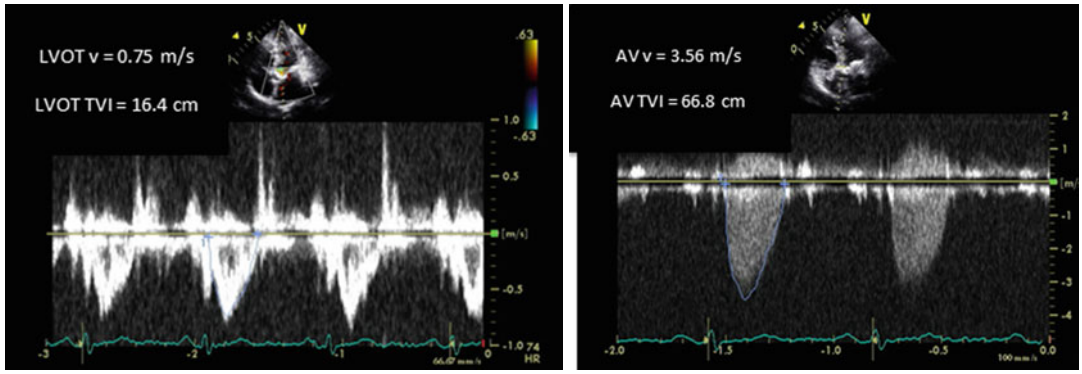

Fig. 8.5 Paradoxically low flow/low gradient severe AS with preserved EF. 82 year-old male presents with syncope, EF 60 %, hypertension, dyslipidemia, pacemaker for high grade AV block, and known aortic stenosis (see Table 8.6)

A recent study described >40 % of patients with PLF/LG AS were reclassified after using a 3D measure of LVOT area in the continuity equation, suggesting that the continuity equation may underestimate the AVA in low flow states and/or a portion of these patients may actually have moderate AS with an overestimation of their AV stenosis.

Some studies have suggested that PLF/LG AS patients are referred later for AVR as compared with patients with normal flow/high gradient (NF/HG) AS, perhaps contributing to the worse clinical outcomes observed in this group [3, 17, 20]. Alternatively, one Doppler study of 1,525 asymptomatic AS patients compared prognosis between those with moderate AS and those with PLF/LG AS [21]. The study showed a similar prognosis in both groups over a follow up period of 46 months [21]. These results were recently challenged by Lancellotti et al. in a paper contending a high rate of patient overlap and misclassification in the previous study with a large percentage of PLF/LG classified patients actually having normal flow dynamics and similar AVAs between groups (PLF/LG AS AVA of 0.99 cm^2 and moderate AS AVA of 1.01 cm^2) [4]. Moreover, this paper validated the poor prognosis of

PLF/LG AS patients quoting a 3-year event-free rate fivefold lower than the NF/HG AS group [4].

Utilizing the dimensionless index in this patient population may be helpful in confirming the diagnosis of severe AS despite a low ΔP as the index may remain in the critical range due to a decreased LVOT velocity and/or time velocity integral in the presence of a low SVI (Table 8.5) [17]. Dobutamine infusion and estimation of the AVA_{proj} has also been proposed in these patients in a similar fashion as those patients with depressed EF.

Of note, approximately 15 % of patients in this group are able to generate high ΔP despite a low flow state [3]. These patients are classified as having low flow/high gradient AS (LF/HG AS) and have better outcomes as compared to PLF/LG AS patients with a 3 year event free rate comparable to NF/LG AS patients [3, 4]. The low flow state in this group may represent an early subclinical marker of intrinsic myocardial dysfunction despite a preserved LVEF [4].

Table 8.6 Paradoxically low flow/low gradient severe AS with preserved EF

Variable	Baseline
LVOT Vmax (m/s)	0.75
LVOT TVI (cm)	16.4
LVOT diameter (cm)	2
SVI (ml/m^2)	33.6
AVA (cm^2)	0.77
AV Vmax (m/s)	3.56
AV TVI (cm)	66.8
ΔP_{mean} (mmHg)	27.2
ΔP_{MIG} (mmHg)	50.7
DI	0.24

Clinical Implications

Determining the true hemodynamic severity of AS is fundamental in the counseling of patients on the need and timing of AVR. In most cases,

Table 8.7 Methods of assessing left ventricular hemodynamic burden

Method	Definition	Calculation/assessment	Change suggesting increased LV hemodynamic load
LV% stroke work loss (SWL)	% of LV work wasted during systole for flow across the AV	$(\Delta P_{mean}/\Delta P_{mean} + SBP) \times 100$ Doppler/invasive	Increase >25 %
Stroke work index (SWI)	Cardiac trans-systemic workload per beat	(MAP-PCWP) × SVI × 0.0136 Invasive	Increase
Cardiac work index (CWI)	Cardiac trans-systemic workload per minute	(MAP – PCWP) × CI × 0.0136 Invasive	Increase
Systemic vascular resistance (SVR)	Representative of static vascular load	(MAP – RAP)/CO Invasive	Increase >25 WU
Systemic arterial compliance (SAC)	Representative of pulsatile vascular load	SVI/PP Doppler/invasive	Decrease ≤0.6 $ml.mmHg^{-1}.m^{-2}$
Valvulo-arterial impedance (Zva)	Cost in mmHg for each mL of blood ejected. global load	SBP + ΔPmean/SVI Doppler/invasive	Increase Z_{va} is >4.5 $mmHg/ml^{-1}/m^2$
Brain natriuretic peptide (BNP)		Laboratory measurement	Increase >500
Myocardial fibrosis		Cardiac MRI	Increase Severe late gadolinium enhancement
Global myocardial longitudinal strain		Speckle tracking echocardiography	Decrease <15 %
Normalized LV stroke work	Global load	LV stroke work/stroke volume Doppler/cardiac MRI	Increase

the severity of AS may be clearly ascertained by Doppler echocardiography and/or cardiac catheterization. In contrast, a proportion of patients may present with a discrepancy between AVA and ΔP with regard to the degree of AS severity, posing an increased challenge in clinical decision making.

As discussed above, the AVA_{proj} may enhance the traditional role of dobutamine echocardiography in further risk stratifying LF/LG AS patients with depressed LVEF [5]. Irrespective of flow, LVEF, or ΔP, patients in this group with an AVA <1.0 cm^2 tend to have better outcomes with AVR as compared to medical therapy alone, albeit with a wide variation in mortality [12, 14]. Moreover, the higher the LVEF and ΔP, the better the clinical outcome following surgery [12, 14]. Accordingly, these patients should not be deprived of surgical consultation solely due to a low ΔP or LV systolic dysfunction.

Patients with severe AS and preserved LVEF have been recently classified into 4 groups based on flow dynamics and trans-valvular gradients: NF/HG, NF/LG, LF/HG, and PLF/LG AS with both NF/LG and PLF/LG exhibiting area-gradient mismatch see (Fig. 8.6) [4]. NF/HG AS remains the most common form of severe AS with a prevalence of 52 % and a 3-year event rate (death or need for surgery) of 33 % [4]. NF/LG AS, considered an early form of the disease, has the best clinical prognosis, followed by NF/HG and LF/HG AS. Reports regarding outcomes of patients with PLF/LG AS are inconsistent, however this group likely carries the worst prognosis [4, 21]. The 2-year cardiac event-free rate was 83 % ± 6 % for NF/LG (52 % of cases), 44 % ± 6 % for NF/HG (31 % of cases), 30 % ± 12 % for LF/HG (10 % of cases), and 27 % ± 13 % for LF/LG (7 % of cases) groups in one study [4]. The BNP levels were 22 (13–44), 47.5 (32–74), 114 (68–133), 78 (66–101) pg/dl, respectively [4]. The value of Z_{va} in predicting outcomes in each subgroup requires further study. Brain natriuretic peptide (BNP) may also carry prognostic implications as studies have shown that as LV longitudinal strain declines, myocardial fibrosis and BNP levels increase in a manner that parallels the prognosis of the various subgroups mentioned above [4, 22]. A suggested approach for the evaluation of patients with AS and area-gradient mismatch is outlined in Fig. 8.7.

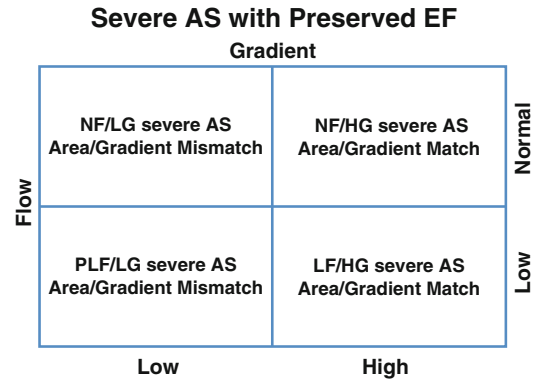

Fig. 8.6 Clinical evaluation of AS severity

Conclusion

AS severity is primarily determined by invasive and non-invasive estimations of AVA and ΔP. Uncertainty with regard to AS severity may occur when a mismatch between area and gradient determinations are present. The cause of such discrepancies must be elucidated so as to best counsel patients on the most ideal treatment strategy.

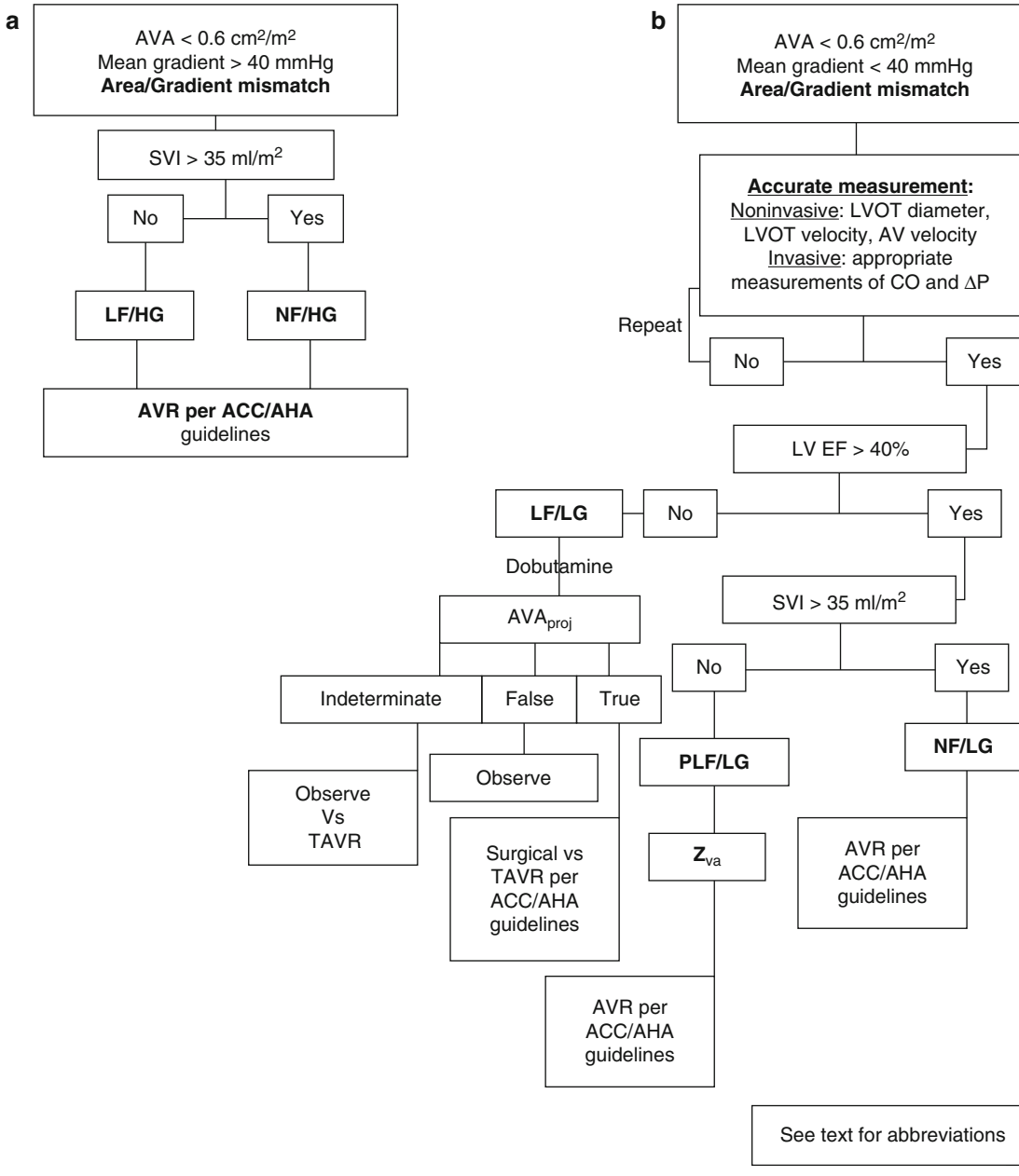

Fig. 8.7 (**a**, **b**) Evaluation and management of patients with aortic stenosis and area/gradient mismatch, compared to those with area/gradient match

References

1. Bonow RO, Carabello BA, Kanu C, et al. ACC/AHA 2006 guidelines for the management of patients with valvular heart disease. Circulation. 2006;114: e84–231.
2. Vahanian A, Alfieri O, Andreotti F, et al. Guidelines for the management of valvular heart disease. Eur Heart J. 2012;33:2451–96.
3. Dumesnil JG, Pibarot P, Carabello B. Paradoxical low flow and/or low gradient severe aortic stenosis despite preserved left ventricular ejection fraction: implications for diagnosis and treatment. Eur Heart J. 2010; 31:281–9.
4. Lancellotti P, Magne J, Donal E, et al. Clinical outcome in asymptomatic severe aortic stenosis, insights from the new proposed aortic stenosis grading classification. J Am Coll Cardiol Img. 2012;3:235–43.
5. Burwash IG. Low-flow, low-gradient aortic stenosis: from evaluation to treatment. Curr Opin Cardiol. 2007;22:84–91.
6. Pibarot P, Dumesnil JG, Clavel MA. Paradoxical low flow, low gradient aortic stenosis despite preserved ejection fraction. ACVD. 2008;101:595–6.
7. Abbas AE, Franey LM, Goldstein J, Lester S. Aortic valve stenosis: to the gradient and beyond – the mismatch between area and gradient severity. J Interv Cardiol. 2013;26:183–94.
8. Oh JK, Seward JB, Tajik AJ. The echo manual. 3rd ed. Philadelphia: Lippincott Williams & Wilkins; 2007.
9. Baumgartner H, Hung J, Bermejo J, et al. Echocardiographic assessment of valve stenosis: EAE/ASE recommendations for clinical practice. J Am Soc Echocardiogr. 2009;22(1):1–23.
10. Minners J, Allgeier M, Gohlke-Baerwolf C, et al. Inconsistent grading of aortic valve stenosis by current guidelines: haemodynamic studies in patients with apparently normal left ventricular function. Heart. 2010;96:1463–8.
11. Clavel MA, Fuchs C, Burwash IG, et al. Predictors of outcomes in low-flow, low-gradient aortic stenosis: results of the multicenter TOPAS study. Circulation. 2008;118:S234–42.
12. Bermejo J, Yotti R. Low-gradient aortic valve stenosis: value and limitations of dobutamine stress testing. Heart. 2007;93:298–302.
13. de Filippi CR, Willett DL, Brickner ME, et al. Usefulness of dobutamine echocardiography in distinguishing severe from non-severe valvular aortic stenosis in patients with depressed left ventricular function and low transvalvular gradients. Am J Cardiol. 1995;75:191–4.
14. Nishimura RA, Grantham A, Connolly HM, et al. Low-output, low-gradient aortic stenosis in patients with depressed left ventricular systolic function: the clinical utility of the dobutamine challenge in the catheterization laboratory. Circulation. 2002;106:809–13.
15. Blais C, Burwash IG, Mundigler G, et al. Projected valve area at normal flow rate improves the assessment of stenosis severity in patients with low-flow, low-gradient aortic stenosis. Circulation. 2006;113:711–21.
16. Mascherbauer J, Schima H, Rosenhek R, et al. Value and limitations of aortic valve resistance with particular consideration of low flow – low gradient aortic stenosis: an in vitro study. Eur Heart J. 2004;25: 787–93.
17. Hachicha Z, Dumesnil JG, Bogarty P, et al. Paradoxical low-flow, low-gradient severe aortic stenosis despite preserved ejection fraction is associated with higher afterload and reduced survival. Circulation. 2007;115:2856–64.
18. Cramariuc D, Cioffi G, Rieck AE, et al. Low-flow aortic stenosis in asymptomatic patients: valvular arterial impedance and systolic function from the seas substudy. J Am Coll Cardiol Img. 2009;2:390–9.
19. Briand M, Dumesnil JG, Kadem L, et al. Reduced systemic arterial compliance impacts significantly on left ventricular afterload and function in aortic stenosis: implications for diagnosis and treatment. J Am Coll Cardiol. 2005;46:291–8.
20. Barasch E, Fan D, Chukwu EO, et al. Severe isolated aortic stenosis with normal left ventricular systolic function and low trans-valvular gradients: pathophysiologic and prognostic insights. J Heart Valve Dis. 2008;17:81–8.
21. Jander N, Minners J, Holme I, et al. Outcome of patients with low-gradient "severe" aortic stenosis and preserved ejection. Circulation. 2011;123(8): 887–95.
22. Daneshvar SA, Rahimtoola SH. Valve prosthesis-patient mismatch. a long term perspective. J Am Coll Cardiol Img. 2012;60:1123–35.

9 Reverse Area and Gradient Mismatch: The Discordance of a Large Valve Area and High Gradients

Amr E. Abbas and Steven J. Lester

Abstract

In previous chapters, we have defined "*Area/gradient match*" or concordance as present when criteria for AS severity is met by both gradient (ΔP) and area variables. Clinical decision making in these cases is rather straightforward and referral for aortic valve replacement, in the appropriate clinical circumstance, is the rule.

"*Area/gradient mismatch*" was discussed in detail in the previous chapter and refers to the situations where AS is severe by area but not by gradient criteria. Less commonly, and conversely, an elevated gradient may be present across the aortic valve (AV) in the absence of severe decrease in aortic valve area (AVA); and this has been referred to as "*reverse area/gradient mismatch*" or discordance. This later form of area/gradient severity discordance has not received as much emphasis in the literature as the former and yet maybe present in both native and prosthetic valves ($AV_{prosthesis}$). In these patients, Doppler-derived gradients and areas may not correspond to those obtained invasively, hence creating a "*Doppler-catheter mismatch*" which may add further challenges in the appropriate determination of the AS severity.

Errors of measurements and assumption, alterations in trans aortic valve flow (Q) and pressure recovery (P_{rec}), and paravalvular obstructions may account for a significant portion of this mismatch phenomenon. P_{rec} may also account for the discrepancy between Doppler- and catheter-derived estimations of AS severity.

A.E. Abbas, MD, FACC, FSCAI, FSVM, FASE, RPVI (✉)
Department of Cardiovascular Medicine,
Beaumont Health, Oakland University/William Beaumont School of Medicine, Royal Oak, MI, USA
e-mail: aabbas@beaumont.edu

S.J. Lester, MD
Department of Medicine, Mayo Clinic,
Scottsdale, AZ, USA

A.E. Abbas (ed.), *Aortic Stenosis: Case-Based Diagnosis and Therapy*,
DOI 10.1007/978-1-4471-5242-2_9

Keywords
Aortic stenosis severity • Reverse area/gradient mismatch • Doppler/catheter mismatch • Causes of reverse area/gradient mismatch • Paravalvular obstruction • Eccentric jet

Introduction

In previous chapters, we have defined "*Area/gradient match*" or concordance as present when criteria for AS severity is met by both gradient (ΔP) and area variables [1]. Clinical decision making in these cases is rather straightforward and referral for aortic valve replacement, in the appropriate clinical circumstance, is the rule.

"*Area/gradient mismatch*" [1] was discussed in detail in the previous chapter and refers to the situations where AS is severe by area but not by gradient criteria. Less commonly, and conversely, an elevated gradient may be present across the aortic valve (AV) in the absence of severe decrease in AVA; and this has been referred to as "*reverse area/gradient mismatch*" or discordance [1]. This later form of area/gradient severity discordance has not received as much emphasis in the literature as the former and yet maybe present in both native and prosthetic valves ($AV_{prosthesis}$). In these patients, Doppler-derived gradients and areas may not correspond to those obtained invasively [2], hence creating a "*Doppler-catheter mismatch*" which may add further challenges in the appropriate determination of the AS severity.

Errors of measurements and assumption, alterations in trans aortic valve flow (Q) and pressure recovery (P_{rec}), and paravalvular obstructions may account for a significant portion of this mismatch phenomenon [1, 3, 4]. P_{rec} may also account for the discrepancy between Doppler- and catheter-derived estimations of AS severity [4]. Patients with $AV_{prosthesis}$ may also experience any of the above described mismatch phenomenon leading to concerns regarding prosthetic function. In addition, prosthesis-specific clinical scenarios of reverse area/gradient discordance such as prosthesis-patient mismatch (PPM) and localized pressure loss through the central orifice of mechanical bileaflet aortic valve prosthesis may also occur.

This chapter will review the various causes of reverse area/gradient mismatch through clinical case examples.

Reverse Area/Gradient Mismatch

A recent study utilizing CTA suggested the incidence of this category to be around 2–3 % in patients with moderate to severe AS when using the effective orifice area (EOA) [5]. However, as the EOA is derived from ΔP measurements, both invasively and non-invasively, it is usually proportionately low to the degree of the transvalvular ΔP. Conversely, the geometric orifice area (GOA) remains non-severe in these cases and in the case of prosthetic valves, the occluder motion and/or bioprosthesis leaflets reveal no restriction or stenosis and remain in the expected range for prosthesis area. Hence, this discordance more commonly occurs between the GOA and the estimated ΔP and its actual incidence is unknown but likely higher.

Causes of Reverse Area-Gradient Mismatch in Native Valves

Errors of Measurement and/or Assumption

As previously discussed, **noninvasively**, ΔP across the aortic valve is generally determined on the principles of the Bernoulli equation:

$$\Delta P = 1/2\rho\left(V_2^{2-}V_1^2\right)\left(convective\,acceleration\right) + \rho_{prox}\int^{max}\left(dv/dt\right)*ds\begin{pmatrix} flow\,acceleration \\ +R\left(\mu\right)\left(viscous\,losses\right)\end{pmatrix}.$$

It is further modified in clinical cardiology as:

$$\Delta P = 4V_2^2 - 4V_1^2.$$

V_2 represents the Doppler derived blood flow velocity distal to the valve or the aortic valve velocity (AV_{vel}) and V_1 the proximal blood flow velocity or the left ventricular outflow velocity (LVOT V_1).

In the presence of severe AS, V_2 is usually significantly greater than V_1 and thus V_1 is omitted and the equation is further simplified into:

$$\Delta P = 4\left(V_2^2\right).$$

Errors of assumption occur when V_1 is omitted and the simplified equation is applied, and V_1 is >1.5 m/s as seen with hyperdynamic states, dynamic outflow obstruction, and moderate to severe aortic regurgitation or when V_2 is <3.0 m/s. This causes an overestimation of the noninvasively derived ΔP. In such cases, V_1 should be included in the equation [6–8].

Simplification of the Bernoulli equation also neglects the final term in the calculation, R (μ), which represents energy loss due to viscous friction, where R is viscous resistance and μ is viscosity. Though less common, failing to recall this component may result in an overestimation of pressure gradients in anemic patients [1] or an underestimation in milder degrees of AS with laminar flow where viscous losses are more significant [9].

Erroneous noninvasive overestimates of ΔP may also occur due to inadvertently mistaking an eccentric mitral regurgitation jet for AS jet [8] (**Case 1**, **seen in** Fig. 9.1). This is particularly true when the mitral regurgitation jet is eccentric as with mitral valve prolapse, with hypertrophic obstructive cardiomyopathy and associated systolic anterior motion of the mitral valve leaflets and mitral regurgitation, and with the use of the non-imaging probe (Pedoff). Less commonly, tricuspid regurgitation jet may also be mistaken for aortic stenosis.

The aortic stenosis spectral flow pattern is a systolic ejection flow and occurs upon opening of the aortic valve, progresses to a peak at some point during systole and ceases at the closure of the aortic valve. As this flow occurs during left ventricular ejection only, it will not be present during isovolumic ventricular contraction time (IVCT) or isovolumic ventricular relaxation time (IVRT). This fact helps differentiate the aortic stenosis flow pattern from the holosystolic flow of mitral insufficiency or tricuspid insufficiency. These latter two flow patterns, although occasionally confused with aortic stenosis due to their occurrence during systole, are holosystolic in nature. These regurgitant jets therefore begin immediately upon cessation of diastolic inflow velocities through the AV valves and continue throughout systole until, and sometimes into the next diastolic flow pattern. Careful examination of the timing of the turbulent systolic jet low pattern is necessary to avoid confusion and mistaking these jets for an aortic stenotic flow pattern.

Systolic turbulence due to left ventricular outflow tract obstruction may be noted from the same windows used to interrogate the aortic valve, particularly when using the Pedoff probe. The continuous wave flow pattern in this pathologic entity differ from aortic stenosis in that the peak velocity of the jet tends to be in a much later part of systole and tends to be maximal in the late phase of systole and the velocity is usually negligible or very low in the early to mid-portion of systole.

Invasively, ΔP is obtained via a double lumen single catheter, dual catheters, or pull back of a single catheter across the AV. Poor balancing, air bubbles in transducers, or the positioning of the transducer either too high or too low in relation to the patient may account for errors. Moreover, utilizing the pressure difference between the left ventricular catheter and the femoral line rather than the ascending aorta as a surrogate for transaortic gradient may overestimate ΔP in the presence of descending aortic or iliac stenosis [10]. Inherent errors in estimating the cardiac output may also account for errors of area measurement as may occur with utilizing an erroneous constant, utilizing estimated rather than measured O_2 consumption with Fick method, or using the thermodilution method with severe tricuspid regurgitation, atrial fibrillation, or low cardiac output [11].

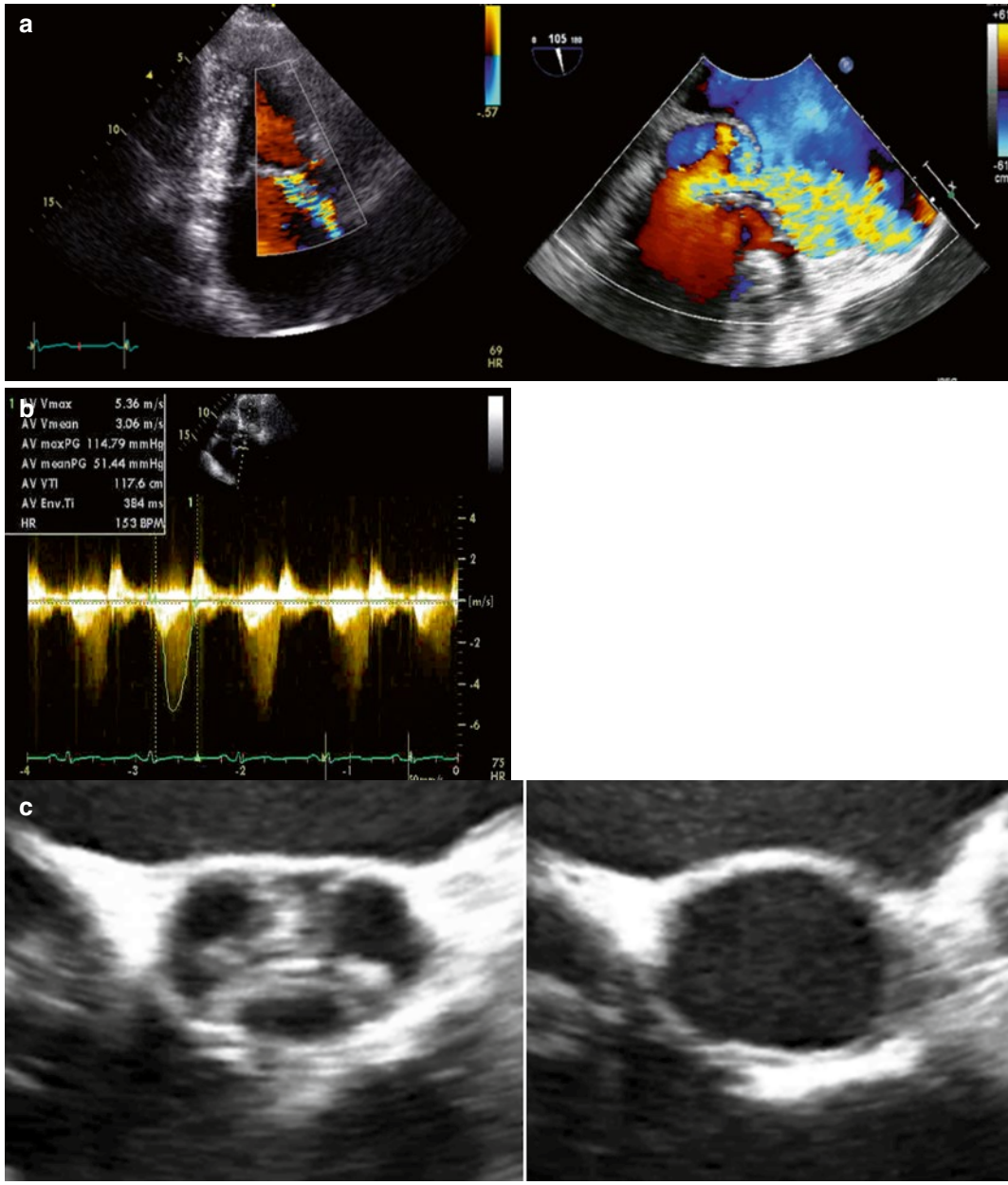

Fig. 9.1 Case 1: Error of Measurement. 50 year/old female presents for echocardiographic evaluation after her primary care physician noted a new murmur on routine physical examination. Echo reveals markedly eccentric severe mitral regurgitation jet due to severe prolapse of the posterior mitral leaflet on TTE (**a**-*left*) and TEE (**a**-*right*). Doppler signal is wrongfully noted as AV Doppler, which is actually that of the eccentric mitral regurgitation jet (**b**). Normal Excursion of the AV is noted on 2D (**c**)

High Flow States

Due to the quadratic and direct relationship between pressure gradient and flow, a high flow state may cause elevated gradients (both Doppler ΔP_{max} and invasive ΔP_{net}) in the absence of significant AS. Moreover, as note above, high flow may increase the LVOT V_1 component of the simplified Bernoulli equation to >1.5 m/s and ignoring it will also overestimate ΔP.

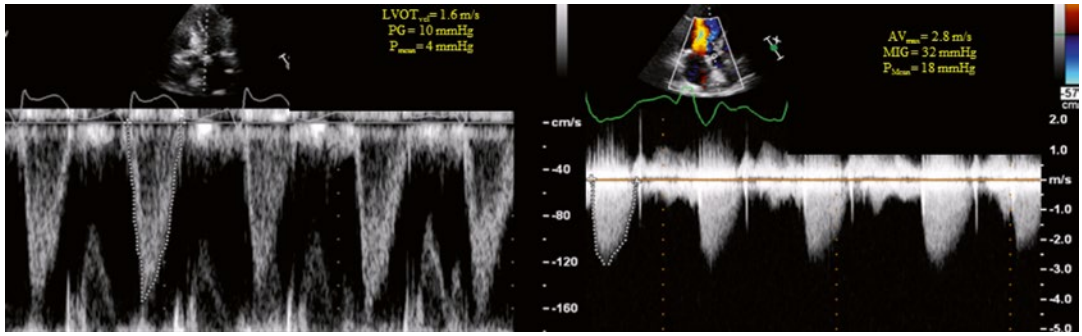

Fig. 9.2 Case 2: High flow states. 64 year/old male on chronic hemodialysis, admitted for fevers/chills. The patient was found to have sepsis, likely secondary to a chronic indwelling line infection. Trans-thoracic echocardiogram was initially obtained to evaluate for obvious cardiac valve vegetation. Pulse wave Doppler (*left*) and Continuous wave Doppler (*right*) across the AV demonstrating increased velocities as well as an AV velocity <3 m/s. Thus the modified Bernoulli rather than the simplified equation should be used $\Delta P = 4V_2^2 - 4V_1^2$. The actual ΔP_{MIG} across the AV is $\Delta P_{MIG} 32 - 10 = 22 mmHg$

High flow may occur with fever, severe anemia, pregnancy, thyrotoxicosis, arterio-venous fistulas, and thiamine deficiency [8]. **Case 2, seen in** Fig. 9.2, demonstrates a patient on hemodialysis admitted with fever and chills causing a hyperdynamic state with increased flow across the AV.

Conversion of a high flow/high gradient AS in the presence of a dialysis shunt to a paradoxically low flow low gradient AS with shunt compression has been reported [12]. In a patient on dialysis with an AV fistula and mild to moderate AS, the increased flow from the AV shunt, may increase the gradient noted on both Doppler and catheterization into the severe range. In addition, the cardiac output may be markedly elevated by invasive measures. This leads to a large AVA by the Gorlin equation in the mild to moderate range of severity. However, the increase flow may only marginally increase the Doppler LVOT TVI, causing the Doppler-estimated AVA to remain in the severe range. Hence, reverse area/gradient mismatch will be only noted on cardiac catheterization.

In addition, aortic regurgitation may also increase transaortic flow leading to an increase in the AV_{vel} and thus the ΔP, particularly in the presence of combined valve stenosis and regurgitation. In patients with at least moderate combined AV disease, the progressive increase AV_{vel} has been recently linked to worse outcomes, especially in patients with bicuspid aortic valve disease [13].

Pressure Recovery

In the presence of significant P_{rec}, reverse area/gradient mismatch is only present by Doppler-derived mean gradient (ΔP_{mean}) and EOA assessments of AS severity. However, catheter-derived ΔP_{mean} is lower and concordant to the higher invasively derived EOA resulting in Doppler/catheter discordance. The P_{rec} phenomenon is clinically relevant in patients with a small ascending aorta diameter and moderate aortic stenosis [14–16] (**Case 3, seen in** Fig. 9.3).

In a study of 1,563 patients with AS, 47.5 % initially classified as severe were reclassified as moderate after accounting for P_{rec} [4]. A clinically relevant P_{rec} (>20 % of ΔP_{max}) was present in 16.8 % of patients [4]. After accounting for P_{rec} via calculation of energy loss index (ELI), reclassification into moderate AS occurred more often in patients with a smaller ascending aorta (<3.0 cm) and lower trans-aortic velocities, regardless of flow state. However, the absolute magnitude of P_{rec} was greater in the presence of higher trans-aortic velocities (>3.33 m/s) [4]. This was discussed in more detail in Chap. 3.

Eccentric Jet

Conversely, in the presence an eccentric jet across the AV (as in cases of a bicuspid AV, non uniform calcification of cusps, and uneven restriction of AV leaflets) (Fig. 9.4), there is an increase in pressure loss as the eccentric jet collides with the ascending aortic wall with resultant energy loss

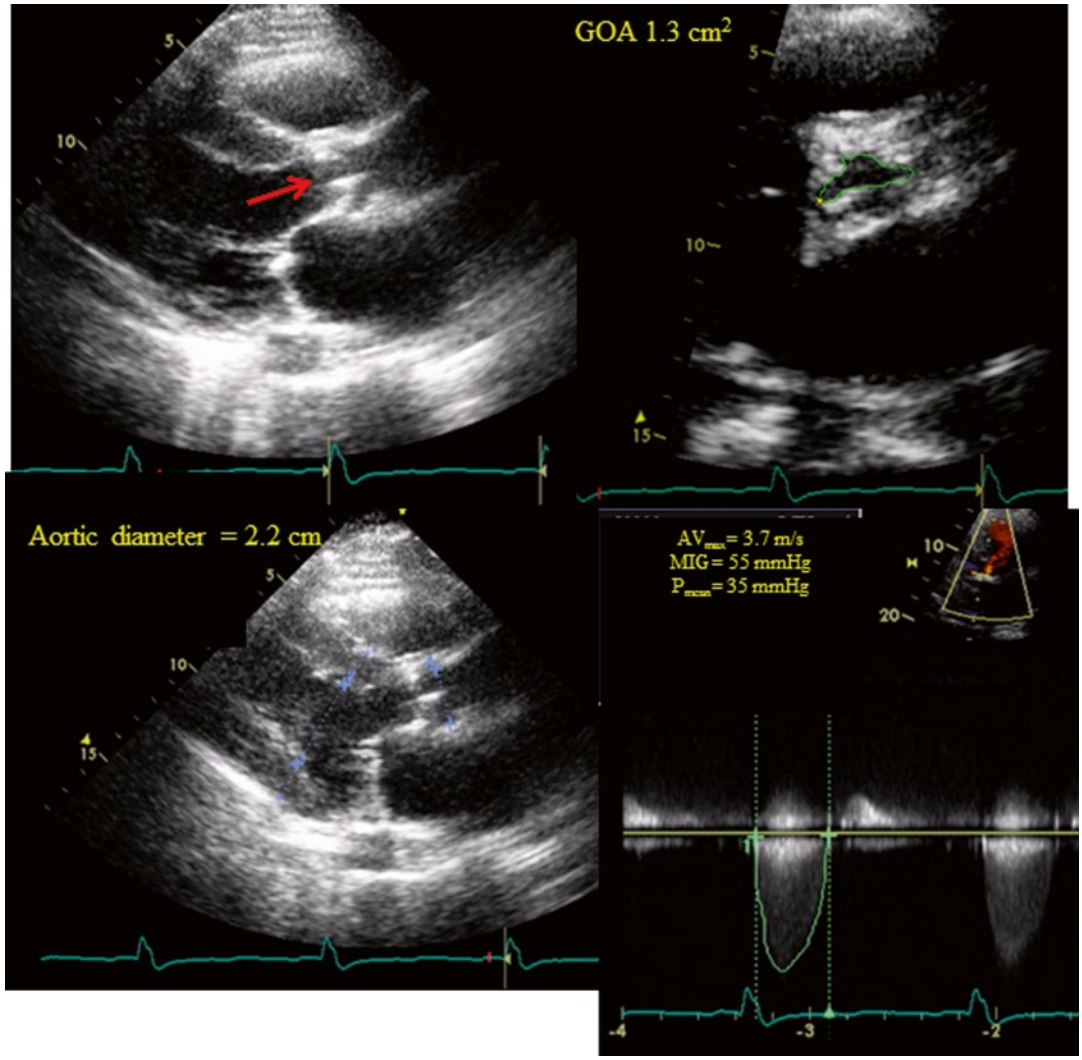

Fig. 9.3 Case 3: Pressure recovery: significant pressure recovery in a patient with moderate aortic stenosis and small aortic diameter (Doppler-only reverse area/gradient mismatch). 80 year/old female with a history of an undetermined degree of aortic stenosis presents for TAVR evaluation. **Echocardiography**: AV_{vel} : 3.5 m/s, **ΔPmean**: **30mmHg**, ΔP_{MIG} : 50mmHg (*bottom right*), Dimensionless index (VTI): 0.16, **EOADop (VTI): 0.6 cm²**, iEOA: 0.33 cm^2/m^2, **GOA by planimetry is 1.3 cm²** (*top right*), aortic diameter: 2.2 cm (*bottom left*), $ELCo = (3.79 * 0.6 / 3.79 - 0.6) = 0.715$, **noninvasive absolute P_{rec}** = 14 mmHg (using ΔP_{mean}), relative P_{rec} (P_{rec}/Doppler ΔP_{mean}) 15/34 = 44 %. Note that the AV is thickened and restricted (*red arrow*, *top left*), however, appears only moderately stenosed. **Catheterization**: $D\mathbf{P_{mean}}$: **18mmHg**, DP_{PPG} 21mmHg, $\mathbf{EOA_{cath}}$ 1.0**cm²**, iEOA : 0.6cm^2 / m^2, **Invasive absolute P_{rec}** (**Doppler $D\mathbf{P_{mean}}$ Catheter $D\mathbf{P_{mean}}$**) = 35 − 18 = 17mmHg, Relative P_{rec} (P_{rec} / Doppler DP_{mean}) 17 / 35 = 49%

due to heat, flow separation, and vortex formation. The latter will also cause a decrease in the absolute and relative P_{rec} [17–20]. As a result of both increased in pressure loss as well as decreased P_{rec}, both the Doppler- and catheter-derived ΔP_{mean} will be higher compared to the GOA. As such, there is Doppler/catheter concordance and reverse area/gradient mismatch is present on both Doppler and catheter-derived assessments. The greatest proportion of increase in both Doppler ΔP_{max} and catheter $\Delta P_{net,}$ and decline in EOA induced by jet eccentricity occurs by an angle of 30° and to a

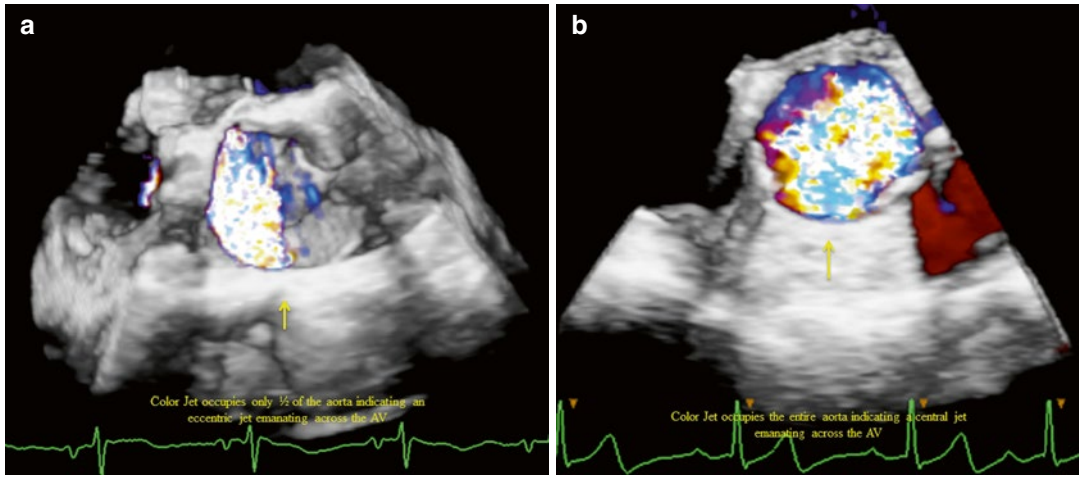

Fig. 9.4 Eccentric (**a**) (*left*) and centric (**b**) (*right*) jets across the aortic valve as viewed above the valve from the aorta as demonstrated on 3D color in two different

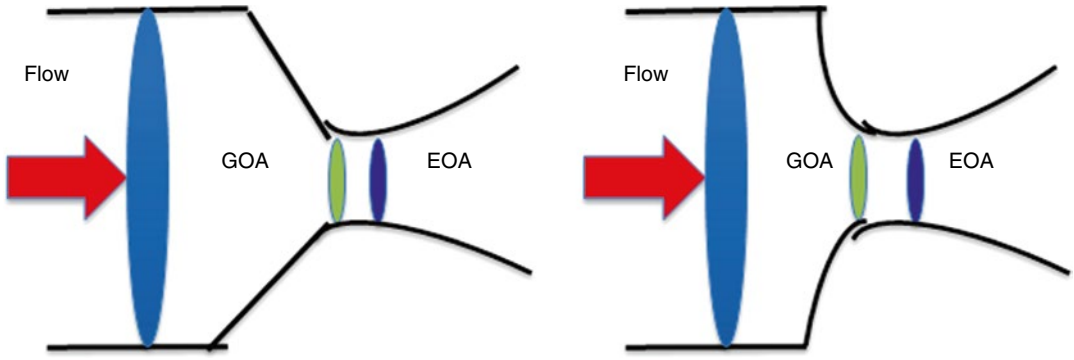

Fig. 9.5 The relationship between GOA, EOA, and the coefficient of orifice contraction (EOA/GOA). With a more gradually narrowed GOA (*left*), the EOA is almost equal to the GOA and the CC is close to 1. However, with a more abrupt narrowing (*right*), the EOA is more distal and smaller than the GOA

higher degree in the presence of more severe AS [18]. We have recently published a review highlighting several cases of an eccentric jet leading to reverse area/gradient mismatch [17].

Aortic Valve Geometry

As mentioned above, a pliable domed AV with a gradually narrowed orifice (funnel-shaped) will have a larger EOA for a given gradient that is almost similar to the GOA in dimension (a higher coefficient of orifice contraction) (Fig. 9.5). Conversely, a relatively flat AV with abrupt narrowing (sharp-edged) will lead to increase in disparity between the EOA and the GOA and a smaller EOA for a given gradient and [21] with reverse area gradient mismatch. A bicuspid AV will lead to a smaller EOA and higher ΔP_{mean} for a given GOA with a low coefficient of orifice contraction [22].

Increased LVOT Diameter

Similarly, increased LVOT diameter will lead to more initial drop of pressure as blood flow converges towards the AV. Thus, with larger LVOT diameters, there is an elevation in both Doppler ΔP_{max} and invasive ΔP_{net} that is disproportionate to the degree of area stenosis. However, Doppler and invasive gradients are close to each other with a reverse area/gradient mismatch noted by both modalities [18–20]. Thus for a given geometric AVA, a larger LVOT diameter

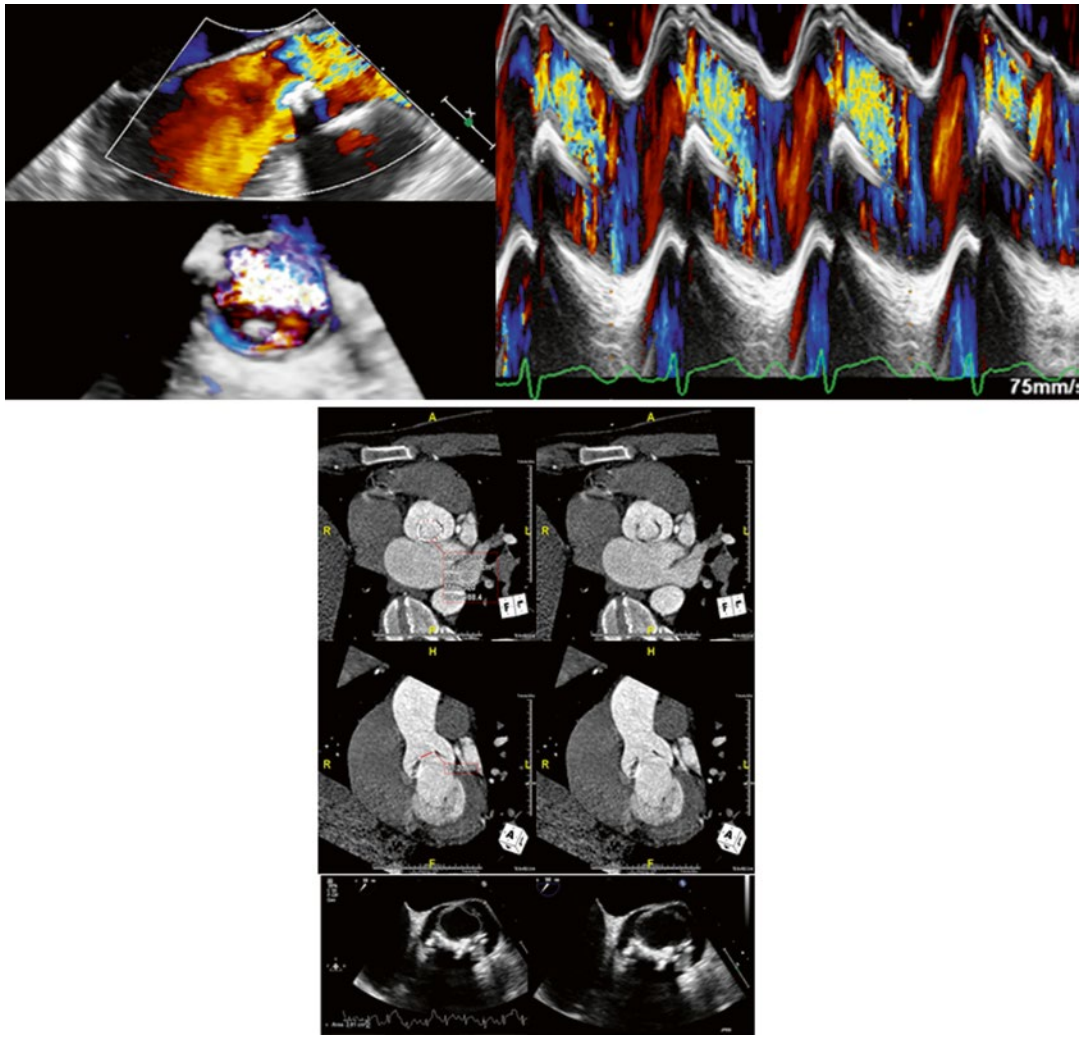

Fig. 9.6 Case 4: Pressure recovery: insignificant pressure recovery and high transaortic valve flow in a patient with a bicuspid aortic valve. (Doppler- and invasive- reverse area/gradient mismatch). 24 year/old male with a bicuspid AV and an eccentric jet, moderate to severe aortic regurgitation, and mildly dilated aortic root (3.6 cm) all leading to marked increase and concordance (due to no significant P_{rec}) of both Doppler and catheter derived ΔP, despite non severe AS by planimetry via CTA and TEE. **Echocardiography**: **ΔP_{mean}: 57 mmHg**, ΔP_{MIG}: 92 mmHg, **EOA (VTI)**: **1.1 cm2**. **GOA by planimetry is 2.61 cm²**. An eccentric jet is demonstrated by Color Doppler (*top left*), Color M-Mode (*right*), and Color 3D (*bottom left*). **Catheterization**: **ΔP_{mean} 50 mmHg**, **EOA 1.2 cm²**, +3 to +4 aortic regurgitation. **CTA and TEE Planimetry**: TEE GOA 2.61 cm^2, CTA GOA 2.54 cm^2 (*bottom*)

yields a higher gradient, higher AV_{Vel}, and a smaller dimensionless index (DI). Moreover, the larger the LVOT size compared to that of the GOA, the lower the EOA and the contraction coefficient with disproportionately high gradients [11].

The impact of LVOT diameter on Doppler-derived P_{mean} was further elucidated in a recent Doppler study of about 10,000 patients. In this study, an AVA of 1 cm^2 corresponded to a P_{mean} of 42 mmHg, AV_{Vel} of 4.1 m/s, and a DI of 0.22 in patients with a large $LVOT_D$ (>2.3 cm). While it corresponded to a P_{mean} of 35 mmHg, AV_{Vel} 3.8 m/s, and a DI of 0.29 in patients with an average $LVOT_D$ (2–2.2 cm). Finally, it corresponded to a P_{mean} of 29 mmHg, AV_{Vel} 3.5 m/s, and a DI of 0.36 in patients was with a small $LVOT_D$ (1.7–1.9 cm) [23].

All the above factors may occur independently or simultaneously. A patient with a bicuspid aortic

valve, dilated aorta, eccentric jet, moderate to severe aortic regurgitation may experience markedly elevated Doppler and invasive gradients across the AV, despite the absence of severe reduction in the GOA, is demonstrated in **Case 4**, **seen in** Fig. 9.6.

Causes of Reverse Area-Gradient Mismatch in Prosthetic Aortic Valves

Because $AV_{prosthesis}$ annuli and struts occupy more space than the native valve apparatus, a higher ΔP is expected, even when the $AV_{prosthesis}$ is functioning normally. Stentless bio $AV_{prosthesis}$ has the least impact on ΔP, followed by stented bio $AV_{prosthesis}$ and finally mechanical prostheses, which generate the highest gradient. The smaller cross-sectional area of smaller-sized $AV_{prosthesis}$ results in a larger relative obstruction of aortic outflow and higher ΔP.

As such, disproportionately elevated pressure gradients across $AV_{prosthesis}$ may occur in the absence of true $AV_{prosthesis}$ stenosis. This may be flow related, P_{rec} related, or secondary to a misalignment of an $AV_{prosthesis}$ in relation to the aorta resulting in an eccentric jet.

In addition, other causes of reverse area/gradient mismatch occur that are specific to $AV_{prosthesis}$ are outlined below.

Localized High Gradient in Central Orifice of Bileaflet Mechanical Valves

In the presence of mechanical bileaflet (and caged-ball) $AV_{prosthesis}$, a smaller central orifice may give rise to a high velocity jet that corresponds to a localized significant pressure loss at the mechanical valve. This pressure is recovered just distal to the $AV_{prosthesis}$ once the central flow reunites with flows originating from the lateral orifices [24]. Doppler-derived ΔP_{max}, but not catheter-derived ΔP_{net}, will overestimate the net pressure drop across the valve, and thus the gradient. This again results in an increase in the discrepancy between both Doppler and invasive measurements and a reverse area/gradient mismatch on Doppler only [24]. This condition may be exaggerated with very small valves (<19 mm) and with high flow conditions. Fluoroscopy, CT, and TEE may help visualize the mechanical leaflets and exclude prosthesis obstruction. Detailed observational data on expected valve gradients of normally functioning prosthetic aortic valves by valve type and size have been published and usually account for this phenomenon [24]. Some authors sometimes view this phenomenon as a form of P_{rec} and a similar mechanism can occur to a lesser extent with stented bioprosthesis (Fig. 9.7).

Prosthesis-Patient Mismatch (PPM)

As mentioned above, $\Delta P = Q^2/(K \times EOA^2)$ where K is constant. Thus for gradients to remain low, the EOA must be proportionate to the flow requirements, that under resting conditions, are related to BSA [13]. Thus for larger people with higher cardiac output (CO), the EOA has to be proportionately larger to accommodate increased flow and keep ΔP low.

PPM is a condition that occurs when the iEOA of a prosthetic valve is <0.85 cm/m^2 in the presence of elevated gradients across the prosthetic valve [25, 26] and is severe at <0.65 cm/m^2; in other words, the prosthetic EOA is too small for the patient's BSA and hence his CO (Fig. 9.8). Various reports on its significance exist, however, it is important to distinguish PPM from elevated gradients due to P_{rec} and true prosthetic stenosis. Expected iEOA and GOA have also been used to predict PPM [25, 26], albeit with debated validity.

The Doppler velocity index (DVI, ratio of LVOT velocity/AV prosthetic velocity), contour of the velocity jet, acceleration time (AT, time from onset to peak velocity jet), ejection time (ET), AT/ET, difference between expected $AV_{prosthesis}$ EOA and EOA_{Dop} may help distinguish true $AV_{prosthesis}$ stenosis, PPM and elevated velocities due to P_{rec}, errors, and increased flow [24, 27] (Fig. 9.9). Moreover, identifying normal mechanical $AV_{prosthesis}$ function on fluoroscopy (opening angle </>30°, or leaflet mobility on TEE or CTA may assist with identifying PPM [28, 29]. A patient with PPM of a mechanical $AV_{prosthesis}$ is demonstrated in **case 5**, **seen in** Fig. 9.10.

It is important to note that increased flow in a patient with a small aorta and an $AV_{prosthesis}$ may lead to an increase in ΔP_{max} (via increased flow

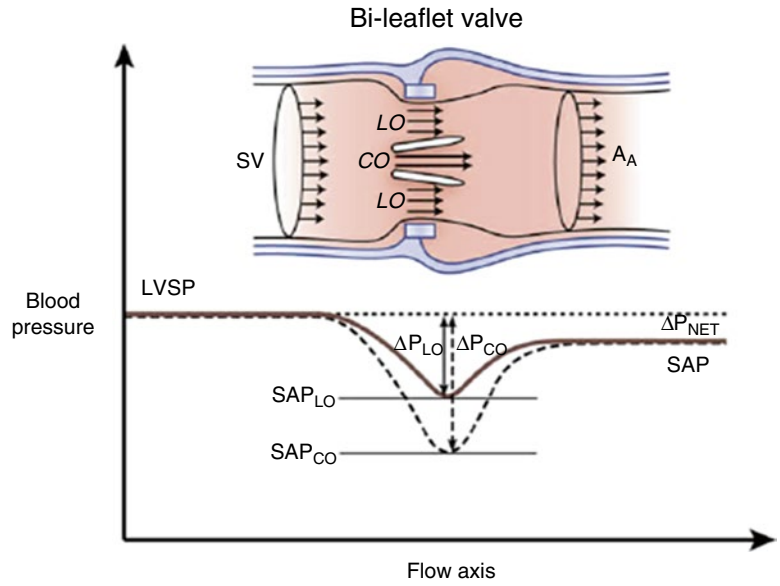

Fig. 9.7 In the presence of mechanical bileaflet (and caged-ball) $AV_{prosthesis}$, a smaller central orifice may give rise to a high velocity jet that corresponds to a localized significant pressure loss at the mechanical valve. This pressure is recovered just distal to the $AV_{prosthesis}$ once the central flow reunites with flows originating from the lateral orifices. Doppler-derived ΔP_{max}, but not catheter-derived ΔP_{net}, will overestimate the net pressure drop across the valve, and thus the gradient. This again results in an increase in the discrepancy between both Doppler and invasive measurements and a reverse area/gradient mismatch on Doppler only (From Zoghbi et al. [24] with permission

and presence of an $AV_{prosthesis}$) with an increase in absolute P_{rec} and a corresponding decrease in ΔP_{net} (due to a small aorta and a $AV_{prosthesis}$) causing even a further discrepancy between Doppler ΔP_{max} and invasive ΔP_{net}. PPM should not be assumed in patients with small [19, 21] sizes of a bileaflet mechanical valve due to the previously described phenomenon of localized high velocity/gradient of the central orifice and significant recovery of pressure with stream realignment upstream.

Paravalvular Obstruction: Sub or Supra-valvular Aortic Obstruction

In patients with either sub- or supra-valvular aortic stenosis, the GOA and valve motion may be preserved, despite an elevated pressure gradient across the aortic valve.

Left ventricular outflow obstruction (by membranes, hypertrophied septum, or a struts of a stented mitral valve bioprosthesis) and supra-valvular obstruction may also be present and account for elevated gradients across the aortic valve (and LVOT and aortic root) despite a normal aortic valve GOA and valve motion.

The para aortic membranes may be better visualized with off axis TTE views, TEE, as well as CT and MRI in some instances.

Subaortic Membrane

Sub valvular aortic stenosis is somewhat more common than the supra valvular form. It may also occur as a part of a syndrome as Shone's complex or occur in isolation. Sub aortic membranes, muscular ridges, and tunnels can also account for the obstruction. Damage to the aortic valve from the eccentric high velocity jet may lead to aortic valve regurgitation further increasing the hemodynamic burden on the left ventricle [6].

Case 6A, **seen in** Fig. 9.11, demonstrates a case of a sub-aortic membrane causing an elevated trans AV gradient in the absence of aortic

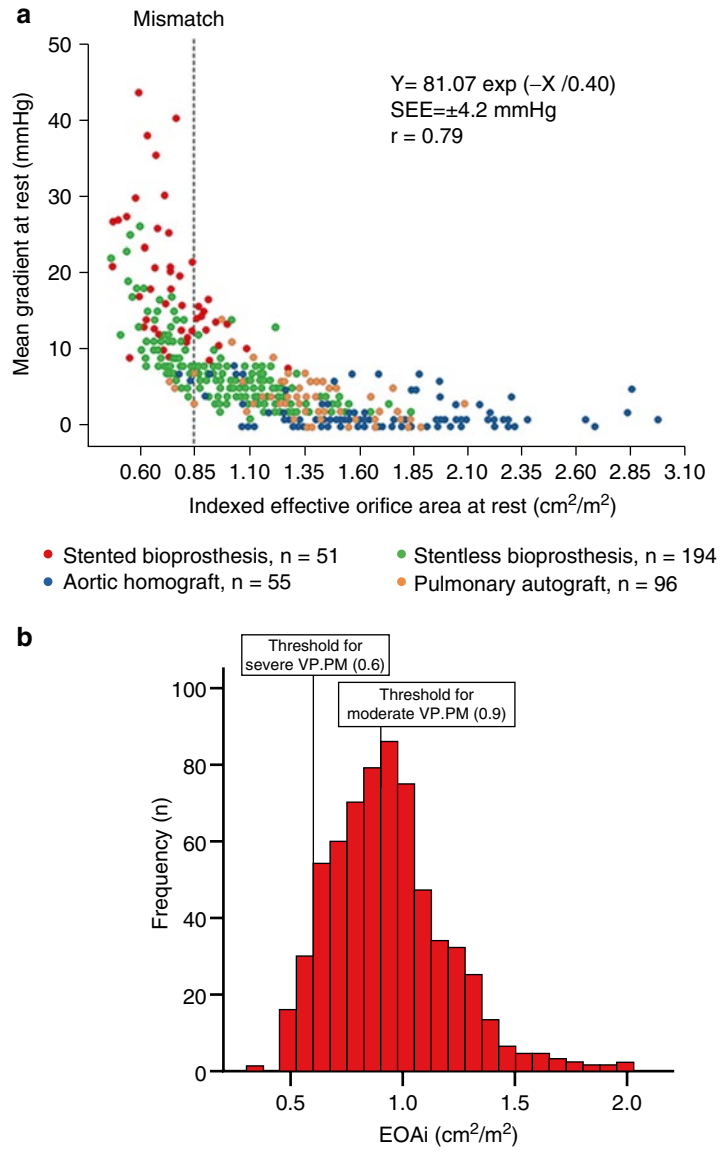

Fig. 9.8 The curvilinear relationship between ΔP_{mean} and EOA in various bio $AV_{prosthesis}$, PPM is present when iEOA <0.85 cm^2 *top* (**a**). *Bottom* (**b**) diagram shows the iEOA after implanting the same valve (Edwards perimount 23) in different patients, demonstrating that most individuals would have moderate PPM, many would have mild, and a few would have severe PPM depending on their BSA (**a**) (From Daneshvar and Rahimtoola [26])

stenosis. In addition, there is evidence of aortic regurgitation in the same patient.

Hypertrophic Obstructive Cardiomyopathy

Case 6B, **seen in** Fig. 9.12, demonstrates a dagger-shape Doppler signal suggestive of hypertrophic obstructive cardiomyopathy (HCM) with no valvular stenosis. Demonstration of an intracavitary or outflow gradient on catheterization as well as the Brokenborough effect may demonstrate the presence of a dynamic outflow obstruction due to HCM or hypertension and left ventricular hypertrophy [10].

Supra-aortic Obstruction

Supra valvular aortic stenosis is exceedingly rare and may present either in isolation or as a part of congenital syndromes as William's Syndrome. It may occur in the form of membranes, muscular ridges, or tunneling of the ascending aorta. Associated features of patients with William's

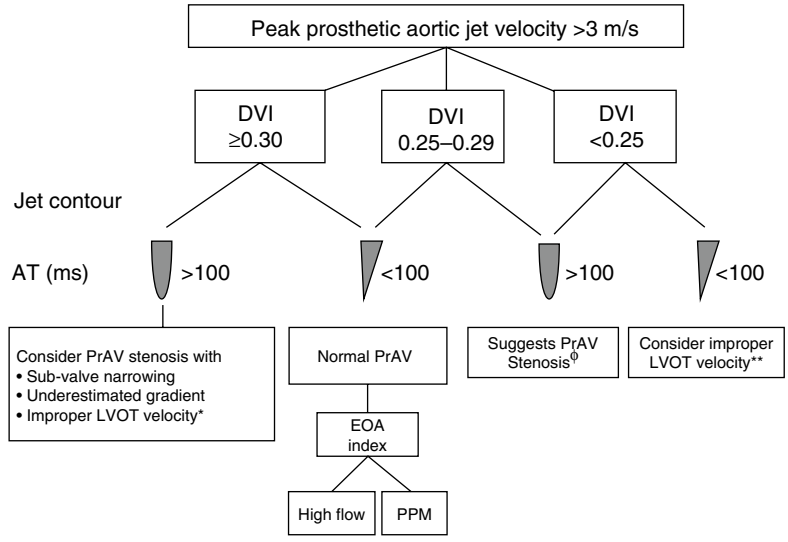

Fig. 9.9 Differentiating elevated gradients across $AV_{prosthesis}$ by Doppler. Recent evidence suggests that a DVI cutoff of <0.35, > 1 SD between projected and actual EOA, and a closing angle <30° on fluoroscopy for mechanical valves suggest $AVA_{prosthesis}$ stenosis

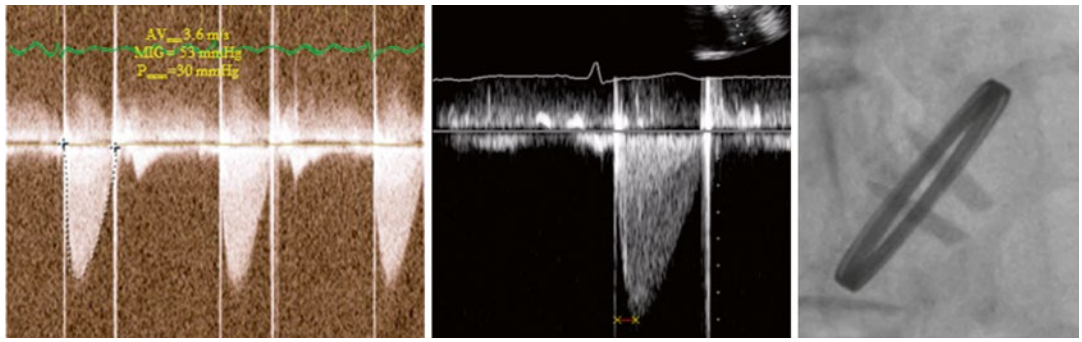

Fig. 9.10 Case 5: Patient prosthesis mismatch. A 69 year/old female with a history of a bileaflet mechanical AV prosthesis presents after routine echocardiography. **Doppler Echocardiography**: The $\mathbf{\Delta P_{mean} = 30\ mmHg}$, $\Delta P_{MIG} = 53$ mmHg (*Left*), **iEOA is 0.62 cm^2/m^2**. There is a triangular jet contour with a DVI: 0.26. The acceleration time is normal at 60 msec (*Center*). **Fluoroscopy**: Demonstrating normal, unrestricted opening of the mechanical aortic valve leaflets (*Right*)

Syndrome are elfin features, self-mutilations, and developmental issues [6].

Suprasternal views may help demonstrate the presence of supra aortic membranes.

Case 6C, **seen in** Fig. 9.13, demonstrates a case of a supra-aortic membrane causing an elevated trans AV gradient in the absence of aortic stenosis. The suprasternal view best visualizes the membrane.

Mitral Valve Prosthesis

LVOT obstruction may also occur following mitral valve prosthesis that protrudes into the LV outflow, especially in the setting of basal septal hypertrophy (**Case 6D**, **seen in** Fig. 9.14). This usually occurs with bioprosthetic valves as with this patient and following a reoperation with mechanical mitral valve prosthesis, the elevated transaortic gradient resolved.

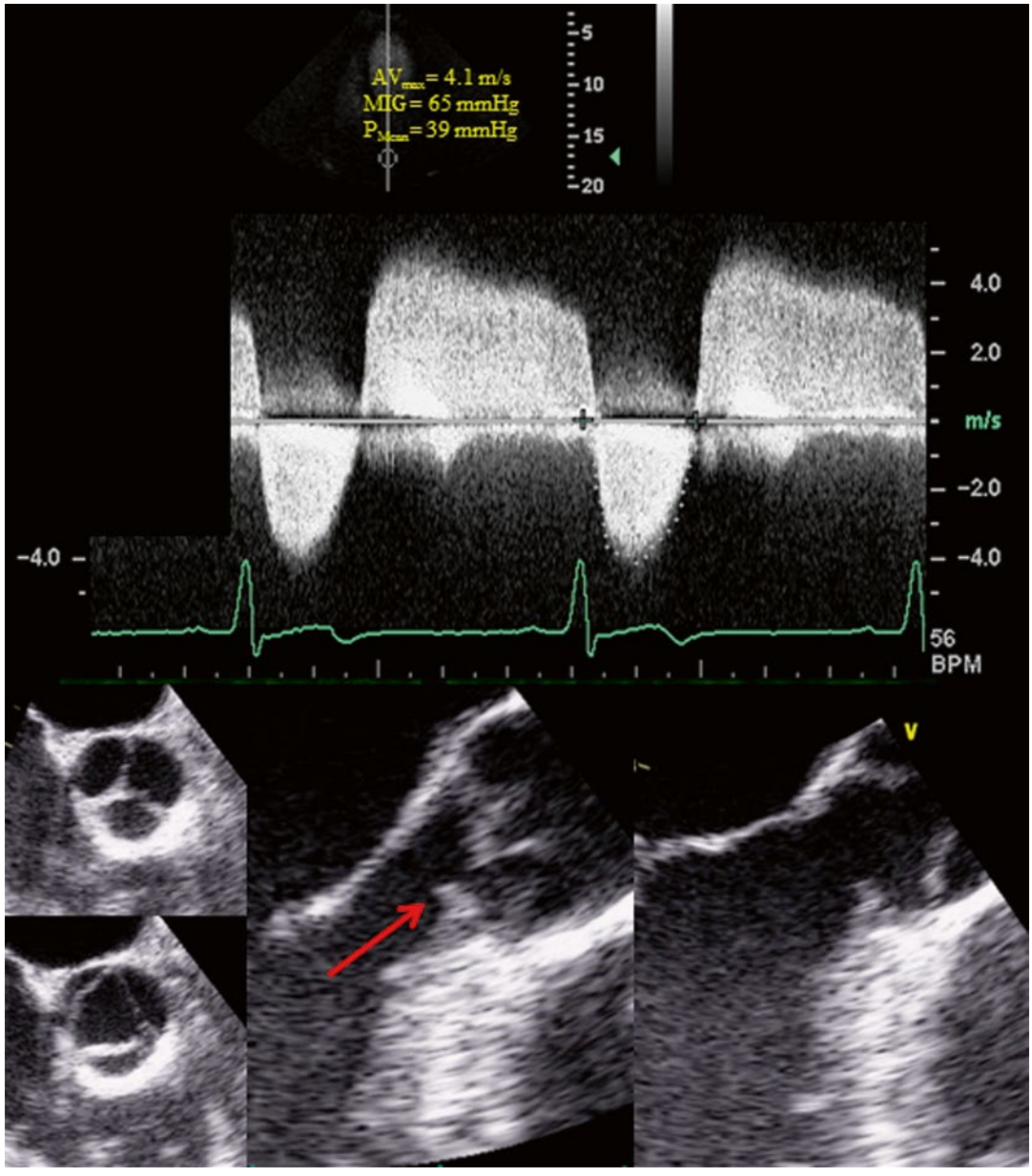

Fig. 9.11 Case 6: Para-valvular obstruction. A Subaortic membrane: 26 year old, asymptomatic male presents for echocardiographic evaluation of a harsh, systolic murmur. Pressure gradients across the aortic valve are determined to be elevated despite a normal appearing valve. **Echocardiographic Data** (**TTE**), ***Top panel***: $\mathbf{\Delta P_{mean}}$: **39 mmHg**, ΔP_{MIG}: 67 mmHg. Severe AS by gradient is suggested, however, the visualized aortic valve does not show leaflet restriction. There is also moderate to severe aortic regurgitation. **Echocardiographic Data** (**TEE**) ***Bottom panel***: Tri-leaflet AV with normal function and a subaortic membrane (*red arrow*) are visualized, which is semi-lunar in structure, and accounts for the elevated velocities noted on TTE

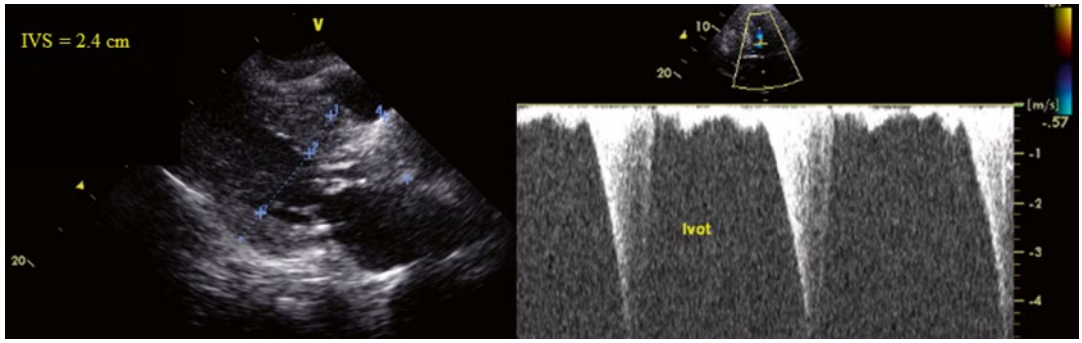

Fig. 9.12 Case 6B. Hypertrophic obstructive cardiomyopathy: 47 year/old male presents for echocardiographic evaluation after a syncopal event and systolic murmur on physical examination **Echocardiographic Data** (**TTE**): Moderate to severe concentric LVH noted with septal wall hypertrophy (*left*). An elevated dagger-shape, late-systolic peaking Doppler jet (**peak LVOT gradient**: **65 mmHg**) (*right*) may help identify dynamic outflow tract obstruction due to hypertrophic cardiomyopathy or hypertension

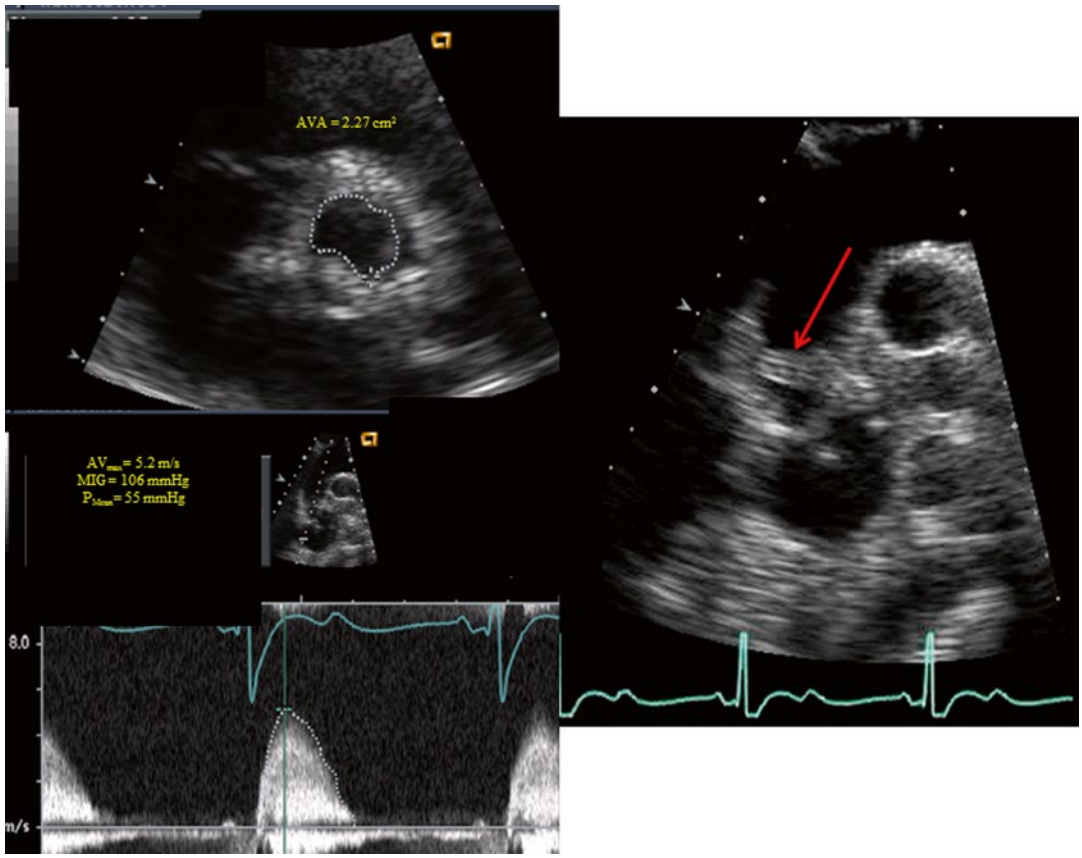

Fig. 9.13 Case 6C. Supravalvular obstruction: 55 year/old female evaluated for possible aortic stenosis due to elevated pressure gradients determined by Doppler echocardiography. **Echocardiographic Data**: A supravalvular membrane (*red arrow*) is noted with **ΔP_{mean} of 54 mmHg**, ΔP_{MIG} of 106 mmHg. The "AVA EOA", is 0.75 cm^2. The AV displays adequate leaflet excursion with **GOA planimetry of 2.3 cm^2** yet creating an elevated ΔP despite non- severe valvular AS

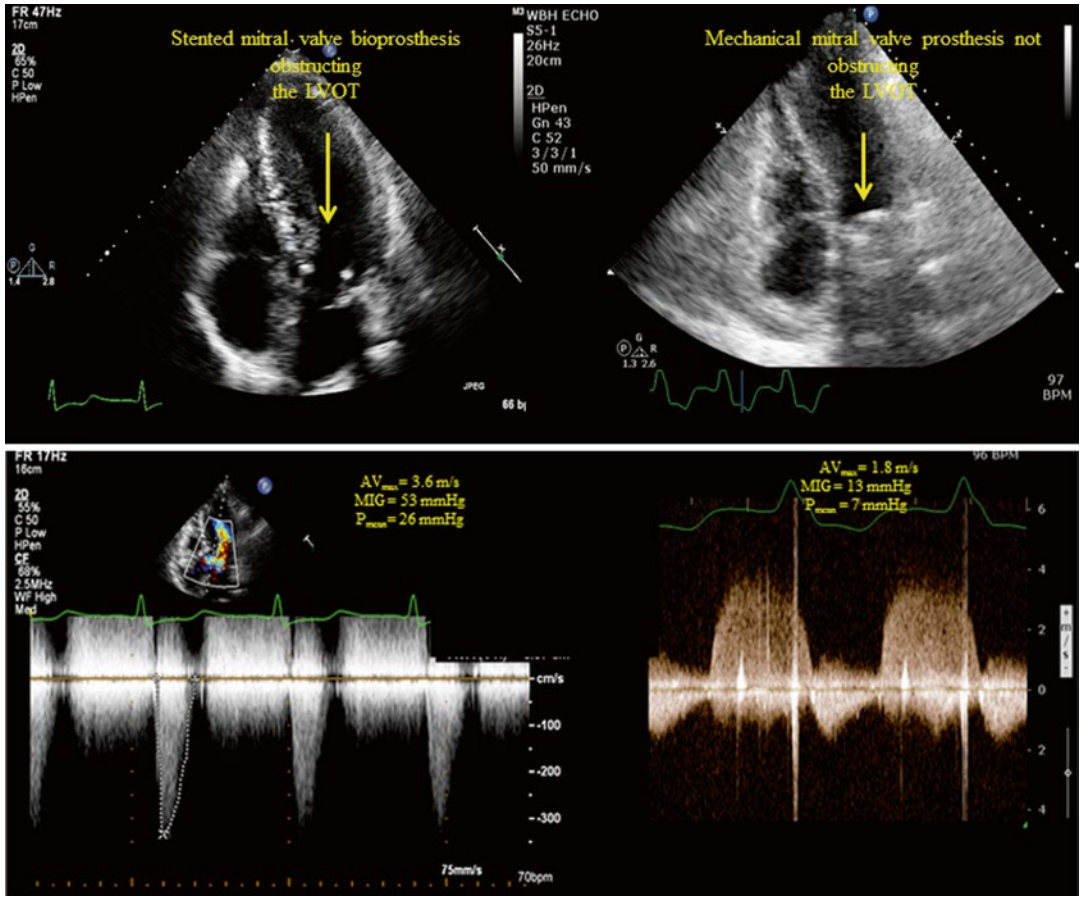

Fig. 9.14 Case 6D. Subvalvular obstruction due to mitral valve prosthesis: 56 year/old female with H/O HOCM and moderate to severe mitral regurgitation underwent mitral valve replacement with a stented bioprosthesis and minimal myomectomy. Few months later, she presented with elevated gradients across the AV and marked dyspnea on exertion (*left panel top* and *bottom*), $AV_{vel} = 3.6$ m/s with a P_{mean} of 26 mmHg. Patient underwent further reduction myomectomy and replacement with a lower profile mechanical valve with improvement in symptoms and transaortic gradient (*right panel*, *top* and *bottom*), $AV_{vel} = 1.8$ m/s with a P_{mean} of 7 mmHg

Conclusion

Reverse area gradient mismatch occurs when elevated ΔP are present despite the absence of severely reduced GOA. This may manifest with either Doppler and catheter discordance or concordance. After ruling out sub or supravalvular obstruction, assessing the GOA, aortic root and LVOT diameters, as well as number of cusps and nature of prosthesis via TEE, CT, MRI, and fluoroscopy (in case of mechanical prosthesis) may assist with resolving the area/gradient discrepancy. Moreover, considering the presence of an eccentric jet or utilizing other measures of AS severity as ELI and recovered P_{rec} that account for the P_{rec} may prove valuable. Considering high flow states as well as assessing for aortic regurgitation severity may also help in cases with high flow states and combined valve pathology [13, 30]. Utilizing these techniques is imperative to assess the true severity of aortic valve stenosis. A suggested approach for the evaluation of patients with AS and reverse area/gradient mismatch is outlined in Fig. 9.15.

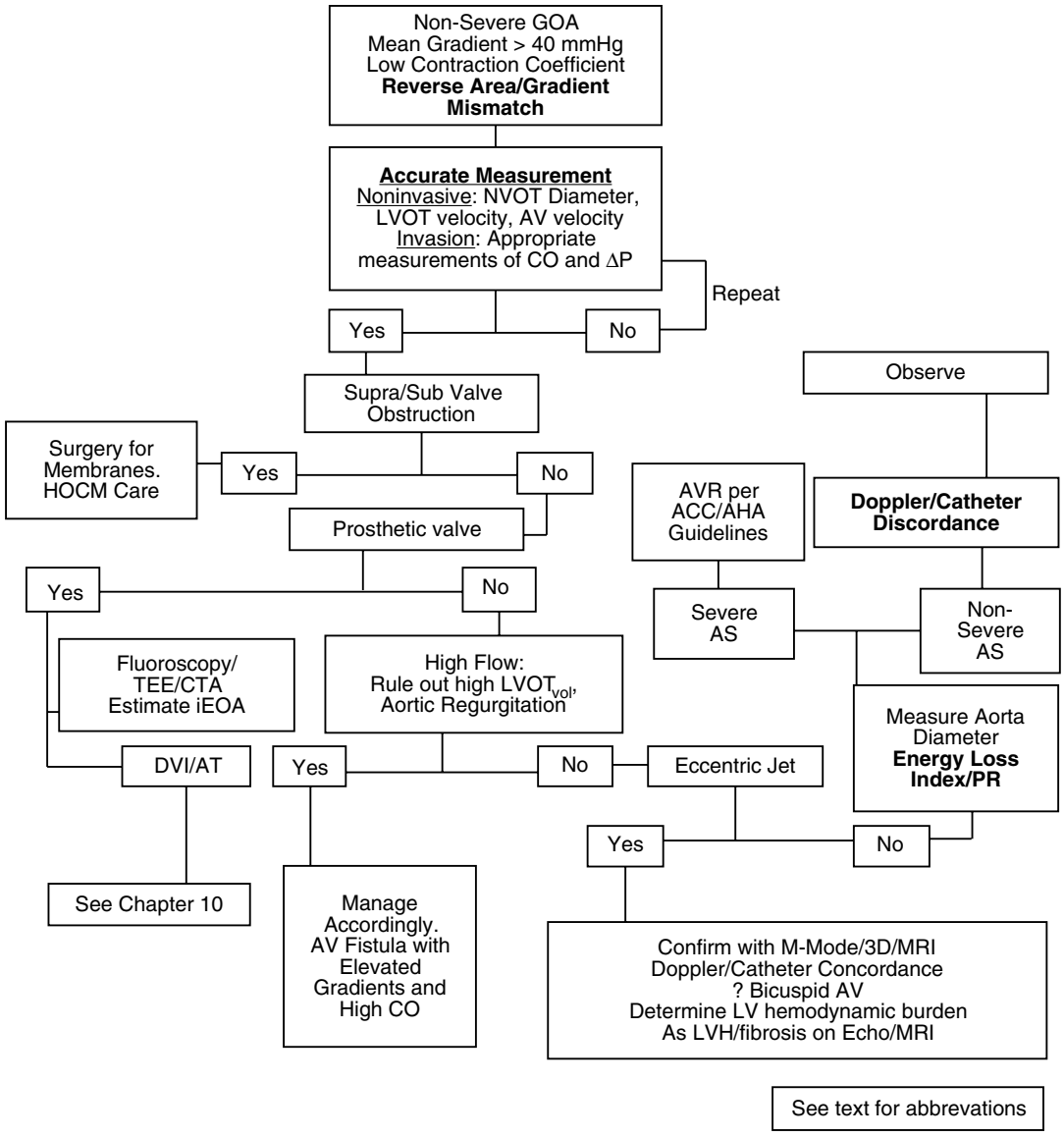

Fig. 9.15 Management outline for patients with reverse area gradient mismatch

References

1. Abbas AE, Franey LM, Goldstein J, Lester S. Aortic valve stenosis: to the gradient and beyond-the mismatch between area and gradient severity. J Interv Cardiol. 2013;26(2):183–94.
2. Oh JK, Taliercio CP, Holmes Jr DR, et al. Prediction of the severity of aortic stenosis by Doppler aortic valve area determination: prospective Doppler-catheterization correlation in 100 patients. J Am Coll Cardiol. 1988;11:1227–34.
3. Dumesnil JG, Pibarot P, Carabello B. Paradoxical low flow and/or low gradient severe aortic stenosis despite preserved left ventricular ejection fraction: implications for diagnosis and treatment. Eur Heart J. 2010;31:281–9.
4. Bahlmann E, Cramariuc D, Gerdts E, et al. Impact of pressure recovery on echocardiographic assessment of asymptomatic aortic stenosis. A SEAS substudy. JACC Cardiovasc Imaging. 2010;3:555–62.
5. Clavel MA, Messika-Zeitoun D, Pibarot P, Aggarwal SR, Malouf J, Araoz PA, Michelena HI, Cueff C, Larose E, Capoulade R, Vahanian A, Enriquez-Sarano M. The complex nature of discordant severe calcified aortic valve disease grading: new insights from combined Doppler echocardiographic and computed tomographic study. J Am Coll Cardiol. 2013;62(24):2329–38.

6. Nishimura RA, Otto CM, Bonow RO, Carabello BA, Erwin JP, Guyton RRA, O'Gara PT, Ruiz CE, Skubas NJ, Sorajja P, Sundt TM, Thomas JM. ACC/AHA guideline for the management of patients with valvular heart disease. J Am Coll Cardiol. 2014. doi:10.1016/j.jacc.2014.02.536.
7. Vahanian A, Alfieri O, Andreotti F, et al. Guidelines for the management of valvular heart disease. Eur Heart J. 2012;33:2451–96.
8. Baumgartner H, Hung J, Bermejo J, et al. Echocardiographic assessment of valve stenosis: EAE/ASE recommendations for clinical practice. J Am Soc Echocardiogr. 2009;22(1):1–23.
9. Adams JC, Jiamsripong P, Belohlavek M, McMahon EM, Marupakula V, Heys J, Chaliki HP. Potential role of Reynolds number in resolving Doppler- and catheter- based transvalvular gradient discrepancies in aortic stenosis. J Heart Valve Dis. 2011;20:159–64.
10. Carabello BA, Grossman W. Grossman's cardiac catheteization, angiography, and intervention, 6th ed. Lippincott Williams & Wilkins: Philadelphia; 2000.
11. Saikrishnan N, Kumar G, Sawaya FJ, Lerakis S, Yoganathan AP. Accurate assessment of aortic stenosis: a review of diagnostic moalities and hemodynamics. Circulation. 2014;129:244–53.
12. Ennezat PV, Marechaux S, Pibarot P. From excessive high-flow, high-gradient to paradoxical low-flow, low-gradient aortic valve stenosis: hemodialysis arteriovenous fistula model. Cardiology. 2010;116(1):70–2.
13. Zilberszac R, Gabriel H, Schemper M, Zahler D, Czerny M, Maurer G, Rosenhek R. Outcome of combined stenotic and regurgitant aortic valve disease. J Am Coll Cardiol. 2013;61(14):1489–95.
14. Garcia D, Pibarot P, Dumesnil JG, Sakr F, Durand LG. Assessment of aortic valve stenosis severity: a new index based on the energy loss concept. Circulation. 2000;101(7):765–71.
15. Bahlmann E, Gerdts E, Cramariuc D, Gohlke-Baerwolf C, Nienaber CA, Wachtell K, Seifert R, Chambers JB, Kuck KH, Ray S. Prognostic value of energy loss index in asymptomatic aortic stenosis. Circulation. 2013;127:1149–56.
16. Levine RA, Schwammenthal E. Stenosis is in the eye of the observer: impact of pressure recovery on assessing aortic valve area. J Am Coll Cardiol. 2003;41(3):443–5.
17. Abbas AE, Franey LM, Lester S, Raff G, Gallagher MJ, Hanzel G, Safian RD, Pibarot P. The role of jet eccentricity in generating disproportionately elevated transaortic pressure gradients in patients with aortic stenosis. Echocardiography. 2015;32(2):372–82.
18. VanAuker MD, Chandra M, Shirani J, Strom JA. Jet eccentricity: a misleading source of agreement between Doppler/catheter pressure gradients in aortic stenosis. J Am Soc Echocardiogr. 2001;14(9):853–62.
19. Donal E, Novaro GM, Deserrano D, Popovic ZB, Greenberg NL, Richards KE, Thomas JD, Garcia MJ. Planimetric assessment of anatomic valve area overestimates effective orifice area in bicuspid aortic stenosis. J Am Soc Echocardiogr. 2005;18(12):1392–8.
20. Richards KE, Deserranno D, Donal E, Greenberg NL, Thomas JD, Garcia MJ. Influence of structural geometry on the severity of bicuspid aortic stenosis. Am J Physiol Heart Circ Physiol. 2004;287(3):H1410–6.
21. Bach D. Echo/Doppler evaluation of hemodynamics after aortic valve replacement: principles of interrogation and evaluation of high gradients. J Am Coll Cardiol Img. 2010;3:296–304.
22. Garcia D, Pibarot P, Landry C, Allard A, Chayer B, Dumesnil JG, Durand LG. Estimation of aortic valve effective orifice area by Doppler echocardiography: effects of valve inflow shape and flow rate. J Am Soc Echocardiogr. 2004;17(7):756–65.
23. Michelena HI, Margaryan E, Miller FA, Eleid M, Maalouf J, Suri R, Messika-Zeitoun D, Pellikka PA, Enriquez-Sarano M. Inconsistent, echocardiographic grading of aortic stenosis: is the left ventricular outflow tract important? doi:10.1136/heartjnl-2012-302881.
24. Zoghbi WA, Chambers JB, Dumesnil JG, Foster E, Gottdiener JS, Grayburn PA, Khandheria BK, Levine RA, Marx GR, Miller Jr FA, et al. Recommendations for evaluation of prosthetic valves with echocardiography and doppler ultrasound. J Am Soc Echocardiogr. 2009;22(9):975–1014; quiz 1082–4.
25. Schobel WA, Voelker W, Haase KK, Karsch KR. Extent, determinants and clinical importance of pressure recovery in patients with aortic valve stenosis. Eur Heart J. 1999;20(18):1355–63.
26. Daneshvar SA, Rahimtoola SH. Valve prosthesis-patient mismatch. A long term perspective. J Am Coll Cardiol Img. 2012;60:1123–35.
27. Pibarot P, Dumesnil JG. Valve prosthesis–patient mismatch, 1978 to 2011. From original concept to compelling evidence. J Am Coll Cardiol Img. 2012;60:1136–9.
28. Smadi O, Garcia J, Pibarot P, Gaillard E, Hassan I, Kadem L. Accuracy of Doppler-echocardiographic parameters for the detection of aortic bileaflet mechanical prosthetic valve dysfunction. Eur Heart J Cardiovasc Imaging. 2013. doi:10.1093/ehjci/jet059.
29. Muratori M, Montorsi P, Maffessanti F, Teruzzi G, Zoghbi WA, Gripari P, Tamborini G, Ghulam Ali SG, Fusini L, Fiorentini C, Pepi M. Dysfunction of bileaflet aortic prosthesis accuracy of echocardiography versus fluoroscopy. J Am Coll Cardiol Img. 2013;6:196–205.
30. Burwash IG. Low-flow, low-gradient aortic stenosis: from evaluation to treatment. Curr Opin Cardiol. 2007;22:84–91.

Prosthetic Aortic Valves and Diagnostic Challenges

10

Michael J. Gallagher

Abstract

Stenosis of bioprosthetic or mechanical aortic valves can occur due to valve degeneration, pannus formation, thrombosis, and endocarditis. Prosthetic valve stenosis is characterized by elevated trans-aortic velocities and gradients; however, it is imperative to realize that the mere presence of an elevated gradient across an aortic valve prosthesis is not sufficient to diagnose prosthesis stenosis. This chapter will review the valve design and types, causes of prosthetic aortic valve stenosis, approach to evaluate patients with elevated trans-aortic prosthesis gradient, as well as the complimentary role of CT and MRI.

Keywords

Prosthetic aortic valves • Bioprosthetic aortic valves • Mechanical aortic valves • Prosthetic valve stenosis • Causes of prosthetic valve aortic stenosis

Prosthetic Aortic Valves and Diagnostic Challenges

Stenosis of bioprosthetic or mechanical aortic valves can occur due to valve degeneration, pannus formation, thrombosis, and endocarditis. Prosthetic valve stenosis is characterized by elevated trans-aortic velocities and gradients; however, it is imperative to realize that the mere presence of an elevated gradient across an aortic valve prosthesis is not sufficient to diagnose prosthesis stenosis. This chapter will review the valve design and types, causes of prosthetic aortic valve stenosis, approach to evaluate patients with elevated trans-aortic prosthesis gradient, as well as the complimentary role of CT and MRI.

M.J. Gallagher, MD, FACC
Department of Cardiovascular Medicine,
Beaumont Health, Oakland University/William
Beaumont School of Medicine, Royal Oak, MI, USA
e-mail: Mgallagher@beaumont.edu

Valve Design and Types

The ideal prosthetic aortic valve should replicate the function and durability of a native aortic valve. No prosthetic aortic valve is perfect, and evaluation of patients with abnormal prosthetic valve function is one of the most difficult challenges a clinician faces. Selection of a proper

A.E. Abbas (ed.), *Aortic Stenosis: Case-Based Diagnosis and Therapy*,
DOI 10.1007/978-1-4471-5242-2_10

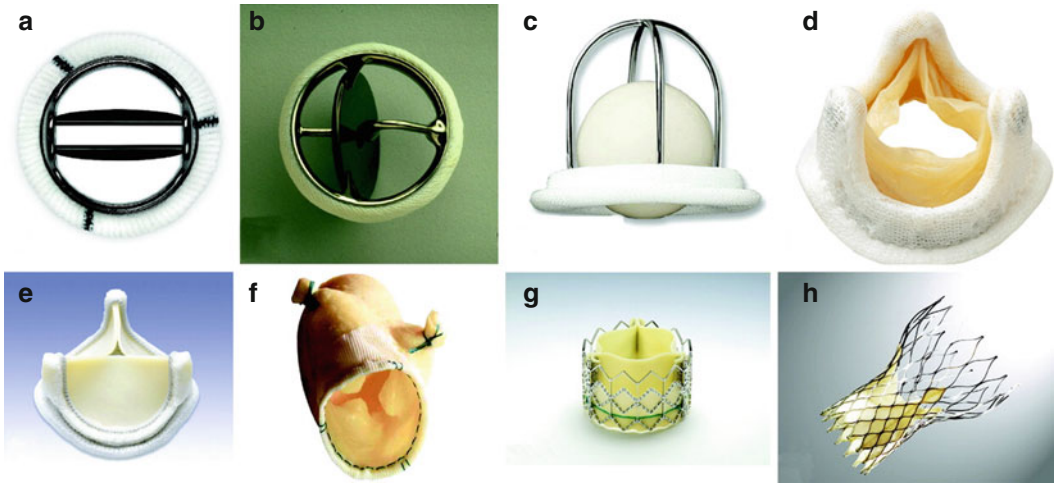

Fig. 10.1 Different types of prosthetic valves. (**a**) Bileaflet mechanical valve (St Jude); (**b**) monoleaflet mechanical valve (Medtronic Hall); (**c**) caged ball valve (Starr-Edwards); (**d**) stented porcine bioprosthesis (Medtronic Mosaic); (**e**) stented pericardial bioprosthesis (Carpentier-Edwards Magna); (**f**) stentless porcine bioprosthesis (Medtronic Freestyle); (**g**) percutaneous bioprosthesis expanded over a balloon (Edwards Sapien); (**h**) self-expandable percutaneous bioprosthesis (CoreValve) (From Pibarot and Demesnil [3] with permission)

valve involves trade-offs between the advantages and disadvantages of the valve type [1]. Prosthetic valve types are grouped into biologic (tissue) and mechanical valves. Figure 10.1 provides examples of commonly used prosthetic valves [2, 3].

Bioprosthetic Valves

Bioprosthetic valves can be classified according to their species origin, nature of tissue used, whether or not they are mounted on a stent, whether they are placed surgically or percutaneously, and the site of placement.

A. A tissue valve is an actual valve or biological tissue derived from:
   (a) Animals (heterograft or xenograft): Bovine or porcine
   (b) Humans (homograft or allograft): the Ross procedure describes transposing of the patient's pulmonic valve in the aortic position and placing a bioprosthetic valve in the pulmonic position.

B. A tissue valve is made of biologic tissue derived from:
   (a) Aortic valve tissue: usually porcine in origin and consists of three porcine aortic valve leaflets cross-linked with glutaraldehyde.
   (b) Pericardial tissue: pericardial valves are usually derived from sheets of bovine pericardium.

C. A tissue valve may either be a:
   (a) Stented bioprosthesis: This may consistent of sheets of bovine pericardium mounted inside or outside a supporting stent or a porcine aortic valve mounted on a metallic or polymer supported stent.
   (b) Stentless bioprosthesis: may also be either porcine aortic valves or derived from bovine pericardium and are devoid of stent in an attempt to improve valve hemodynamics and durability.

D. A tissue valve may either be placed:
   (a) Surgically: surgical aortic valve replacement (SAVR) through either a full sternotomy or minimally invasive surgery through a hemisternotomy or a right thoracotomy.
   (b) Percutaneously: Transaortic valve replacement (TAVR) that may be implanted through a transfemoral, transaortic, and transapical approaches. Other

alternatives may include a transcaval approach where the valve is placed through the femoral vein and then through an IVC-aortic created connection as well as a transsubclavian approach. TAVR valves may either be placed as balloon expandable or self expandable techniques.

E. A tissue valve may either be placed:
   (a) Annular: at the level of the aortic annulus
   (b) Supra-annular: This is designed to lift the valve out of the annulus in order to minimize the resistance contained in the annulus.

The most common aortic position tissue valve is a **stented aortic valve xenograft**. These aortic valves are extracted, preserved, and fixed within a mount attached to a Dacron sewing ring. Pericardial prosthetic valve leaflets are typically comprised of pericardial tissue sewn on to **stent posts**.

Stentless bioprostheses are also commonly used in the aortic position. Stentless xenograft valves are usually made from a preparation of a porcine aorta. This type of valve is supported by a "cuff" and does not require rigid stents. These valves (e.g. Medtronic Freestyle) are porcine aortic valves that include the annulus, valve and aortic root. Tissue valves have the advantage of non-thrombogenicity such that long term anticoagulation is not necessary, however the durability of a tissue valve is limited. Stentless bioprosthesis and pulmonary autografts may have a temporary increase in the gradients for 3 months after surgery due to edema between the prosthesis and the aortic wall or because of outflow tract remodelling that usually regress.

Mechanical Valves

Mechanical valves are classified as caged ball and tilting disk designs.

A. The caged ball (e.g. Starr-Edwards) valves: they are no longer implanted. They consisted of a silastic ball with a circular sewing ring and a cage formed by three metal arches. Patients with these types of valves implanted require physicians to be versed in their special characteristics and echo image.
B. Tilting Discs: Several tilting disk valves are in use, including:
   (a) Single tilting disk valves or monoleaflet valves (e.g. Bjork Shiley, Medtronic Hall, Omniscience): these are secured by lateral or central struts and the resultant two valve orifices are of different sizes
   (b) Bileaflet tilting disk valves (e.g. St Jude Medical and Carbomedics): these are made of two semilunar disks attached to a rigid valve ring by small hinges and there are three resultant valve orifices; one smaller central and two larger peripheral ones.

The most frequent mechanical aortic valve implanted is the **bileaflet tilting disk valve**. These valves differ among manufacturers based upon the design, shape and angle of opening of the leaflets, and design and shape of the housing and sewing ring. The major disadvantages of mechanical valves are related to the necessity for life long anticoagulation with warfarin, whereas durability is the major advantage.

Causes of Prosthetic Valve Aortic Stenosis

The most common causes of prosthetic aortic valve stenosis are **valve degeneration** (**causing bioprosthetic valve stenosis or regurgitation**), **pannus formation**, **valve thrombosis**, **and rarely endocarditis** (Fig. 10.2). Both bioprosthetic and mechanical vales are at risk of fibrous tissue or pannus overgrowth causing prosthetic stenosis. This is more common than valve thrombosis, which occurs more commonly in mechanical valves and presents with thrombo-embolic complications or an incidental finding on echocardiography, although critical valve thrombosis

is uncommon. In addition to type of valve, the risk of thrombosis is also related to patient factors as left ventricular function, left atrial size, atrial fibrillation and most commonly is related to coagulopathy or lack of adherence to anticoagulation. The role of the novel anticoagulants in thromboembolic prevention in patients with mechanical valves is unclear. The CATHAR trial (Comparison of Antithrombotic Treatments After Aortic Valve Replacement, clinical trial number NCT02128841) will compare the role of Rivaroxaban (Xarelto) to warfarin in patients with mechanical valves. However, RE-ALIGN study found an increased risk of stroke and higher bleeding in patients who received a mechanical heart valve and were treated with Dabigatran (Pradaxa) as compared to warfarin [4].

Obstruction of homografts or Stentless bioprosthesis with thrombus or pannus is less frequent than mechanical or stented bioprosthesis. In a study of 251 patient with prosthetic valve malfunction requiring reoperation, the linearinzed rate of pannus formation was 0.24 %/patient-year (48/251) and that of thrombosis was 0.15 % (29/251) [2].

The distinction between thrombus, pannus, and endocarditis as the underlying etiology of obstruction is essential if thrombolytic therapy or surgery is contemplated. Using TEE along with clinical parameters, the following features may help differentiate the different etiologies of prosthetic valve stenosis (Fig. 10.2):

1. **Pannus Formation**: this includes a **small echodense echocardiographic mass** on the valve that may not be visible in 30 % of the time and is more common in the aortic position. It is usually associated with a longer and gradual duration and onset of symptoms.
2. **Valve Thrombosis**: thrombi present as **larger masses with more echolucency** compared to pannus. They more commonly present with shorter duration of symptoms and more abrupt onset, with a history of inadequate anticoagulation. Moreover, TEE is more likely to detect abnormal prosthetic valve motion with an occasional catastrophic presentation.

   Patients with NYHA class I and II and who have recent symptom onset and thrombi with a resultant aortic valve area <0.8 cm^2 are candidates for lytic therapy if IV heparin fails. Conversely, patients with mobile or larger thrombi or class III and IV symptoms should undergo emergency surgery. Baseline TEE and follow up serial Doppler of the prosthetic valves is essential with thrombolytic therapy. It is to be noted that both pannus and thrombus can occur together and after successful lytic therapy. Follow up Doppler to diagnose residual pannus is essential to avoid valve re-thrombosis.
3. **Vegetations from endocarditis**: These tend to occur in the valve ring area and can affect valve function by interrupting the valve leaflet, stent, or occluder and cause prosthetic stenosis (or regurgitation). **Vegetations are usually irregularly shaped and mobile with independent movement**. Differentiating vegetations from thrombus, sutures, and pledgets, can be difficult, and comparison to previous or post-operative baseline studies may be essential. Moreover, interpreting the echocardiographic image in the context of the clinical picture (fever, positive blood cultures, etc.) will also aid with the diagnosis of prosthetic valve endocarditis [2].

Hemodynamics and Anticipated Gradients of Prosthetic Valves

The initial suspicion of abnormal prosthetic valve function is often the **discovery of a new murmur** or the incidental finding of a **high transprosthetic gradient**. Most of the relevant information regarding the function of a prosthetic valve is obtained from a thorough and quantitative Doppler examination. The range of normal, or anticipated gradients across a prosthetic aortic valve vary depends on the **size** of the prosthesis as well as the **type** of valve (i.e. mechanical valve, stented and stent-less bioprostheses, transcatheter valves, have a decreasing expected trans valve gradient in that order) [2].

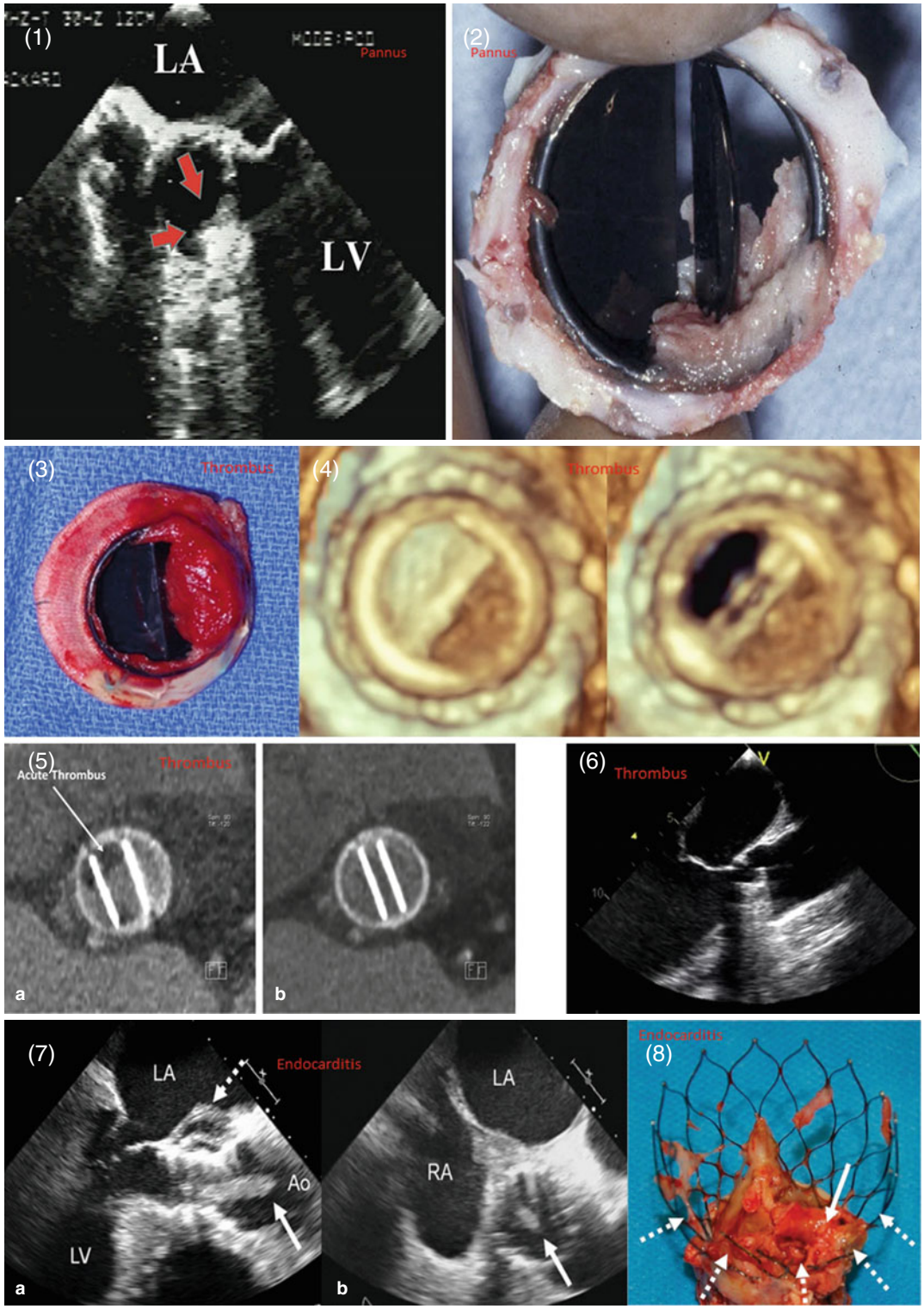

Fig. 10.2 Causes of prosthetic aortic valve stenosis: pannus formation (1–2), thrombus formation (3–6), and vegetation (7–8): (From Zoghbi et al. [2]; Extract from the Educational Case on "Mechanical Valve Thrombosis" by Prof. D. Messika-Zeitoun and Dr C. Cimadevilla, members of the ESC Working Group on valvular heart diseases. Retrieve the full case on http://www.escardio.org/communities/Working-Groups/valvular/education/featured-cases/Pages/mechanical-valve-thrombosis.aspx; and Orban et al. [25] with permission)

In general, Doppler gradients across normally functioning prosthetic valves resemble those obtained across a native valve with mild aortic stenosis. The hemodynamics and blood flow characteristics can differ substantially between the various prosthetic aortic valve types and according to patient characteristics.

The **normal** pattern of flow through stented aortic bioprostheses is typically a **circular central flow** field with a **peak velocity** between 2 and 3 m/s, corresponding to a **mean pressure gradient** of 10–15 mmHg, along with a **triangular shape** of the velocity contour with an early systolic maximal velocity. Importantly, high gradients may be seen across normal valves with a small size: for example a 29 mm St. Jude bileaflet valve may have a maximum gradient of 18 mmHg, while a 19 mm Carpentier-Edwards bio-prosthetic stented valve may have a normal maximum gradient of 43 mmHg. The hemodynamics of tissue valves vary significantly based upon the valve type, structure and size [5].

In general, lower profile valves such as stentless substitutes (stentless bioprostheses, aortic homografts) tend to have lower trans-prosthetic gradients than stented valves. In addition, transcatheter aortic valve replacement (TAVR) is associated with minimal gradients owing to the low profile of the valve.

See Table 10.1 for the different types of prosthetic valves and range of "normal" (anticipated) gradients depending on the type and size of valve prosthesis.

Algorithmic Approach to Evaluate Prosthetic Aortic Valve Function

A baseline echocardiogram soon after AVR, is invaluable to evaluate future tans-aortic gradients across the prosthetic valve. The guidelines suggest the first post-operative echo performed within 2-4 weeks after anemia has resolved, wound healed, and patient ambulating. No further echocardiograms are recommended except annually after 10 years with bioprosthetic valves and with development of signs or symptoms suggestive of any valve dysfunction.

Distinguishing prosthetic aortic valve stenosis from other causes of increased trans AV velocities and gradients is essential. Multiple diagnostic modalities that have been suggested to assist with the diagnosis include:

1. **TTE and TEE 2D and Doppler echocardiography**: It should be noted that shadowing from the prosthetic valves might obscure adequate visualization of leaflet structure and mobility. In addition, adequate visualization of the cause of prosthetic valve stenosis may be best detected by TEE as compared to TTE. Doppler parameters have been suggested to help evaluate the hemodynamic impact in addition to the pathological diagnosis.
2. **Stress echocardiography**: The use of supine bike and dobutamine echocardiography are preferred to treadmill exercise due to the rapid decline to baseline hemodynamics with the latter.

   Normally functioning stentless valves and stented bovine pericardial valves have the lowest resting and exercise gradients with a resultant minimal increase in mean pressure gradient from about 6 mmHg at rest to 9 mmHg during stress. Conversely, porcine valves are relatively more obstructive and generate higher resting and exercise gradients. In one study, there was an increase in mean gradient from 19 to 28 mmHg during stress with the Medtronic intact porcine valve. Mechanical valves generate the highest Doppler gradients in part due to flow acceleration in the smaller central orifice of a bi-leaflet mechanical valve. Upstream from the valve, the central jet reunites with the lateral jets with resultant recovery of pressure and decrease in transvalvular pressure gradient. The diagnostic change in mean gradient from rest to exercise is unknown. However, an increase in trans-valvular gradient by greater than 15 mmHg with exercise, in a symptomatic patient without ischemia, is highly suggestive of abnormal valve dynamics. Dobutamine echocardiography may also be used when low flow/low gradient severe prosthetic valve stenosis is suspected similar to what is described in the native valves.

Table 10.1 Normal Doppler echocardiography values for selected prosthetic aortic valves

Cryolilfe *Stentless*	19 21 23 25 27		9.0 ± 2.0 6.6 ± 2.9 6.0 ± 2.3 6.1 ± 2.6 4.0 ± 2.4	1.5 ± 0.3 1.7 ± 0.4 2.3 ± 0.2 2.6 ± 0.2 2.8 ± 0.3
Edwards Duromedics *Bileaflet*	21 23 25 27	39.0 ± 13 32.0 ± 8.0 26.0 ± 10.0 24.0 ± 10.0		
Edwards Mira *Bileaflet*	19 21 23 25		18.2 ± 5.3 13.3 ± 4.3 14.7 ± 2.8 13.1 ± 3.8	1.2 ± 0.4 1.6 ± 0.4 1.6 ± 0.6 1.9
Hancock *Stented porcine*	21 23 25	18.0 ± 6.0 16.0 ± 2.0 15.0 ± 3.0	12.0 ± 2.0 11.0 ± 2.0 10.0 ± 3.0	
Hancock II *Stented porcine*	21 23 25 29	34.0 ± 13.0 22.0 ± 5.3 16.2 ± 1.5	14.8 ± 4.1 16.6 ± 8.5 10.8 ± 2.8 8.2 ± 1.7	1.3 ± 0.4 1.3 ± 0.4 1.6 ± 0.4 1.6 ± 0.2
Homograft *Homograft valves*	17–19 19–21 20–21 20–22 22 22–23 22–24 24–27 26 25–28	1.7 ± 0.3 0.4 ± 0.6	9.7 ± 4.2 7.9 ± 4.0 7.2 ± 3.0 5.6 ± 3.1 6.2 ± 2.6	4.2 ± 1.8 5.4 ± 0.9 3.6 ± 2.0 3.5 ± 1.5 5.8 ± 3.2 2.6 ± 1.4 5.6 ± 1.7 2.8 ± 1.1 6.8 ± 2.9 6.2 ± 2.5
Intact *Stented porcine*	19 21 23 25 27	40.4 ± 15.4 40.9 ± 15.6 32.7 ± 9.6 29.7 ± 15.0 25.0 ± 7.6	24.5 ± 9.3 19.6 ± 8.1 19.0 ± 6.1 17.7 ± 7.9 15.0 ± 4.5	1.6 ± 0.4 1.6 ± 0.4 1.7 ± 0.3
Ionescu-Shiley *Stented bovine pericardial*	17 19 21 23	23.8 ± 3.4 19.7 ± 5.9 26.6 ± 9.0	13.3 ± 3.9 15.6 ± 4.4	0.9 ± 0.1 1.1 ± 0.1
Labcor Santiago *Stented bovine pericardial*	19 21 23 25	18.6 ± 5.0 17.5 ± 6.6 14.8 ± 5.2 12.3 ± 3.4	11.8 ± 3.3 8.2 ± 4.5 7.8 ± 2.9 6.8 ± 2.0	1.2 ± 0.1 1.3 ± 0.1 1.8 ± 0.2 2.1 ± 0.3
Labcor Synergy *Stented porcine*	21 23 25 27	24.3 ± 8.1 27.3 ± 13.7 22.5 ± 11.9 17.8 ± 7.0	13.3 ± 4.2 15.3 ± 6.9 13.2 ± 6.4 10.6 ± 4.6	1.1 ± 0.3 1.4 ± 0.4 1.5 ± 0.4 1.8 ± 0.5
MCRI On-X *Bileaflet*	19 21 23 25	21.3 ± 10.8 16.4 ± 5.9 15.9 ± 6.4 16.5 ± 10.2	11.8 ± 3.4 9.9 ± 3.6 8.6 ± 3.4 6.9 ± 4.3	1.5 ± 0.2 1.7 ± 0.4 1.9 ± 0.6 2.4 ± 0.6

(continued)

Table 10.1 (continued)

Medtronic Advantage *Bileaflet*	23 25 27 29		10.4 ± 3.1 9.0 ± 3.7 7.6 ± 3.6 6.1 ± 3.8	2.2 ± 0.3 2.8 ± 0.6 3.3 ± 0.7 3.9 ± 0.7
Medtronic Freestyle *Stentless*	19 21 23 25 27	11.0 ± 4.0	13.0 ± 3.9 9.1 ± 5.1 8.1 ± 4.6 5.3 ± 3.1 4.6 ± 3.1	1.4 ± 0.3 1.7 ± 0.5 2.1 ± 0.5 2.5 ± 0.1
Medtronic Hall *Single tilting disc*	20 21 23 25 27	34.4 ± 13.1 26.9 ± 10.5 26.9 ± 8.9 17.1 ± 7.0 18.9 ± 9.7	17.1 ± 5.3 14.1 ± 5.9 13.5 ± 4.8 9.5 ± 4.3 8.7 ± 5.6	1.2 ± 0.5 1.1 ± 0.2 1.4 ± 0.4 1.5 ± 0.5 1.9 ± 0.2
Medtronic Mosaic *Stented porcine*	21 23 25 27 29	23.8 ± 11.0 22.5 ± 10.0	14.2 ± 5.0 13.7 ± 4.8 11.7 ± 5.1 10.4 ± 4.3 11.1 ± 4.3	1.4 ± 0.4 1.5 ± 0.4 1.8 ± 0.5 1.9 ± 0.1 2.1 ± 0.2
Mitroflow *Stented bovine pericardial*	19	18.6 ± 5.3	13.1 ± 3.3	1.1 ± 0.2
Monostrut Bjork-Shiley *Single tilting disc*	19 21 23 25 27	27.5 ± 3.1 20.3 ± 0.7	27.4 ± 8.8 20.5 ± 6.2 17.4 ± 6.4 16.1 ± 4.9 11.4 ± 3.8	
Prima *Stentless*	21 23 25	28.8 ± 6.0 21.5 ± 7.5 22.1 ± 12.5	13.7 ± 1.9 11.5 ± 4.9 11.6 ± 7.2	1.4 ± 0.7 1.5 ± 0.3 1.8 ± 0.5
Omnicarbon *Single tilting disc*	21 23 25 27	37.4 ± 12.8 28.8 ± 9.1 23.7 ± 8.1 20.1 ± 4.2	20.4 ± 5.4 17.4 ± 4.9 13.2 ± 4.6 12.4 ± 2.9	1.3 ± 0.5 1.5 ± 0.3 1.9 ± 0.5 2.1 ± 0.4
Omniscience *Single tilting disc*	21 23	50.8 ± 2.8 39.8 ± 8.7	28.2 ± 2.2 20.1 ± 5.1	0.9 ± 0.1 1.0 ± 0.1
Starr Edwards *Caged ball*	23 24 26 27 29	32.6 ± 12.8 34.1 ± 10.3 31.8 ± 9.0 30.8 ± 6.3 29.0 ± 9.3	22.0 ± 9.0 22.1 ± 7.5 19.7 ± 6.1 18.5 ± 3.7 16.3 ± 5.5	1.1 ± 0.2 1.1 ± 0.3
Sorin Bicarbon *Bileaflet*	19 21 23 25	30.1 ± 4.5 22.0 ± 7.1 16.8 ± 6.1 11.2 ± 3.1	16.7 ± 2.0 10.0 ± 3.3 7.7 ± 3.3 5.6 ± 1.6	1.4 ± 0.1 1.2 ± 0.4 1.5 ± 0.2 2.4 ± 0.3
Sorin Pericarbon *Stentless*	19 21 23	36.5 ± 9.0 28.0 ± 13.3 27.5 ± 11.5	28.9 ± 7.3 23.8 ± 11.1 23.2 ± 7.6	1.2 ± 0.5 1.3 ± 0.6 1.5 ± 0.5

Table 10.1 (continued)

St. Jude Medical Haem Plus *Bileaflet*	19 21 23	28.5 ± 10.7 16.3 ± 17.0 16.8 ± 7.3	17.0 ± 7.8 10.6 ± 5.1 12.1 ± 4.2	1.9 ± 0.1 1.8 ± 0.5 1.7 ± 0.5
St. Jude Medical Regent *Bileaflet*	19 21 23 25 27	20.6 ± 12 15.6 ± 9.4 12.8 ± 6.8 11.7 ± 6.8 7.9 ± 5.5	11.0 ± 4.9 8.0 ± 4.8 6.9 ± 3.5 5.6 ± 3.2 3.5 ± 1.7	1.6 ± 0.4 2.0 ± 0.7 2.3 ± 0.9 2.5 ± 0.8 3.6 ± 0.5
St. Jude Medical Standard *Bileaflet*	19 21 23 25 27 29	42.0 ± 10.0 25.7 ± 9.5 21.8 ± 7.5 18.9 ± 7.3 13.7 ± 4.2 13.5 ± 5.8	24.5 ± 5.8 15.2 ± 5.0 13.4 ± 5.6 11.0 ± 5.3 8.4 ± 3.4 7.0 ± 1.7	1.5 ± 0.1 1.4 ± 0.4 1.6 ± 0.4 1.9 ± 0.5 2.5 ± 0.4 2.8 ± 0.5
St. Jude Medical *Stentless*	21 23 25 27 29	22.6 ± 14.5 16.2 ± 9.0 12.7 ± 8.2 10.1 ± 5.8 7.7 ± 4.4	10.7 ± 7.2 8.2 ± 4.7 6.3 ± 4.1 5.0 ± 2.9 4.1 ± 2.4	1.3 ± 0.6 1.6 ± 0.6 1.8 ± 0.5 2.0 ± 0.3 2.4 ± 0.6

Modified from Zoghbi et al. [2] with permission

3. **CTA** of the mechanical prosthetic valve occluder motion.
4. The difference between **projected and measured EOAi**. If the measured EOA is less than the projected EOA - 1 standard deviation (SD), prosthetic stenosis should be suspected. If it is less than the projected EOA - 2 SD, there is a high likelihood of significant stenosis.
5. The **geometric orifice area** of the prosthetic valve.
6. **Fluoroscopy** of mechanical prosthetic valve occluder motion: Opening angle of <30° on fluoroscopy of a mechanical prosthesis also suggests stenosis.

A trans aortic high velocity/gradient alone is not sufficient evidence that a prosthetic aortic valve demonstrates significant stenosis. Although there is a broad spectrum of "normal" or anticipated gradients depending upon the type of surgical prosthesis used, general guidelines have been proposed by the ASE writing group regarding the parameters that should be routinely measured during the echocardiographic assessment of prosthetic aortic valve function.

Figure 10.3 outlines the American Society of Echocardiography – Prosthetic Valve (ASE – PV) algorithmic approach for evaluation of prosthetic aortic valves under normal (or near normal) flow conditions [6]. Although the proposed approach provides a general framework for the sonographer and echocardiographer, multiple factors influence the accuracy and reliability of the semi-quantitative and quantitative parameters.

A careful assessment of all clinical, invasive and imaging data is necessary in evaluation of such complex patients. Importantly, this algorithm does not apply to valves that simulate a "normal" aortic valve flow characteristics such as stentless aortic valves, homografts and percutaneous aortic valves (i.e. TAVR).

The initial suspicion of prosthetic valve dysfunction is often an ***elevated trans-prosthetic velocity*** detected during a routine echocardiogram assessment. A thorough echocardiographic assessment is necessary for optimal assessment of aortic valve function. Comparison with a "baseline" study of valve function and Doppler indices obtained soon after surgery is extremely helpful. The

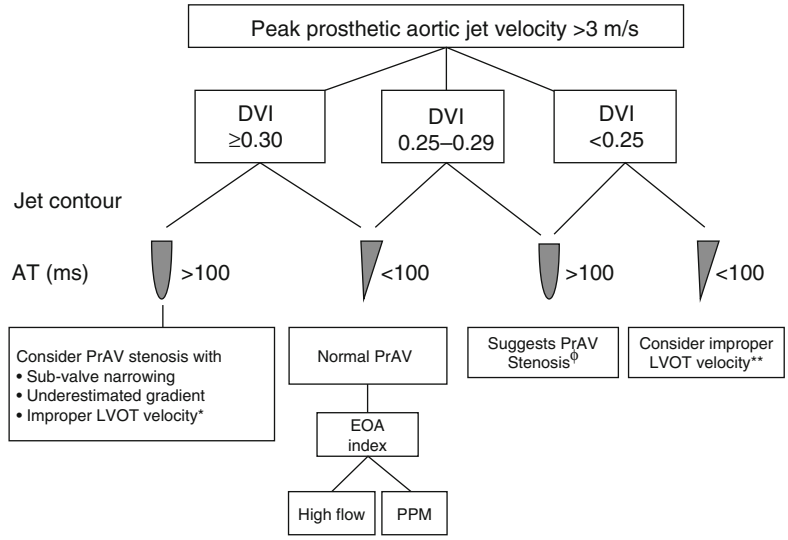

Fig. 10.3 Algorithm for evaluation of prosthetic valve function (From Zoghbi et al. [2] with permission)

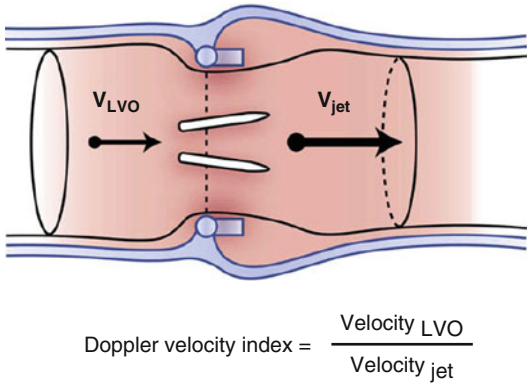

Fig. 10.4 Doppler velocity index ratio (From Zoghbi et al. [2] with permission)

type and size of the prosthetic valve should be noted, as well as measurements of the aortic root and ascending aorta.

Important Doppler echocardiographic quantitative parameters of prosthetic valve function (see Figs. 10.3 and 10.4; Tables 10.1 and 10.2) include determination of:

1. **The peak velocity across the valve**: AV_{vel} (A value greater than 3 m/s is considered abnormal)
2. **The peak and mean gradients**: ΔP_{MIG} and ΔP_{mean}. Both 1 & 2 are more affected by transvalvular flow than the other parameters and may be non elevated despite prosthetic valve stenosis in low flow states (prosthesis area/gradient mismatch)
3. **Doppler velocity index** (**DVI**): ratio of the LVOT velocity ($LVOT_{vel}$) divided by the peak velocity of the AV jet ($DVI = LVOT_{vel}/AV_{vel}$) [7] (A value less than 0.3 and DVI is less dependent on flow especially less than 0.25 is abnormal) (Fig. 10.4)
4. **Calculated prosthetic aortic valve effective orifice area** ((**EOA = (CSA LVOT × VTI LVO)/VTI jet**)): "The LVOT diameter should be measured apically to the prosthesis in the zoomed parasternal long view. The LVOT diameter is not the inner prosthesis stent, strut, or ring and it should not be substituted for the labelled prosthesis size." This is true for surgical valves and for balloon expandable trans-catheter valves. However, for self expandable valves, measuring the LVOT diameter within the proximal portion of the stent 5-10 mm below the leaflets is recommended. (Fig. 10.5)
5. **Acceleration time** (**AT**): [8] (A cutoff AT value of 100 ms has been shown to differentiate between normal and obstructive valves)
6. **Ejection time** (**ET**):
7. **AT/ET**: a value >0.4 suggests prosthesis stenosis
8. **Shape of the AV jet contour**: (triangular versus bullet shaped)

Obstruction of the valve is considered when the **AVvel is >3 m/s and the DVI is <0.25**; a

Table 10.2 Echocardiography Doppler parameters of normal and abnormal prosthetic valve function (*)

Parameter	Normal	Possible stenosis	Suggests significant stenosis
Peak velocity (m/s)[a]	<3	3–4	>4
Mean gradient (mmHg)[a]	<20	20–35	>35
DVI	≥0.30	0.29–0.25	<0.25
EOA (cm^2)	Triangular, early peaking	Triangular to intermediate	Rounded, symmetrical contour
AT (ms)	<80	80–100	>100

Modified from Zoghbi et al. [2] with permission
*PrAV p*rosthetic aortic valve
*In conditions of normal or near normal stroke volume (50–70 mL) through the aortic valve
[a]These parameters are more affected by flow, including concomitant AR

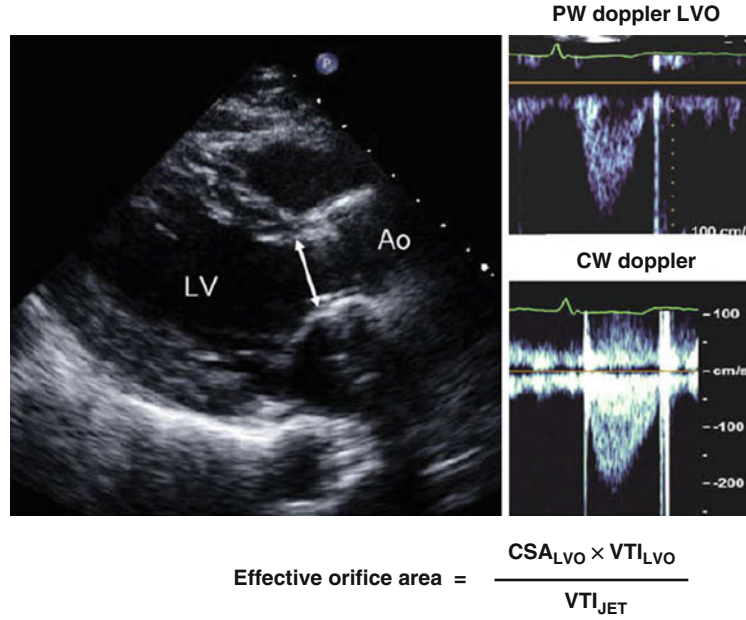

Fig. 10.5 Calculation of the effective orifice area (From Zoghbi et al. [2] with permission)

rounded contour jet velocity with a late peaking envelope (i.e. **longer acceleration time**) increases the suspicion for prosthetic aortic valve disease. It is not uncommon, however, for discordance between parameters and other imaging/clinical data. The following cases outline important considerations and caveats in application of the ASE – PV algorithmic.

ASE: PV Algorithm Case Illustration

Errors in Measurement

The principals used in evaluation of prosthetic aortic valves are similar to those used in native aortic valve assessment. Continuous wave and pulsed wave Doppler and color Doppler are par-

amount in determining the flow characteristics of the prosthetic valve function. The Doppler study must be performed with a variety of transducer positions to detect the maximal jet velocity across the valve. From these Doppler recordings, maximal and mean pressure gradients and the effective orifice area can be calculated. Importantly, the maximum continuous wave velocity can be increased without stenosis, such as in cases of *high output state*, *prosthesis patient mismatch*, *local flow acceleration* through the central orifice of a bileaflet tilting discs, and the concomitant presence of *prosthetic valvular regurgitation*.

In order to obtain the left ventricular outflow tract (**LVOT**) **velocity**, a pulsed wave (PW) sample volume is placed adjacent to the prosthesis, taking care to avoid the region of sub-valvular acceleration – sample volume usually requires a position 5–10 mm toward the apex to avoid acceleration. This is especially true for surgical valves. For balloon expandable trans-catheter valves, LVOT velocity should be measured immediately proximal to the apical border of the stent. However, for self expandable valves, measuring within the proximal portion of the stent 5-10 mm below the leaflets is recommended. The LVOT pulsed wave Doppler envelope should have minimal spectral broadening with a well-defined peak. The highest velocities and most laminar flow generally occurs at the center of the annulus. If the pulse volume is placed (incorrectly) within the zone of flow acceleration, this can lead to an artificially high Doppler velocity index as well as an artificially high aortic valve area calculated by the continuity equation, thus underestimating the severity of valve stenosis (see example below). Importantly, improper placement of the LVOT sample volume too far from the prosthetic aortic valve can lead to an under estimation of the LVOT velocity and over estimation of the severity of valve stenosis (see Fig. 10.3). Another potential source of error in estimating the aortic valve area is inaccurate measurement of the **left ventricular outflow tract area**. When necessary, trans-esophageal imaging can be used for an accurate LVOT measurement [9]. Doppler misalignment and interrogation of other jets (as mitral regurgitation) may also occur as with native valves and has been described before.

Patient Example 1

67-year-old female with a history of mechanical aortic valve replacement in 1998 (Bi-leaflet St Jude Epic Porcine Prosthesis) with progressive dyspnea on exertion.

Echocardiogram demonstrated LVEF: 60 %. Mean AV gradient: 24 mmHg. Peak AV gradient: 48 mmHg (Fig. 10.6). Peak AV velocity 3.5 m/s. AVA (VTI): 0.9 cm^2., DVI: 1.19/3.3 = 0.33. Effective orifice area = (CSA lvo × VTI lvo)/VTIprav = 3.14×0.95^2 (24.2/71.4) = 0.9 cm^2. Mechanical AV appeared stenotic visually. Left heart catheterization and valve fluoroscopy was performed, demonstrating only one of two functional mechanical aortic valve leaflets (Fig. 10.7).

On further examination, it was found that when obtaining LVOT velocities, the pulse wave sample was placed too close to the aortic valve prosthesis (Position 1, more aortic), thus elevating the LVOT velocities and falsely increasing the DVI (Fig. 10.8). When the study was repeated with correction of the PW sample (Position 2, more apical), a DVI was determined to be in the severe range (0.82/3.60 = 0.23) (Fig. 10.9). Surgery confirmed the findings of a single functioning mechanical leaflet with a large area of tissue ingrowth beneath the valve resulting in prosthetic valve stenosis.

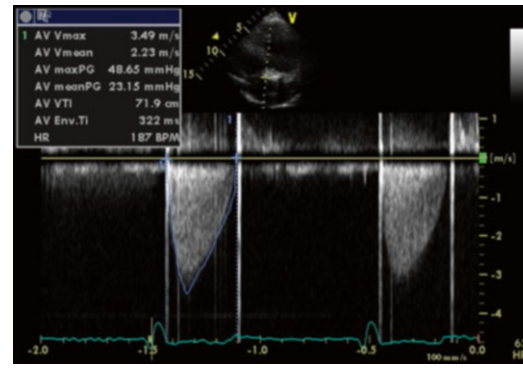

Fig. 10.6 Continuous Wave (*CW*) Doppler of the aortic valve mechanical prosthesis

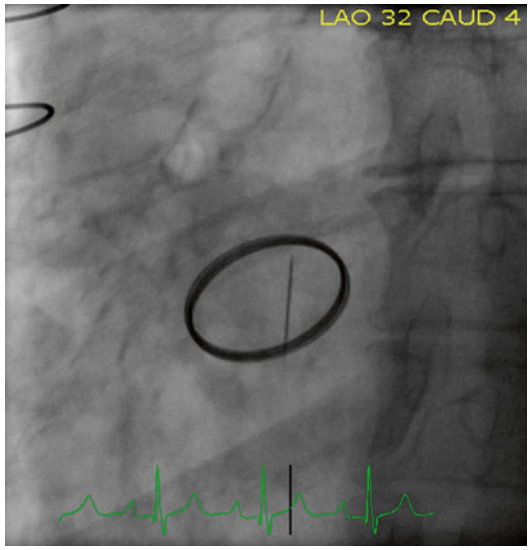

Fig. 10.7 Fluoroscopy demonstrating a single functioning mechanical valve leaflet

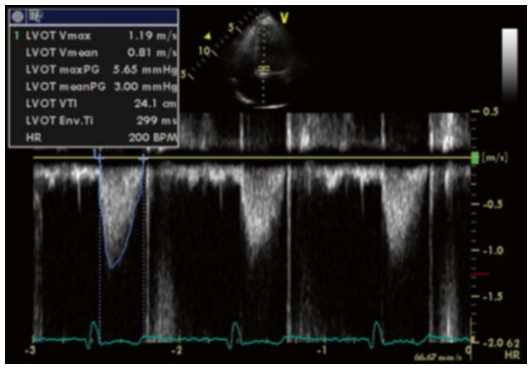

Fig. 10.8 Left Ventricular Outflow Tract (*LVOT*) Pulsed Wave (*PW*) Doppler Position 1 (too close to flow convergence adjacent to the prosthetic valve)

Importance of Qualitative Indices in the Assessment of Prosthetic Valve Stenosis

High trans-prosthetic gradients may not be evident in the case of low cardiac output, even in the presence of obstruction. The sum of velocities taken at the LVOT using pulsed wave Doppler is called the velocity time integral (VTI). The VTI is equal to stroke distance, and used to calculate stroke volume (SV = VTI × CSA LVOT). In patients with reduced left ventricular function, the aortic flow velocity and gradients can be

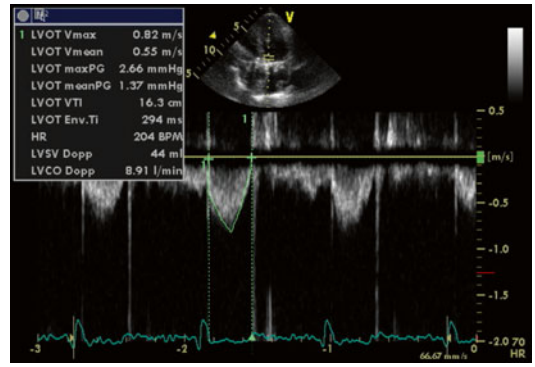

Fig. 10.9 Left Ventricular Outflow Tract (*LVOT*) Pulsed Wave (*PW*) Doppler position 2 (moved more apically to avoid flow convergence and acceleration of flow and falsely elevated LVOT velocity)

deceptively low. In such cases, the LVOT velocity time integral also decreases due to low stroke volume, and consequently the calculated DVI remains in a severe range. In such cases, the contour of the velocity through the prosthesis is a valuable index of valve function that is used in conjunction with other quantitative values. In normal prosthetic valves, there is a triangular shaped to the velocity with a rapid acceleration time (AT). With prosthetic valve dysfunction, a more rounded velocity contour is seen with a prolonged AT peaking often in mid ejection (a cutoff AT value of 100 ms has been shown to differentiate between normal and obstructive valves) [10].

Patient Example 2

81-year-old with a history of rheumatic valve disease, history of multivessel bypass graft surgery and mechanical aortic valve replacement in 2003 (19 mm St. Jude Regent valve). The patient presented with progressive dyspnea on exertion.

Transthoracic echocardiogram demonstrated ejection fraction 50 %, Mean AV gradient: 24 mmHg. Peak AV gradient: 42 mmHg. Peak AV velocity 3.2 m/s, DVI: 0.58/3.24=0.18 (Figs. 10.10 and 10.11). Rounded velocity contour was seen with an acceleration time of 150 ms. Mechanical AV was difficult to see on transthoracic and transesophageal imaging. Therefore a functional

cardiac CT angiogram was performed for assessment of bypass graft anatomy as well as valve function (Figs. 10.12a–d and 10.13). These studies demonstrated one fixed mechanical valve leaflet. This case example highlights the concept that a dysfunctional aortic valve prosthesis may have a normal peak velocity and mean gradient (i.e. as seen in low flow states and area/gradient mismatch).

Valve Prosthesis: Patient Mismatch (VP-PM)

One of the most common causes of a high gradient across a prosthetic aortic valve is valve prosthesis – patient mismatch (VP-PM). VP-PM occurs when the indexed EOA (EOAi) is reduced, this occurs when the size of the prosthetic valve orifice is too small in relation to the patient's body size. Severe VP-PM is associated with increased mortality especially in the subset of patients who

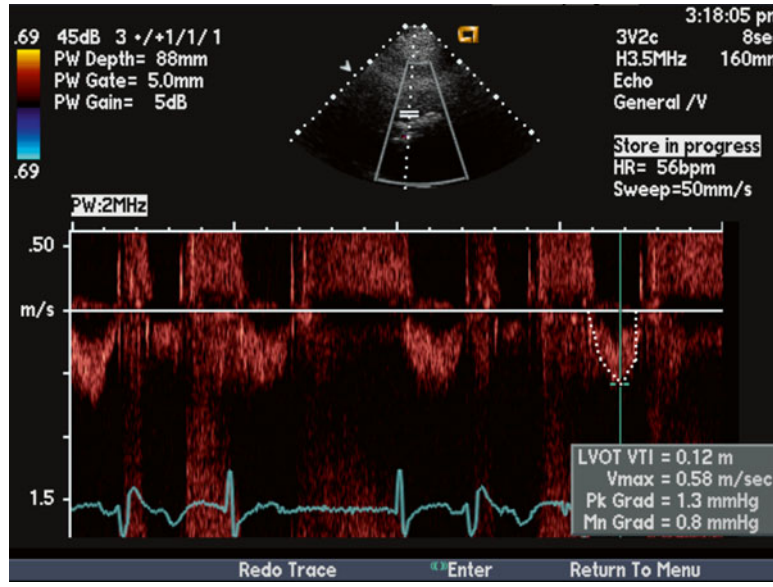

Fig. 10.10 Pulsed wave Doppler of LVOT

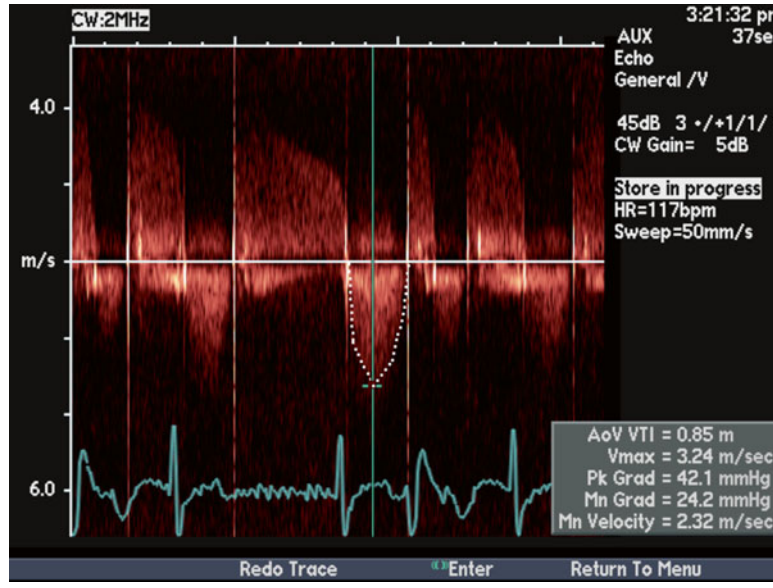

Fig. 10.11 Continuous wave Doppler across prosthetic mechanical aortic valve

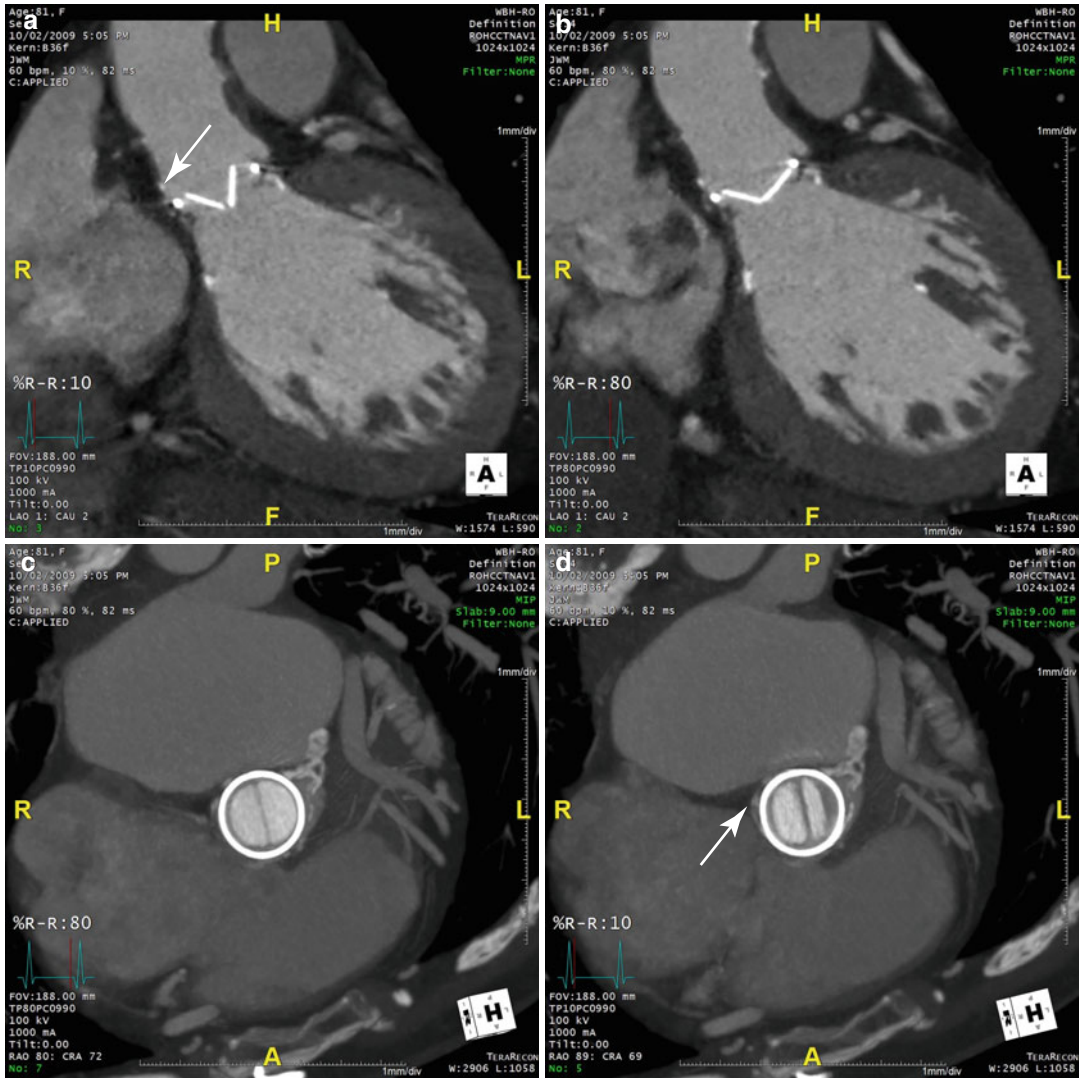

Fig. 10.12 In systole (**a** and **d**) and diastole (**b** and **c**). Fixed leaflet is highlighted by the *arrow*. (**a**–**d**) Functional gated cardiac CT angiography demonstrating dynamic valve motion and the presence of one fixed leaflet

are < 70 years of age, have a BMI < 30, and with low left ventricular systolic function.

The most commonly used measures of valve size are the **measured EOAi** and the **projected EOAi** [11]. The measured (or observed) EOAi is calculated based upon echo doppler data, while the projected EOAi is based upon reference data that provide the expected EOA for the labeled size and model of the valve that was implanted [7, 12]. The majority of studies that have examined the VP-PM have used cut off values of <0.85 cm^2/m^2 for moderate VP- PM and <0.65 cm^2/m^2 for severe VP-PM [13]. The American Society of echocardiography 2009 guidelines for assessment of prosthetic valves have endorsed these definitions. Therefore, to avoid any significant gradient at rest or with exercise, the projected EOAi of the aortic valve prosthesis should be no less than 0.85–0.9 cm^2/m^2. In the patient example outlined below (with a body surface area of 1.6 m^2), the ideal minimal value E0A to avoid VP-PM is 1.36 cm^2 (Pibarot JACC 2000). This patient underwent AVR utilizing a 23 mm St Jude with a projected EOA of 1.5 cm^2 (and projected EOAi = 1.0 cm^2/m^2).

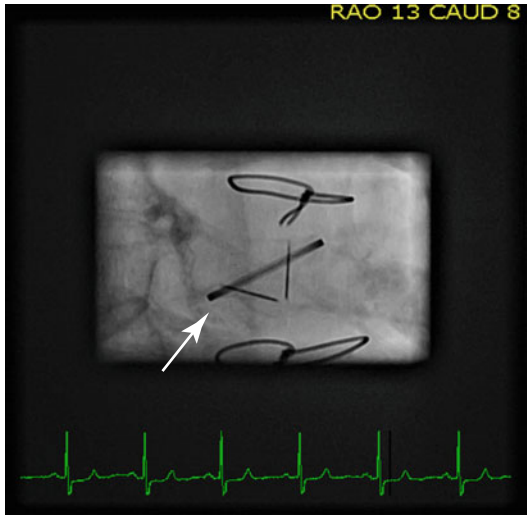

Fig. 10.13 Fluoroscopy of mechanical valve motion demonstrating one fixed leafet

Fortunately, there have been significant improvements in design of valve prostheses that provide a better hemodynamic performance. As a result, with careful attention to appropriate valve sizing and selection, the incidence of significant mismatch has declined. PPM should not be assumed in patients with small (19, 21) sizes of a bileaflet mechanical valve due to the previously described phenomenon of localized high velocity/gradient of the central orifice and significant recovery of pressure with stream realignment upstream. In summary, VP-PM is considered present when the inserted prosthetic valve is too small relative to patient body size and therefore causes a higher-than-expected gradient through a normally functioning prosthetic valve.

Patient Example 3

66-year-old female (51 kg, 66 in., body surface area 1.57 m^2) with history of COPD underwent mechanical aortic valve replacement in 2002 (23 mm St Jude Valve Conduit) due to severe aortic insufficiency associated with annulo-aortic ectasia, with ascending aortic dilation and EF 45 % at the time of initial surgery. Patient was admitted with progressive dyspnea on exertion.

Transthoracic echocardiogram demonstrated ejection fraction 55 %, Mean AV gradient: 30 mmHg. Peak AV gradient: 53 mmHg. Peak AV velocity 3.6 m/s, LVOT velocity 0.78 m/s, DVI: 0.78/3.6 = 0.21 (Figs. 10.14, 10.15, and 10.16). Triangular velocity contour was seen with an acceleration time of 90 ms. the aortic valve area calculated by VTI equals 0.97 cm^2. The indexed EOA equals 0.62 (BSA = 1.6). Manufacturer provided EOA = 1.6 cm^2 for 23 mm St Jude Standard valve (Chafizadeh et al. Circulation 1991), thus projected EOAi = 1.0 cm^2/m^2) The patient underwent fluoroscopy and was found to have normal tilting disc motion. These findings suggest valve prosthesis-patient mismatch (VP-PM).

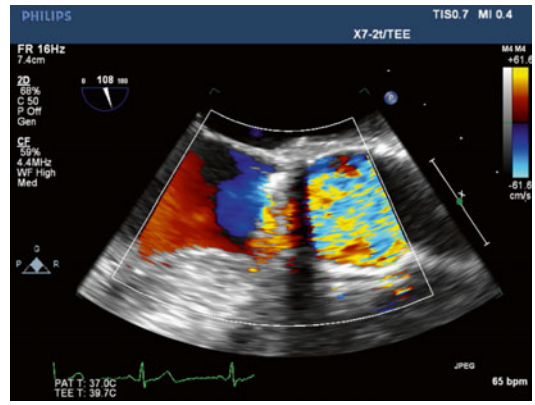

Fig. 10.14 Color Doppler through the mechanical aortic valve on trans-esophageal imaging

Role of Cardiac CT and Cardiac MRI for Assessment of Prosthetic Valve Complications

The assessment of prosthetic valve function remains a significant challenge to clinicians. Proper identification of prosthetic leaflet motion by transthoracic and trans-esophageal echocardiography has been shown to be poorly feasible in a subset of patients [14, 15]. As outlined above, use of gradients alone can be limited as gradients dependent on flow magnitude as well as patient size and valve type. In cases of suspected or equal vocal prosthetic

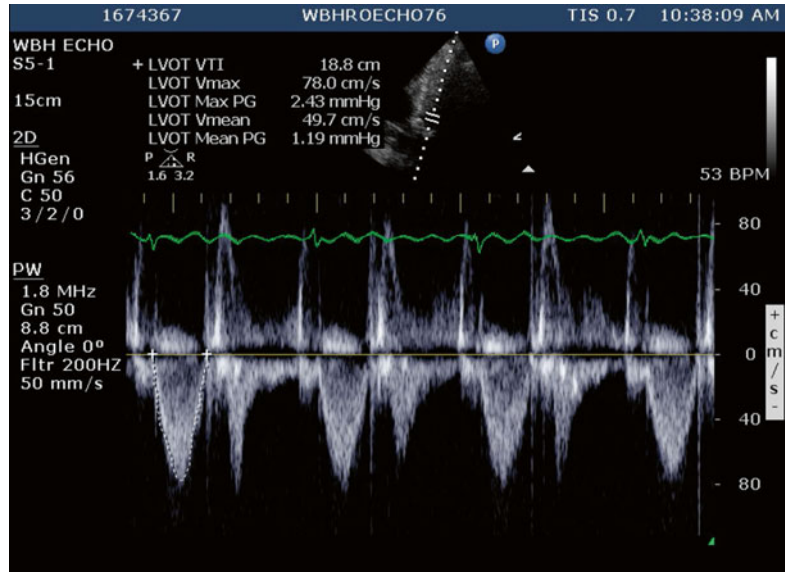

Fig. 10.15 PW Doppler across the left ventricular outflow tract

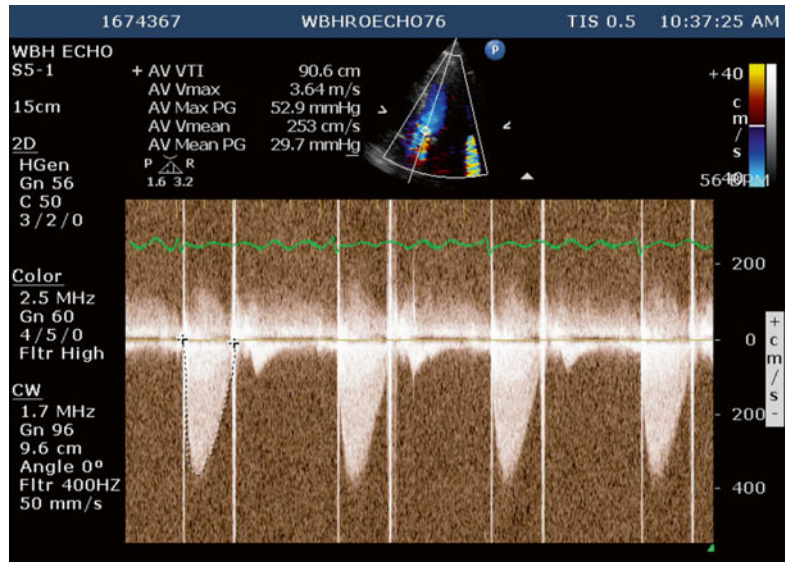

Fig. 10.16 CW Doppler imaging across the mechanical aortic valve. The CW jet contour is triangular and early peaking (AT < 100 ms), consistent with the absence of prosthetic valve stenosis as what may occur with VP-PM. Other causes of increased trans-valve gradient in the absence of stenosis include high flow states, pressure recovery, or any combination of the above

valve function, complementary data can be obtained from fluoroscopy as well as CT and cardiac MRI imaging. The following case examples will outline the role of cardiac CT and MR imaging in the diagnosis of prosthetic valve disease as well as complications of prosthetic aortic valves.

Cardiac CT

Multi-detector CT has rapidly evolved into an important cardiovascular imaging tool for assessment of patients with suspected coronary artery disease. More recently, cardiac CT has been used for assessment of native and prosthetic valvular disease [16–18]. Assessment of valve disease requires electrocardiographic gating to study the valve motion of the prosthesis over the entire cardiac cycle. Cine mode of leaflet motion can be assessed to evaluate mechanical valve motion with minimal artifact (see above patient examples). Assessment of tissue prosthetic valve motion is more challenging, however CT does permit characterization of

perivalvular structures (i.e. aortic root, mediastinal structures, abscess formation, etc.) that are not well visualized upon echocardiography. More recently, use of positron emission tomography/commuted tomography has been shown to be a helpful technique for diagnosing prosthetic valve endocarditis, especially in the case of initial negative echocardiography results [19, 20].

As outlined in the previous case, fluoroscopy and /or functional CT imaging can be complementary and useful diagnostic studies in patients with diagnostic challenges. Such complementary information is useful in patients with low gradients and low cardiac output, as well as in patients with a high gradient where the possibility of patient prosthesis mismatch cannot be excluded [21, 22]. Fluoroscopy and gated cardiac CT are rapid, inexpensive and very active at techniques to evaluate tilting disc prosthetic function. In cases where additional coronary or aortic imaging is indicated (i.e. evaluate location or patency of bypass grafts, younger patients without suspicion for coronary artery disease, evaluation of the aortic root or other pathology), functional gated cardiac CT is a useful adjunct. Such complementary imaging is especially useful in states where a high gradient might be related to a high flow state (such as sepsis, etc.) or improper interrogation through the smaller central orifice of a bi-leaflet mechanical valve. The following cases illustrate such a caveat.

Patient Example 4

48-year-old female with a history of congenital aortic stenosis, underwent mechanical aortic valve replacement as a 24-year-old (CarboMedics). Over the past year she has developed progressive shortness of breath complicated by new anemia requiring a blood transfusion.

Transthoracic echocardiogram revealed an ejection fraction of 65 %, prosthetic aortic peak velocity of 4.0 m/s, peak gradient 63 mmHg, mean gradient 36 mmHg. Doppler velocity index = 0.275, AT = 105 ms (Fig. 10.17). Trans-esophageal echocardiogram revealed similar hemodynamics, the aorta was moderately dilated measuring 42 mm in maximum dimension. Left main appeared aneurysmal measuring 12 mm (Fig. 10.18a, b).

Functional gated cardiac CT study was performed to assess the coronary anatomy, left main aneurysm, aortic root and mechanical disk motion. This revealed normal mechanical valve leaflet motion, dilated aortic root, aneurysmal left main ostium and no evidence of coronary artery disease (Figs. 10.19 and 10.20a, b). It was felt that the patient's elevated gradients were due to a higher estimated flow velocity associated with an eccentric jet (off-axis relationship of prosthetic aortic valve with aneurysmal aortic root), yielding an over estimation of the gradient and underestimation of the effective orifice area [23].

Patient Example 5

74-year-old male presented 9 months after redo aortic valve replacement and repair of a sub-valvular abscess with a bovine pericardial patch. Patient presented with fever, leukocytosis and bacteremia (staph epidermitis).

Transesophageal echocardiogram demonstrated a recurrent subvalvular leak as well as a perivalvular leak. The extent of the involvement was not well defined by transesophageal echocardiogram (Fig. 10.21).

Coronary CT angiogram was performed for assessment of bypass graft anatomy as well as the presumed abscess. CT demonstrated a large pseudoaneurysm/abscess cavity surrounding the posterior and lateral aspect of the aortic root. The extent of abscess/cavity involvement was well defined by CT and noted a free and open communication with the non-coronary cusp adjacent to the sewing region. The CT angiogram provided useful information to guide a redo sternotomy, composite descending aorta and aortic valve replacement, Decadron interposition graft, and coronary artery ostia reimplantation (Figs. 10.22, 10.23, 10.24, and 10.25).

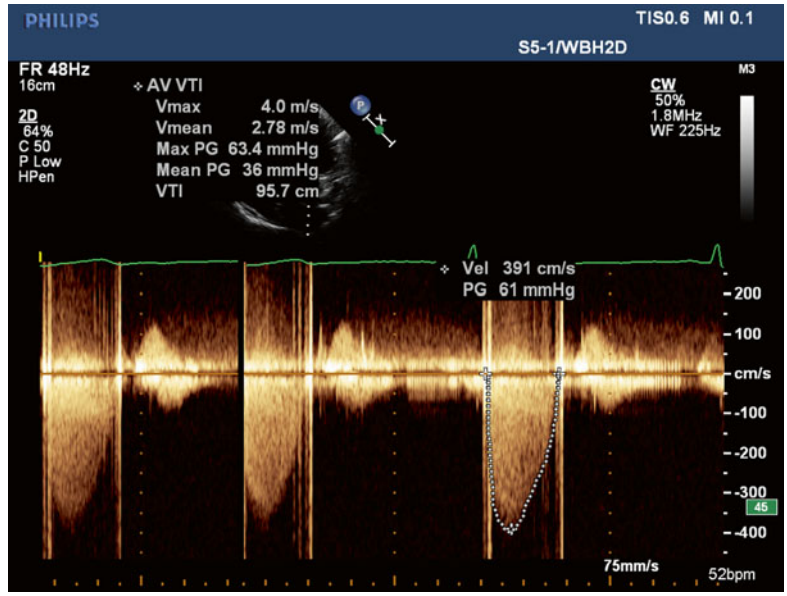

Fig. 10.17 Transthoracic CW gradient across mechanical aortic valve

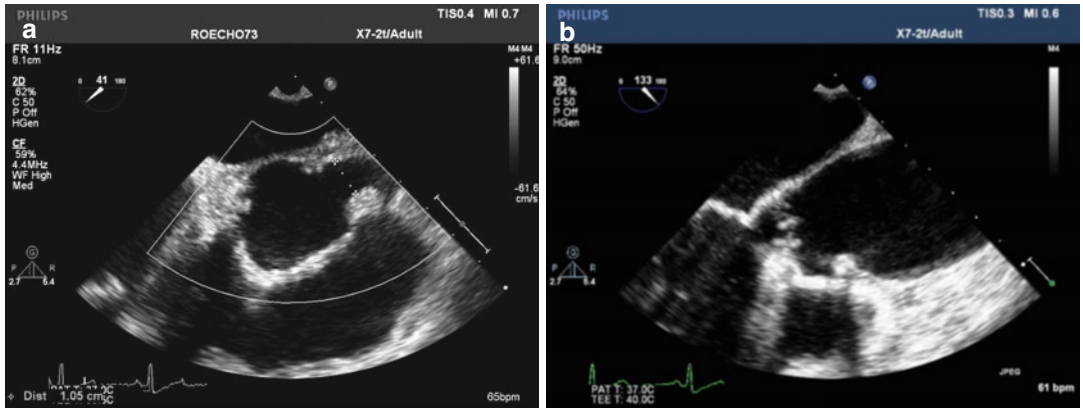

Fig. 10.18 Transesophageal echo images of mechanical aortic valve and left main coronary artery short axis (**a**) and long axis (**b**)

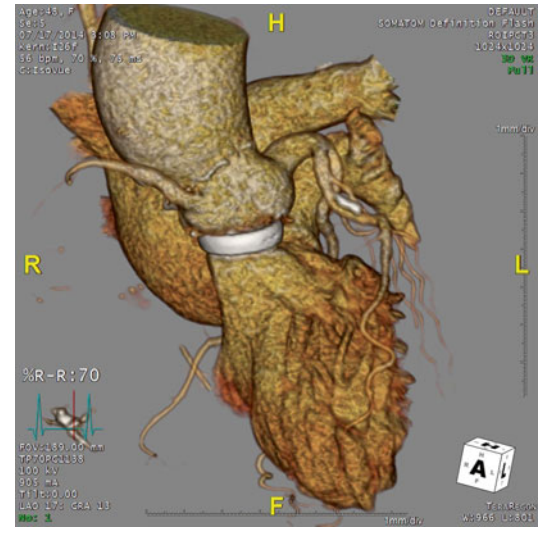

Fig. 10.19 ECG gated CT angiogram of left main and aortic root

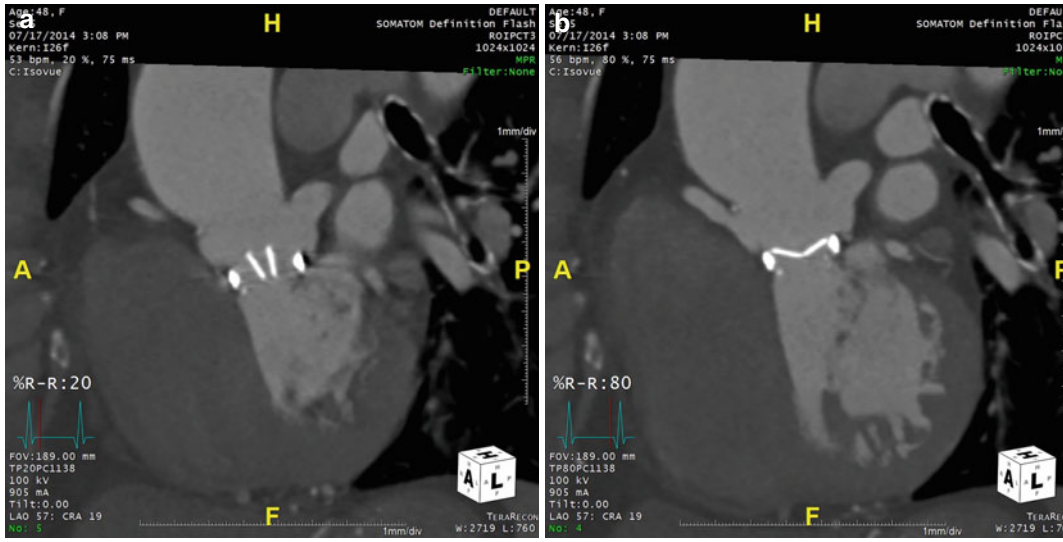

Fig. 10.20 ECG gated CT angiogram of mechanical aortic valve (**a**) systole and (**b**) diastole

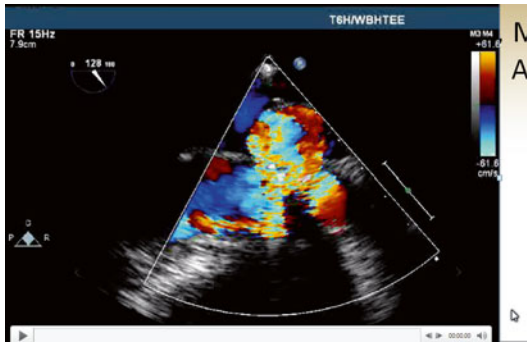

Fig. 10.21 Trans-esophageal image of sub-valvular and peri-valvular leak

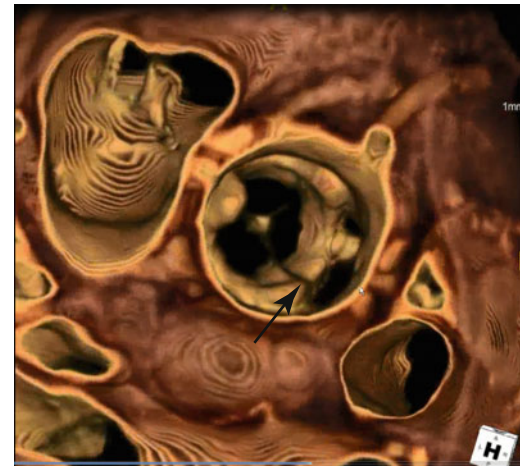

Fig. 10.23 ECG-gated functional Cardiac CT demonstrating large pseudo-aneurysm/abscess cavity (arrow)

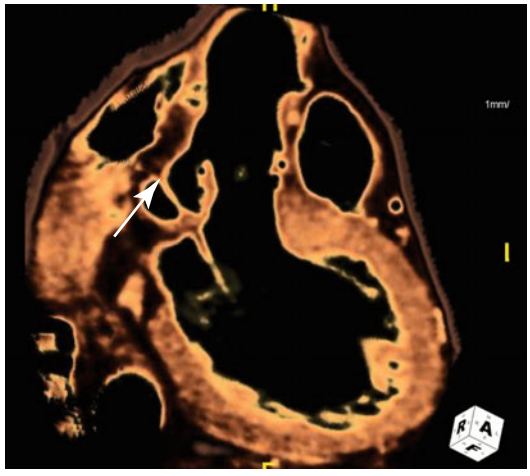

Fig. 10.22 ECG-gated functional cardiac CT demonstrating large pseudo-aneurysm/abscess cavity (arrow)

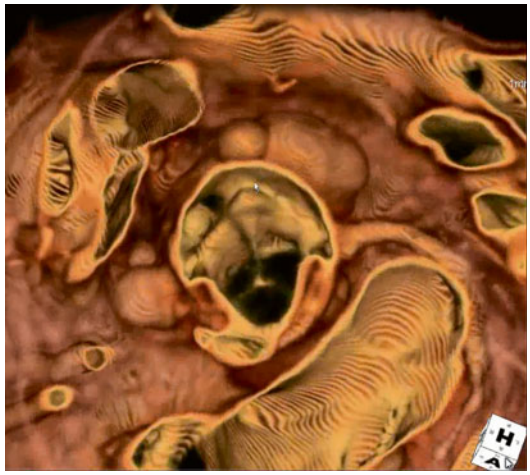

Fig. 10.24 ECG-gated functional Cardiac CT demonstrating large pseudo-aneurysm/abscess cavity

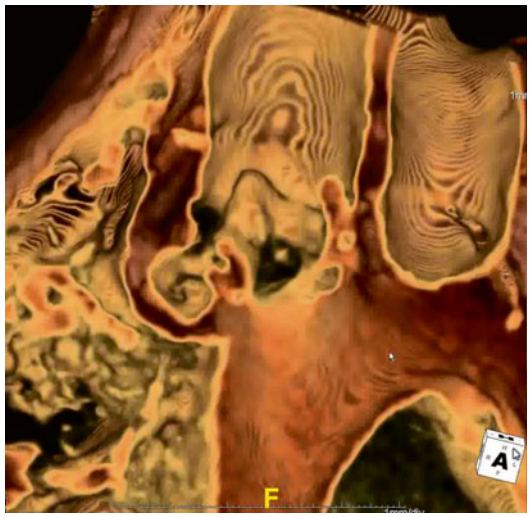

Fig. 10.25 ECG-gated functional cardiac CT demonstrating large pseudo-aneurysm/abscess cavity

Cardiac MRI

Cardiac MRI has been shown to be safe for evaluation of most cardiac valve prostheses. Importantly, prosthetic valve artifacts can affect the ability to visualize leaflet motion, particularly in the setting of mechanical valve prostheses. **Quantification of aortic regurgitation** can be well assessed using cardiac MRI in the assessment of prosthetic valve regurgitation. Phase contrast velocity encoded MRI imaging within the aortic root allows accurate quantitation of the degree of regurgitation. As outlined in the cases below, cardiac MRI may be a useful adjunct in the assessment of patients with bioprosthetic valve disease. Although mechanical prostheses result in metallic imaging artifacts, selective use of cardiac MRI may be complementary in patients with prosthetic valve complications as outlined in the case below [24].

Patient Example 6

46 year old female with a history of aortic dissection requiring Bentall aortic repair with mechanical aortic valve replacement. One decade after surgery, the patient presented with fever, rigors, dyspnea and blood cultures growing gram positive cocci.

Trans-thoracic and trans-esophageal imaging (Fig. 10.26) demonstrated dehiscence of the mechanical valve with pseudoaneurysm formation. Prior to re-do sternotomy and replacement of ascending aortic valve conduit, the patient underwent Cardiac MRI imaging to better delineate the pseudo-aneurysm and peri-aortic complication. Cardiac MRI revealed a large pseudo aneurysm with superior displacement of the mechanical valve above the aortic annulus (Figs. 10.27 and 10.28). Surgical findings revealed dehiscence of the entire valve conduit from the annulus with a very large pseudoaneurysm and extensive purulent tissue around the site.

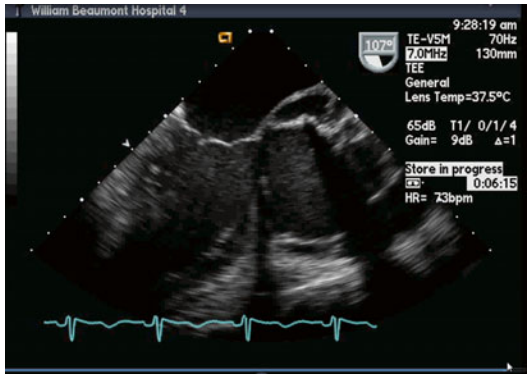

Fig. 10.26 Trans-esophageal echocardiography image of the mechanical aortic valve dehiscence

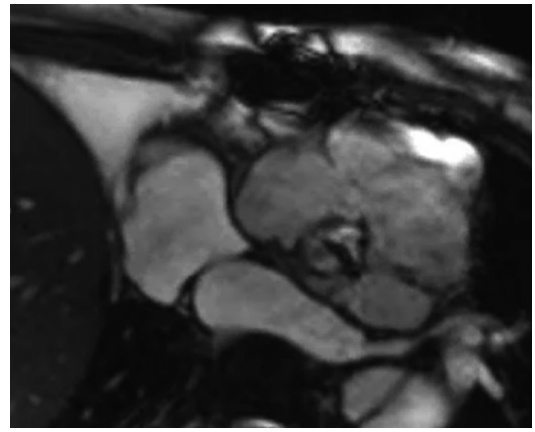

Fig. 10.28 Cardiac MRI images of the mechanical aortic valve dehiscence and circumferential pseudo-aneurysm formation of the valve conduit

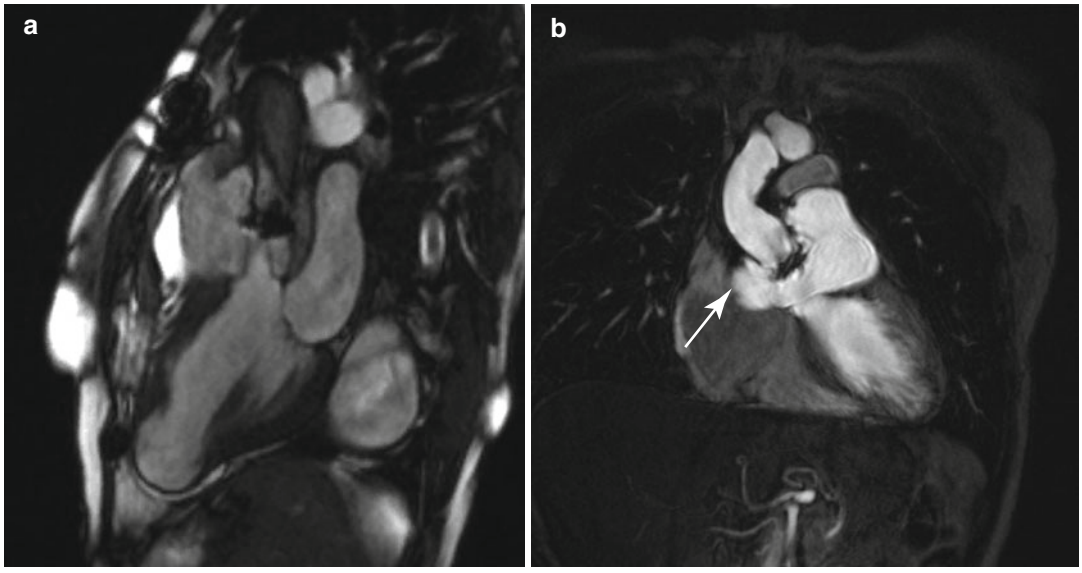

Fig. 10.27 Cardiac MRI images of the mechanical aortic valve dehiscence and circumferential pseudo-aneurysm formation of the valve conduit (**a**) 3 chamber long axis cine view, (**b**) chest MRA of the LVOT and aorta. Arrow highlights the pseudo-aneurysm

References

1. Rahimtoola SH. Choice of prosthetic heart valve for adult patients. J Am Coll Cardiol. 2003;41:893–904.
2. Zoghbi WA, Chambers JB, Dumesnil JG, Foster E, Gottdiener JS, Grayburn PA, et al. Recommendations for evaluation of prosthetic valves with echocardiography and Doppler ultrasound: a report from the American Society of Echocardiography's Guidelines and Standards Committee and the Task Force on Prosthetic Valves, developed in conjunction with the American College of Cardiology Cardiovascular Imaging Committee, Cardiac Imaging Committee of the American Heart Association, the European Association of Echocardiography, a registered branch of the European Society of Cardiology, the Japanese Society of Echocardiography and the Canadian Society of Echocardiography, endorsed by the American College of Cardiology, American Heart Association, European Association of Echocardiography, a registered branch of the European Society of Cardiology, the

Japanese Society of Echocardiography, and Canadian Society of Echocardiography. J Am Soc Echocardiogr. 2009;22:975–1014.
3. Pibarot P, Demesnil JG. Valvular heart disease: changing concepts in disease management prosthetic heart valves: selection of the optimal prosthesis and long-term management. Circulation. 2009;119: 1034–48.
4. Eikelboom JW M.D., Connolly SJ M.D., Brueckmann M M.D., Granger CB M.D., Kappetein AP M.D., Ph.D., Mack MJ M.D., Blatchford J C.Stat., Devenny K B.Sc., Friedman J M.D., Guiver K M.Sc., Harper R Ph.D., Khder Y M.D., Lobmeyer MT Ph.D., Maas H Ph.D., Voigt J-U M.D., Simoons ML M.D., Van de Werf F M.D., Ph.D., RE-ALIGN Investigators. Dabigatran versus warfarin in patients with mechanical heart valves. N Engl J Med. 2013;369:1206–14.
5. Rajani R, Mukherjee D, Chambers JB. Doppler echocardiography in normally functioning replacement aortic valves: a review of 129 studies. J Heart Valve Dis. 2007;16:519–35. 332.
6. Baumgartner H, Khan S, DeRobertis M, Czer L, Maurer G. Effect of prosthetic aortic valve design on the Doppler-catheter gradient correlation: an in vitro study of normal St. Jude, Medtronic-Hall, Starr-Edwards and Hancock valves. J Am Coll Cardiol. 1992;19(2):324.
7. Chafizadeh ER, Zoghbi WA. Doppler echocardiographic assessment of the St. Jude Medical prosthetic valve in the aortic position using the continuity equation. Circulation. 1991;83:213–23.
8. Rothbart RM, Castriz JL, Harding LV, Russo CD, Teague SM. Determination of aortic valve area by two-dimensional and Doppler echocardiography in patients with normal and stenotic bioprosthetic valves. J Am Coll Cardiol. 1990;15:817–24.
9. Zabalgoitia M, Herrera CJ, Chaudhry FA, Calhoon JH, Mehlman DJ, O'Rourke RA. Improvement in the diagnosis of bioprosthetic valve dysfunction by transesophageal echocardiography. J Heart Valve Dis. 1993;2:595–603.
10. Ben Zerky S, Saad RM, Little SH, Zoghbi WA. Flow acceleration time: a novel diagnostic parameter for prosthetic aortic valve stenosis [abstract]. Circulation. 2008;118:S1069.
11. Daneshvar SA, Rahimtoola SH. Valve prosthesis-patient mismatch (VP-PM). A long-term perspective. J Am Coll Cardiol. 2012;60:1123–35.
12. Pibarot P, Dumesnil JG. Hemodynamic and clinical impact of prosthesis-patient mismatch in the aortic valve position and its prevention. J Am Coll Cardiol. 2000;36:1131–41.
13. Pibarot P, Dumesnil JG. Valve prosthesis-patient mismatch, 1978 to 2011. From original concept to compelling evidence. J Am Coll Cardiol. 2012;60(13): 1136–9.
14. Mohr-Kahaly S, Kupferwasser I, Erbel R, et al. Value and limitations of transesophageal echocardiography in the evaluation of aortic prostheses. J Am Soc Echocardiogr. 1992;6:12–20.
15. Muratori M, Montorsi P, Teruzzi G, et al. Feasibility and diagnostic accuracy of quantitative assessment of mechanical prostheses leaflet motion by transthoracic and transesophageal echocardiography in suspected prosthetic valve dysfunction. Am J Cardiol. 2006;97:94–100.
16. Habets J, Mali P, Budde RP. Multidetector CT angiography in evaluation of prosthetic heart valve dysfunction. Radiographics. 2012;32(7):1893–905.
17. Tsai IC, Lin YK, Chang Y. Correctness of multidetector row computed tomography for diagnosing mechanical prosthetic heart valve disorders using operative findings as a gold standard. Eur Radiol. 2009;19(4):857–67.
18. Chenot F, Montant P, Goffinet C. Evaluation of anatomic valve opening and leaflet morphology in aortic valve bioprosthesis by using multidetector CT: comparison with transthoracic echocardiography. Radiology. 2010;255(2):377–85.
19. Saby L, Laas O, Habib G, Cammilleri S, Mancini J, Tessonnier L, et al. Positron emission tomography/computed tomography for diagnosis of prosthetic valve endocarditis. Increased valvular 18F-Fluorodeoxyglucose uptake as a novel major criterion. J Am Coll Cardiol. 2013;61:2374–82.
20. Millar BC, Prendergast BD, Alavi A, Moore JE. 18-FDG-positron emission tomography (PET) has a role to play in the diagnosis and therapy of infective endocarditis and cardiac device infection. Int J Cardiol. 2013;167:1724–36.
21. Muratori M, Montorsi P, Maffessanti F, Teruzzi G, Zoghbi WA, et al. Dysfunction of bileaflet aortic prosthesis. Accuracy of Echocardiography versus fluoroscopy. J Am Coll Cardiol Img. 2013;6:196–205.
22. Ueda T, Teshima H, Fukunaga S, Aoyagi S, Tanaka H. Evaluation of prosthetic valve obstruction on electrocardiographically gated multidetector-row computed tomography. Identification of sub-prosthetic pannus in the aortic position. Circ J. 2013;77:418–23.
23. Abbas AE, Franey LM, Goldstein J, Lester S. Aortic valve stenosis: to the gradient and beyond – the mismatch between area and gradient severity. J Interv Cardiol. 2013;26:183–94.
24. Pham N, Zaitoun H, Mohammed TL, DeLaPena-Almaguer E, Martinez F, Novaro GM, Kirsch J. Complications of aortic valve surgery: manifestations at CT and MR imaging. Radiographics. 2012;32:1873–92.
25. Orban M, Sinnecker D, Mair H, Nabauer M, Kupatt C, Schmitz C, Massberg S, Laugwitz KL, Barthel P. Transcatheter aortic-valve endocarditis confirmed by transesophageal echocardiography. Circulation. 2013;127:e265–6.

Risk Prediction Models, Guidelines, Special Populations, and Outcomes

11

Michael J. Mack and Amr E. Abbas

Abstract

This chapter will discuss risk prediction models for aortic valve replacement, review of the most recent guidelines regarding aortic stenosis, specific patient populations with aortic stenosis, and the valve academic research consortium (VARC) consensus regarding standardized endpoint definitions for transcatheter aortic valve replacement (TAVR).

Keywords

Risk prediction models for aortic valve replacement • Guidelines for aortic stenosis • Valve academic research consortium (VARC) • Transcatheter aortic valve replacement (TAVR) • Aortic stenosis during pregnancy

Introduction

This chapter will discuss risk prediction models for aortic valve replacement, review of the most recent guidelines regarding aortic stenosis, specific patient populations with aortic stenosis, and the valve academic research consortium (VARC) consensus regarding standardized endpoint definitions for transcatheter aortic valve replacement (TAVR).

M.J. Mack, MD
Department of Cardiovascular Disease, Baylor Scott & White Health, Plano, TX, USA

A.E. Abbas, MD, FACC, FSCAI, FSVM, FASE, RPVI (✉)
Department of Cardiovascular Medicine, Beaumont Health, Oakland University/William Beaumont School of Medicine, Royal Oak, MI, USA
e-mail: aabbas@beaumont.edu

Risk Prediction Models

Background

Risk scores are predicted probabilities calculated from a multivariable logistic regression model calibrated on data from within a fixed time [1]. Their accuracy is limited to the patient population and time period from which they were derived. They have been used in various fields of medicine in an attempt to "predict" patient outcomes following a disease process or treatment provided while accounting for general and patient-specific confounding factors. Their goal is to provide a

A.E. Abbas (ed.), *Aortic Stenosis: Case-Based Diagnosis and Therapy*,
DOI 10.1007/978-1-4471-5242-2_11

patient specific outcome expectation and also a quality assurance metric by calculating an observed to expected outcome ratio (O/E) so as to compare therapies and institutions (and possibly individual clinicians in the near future).

An O/E <1 means that patient outcomes at that institution is better than expected based on the historical cohort [1]. In addition, in comparing two different treatment modalities, the therapy with lower O/E ratios suggests a more favorable outcome based on the patient's current comorbidities. It should be noted, that the use of risk prediction models in a given institution with reasonable reliability is appropriate only if institutional outcome are within 1 standard deviation of the STS average O/E ratio for the procedure [2].

Risk models were initially derived, in their primordial form, in response to public reporting of outcomes data in a raw, unrisk-adjusted form following cardiac bypass surgery by the US Health Care Financing Agency (HCFA), the precursor to Medicare, to compare providers and their outcomes in 1984 [1]. However, not accounting for the "case-mix" challenged the simple notion of comparing unadjusted patient outcome data [3]. Moreover, the need for risk models for various diseases, therapies, procedures, and surgeries lead to the surge of current risk prediction models.

The ability to account for various patient-specific baseline variables, severity of illness, unknown confounding factors, and chance is the challenge that faces all risk model predictions [1]. Undoubtedly, the presence of multiple risk models to assess outcomes in patients presenting with the same disease entity, or undergoing the same surgical procedure reflects the lack of a single model that can accurately predict outcome. Moreover, in reality, only optimally reflect the population they were tested in and the accuracy and completion of the data and data points they were derived from (garbage in, garbage out!).

In the field of cardiac surgery, the Society of Thoracic Surgeons (STS) established a committee for the development of The STS National Cardiac Database, which was formally established in 1989 [1]. The earlier STS models for isolated valve surgery were based on data from 1994 to 1997 and did not include data on mitral valve repair [1, 3]. In 2009, based on data from 2002 to 2006 and in an analysis of over 100,000 patients, the STS cardiac risk surgery models for isolated different valve surgeries (isolated aortic and mitral valve replacement and mitral valve repair) and combined CABG and valve surgery were released [3]. Moreover, combined valve surgery models have been developed.

In addition to classic risk prediction models, other parameters to predict outcome in both surgical (SAVR) and trans-catheter aortic valve replacement (TAVR) have been studied as 6-min walk test, frailty score testing [4], and aortic calcifications (porcelain aorta) [1, 2, 4]. In addition to the aforementioned, surgeons frequently use the classic "eye ball" test of the patient prior to proceeding with valve surgery.

Development and Limitations

Three techniques [1] have been used for development of cardiac surgery risk models.

1. Bayesian models: Initially used for the STS database to account for the significant amount of missing data.
2. Logistic regression models: This is the most common statistical technique used and there is some evidence that they perform better [5]. The STS, New York State [6], the Veterans Administration [7], and the Northern New England Cardiovascular Disease Study Group use this model [8]
3. Simple additive scores: With weights derived from logistic regression models. The Parsonnet score [9], and the additive European System for Cardiac Operative Risk Evaluation (EuroSCORE) [10] use this method.

Limitations of risk prediction models includes the following:

1. As mentioned above, risk algorithms are accurate only for the population and in the time frame in which they are developed and

validated. If new confounding variables are discovered or novel technologies or techniques emerge over time, the data may not be accurate. An example is that the early STS database did not include mitral valve repair operations [3]. Similarly, extrapolating the risk prediction models for SAVR likely does not accurately apply to TAVR.

2. Accuracy is diminished at the extremes of the population studied (the tail of the bell-shaped curve), where there are too few patients upon which to build a statistically valid model. This is where high-risk patients with severe aortic stenosis reside accounting for some of the overestimation of risk seen with many models [11, 12]
3. Data that has not been collected due to its *infrequency* (e.g., porcelain aorta, liver disease), due to *lack of its consideration* as a confounding variable (e.g., frailty, severe pulmonary hypertension, severe right ventricular dysfunction), or due to *plain omission* (e.g., internal mammary or other conduit crossing the midline and/or adherent to posterior sternal table, hostile chest from prior surgery, radiation, kyphoscoliosis, pleural adhesions) will not be accounted for in the risk models developed and thus their impact on therapy will not included.
4. An appropriate balance between the need to account for complete and accurate confounding variables on one hand and the ease of use and availability of this data on the other hand allows these models to be used in every patient and for routine decision making. Simpler models, albeit less accurate, may find themselves used on a more regular basis than more accurate, but also more tasking models.

Comparing Different Surgical Risk Models for Aortic Valve Replacement

When comparing different risk algorithms, it is important to distinguish the different time-defined endpoints (in-hospital versus 30 day mortality) [1]. Early mortality, as defined by the STS, includes all deaths occurring before 30 days whether in or out of the hospital and any death occurring in the hospital at any time. Other risk prediction models for early mortality include only in-hospital mortality will underreport approximately 40 % of the deaths as reported by 30 day outcome reporting. For example, in most TAVR series where both in-hospital and 30-day outcomes are reported the mortality is approximately 5 % and 7 % respectively.

The advantage of reporting in-hospital mortality is that the data are more easily collected and probably more accurate. The disadvantage, however, is that very ill postoperative patients who are quite likely to die are frequently discharged to long-term acute care or skilled nursing facilities less than 30 days after surgery and are therefore not counted [1].

In a 2012 analysis of EuroSCORE II outcome data, for example, in which hospital mortality is around 4 %, adding 30-day mortality increases the reported mortality by about 0.6 % (a 15 % relative increase), and adding 90-day mortality increases it further by about 0.9 %.

Surgical Risk Models

At least 12 risk algorithms have been developed in various populations and differing periods to predict outcomes after surgical AVR (Table 11.1). The two most widely used are the Logistic EuroSCORE and the STS Predicted Risk of Mortality and they will be discussed in more details [13–15]

Table 11.1 Surgical risk prediction models for surgical AVR

Society of thoracic surgeons predicted risk of mortality v.2.73
Additive EuroSCORE
Logistic EuroSCORE
EuroSCORE II
Ambler
Northern New England
New York State
Providence Health System
Veterans Affairs Risk Score
Age, Creatinine, Ejection Fraction (ACEF) Score
Australian AVR Score
German Aortic Valve Score

1. **EuroSCORE**: The EuroSCORE risk predictive models include the additive and logistic EuroSCORE as well as the EuroScore II.
   (a) **The additive EuroSCORE model**: It was developed in 1995 and was derived from a population of 15,000 patients and from eight different countries in Europe. Twelve variables were considered in the additive EuroSCORE that were deemed predictive of early mortality.
   (b) **The logistic EuroSCORE model**: This was derived from the additive model and includes 18 variables. However, being based on a relatively small sample, many years ago, and in Europe, it tends to overestimate the actual surgical risk. As such, it has not been used in the any of the TAVR trials or in common clinical use in the US to predict surgical mortality [11, 12]
   (c) **The EuroSCORE II model**: This updated score was derived from more than 22,000 patients operated on between May and July 2010 in 43 countries worldwide. It includes all cardiac procedures and now has 18 covariates predictive of surgical aortic valve mortality. Its incremental benefit remains in question, especially as pertains to surgical AVR. Chalmers et al. [16] applied the model to a 5,500-patient cohort and concluded that EuroSCORE II is globally better calibrated than the EuroSCORE and found better overall discrimination, with a c-index of 0.79 (old model 0.77) and its best performance in mitral (0.87) and coronary (0.79) surgery; Euro SCORE II was weakest in isolated AVR (c-index 0.69), only marginally better than the old model (0.67) [16].
2. **The STS Predicted Risk of Mortality (PROM)**: The model was developed in a later era (2002–2006) in the United States with use of data from over 67,000 patients undergoing only isolated AVR. Twenty-four covariates for mortality have been identified. At least two series have found the STS PROM to be a better predictor of early mortality than the Logistic EuroSCORE, especially in the higher-risk patients undergoing AVR [17, 18]. The STS PROM has now been updated from version 2.73 to version 2.81. As with all risk algorithms, calibration drift occurs as the original data set becomes dated, and the algorithm will need to be updated once sufficient numbers of patients are available for the new version that has in addition captured the new possible predictors. The STS online risk calculator is capable of calculating major morbidity in addition to mortality after surgical AVR [19]. The weighting of the various risk factors is recalibrated with each new version of the STS Adult Cardiac Database according to the most recent data uploaded by the 1,005 cardiac surgery programs in the United States that participate in the database. STS version 2.81 includes 9 outcome points; risk of mortality, morbidity or mortality, long length of stay, short length of stay, permanent stroke, prolonged ventilation, DSW infection, renal failure, and reoperation.

   A composite score from the STS was released in 2012 from observation studies of 3 years (June 2007–July 2010) and 5 years (June 2005–July 2010). This score was based solely on outcomes, including risk-standardized mortality and any-or-none risk-standardized morbidity (occurrence of sternal infection, reoperation, stroke, renal failure, or prolonged ventilation) [20].

   Rankin et al. [21] have also published a risk prediction for multiple valve operations.
3. Less commonly used models include:
   A. The **Ambler Score** was developed from a national database from the Society of Cardiothoracic Surgeons of Great Britain and Ireland on 32,839 patients who underwent heart valve surgery between April 1995 and March 2003 [22].
   B. The **Northern New England risk model** was derived from eight Northern New England Medical Centers in the period January 1991 through December 2001. In this model, 8,943 patients undergoing heart valve surgery were analyzed, and 11 variables in the aortic model were found to be predictive of adverse outcomes [23].

They included older age, lower body surface area, prior cardiac operation, elevated serum creatinine level, prior stroke, New York Heart Association (NYHA) functional class IV, heart failure, atrial fibrillation, acuity, year of surgery, and concomitant CABG.

C. The **Age**, **Creatinine**, **Ejection Fraction score**, previously mentioned, analyzed 29,659 consecutive patients who underwent elective cardiac operations in 14 Italian institutions from 2004 to 2009 [24, 25]. Using only three variables, age serum creatinine and ejection fraction, Ranucci et al. [24, 25] found that for all deciles of risk distribution, the Logistic EuroSCORE significantly overestimated mortality risk and that the Age, Creatinine, Ejection Fraction score slightly overestimated the mortality risk in very-low-risk patients and significantly underestimated the mortality risk in very-high-risk patients, correctly estimating the risk in 7 of 10 deciles. The accuracy of the Age, Creatinine, Ejection Fraction score was acceptable (AUROC 0.702) and at least comparable to the Logistic EuroSCORE calculation.

D. The **Australian AVR score** is based on 3,544 AVR procedures performed between 2001 and 2008. It contains the following predictors: age, NYHA functional class, left main disease, infective endocarditis, cerebrovascular disease, renal dysfunction, previous cardiac surgery, and estimated ejection fraction. The final model (AVR-Score) obtained an average AUROC of 0.78 for early mortality [26].

4. **Models for TAVR**:

With the emergence of percutaneous approaches to AVR, there has been an interest in developing predictive risk models for the management of patients who are candidates for TAVR. The most commonly used model has been the STS PROM which was not developed nor originally intended for this procedure and may not necessarily be the most accurate method for this patient population [27]. Among the factors leading to inaccuracy include:

A. TAVR patients are at the extremes of risk, where the current risk models fail because there are too few patients at the higher extremes of risk to be able to have robust discrimination of risk.

B. The variables that may play significant roles in risk, including porcelain aorta, previous radiation therapy, liver disease, and frailty were included in the risk model.

C. Some of the morbidity data included in the model do not pertain to the TAVR procedure (risk of sternal infection with the trans-femoral approach)

In order to help address some of the inadequacies of the current risk prediction models in adults undergoing aortic valve procedures, the **German Aortic Valve Registry** (**GARY**) has developed the German Aortic Valve Score [28]. It is based on 11,794 patients undergoing surgical AVR or TAVR in Germany in 2008. Using multiple logistic regression, Kötting et al. [28] identified 15 risk factors influencing in-hospital mortality. Among the most important factors determined to predict risk were age, body mass index, renal disease, urgent status, and left ventricular function. The risk model had a high degree of discrimination, with an AUROC of 0.808.

The model does, however, have many limitations including:

A. It was developed on the basis of patients treated in 2008 and may already be not applicable to technologies currently involved in TAVR.

B. Patients undergoing TAVR constituted only 5.1 % (573/11,147) of the study population, limiting the specific application to transcatheter valve risk prediction. Also, TAVR was performed in only 25/81 participating institutions, again limiting the "generalizability" of the score.

C. The model was developed for inter-hospital comparisons only and therefore can predict only overall outcomes in German hospitals. Comparisons can be made of overall program

outcomes between various centers, but it cannot be used to discriminate among different procedures, approaches, or devices.

D. It also cannot as yet determine whether an individual patient should undergo surgical AVR or TAVR or whether a specific device or approach is preferable. It is also likely that different factors constitute different risk profiles for different procedures. For example, frailty may be weighted more when considering surgical AVR compared to TAVR. The risks may not be the same for the different approaches for TAVR, because severe lung disease may be a significant factor impacting outcomes with the transapical approach but not the transfemoral approach.
E. The model was created from a derivation sample due to the small sample size of TAVR procedures in the study, and no validation sample was examined, so the model needs to be validated externally in other populations.
F. This model is based on in-hospital mortality, which is lower than the 30-day definition of mortality used by the STS algorithm.

A true TAVR-specific risk model needs to be developed, and at least two efforts are under way.

1. The **European registries of the SAPIEN Valve** (Edwards Lifesciences, Irvine, California): This identified that patients with the transapical approach (n=575) suffered more comorbidities than transfemoral patients (n=463) with a significantly higher logistic EuroSCORE (29 % versus 25.8 %; P=0.007). On Multivariable analysis identified logistic EuroSCORE, renal disease, liver disease, and smoking as variables with the highest hazard ratios for 1-year mortality whereas carotid artery stenosis, hyperlipidemia, and hypertension were associated with lower mortality [29].
2. **The U.S. Placement of AoRTic TraNscathetER Valve** (**PARTNER**) **Trial**, and data obtained in Continued Access patients are being collated and analyzed to develop a TAVR-specific algorithm, and the STS/American College of Cardiology Transcatheter Valve Therapy (**STS/ACC TVT**) Registry in the United States now has sufficient patients enrolled for a risk algorithm to be developed. Validation of a TAVR-specific risk algorithm between these two populations is planned. Data from the TVT registry of 7,710 patients who underwent TAVR were published and revealed that the observed incidence of in-hospital mortality was 5.5 %. The major complications included stroke (2.0 %), dialysis-dependent renal failure (1.9 %), and major vascular injury (6.4 %). Median hospital stay was 6 days. Among patients with available follow-up at 30 days (n=3133), the incidence of mortality was 7.6 %, an major complications included a stroke in 2.8 %, new dialysis in 2.5 %, and reintervention in 0.5 % [30].

The most recent valve guidelines present a novel approach for evaluation of surgical and interventional risk for AVR [2]. This model (Table 11.2) includes several factors in addition to the STS PROM risk prediction model including:

1. **STS PROM**: low risk (<4 %), intermediate risk (4–8 %), high risk (>8 %), and prohibitive (predicted risk of death or major morbidity >50 % at 1 year)
2. **Frailty**: Seven frailty indices: Katz Activities of Daily Living (independence in feeding, bathing, dressing, transferring, toileting, and urinary continence) and independence in ambulation or gait speed (no walking aid or assist required or 5-m walk in <6 s). Other scoring systems can be applied to calculate no, mild-, or moderate-to-severe frailty as dominant hand grip strength and serum albumin
3. **Major organ system compromise not to be improved postoperatively**: This includes; Cardiac—severe LV systolic or diastolic dysfunction or RV dysfunction, fixed pulmonary hypertension; CKD stage 3 or worse; pulmonary dysfunction with FEV1 <50 % or DLCO2 <50 % of predicted; CNS dysfunction (dementia, Alzheimer's disease, Parkinson's disease, CVA with persistent physical limitation); GI dysfunction—Crohn's disease, ulcerative colitis, nutritional impairment, or serum albumin <3.0; cancer—active malignancy; and liver—any history of cirrhosis, variceal bleeding, or elevated INR in the absence of VKA therapy

Table 11.2 Combined evaluation of surgical and interventional risk for aortic valve replacement

	Low risk (must meet all criteria in this column)	Intermediate risk (any 1 criterion in this column)	High risk (Any 1 criterion in this column)	Prohibitive risk (any 1 criterion in this column)
STS PROM	<4 % AND	4–8 % OR	>8 % OR	Predicted risk with surgery of death or major morbidity (all-cause) >50 % at 1 year OR
Frailty	None AND	1 Index (mild) OR	≥2 Indices (moderate to severe) OR	
Major organ system compromise not to be improved postoperatively	None AND	1 Organ system OR	No more than 2 organ systems OR	≥3 Organ systems OR
Procedure-specific impediment	None	Possible procedure-specific impediment	Possible procedure-specific impediment	Severe procedure-specific impediment

4. **Procedure specific impediment**: tracheostomy present, heavily calcified ascending aorta, chest malformation, arterial coronary graft adherent to posterior chest wall, or radiation damage

More recently, several factors have been evaluated as risk predictors in patients undergoing TAVR including:

1. **Diabetes**: In an analysis of the FRANCE 2 registry, the investigators noted an interaction between the presence of diabetes, delivery approach and clinical outcome: In those who underwent femoral access TAVR, the rate of death or stroke at 1 year was similar in diabetic and nondiabetic patients (19.9 % and 20.6 %, respectively; p = 0.67), but in those who underwent nonfemoral TAVR, the rate was lower in diabetic versus nondiabetic patients (19 % vs. 30.3 %, respectively; p = 0.001) [31].
2. **Chronic kidney disease**: In a study published by Allende et al., a history of atrial fibrillation (HR, 2.29; p = 0.001) and dialysis therapy (HR, 1.86; p = 0.009) on multivariate analysis, were predictors of mortality in advanced CKD patients. Patients with advanced CKD on dialysis and with a history of AF had a mortality rate of 71 % at 1 year and 100 % at 2 years, compared with 20.1 % and 28.4 %, respectively, in patients who had advanced CKD but neither of these two risk factors (p < 0.001) [32].
3. **Gender Difference**: In an analysis of the PARTNER trial to determine the effect of sex on TAVR and SAVR outcomes, Procedural mortality trended lower with TAVR versus SAVR for female patients (6.8 % vs. 13.1 %; p = 0.07), although procedural stroke rates were higher (5.4 % vs. 0.7 %; p = 0.02) because of higher stroke incidence in the transfemoral arm. The difference in mortality favoring TAVR was significant at 6 months (12.2 % vs. 25.8 %; p < 0.01) and 2 years (28.2 % vs. 38.3 %; hazard ratio [HR]: 0.67; p = 0.049) [33].
4. **Pulmonary hypertension**: In analysis of the FRANCE two registry, The investigators concluded that pulmonary hypertension (defined as systolic pulmonary hypertension ≥40 mmHg) in patients with severe aortic stenosis undergoing TAVR was associated with increased 1-year mortality (28 % for systolic pulmonary hypertension ≥40 mmHg vs. 22 % for systolic pulmonary hypertension <40 mmHg; p = 0.032) [34].
5. **Mitral Regurgitation**: In a multicenter registry analysis of patients undergoing TAVR with the CoreValve revalving system, patients with severe or moderate MR had significantly higher mortality rates at 1 month and 1 year after TAVR compared to those with mild or no MR. At these time points, the mortality rates between those with moderate or severe MR were comparable [35].
6. **Chronic Obstructive Pulmonary Disease (COPD)**: In a study of 319 patients with undergoing TAVR, survival rates at 1 year were 70.6 % in COPD patients and 84.5 % in patients

without COPD (p=0.008). COPD was an independent predictor of cumulative mortality after TAVR (hazard ratio: 1.84; 95 % confidence interval: 1.08–3.13; p=0.026). COPD patients exhibited less (p=0.036) improvement in NYHA functional class. Among COPD patients, a shorter 6 min walk test (6MWT) distance predicted cumulative mortality (p=0.013), whereas poorer baseline spirometry results (FEV1 [forced expiratory volume in the first second of expiration]) determined a higher rate of periprocedural pulmonary complications (p=0.040). TAVR was futile in 40 COPD patients (42.5 %) and a baseline 6MWT distance <170 m best determined the lack of benefit after TAVR (p=0.002) [36].

7. **Tricuspid Regurgitation** (**TR**): In a study of 518 patients undergoing TAVR, patients were divided into either those with moderate/severe TR (79 patients) versus none/mild TR. Significant TR was associated with more comorbidities. However, was not an independent predictor of 2-year mortality. Prespecified subgroups showed an interaction between TR and left ventricular systolic function (Pinteraction=0.047). Interestingly, moderate/severe TR was significantly related to mortality only in patients with left ventricular ejection fraction (LVEF) >40 % (adjusted OR: 2.01, CI: 1.05–3.84, P=0.036). In patients with LVEF ≤40 %, TR had no significant impact on all-cause mortality (adjusted OR: 1.04, CI: 0.34–3.16, P=0.946). No significant interactions were identified regarding patients with perioperative moderate/severe mitral regurgitation (Pinteraction=0.829) and patients with baseline systolic pulmonary artery pressure ≥60 mmHg (Pinteraction=0.669) [37].
8. **STS >15**: The survival benefit of TAVR seems to diminish in patients with high STS score. In the PARTNER trial 2 year mortality data, there was no survival benefit for TAVR in patients with an STS score >15 in comparison to standard therapy. At ACC 2014, the TVT 1-year registry data were presented and revealed a 40 % mortality in patients with an STS score >15, compared to just over 26 % in the entire cohort [38].
9. **TVT registry**: Acting as a "real world" experience, at the ACC 2014, the 1-year data were presented for 5980 patients and revealed a mortality rate of 26 % and a stroke rate of 3.6 %. Male gender, COPD, impaired renal function, non trans-femoral access site, and STS score >15 were independent predictors of death. Female gender appeared the only independent predictor of stroke [38].
10. **Frailty**: Mortality may be as high as 32.7 % in frail patients compared to 15.9 % in non frail patients.
11. **Liver disease**: For patients with model for end stage liver disease (MELD) < 20 and Child Turcotte Pugh (CTP) class < C, outcomes are acceptable However, higher grades of liver disease are unknown.

As mentioned above, risk prediction models for SAVR have been developed to identify and guide operative risk for patients with severe AS. Despite its development as a surgical model, the STS PROM has also been utilized to risk stratify patients undergoing TAVR. Current risk models dedicated to patients undergoing TAVR are underway.

The Heart Valve Team, Heart Valve Center of Excellence

Management of patients with valvular heart disease has traditionally involved a variety of cardiology-related personnel. These may include a cardiologist who evaluates the patients clinically, another who interprets the non-invasive imaging diagnostic modality, an invasive cardiologist who performs the pre-AVR cardiac catheterization or obtains further invasive hemodynamic data, a cardiac anesthesiologist who monitors the patient intra-operatively, and a cardiac surgeon who evaluates the patient's surgical candidacy. In addition, the echosonographer, and cardiac, ICU and OR nurses remain an integral part of the management team.

With the advent of percutaneous approaches for the management of valvular heart disease, patients who were previously deemed inopera-

tive or at a high surgical risk have been considered as candidates for TAVR. The need for simultaneous, detailed and thorough evaluation of these patients has lead to the development of the ***Heart Valve Team*** to address the management of these patients with complex severe valvular heart disease.

In the most recent guidelines, the presence of a heart valve team for optimal patient selection for available procedures through a comprehensive understanding and analysis of the risk-benefit ratio of different treatment strategies and detailed counseling with the patient and family has been given a class I status.

The optimal care of the patients with complex valve disease is best performed in centers that can provide all options for diagnosis and management including the complex valve surgeries, transcatheter options, and advanced diagnostic modalities. This has lead to the development of ***Heart Valve Centers of Excellence***.

These Centers of Excellence:

1. Are composed of experienced healthcare providers with expertise from multiple disciplines.
2. Offer all available options for diagnosis and management, including complex valve repair, aortic surgery, and transcatheter therapies
3. Participate in regional or national outcome registries (as the post marketing registries and the TVT)
4. Demonstrate adherence to national guidelines
5. Participate in continued evaluation and quality improvement processes to enhance patient outcomes
6. Publically report mortality and success rates. Decisions about intervention at the center should be dependent on the center's publically available mortality rates and operative outcomes.

Novel Guidelines and Aortic Valve Replacement

The European society of cardiology (ESC) and the European association of cardiothoracic surgery (EACTS) published in 2012 [39] and the American heart association (AHA) and American college of cardiology guidelines were published in 2014 [2] and have both agreed on the definition of severe aortic valve stenosis (valve area $\leq$1 cm^2, mean gradient $\geq$40 mmHg, aortic velocity >4 m/s, and indexed valve area $\leq$0.6 cm^2). However, very severe aortic stenosis is defined as an aortic velocity of $\geq$5 m/s in the ACC/AHA guidelines and as $\geq$5.5 m/s in the ESC/EACTS guidelines.

The novelty in the 2014 ACC/AHA guidelines was the presence of stages for AS akin to that of heart failure. At risk (stage A), progressive AS (stage B), asymptomatic severe AS (stage C), and symptomatic severe AS (stage D) are the four stages of AS identified in the guidelines.

The indications for SAVR remain largely unchanged as demonstrated below for both the ACC/AHA (Tables 11.3 and 11.4) and ESC/EACTS (Table 11.5). However, given the results of the recent TAVR trials, TAVR has been introduced as an option in patients with severe AS and with prohibitive, or high surgical risk after discussion with a heart team and with a life expectancy >1 year TAVR (Tables 11.4 and 11.6). Another new indication introduced is the presence of very severe AS (velocity >5 m/s, >5.5 m/s) in the absence of symptoms with a low surgical risk.

Flow charts detailing the management of patients with AS in both guidelines are highlighted in Figs. 11.1 and 11.2.

Special Populations with Severe Aortic Stenosis

Certain patient populations require special considerations when they suffer aortic stenosis. Patients that require additional diagnostic tools, exhibit increased likelihood of worse outcomes, or need alternative treatment plans fall into this category. These patients include

1. Pregnant patients,
2. Patients with low flow status with and without preserved left ventricular ejection fraction,
3. Patients with AS undergoing non-cardiac surgery,

Table 11.3 ACC/AHA timing of intervention

ACC/AHA recommendations: timing of intervention	COR	LOE
AVR is recommended for symptomatic patients with severe high-gradient AS who have symptoms by history or on exercise testing (stage D1)	**I**	**B**
AVR is recommended for asymptomatic patients with severe AS (stage C2) and LVEF ≤50 %	**I**	**B**
AVR is indicated for patients with severe AS (stage C or D) when undergoing other cardiac surgery	**I**	**B**
AVR is reasonable for asymptomatic patients with very severe AS (stage C1, aortic velocity ≥5.0 m/s) and low surgical risk	**IIa**	**B**
AVR is reasonable in asymptomatic patients (stage C1) with severe AS and decreased exercise tolerance or an exercise fall in BP	**IIa**	**B**
AVR is reasonable in symptomatic patients with low-flow/low-gradient severe AS with reduced LVEF (stage D2) with a low-dose dobutamine stress study that shows an aortic velocity ≥4.0 m/s (or mean pressure gradient ≥40 mmHg) with a valve area ≤1.0 cm^2 at any dobutamine dose	**IIa**	**B**
AVR is reasonable in symptomatic patients who have low-flow/low-gradient severe AS (stage D3) who are normotensive and have an LVEF ≥50 % if clinical, hemodynamic, and anatomic data support valve obstruction as the most likely cause of symptoms	**IIa**	**C**
AVR is reasonable for patients with moderate AS (stage B) (aortic velocity 3.0–3.9 m/s) who are undergoing other cardiac surgery	**IIa**	**C**
AVR may be considered for asymptomatic patients with severe AS (stage C1) and rapid disease progression and low surgical risk	**IIb**	**C**

Table 11.4 ACC/AHA choice of AVR

ACC/AHA recommendations: choice of SAVR or TAVR	COR	LOE
Surgical AVR is recommended in patients who meet an indication for AVR with low or intermediate surgical risk	I	A
For patients in whom TAVR or high-risk surgical AVR is being considered, members of a Heart Valve Team should collaborate to provide optimal patient care	I	C
TAVR is recommended in patients who meet an indication for AVR for AS who have a prohibitive surgical risk and a predicted post-TAVR survival ≥12 months	I	B
TAVR is a reasonable alternative to surgical AVR in patients who meet an indication for AVR and who have high surgical risk	IIa	B
Percutaneous aortic balloon dilation may be considered as a bridge to surgical or transcatheter AVR in severely symptomatic patients with severe AS	IIb	C
TAVR is not recommended in patients in whom existing comorbidities would preclude the expected benefit from correction of AS	III: No Benefit	B

4. Patients with mixed valve disorders and additional outflow obstruction
5. Patients with asymptomatic severe AS
6. Patients with bicuspid aortic valve disease
7. Patients with coronary artery disease,
8. Patients with significant comorbidities as pulmonary hypertension, chronic obstructive pulmonary disease, end stage renal disease, and diabetes fall into this category.

Patient populations with significant comorbidities are included in the risk prediction models noted above and patients with low flow states and AS have been discussed elsewhere in this book.

The following section will focus on pregnancy in patients with severe AS, patients with AS undergoing non-cardiac surgery, patients with mixed valvular disease and additional outflow obstruction, asymptomatic severe AS, bicuspid aortic valve disease, and patients with AS and coronary artery disease.

Pregnancy and Aortic Stenosis

Pregnant patients with aortic stenosis constitute a unique population due to the risk posed onto the mother and fetus, the hemodynamic burden of pregnancy, and the limited options for treatment during pregnancy.

Table 11.5 ESC/EACTS indications for SAVR

ESC/EACTS recommendations: indications for SAVR	COR	LOE
AVR is recommended for patients with severe AS and any symptoms related to AS	**I**	**B**
AVR is recommended for asymptomatic patients with severe AS and systolic LV dysfunction LVEF ≤50 % not due to another cause	**I**	**B**
AVR is indicated for patients with severe AS when undergoing CABG, surgery of the ascending aorta, or another valve	**I**	**B**
AVR is reasonable in asymptomatic patients (with severe AS and abnormal exercise test showing symptoms on exercise clearly related to AS	**I**	**C**
AVR should be considered in high risk patients with severe symptomatic AS who are suitable for TAVR, but in whom surgery is favored by a "heart team" based on individual risk profile and anatomic suitability	**IIa**	**C**
AVR is reasonable for asymptomatic patients with very severe AS (aortic velocity ≥5.5 m/s) and low surgical risk	**IIa**	**C**
AVR is reasonable in asymptomatic patients (stage C1) with severe AS and an exercise fall in BP below baseline	**IIa**	**C**
AVR is reasonable in symptomatic patients with low-flow/low-gradient severe AS with reduced LVEF (with evidence of flow reserve)	**IIa**	**C**
AVR is reasonable in symptomatic patients who have low-flow/low-gradient severe AS who are normotensive and have an LVEF ≥50 % after careful confirmation of severe AS	**IIa**	**C**
AVR is reasonable for patients with moderate AS (aortic velocity 3.0–3.9 m/s) who are undergoing CABG, surgery of the ascending aorta, or another valve	**IIa**	**C**
AVR may be considered for asymptomatic patients with severe AS and rapid disease progression >0.3 m/s/year and low surgical risk	**IIa**	**C**
AVR is reasonable in symptomatic patients with low-flow/low-gradient severe AS with reduced LVEF (without evidence of flow reserve)	**IIb**	**C**
AVR may be considered for asymptomatic patients with severe AS and low surgical risk if one or more is present:	**IIb**	**C**
1. Markedly elevated natriuretic peptide levels confirmed by repeated measurements and without other explanations		
2. Increase of mean gradient by 20 mmHg with exercise		
3. Excessive LVH in the absence of hypertension		

Table 11.6 ESC/EACTS indications for TAVR

ESC/EACTS recommendations: indications for TAVR	COR	LOE
TAVR should only be undertaken with a multidisciplinary heart team including cardiologists, cardiac surgeons and other specialists if needed	I	C
TAVR should only be performed with cardiac surgery on site	I	C
TAVR is recommended in patients who meet an indication for AVR for AS who have a prohibitive surgical risk and a predicted post-TAVR survival ≥12 months and are likely to gain improvement in their quality of life	I	B
TAVR is a reasonable alternative to surgical AVR in patients who meet an indication for AVR and who have high surgical risk	IIa	B

During pregnancy, increased cardiac output and heart rate as well as decreased afterload contribute to hemodynamic decompensation in the presence of severe aortic stenosis. In addition, any superimposed hemodynamic stress, such as infection or anemia, can lead to clinical decompensation. The most common etiology of AS in women of childbearing age in developed countries is usually unicuspid or bicuspid valve [2, 40, 41]. In addition, these patients can also suffer an aortopathy, which places the patients at increased risk of aortic complications during pregnancy.

The management of patients with valve stenosis should ideally begin *before conception* [2, 40, 41].

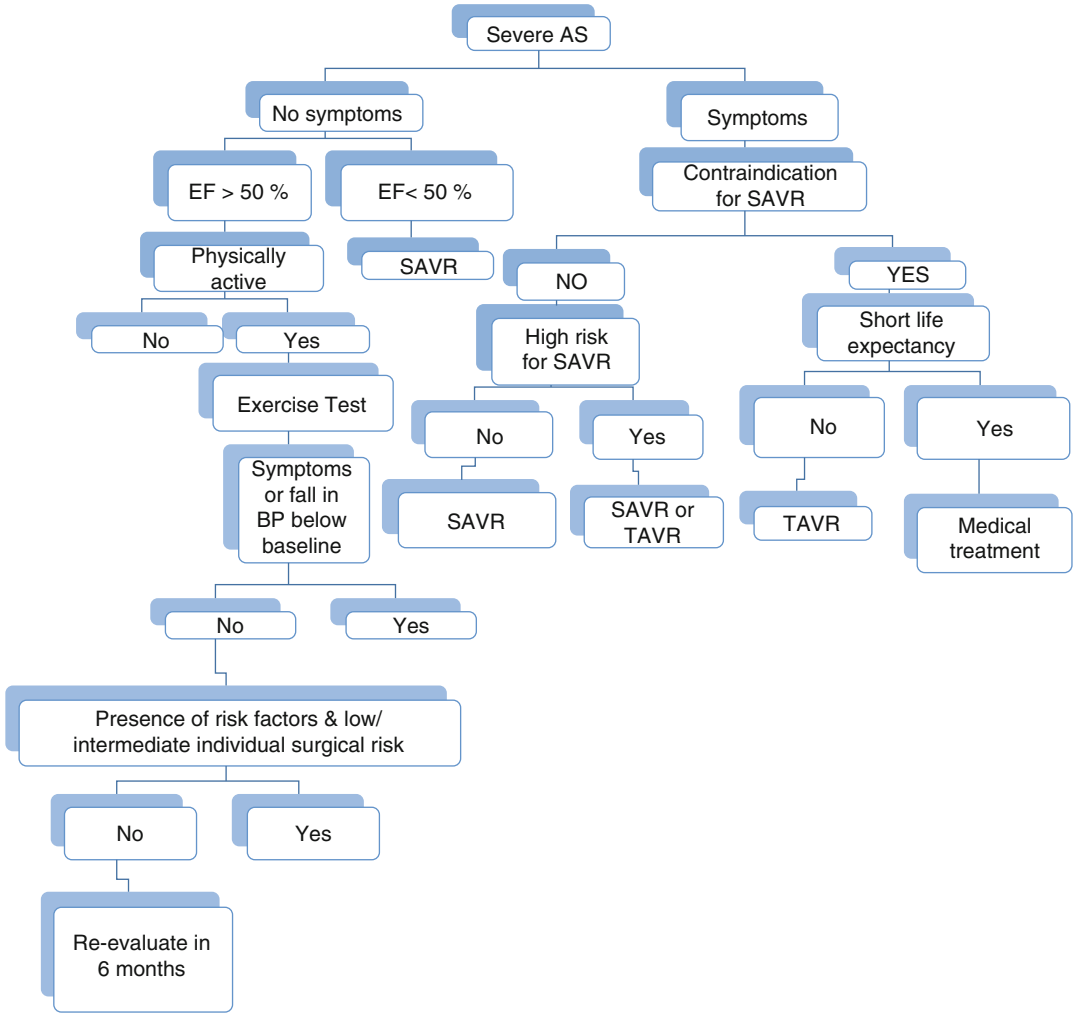

Fig. 11.1 ESC/EACTS: management of severe AS

1. The risks of proceeding with pregnancy must be fully discussed with the patient. **Symptomatic patients and patients with severe aortic stenosis**, regardless of symptoms, should be cautioned against pregnancy or should undergo an intervention such as AVR or percutaneous aortic balloon dilation before conception.
2. Assessment of functional capacity, severity of stenosis, and the status of the left ventricle and pulmonary pressures are necessary to determine the risk of pregnancy and delivery in patients with valve stenosis. Symptomatic patients have an increased risk of sudden clinical deterioration and even death during pregnancy. Asymptomatic patients may undergo exercise testing obtain an objective assessment of exercise tolerance
3. Drugs with potential harmful effects on the fetus must be identified.
4. Counseling regarding all these areas should be performed by a cardiologist with expertise in managing patients with VHD during pregnancy.

If *pregnancy* is contemplated, arrangements should be made for the patient to be monitored in a tertiary care center with a dedicated Heart Valve Team of cardiologists, surgeons, anesthesiologists,

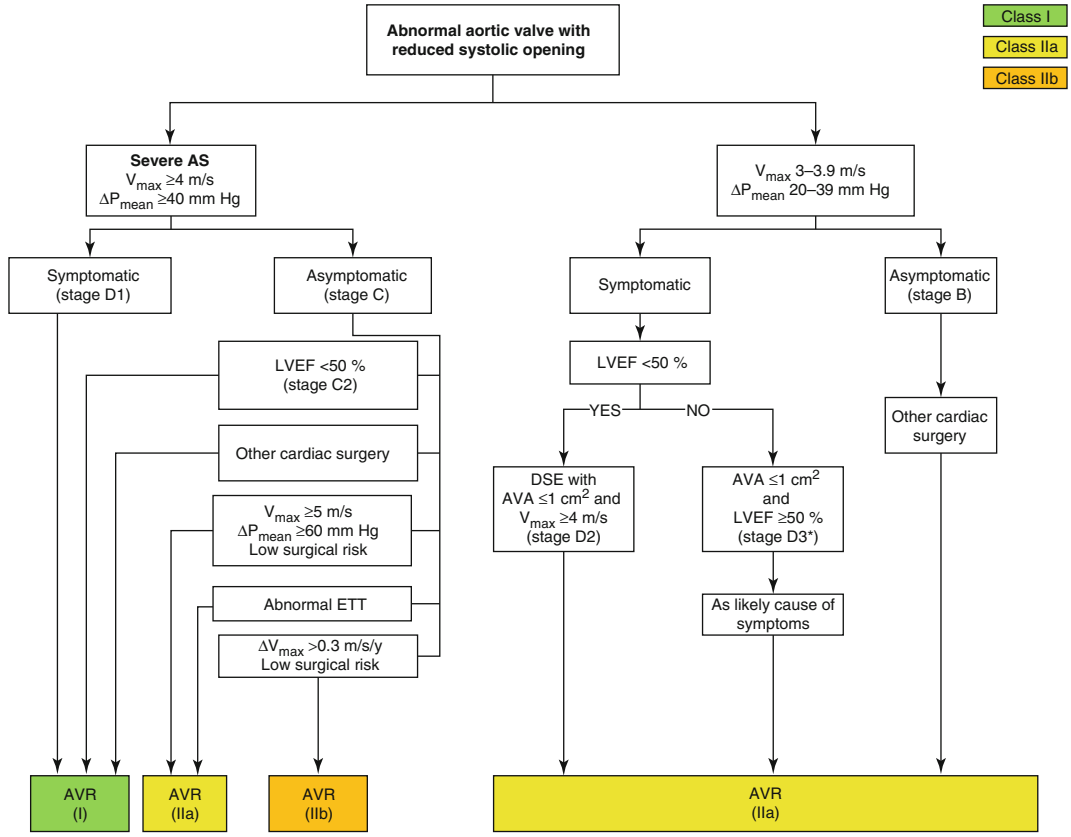

Fig. 11.2 ACC/AHA: management of AS

and obstetricians who have expertise in managing high-risk cardiac patients (Class 1) [2, 41]. Cardiac diagnostics, hemodynamic monitoring, and prevention of cardiovascular complications are required to prevent complications that may occur as pulmonary edema, arrhythmias, and even maternal death.

Timing and mode of *delivery* should be discussed jointly and carried out by the Heart Valve Team, with close hemodynamic monitoring during and up to 24 h after delivery. Clinical deterioration during pregnancy may persist after delivery and increase the probability of late interventions in this population [42].

Issues related to pregnancy in patients with aortic stenosis are highlighted as follows:

1. Echocardiography allows quantitative evaluation of the severity of aortic stenosis and any associated abnormalities. Peak and mean aortic gradients predictably rise during pregnancy because of increased cardiac output and transaortic flow. Aortic valve area, however, should remain unchanged.
2. Patients with mild-to-moderate AS usually tolerate pregnancy without adverse cardiovascular events.
3. Although aortic stenosis increases maternal risk, many patients can be managed medically. Even when stenosis is severe, maternal mortality is rare [40, 43–47]. Earlier studies demonstrated a very poor outcome for pregnant patients with severe AS with a maternal mortality rate of 17 % and fetal and neonatal mortality rate of 32 %. Subsequent studies reported better outcomes, however, a progressive course as well as a sudden deterioration and even death may still occur, despite meticulous medical care during pregnancy and delivery [2, 41].

(a) Symptoms typically increase by one NYHA functional class in about one half of patients. HF develops in 10–44 % [43–48] of patients and arrhythmias in up to 25 %, even if they were asymptomatic before pregnancy.
(b) There is an increased incidence of hypertensive emergencies that occur during pregnancy in patients with severe AS, possibly related to poor placental perfusion.
(c) All prosthetic valve types pose major problems during pregnancy. Patients with mechanical prostheses require continued anticoagulation throughout pregnancy to prevent valve thrombosis and systemic embolism. However, anticoagulation has risks for both the mother and the fetus. Bioprostheses have a limited life span, particularly in the younger patient, and controversy persists as to whether there is acceleration of valve degeneration during pregnancy [2, 46].
(d) Fetal outcomes are also worse in patients with severe AS. Fetal complications include preterm birth, intrauterine growth retardation, and low birth weight and can occur in up to 25 % of pregnant women with moderate and severe AS [46].
(e) The risk of neonatal complication is also high, occurring in as many as 25 % of pregnancies in women with aortic stenosis [41]. The most common neonatal complications are prematurity and being small for gestational age, which may be the result of reduced placental perfusion [46, 49, 50]

Management of Aortic Stenosis During Pregnancy

AS is a fixed mechanical obstruction and therefore medical therapy is of limited efficacy. If symptoms occur, treatment options include bed rest, diuretics, oxygen supplement, and use of beta-blockers to increase LV and coronary diastolic filling times Both SAVR and percutaneous aortic balloon dilation are high-risk procedures during pregnancy for both the mother and the fetus and should only be performed if there is hemodynamic deterioration or severe NYHA class III to IV HF symptoms in centers with sufficient expertise (Class IIa) [2, 41].

Percutaneous aortic balloon dilation during pregnancy has better results in patients with the noncalcified bicuspid aortic valve but may result in severe AR due to a tear in an aortic valve cusp. Limited fluoroscopy time with appropriate lead shielding of the fetus is necessary. Intervention is preferable after 20 weeks of gestation because it is safer for the fetus [2, 41, 46, 51–53].

If SAVR is considered, high pump flows and normothermic perfusion should be used to protect the fetus during cardiopulmonary bypass, with the shortest pump time possible. Continued monitoring of the fetus should be performed. Valve surgery during pregnancy is high risk, with a 30–40 % fetal mortality rate and up to 9 % maternal mortality rate reported. It should be reserved only for patients with severe, intractable symptoms unresponsive to bed rest and medical therapy. There is no ideal time during pregnancy to perform surgery, so timing is based on the combination of the clinical status of the mother and the fetus. The period between the 20th and 28th weeks of pregnancy appears to be safest for the fetus in terms of risk of malformation and premature delivery. If the mother can carry the fetus to full maturity, a combined cesarean section followed by cardiac operation can be planned [2, 41].

As TAVR is more widely used, there may be opportunities for use in the rare circumstances of valvuloplasty failure or need for traditional surgical AVR.

Perioperative Risk Assessment in Patients with Severe Aortic Stenosis Undergoing Noncardiac Surgery

Data regarding patients with aortic stenosis undergoing noncardiac surgery is conflicting. It has been estimated that the rate of cardiac complications in patients with undiagnosed severe aortic stenosis undergoing noncardiac surgery is between 10 and 30 % [2]. However, most of the

data has been obtained from multiple studies with no clear assessment or reporting of true severity, symptom state, associated valvular disease, or ventricular function. Increased mortality, cardiac complications including myocardial infarction, arrhythmias (especially atrial fibrillation), and intraoperative hypotension have been the most reported complications [54]. The following variables appear to be truly associated with increased risk of perioperative complications in patients with severe aortic stenosis:

1. Mean gradient >45–50 mmHg
2. Left ventricular systolic dysfunction
3. Symptomatic aortic stenosis
4. Associated significant valve disease especially mitral regurgitation
5. >18 mmHg increase in gradient with exercise
6. Significant coronary artery disease

Advances in surgical and anesthetic techniques with aggressive treatment of low blood pressure and arrhythmias and avoiding tachycardia and close postoperative management allow non cardiac surgery in these patients possible with an acceptable risk. Intravascular volume should be titrated at a level that ensures an adequate forward cardiac output without an excessive rise in left atrial pressure. This can be achieved by ensuring adequate volume replacement with guidance from central venous or pulmonary pressures or dynamic pulsatility indices, and monitoring LV chamber size with intraoperative TEE may be particularly useful [2]. Intra- and postoperative monitoring of BP and intracardiac volume are implemented starting in the preoperative period and continuing until hemodynamics are stable, which may be as long as 24–48 h after the procedure.

Either phenylephrine or norepinephrine can be used to raise the BP; without adversely affecting LV systolic and diastolic function. Instances of systemic hypertension should be treated preferentially with arterial dilators, such as short-acting calcium channel blockers instead of preload-reducing agents such as nitroglycerin [2].

In patients who are asymptomatic severe aortic valve stenosis with preserved systolic ventricular function and no other valve disease, the role of balloon valvuloplasty (BAV) is questionable and their prognosis appears favorable a. However, BAV may be needed in patients who are hemodynamically unstable as a "bridge to aortic valve surgery". Patients with low flow/low gradient aortic stenosis with preserved ejection fraction do not seem to incur additional perioperative risk [54].

Aortic Stenosis in Association with Other Valvular Diseases

Patients with rheumatic heart disease, and less commonly degenerative valve disease may suffer from mixed valvular disease. In general, there is paucity of data to objectively guide management of AS in the presence of associated valve disease and/or non-valvular obstruction as subaortic membrane and hypertrophic obstructive cardiomyopathy [2]. For patients with mixed valve disease and a predominant lesion, the need for intervention should generally follow recommendations for a pure dominant lesion. This consideration should be undertaken with attention to:

1. Symptoms,
2. Severity of valve disease,
3. Left ventricular remodeling,
4. Operative risk, and
5. The expected surgical outcome.

For those patients with symptoms of uncertain origin, valve intervention may be considered when there are clinical findings or data supportive of significant pathological consequences of the mixed valve lesion. Supportive abnormalities include objective evidence of functional limitation (e.g., severely reduced peak myocardial oxygen consumption attributable to impaired cardiac output) and significantly elevated atrial or ventricular pressures [2]. Exercise hemodynamic studies should be considered for those patients with symptoms that do not match and are out of proportion to the resting hemodynamic findings. Timing of intervention must be individualized because coexistence of multiple valve lesions may have pathological consequences that are incremental to the effects of either lesion alone.

Aortic stenosis (AS) is seen most frequently in association with mitral valve disease, stenosis and regurgitation, as well as aortic regurgitation. Additionally. AS, particularly in the setting of bicuspid valve disease may also be present with subvalvular fixed aortic stenosis adding to the hemodynamic burden on the left ventricle. Similarly, in patients with AS, the presence of left ventricular (LV) hypertrophy, particularly at the basal septum, may also add an additional component of dynamic obstruction to ventricular ejection, interfere with appropriate non-invasive gradient estimation [55], and may have implications during surgical (SAVR) or transcatheter aortic valve replacement (TAVR).

In regards to *mixed aortic and mitral valve disease*, it is difficult to assess the true severity of aortic stenosis in the presence of mitral valve disease by either invasive and non-invasive methods since one valve disease affects criteria used to gage severity of the other. It is also challenging to attribute symptoms to one particular lesion versus the other.

Finally, the *coexistence of AS and AR* may have pathological consequences that are incremental to the effects of either of these disease states alone. As a result, patients with mixed disease may require serial evaluations at intervals earlier than recommended for single valve lesions [2]. Consequently, the appropriate timing for serial evaluations of these patients remains uncertain. For patients with predominant lesions (i.e., stenosis or regurgitation), serial evaluations in accordance with recommendations for the predominant valve lesion are generally recommended [2]. Additionally, the timing of intervention must be individualized because coexistence of stenosis and regurgitation may have pathological consequences that are incremental to the effects of either lesion alone.

Aortic Stenosis with Aortic Regurgitation

For the majority of patients with mixed aortic valve disease, one valve lesion usually predominates, as such; the symptoms and pathophysiology resemble those of a pure dominant lesion [2].

For patients with mixed aortic disease and predominant AS, a high gradient and small valve area will be present. Pressure overload results in concentric LV myocardial hypertrophy, usually without chamber enlargement except in late stages of the disease. Symptoms may be present in patients with predominant AS with or without alterations in chamber morphology. Conversely, for patients with mixed aortic disease and predominant AR, the aortic velocity and gradient may be significantly elevated due to regurgitation in the setting of AS, but the aortic valve area is relatively large. Patients with predominant AR will have both pressure and volume overload, resulting in marked increases in LV volume. In these patients, symptoms may be relatively latent due to preload recruitment with compensatory eccentric hypertrophy [2]. In patients with at least moderate combined AV disease, the progressive increase in transaortic valve velocity has been recently linked to worse outcomes, especially in patients with bicuspid aortic valve disease [56]. In the same study, asymptomatic patients with combined aortic valve disease can be safely followed until surgical criteria defined for aortic stenosis, aortic regurgitation, or the aorta are reached. However, high event rates can be expected even in younger patients and those with only moderate disease [56]. For patients with mixed AS/AR, the appropriate interventional therapy is determined by guidelines for the predominant valve lesion with consideration of the severity of the concomitant valve disease. For example, in a patient with predominant AS, TAVR may be considered in patients with moderate but not severe AR, whereas SAVR may be a therapeutic option regardless of severity of mixed valve disease [2].

AS with Moderate or Severe Mitral Stenosis (MS)

In rheumatic heart disease, the mitral valve is almost always involved, and the combination of both mitral and aortic valve disease is the second most common valve pathology [2, 57]. However, the combination of severe stenosis of both valves

without significant regurgitation is uncommon. When both lesions are severe, physical findings are more suggestive of severe MS and the physical findings and murmur of AS are commonly obscured. The presence of left ventricular hypertrophy on EKG or echocardiography, delayed carotid upstrokes, or a systolic ejection murmur in the setting of severe MS may suggest the presence of concomitant AS.

MS results in low cardiac output because of inadequate left ventricular (LV) filling leading to a lower trans aortic valve gradient for the same aortic valve area. Moreover, it may cause paradoxically low flow/low gradient aortic stenosis in the setting of a preserved ejection fraction. As such, evaluation of the geometric aortic valve area by TEE, CT, or MRI planimetry, calculation of the aortic valve calcium score, and the dimensionless index may all assist in determining the true severity of the aortic stenosis.

AS in Association with Mitral Regurgitation (MR)

Severe AS in association with significant MR is the least common combination of valvular lesions in rheumatic heart disease [57]. However, it is not infrequently seen in elderly patients with degenerative valve disease, and usually one lesion predominates.

As discussed above and similar to MS, MR also produces low cardiac output state resulting in low-gradient/low-flow aortic stenosis and may result in underestimation of gradients across the aortic valve. Conversely, MR severity may be overestimated due to increased afterload and even without mitral valve surgery; the MR may improve following AVR due to decreased intraventricular pressure.

When severe, both lesions produce undesirable concordant hemodynamic effects. The elevated afterload from AS augments the severity of MR, the MR itself reduces end-systolic volume and thereby mitigates the beneficial effect of increased preload on LV performance. The result is a much decline in forward stroke volume [57]. If AS is the dominant lesion, then the patient will more commonly develop symptoms such as syncope and angina and the physical examination is likely to reveal delayed carotid upstroke and LV fourth heart sound (S4). In addition, the systolic murmur is usually well heard in right second intercostal space and radiates into carotids and not to back. However in patients, who have predominant MR, easy fatigability and exertional dyspnea are the main symptoms and on auscultation LV third heart sound (S3) is found. If both lesions are significant, then the symptoms and the physical findings will overlap [57].

Aortic Stenosis in Association with Basal Septal Hypertrophy

Patients with AS invariably develop hypertrophy that is usually, but not always concentric. When asymmetrical basal septal hypertrophy is present in patients with AS, It may confound the diagnosis and management of valvular AS. The first dilemma is **whether there is associated HOCM**. Asymmetric basal septal hypertrophy can occur in 10 % of patients with AS [57]. The absence of severe LVH (<25 mm), the presence of concentric hypertrophy, the lack of systolic anterior motion of the mitral valve, and the negative family history make the diagnosis of concomitant HOCM less likely and the septal hypertrophy can be attributed to AS [57]. The second question is **what is the gradient attributed to each pathology**; **valvular and subvalvular**? Doppler echocardiography is not useful in the presence of serial stenoses to determine the individual gradient attributed to each pathology and an invasive strategy should be obtained [55]. In some patients, early to mid systolic spectral Doppler waveform of valvular AS and the late-peaking systolic waveform (dagger-shaped) of dynamic left ventricular outflow tract (LVOT) obstruction may both be clearly seen as two separate traces and permitting the estimation of the mean AS gradient with reasonable accuracy. However, the assessment of the geometric aortic valve area with the methods described above and the aortic valve calcium core may be required to better assess the true aortic valve severity. Finally, **how**

does this affect SAVR and TAVR? The choice of the valve type in TAVR as well as the decision to undergo myectomy in addition to SAVR needs to be determined in patients with asymmetric basal septal hypertrophy. The removal of the fixed LV outflow obstruction with SAVR increases the velocity of blood across the LVOT and may augment the venturi forces resulting in SAM of mitral leaflets and functional LV outflow obstruction (ASH-crash) [57]. However, it should be remembered that myectomy is not free of complications and can result in conduction abnormalities and iatrogenic ventricular septal defect formation. Therefore, it is recommended that only those patients with SAM and subaortic gradients who have narrow LVOT area (<4 cm^2) and adequate septal thickness (>18 mm) should undergo myectomy along with SAVR [57].

Asymptomatic Severe AS

Calcific AS is a progressive disease, and once moderate AS is present, the likelihood of symptom onset within 5 years is significant. Predictors of rapid disease progression include *older age*, more severe valve *calcification*, and a faster rate of *hemodynamic progression* on serial studies [2]. Besides these parameters, the recent evidence has also highlighted the significance of *subclinical LV systolic dysfunction* in these patients. Newer echocardiographic modalities such as speckle-tracking based strain measurement have been studied as methods to identify these latter group of patients. However, more data is required before strain measurement can be routinely recommended for this purpose [57].

The guidelines recommend undergoing AVR in patients with truly ***asymptomatic*** AS in the following scenarios [2]:

1. **CLASS I**, **LEVEL of EVIDENCE B**: Severe AS with decreased systolic opening of a calcified valve, with velocity >4 m/s or mean gradient >40 mmHg and an ejection fraction <50 %.
2. **CLASS I**, **LEVEL of EVIDENCE B**: Severe AS with velocity >4 m/s or mean gradient >40 mmHg in patients undergoing cardiac surgery for another indication.
3. **CLASS IIa**, **LEVEL of EVIDENCE B**: Very severe AS with decreased systolic opening of a calcified valve, with velocity >5 m/s or mean gradient >60 mmHg in low surgical risk patients
4. **CLASS IIa**, **LEVEL of EVIDENCE B**: Severe AS with decreased systolic opening of a calcified valve, with velocity 4–4.9 m/s or mean gradient 40–59 mmHg, and an exercise test demonstrating a decreased exercise tolerance compared to age and sex matched controls, or a fall in systolic blood pressure below baseline or failure to increase blood pressure by at least 20 mmHg.
5. **CLASS IIa**, **LEVEL of EVIDENCE C**: Moderate AS with velocities of 3–3.9 m/s or mean gradients between 20 and 39 mmHg in patients undergoing cardiac surgery for another indication.
6. **CLASS IIb**, **LEVEL of EVIDENCE C**: Severe AS with velocity >4 m/s or mean gradient >40 mmHg in low surgical risk patients (STS score <4 with an estimated operative mortality of <1.5 % in Heart valve centers of excellence) with an increase in aortic velocity of >0.3 m/s/year.

Aortic Stenosis in Bicuspid Aortic Valve (BAV)

The bicuspid aortic valve is usually comprised of two unequal sized leaflets. The most common fusion pattern is the typical pattern involving the fusion of the ***right and left cusps***. The second most common pattern is the atypical pattern involving fusion of the ***right and noncoronary cusps*** [57]. Most patients with a bicuspid aortic valve will develop AS or AR over their lifetime [2]. Most patients with BAV disease develop severe calcific AS, usually presenting after 50 years of age. AS more commonly results when there is typical configuration of cusp fusion (right and left). As previously discussed, patient with a BAV and AS will develop a higher gradient for a given geometrical valve area compared to those

with trileaflet valves. This is due to jet eccentricity, associated aortic regurgitation, and a dilated aorta with limited or absent pressure recovery.

Twenty percent of the patients with BAV develop AR, usually requiring AVR between the age group of 10 and 40 years of age. The causes of AR in BAV are usually prolapse or fibrotic retraction of the aortic cusps and dilatation of sinotubular junction. Endocarditis occurs more commonly when AR is present and can occur up to 30 % of cases [57]. Combined aortic stenosis and regurgitation can also occur to variable degrees and the indications for SAVR remain the same as that for a trileaflet valve. However, the role of TAVR in patients with BAV has been limited and those patients were excluded in clinical trials.

Bicuspid aortic valves are frequently associated with aortic dilation either at the level of the sinuses of Valsalva or, more frequently, in the ascending aorta. In some patients, severe aneurysmal aortic dilation may develop. The incidence of aortic dilation is higher in patients with fusion of the *right and noncoronary cusps* than the more common phenotype of fusion of the right and left coronary cusps. Some studies have suggested that fusion of the right and left coronary cusps pattern is more often associated with dilatation of the aortic root and asymmetric dilatation of the tubular ascending aorta than the right and noncoronary cusps fusion pattern, which usually results in dilatation of aortic arch. Although the severity of AR is shown to correlate with the risk of aortic root dilatation and aortic dissection, the dilatation of aortic root can be seen even in the absence of significant AR. In contrast, aortic dissection is relatively uncommon in patients with AS with mild to moderate aortic root dilatation. In 20–30 % of patients with bicuspid valves, other family members also have bicuspid valve disease and/or an associated aortopathy.

Indications for repair of the aortic sinuses or replacement of the ascending aorta in patients with BAV are the following [2]:

1. **CLASS I**, **LEVEL of EVIDENCE B**: if the diameter of the aortic sinuses or ascending aorta >5.5 cm.
2. **CLASS IIa**, **LEVEL of EVIDENCE C**: if the diameter of the aortic sinuses or ascending aorta >5 cm and a risk factor for dissection is present (if the rate of diameter increase >0.5 cm/year, or in the presence of a family history of dissection).
3. **CLASS IIa**, **LEVEL of EVIDENCE C**: if the diameter of the ascending aorta >4.5 cm and the patient is undergoing surgery for AVR

Other variables in consideration is the ratio of aortic area to body height greater than 10 cm^2/m or the ratio of aortic diameter to body surface area greater than 4.25 cm/m^2 in the presence of a small body size, the presence of coarctation of the aorta, and the desire for pregnancy.

Evaluation of Coronary Artery Disease Prior to AVR

As a **class 1**, **level of evidence C**, selective coronary angiography is indicated in patients with AS prior to SAVR in patients with angina, objective evidence of ischemia, decreased LV ejection fraction, history of coronary artery disease, presence of coronary risk factors, age >40 years for males and in postmenopausal women [2]. Coronary CTA may be considered in patients with low and intermediate pretest probability and in one study was able to avoid invasive angiography in 69 % of the population [2]. Prior to TAVR, knowledge of coronary anatomy is required and may be related to recovery of LV ejection fraction following the procedure [2].

Although combined CABG and AVR increases cross-clamp time and has the potential to increase perioperative MI and early postoperative mortality compared with patients without CAD undergoing isolated valve surgery, in several series, combined CABG had little or no adverse effect on operative mortality. Moreover, combined CABG and valve operation reduces the rates of perioperative MI, operative mortality and late mortality, and morbidity compared with patients with significant CAD who do not undergo revascularization at the time of valve operation. It has become standard practice to bypass all significant coronary artery stenoses when possible in patients undergoing valve surgery.

The alternative in some patients of a hybrid approach of surgical valve replacement and PCI is attractive, but there are no data at this time to support this approach. Incomplete revascularization is associated with greater postoperative LV systolic dysfunction and reduced survival rates after surgery compared with patients who receive complete revascularization [2]. In patients with a significant stenosis of the left anterior descending artery, a left internal thoracic artery graft should be used if possible. There are no adequate data to fully support the use of concomitant CABG in all patients with asymptomatic CAD undergoing SAVR.

The Valve Academic Research Consortium (VARC) Consensus Document

The Valve Academic Research Consortium established an independent collaboration between Academic Research organizations and specialty societies (cardiology and cardiac surgery) in the USA and Europe. Two meetings, in San Francisco, California (September 2009) and in Amsterdam, the Netherlands (December 2009), including key physician experts, and representatives from the US Food and Drug Administration (FDA) and device manufacturers, were focused on creating consistent endpoint definitions and consensus recommendations for implementation in TAVR clinical research programs. Consensus criteria were developed for the following endpoints: mortality, myocardial infarction, stroke, bleeding, acute kidney injury, vascular complications, and prosthetic valve performance. Composite endpoints for TAVR safety and effectiveness were also recommended [58].

The aim of the current Valve Academic Research Consortium (VARC)-2 initiative was to revisit the selection and definitions of TAVR clinical endpoints to make them more suitable to the present and future needs of clinical trials [59]. In addition, this document is intended to expand the understanding of patient risk stratification and case selection. Two in-person meetings (held in September 2011 in Washington, DC, USA, and in February 2012 in Rotterdam, Netherlands) involving VARC study group members, independent experts (including surgeons, interventional and non-interventional cardiologists, imaging specialists, neurologists, geriatric specialists, and clinical trialists), the US Food and Drug Administration (FDA), and industry representatives, provided much of the substantive discussion from which this VARC-2 consensus manuscript was derived. This document provides an overview of risk assessment and patient stratification that need to be considered for accurate patient inclusion in studies. Working groups were assigned to define the following clinical endpoints: mortality, stroke, myocardial infarction, bleeding complications, acute kidney injury, vascular complications, conduction disturbances and arrhythmias, and a miscellaneous category including relevant complications not previously categorized. Furthermore, comprehensive echocardiographic recommendations are provided for the evaluation of prosthetic valve (dys)function. Definitions for the quality of life assessments are also reported. These endpoints formed the basis for several recommended composite endpoints. This data is presented in the supplement at the end of this chapter (Appendix "VARC-2 definitions").

Conclusions

Management of patients with severe AS and associated cardiac or systemic comorbidities requires a heart team approach to deliver the optimum care for these high-risk patients. Multiple risk prediction models for SAVR are available and specific models for TAVR are under way.

Appendix: VARC-2 Definitions

All-cause mortality
Cardiovascular mortality
Any of the following criteria
Death due to proximate cardiac cause (e.g. myocardial infarction, cardiac tamponade, worsening heart failure)
Death caused by non-coronary vascular conditions such as neurological events, pulmonary embolism, ruptured aortic aneurysm, dissecting aneurysm, or other vascular disease
All procedure-related deaths, including those related to a complication of the procedure or treatment for a complication of the procedure

All-cause mortality
All valve-related deaths including structural or non-structural valve dysfunction or other valve-related adverse events
Sudden or unwitnessed death
Death of unknown cause
Non-cardiovascular mortality Any death in which the primary cause of death is clearly related to another condition (e.g. trauma, cancer, suicide)

Myocardial infarction
Peri-procedural MI (≤72 h after the index procedure)
New ischaemic symptoms (e.g. chest pain or shortness of breath), or new ischaemic signs (e.g. ventricular arrhythmias, new or worsening heart failure, new ST-segment changes, haemodynamic instability, new pathological Q-waves in at least two contiguous leads, imaging evidence of new loss of viable myocardium or new wall motion abnormality) AND
Elevated cardiac biomarkers (preferable CK-MB) within 72 h after the index procedure, consisting of at least one sample post-procedure with a peak value exceeding 15× as the upper reference limit for troponin or 5× for CK-MB[a]. If cardiac biomarkers are increased at baseline (>99th percentile), a further increase in at least 50 % post-procedure is required AND the peak value must exceed the previously stated limit
Spontaneous MI (>72 h after the index procedure) Any one of the following criteria
Detection of rise and/or fall of cardiac biomarkers (preferably troponin) with at least one value above the 99th percentile URL, together with the evidence of myocardial ischaemia with at least one of the following:
Symptoms of ischaemia
ECG changes indicative of new ischaemia [new ST-T changes or new left bundle branch block (LBBB)]
New pathological Q-waves in at least two contiguous leads
Imaging evidence of a new loss of viable myocardium or new wall motion abnormality
Sudden, unexpected cardiac death, involving cardiac arrest, often with symptoms suggestive of myocardial ischaemia, and accompanied by presumably new ST elevation, or new LBBB, and/or evidence of fresh thrombus by coronary angiography and/or at autopsy, but death occurring before blood samples could be obtained, or at a time before the appearance of cardiac biomarkers in the blood.
Pathological findings of an acute myocardial infarction

[a]Previously in the original VARC it was 10× and 5× for troponin and CK-MB, respectively

Stroke and TIA
Diagnostic criteria
Acute episode of a focal or global neurological deficit with at least one of the following: change in the level of consciousness, hemiplegia, hemiparesis, numbness, or sensory loss affecting one side of the body, dysphasia or aphasia, hemianopia, amaurosis fugax, or other neurological signs or symptoms consistent with stroke
Stroke: duration of a focal or global neurological deficit ≥24 h; OR <24 h if available neuroimaging documents a new haemorrhage or infarct; OR the neurological deficit results in death
TIA: duration of a focal or global neurological deficit <24 h, any variable neuroimaging does not demonstrate a new haemorrhage or infarct
No other readily identifiable non-stroke cause for the clinical presentation (e.g. brain tumour, trauma, infection, hypoglycaemia, peripheral lesion, pharmacological influences), to be determined by or in conjunction with the designated neurologist[a]
Confirmation of the diagnosis by at least one of the following
Neurologist or neurosurgical specialist
Neuroimaging procedure (CT scan or brain MRI), but stroke may be diagnosed on clinical grounds alone
Stroke classification
Ischaemic: an acute episode of focal cerebral, spinal, or retinal dysfunction caused by infarction of the central nervous system tissue
Haemorrhagic: an acute episode of focal or global cerebral or spinal dysfunction caused by intraparenchymal, intraventricular, or subarachnoid haemorrhage
A stroke may be classified as undetermined if there is insufficient information to allow categorization as ischaemic or haemorrhagic
Stroke definitions[b]
Disabling stroke: an mRS score of 2 or more at 90 days and an increase in at least one mRS category from an individual's pre-stroke baseline
Non-disabling stroke: an mRS score of <2 at 90 days or one that does not result in an increase in at least one mRS category from an individual's pre-stroke baseline

mRS modified Rankin Scale

[a]Patients with non-focal global encephalopathy will not be reported as a stroke without unequivocal evidence of cerebral infarction-based upon neuroimaging studies (CT scan or brain MRI)

[b]Modified Rankin Scale assessments should be made by qualified individuals according to a certification process

Bleeding
Life-threatening or disabling bleeding
Fatal bleeding (*BARC type 5*) OR
Bleeding in a critical organ, such as intracranial, intraspinal, intraocular, or pericardial necessitating pericardiocentesis, or intramuscular with compartment syndrome (*BARC type 3b and 3c*) OR
Bleeding causing hypovolaemic shock or severe hypotension requiring vasopressors or surgery (*BARC type 3b*) OR
Overt source of bleeding with drop in haemoglobin ≥5 g/dl or whole blood or packed red blood cells (RBCs) transfusion ≥4 units[a] (*BARC type 3b*)
Major bleeding (*BARC type 3a*)
Overt bleeding either associated with a drop in the haemoglobin level of at least 3.0 g/dl or requiring transfusion of two or three units of whole blood/RBC, or causing hospitalization or permanent injury, or requiring surgery AND
Does not meet criteria of life-threatening or disabling bleeding
Minor bleeding (*BARC type 2 or 3a, depending on the severity*)
Any bleeding worthy of clinical mention (e.g. access site haematoma) that does not qualify as life-threatening, disabling, or major

BARC Bleeding Academic Research Consortium [29], *RBC* red blood cell

[a]Given that one *unit* of packed RBC typically will raise the haemoglobin concentration by 1 g/dl, an estimated decrease in haemoglobin will be calculated

Acute kidney injury (AKIN classification[a])
Stage 1
Increase in serum creatinine to 150–199 % (1.5–1.99× increase compared with baseline) OR increase of ≥0.3 mg/dl (≥26.4 mmol/l) OR
Urine output <0.5 ml/kg/h for >6 but <12 h
Stage 2
Increase in serum creatinine to 200–299 % (2.0–2.99× increase compared with baseline) OR
Urine output <0.5 ml/kg/h for >12 but <24 h
Stage 3[b]
Increase in serum creatinine to ≥300 % (>3× increase compared with baseline) OR serum creatinine of ≥4.0 mg/dl (≥354 mmol/l) with an acute increase of at least 0.5 mg/dl (44 mmol/l) OR
Urine output <0.3 ml/kg/h for ≥24 h OR
Anuria for ≥12 h

The increase in creatinine must occur within 48 h

[a]Mehta et al. [31]

[b]Patients receiving renal replacement therapy are considered to meet Stage 3 criteria irrespective of other criteria

Vascular access site and access-related complications
Major vascular complications
Any aortic dissection, aortic rupture, annulus rupture, left ventricle perforation, or new apical aneurysm/pseudo-aneurysm OR
Access site or access-related vascular injury (dissection, stenosis, perforation, rupture, arterio-venous fistula, pseudoaneurysm, haematoma, irreversible nerve injury, compartment syndrome, percutaneous closure device failure) *leading to* death, life-threatening or major bleeding[a], visceral ischaemia, or neurological impairment OR
Distal embolization (non-cerebral) from a vascular source requiring surgery or resulting in amputation or irreversible end-organ damage OR
The use of unplanned endovascular or surgical intervention *associated* with death, major bleeding, visceral ischaemia or neurological impairment OR
Any new ipsilateral lower extremity ischaemia documented by patient symptoms, physical exam, and/or decreased or absent blood flow on lower extremity angiogram OR
Surgery for access site-related nerve injury OR
Permanent access site-related nerve injury OR
Minor vascular complications
Access site or access-related vascular injury (dissection, stenosis, perforation, rupture, arterio-venous fistula, pseudoaneuysms, haematomas, percutaneous closure device failure) *not leading to* death, life-threatening or major bleeding[a], visceral ischaemia, or neurological impairment OR
Distal embolization treated with embolectomy and/or thrombectomy and not resulting in amputation or irreversible end-organ damage OR
Any unplanned endovascular stenting or unplanned surgical intervention not meeting the criteria for a major vascular complication OR
Vascular repair or the need for vascular repair (via surgery, ultrasound-guided compression, transcatheter embolization, or stent-graft) OR
Percutaneous closure device failure
Failure of a closure device to achieve haemostasis at the arteriotomy site leading to alternative treatment (other than manual compression or adjunctive endovascular ballooning)

[a]Refers to VARC bleeding definitions

Conduction disturbances and arrhythmias
Up to 72 h, continuous rhythm monitoring is recommended in order to maximize the detection of arrhythmias
Data elements to be collected should include

Conduction disturbances and arrhythmias
Baseline conduction abnormalities, paroxysmal or permanent atrial fibrillation (or flutter), and the presence of permanent pacemaker[a]
Implant-related new or worsened cardiac conduction disturbance (new or worsened first-degree atrioventricular (AV) block, second-degree AV block (Mobitz I or Mobitz II), third-degree AV block, incomplete right bundle branch block, right bundle branch block, intraventricular conduction delay, left bundle branch block, left anterior fascicular block, or left posterior fascicular block, including block requiring a permanent pacemaker implant
Persistent or transient high-degree AV block. High-grade AV block is persistent if it is present *every* time the underlying rhythm is checked
New permanent pacemaker implantation, with precision of the indication and the number of days post-implant of the placement of new permanent pacemaker
New-onset atrial fibrillation (or flutter)[b]
Any new arrhythmia resulting in haemodynamic instability or requiring therapy[c]

[a]Type of permanent pacemaker should be recorded (e.g. defibrillator, single vs. dual chamber, biventricular)
[b]New-onset atrial fibrillation (or flutter) is diagnosed as any arrhythmia within hospitalization that has the ECG characteristics of atrial fibrillation (or flutter) and lasts sufficiently long to be recorded on a 12-lead ECG, or at least 30 s on a rhythm strip
[c]Therapy includes electrical/medical cardioversion or initiation of a new medication (oral anticoagulation, rhythm, or rate controlling therapy)

Other TAVI-related complications
Conversion to open surgery
Conversion to open sternotomy during the TAVI procedure secondary to any procedure-related complications
Unplanned use of cardiopulmonary bypass (CPB)
Unplanned use of CPB for haemodynamic support at any time during the TAVI procedure
Coronary obstruction
Angiographic or echocardiographic evidence of a new, partial or complete, obstruction of a coronary ostium, either by the valve prosthesis itself, the native leaflets, calcifications, or dissection, occurring during or after the TAVI procedure
Ventricular septal perforation
Angiographic or echocardiographic evidence of a new septal perforation during or after the TAVI procedure
Mitral valve apparatus damage or dysfunction
Angiographic or echocardiographic evidence of new damage (chordae papillary muscle, or to the leaflet) to the mitral valve apparatus or dysfunction (e.g. restrictions due to the THV) of the mitral valve during or after the TAVI procedure
Cardiac tamponade
Evidence of a new pericardial effusion associated with haemodynamic instability and clearly related to the TAVI procedure
Endocarditis
Any one of the following
Fulfilment of the Duke endocarditis criteria[a]
Evidence of abscess, paravalvular leak, pus, or vegetation confirmed as secondary to infection by histological or bacteriological studies during a re-operation
Findings of abscess, pus, or vegetation involving a repaired or replaced valve during an autopsy
Valve thrombosis
Any thrombus attached to or near an implanted valve that occludes part of the blood flow path, interferes with valve function, or is sufficiently large to warrant treatment. Note that valve-associated thrombus identified at autopsy in a patient whose cause of death was not valve-related should not be reported as valve thrombosis
Valve malpositioning
Valve migration
After initial correct positioning, the valve prosthesis moves upwards or downwards, within the aortic annulus from its initial position, with or without consequences
Valve embolization
The valve prosthesis moves during or after deployment such that it loses contact with the aortic annulus
Ectopic valve deployment
Permanent deployment of the valve prosthesis in a location other than the aortic root
TAV-in-TAV deployment
An additional valve prosthesis is implanted within a previously implanted prosthesis because of suboptimal device position and/or function, during or after the index procedure

Prosthetic valve dysfunction			
	Prosthetic aortic valve stenosisa		
	Normal	Mild stenosis	Moderate/severe stenosis
Quantitative parameters (flow-dependent)[b]			
Peak velocity (m/s)	<3 m/s	3–4 m/s	>4 m/s
Mean gradient (mmHg)	<20 mmHg	20–40 mmHg	>40 mmHg
Quantitative parameters (flow-independent)			
Doppler velocity index[c]	>0.35	0.35–0.25	<0.25
Effective orifice area[d]	>1.1 cm^2	1.1–0.8 cm^2	<0.8 cm^2
Effective orifice area[e]	>0.9 cm^2	0.9–0.6 cm^2	<0.6 cm^2
	Prosthesis–patient mismatch (PPM)		
	Insignificant	Moderate	Severe
Indexed effective orifice area[f] (cm^2/m^2)	>0.85 cm^2/m^2	0.85–0.65 cm^2/m^2	<0.65 cm^2/m^2
Indexed effective orifice area[g] (cm^2/m^2)	>0.70 cm^2/m^2	0.90–0.60 cm^2/m^2	<0.60 cm^2/m^2
	Prosthetic aortic valve regurgitation		
	Mild	Moderate	Severe
Semi-quantitative parameters			
Diastolic flow reversal in the descending aorta—PW	Absent or brief early diastolic	Intermediate	Prominent, holodiastolic
Circumferential extent of prosthetic valve paravalvular regurgitation (%)[h]	<10 %	10–29 %	≥30 %
Quantitative parameters[c]			
Regurgitant volume (ml/beat)	<30 ml	30–59 ml	≥60 ml
Regurgitant fraction (%)	<30 %	30–49 %	≥50 %
EROA (cm^2)	0.10 cm^2	0.10–0.29 cm^2	≥0.30 cm^2

[a]In conditions of normal or near normal stroke volume (50–70 ml)
[b]These parameters are more affected by flow, including concomitant aortic regurgitation
[c]For LVOT >2.5 cm, significant stenosis criteria is <0.20
[d]Use in setting of BSA ≥1.6 cm^2 (note: dependent on the size of the valve and the size of the native annulus)
[e]Use in setting of BSA <1.6 cm^2
[f]Use in setting of BMI <30 kg/cm^2
[g]Use in setting of BMI ≥30 kg/cm^2
[h]Not well-validated and may overestimate the severity compared with the quantitative Doppler

References

1. Mack MJ. Risk assessment for valvular heart disease. Valvular heart disease. A companion to Braunwald's heart disease. 4th ed. Philadelphia: Elsevier; 2013.
2. Nishimura RA, Otto CM, Bonow RO, Carabello BA, Erwin JP, Guyton RRA, O'Gara PT, Ruiz CE, Skubas NJ, Sorajja P, Sundt TM, Thomas JM. 2014 ACC/AHA guideline for the management of patients with valvular heart disease. J Am Coll Cardiol. 2014. doi:10.1016/j.jacc.2014.02.536.
3. O'Brien SM, Shaian DM, Filardo G, Ferraris VA, Haan CK, Rich JB, Normand ST, DeLong ER, Shewan CM, Dokholyan RS, Eterson ED, Edwards FH, Anderson RP, The Society of Thoracic Surgeons. Cardiac surgery risk models: part 2-isolated valve surgey. Ann Thorac Surg. 2008;88(1):S23–42.
4. Afilalo J, Alexander KP, Mack MJ, et al. Frailty assessment in the cardiovascular care of older adults. J Am Coll Cardiol. 2014;63:747–62.
5. Marshall G, Grover FL, Henderson WG, et al. Assessment of predictive models for binary outcomes: an empirical approach using operative death from cardiac surgery. Stat Med. 1994;13:1501–11.
6. Hannan EL, Kilburn Jr H, O'Donnell JF, et al. Adult open heart surgery in New York State: an analysis of risk factors and hospital mortality rates. JAMA. 1990;264:2768–74.
7. Grover FL, Shroyer AL, Hammermeister KE. Calculating risk and outcome: the veterans affairs database. Ann Thorac Surg. 1996;62:S6–11.

8. O'Connor GT, Plume SK, Olmstead EM, et al. Multivariate prediction of in-hospital mortality associated with coronary artery bypass graft surgery. Northern New England Cardiovascular Disease Study Group. Circulation. 1992;85:2110–8.
9. Parsonnet V, Dean D, Bernstein AD. A method of uniform stratification of risk for evaluating the results of surgery in acquired adult heart disease. Circulation. 1989;79:I3–12.
10. Nashef SA, Roques F, Michel P, et al. European system for cardiac operative risk evaluation (EuroSCORE). Eur J Cardiothorac Surg. 1999;16: 9–13.
11. Osswald BR, Gegouskov V, Badowski-Zyla D, et al. Overestimation of aortic valve replacement risk by EuroSCORE: implications for percutaneous valve replacement. Eur Heart J. 2009;30:74–80.
12. Leontyev S, Walther T, Borger MA, et al. Aortic valve replacement in octogenarians: utility of risk stratification with EuroSCORE. Ann Thorac Surg. 2009;87:1440–5.
13. Kappetein AP, Head SJ. Predicting prognosis in cardiac surgery: a prophecy? Eur J Cardiothorac Surg. 2012;41:732–3.
14. Roques F, Nashef SAM, Michel P, et al. Risk factors and outcome in European cardiac surgery: analysis of the EuroSCORE multinational database of 19,030 patients. Eur J Cardiothorac Surg. 1999;15:816–23.
15. Roques F, Michel P, Goldstone AR, et al. The logistic EuroSCORE. Eur Heart J. 2003;24:881–2.
16. Chalmers J, Pullan M, Fabri B, et al. Validation of EuroSCORE II in a modern cohort of patients undergoing cardiac surgery. Eur J Cardiothorac Surg. 2013;43:688–94.
17. Dewey T, Brown D, Ryan WH, et al. Reliability of risk algorithms in predicting early and late operative outcomes in high risk patients undergoing aortic valve replacement. J Thorac Cardiovasc Surg. 2008;135: 180–7.
18. Conradi L, Seiffert M, Treede H, et al. Transcatheter aortic valve implantation versus surgical aortic valve replacement: a propensity score analysis in patients at high surgical risk. J Thorac Cardiovasc Surg. 2012; 143:64–71.
19. Online STS Risk Calculator. < http://riskcalc.sts.org.
20. Shahian DM, He X, Jacobs JP. The society of thoracic surgeons isolated Aortic Valve Replacement (AVR) composite score: a report of the STS quality measurement task force. Ann Thorac Surg. 2012;94:2166–71.
21. Rankin SJ, He X, O'Brien SM. The society of thoracic surgeons risk model for operative mortality after multiple valve surgery. Ann Thorac Surg. 2013;95: 1484–90.
22. Ambler G, Omar RZ, Royston P, et al. Generic, simple risk stratification model for heart valve surgery. Circulation. 2005;112:224–31.
23. Nowicki ER, Birkmeyer NJ, Weintraub RW, et al. Multivariable prediction of in-hospital mortality associated with aortic and mitral valve surgery in Northern New England. Ann Thorac Surg. 2004;77:1966–77.
24. Ranucci M, Castelvecchio S, Menicanti L, et al. Risk of assessing mortality risk in elective cardiac operations: age, creatinine, ejection fraction, and the Law of Parsimony. Circulation. 2009;119:3041–3.
25. Ranucci M, Castelvecchio S, Conte M. The easier, the better: age, creatinine, ejection fraction score for operative mortality risk stratification in a series of 29,659 patients undergoing elective cardiac surgery. J Thorac Cardiovasc Surg. 2011;142:581–6.
26. Ariyaratne TV, Billah B, Yap CH, et al. An Australian risk prediction model for determining early mortality following aortic valve replacement. Eur J Cardiothorac Surg. 2011;39:815–21.
27. Gummert JF, Funkat A, Osswald B, et al. EuroSCORE overestimates the risk of cardiac surgery: results from the national registry of the German Society of Thoracic and Cardiovascular Surgery. Clin Res Cardiol. 2009;98:363–9.
28. Kötting J, Schiller W, Beckmann A, et al. German aortic valve score: a new scoring system for prediction of mortality related to aortic valve procedures in adults. Eur J Cardiothorac Surg. 2013;43:971–7.
29. Thomas M, Schymic G, Walther T, Himbert D, Lefevre T, Treede H, Eggebrecht H, Rubino P, Colombo A, Lange R, Schwarz RR, Wendler O. One-year outcomes of cohort 1 in the Edwards SAPIEN Aortic Bioprosthesis European Outcome (SOURCE) registry: the European registry of transcatheter aortic valve implantation using the Edwards SAPIEN valve. Circulation. 2011;124(4):425–33.
30. Mack MJ, Brennan M, Brindis R, Carroll J, Edwards F, Grover F, Shahian D, Tuzcu EM, Peterson ED, Rumsfeld JS, Hewitt K, Shewan C, Michaels J, Christensen B, Christian A, O'Brien S, Holmes D. Outcomes following transcatheter aortic valve replacement in the United States. JAMA. 2013;310(19):2069–77.
31. ESC 2014 Late-Breaking Clinical Trial: is TAVI the treatment of choice for high risk diabetic patients with aortic stenosis? Insights from the FRANCE 2 registry. Presented by E Van Belle on September 2.
32. Allende R, Webb JG, Munoz-Garcia AJ, et al. Advanced chronic kidney disease in patients undergoing transcatheter aortic valve implantation: insights on clinical outcomes and prognostic markers from a large cohort of patients. Eur Heart J. 2014;35(38):2685.
33. Williams M, Kodali SK, Hahn RT, et al. Sex-related differences in outcomes after transcatheter or surgical aortic valve replacement in patients with severe aortic stenosis. Insights from the PARTNER trial (Placement of Aortic Transcatheter Valves). J Am Coll Cardiol. 2014;63:1522–8.
34. Lucon A, Oger E, Bedossa M, et al. Prognostic implications of pulmonary hypertension in patients with severe aortic stenosis undergoing transcatheter aortic valve implantation. Study from the FRANCE 2 Registry. Circ Cardiovasc Interv. 2014;7(2):240–7.
35. Bedogni AL, de Marco F, et al. Interplay between mitral regurgitation and transcatheter aortic valve replacement with the corevalve revalving system. A multicenter registry. Circulation. 2013;128:2145–53.

36. Mok M, Nombela-Franco L, Dumont E, Urena M, DeLarochellière R, Doyle D, Villeneuve J, Côté M, Ribeiro HB, Allende, Laflamme J, DeLarochellière H, Laflamme L, Amat-Santos I, Pibarot P, Maltais F, Rodés-Cabau J. Chronic obstructive pulmonary disease in patients undergoing transcatheter aortic valve implantation. Insights on clinical outcomes, prognostic markers, and functional status changes. J Am Coll Cardiol Intv. 2013;6(10):1072–108.
37. Barbanti M, Binder RK, Dvir D, Tan J, Freeman M, Thompson CR, Cheung A, Wood DA, Leipsic J, Webb JG. Prevalence and impact of preoperative moderate/severe tricuspid regurgitation on patients undergoing transcatheter aortic valve replacement. Catheter Cardiovasc Interv. 2014. doi:10.1002/ccd.25512 [Epub ahead of print].
38. One-Year TAVR Mortality and Stroke Data Reassures. Medscape. Apr 01, 2014.
39. Vahanian A, Alfieri O, Andreotti F, et al. Guidelines for the management of Valvular Heart Disease. Eur Heart J. 2012;33:2451–96.
40. Lao TT, Sermer M, MaGee L, et al. Congenital aortic stenosis and pregnancy—a reappraisal. Am J Obstet Gynecol. 1993;169:540–5.
41. Stout KK, Krieger EV. Valvular heart disease in pregnancy. Valvular heart disease. A companion to Braunwald's heart disease. 4th ed. Philadelphia: Elsevier; 2013.
42. Tzemos N, Silversides CK, Colman JM, et al. Late cardiac outcomes after pregnancy in women with congenital aortic stenosis. Am Heart J. 2009;157:474–80.
43. Easterling TR, Chadwick HS, Otto CM, et al. Aortic stenosis in pregnancy. Obstet Gynecol. 1988;72:113–8.
44. Arias F, Pineda J. Aortic stenosis and pregnancy. J Reprod Med. 1978;20:229–32.
45. Shime J, Mocarski EJ, Hastings D, et al. Congenital heart disease in pregnancy: short- and long-term implications. Am J Obstet Gynecol. 1987;156:313–22.
46. Abbas AE, Lester SJ, Connolly H. Pregnancy and the cardiovascular system. Int J Cardiol Cardiol. 2005;98:179–89.
47. Brian Jr JE, Seifen AB, Clark RB, et al. Aortic stenosis, cesarean delivery, and epidural anesthesia. J Clin Anesth. 1993;5:154–7.
48. Hameed A, Karaalp IS, Tummala PP, et al. The effect of valvular heart disease on maternal and fetal outcome of pregnancy. J Am Coll Cardiol. 2001;37:893–9.
49. Yap SC, Drenthen W, Pieper PG, et al. Risk of complications during pregnancy in women with congenital aortic stenosis. Int J Cardiol. 2008;126:240–6.
50. Roberts JM, Gammill HS. Preeclampsia: recent insights. Hypertension. 2005;46:1243–9.
51. Lao TT, Adelman AG, Sermer M, et al. Balloon valvuloplasty for congenital aortic stenosis in pregnancy. Br J Obstet Gynaecol. 1993;100:1141–2.
52. Sreeram N, Kitchiner D, Williams D, et al. Balloon dilatation of the aortic valve after previous surgical valvotomy: immediate and follow up results. Br Heart J. 1994;71:558–60.
53. Banning AP, Pearson JF, Hall RJ. Role of balloon dilatation of the aortic valve in pregnant patients with severe aortic stenosis. Br Heart J. 1993;70:544–5.
54. Samarendra P, Mangione MP. Aortic stenosis and Perioperative risk with Noncardiac surgery. J Am Coll Cardiol. 2015;65:29–302.
55. Santlebury DC, Geske JB, Nishimura RA. Limitations of Doppler echocardiography in the evaluation of serial stenoses. Circ Cardiovasc Imag. 2013;6:850–2.
56. Zilberszac R, Gabriel H, Schemper M, Zahler D, Czerny M, Maurer G, Rosenhek R. Outcome of combined stenotic and regurgitant aortic valve disease. J Am Coll Cardiol. 2013;61(14):1489–95.
57. Grewal HK, Bansal M, Kasliwal RR. Complex issues in aortic valve diseases. In: Valvular heart disease CSI.ORG.IN. 2014.
58. Leon MB, Piazza N, Nikolsky E, Blackstone EH, Cutlip DE, Kappetein AP, et al. Standardized endpoint definitions for transcatheter aortic valve implantation clinical trials: a consensus report from the Valve Academic Research Consortium. J Am Coll Cardiol. 2011;57(3):253–69.
59. Kappetein AP, Head SJ, Genereux P, Piazza N, van Mieghem NM, et al. Updated standardized endpoint definitions for transcatheter aortic valve implantation: the Valve Academic Research Consortium-2 consensus document. J Am Coll Cardiol. 2012;60(15):1438–54.

Surgical Management of Aortic Valve Stenosis

12

Francis L. Shannon, Marc P. Sakwa, and Robert L. Johnson

Abstract

The time-tested management of patients with severe aortic stenosis has been surgical aortic valve replacement (sAVR). The advances in AVR have progressed over the last 60 years with developments in the heart lung machine, type of valve prosthesis, minimally invasive approaches, and transcatheter techniques. There are currently over 80 types of prosthetic valves available for use. This chapter will provide an overview of the various surgical approaches for AVR as well as the types of aortic valve prosthesis.

Keywords

Surgical management of aortic valve stenosis • Aortic valve replacement (AVR) • Surgical aortic valve replacement (sAVR) • Aortic valve prosthesis • Mechanical aortic valve replacement • Auto-graft aortic valve replacement

F.L. Shannon, MD (✉) • M.P. Sakwa
Department of Cardiovascular Surgery,
Beaumont Health, Oakland University School of Medicine, Royal Oak, MI, USA
e-mail: robert.johnson@beaumont.edu

R.L. Johnson, PA-C, BS-Medicine
Department of Cardiovascular Surgery,
Beaumont Health, Royal Oak, MI, USA

A.E. Abbas (ed.), *Aortic Stenosis: Case-Based Diagnosis and Therapy*,
DOI 10.1007/978-1-4471-5242-2_12

Introduction

The time-tested management of patients with severe aortic stenosis has been surgical aortic valve replacement (sAVR). The advances in AVR have progressed over the last 60 years with developments in the heart lung machine, type of valve prosthesis, minimally invasive approaches, and transcatheter techniques. There are currently over 80 types of prosthetic valves available for use. This chapter will provide an overview of the various surgical approaches for AVR as well as the types of aortic valve prosthesis.

Historical Perspective and Background

The first attempts of valve replacement surgery dealt with aortic regurgitation with valves implanted in the descending aorta [1]. With the development of cardiopulmonary bypass and the heart lung machine in the 1950s, it became possible to replace diseased heart valves in their native positions with a prosthetic valve [2]. The first successful surgery with the heart lung machine was on June 30th **1955** and was performed by Harold A. Lyons MD. This was followed by what Dr. L. Henry Edmunds described as the "great valve rush" [3]. The heart lung machine was patented in **1974** (Fig. 12.1) and has E. Weishaar as the inventor [4].

Different aortic valve replacement prosthesis have developed over the years and include mechanical valves, bioprosthetic valves constructed from either bovine pericardial tissue or porcine or human aortic valve leaflets with or without stent struts, and pulmonary valve autograft. The currently available aortic prosthetic manufactures are ATS medical, Edwards life sciences, Medtronic, St. Jude Medical, Sorin group, and On-X life technologies. A list of manufacture specific valves is available on these company's websites and surgeons have inherent preferences in their selection of valves.

Aortic Valve Surgery

The available methods for aortic valve surgery for aortic stenosis include:

Mechanical Aortic Valve Replacement

This was the first attempt to replace an aortic valve and in **1960** the first AVR was performed using a "**ball and cage**" mechanical valve. The most common of these mechanical valves is the Starr-Edwards valve, which was approved by the FDA in **1965**. Mechanical valves have since evolved to a **single leaflet** by Beal, **tilting disk** valves by Bjork Shiley, Omnicarbon, monstrut, and the Hall Medronic approved by the FDA in **1977**, **bi-leaflet** valves as Carbomedics, ATS open pivot, On-X, Coform-X, and St Jude that was also approved in **1977**, and even **tri-leaflets** [2].

The Starr-Edwards valve required a higher anticoagulation threshold and greater concerns regarding hemolytic anemia. The Bjork Shiley suffered a design and construction flaw where the strut would fracture at the site it was welded onto the metal valve ring. The FDA withdrew its approval in **1986** in what was deemed as the "most infamous recall on record". Currently, the most commonly implanted mechanical valve designs are the St Jude bi-leaflet valves and the longevity of these valves is an attractive feature. However, due to the need for anticoagulation, these valves pose a problem in women in the childbearing age and in the pediatric population. In addition, the inability to expand with somatic growth during child development guarantees the need for reoperation if implanted in children.

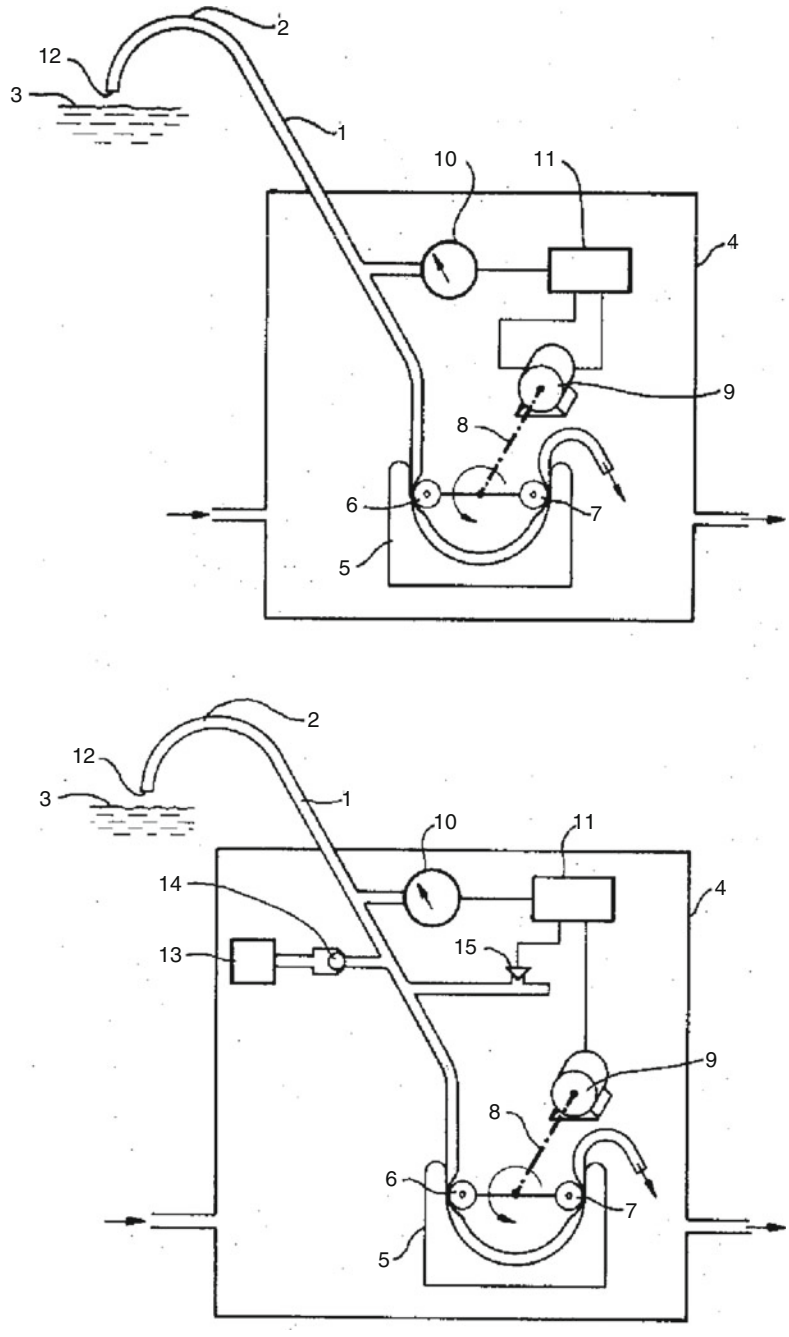

Fig. 12.1 During different operations (top and bottom). The patented diagram for the heart lung machine (From United States Patent [1] 1 Weishaar APPARATUS FOR DRAINING BLOOD FROM A SURGICAL WOUND AND TRANSMISSION TO A HEART-LUNG MACHINE Inventor: Egon Georg Weishaar, 8000 Munich 2, Erzglessereistrasse 29, Munich, Germany Filed: Nov. 15, 1972 Appl. No.: 306.937 with permission)

The prosthetic valves are constructed from material that has biocompatibility, strength, and hardness. The earlier mechanical valves were made of **silicone rubber** and other materials used for valve manufacturing include **silicone carbide** and **pyrolitic carbon**. The latter is a form of carbon developed for the nuclear fuel industry in the 1960s, which has great strength and has been used over the last 30 years in prosthetic valve construction.

Auto-graft Aortic Valve Replacement (Ross Procedure)

Commonly known as the **Ross procedure**, this involves replacing the aortic valve with the patient's own pulmonary valve and then using a pulmonary allograft created from the patient's tissues to replace the pulmonary valve. In a canine model in **1960**, the concept was investigated using auto-transplantation of the pulmonic valve into the descending thoracic aorta of dogs [5]. Pillsbury and Shumway described auto transplantation into the aortic annulus in **1966** [6]. However, Donald Ross reported the first clinical application in **1967** and the surgical approach was named after him [7]. This method provides an excellent hemodynamic profile with no chance of prosthesis-patient mismatch, provides no increased risk of endocarditis, and can grow with child growth. As such, his procedure is highly attractive in the pediatric population obviating the need for anticoagulation or "resizing reoperation" due to child growth. A study comparing the Ross procedure in comparable patients, 18–60 years of age demonstrated no late survival benefit in the first post-operative decade between the Ross procedure and mechanical valve implantation with optimal anticoagulation self-management [8].

Bioprosthetic Aortic Valve Replacement

Bioprosthetic aortic valves can be either derived from animal or human tissue as noted below [9, 10].

A. **Animal tissue valves**: These are either
   (a) **Aortic valve tissue**: typically **stented** porcine as the Hancock and Carpentier-Edwards. These valves are either obtained from *single pig valve* sewn onto a plastic stent the base of which is reinforced with metal as the standard Hancock valve. The system is then covered with Dacron and preserved with glutaraldehyde. On the other hand, the modified Hancock is obtained from *two porcine valves* where the septal porcine aortic valve leaflet in one of the valves, that is normally thicker and stiffer, is replaced by another leaflet from the other porcine valve. Sodium dodecyl sulfate, an anticalcification agent, is used to decrease leaflet mineralization. The Carpentier Edwards valve is sewn to a metal wire stent, which is bent to form three U-shaped prongs. A Dacron skirt covers the base of the wire and the stent
   (b) **Bovine pericardium**: Examples of these **stented** bioprosthetic valves are the Hancock and the Ionescu-Shiley valve that have been discontinued and the Carpentier-Edwards valve that has the pericardial tissue secured to the stent posts to avoid high stress regions and tears. Bovine pericardium valves have excellent hemodynamics and are preferred in patients with a small aortic root sizes (19–21 mm).
   (c) **Stentless valves**: These valves were suggested to have excellent hemodynamic profiles but are more difficult to implant and may require longer bypass times. They are preferred in relatively young active patients with impaired ventricular function and small aortic annulus. They are derived from either
      (i) The entire aortic root and adjacent aorta of a pig after trimming the coronary arteries and are implanted as a block as the Free Style and Prima Plus.
      (ii) Porcine valves as the Toronto, O'brien, and Biocor.

(iii) Bovine pericardium as the Pericarbon
(iv) Equine pericardial tubular valve as the 3F therapeutics valve.

B. **Human tissue valves**: these can be either
(a) Homografts: They are obtained from human tissue valves and are preserved in liquid nitrogen. They do not incite rejection in the host and need to be thawed overnight and as such require knowledge of the required valve size.
(b) Autograft: The Ross described above.

A chronology of the development of bioprosthetic valves is highlighted below:

- **1961**: Robert Frater starts free-hand utilization of autogenous pericardium to create valves or parts of valves. Denaturing the proteins with mercurial solutions, freeze-drying, or formalin treatment was preformed to remove the antigens and avoid tissue rejection.
- **1965**: The first xenograft aortic valve was successfully implanted.
- **1965–1969**: The labs of Robert Carpentier in Paris and Hancock and Nimni in Los Angeles utilize glutaraldehyde as a preservative for the xenografts.
- **1969**: The first aortic porcine valve preserved with glutaraldehyde was implanted.
- The Ionescu-Shiley pericardial bovine valve is subsequently widely used. However, a design error leads high stress forces to cause tears and premature failure and leads to the valve withdrawal.
- **1976**: The Hancock Porcine Valve began being used but is no longer in use because the company went bankrupt.
- **1980**: The Carpentier-Edwards stented pericardial and porcine valves were created.
- **Late 1980s–1990s**: The Stentless valves are created.
- **1990s-early 2000s**: Trans-aortic valve implantation of bioprosthetic valves in porcine and subsequently human models.
- **Current times**: Sutureless aortic valve replacement via MIVS approaches in elderly patients.

Comparison Between Mechanical and Bioprosthetic Aortic Valve

As a general rule, there is no survival benefit of bioprosthetic versus mechanical valve implantation. The main differences is the *higher need for repeat surgery* combined with a *lower risk of major bleeding* in patients receiving a bioprosthetic valve compared to those receiving a mechanical valve [11]. In propensity-matched comparisons, actuarial 15-year mortality rates were 60.6 % with the bioprosthetic aortic valve and 62.1 % with the mechanical valve. Cumulative 15-year stroke rates were 7.7 % and 8.6 % in the two groups, respectively. The reoperation rate was 12.1 % in the bioprosthetic valve group at 15 years and 6.9 % in the mechanical valve group, while major bleeding occurred in 6.6 % of bioprosthesis patients and in 13.0 % of the mechanical-valve group [11].

Comparison Between Stented and Stentless Bioprosthetic Aortic Valves

The data is somewhat conflicting with some data suggesting improved mean gradients, effective orifice areas, faster and more significant ventricular mass regression with stentless valves in exchange for more difficult implantation techniques and longer bypass duration [12–18]. Improvement in the stented prosthetic valve technology somewhat dampened the initial enthusiasm regarding the stentless bioprosthesis share of the market. In 2008, only 12 % of the European market of AVR implantation was using stentless bioprosthesis [19].

Aortic Valve Decalcification

Surgical decalcification of the aortic valve in patients with aortic stenosis was one of the original cardiac surgical operations. The high incidence of restenosis and the emergence of prosthetic valves lead to the abandonment of the procedure. Ultrasound debridement was then introduced and was plagued by a high incidence of restenosis and early and severe aortic regurgitation. As such, surgical repair techniques

of the aortic valve are now on limited in young patients with exclusive aortic regurgitation [20].

Transcatheter Aortic Valve Replacement

Finally, transcatheter aortic valve implantation developed from implantation in a porcine model in 1992 [21], to human experiments by Cribier and others in 2002 [22], initially via an antegrade trans venous-trans-septal- trans-mitral route was developed. With improved profile, trans arterial retrograde implantation via trans femoral, trans aortic, trans apical, trans subclavian, and trans caval-to aortic routes have been performed. Both balloon expandable (Carpentier Edwards) and self-expandable (Medtronic core valve) formats have been developed and have been discussed elsewhere in this book.

Approaches for Surgical Aortic Valve Replacement

Traditionally, conventional full sternotomy (FS) has been the mainstay for surgical aortic valve replacement (sAVR). At our institution, we are fortunate to have a group of progressive surgeons who believe in the value of minimally invasive techniques for aortic valve replacement surgery. Minimally invasive valve surgery (MIVS) for aortic valve replacement (MIAVR) is our mainstay for isolated aortic valve surgery as well as for other institutions with surgeons who are equipped and trained to perform. These techniques are backed by years of experience with conventional FS for AVR.

Right thoracotomy (RT) and upper hemisternotomy (HS) are minimally invasive approaches we are able to customize to each individual patient depending on certain variables outlined in Fig. 12.2. Patient anatomy, comorbidities, need

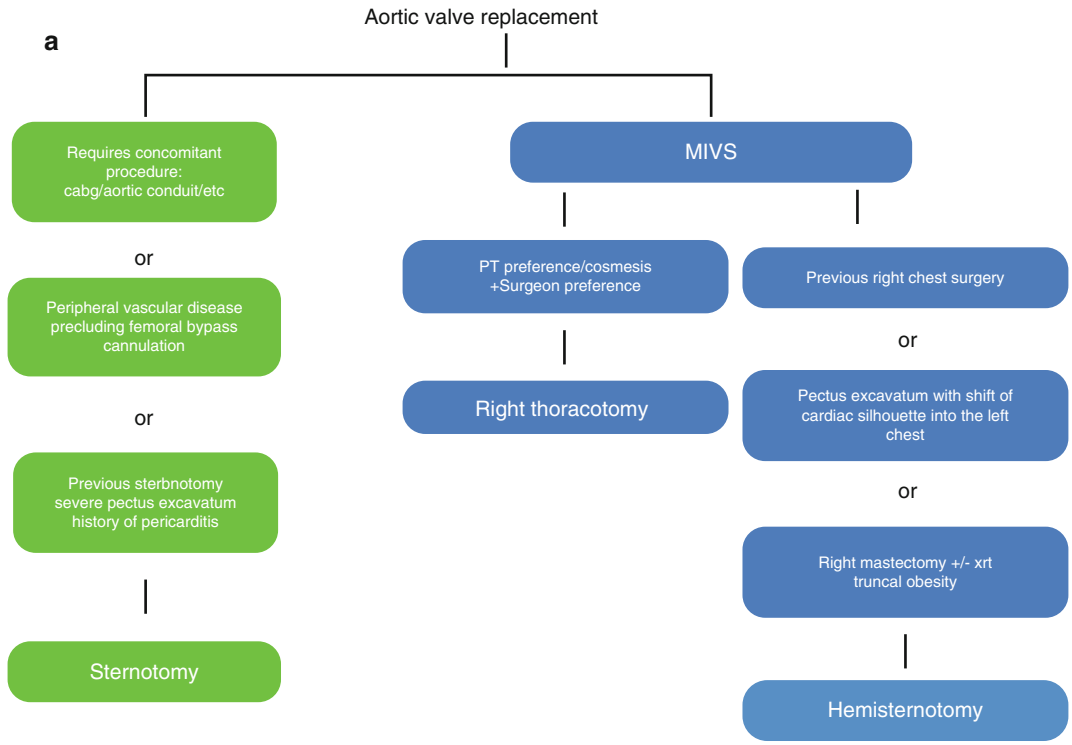

Fig. 12.2 Decision trees for surgical aortic valve replacement. (a) general overview, (b) with coronary artery disease, and © with other valve disease. *MIVS/MIAVR* minimally invasive valve surgery/aortic valve replacement, *AVR* aortic valve replacement, *SVCAD and MVCAD* single and multi vessel coronary artery disease, respectively, *RAT* right anterior thoracotomy, *CAB* coronary artery bypass, *PCI* percutaneous coronary intervention, *LIMA* left interior mammary artery, *MR* mitral regurgitation, *MS* mitral stenosis, *TVR* tricuspid valve regurgitation, *RCA* right coronary artery, *Cx* circumflex, *LAD* left anterior descending artery

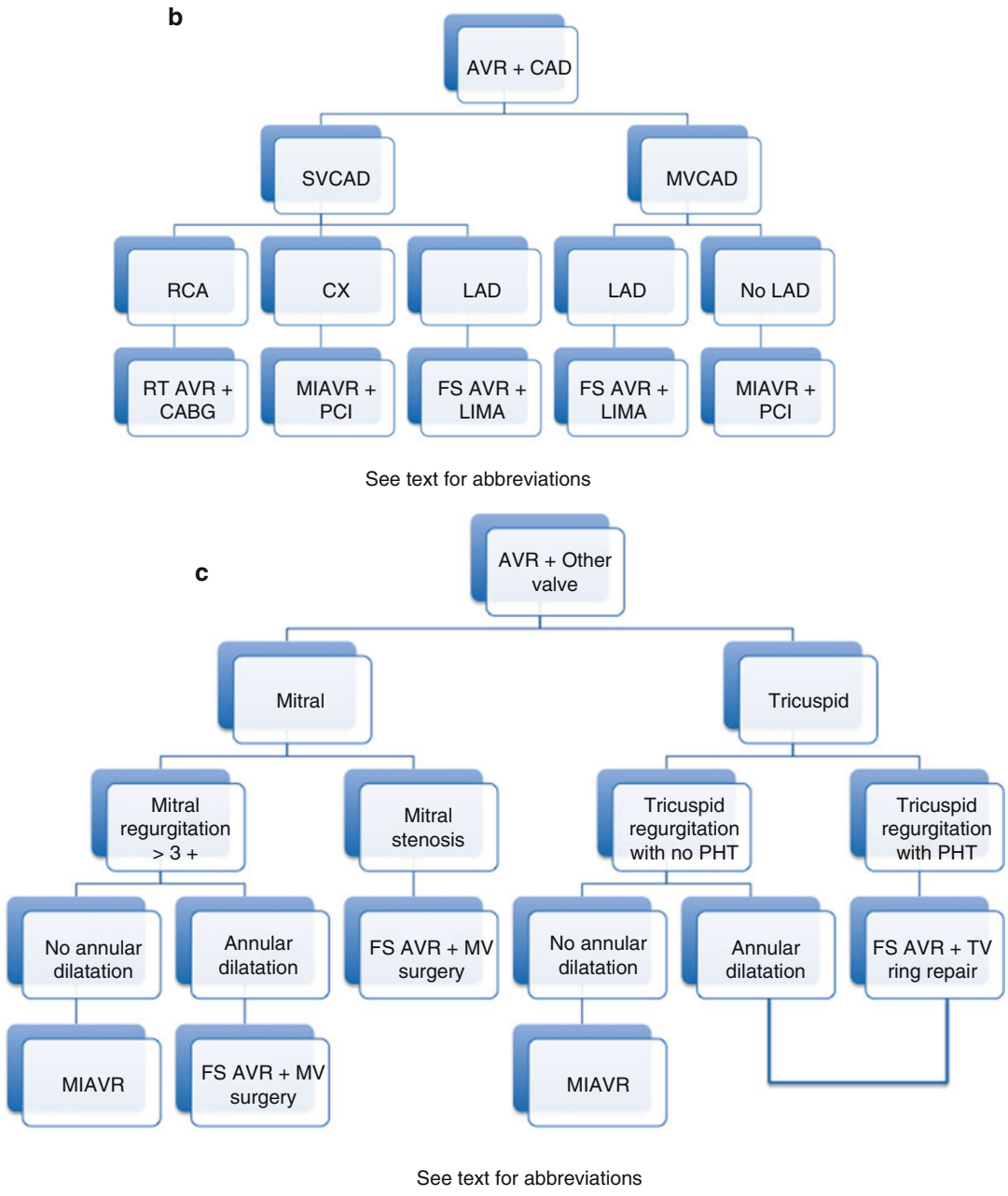

Fig. 12.2 (continued)

for other cardiac surgeries, and patient preference are factors to consider when selecting the best approach. A brief comparison is noted in Table 12.1.

In recent years our program has not only been able to survive, but thrive, due to the minimally invasive techniques. As patients have become more sophisticated and empowered in the decision making of their surgical care, the real advantages of MIAVR have patients and referring physicians seeking out programs for these procedures.

Table 12.1 Comparison or right thoracotomy and hemisternotomy

Property	Hemi-sternotomy	Right anterior thoracotomy
Learning curve	Short (<10 cases)	Long (>30 cases)
Versatility	Ascending aortic cases	RCA bypass
	Vary incision length	Island maze lesion
	Central cannulation	Coronary sinus catheterization
% MIAVR cases done internationally	80 %	20 %
Cosmetic results	Better for men	Preferred by women

Studies that have compared conventional FS to MIAVR have revealed no difference in mortality. However, the major benefit is in the need for transfusion, time to extubation, cardiopulmonary bypass time, incidence of atrial fibrillation, and ICU and post-operative length of stay (Tables 12.2 and 12.3) [23, 24].

A study that have compared 155 patients who underwent HS and 251 patients who underwent RT routes of MIAVR have revealed an increase in procedure time and learning curve for RT compared to HS in exchange for lesser incidence of postoperative atrial fibrillation, lesser ventilation time, ICU stay, and hospital stay. There was no difference in terms of cardiopulmonary time, cross-clamping time, postoperative stroke, re-exploration for bleeding, or blood transfusion (Table 12.4) [25].

Retrospective review of 217 consecutive cases at our institution has shown comparable results between hemisternotomy and right thoracotomy except in transfusion rates. This seems to be an expected result taking into account bleeding from the divided sternum. There was also a higher cardiopulmonary bypass and aortic clamping time with hemisternotomy and lower hospital stay with right thoracotomy.

The following section will provide an image-guided detailed view of various routes of sAVR.

Table 12.2 AVR using ministernotomy versus full sternotomy

Event	Hemi-sternotomy	Full sternotomy	p value
Mortality	0.96 %	0.96 %	NS
Stroke	1.3 %	1.3 %	NS
Renal failure	0.72 %	0.84 %	NS
Sternal wound infection	0.6 %	0.8 %	NS
RBC transfusion (any)	24 %	34 %	<0.0001
Respiratory insufficiency	2.9 %	5.4 %	<0.01
Median time to extubation	5.2 h	6.9 h	<0.0001
ICU length of stay	2 days	3 days	<0.0001
Post op length of stay	9.2 days	12 days	<0.0001

Table 12.3 AVR using right thoracotomy versus full sternotomy

Event	Right anterior thoracotomy	Full sternotomy	p value
Mortality	0.7 %	0.7 %	NS
Stroke	0.7 %	1.5 %	NS
Wound infection	0	0.7 %	NS
Re-exploration bleeding	6.5 %	4.3 %	NS
RBC transfusion (any)	19 %	34 %	<0.006
Median time to extubation	6 h	8 h	<0.02
Median post op LOS	5	6	<0.02
Post op atrial fibrillation	18 %	28 %	<0.03
Cardiopulmonary bypass	121 ± 45	107 ± 32	<0.003

Traditional Full Sternotomy Approach

Median sternotomy is the traditional and most familiar approach to most cardiac surgery procedures.

Table 12.4 MIAVR using right minithoracotomy is associated with better outcome than ministernotomy

Event	Right anterior	Mini sternotomy	p-value
Mortality	1.2	1.3	1
Stroke	1.2	1.3	1
New onset post operative atrial fibrillation	19.5	34.2	0.01
Blood transfusions	20.3	25.8	0.24
ICU stay (day)	1	1	0.001
Ward stay (day)	5	6	0.001
Ventilation time	7	8	0.003
Re-exploration bleeding	4.8	3.2	0.61

The benefits of this approach are:

1. Ease of surgical technique.
2. Ample exposure.

Those benefits are offset by:

1. Post-operative pain associated with dividing the sternum, its subsequent healing or possible non-healing
2. Bleeding from a very vascular marrow
3. Higher incidence of infection compared to minimally invasive techniques.
4. Longer CPB, ICU stay, postoperative stay, and intubation times

Surgical Technique

A. A midline incision is made from the sternal notch to the xiphoid process (Fig. 12.3). The sternum is divided in the midline.
B. The pericardium is opened and the heart centrally cannulated for cardiopulmonary bypass (Fig. 12.4).
C. An aortic cannula is placed through a controlling purse string suture into the aorta just proximal to the takeoff of the innominate artery.
D. The venous cannula is placed in a similar fashion through the right atrial appendage and cardiopulmonary bypass is initiated.

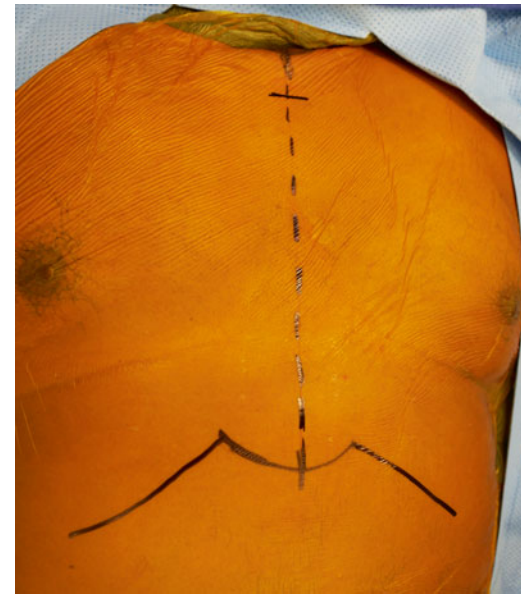

Fig. 12.3 Reference marking for median sternotomy

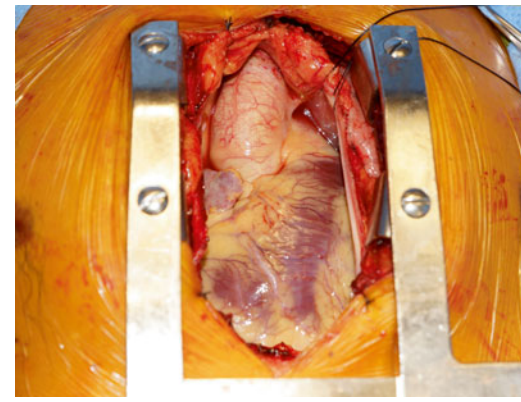

Fig. 12.4 Pericardium reflected back and the aorta and right heart exposed

E. The aorta is cross-clamped just proximal to the aortic cannula.
F. Antegrade cardioplegia is delivered proximal to the clamp.
G. Retrograde cardioplegia can be delivered by a cannula placed through the right atrium into the coronary sinus.
H. Once the heart is arrested, the aorta is incised above the valve.
I. The valve is inspected, debrided, and replaced in the normal fashion (see below).

J. After separating from bypass and removing all cannulas, the sternum is reapproximated with stainless steel wires that are left in place permanently.

Minimally Invasive Aortic Valve Replacement (MIAVR)

MIVS is our preferred technique for isolated aortic valve replacement in patients who qualify.

This technique allows:

1. Optimal exposure
2. Better cosmetics.
3. Faster recovery.

The tried and true techniques of valve repair/replacement through a sternotomy are the same techniques used in the minimally invasive approach. The only true ***absolute*** contraindication for MIVS is a previous sternotomy because residual scarring restricts access and exposure of the aorta can be daunting without a full sternotomy. On the other hand, there are few ***relative*** contraindications for MIVS approach.

A. Severe peripheral vascular disease (iliofemoral) that prohibits femoral arterial cannulation, central cannulation can be done, although more easily in the hemisternotomy approach.
B. Pectus excavatum can displace the heart into the left hemithorax making access to the aorta and aortic valve more difficult.
C. Multi- vessel coronary artery disease that is not amenable to stenting would necessitate full sternotomy and coronary artery bypass grafting.
D. An IVC filter could prevent femoral venous cannulation. However, successful placement of the cannula through the filter without complications can be performed. However, a caval clip is more prohibitive.
E. Thoracic and abdominal aneurysm
F. Greater than four atheromatous disease
G. Stove pipe aorta

Right Thoracotomy Approach

Surgical Technique

A. **Right lung isolation**
Following intubation, a small balloon tipped bronchial isolation catheter is guided down the endotracheal tube using a small caliber flexible endoscope. The balloon is positioned so as to isolate the right lower and middle lobar segments from inflation and ventilation. The deflated right lung is moved out of harms way as we enter the pleural space; this improves visualization of the mediastinal structures and may improve access to the aorta by hyper-inflating the left lung, which pushes the heart further into the right-sided operative field.
B. **Skin incision/exposure**
A 3-in. skin incision is made over the third rib (Fig. 12.5). From this position, the second or third intercostal space can be entered for the best exposure. The incision is carried down into the pleural space and the heart structures are identified. The right internal mammary artery and vein are ligated. The third rib is disarticulated from the sternum and can be directed cephalad or caudal as needed for best exposure to the aorta. The rib will later be reaffixed to the sternum. Soft tissue and rib spreading retractors are placed. The pericardium can now be opened, being careful to identify the phrenic nerve and avoid injury. Retraction stitches are placed around the edge of the pericardium to add exposure (Fig. 12.6).
C. **Femoral cannulation**
A small oblique incision is made in the groin to expose the right common femoral artery and vein for cardiopulmonary bypass cannulation (Fig. 12.7). Vessel loops are placed around the artery proximal and distal to the cannulation for control. Encircling purse strings stitches are then placed at the cannulation sites. The femoral artery is cannulated by the Seldinger technique with either a 16F or 18F cannula depending on the patient's size and the arterial caliber. The femoral vein is cannulated in a similar fashion. The venous

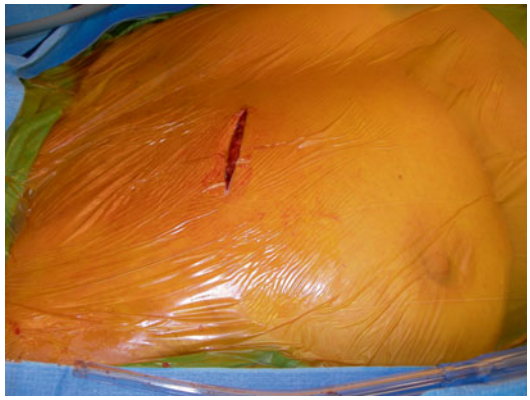

Fig. 12.5 Right thoracotomy skin incision

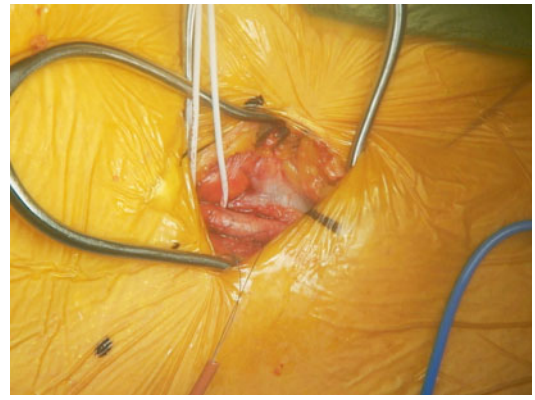

Fig. 12.7 Femoral vessel exposure

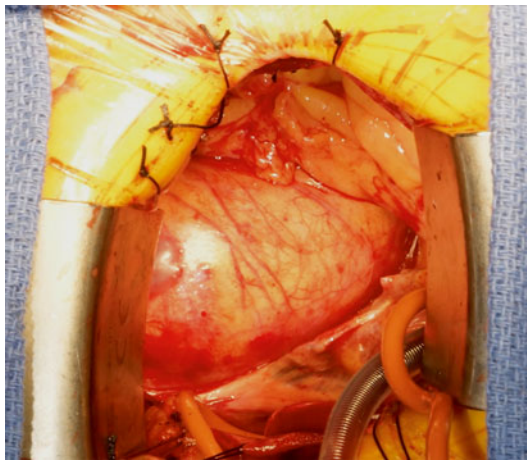

Fig. 12.6 Aortic root and right atrial appendage

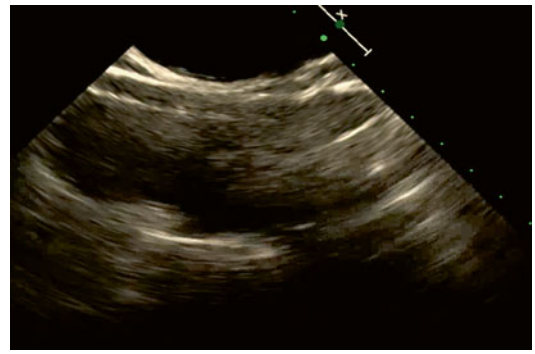

Fig. 12.8 TEE, venous bypass catheter crossing the RA into the SVC

wire is guided into the SVC with aid of TEE (Fig. 12.8). Once the wire is visualized in the SVC, the cannula is passed over and up with the aid of TEE as well. Cannulas are connected to the bypass circuit and cardiopulmonary bypass is initiated (Fig. 12.9).

D. **Cardiac diastolic arrest**
Attention is then returned to the chest. Small encircling purse strings are then placed in the right atrial appendage and the proximal ascending aorta for placement of the retrograde and antegrade perfusion cannulas. A similar purse string is placed in the right superior pulmonary vein in which a cannula will be placed to drain blood from the left atrium/left ventricle while the aortic valve is being replaced. The antegrade and left ventricular cannulas are placed under direct vision while the retrograde cardioplegia cannula is placed is with the aid of TEE. The aortic cross clamp is applied and cardioplegia given antegrade and retrograde in order to induce diastolic arrest. Cardioplegia is again given either retrograde or antegrade directly into the coronary os every 20 min thereafter. CO_2 is introduced into the chest wound in order to displace nitrogen and aid in de-airing the heart when separating from bypass at the end of the case.

E. **Native aortic valve inspection/debridement**
When the heart is arrested, an inverted U incision is made at the base of the aorta to expose the aortic valve. Retraction sutures are placed in the edges of the aortotomy to aid in visualizing the valve. The valve is inspected and annulus/leaflet complex is aggressively debrided in order to maximize the size of the new prosthetic

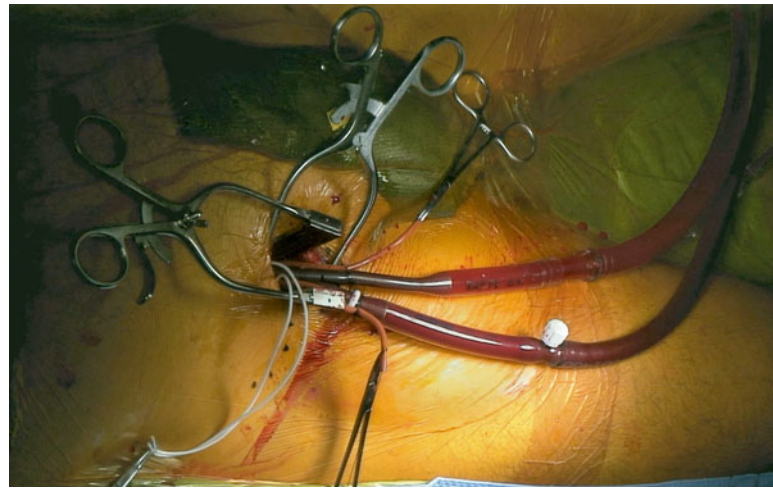

Fig. 12.9 Femoral arterial and venous bypass catheters in place

valve and facilitate healing of the new valve without perivalvular leaks (Fig. 12.10). The aorta is flushed with cold saline to irrigate any remaining debris (Fig. 12.11).

F. **Prosthetic valve sizing and placement**
Each type of prosthetic valve has a separate and distinct set of valve sizers (Fig. 12.12a). These sizers are used to measure the debrided annulus and choose the largest valve to optimize the aortic outlet (Fig. 12.12a, b). The appropriate size also minimizes perivalvular leaks when the valve is seated. 2-0 braided nylon sutures reinforced with felt pledgettes are placed around the annulus and placed into the sewing ring of the new prosthetic valve (Figs. 12.13 and 12.14). The prosthetic valve is tied into its final position and aorta is closed after proper valve seating and functioning is confirmed (Figs. 12.15, 12.16, and 12.17). Epicardial right ventricular pacing wires and chest tubes are placed and secured. The patient is weaned from bypass and all cannulas are removed.

G. **Wound closure**
The third rib is re-approximated to the sternum with a small metal plate and suture (Fig. 12.18). The chest wall is closed in multiple layers (Fig. 12.19), as is the femoral cannulation site.

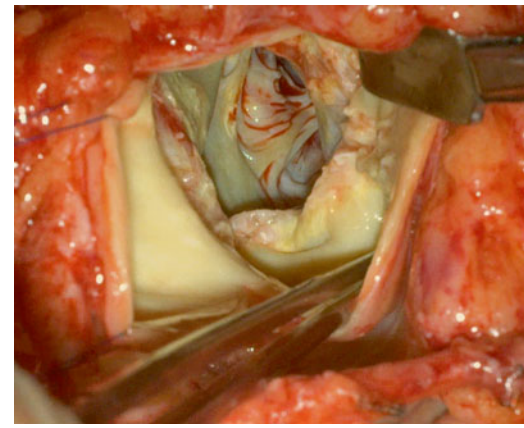

Fig. 12.10 Aortic valve exposure and debridement

Hemisternotomy Approach

As with the right thoracotomy approach, the hemisternotomy approach utilizes the same valve replacement techniques perfected over time used with traditional sternotomy. Although limited, the exposure achieved is more in more line with the full sternotomy. Because of this familiarity, some surgeons are more comfortable with the approach and it has become more widely used for aortic valve replacement than right anterior thoracotomy.

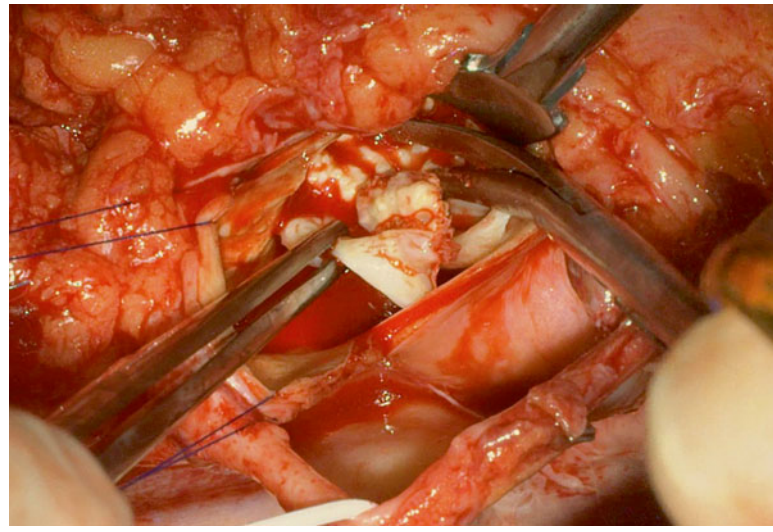

Fig. 12.11 Aortic valve fully excised

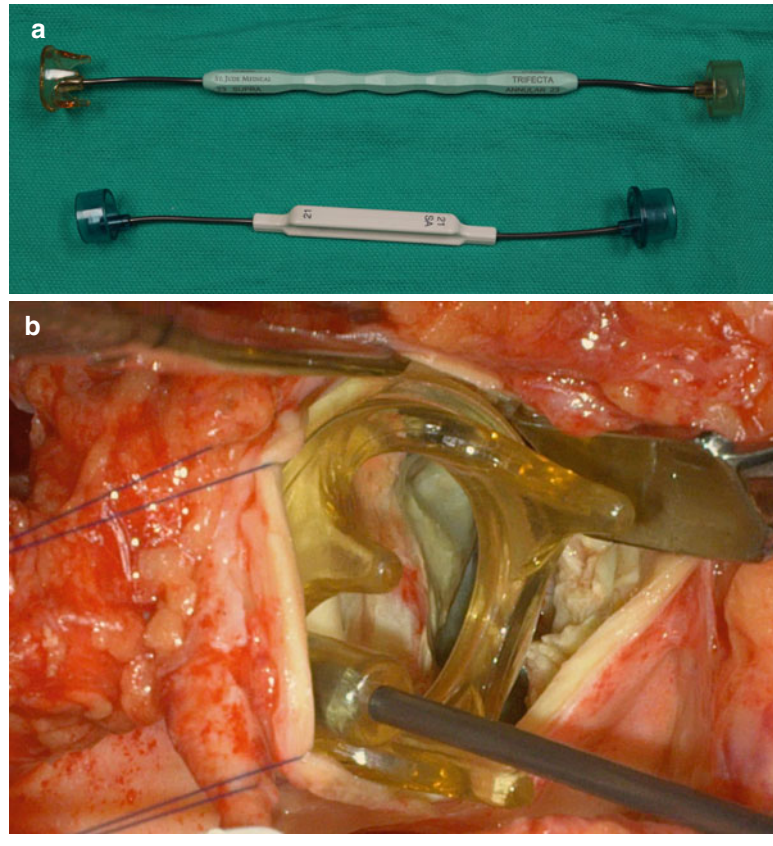

Fig. 12.12 (**a**) Typical aortic valve prosthesis sizers. (**b**) Prosthetic valve sizing

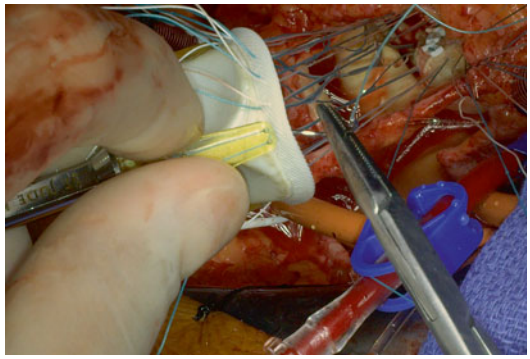

Fig. 12.13 Stitches placed into valve sewing ring

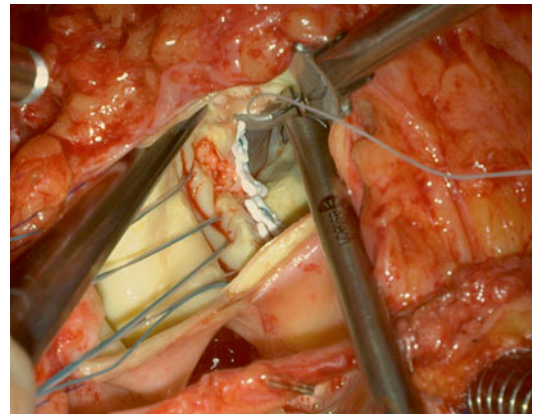

Fig. 12.14 Annular stitches placed

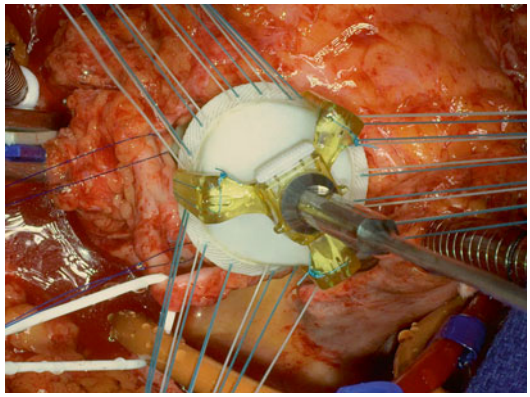

Fig. 12.15 Prosthetic valve lowered in position

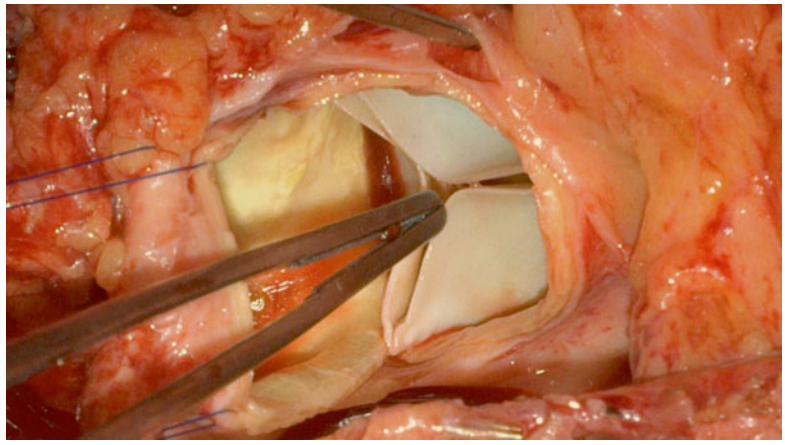

Fig. 12.16 Final position of prosthesis

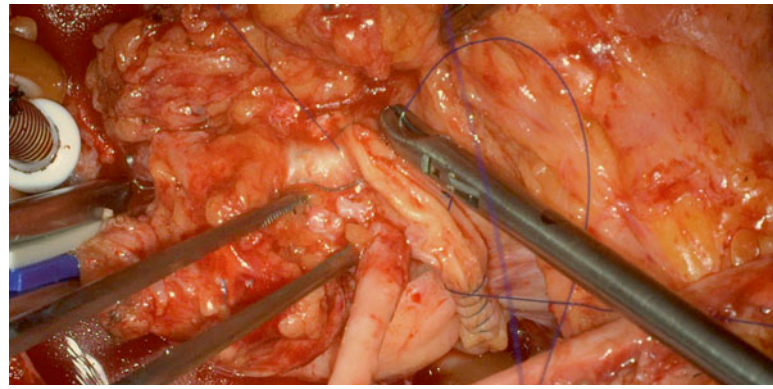

Fig. 12.17 Aorta is closed

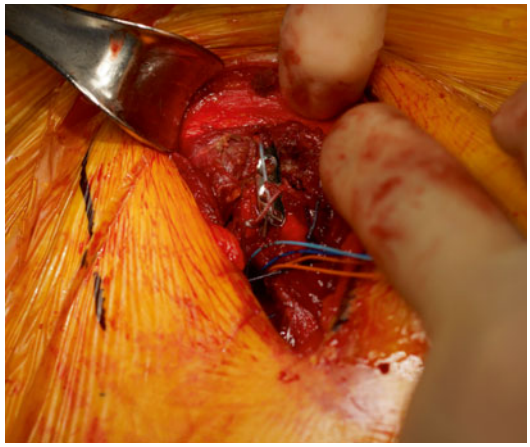

Fig. 12.18 Third rib is reapproximated to the sternum

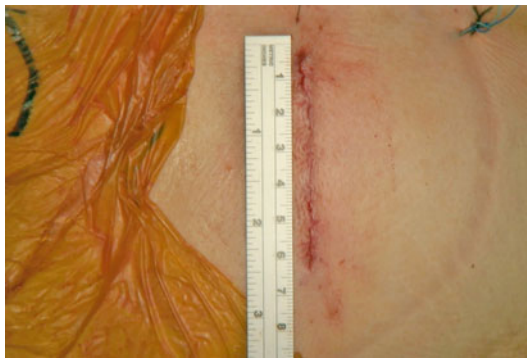

Fig. 12.19 Final wound closure

Surgical Technique

A. **Skin incision/exposure**
A 3-in. midline incision is made over the sternum, from the Angle of Louis to the fourth intercostal space (Fig. 12.20a, b). The skin incision is carried down to the sternum from a line inferior to the sternal notch down to the fourth intercostal space (approximately 3 in.). The reciprocating sternal saw is used to divide the sternum in the midline from the sternal notch and is "J'ed" off into the right third or fourth intercostal space. The pericardium is opened. Retraction stitches are placed around the edge of the pericardium to add exposure. A soft tissue retractor and rib spreading retractor are placed and the aorta is exposed (Fig. 12.21).

B. **Femoral cannulation/Cardiac diastolic arrest/Aortic valve debridement/Prosthetic valve replacement**
The approach is then carried forward in the same manner as the RT procedure (see above). Femoral cannulation, placement of antegrade and retrograde cardioplegia cannulas, and placement of the left ventricular drainage cannula is identical. The heart is arrested and aorta is incised (Fig. 12.22). The calcified aortic leaflets and annulus are aggressively debrided to make room for the largest diameter prosthetic valve. Pledgetted stitches are placed

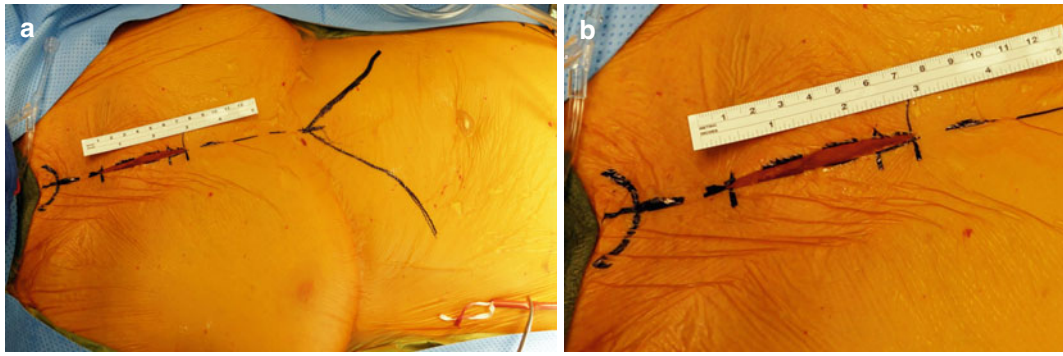

Fig. 12.20 (**a**) Hemisternotomy skin incision. (**b**) Hemisternotomy skin incision (zoomed in)

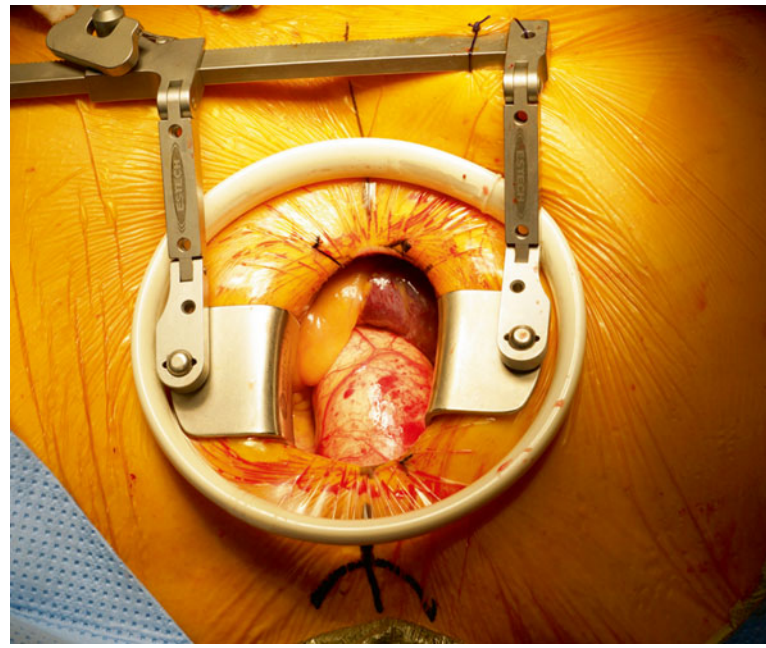

Fig. 12.21 Aortic exposure

around the native annulus and brought through the new prosthetic valve. The valve is tied into place (Fig. 12.23) and the aorta is closed with running, non-absorbable Prolene sutures. Right ventricular epicardial pacing wires and chest tubes are placed and secured. The patient is weaned from bypass and all cannulas are removed. The surgical wounds are closed in multiple layers.

Robotic Aortic Valve Replacement

There have been few reports of robotic aortic valve replacement (Figs. 12.23 and 12.24). As for many of the robotic procedures, the learning curve can be very steep. The working incision is similar in size to a MIVS approach. The cardiopulmonary bypass times are significantly longer than MIVS and surgical technique is

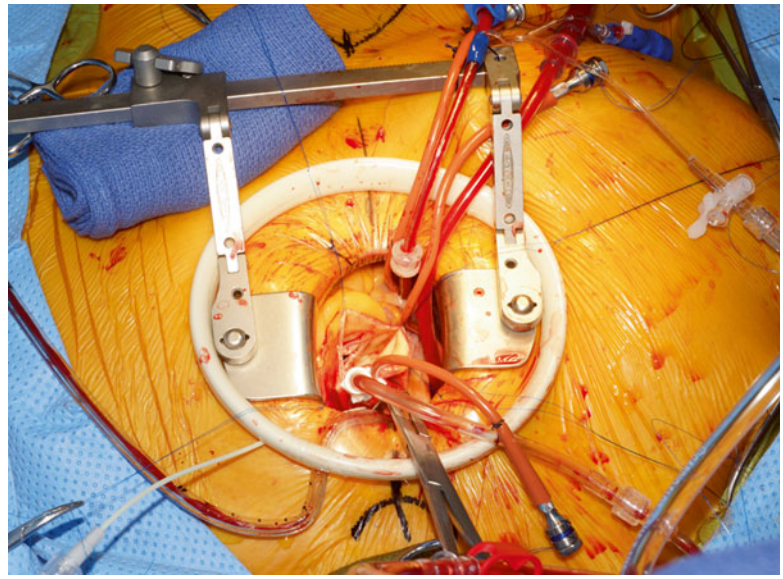

Fig. 12.22 Aortic incision

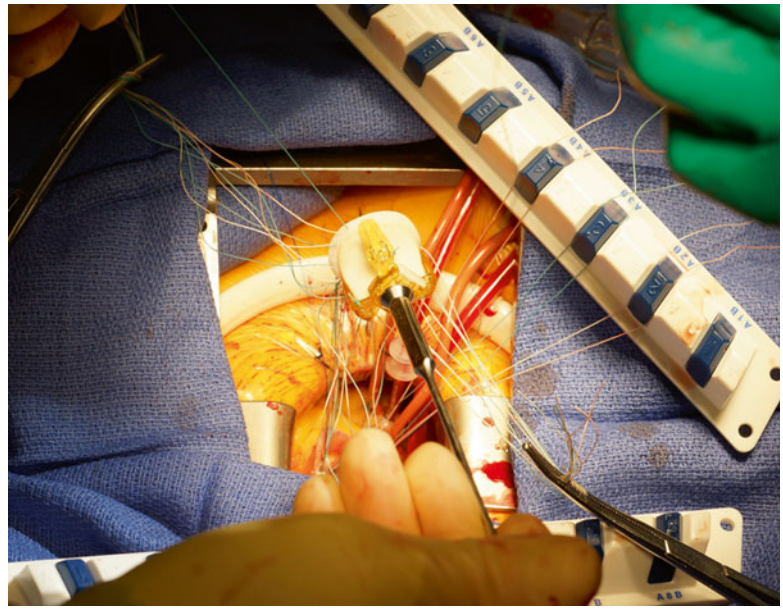

Fig. 12.23 Valve being lowered in place

often compromised by the limits of the robotic access. For these reasons, robotic aortic replacement surgery has not been widely adopted [26, 27].

Sutureless Aortic Valve Replacement

Recent reports suggest that placement of sutureless prosthetic aortic valve prosthesis,

Fig. 12.24 (**a**) Da Vinci robotic system. (**b**) Da Vinci robotic system

especially in elderly patients, may reduce operative times and ventilation times. The Sorin Precaval S, Carpentier-Edwards Perimount, and Medtronic Mosaic have been the majority of tested valves and have been compared to TAVR [28, 29].

Types and Choice of the Prosthetic Aortic Valve

There are multiple choices and manufacturers of tissue and mechanical prosthesis, each having advantages and disadvantages. Every surgeon has

his/her own preferences. Figure 12.25 reveals an example of the most commonly used prosthetic aortic valves, Fig. 12.26 reveals common vendors and their available valves, and Table 12.5 summarizes the new guidelines regarding the choice of prosthetic aortic valves [30].

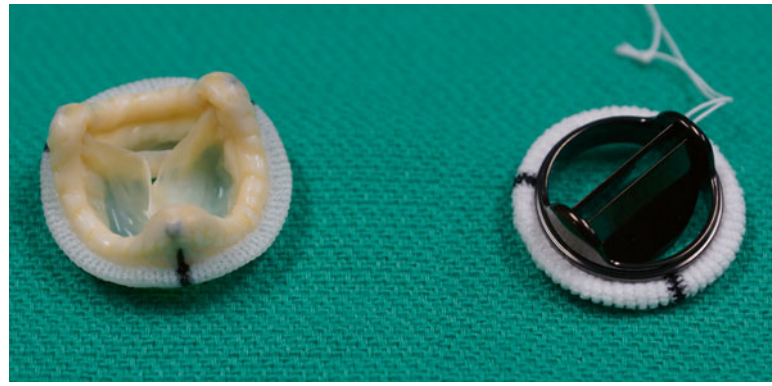

Fig. 12.25 Porcine (*left*) and mechanical (*right*) aortic valve prosthesis

Widely available aortic prosthetic valves

Medtronic	Hancock II (porcine) 21–29 mm	Mosaic (porcine) 19–29 mm	Freestyle (porcinevalve & root) 19–29 mm	Open Pivot (mechanical) 19–29mm 16–26 mm (AP 360)		
On-X	ON–X (mechanical) 19–29 mm					
St Jude	Trifecta (bovine pericardium) 19–29 mm	Epic Supra (porcine) 19–27 mm	Epic (porcine) 21–29 mm	Regent (mechanical) 19–27 mm	HP Series (mechanical) 17–27 mm	Master Series (mechanical) 17–27 mm
Edwards	MagnaEase (bovine pericardium) 19–29 mm	Magna (bovine pericardium) 19–29 mm	Perimount (bovine pericardium) 19–29 mm			
Sorin	Mitroflow (bovine pericardium) 19–27 mm	Carbomedics (mechanical) 17–31 mm				

Fig. 12.26 Widely available prosthetic aortic valves

Table 12.5 Choice of bioprosthetic versus mechanical valves

Guideline recommendation	Class of recommendation	Level of evidence
Decisions of the nature of valve surgery/intervention and prosthetic valve type should be shared	**I**	**C**
Regardless of age, a bioprosthetic valve is recommended, when anticoagulation is contraindicated, cannot be adequately managed, or is not desired	**I**	**C**
In patients younger than 60 years of age with no contraindication to anticoagulation, it is reasonable to undergo a mechanical prosthesis	**IIa**	**B**
In patients greater than 70 years of age, a bioprosthesis in reasonable	**IIa**	**B**
In patients between 60 and 70 years, it is reasonable to under either bioprosthetic or mechanical valve replacement	**IIa**	**B**
In young patients, the Ross procedure, may be considered when anticoagulation is contraindicated, cannot be adequately managed, or is not desired	**IIb**	**C**

Modified from Nishimura et al. [30] with permission
I = Should be performed, IIa = Reasonable to be performed, IIb = Maybe Considered, B = Limited population studies or single randomized trial, C = Very limited or expert opinion

References

1. Hufnagel CA, Harvey WP, Rabil PJ, McDermott F. Surgical correction of aortic insufficiency. Surgery. 1954;35:673–83.
2. Vlahakes GJ. Mechanical heart valves: the test of time. Circulation. 2007;116:1759–60.
3. Edmunds Jr LH. Evolution of prosthetic heart valves. Am Heart J. 2001;141:849–55.
4. Apparatus for draining blood from a surgical wound and transmission to a heart-lung machine US 3799702 A.
5. Lower RR, Stofer RC, Shumway NE. Autotransplantation of the pulmonic valve into the aorta. J Thorac Cardiovasc Surg. 1960;39(5):680–7.
6. Pillsbury RC, Shumway NE. Replacement of the aortic valve with the autologous pulmonic valve. Surg Forum. 1966;17:176–7.
7. Ross DN. Replacement of aortic and mitral valves with a pulmonary autograft. Lancet. 1967;2(7523):956–8.
8. Mokhles MM, Körtke H, Stierle U, Wagner O, Charitos EI, Bogers AJJC, Gummert J, Sievers HH, Takkenberg JJM. Survival comparison of the ross procedure and mechanical valve replacement with optimal self-management anticoagulation therapy. Propensity-matched cohort study. Circulation. 2011;123:31–8.
9. Pibarot P, Dumesnil JG. Prosthetic heart valves: selection of the optimal prosthesis and long-term management. Circulation. 2009;119:1034–48.
10. Kobayashi J. Stentless aortic valve replacement: an update. Vasc Health Risk Manag. 2011;7:345–51.
11. Chiang YP, Chikwe J, Moskowitz AJ, Itagaki S, Adams DH, Egorova NN. Survival and long-term outcomes following bioprosthetic vs mechanical aortic valve replacement in patients aged 50 to 69 years. JAMA. 2014;312(13):1323–9.
12. Dunning J, Graham RJ, Thambyrajah J, et al. Stentless vs stented aortic valve bioprostheses: a prospective randomized controlled trial. Eur Heart J. 2007;28:2369–74.
13. Luciani GB, Auriemma S, Santini F, et al. Comparison of late outcome after stentless versus stented xenograft aortic valve replacement. Semin Thorac Cardiovasc Surg. 2001;13(Suppl I):I136–42.
14. Tamin M, Bove T, Van Belleghem Y, et al. Stentless vs stented aortic valve replacement: left ventricular mass regression. Asian Cardiovasc Thorac Ann. 2005;13:112–8.
15. Borger MA, Carson SM, Ivanov J, et al. Stentless aortic valve are hemodynamically superior to stented valves during mid-term follow-up: a large retrospective study. Ann Thorac Surg. 2005;80:2180–5.
16. Bové T, Bellenghem YV, François K, et al. Stentless and stented aortic valve replacement in elderly patients: factors affecting midterm clinical and hemodynamical outcomes. Eur J Cardio Thorac Surg. 2006;30:706–15.
17. Cohen G, Christakis GT, Joyner CD, et al. Are stentless valves hemodynamically superior to stented valves? A prospective randomized trial. Ann Thorac Surg. 2002;73:767–75.
18. Kunadian B, Vijayalakshmi K, Thornley AR, et al. Meta-analysis of valve hemodynamics and left ventricular mass regression for stentless versus stented aortic valves. Ann Thorac Surg. 2007;84:73–8.
19. Gulbins H, Florath I, Ennker J. Cerebrovascular events after stentless aortic valve replacement during a 9-year follow-up period. Ann Thorac Surg. 2009;86:769–73.
20. Cosgrove DM, Ratliff NB, Schaff HV, Edwards WD. Aortic valve decalcification: history repeated with a new result. Ann Thorac Surg. 1990;49:689–90.

21. Andersen HR, Knudsen LL, Hasenkam JM. Transluminal implantation of artificial heart valves: description of a new expandable aortic valve and initial results with implantation by catheter technique in closed chest pigs. Eur Heart J. 1992;13:704–8.
22. Cribier A, Eltchaninoff H, Bash A, Borenstein N, Tron C, Bauer F, Derumeaux G, Anselme F, Laborde F, Leon MB. Percutaneous transcatheter implantation of an aortic valve prosthesis for calcific aortic stenosis: first human case description. Circulation. 2002;106:3006–8.
23. Johnston DR, Atik FA, Rajeswaran J, et al. Outcomes of less invasive J-incision approach to aortic valve surgery. JTCVS. 2012;144(4):852–8.
24. Glauber M, Miceli A, Gilmanov D, et al. Right anterior minithoracotomy versus conventional aortic valve replacement: a propensity score matched study. JTCVS. 2012;145(5):1222–6.
25. Miceli A, Murzi M, Gilmanov D, et al. Minimally invasive aortic valve replacement using right minithoracotomy is associated with better outcomes than ministernotomy. JTCVS. 2014;148(1):133–7.
26. Suri RM, Burkhart HM, Schaff HV. Robot-assisted aortic valve replacement using a novel sutureless bovine pericardial prosthesis: proof of concept as an alternative to percutaneous implantation. Innovations (Phila). 2010;5(6):419–23.
27. Folliguet TA, Vanhuyse F, Konstantinos Z, Laborde F. Early experience with robotic aortic valve replacement. Eur J Cardiothorac Surg. 2005;28(1):172–3.
28. Gilmanov D, Miceli A, Ferrarini M, et al. Aortic valve replacement through right anterior minithoracotomy: can sutureless technology improve clinical outcomes? Ann Thorac Surg. 2014;98(5):1585–92.
29. Rubino AS, Santarpino G, De Praetere H, et al. Early and intermediate outcome after aortic valve replacement with a sutureless bioprosthesis: results of a multicenter study. JTCVS. 2014;148(3):865–71.
30. Nishimura RA, Otto CM, Bonow RO, Carabello BA, Erwin JP, Guyton RRA, O'Gara PT, Ruiz CE, Skubas NJ, Sorajja P, Sundt TM, Thomas JM. 2014 ACC/AHA guideline for the management of patients with valvular heart disease. J Am Coll Cardiol. 2014. doi:10.1016/j.jacc.2014.02.536.

Balloon Aortic Valvuloplasty

13

Aaron David Berman

Abstract

The role of surgical aortic valve replacement (SAVR) for aortic stenosis (AS) is well established as a lifesaving therapy, conferring improved survival, improved symptomatic status, decreases in left ventricular hypertrophy, and improvement in left ventricular systolic function. However, there remain a group of patients with clinical risk factors in whom the risk of SAVR is felt to be prohibitive due to comorbidities. Such risk factors include advanced age, advanced renal and pulmonary disease, and severe left ventricular dysfunction. Of particular concern were patients with "low gradient" AS in the presence of severe LV dysfunction and low cardiac output. The natural history of this group, treated medically, is dismal, with a 3 year survival of 25 %.

Balloon dilatation of the aortic valve in non-calcified AS in young patients has been performed since 1984 with good short and long term results. Given these results, this technique was adapted for the treatment of high risk patients with AS in the 1980s by a number of groups. The procedure enjoyed some popularity in the mid 1980s in the treatment of a group of patient who otherwise were not candidates for SAVR. Enthusiasm waned, however, with subsequent reports of almost universal early recurrence of symptoms and hemodynamic deterioration, and aortic valvuloplasty was performed relatively infrequently over the subsequent 20 years. However, in the last several years, the success of transcatheter aortic valve replacement (TAVR) has again focused attention on patients who were felt to be at high risk for SAVR, and the role of BAV is being reassessed.

The purpose of this chapter is to review the technique of balloon aortic valvuloplasty (BAV), and its place in the current era of valve interventions.

A.D. Berman, MD, FACC
Department of Cardiology,
William Beaumont Hospital,
Royal Oak, MI, USA
e-mail: aberman@beaumont.edu

A.E. Abbas (ed.), *Aortic Stenosis: Case-Based Diagnosis and Therapy*,
DOI 10.1007/978-1-4471-5242-2_13

Keywords
Balloon aortic valvuloplasty (BAV) • Patho-anatomic mechanism of balloon aortic valvuloplasty (BAV) • Double balloon technique • Rapid ventricular pacing • Immediate hemodynamic results of BAV

Introduction

The role of surgical aortic valve replacement (SAVR) for aortic stenosis (AS) is well established as a lifesaving therapy, conferring improved survival, improved symptomatic status, decreases in left ventricular hypertrophy, and improvement in left ventricular systolic function. However, there remain a group of patients with clinical risk factors in whom the risk of SAVR is felt to be prohibitive due to comorbidities. Such risk factors include advanced age, advanced renal and pulmonary disease, and severe left ventricular dysfunction. Of particular concern were patients with "low gradient" AS in the presence of severe LV dysfunction and low cardiac output [1]. The natural history of this group, treated medically, is dismal, with a 3 year survival of 25 % [2].

Balloon dilatation of the aortic valve in non-calcified AS in young patients has been performed since 1984 with good short and long term results [3–5]. Given these results, this technique was adapted for the treatment of high risk patients with AS in the 1980s by a number of groups [6–9]. The procedure enjoyed some popularity in the mid 1980s in the treatment of a group of patient who otherwise were not candidates for SAVR. Enthusiasm waned, however, with subsequent reports of almost universal early recurrence of symptoms and hemodynamic deterioration, and aortic valvuloplasty was performed relatively infrequently over the subsequent 20 years. However, in the last several years, the success of transcatheter aortic valve replacement (TAVR) has again focused attention on patients who were felt to be at high risk for SAVR, and the role of BAV is being reassessed.

The purpose of this chapter is to review the technique of balloon aortic valvuloplasty (BAV), and its place in the current era of valve interventions.

Historical Considerations

Surgical debridement of the stenotic aortic valve was first performed in the late 1940s. These initial attempts at aortic valve debridement were done via blind tranapical or transaortic valvulotomy and have been well detailed by Brock [10] and Harken [11]. This procedure carried a high risk of intraoperative mortality. With the advent of cardiopulmonary bypass, debridement of the calcific aortic valve could be performed under direct vision [12]. Mortalities of 10–34 % were described [13, 14], and this procedure was largely abandoned after the wide availability of prosthetic valves.

The failure of these attempts at aortic valve debridement after the success of blind and open procedures for the treatment of mitral stenosis was not in retrospect unexpected, given the pathology of calcific adult aortic stenosis compared to the pathology of mitral stenosis, which is almost exclusively rheumatic in origin. The pathology of rheumatic mitral stenosis, with commissural fusion as the predominant abnormality (especially in the young) allowed durable palliation by separation of the commissures either by blind or open procedures. This predicted the later success of balloon mitral valvuloplasty, first performed in 1984 by Inoue [15]. The surgical experience with calcific aortic stenosis as outlined above did not portend well for the long term success of BAV.

Patho-anatomic Mechanism of Balloon Aortic Valvuloplasty (BAV)

The pathology of aortic valve stenosis is characterized by thickening and calcification of the aortic leaflets. Unlike the pathology of mitral stenosis,

commissural fusion plays very little role in valve leaflet restriction, although there may be minor calcific bridging at the attachment to the aortic wall. Calcific nodules are visible on the aortic side of the valve. More recently, it has become apparent that the process of "senile degenerative" aortic stenosis is not due entirely to passive accretion of calcium. The valve leaflets are thickened and made dysfunctional by an active atherosclerotic process, Foam cells and free cholesterol crystals are found within the stenotic aortic valve. As one pushes a finger across the valve from the ventricular side of an intraoperative or postmortem specimen, significant force is need to push the leaflets apart, yet little visible change is made to them as the finger is withdrawn.

The mechanism of improvement in aortic valve orifice with aortic valvuloplasty has been postulated to be a combination of annular stretching, macro- and microfractures of the leaflets, and possible separation of partially fused commissures in a minority of cases. Numerous investigators [14–18] have demonstrated these findings in surgical and autopsy specimens. It was found that discrete calcific fractures could be visualized and that leaflet pliability (at least transiently) improved. These postulated mechanisms had some early detractors [19, 20], but have largely been accepted. A universal finding from these early studies was the lack of liberation of any obvious calcific debris by balloon dilatation, with the feeling that it was likely that the calcific deposits remained endothelialized and were not likely to embolize. Further, it was found that dilatation of the valves with 20 mm balloons rarely caused damage, but that in one case, the use of a 25 mm balloon resulted in leaflet avulsion [17].

Technique

The technique of BAV had undergone very little change for most of the 1990s, but in the last 10 years, minor modifications in the procedure have been introduced which may enhance the safety, if not the efficacy of the procedure.

Access to the aortic valve can be achieved via an antegrade transseptal approach or via a retrograde approach from the femoral artery. In experienced hands, the antegrade approach yields similar hemodynamic results [21]. Access may also be obtained from the brachial approach albeit with an increased risk arterial injury.

The balloon size used for dilatation is generally 20 mm. Balloons as small as 15 mm may be used in cases of critical AS in smaller patients. The double balloon technique, wherein two balloons are introduced across the valve and inflated together has also been described [22, 23] and more recently, has been described guided by CT scanning of the aortic annulus to help determine balloon size [24]. The use of bifoil or trefoil (two or three balloons mounted on one shaft) has been described. These latter balloon configurations carry the theoretical benefit of allowing more blood flow during balloon inflation, making inflations better tolerated.

The technique of retrograde BAV broadly involves achieving vascular access with a large (12–13F) sheath, and crossing the aortic valve in the standard retrograde fashion. At that point, a 0.035″ 260 cm J tipped guidewire with a large secondary curve to deflect the balloon tip from the myocardium is exchanged in. The valvuloplasty balloon is then advanced and positioned across the valve, inflated manually for approximately 5 s, depending upon the hemodynamic response to balloon inflation, deflated and withdrawn from the valve into the ascending aorta. After several inflations, a pigtail catheter is exchanged back in and repeat hemodynamic measurements obtained. Following BAV, supravalvular aortography is not routinely done, but can be performed if there is suspicion clinically or hemodynamically of worsening aortic regurgitation. When a satisfactory hemodynamic result is obtained, the procedure is concluded. In the past, sheaths were removed when the ACT was less than 180 and manual compression applied to obtain hemostasis. This last step has changed over the years, with the introduction of vascular closure devices, as will be discussed.

Several modifications to BAV have been made over the years. The use of rapid ventricular pacing to decrease cardiac output and pulse pressure (Fig. 13.1) prior to balloon inflation has been well

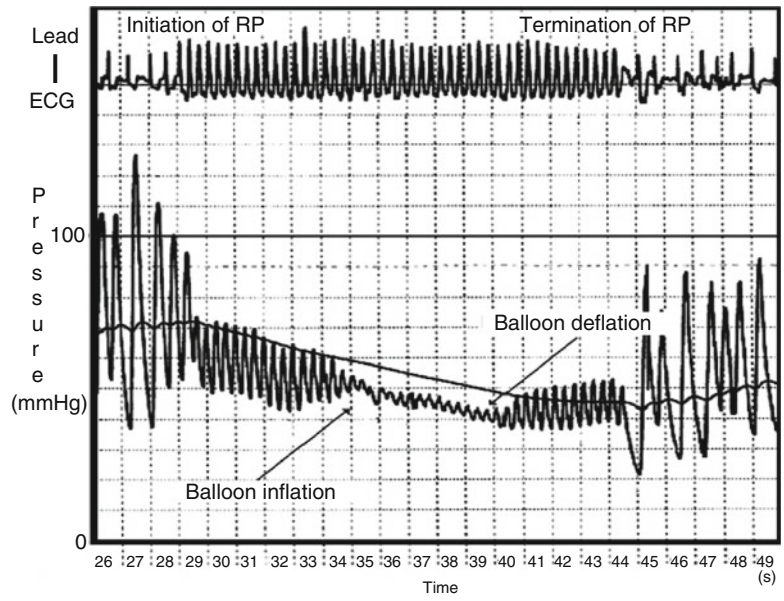

Fig. 13.1 Hemodynamics during rapid right ventricular pacing. Systolic pressure and pulse pressure fall with rapid pacing, and nearly vanish with balloon inflation (From Witzke et al. [26] with permission)

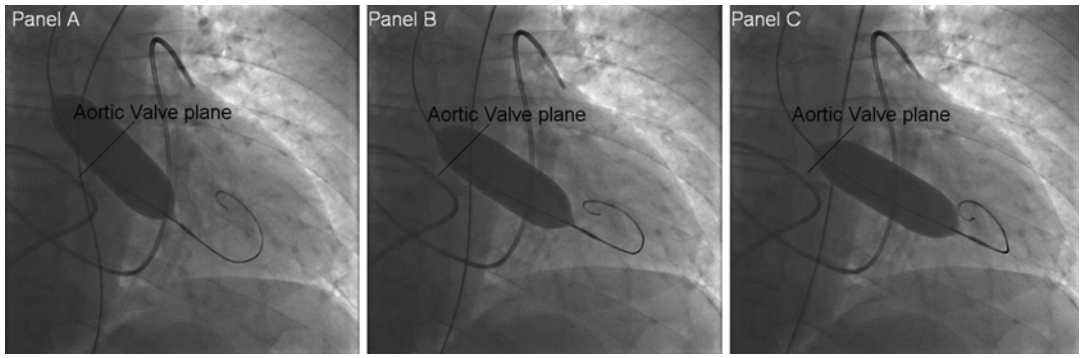

Fig. 13.2 Watermelon seeding of the balloon without rapid pacing. Note the exaggerated "J" on the wire to deflect the balloon from the myocardium (From Witzke et al. [26] with permission). A-C, progressive balloon watermelon seeding

described [24, 25]. In this technique, right ventricular pacing is secured and tested at rates of 180–200, with a goal of decreasing systolic pressure to the 50–70 mmHg range. Once the balloon is across the valve, pacing is initiated and a 5 s inflation performed. Pacing is then stopped and the balloon immediately deflated and withdrawn into the ascending aorta. This decreases the tendency of the valvuloplasty balloon to "watermelon seed" (Fig. 13.2) back and forth across the valve, thus decreasing the possibility of ventricular perforation and allowing for a more effective dilatation. Although not subjected to randomized study, this technique seems safe with no myocardial perforations reported by Sack [25] in a modestly sized series of 75. In Witzke's series of 149 patients, two developed tamponade in the "no-pacing" group versus none in the rapid pacing group [26]. The additional theoretical benefit of this technique is that it may allow for shorter balloon inflations and

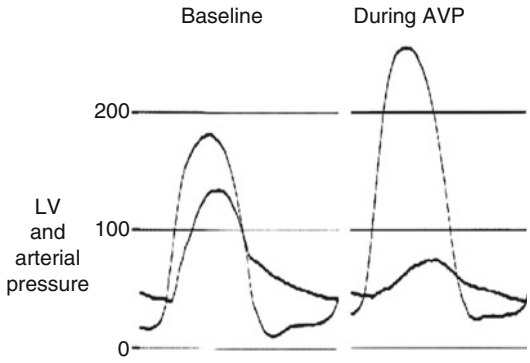

Fig. 13.3 Hemodynamics during balloon inflation. With loss of aortic pressure but marked elevation in LV generated pressure (From Carroll [61] with permission)

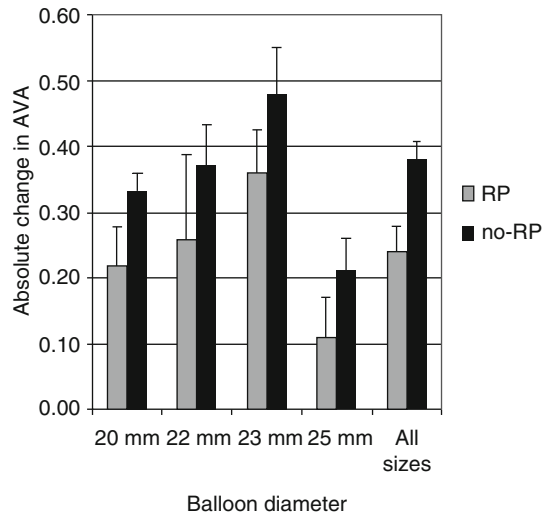

Fig. 13.4 Changes in aortic valve area with and without RV pacing

may mitigate the marked rise in left ventricular pressure seen during BAV (Fig. 13.3), thus decreasing subendocardial ischemia. However, rapid pacing could likewise increase ischemia particularly in patient with coronary artery disease, although in the above mentioned series, there was no difference in outcomes in patients with and without coronary artery disease. This may also reflect the tendency to perform percutaneous coronary revascularization prior to BAV. One finding of some concern was the slight decrease in hemodynamic benefit of BAV in patients undergoing rapid pacing in Witzkes's series (Fig. 13.4). In this retrospective series, the mean aortic gradient fell from 48 to 31 mmHg in the pacing group, and 46–25 mmHg in the non-pacing group with a concomitantly smaller improvement in aortic valve area in the pacing group. One hypothetical reasons for this could include the motion of the balloon in the non-pacing group actually contributing to the improvement in gradient reduction. More likely is perhaps in increase in stunning in the paced group, making early hemodynamic measurements less reliable. At this time, rapid ventricular pacing has become a standard part of BAV, although one of the new balloons now available (see below) may decrease the need for this technique.

Another modification that has made BAV technically safer is the introduction of different balloon shapes and materials. The only balloons available in the early years of balloon valvuloplasty were made by Mansfield (Billerica, MA) and had large shafts and bulky balloons that once inflated, could only come out through a very large sheath. More often, these balloons were inserted through a 12F sheath and once BAV was complete, the deflated balloon and sheath were removed "en-block" over a still wire and a new 12F or larger sheath was inserted. This left a large and perhaps ragged arteriotomy and led to the high incidence of vascular injury and transfusion seen in the early valvuloplasty experience. Newer, lower profile balloons made of more foldable, less bulky polymers such as the Z-Med balloon (Braun Interventional Systems, Bethlehem PA), the True balloon (Bard, Tempe Az) and the Tyshak balloon (Numed, NY), have made vascular access easier, and although difficult to demonstrate in studies, have made vascular complications less frequent. The Inoue balloon (Toray Medical, Houston Tx), initially designed for mitral balloon valvuloplasty, has been adapted for BAV [27–29] with good hemodynamic and clinical results, entirely bypassing the issue of large bore arterial access if the antegrade

Table 13.1 Common types of valvuloplasty balloons

Balloons	Z-Med/Z-Med II/NuCLUES/ NuCLEUS-X/TYSHAK/TYSHAK II	V8	True balloon
Advantages	Quick inflation and deflation time Short flexible distal tip with short balloon taper aids maneuverability through tortuous anatomy Coaxial haft design provides enhanced column strength and pushability Z-Med II provides higher strength and in some instances a larger introducer	Designed to lock into valve, limiting movement Shape maintained reducing likelihood of annular rupture Quick inflation and deflation time	True reliable sizing Fast Rupture resistant
Balloon diameter (mm)	Z-Med: 10–25, Z-Med II: 5–25, Z-Med II TAVR: 20–25, NuCLEUS-X: 18–30	Waist: 17–23 mm/bulbous segment: 22–27.5 mm	20–26 mm
Balloon length (cm)	Z-Med: 2–4, Z-Med II: 2–6, Z-Med II TAVR: 4.5, NuCLEUS: 4–6		4.5 cm
Introducer size (Fr)	Z-Med: 7–12, Z-Med II: 6–14, Z-Med II TAVR: 11–12, NuCLEUS: 10–14	12 Fr	11–13 Fr
Shaft size (Fr)	Z-Med: 6–9, Z-Med II: 5–9, Z-Med II TAVR: 10, NuCLEUS: 9		
Usable length (cm)	Z-Med: 100, Z-Med II: 100, Z-Med II TAVR: 110, NuCLEUS: 110		110 cm
Guide wire (inches)	Z-Med: 0.035, Z-Med II: 0.025–0.035, Z-Med II TAVR: 0.035, NuCLEUS: 0.035	0.035 in.	
Rated burst (ATM)	Z-Med: 9–3, Z-Med II: 15–4, Z-Med II TAVR: 5–4, NuCLEUS: 4–2		
Nominal pressure (ATM)	Z-Med: 4–2, Z-Med II: 6–2, Z-Med II TAVR: 2	Inflation volume: 17 mm/16 cc, 19 mm/20 cc, 21 mm/23 cc, 23 mm/27 cc	

technique is used. To utilize this technique, significant transseptal experience is mandatory, and care needs to be taken to preserve a large loop in the ventricle around the anterior mitral leaflet to prevent damage to this structure and catastrophic mitral insufficiency. Another other novel design balloon is the V8 balloon (InterValve Inc, Plymouth MN). This balloon with a 12F shaft, is hourglass shaped and is sized by the waist in the hourglass which naturally seats itself in the stenotic valve as it is expanded, applying force directly on to the valve and also limiting the "watermelon seeding" motion of the balloon. This has lessened the need for the rapid ventricular pacing described above.

Perhaps the most dramatic change in retrograde BAV technique has been the adaptation of closure devices of various types to the large arteriotomy defects left by the large sheaths involved in BAV. Since they are involved directly in the prevention of vascular complications, they will be described in full in that section.

A list of commonly used valvuloplasty balloons and their manufacturers is listed in Table 13.1 and Fig. 13.5 demonstrates some of the commercially available balloons.

Immediate Hemodynamic Results

The immediate hemodynamic results of BAV have been well described in many single center series as well as the Mansfield BAV Registry. These are summarized in Table 13.2. In these large experiences, the immediate hemodynamic effects of BAV are fairly uniform, with roughly a halving of the transaortic gradient and an increase in calculated aortic valve area of 0.3–0.4 cm^2.

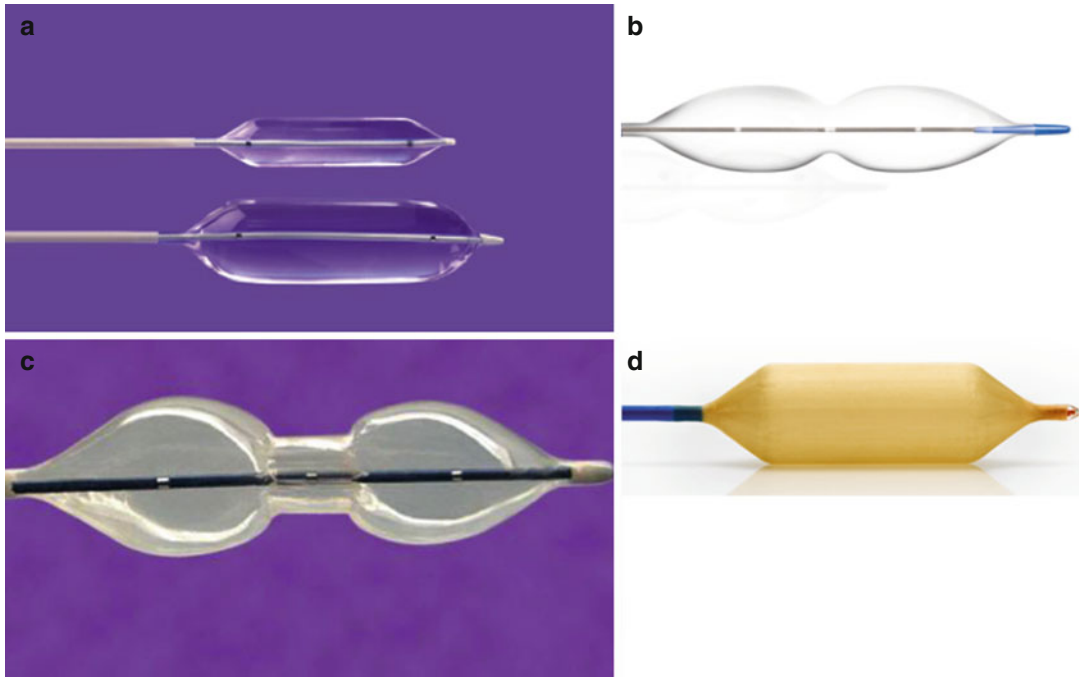

Fig. 13.5 Commonly available valvuloplasty balloons: *top left* (**a**) Z-Med, *bottom left* (**c**) NuCLEUS, *top right* (**b**) V8, and *bottom right* (**d**) True balloon

Table 13.2 Immediate hemodynamic effects of BAV: large series

Reference	N	AVA-pre cm^2	AVA-post cm^2	Mean gradient pre	Mean gradient post
Safian [6]	170	0.6	0.9	71	36
Letac [7]	218	0.5	0.9	72	29
McKay [8]	492	0.5	0.8	60	30
Lewin [9]	125	0.6	1.0	70	30
Ben-Dor [30]	262	0.6	1.0	–	–
Kapadia [31]	99	0.6	1.0	46	21
Khawaja [32]	423	0.6	0.8	62	28

The age of the patient seems not to affect the acute hemodynamic outcome [33]. Other hemodynamic effects include a very modest change in cardiac output as well as an increase in central aortic systolic pressure. Immediate changes in right and left heart filling pressures are usually modest in nature. Although larger balloons and multiple balloon techniques have been utilized to improve the acute hemodynamic results, these may come at the cost of increased risk of aortic root disruption or leaflet avulsion. In a large series from the UK [32] there was a weakly positive correlation between both the balloon size and balloon/annulus ration with percent change in aortic valve area, although neither had any effect on mortality or long-term outcome. In a small consecutive series [29], it was suggested that the antegrade Inoue technique resulted in a slightly better hemodynamic result than the standard retrograde technique. The final balloon diameter was larger in the antegrade group than the retrograde group. This series of 13 patients is more hypothesis generating than definitive, and at this point there is no particular technique that has been shown to consistently deliver better acute hemodynamic results.

Acute Complications

To evaluate the potential for catastrophic complications of BAV, Safian et al. [17] performed 33 postmortem BAV procedures, and 6 intraoperative

Table 13.3 Acute complications of BAV

Reference	N	Death (%)	CVA (%)	Cardiac perforation (%)	AMI (%)	Acute aortic insufficiency (%)	Vascular injury (%)
Cribier [33]	334	4.5	1.4	0.6	0.3	0	13.1
Safian et al. [17]	225	3.1	0.4	1.2	0.5	0.8	7.5
Block and Palacios [36]	162	7.0	2.0	0	0	0	7.0
Lewin [9]	125	10.4	3.2	0	1.6	1.6	9.6
Total	846	5.4	1.5	0.6	0.5	0.5	10.6

From Safian et al. [35] with permission

procedures. As described earlier, the mechanism of aortic valve lumen enlargement was elucidated. Fracture of calcific nodules was visually seen in 16 valves, separation of fused commissures were seen in 5 valves (three of the cases were rheumatic), and grossly inapparent microfractures in 12 valves. Leaflet avulsion occurred in one valve that had been dilated with an oversized balloon. The dilated valves were carefully washed for debris and no calcific debris could be recovered. Moreover, no valve ring disruption or mid leaflet tears occurred. With data from this center and others suggesting that major catastrophes should be unlikely, many centers embarked on BAV programs in the mid 1980s.

The most serious complications of BAV that have been reported are death, athero/thromboembolic complications, complications causing disruption of the aortic root or aortic leaflets causing massive aortic regurgitation, myocardial infarction and peripheral vascular injury due to the large size sheaths used. Ventricular perforation has also been reported. Conduction may also be expected, given the proximity of the aortic annulus to the conduction system. In one series [34], the incidence of new conduction defects was 8.5 %, with only 1.5 % of patients required permanent pacing. The risk of new conduction defects was related to the ratio of balloon size to left ventricular outflow tract (1.2 in patients with new conduction defects, 1.15 in patient with no new defect).

Acute complications from major series are shown in Table 13.3 [35]. Mortality rates of 3–10 % as noted are likely due to the high risk nature of these patients, with advanced age and multiple comorbities. The risk of BAV may be reduced by adoption of some of the modifications to the technique as outlined above. In a more contemporary series of 334 patients [34], the mortality was 1.5 %.

As noted, the most common complication of BAV when done in the retrograde fashion is vascular injury. Transfusion rates in excess of 15 % were reported in most early series of BAV, when manual compression or planned surgical removal of the sheaths were the only options for hemostasis. Suture mediated (Proglide 6F, Abbott Vascular Devices, Redwood City CA) and collagen based techniques (Angioseal 8F, St. Jude Medical, St. Paul, MN) have both been adapted to large sheath sizes, and have been utilized for vascular closure after BAV. They been demonstrated to decrease the incidence of vascular complication and transfusion [37, 38]. Although direct comparisons are difficult due to the non-randomized nature of these studies, it appears that in patients with suitable anatomy (lack of severe atherosclerotic obstruction, well placed arteriotomy site), these devices do decrease complications as well as improve the patient experience.

Long-Term Followup

The modest improvements in hemodynamics [39] and symptoms afforded by BAV are relatively short-lived, limiting the widespread application of the procedure. Very high rates of recurrent symptoms, repeat procedures or death (Table 13.4) have relegated the procedure to an

Table 13.4 Long term followup following BAV

Reference	N	Followup (mo)	Symptom recurrence (%)	Death (%)	Re-BAV (%)	AVR (%)
Kuntz [40]	205	24 ± 12	82	40	22	27
Block [41]	84	5.5 ± 0.3	56	28	18	–
O'Neill [42]	492	12		36		
Lewin [9]	125	12.3 ± 4	54	32	8	4

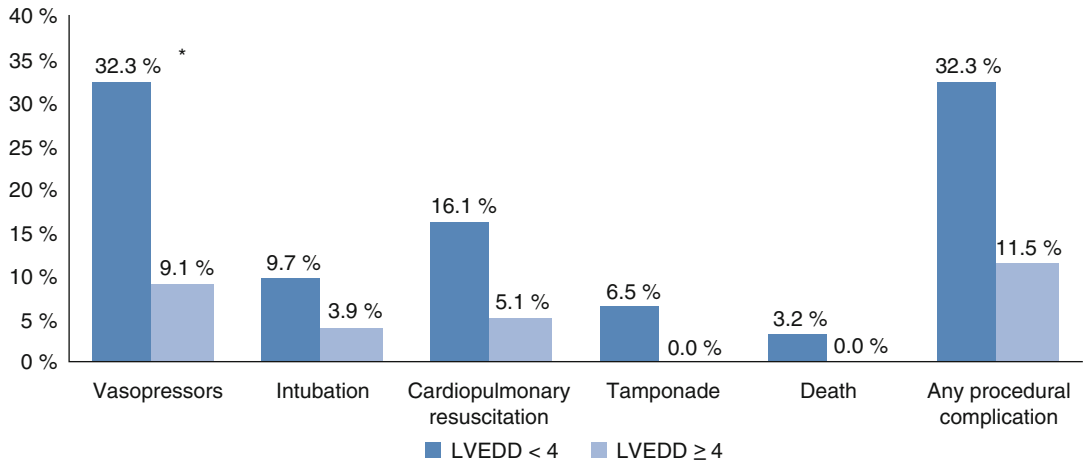

Fig. 13.6 Complications in patients with smaller LV chamber sizes (From Don et al. [46] with permission)

almost exclusively palliative or "boutique" role, although with increasing application of transarterial valve replacement (TAVR), there is more interest in the use of BAV as a "bridging procedure" as a prelude to TAVR. In a more contemporary BAV series from the United Kingdom [32] involving 423 patients, the 1 year mortality was 36.3 %, with 18.3 % of patients undergoing TAVR following BAV and 7.0 % of patients undergoing SAVR.

A number of investigators have identified clinical and hemodynamic predictors of response to BAV [32, 40, 43, 44]. Lower initial left ventricular and systemic systolic pressure, the presence of coronary artery disease, elevated pulmonary artery pressure and lower left ventricular ejection fraction have all been demonstrated to predict poorer outcome. In one study of 205 patients [40], the aortic systolic pressure, pulmonary capillary wedge pressure, and percent reduction in peak aortic valve gradient were predictors of event-free survival in multivariate analysis. Urgent or emergent presentation likewise was a predictor of poor outcome, although the use of BAV as a potential lifesaving procedure on patients with cardiogenic shock and critical aortic stenosis has been described [45]. More recently, patients with small LV diastolic dimensions undergoing BAV have been noted to have poorer outcomes and a higher acute complication rate ([46], Fig. 13.6).

Mechanisms of Clinical Improvement

Balloon aortic valvuloplasty results in only modest immediate changes in cardiac filling pressures and cardiac output, yet the majority of patients undergoing the procedure have improvement in symptoms. Improvement in systolic function in patients with depressed ejection fractions at baseline have been well documented [47–49] although the response of the ejection fraction to BAV is

heterogenous and may relate to concomitant coronary artery disease and other comorbidities. Symptomatic improvement may also be due in part to improved diastolic function [50, 51], as well as improvement in the magnitude of mitral regurgitation [52, 53].

Miscellaneous Applications

BAV has been proposed [54–56] as a palliative procedure in patients in need of non-cardiac surgery in who are either not candidates for SAVR or who are felt to be at high risk for SAVR. The 2014 ACC/AHA guidelines for management of cardiac conditions for noncardiac surgery discuss BAV as an option in patients with severe symptomatic aortic stenosis in need of noncardiac surgery. No specific recommendation is made. It would seem reasonable to consider BAV in this population particularly in patients with impaired left ventricular function or relative hypotension, as this group might be expected to tolerate general anaesthesia and fluid shifts especially poorly.

Bioprosthetic aortic valve stenosis is likely to be seen more frequently as more valves are placed and the population ages, although regurgitation is a more common mode of valve failure. There are scattered reports of balloon dilatation of aortic valves [57–60], with few successes and several catastrophic complications reported of leaflet damage and severe aortic regurgitation. In light of the limited and somewhat discouraging clinical experience, balloon dilatation of bioprostheses in the aortic position cannot be supported as a viable alternative in these patients, although there are TAVR registries evaluating this new technology in this group of patients.

Summary

Initially performed in the 1980s, Balloon aortic valvulplasty enjoyed a short period of enthusiastic popularity, as physicians, perhaps encouraged by the experience of BAV in young patients with noncalcific aortic valve stenosis, sought a way to treat patients with calcific AS who were poor candidates for SAVR by virtue of very advanced age, debility, and other comorbidities. As the disappointing results regarding symptomatic recurrence and hemodynamic deterioration became apparent, the procedure was performed very infrequently during the 1990s. However, with the advent of TAVR, attention is again focused on this very ill and aged group of patients, many of whom are awaiting TAVR but need short term therapy while their evaluation is being done. With the technical improvements in the procedure, and the new need for a bridge, BAV may again become an important procedure in the armentarium of treatment of advanced calcific aortic stenosis.

References

1. O'Keefe JH, Vlietstra RE, Bailey KR, Holmes DR. Natural history of candidates for balloon aortic valvuloplasty. Mayo Clin Proc. 1987;62:986–91.
2. Carabello BA, Breen LH, Grossman W, Cohn LH, Koster K, Collins JJ. Hemodynamic determinants of prognosis of aortic valve replacement in critical aortic stenosis and advanced congestive heart failure. Circulation. 1980;62(1):42–7.
3. Lababidi Z, Wu JR, Walls JT. Percutaneous balloon aortic valvuloplasty: results in 23 patients. Am J Cardiol. 1984;53:194–9.
4. Rosenfeld HM, Landzberg MJ, Perry SB, Colan SD, Keane JF, Lock JE. Balloon aortic valvuloplasty in the young adult with congenital aortic stenosis. Am J Cardiol. 1994;73:1112–7.
5. Maskatia SA, Ing FF, Justino H, Crystal MA, Mullins CE, Mattamal RJ, Smith EO, Petit CJ. Twenty-five year experience with balloon aortic valvuloplasty for congenital aortic stenosis. Am J Cardiol. 2011;108:1024–8.
6. Safian RD, Berman AD, Diver DJ, McKay LL, Come PC, Riley MF, Warren SE, Cunningham MJ, Wyman RM, Weinstein JS, Grossman W, McKay RG. Balloon aortic valvuloplasty in 170 consecutive patients. N Engl J Med. 1988;319:125–30.
7. Letac B, Cribier A, Koning R, Bellefleur J. Results of percutaneous transluminal valvuloplasty in 218 patients with valvular aortic stenosis. Am J Cardiol. 1988; 62:598–605.
8. Mckay RG. The Mansfield scientific aortic valvuloplasty registry: overview of acute hemodynamic results and procedural complications. J Am Coll Cardiol. 1991;17:485–91.
9. Lewin RF, Dorros G, King JF, Mathiak L. Percutaneous transluminal aortic valvuloplasty: acute outcome and followup in 125 patients. J Am Coll Cardiol. 1989; 14:1210–7.

10. Brock R. Surgical treatment of aortic stenosis. Br Med J. 1957;1:1020–8.
11. Harken DF, Black H, Taylor WJ, Thrower WB, Soroff HS, Bush V. Am J Cardiol. 1959;4(2):135–46.
12. Kirklin JW, Mankin HT. Open operation in the treatment of calcific aortic stenosis. Circulation. 1960;21:578–86.
13. Hurley PJ, Lowe JB, Barratt-Boyes BG. Debridement-valvotomy for aortic stenosis in adults. A followup of 76 patients. Thorax. 1967;22:314–9.
14. Hufnagel CA, Conrad PW. Calcific aortic stenosis. N Engl J Med. 1962;266(2):72–6.
15. Inoue K, Owaki T, Nakamura T, Kitamura F, Miyamoto N. Clinical application of transvenous mitral commisurotomy by a new balloon catheter. J Thorac Cardiovasc Surg. 1984;87(3):394–402.
16. Kalan JM, Mann JM, Leon MB, Pichard A, Kent KM, Roberts WC. Morphologic findings in stenotic aortic valves that have had "successful" percutaneous balloon dilatation. Am J Cardiol. 1988;62:152–4.
17. Safian RD, Mandell VS, Thurer RE, Hutchins GM, Schnitt SJ, Grossman W, McKay RG. Postmortem and intraoperative balloon valvuloplasty of calcific aortic stenosis in elderly patients. J Am Coll Cardiol. 1987;9:655–60.
18. Isner JM, Samuels DA, Slovenkai GA, Halburka KR, Hougen TJ, Desnoyers MR, Fields CD, Salem DN. Mechanism of aortic balloon valvuloplasty: fracture of valvular calcific deposits. Ann Intern Med. 1988; 108:377–80.
19. Robicsek F, Harbold NB, Daugherty HK, Cook JW, Seele JG, Hess PJ, Gallagher JJ. Balloon valvuloplasty in calcified aortic stenosis: a cause for caution and alarm. Ann Thorac Surg. 1988;45:515–25.
20. Robicsek F, Harbold NB, Scotten LN, Walker DK. Balloon dilatation of the stenosed aortic valve: how does it work? Why does it fail? Am J Cardiol. 1990;65:761–6.
21. Block PC, Palacios IF. Comparison of hemodynamic results of anterograde versus retrograde percutaneous balloon aortic valvuloplasty. Am J Cardiol. 1987;60(59):659.
22. Dorros G, Lewin RF, King JF, Janke LM. Percutaneous transluminal valvuloplasty in calcific aortic stenosis: the double balloon technique. Catheter Cardiovasc Diagn. 1987;13:151–6.
23. Isner JM, Salen DN, Desnoyers MR, Fields CD, Halaburka KR, Slovenkai GA, Hougen TJ, Eichorn EJ, Rosenfield K. Dual balloon technique for valvuloplasty of aortic stenosis in adults. Am J Cardiol. 1988;61:593–9.
24. Inohara T, Hayashida K, Fukuda K. Double balloon aortic valvulplasty in TAVI era: insight from intracardiac echocardiography and multidetector computed tomography findings. J Invasive Cardiol. 2014;26(7):e95–7.
25. Sack S, Kahlert P, Khandanpour S, Naber C, Philipp S, Mohlenkamp S, Sievers B, Hagen K, Erbel R. Revival of an old method with new techniques: balloon aortic valvuloplasty of the calcified aortic stenosis in the elderly. Clin Res Cardiol. 2008;97:288–97.
26. Witzke C, Don CW, Cubeddu R, Herrero-Garibi J, Pomerantzev E, Caldera A, McCarty D, Inglessis I, Palacios I. Impact of rapid ventricular pacing during percutaneous balloon aortic valvuloplasty in patients with critical aortic stenosis: should we be using it? Catheter Cardiovasc Interv. 2010;75:444–52.
27. Bhargava B, Agarwal R, Yadav R, Bahl V, Manchanda S. Percutaneous balloon aortic valvuloplasty during pregnancy: use of the Inoue balloon and the physiologic antegrade approach. Catheter Cardiovasc Diagn. 1998;45:422–5.
28. Sakata Y, Syed Z, Salinger M, Feldman T. Percutaneous balloon aortic valvuloplasty: antegrade transseptal vs. conventional retrograde transarterial approach. Catheter Cardiovasc Interv. 2005;64:314–21.
29. Eisenhauer A, Hadjipetrou P, Piemonte T. Balloon aortic valvuloplasty revisited: the role of the Inoue balloon and transseptal antegrade approach. Catheter Cardiovasc Interv. 2000;50:484–91.
30. Ben-Dor I, Pichard A, Satler L, Goldstein S, Syed A, Gaglia M, Weissman G, Maluenda G, Gonzalez M, Wakabayashi K, Collins S, Torguson R, Okubagzi P, Xue Z, Kent K, Lindsay J, Waksman R. Complications and outcome of balloon aortic valvuloplasty in high-risk or inoperable patients. J Am Coll Cardiol Intv. 2010;3:1150–6.
31. Kapadia S, Goel S, Yuksel U, Agarwal S, Pettersson G, Svensson L, Smedira N, Whitlow P, Lytle B, Tuzcu E. Lessons learned from balloon aortic valvuloplasty experience from the pre-transcatheter aortic valve implantation era. J Interv Cardiol. 2010;23:499–508.
32. Khawaja M, Sohal M, Valli H, Dworakowski R, Pettit S, Roy D, Newton J, Schneider H, Manoharan G, Doshi S, Muir D, Roberts D, Nolan J, Gunning M, Densem C, Spence M, Chowdhary S, Mahadevan V, Brecker S, MacCarthy P, Mullen M, Staples R, Prendergast B, de Belder A, Thomas M, Redwood S, Hildick-Smith D. Standalone balloon aortic valvulplasty: indications and outcomes from the UK in the transcatheter valve era. Catheter Cardiovasc Interv. 2013;81:366–73.
33. Cribier A, Gerber L, Letac B. Percutaneous balloon aortic valvuloplasty: the French experience. In: Topol EJ, editor. Textbook of interventional cardiology. Philadelphia: WB Saunders; 1990. p. 849.
34. Laynez A, Ben-Dor I, Hauville C, Xue Z, Satler L, Kent K, Pichard A, Lindsay J, Waksman R. Frequency of cardiac conduction disturbances after balloon aortic valvuloplasty. Am J Cardiol. 2011;108:1311–5.
35. Safian R, Kuntz R, Berman A. Aortic valvuloplasty. Cardiol Clin. 1991;9(2):289–99.
36. Block P, Palacios I. Aortic and mitral vavluloplasty: the United States experience. In: Topol EJ, editor. Textbook of interventional cardiology. Philadelphia: WB Saunders; 1990. p. 831.
37. Ben-dor I, Looser P, Bernardo N, Maluenda G, Torguson R, Zue Z, Lindsay J, Pichard A, Satler L, R W. Comparison of closure strategies after balloon aortic valvuloplasty: suture mediated versus collagen based versus manual. Catheter Cardiovasc Interv. 2011;78:119–24.
38. O'Neill B, Singh V, Kini A, Mehran R, Jacobs E, Knopf D, Alfonso C, Martinez C, Martinezclark P, O'Neill W, Heldman A, Yu J, Baber U, Kovacic J,

Dangas G, Sharma S, Sartori S, Cohen M. The use of vascular closure devices and impact on major bleeding and net adverse clinical events (NACESs) in balloon aortic valvuloplasty: a sub-analysis of the BRAVO study. Catheter Cardiovasc Interv. 2013;83: 148–53.
39. Bashore T, Davidson C. Followup recatheterization after balloon aortic valvuloplasty. J Am Coll Cardiol. 1991;17(5):1188–95.
40. Kuntz R, Tosteson A, Berman A, Goldman L, Gordon P, Leonard B, McKay R, Diver D, Safian R. Predictor of event-free survival after balloon aortic valvuloplasty. N Engl J Med. 1991;325:17–23.
41. Block P, Palacios I. Clinical and hemodynamic followup after percutaneous aortic valvuloplasty in the elderly. Am J Cardiol. 1988;62:760–3.
42. O'Neill W. Predictors of long-term survival after percutaneous balloon aortic valvuloplasty: report of the Mansfield scientific balloon aortic valvuloplasty registry. J Am Coll Cardiol. 1991;17:193–8.
43. Reeder G, Nishimura R, Holmes D. Patient age and results of balloon aortic valvuloplasty: the Mansfield scientific registry experience. J Am Coll Cardiol. 1991;17:909–13.
44. Sherman W, Hershman R, Lazzam C, Cohen M, Ambrose J, Gorlin R. Balloon valvuloplasty in adult aortic stenosis: determinants of clinical outcome. Ann Intern Med. 1989;110:421–5.
45. Moreno P, Jang I, Newell J, Block P, Palacios I. The role of percutaneous aortic balloon valvuloplasty in patients with cardiogenic shock and critical aortic stenosis. J Am Coll Cardiol. 1994;23:1071–5.
46. Don C, Gupta P, Witzke C, Kesarwani M, Cubeddu R, Inglessias I, Palacios I. Patients with small left ventricular size undergoing balloon aortic valvuloplasty have worse intraprocedural outcomes. Catheter Cardiovasc Interv. 2012;80:946–54.
47. McKay R, Safian R, Lock J, Diver D, Berman A, Warren S, Come P, Baim D, Mandell V, Royal H, Grossman W. Assessment of left ventricular and aortic valve function after aortic balloon valvuloplasty in adult patients with critical aortic stenosis. Circulation. 1987;75(1):192–203.
48. Safian R, Warren S, Berman A, Diver D, McKay L, Come P, Grossman W, McKay R. Improvement in symptoms and left ventricular performance after balloon aortic valvuloplasty in patients with aortic stenosis and depressed left ventricular ejection fraction. Circulation. 1988;78(1):1181–91.
49. Harpone D, Davidson C, Skelton T, Kisslo K, Jones R, Bashore T. Early and late changes in left ventricular systolic performance after percutaneous aortic balloon valvuloplasty. Am J Cardiol. 1990;66:327–32.
50. Sheikh K, Davidson C, Honan M, Skelton T, Kisslo K, Bashore T. Changes in left ventricular diastolic performance after aortic balloon valvuloplasty: acute and late effects. J Am Coll Cardiol. 1990;16:795–803.
51. Stoddard M, Vandormael M, Pearson A, Gudipati C, Kern M, Deligonul U, Labovitz A. Immediate and short term effects of aortic balloon valvulplasty on left ventricular diastolic function and filling in humans. J Am Coll Cardiol. 1989;14:1218–28.
52. Come P, Riley MF, Berman A, Safian R, Waksmonski C, McKay R. Serial assessment of mitral regurgitation by pulsed Doppler echocardiography in patients undergoing balloon aortic valvuloplasty. J Am Coll Cardiol. 1989;14:677–82.
53. Maluenda G, Ben-Dor I, Laynez-Carnicero, Barbash I, Sardi G, Gaglia M, MItulescu L, Torguson R, Goldstein S, Wang Z, Suddath W, Kent K, Satler L, Pichard A, Wakman R. Changes in mitral regurgitation after balloon aortic valvuloplasty. Am J Cardiol. 2011;108:1777–82.
54. Hayes S, Holmes D, Nishimura R, Reeder G. Palliative percutaneous aortic balloon valvuloplasty before noncardiac operations and invasive diagnostic procedures. Mayo Clin Proc. 1989;64:753–7.
55. Roth R, Palacios I, Block P. Percutaneous aortic balloon valvuloplasty: its role in the management of patients with aortic stenosis. Requiring major noncardiac surgery. J Am Coll Cardiol. 1989;13:1039–41.
56. Levine M, Berman A, Safian R, Diver D, McKay R. Palliation of valvular aortic stenosis by balloon valvuloplasty as preoperative preparation for noncardiac surgery. Am J Cardiol. 1988;62:1309–10.
57. Kirwan K, Richardson G, Rothman M. Is there a role for balloon valvuloplasty in patients with stenotic aortic bioprosthetic valves? Catheter Cardiovasc Interv. 2004;63:251–3.
58. McKay C, Waller B, Hong R, Rubin N, Reid C, Rahimtoola S. Problems encountered with catheter balloon valvuloplasty of bioprosthetic aortic valves. Am Heart J. 1988;115(2):463–5.
59. Orbe L, Sobrino N, Mate I, Oliver J, Rico J, Frutos A, Dominguez F, Mesa J, Sobrino J. Effectiveness of balloon percutaneous valvuloplasty for stenotic bioprosthetic valves in different positions. Am J Cardiol. 1991;68:1719–21.
60. Dejam A, Hokinson M, Laham R. Repeated successful balloon valvuloplasty of a bioprosthetic aortic valve in a nonagenarian. Catheter Cardiovasc Interv. 2011;77:589–92.
61. Carroll J. Optimizing technique and outcomes in structural heart disease interventions: rapid pacing during aortic valvuloplasty? Catheter Cardiovasc Interv. 2010;75:453–4.

Imaging for Transcatheter Aortic Valve Replacement

14

Karl K.C. Poon

Abstract

Transcatheter aortic valve replacements (TAVRs) have revolutionized the treatment of aortic stenosis (AS). There have been few, if any, interventional devices in recent memory with such marked clinical impact on patient outcomes. TAVR has been firmly established as an alternative to surgical aortic valve replacement (SAVR) at least in patients deemed high or prohibitive surgical risk. Through the development of transcatheter heart valves (THVs), there have been a renewed interested in the role of imaging for TAVR planning, particularly the routine utilization of multislice computed tomography (MSCT). MSCT has significant advanced the understanding of the aortic complex and highlighted the potential challenges and limitation of the THV technology. Conventional follow up echocardiography had played a key role in highlighting the importance of paravalvular regurgitation in patient outcomes. The future for THV is exciting and its success will depend on the incorporation of data from MSCT and echocardiography to ensure this disruptive technology will one day equal and surpass the gold standard of SAVRs.

Keywords

Transcatheter aortic valve replacements (TAVRs) • Transcatheter heart valves (THVs) • Multislice computed tomography (MSCT) • Paravalvular regurgitation • Two-dimensional transthoracic echocardiography (2D-TTE) • Two-dimensional transesophageal echocardiography (2D-TEE) • Three-dimensional transesophageal echocardiography (3D-TEE)

K.K.C. Poon, MBBS
Cardiology Program, The Prince Charles Hospital,
Chermside, QLD, Australia
e-mail: karl_poon@health.qldl.gov.au

A.E. Abbas (ed.), *Aortic Stenosis: Case-Based Diagnosis and Therapy*,
DOI 10.1007/978-1-4471-5242-2_14

Introduction

Transcatheter aortic valve replacements (TAVRs) have revolutionized the treatment of aortic stenosis (AS). There have been few, if any, interventional devices in recent memory with such marked clinical impact on patient outcomes. TAVR has been firmly established as an alternative to surgical aortic valve replacement (SAVR) at least in patients deemed high or prohibitive surgical risk. Through the development of transcatheter heart valves (THVs), there have been a renewed interested in the role of imaging for TAVR planning, particularly the routine utilization of multislice computed tomography (MSCT). MSCT has significant advanced the understanding of the aortic complex and highlighted the potential challenges and limitation of the THV technology. Conventional follow up echocardiography had played a key role in highlighting the importance of paravalvular regurgitation in patient outcomes. The future for THV is exciting and its success will depend on the incorporation of data from MSCT and echocardiography to ensure this disruptive technology will one day equal and surpass the gold standard of SAVRs.

Transcatheter heart valves (THV) have transformed the treatment of aortic stenosis. It has been shown to provide similar outcomes to traditional surgical aortic valve replacements (SAVR) in high surgical risk aortic stenosis patients [1, 2] and better outcomes over conservative approach in inoperable patients [3, 4]. Ongoing randomized studies are being conducted to evaluate its emerging role in the intermediate surgical risk group of patients. Over the past decade, much has been learnt about transcatheter aortic valve replacements (TAVR) since feasibility was first demonstrated in 2002 in a critically unwell 57-year-old patient [5]. Whilst there is enormous potential in this technology, there have been important lessons learnt in its decade long history of clinical use. The THV is a complete paradigm shift from the surgical management of severe AS and has introduced unique issues such as management of concomitant coronary artery disease, concomitant valvular disease, calcification in the aortic apparatus, and paravalvular regurgitation.

Perhaps the most important lesson over the past decade has been the inadequacy of traditional two dimensional imaging such as echocardiography, and the mandatory role three dimensional imaging plays in the assessment of the aortic apparatus, and the management of the THV implant and possibly even follow up. In SAVR, the aortic annulus and apparatus would be visually inspected, potential issues such as calcification addressed, prior to selecting and implanting the appropriately sized surgical valve. With the current THV technology, information relating to the nature and morphology of the AS, extent and location of calcification, aorto-ventricular fluoroscopic implant angle, and aortic annulus diameter and area, are all obtained prior to the actual implant.

This chapter will therefore examine the evolution of imaging for TAVR. It will focus on the various aspects of imaging crucial to an ideal implant, focussing on the various modalities including traditional transthoracic echocardiography, transesophageal echocardiography, to newer techniques such as 3D echocardiographic imaging, the important role of multi-slice computed tomography (MSCT) as well as other future imaging techniques. The chapter will be divided into the pre-procedural, procedural and post-procedural phases of the TAVR imaging process.

Pre-procedural Planning

Two-Dimensional Transthoracic Echocardiography (2D-TTE)

Despite the advent of newer imaging modalities, a 2D-TTE remains fundamental in the imaging of AS. TTE establishes the indication for intervention – that of severe AS or rapidly worsening AS. TTE also provides important information, such as ventricular function and co-existent valvular disease. Lastly, 2D-TTE provides basic information on the sizing and calcium burden of the aortic annulus, and had traditionally been

crucial in guiding THV size choices, although this is rapidly supplanted by the use of MSCT.

Severity of Aortic Stenosis

The current indication for AS intervention remains unchanged despite the introduction of a less invasive approach. The threshold of intervention is well established [6]. The current guidelines from both the European Society of Cardiology [7] and American College of Cardiology [8] rely heavily on echocardiography to establish the severity for intervention (Chap. 11). Both guidelines have also adopted TAVR as a Class IIa recommendation for high risk or extreme risk/inoperable patients.

In the presence of a normally functioning left ventricle, both flow mediated and derived indices can be used; namely, peak transaortic velocity (Vmax) of >4 m/s and mean gradient of >40 mmHg; derived valve area of <1 cm^2 based on the continuity equation. This has been previously discussed in details.

Paradoxical Low Flow Low Gradient Aortic Stenosis

Paradoxical low flow low gradient (PLFLG) AS represents a distinct entity without the AS group of patients and may exhibit a different natural history [9, 10]. PLFLG AS is defined by a low flow state of stroke volume index <35 mL/m^2 [11]. This entity has been thoroughly described in Chap. 8. The routine adoption of MSCT in the assessment of potential candidates for TAVR has advanced knowledge [12, 13] in this difficult to diagnose entity. There is only limited experience of TAVR in PLFLG [14, 15] but the limited data thus far suggest that, akin to SAVR, TAVR improves survival in patients with PLFLG AS over conventional medical therapy alone. Low flow is also a powerful predictor of adverse outcomes in TAVR [16]. It should also be emphasized patients PLFLG AS essentially have a restrictive physiology and paravalvular regurgitation is poorly tolerated.

Aortic Regurgitation

The impact of pre-existing aortic regurgitation in a patient with severe AS undergoing TAVR is not well characterized. This may be particularly relevant in patients who had significant, moderate to severe paravalvular regurgitation (PVR), post TAVR due to poorly sized THV or heavy calcification. It remains purely hypothesis generating whether patients with pre-existing aortic regurgitation may tolerate post-TAVR PVR better.

The use of THV in native aortic regurgitation is not well assessed either. This has been shown to be feasible in several case series [17–19] with both conventional THVs designed for aortic stenosis, as well as dedicated devices [20, 21]. However, challenges remain in transcatheter treatment of aortic regurgitation. In particular, the fluoroscopic placement can be challenging in the absence of aortic leaflet calcification, raising concerns of stability of the THV, as well as the sometimes co-existing aortic dilatation precluding an appropriately anchored or sized THV.

The treatment of native valve aortic regurgitation with TAVR with current THV devices therefore should be reserved for patients with no other options.

Left and Right Ventricular Function

The status of the left ventricle has significant implication in the outcome of conventional SAVR. The impact of left ventricular dysfunction, i.e. classic low flow low gradient AS, is becoming better defined in the TAVR arena through data gathered from registries and RCT [15, 22–26]. It appears impaired left ventricular function carries a negative impact on mortality with TAVR, although whether this impact may be less so than in a matched SAVR candidate is unclear.

There is much less data on the impact of right ventricular impairment on TAVR outcome. Likewise, there is only limited information on the impact of pulmonary hypertension [27–29] on TAVR outcomes. It stands to reasons if the pulmonary hypertension is left sided driven, i.e. pulmonary venous hypertension, it should respond satisfactorily to TAVR.

Mitral Regurgitation

Several studies had addressed the impact on coexisting MR. These have demonstrated that MR tends to diminish post TAVR although it does

impact negatively on TAVR outcome [30–33]. It remains a difficult dilemma in patients with severe MR whether TAVR is an acceptable treatment option given the concomitant MR is difficult to treat with the current iteration of percutaneous devices [34]. The several registries [30–33] demonstrated the majority derived a reduction in MR, although it is unclear whether such reduction in MR is associated with better TAVR outcomes.

THV Sizing

One of the biggest lessons from the past decade of TAVR development is the inadequacy of two-dimensional imaging in the assessment of the aortic apparatus. With traditional surgery, TTE provides a satisfactory guide to the appropriate prosthesis size. Whilst prosthesis-patient mismatch is a well-recognized issue, minor errors is prosthesis size are corrected during implantation with sutures to ensure no significant PVR occurs. This is not possible with THV and errors in sizing translate to possibly severe PVR or aortic hematoma, dissection or rupture.

The limitation of TTE in THV sizing stems from the fact that the aortic annulus is almost always ovoid and a single diameter obtained from the parasternal long axis view on TTE is simply insufficient to provide the correct THV sizing information. This important concept will be expanded in the following section on MSCT.

Two-Dimensional Transesophageal Echocardiography (2D-TEE)

In the early days of TAVR, TEE was often used to better understand THV sizing. This was particularly the case in TTE with poor image quality. It was conventional wisdom that the measured aortic annulus on TEE was generally 1 mm larger than that from TTE. In patients with absolute contraindication to MSCT such as severe chronic kidney disease, TEE may still have a role in preprocedural planning. The need for TEE for preprocedural planning has very much diminished with the advent of MSCT.

Three-Dimensional Transesophageal Echocardiography (3D-TEE)

3D TEE potentially bypasses the limitation of 2D TTE/TEE in assessing the aortic annulus. Several groups have published their findings suggesting superiority and reproducibility of this method over 2D TEE [35, 36], benchmarked against MSCT [37, 38]. However, the spatial resolution for echocardiography is inherently inferior to MSCT. The use of 3D TEE is likely limited to centers with such expertise and more data is required to demonstrate its equivalent of MSCT in guiding THV sizing algorithm. It should be considered when good MSCT data is not available.

Cardiac Catheterization

Coronary angiography and aortography have always been important in SAVR planning and remain the case for TAVR. The optimal management of concomitant coronary artery disease remains unclear. Several reports [39–42] have provided reassuring data that concomitant CAD can either be treated with percutaneous coronary stents or with medical therapy with generally no significant adverse impact on TAVR outcome with regards to mortality or MACE. Ongoing trials (ACTIVATION, ISRCTN 75836930) may elucidate the optimal treatment of concomitant CAD.

Cardiac catheterization may also provide further information on the severity of aortic stenosis through invasive means. This is particularly pertinent if there is uncertainty on the severity of aortic stenosis.

Aorto-ilio-femoral Angiography

Invasive angiography with a calibrated pigtail catheter may be useful to provide information on iliofemoral calibre for transfemoral TAVR. This was traditionally the method of choice for assessing the iliac and femoral arteries calibres.

However this is now very much surpassed by MSCT, which provides 3D reconstruction of iliofemorals as well as providing detailed information on the circumferential and longitudinal extent and location of calcium.

Multi-slice Computed Tomography

MSCT represents perhaps the single most important paradigm shift in the development of TAVR, and arguably supplants all other imaging modalities in understanding the aortic apparatus [43].

The use of MSCT in SAVR was at best considered a novel concept, perhaps useful in assessing aortic root calcification for aortic root annulation. Over the years, MSCT has progressed from merely a research tool in understanding the aortic annulus, particularly demonstrating the inadequacy of TTE, to demonstrating prospectively its superior in minimizing PVR, to now becoming the imaging modality of choice in TAVR.

There are several specific applications of MSCT in TAVR – THV sizing algorithm, optimal fluoroscopic implant angle prediction, quantification of calcium burden, and peripheral vasculature for TAVR access determination. In all these areas, one could argue MSCT remains the gold standard imaging tool.

THV Sizing

The critical benefit MSCT offers is the ability for three dimensional reconstruction of the aortic annulus, such that the annulus is appreciated correctly enface. Whilst the use of 3DTEE has improved the accuracy of echocardiographic assessment, MSCT remains the gold standard. This derived aortic annulus is completely coaxial to LVOT/Aortic axis, as opposed to the misguided TTE or TEE measurement of the LVOT diameter [44].

With the ability to reconstruct the aortic annulus enface, MSCT has enabled the measurement of various parameters at the aortic annulus. These include maximum diameter, minimum diameter and mean diameter, aortic annulus area and aortic annulus perimeter [45, 46].

The best-validated parameter, at least in the setting of balloon expandable valves, is arguably that of ***aortic annulus area*** [47, 48]. There is prospective multicentre data [49] demonstrating that valve choices based on MSCT derived areas may be associated with less frequent and severe PVR. When fully expanded, each balloon expandable THV produces a nominal circular area (e.g. a 23 mm Edwards Sapien XT THV has an area of 4.15 cm^2). The current data suggests an area oversizing up to 10 % the nominal area. [Case] The use of judicious oversizing in this algorithm has led to a reduction of PVR.

The data is much more limited on self-expanding THVs and it remains controversial as to the best means for THV sizing. It appears that self-expanding THVs may be better sized via the ***perimeter*** of the reconstructed annulus. Prospective data on the use of either perimeter or area in sizing self-expanding THVs are eagerly awaited.

Regardless of the implanter's preference for perimeter or area for valve sizing, it's important to assess the aortic annulus correctly. It's generally recommended that gated MSCTs are used, and a 30–40 % RR interval in systole time point be used to standardize measurement of the aortic annulus. More importantly, it's paramount to be coaxial to the aortic annulus.

There are various proprietary computer programs available nowadays allowing the cardiologist to reconstruct the aortic apparatus. We advocate the centerline spinning technique advocated by others [50]. A centreline is carefully constructed through the aorto-ventricular axis. Once this is achieved, then the bottom of each cusp is "picked up" by the spinning of the axis such that the aortic annulus can be ascertained to be on axis.

A definitive guide to the measurement of the aortic annulus will be beyond the scope of this chapter. In experienced hands, the interobserver variability of this aortic annulus assessment method is with 0.1 cm^2 [51].

Aortic Apparatus Calcification

MSCT also provides crucial information on the extent and location of calcification in the aortic valve. These data have been correlated with the likelihood of PVR post implant [25, 52–54]. It remains controversial as to whether eccentricity or location of calcification is more important or whether the overall extent of calcification has a stronger impact of PVR. Initial research focused on aortic calcification as a continuum, represented by a total calcium score. More recent research focused on the distribution and location of calcium. The later seems more intuitive – a homogenous circumferential extent of calcification may be preferable to a single large nodule of calcium at the LVOT precluding uniform expansion of a THV.

It remains unclear how this information may translate to clinical practice. Whilst it's generally agreed that calcification adverse affects TAVR outcome, what to do with the calcification remains to be defined. Certainly, calcification debridement catheters remain in a very embryonic stage of development. It's foreseeable that one THV may be better than another type of THV for eccentric calcification although this is pure conjecture at this point in time. Calcification certainly has been correlated with the need for post-dilatation of the THV as well as CVA. Much more research will be needed on the management of aortic calcification in the future.

Optimal Fluoroscopic Projection

One of the important requirements for appropriate placement of the THV along the aortoventricular axis is that of an optimal fluoroscopic angle. If the optimal fluoroscopic angle is not used for the THV placement, no matter how the THV is adjusted along the aotroventricular axis, it is unlikely to lead to a perfect placement of the THV in the aortic annulus achieving a perfect seal. This is the case with both balloon expandable and self -expanding THVs.

One of the greatest benefits of pre-procedural MSCT is the infinitely rotatable aortic annulus. In theory, there are infinite combinations of C-arm angles (any combination of LAO/RAO vs. Cranial/Caudal) that will completely perpendicularize or coaxialize the aortic annulus on fluoroscopy. This is the so-called "line of perpendicularity" [55, 56]. One could conclude if these angles are therefore most accurate as a representation of the true aorto-ventricular axis. However, practically the ideal fluoroscopic angle will allow the three cusps to be seen on plane such that on angiography this can be easily identified. Out of the three such angles, generally only one will be practical given space constraint.

Despite the infinitely maneurability of the MSCT aortic annulus, there is still often discrepancy between the MSCT predicted "perfect implant angle" and the ontable fluoroscopic angle [56, 57]. This is most likely explained by different patient positioning during MSCT and the TAVR procedure. The MSCT guided angle is generally quite accurate and in the absence of rotational angiography and it's generally advocated that an MSCT predicated angle be obtained prior to implant.

MSCT Vasculature Assessment

There is more and more data on the use of MSCT in assessing the peripheral vessels for transfemoral TAVR access [58–60]. This again capitalizes on the reconstruction ability of MSCT, allowing the center-line to be deployed to any vessel of interest to allow a coaxial assessment of the true calibre of vessels. This is the reason why invasive assessment of the aorto-ilio-femoral vessels is becoming less important, particular given its inherent limitation of only being a two dimensional assessment.

MSCT allows calcium to be much better appreciated and this has important implications on transfemoral access. The extent of calcium on the arterial wall, expressed as a percent of arc (e.g. 50 % circumferential calcium), can dictate importantly how "stretchable" a vessel behaves. Most operators would regard a calcium free 6 mm diameter vessel as preferable to a heavily calcified 7 mm diameter vessel. The same information on calcification may also be used for transaortic access such that a calcium free spot can be used for aortic cannulation for transaortic TAVR.

Procedural Planning

Fluoroscopy and Angiography

Conventional fluoroscopy is of course the mainstay of imaging in TAVR. Optimal fluoroscopy is crucial the success at every stage of TAVR. Many centres are now adopting hybrid theatres for TAVR although TAVR can certainly be performed in conventional catheterization laboratories as long as space is amenable to the often multiple team members involved. A hybrid theatre theoretically allows much more liberal space utilization and is often preferable for the surgical team should emergency sternotomy or cardiac surgery is necessary.

Optimal fluoroscopic guidance is absolutely crucial for a perfect THV placement. This is generally applicable to all manners of structural heart interventions [61]. In conventional percutaneous coronary interventions, the placement of the coronary stent requires a mere two-dimensional adjustment along the coronary axis. Structural heart interventions, particular TAVR and left atrial appendage interventions require important appreciations of the three dimensional natures of large devices in the cardiac chambers. Put simply, unlike PCI, there's an added complexity of "depth" involved in the placement of such large prosthesis [61].

To achieve the optimal implant angle in the absence of pre-procedural MSCT, a pigtail catheter should be placed in the right aortic sinus. The first aortogram should be performed at between caudal 5 and 10°. The subsequent adjustment to the fluoroscopic angle will then depend on the relationship of the right coronary sinus with the other sinuses. This is the so-called "***follow the right cusp***" rule [62]. In general, it is almost always possible to achieve an ideal angle with fewer than three aortograms. We generally will not pursue further aortography unless the attained angle is grossly inaccurate due to contrast concerns.

Valve-in-Valve Fluoroscopy

TAVR in failed bioprosthetic surgical valves have been shown to be feasible [63]. There are several unique issues with this demonstrated in multicentre registries. Coronary obstruction, residual gradient particularly in originally undersized surgical bioprotheses, and malposition are the three distinguishing features of TAVR valve in valve. To that end, a special mention needs to be made of the fluoroscopic landmarks of various bioprosthetic valves. Complete coverage of this topic is beyond the scope of this chapter. There are however several important points. First, the nominal valve size translates to significantly different inner diameter and the manufacturer's published measurement should be sought [64, 65]. Second, the fluoroscopic landmark of each surgical bioprosthesis vary widely and several publications have defined the fluoroscopic appearance of the commonly used SAVR, this particularly being the case with stentless valve [65, 66]. The specific design of the surgical valves, particularly stentless valves, needs to be appreciated in order to place the valve in an appropriate location.

Rotational Angiography

Certain proprietary imaging systems allow the use of rotational C-arm angiography. This mimics computed tomography during the procedure. During rotational angiography, to minimize motion artefact, breathing is halted and rapid pacing undertaken. Aortography is then undertaken in the usual manner but the C-arm rotates 180°. Usually 25 mL of contrast diluted to a total volume of 100 mL will be sufficient for satisfactory opacification. The computer algorithm is then able to generate a reconstructed three dimensional aorta allowing the operator to rotate at free will, allowing the optimal projection angle to be achieved.

There is thus far limited data as to the clinical benefit of rotational angiography [67–69]. It appears to improve the probability of attaining the optimal projection angle, even over MSCT predicted angle [55, 67]. One theoretical benefit of obtaining the perfect fluoroscopic projection angle is aortic annulus is perfectly coaxial to the THV and the operator is more likely to place the THV absolutely at the right plane. There is only

limited evidence in balloon expandable THVs in regards to surrogate markers such as incidence of THV malpositioning and PVR [67, 69]. The later concept is much more difficult to demonstrate given THV placement is but one factor for PVR, and it's intuitive that THV sizing is much more important a factor. An undersized THV however perfectly aligned will still produce PVR, a perfectly sized or slightly oversized THV may still lead to no PVR as long as the sealing zone of the THV is in contact with the aortic annulus. Several groups have investigated other use for rotational angiography including aortic annulus sizing for TAVR [70], TAVR follow up assessment [71, 72] as well as femoral calibre assessment [73]. Much more data is needed for this to be validated.

Transesophageal Echocardiography

Traditionally TEE is used routinely in balloon expandable THV for precise placement. This provides additional guidance to pure fluoroscopic landmarks. For patients undergoing THV under conscious sedation, such as self-expanding THVs or patients with contraindication to invasive ventilation such as severe lung disease, TEE is often omitted.

As experience accumulates the necessity for TEE guidance during THV placement per se diminishes. However, the most important contribution for TEE during TAVR is probably the more accurate assessment of PVR it achieves over traditional Sellers [74] quantification of aortic regurgitation. Whilst it's sometimes claimed it's possible to differentiate PVR from central aortic incompetence on angiography, echocardiography is the only definitive means to make such a differentiation.

In situation where TEE is not contraindicated, we generally advocate the use of TEE.

TEE quantifies the often multiple jets in PVR well, evaluates THV function immediately and occasionally diagnoses rare complication such as stuck leaflet (reported in both first and second generation Edwards balloon expandable THV), and allows decision to be made immediately for the need for postdilatation or a second THV. TEE is indispensible in the periprocedural management of PVR immediately after THV placement. An example is an oversized THV based on MSCT measurement, particularly in a heavily calcified aortic valve. TEE assessment will allow accurate quantification of PVR. If the THV is perfectly placed, any degree of PVR may be somewhat unexpected and post dilatation may then be appropriate to ensure adequate expansion of the THV in this calcified aortic apparatus.

3D-TEE may be useful during the index TAVR procedure although data is limited [75, 76].

Post Procedural Imaging

Transthoracic Echocardiography

TTE is the single most important imaging modality for TAVR follow up. MSCT post TAVR are done in some centres for mainly research purposes [77, 78], such as to assess expansion of the stent frame and correlate this with underlying aortic calcification or annular eccentricity. Likewise, fluoroscopy is occasionally undertaken to assess deformity or recoil in balloon expandable THVs for research purposes [79]. Neither MSCT nor fluoroscopy however is routine in current clinical practice.

TTE is mandatory for follow up as would be expected for any valvular prosthesis. SAVRs have been shown to be prone to surgical dehiscence, PVR, or late failure such as stenosis or regurgitation in bioprosthetic valves. Given the lack of long term data for THVs [80], TTE is therefore critical in follow up in this relatively recent bioprosthetic device and track its long-term durability.

Without a doubt however, one of the most important, and unfortunately frequent, complications for TAVR is PVR. Some would content this has been an Achilles heel for THV technology [81]. In conventional SAVR, PVR is extremely rare and almost unacceptable due to the nature of surgical suture anchoring the

SAVR and hostile calcium is debrided to avoid malapposition or dehiscence of the SAVR. In TAVR, calcium is pushed onto the LVOT by the THV itself stent strut achieving a satisfactory seal. Whilst it's generally considered that the THV has sufficient radial strength to prevent significant recoil, the residual calcium occasionally prevents optimal apposition or expansion of the THV leaving gaps in at annular contact points like a doorstop.

In the early days of TAVR, particularly in the early European registries, PVR was poorly captured [82, 83]. Indeed in the early days, feasibility and survival were almost the sole focus. Post implant gradient, indicative of a satisfactory orifice and thus treatment outcome, was sometimes the only reported THV parameter for follow up. It was only in the late 2000s when systemic assessment of PVR in these registry data became more the standard [84, 85].

TAVR-PVR is almost a new pathological entity by virtue of its frequency and severity compared to SAVR [81]. In the PARTNER RCT [86], as in all preceeding registries, the majority of TAVR were associated with a degree of PVR, and more concerning, up to 20 % of those would be classed as moderate to severe [87, 88]. The implication of such frequent moderate PVR was clarified in the 2-year data for PARTNER [86] where even mild PVR was associated with a mortality penalty. Whilst whether mild PVR is really associated with increased mortality continues to cause intense debate [89], most operators would concede at least moderate PVR is associated with increased mortality.

The biggest challenge to PVR assessment in TAVR is the unique signature of TAVR-PVR unlike most previous SAVR PVR, and thus a lack of standardized or validated quantification. Until the advent of the VARC (Valve Academic Research Consortium) definition of mild, moderate and severe PVR, there was little standardized classification of PVR. Whilst an expert consensus document, there is as yet no formal validation of VARC or VARC2 criteria [90, 91], partly confounded by the lack of a definitive gold standard assessment of PVR.

TAVR-PVR often manifests as multiple jets, possibly of varying significance. This creates difficulty both in obtaining satisfactory images and interpretation.

Whilst the VARC definition (Tables 14.1 and 14.2) is the best tool currently available, there is no gold standard for PVR classification. Indeed, as an entity the VARC classification has yet to be tested and validated and currently is no more than an expert consensus. Until such time that PVR can be benchmarked against a gold standard much more research into its interpretation is needed. MRI appears to be an attractive method as it's volumetric and takes into the totally of the regurgitant volume which presumably is the important index causing left ventricular adverse effect. Recent MRI data [92] suggested that quantification of PVR with echocardiography, at least benchmarked against MRI, may underestimate the severity.

The strength of the VARC definition may be that it's generally inclusive and acknowledges the fact that not one single parameter is sufficient for determining the severity of PVR. Important new parameters, such as the extent of PVR across the circumference of the annulus, expressed as a percentage, to the use of RVOT/LVOT regurgitant fraction, are incorporated to traditional Doppler colour flow as width of jet, and extend of jet into the ventricle.

Given the lack of standardization in previous reports, it remains to be defined the natural history of PVR in TAVR. There is likely inter-observer variability in non-core lab reported PVR. It's unclear whether PVR generally worsens over time [93], what medication may retard its progress [89], or whether it tends to improve as the previously hypertrophied left ventricle remodels after the aortic stenosis is relieved.

The temporal trend for PVR is important to guide whether TAVR PVR needs to be percutaneously treated or whether medical therapy may suffice. There have been various reports of percutaneous delivery of off label vascular plug into severe PVR to seal of defects between the THV and aortic annulus [94–97]. The observational data remains limited but generally demonstrated an improvement in PVR severity.

Table 14.1 VARC definitions of PVR. VARC prosthetic aortic valve regurgitation criteria (central and paravalvular)

Parameter	Mild	Moderate	Severe
Valve structure and motion			
Mechanical or bioprosthetic	Usually normal	Usually abnormal	Usually abnormal
Structural parameters			
Left ventricular size	Normal	Normal/mildly dilated	Dilated
Doppler parameters (qualitative or semi-quantitative)			
Jet width in central jets (% LVO diameter): color[a]	Narrow (≤25 %)	Intermediate (26–64 %)	Large (≥65 %)
Jet density: CW Doppler	Incomplete or faint	Dense	Dense
Jet deceleration rate (PHT, ms): CW Doppler[b]	Slow (>500)	Variable (200–500)	Steep (<200)
LV outflow vs. pulmonary flow: PW Doppler	Slightly increased	Intermediate	Greatly increased
Diastolic flow reversal in the descending aorta:			
PW Doppler	Absent or brief early diastolic	Intermediate	Prominent, holodiastolic
Circumferential extent of paraprosthetic AR (%)[c]	<10	10–20	>20
Doppler parameters (quantitative)			
Regurgitant volume (mL/beat)	<30	30–59	>60
Regurgitant fraction (%)	<30	30–50	>50

AR aortic regurgitation, *CW* continuous wave, *LVO* left ventricular outflow, *PW* pulsed wave
[a]Parameter applicable to central jets and is less accurate in eccentric jets
[b]Influenced by left ventricular compliance
[c]For paravalvular aortic regurgitation

Table 14.2 VARC-2 definitions for PVR

	Prosthetic aortic valve regurgitation		
	Mild	Moderate	Severe
Semi-quantitative parameters			
Diastolic flow reversal in the descending aorta – PW	Absent or brief early diastolic	Intermediate	Prominent, holodiastolic
Circumferential extent of prosthetic valve paravalvular regurgitation (%)	<10 %	10–29 %	≥30 %
Quantitative parameters			
Regurgitant volume (ml/beat)	<30 ml	30–59 ml	≥60 ml
Regurgitant fraction (%)	<30 %	30–49 %	≥50 %
EROA (cm^2)	0.10 cm^2	0.10–0.29 cm^2	≥0.30 cm^2

Case Presentations and Imaging Considerations

Case 1: Aortic Stenosis Echocardiography

Figure 14.1a, b show TTE with good image quality can provide important and accurate information of aortic valvar apparatus including LVOT diameter, sinus height, sinotubular junction dimension and degree of calcification. Figure 14.1c shows critical aortic stenosis with a transaortic Doppler velocity of 7.5 m/s. In Fig. 14.1d, e, accurate calculation of aortic valve area relies on accurate determination of LVOT diameter; calcification in the RCC as reflected on the parasternal short axis as well. Whilst TTE with good image quality can provide important information on calcium burden, MSCT remains the gold standard.

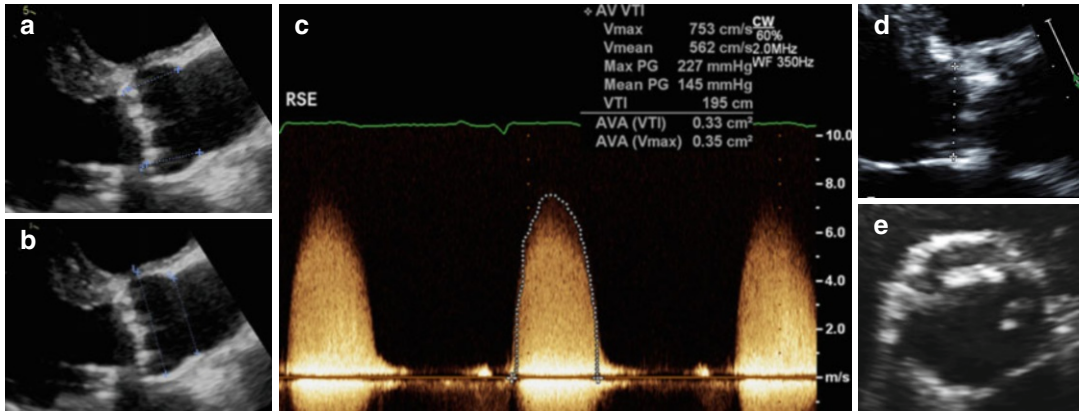

Fig. 14.1 Aortic stenosis echocardiography. (**a**) Sinotubular height, (**b**) annular and sinotubular dimensions, (**c**) CW of the aortic valve, (**d**) LVOT measurement, and (**e**) short axis of the aortic valve

Case 2: Dobutamine Stress Echocardiography

In aortic stenosis with impaired left ventricular systolic function, the transaortic gradient may be underestimated due to poor ventricular function or that the aortic stenosis is indeed less than severe. In this case, the use of dobutamine demonstrated contractile reserve (23 % increase in SV) as well as moderate AS only with the increased ventricular function pushing open the aortic leaflets better (Fig. 14.2).

Case 3: TTE vs. MSCT

Figure 14.3 shows the spatial resolution of MSCT is far superior to TTE. This is particular obvious in calcium quantification. Additionally, the ovoid nature of the aortic annulus is well appreciated in MSCT (Fig. 14.3e vs. Fig. 14.3c). Note suggestion of in the aortomitral continuity well demonstrated on MSCT (Fig. 14.3a vs. Fig. 14.3d). Calcium is likely an important area of research for the TAVR technology.

Case 4: 3mensio Workup

Commercially available 3D reconstruction computer program, such as this 3mensio example (3mensio®, Pie Medical Imaging BV, Netherlands) shown in Fig. 14.4, vastly improves annular plane determination, thus allowing coaxial assessment of the aortic valvular structure. Unlike traditional method without 3D reconstruction, which required many steps of adjustment focusing on each aortic sinus, 3D reconstruction allows the determination of a centerline (yellow line in Fig. 14.4a, b). Once this line is achieved, in Fig. 14.4c, the tangential plane, the cross hair can be spun around the annulus, ensuring that this particular plane transects the bottom of each sinus (Fig. 14.4a, b), the so-called "spinning the line" technique. Once this is achieved, in Fig. 14.4d, a favorable angle for the operators can be selected for implantation angle, to ensure coaxial placement of the aortic root on fluoroscopy.

Case 5: THV Sizing Dilemma

In Fig. 14.5a, MSCT reconstruction yielded an aortic annulus area of 4.13 mm^2, with moderate eccentricity but a focal calcium, extending into a severe aorto-mitral continuity calcification. TTE yielded an LVOT diameter of 22 mm. Borderline for a 23 mm Edwards SAPIEN THV but given the calcification this THV was chosen. In Fig. 14.5b, 23 mm THV placed with severe focal paravalvular regurgitation, likely due to calcification. A second THV with further postdilatation did not significant mitigate PVR. A 10×5 mm vascular plug (arrow) was placed reducing PVR to one fourth (Fig. 14.5d) from four fourths (Fig. 14.5c).

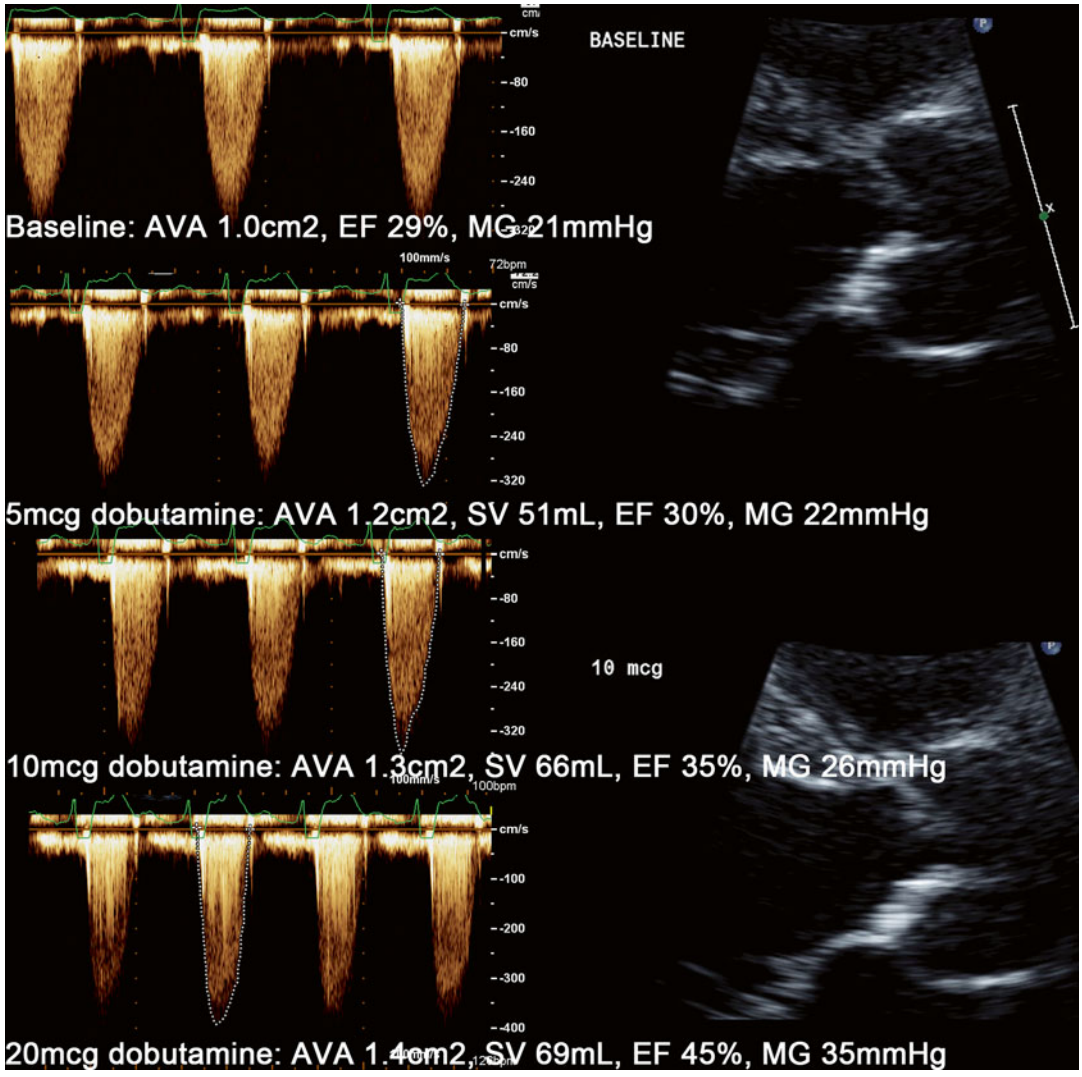

Fig. 14.2 Dobutamine stress echocardiography. From top to bottom; at baseline, 5 mcg, 10 mcg, and 20 mcg of dobutamine. Note how the stroke volume, gradient, and aortic valve area are increasing. Note how the aortic valve on 2D echocardiography appears to be opening further with increased flow

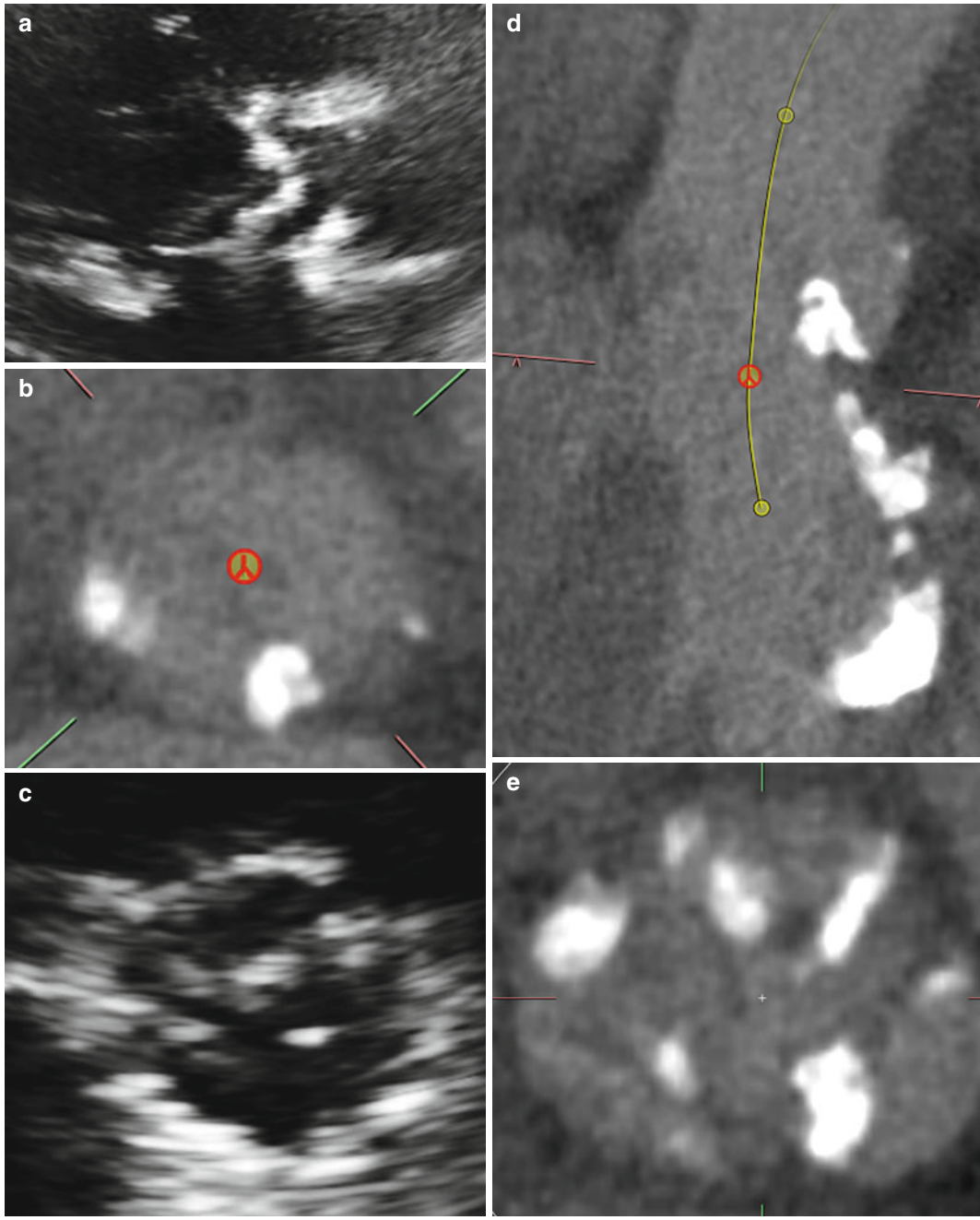

Fig. 14.3 (**a**–**e**) TTE vs. MSCT of the aortic valve apparatus. (**a**) and (**c**) TTE, and (**b**), (**d**), (**e**) MSCT

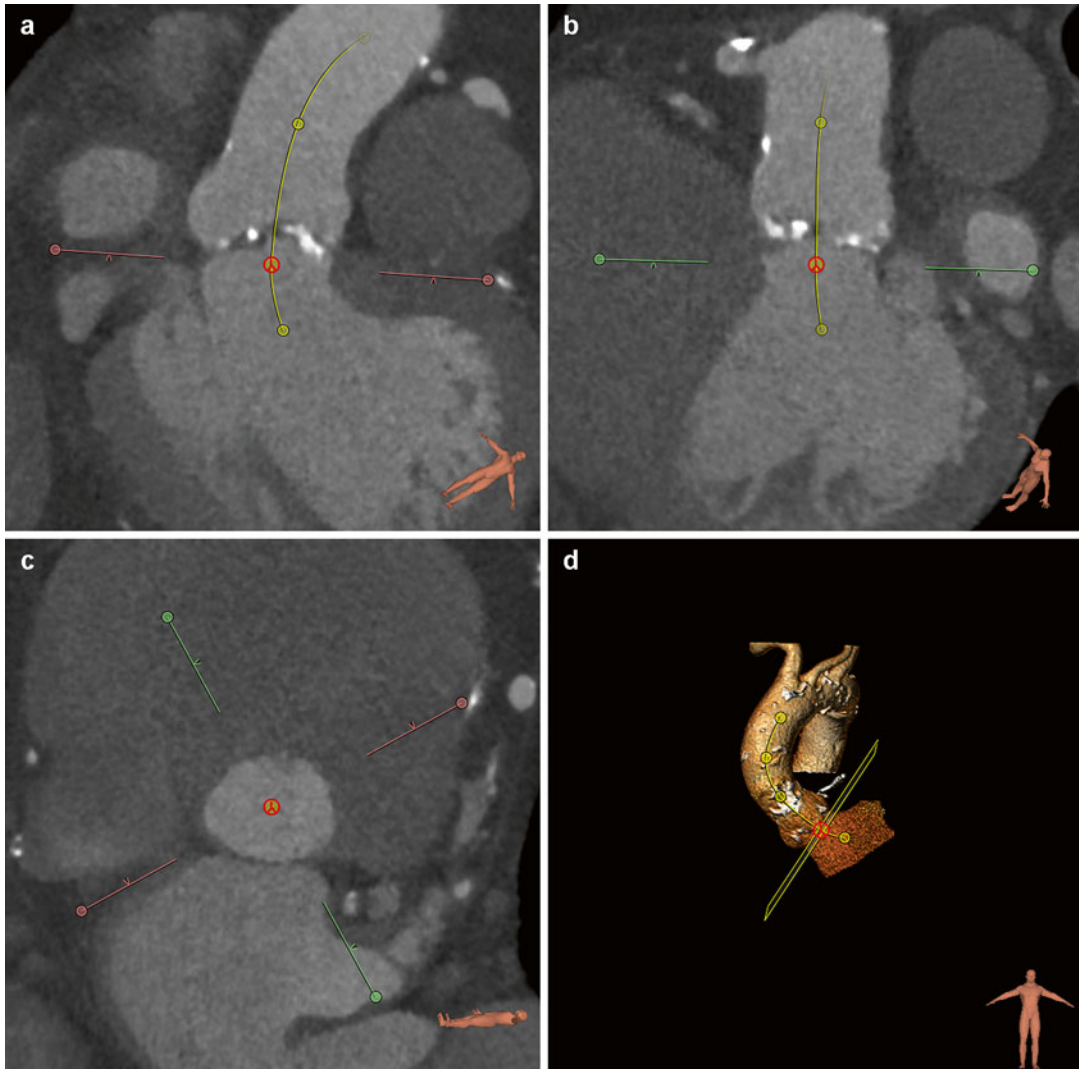

Fig. 14.4 (**a**–**d**) 3mensio workup for identifying and measuring the aortic annulus

Case 6: MSCT Pitfalls

Figure 14.6 shows examples of poorly performed MSCT. Figure 14.6a shows contrast poorly captured in left ventricular outflow tract and most contrast density in descending aorta (Fig. 14.6c). To obtain an accurate aortic annulus measurement sufficient contrast is needed in the left ventricle. In Fig. 14.6d the double shadow in the outline of the aorta and aortic annulus, likely to be patient movement artifact. This significantly compromises the accuracy of annulus measurement.

Case 7: Bicuspid Aortic Valve

A 68 year old with previous coronary bypass grafts adherent to his sternum has now developed severe symptomatic bicuspid aortic stenosis. Figure 14.7a shows bicuspid aortic valve with moderate leaflet tip calcification – the presence

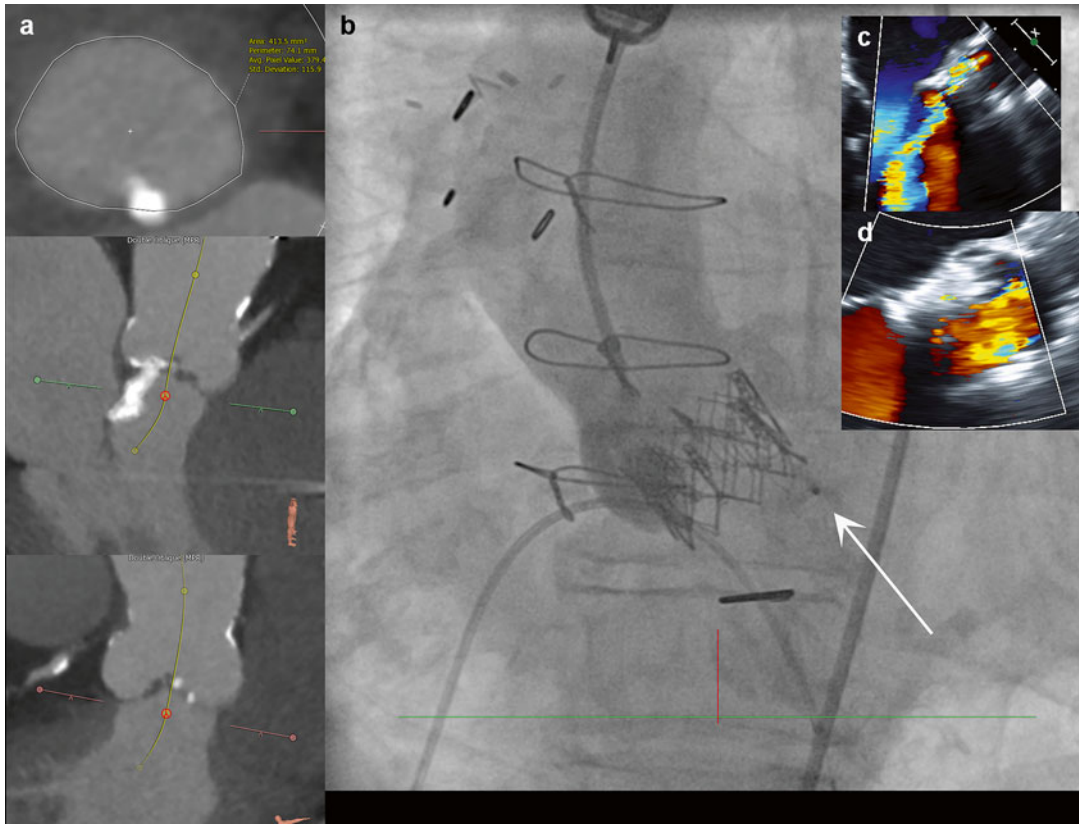

Fig. 14.5 (**a**–**d**) THV sizing dilemma with PVR and need for a vascular plug

of calcification is important to ensure satisfactory anchoring of THV. Figure 14.7b shows MSCT annular determination (area 5.41 cm^2; perimeter 84.1 mm). Figure 14.7c–e show difficult to determine annular plane given bicuspid nature, MSCT demonstrating no prohibitive sinotubular junction or aortic root dilatation. Figure 14.7f shows successful transapical implant of a 29 mm Edwards Sapien XT ® THV. Figure 14.7g shows D4 post THV TTE showing trivial paravalvular regurgitation (blue jet).

Case 8: Vasculature Reconstruction

Figure 14.8a shows conventional angiography of ilio-femoral axis, with a marker pigtail with 10 mm interval markers. Figure 14.8b shows MSCT 3D rendered image of vascularture providing information of tortuosity and calcification not attainable from angiography. Figure 14.8c shows proprietary program such as 3mension providing phantom "straightened" artery and caliber of a 18Fr sheath (see yellow straight line).

Case 9: Edwards and CoreValve Fluoroscopy

Edwards (upper panel) and CoreValve (lower panel) fluoroscopy revealing excellent, acceptable, and poor implantation position (left, middle, and right, respectively) (Fig. 14.9).

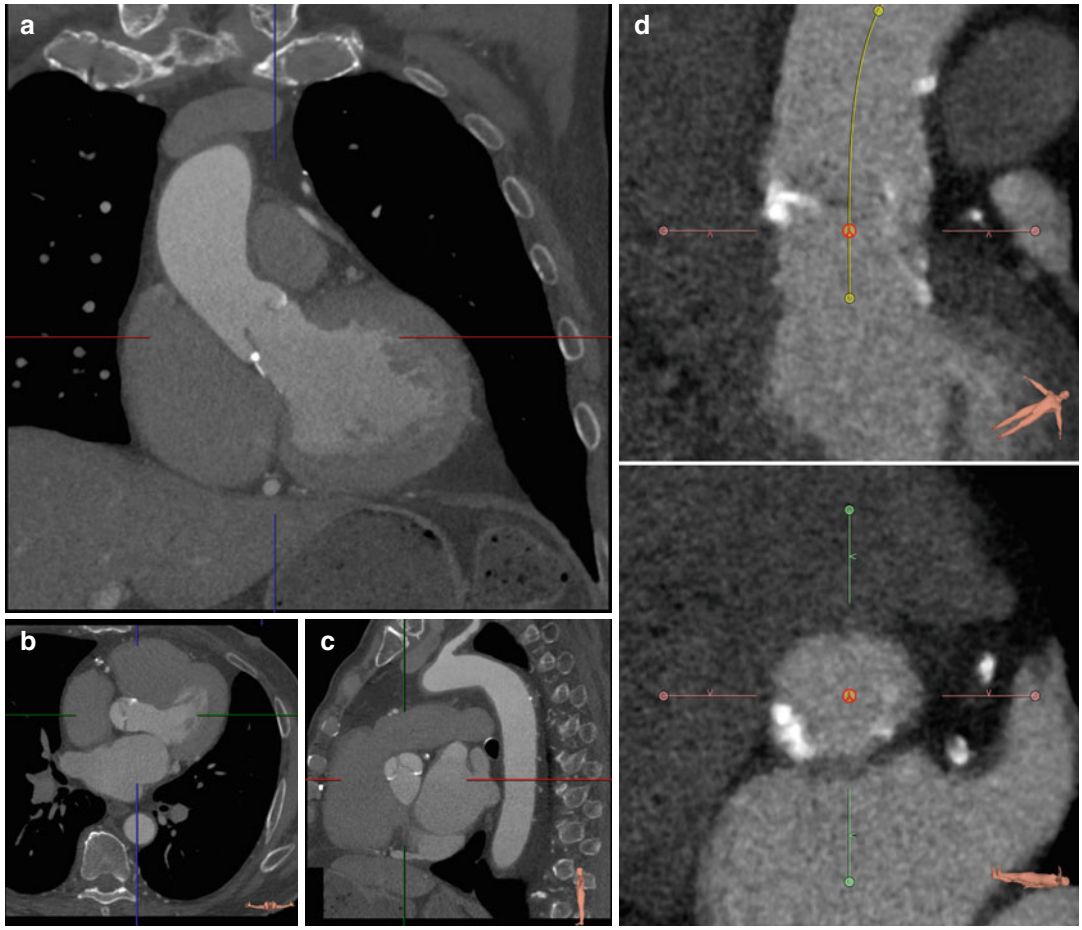

Fig. 14.6 (**a**–**d**) MSCT pitfalls with poor annular contrast opacification on MSCT

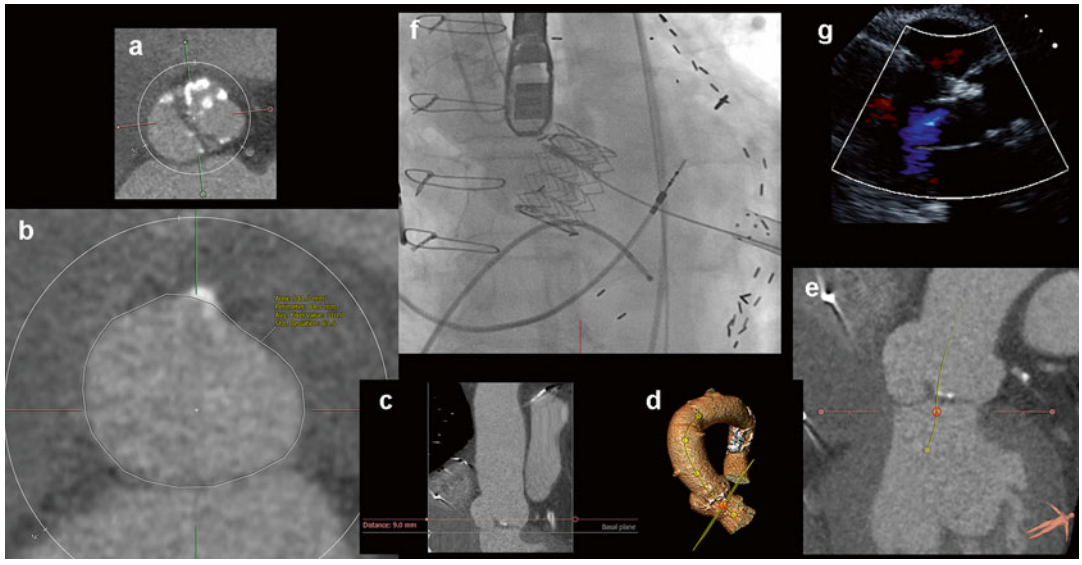

Fig. 14.7 (**a**–**g**) Bicuspid aortic valve (**a**–**e**) 3mensio, (**f**) TAVR implantation, and (**g**) echocardiography

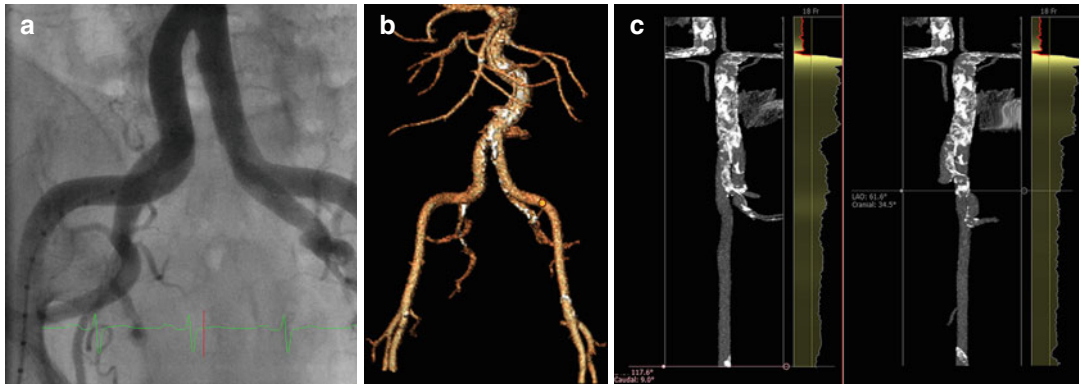

Fig. 14.8 (**a**–**c**) Vasculature reconstruction with 3 mensio

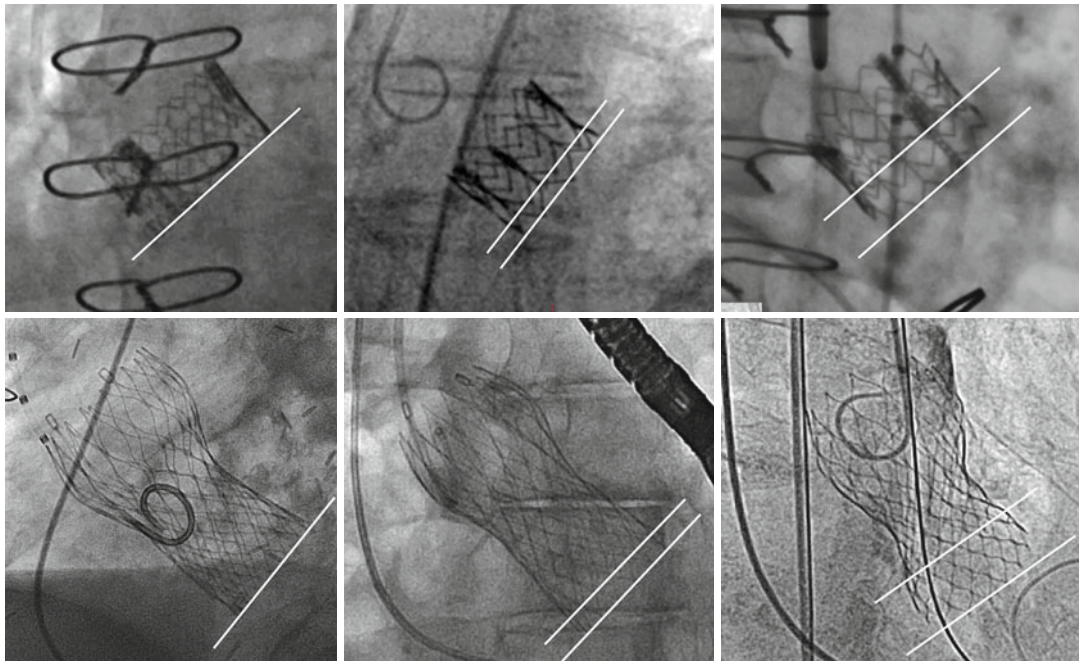

Fig. 14.9 Edwards (*top panels*) and CoreValve (*bottom panels*) fluoroscopy revealing excellent (*left panels*), adequate (*middle panels*), and poor (*right panels*)

Future Perspective

- Magnetic resonance imaging – thus far there is little data on the use of MRI in TAVR planning. There is some MRI data on the aortic root dynamics on systole compared to diastole. The most promising data may be the volumetric assessment of the regurgitant flow possible with MRI [92].
- Paravalvular regurgitation – whilst second generation THVs such as Lotus (SADRA) or Edwards 3 seem to have significant reduced the incidence of moderate to severe PVR, much research is still needed in this area. The temporal pattern to PVR, the individual patient factors contributing to an adverse outcome, and the role of medications in treating PVR are but some of the areas to be defined. A most

pressing area is standardization and validation of PVR. Quantification of PVR remains challenging, and despite the expert consensus of VARC2 definition, the later still needs to be formally validated. Mitigation of PVR is an important prerequisite for the extending the TAVR to a lower risk group of patients.

- MSCT – better understanding of calcification – how best to decide THV choice based on calcium

Conclusion

TAVR has transformed the management of aortic stenosis. Two large RCTs comparing two different THV platform to SAVR and many ongoing registries have demonstrated the importance of this technology and in the foreseeable future, superiority to SAVR, particularly in intermediate to high risk subset. Without doubt with improvement in each iteration of the technology it is likely TAVR will one day become the dominant treatment option for aortic stenosis. Concurrent with this TAVR development has been the enormous improvement in understanding of the complex three dimensional aortic valve apparatus through advancement in imaging modalties particularly through the use of three dimensional imaging such as MSCT. The same lessons learnt from TAVR are now extending to other structural heart disease interventions such as left atrial appendage closure devices. It would not be an exaggeration to claim that TAVR is now equivalent if not superior to SAVR in high risk patients mostly due to mitigation of issues related to imaging techniques and THV design and size algorithm over the years. Imaging, particularly MSCT, will likely play a pivotal role in enhancing THV design and probably will contribute to individualized THV choice in the future based on specific aortic annulus size, calcification, aorto-ventricular angulation and other as yet to be defined important parameters. It therefore behoves the interventional cardiologist and cardiac surgeon to enhance their imaging knowledge through close collaboration with the imaging specialist in the heart team. The issues and techniques highlighted in this chapter will surely evolve, be improved and hopefully in doing so this will propel this disruptive technology to be the forefront of aortic stenosis treatment.

References

1. Adams DH, Popma JJ, Reardon MJ. Transcatheter aortic-valve replacement with a self-expanding prosthesis. N Engl J Med. 2014;371(10):967–8.
2. Smith CR, et al. Transcatheter versus surgical aortic-valve replacement in high-risk patients. N Engl J Med. 2011;364(23):2187–98.
3. Popma JJ, et al. Transcatheter aortic valve replacement using a self-expanding bioprosthesis in patients with severe aortic stenosis at extreme risk for surgery. J Am Coll Cardiol. 2014;63(19):1972–81.
4. Leon MB, et al. Transcatheter aortic-valve implantation for aortic stenosis in patients who cannot undergo surgery. N Engl J Med. 2010;363(17):1597–607.
5. Cribier A, et al. Percutaneous transcatheter implantation of an aortic valve prosthesis for calcific aortic stenosis: first human case description. Circulation. 2002;106(24):3006–8.
6. Turina J, et al. Spontaneous course of aortic valve disease. Eur Heart J. 1987;8(5):471–83.
7. Joint Task Force on the Management of Valvular Heart Disease of the European Society of Cardiology, et al. Guidelines on the management of valvular heart disease (version 2012). Eur Heart J. 2012;33(19):2451–96.
8. Nishimura RA, et al. 2014 AHA/ACC guideline for the management of patients with valvular heart disease: a report of the American College of Cardiology/American Heart Association Task Force on practice guidelines. Circulation. 2014;129(23):e521–643.
9. Eleid MF, et al. Flow-gradient patterns in severe aortic stenosis with preserved ejection fraction: clinical characteristics and predictors of survival. Circulation. 2013;128(16):1781–9.
10. Mohty D, et al. Outcome and impact of surgery in paradoxical low-flow, low-gradient severe aortic stenosis and preserved left ventricular ejection fraction: a cardiac catheterization study. Circulation. 2013;128(11 Suppl 1):S235–42.
11. Hachicha Z, et al. Paradoxical low-flow, low-gradient severe aortic stenosis despite preserved ejection fraction is associated with higher afterload and reduced survival. Circulation. 2007;115(22):2856–64.
12. Clavel MA, et al. The complex nature of discordant severe calcified aortic valve disease grading: new insights from combined Doppler echocardiographic and computed tomographic study. J Am Coll Cardiol. 2013;62(24):2329–38.

13. Clavel MA, et al. Impact of aortic valve calcification, as measured by MDCT, on survival in patients with aortic stenosis: results of an international registry study. J Am Coll Cardiol. 2014;64(12):1202–13.
14. O'Sullivan CJ, et al. Clinical outcomes of patients with low-flow, low-gradient, severe aortic stenosis and either preserved or reduced ejection fraction undergoing transcatheter aortic valve implantation. Eur Heart J. 2013;34(44):3437–50.
15. Herrmann HC, et al. Predictors of mortality and outcomes of therapy in low-flow severe aortic stenosis: a Placement of Aortic Transcatheter Valves (PARTNER) trial analysis. Circulation. 2013;127(23):2316–26.
16. Le Ven F, et al. Impact of low flow on the outcome of high-risk patients undergoing transcatheter aortic valve replacement. J Am Coll Cardiol. 2013;62(9): 782–8.
17. Wendt D, et al. Transapical transcatheter aortic valve for severe aortic regurgitation: expanding the limits. JACC Cardiovasc Interv. 2014;7(10):1159–67.
18. Testa L, et al. CoreValve implantation for severe aortic regurgitation: a multicentre registry. EuroIntervention. 2014;10(6):739–45.
19. Roy DA, et al. Transcatheter aortic valve implantation for pure severe native aortic valve regurgitation. J Am Coll Cardiol. 2013;61(15):1577–84.
20. Roy D, Sharma R, Brecker SJ. Native aortic valve regurgitation: transcatheter therapeutic options. EuroIntervention. 2013;9(Suppl):S55–62.
21. Pasupati S, et al. Transcatheter solution for pure aortic insufficiency. JACC Cardiovasc Imaging. 2014;7(3): 315–8.
22. Elmariah S, et al. Outcomes of transcatheter and surgical aortic valve replacement in high-risk patients with aortic stenosis and left ventricular dysfunction: results from the Placement of Aortic Transcatheter Valves (PARTNER) trial (cohort A). Circ Cardiovasc Interv. 2013;6(6):604–14.
23. Sannino A, et al. Increased mortality after transcatheter aortic valve implantation (TAVI) in patients with severe aortic stenosis and low ejection fraction: a meta-analysis of 6898 patients. Int J Cardiol. 2014;176(1): 32–9.
24. Elhmidi Y, et al. Transcatheter aortic valve implantation in patients with LV dysfunction: impact on mortality and predictors of LV function recovery. J Invasive Cardiol. 2014;26(3):132–8.
25. Koos R, et al. Impact of aortic valve calcification severity and impaired left ventricular function on 3-year results of patients undergoing transcatheter aortic valve replacement. Eur Radiol. 2013;23(12):3253–61.
26. Fraccaro C, et al. Transcatheter aortic valve implantation in patients with severe left ventricular dysfunction: immediate and mid-term results, a multicenter study. Circ Cardiovasc Interv. 2012;5(2):253–60.
27. Lucon A, et al. Prognostic implications of pulmonary hypertension in patients with severe aortic stenosis undergoing transcatheter aortic valve implantation: study from the FRANCE 2 registry. Circ Cardiovasc Interv. 2014;7(2):240–7.
28. Durmaz T, et al. The effect of transcatheter aortic valve implantation on pulmonary hypertension. Echocardiography. 2014.
29. Roselli EE, et al. Pulmonary hypertension is associated with worse early and late outcomes after aortic valve replacement: implications for transcatheter aortic valve replacement. J Thorac Cardiovasc Surg. 2012;144(5):1067–74 e2.
30. Sannino A, et al. Meta-analysis of mortality outcomes and mitral regurgitation evolution in 4,839 patients having transcatheter aortic valve implantation for severe aortic stenosis. Am J Cardiol. 2014;114(6): 875–82.
31. Khawaja MZ, et al. Impact of preprocedural mitral regurgitation upon mortality after transcatheter aortic valve implantation (TAVI) for severe aortic stenosis. Heart. 2014;100(22):1799–803.
32. Barbanti M, et al. Impact of preoperative moderate/severe mitral regurgitation on 2-year outcome after transcatheter and surgical aortic valve replacement: insight from the Placement of Aortic Transcatheter Valve (PARTNER) Trial Cohort A. Circulation. 2013;128(25):2776–84.
33. Bedogni F, et al. Interplay between mitral regurgitation and transcatheter aortic valve replacement with the CoreValve revalving system: a multicenter registry. Circulation. 2013;128(19):2145–53.
34. Madder RD, et al. The first report of transcatheter aortic valve implantation and percutaneous mitral valve repair in the same patient. JACC Cardiovasc Interv. 2011;4(7):824.
35. Altiok E, et al. Comparison of two-dimensional and three-dimensional imaging techniques for measurement of aortic annulus diameters before transcatheter aortic valve implantation. Heart. 2011;97(19): 1578–84.
36. Husser O, et al. Impact of three-dimensional transesophageal echocardiography on prosthesis sizing for transcatheter aortic valve implantation. Catheter Cardiovasc Interv. 2012;80(6):956–63.
37. Khalique OK, et al. Aortic annular sizing using a novel 3-dimensional echocardiographic method: use and comparison with cardiac computed tomography. Circ Cardiovasc Imaging. 2014;7(1):155–63.
38. Jilaihawi H, et al. Aortic annular sizing for transcatheter aortic valve replacement using cross-sectional 3-dimensional transesophageal echocardiography. J Am Coll Cardiol. 2013;61(9):908–16.
39. Masson JB, et al. Impact of coronary artery disease on outcomes after transcatheter aortic valve implantation. Catheter Cardiovasc Interv. 2010;76(2):165–73.
40. Dewey TM, et al. Effect of concomitant coronary artery disease on procedural and late outcomes of transcatheter aortic valve implantation. Ann Thorac Surg. 2010;89(3):758–67; discussion 767.
41. Wenaweser P, et al. Impact of coronary artery disease and percutaneous coronary intervention on outcomes in patients with severe aortic stenosis undergoing transcatheter aortic valve implantation. EuroIntervention. 2011;7(5):541–8.

42. Khawaja MZ, et al. The effect of coronary artery disease defined by quantitative coronary angiography and SYNTAX score upon outcome after transcatheter aortic valve implantation (TAVI) using the Edwards bioprosthesis. EuroIntervention. 2014.
43. Achenbach S, et al. SCCT expert consensus document on computed tomography imaging before transcatheter aortic valve implantation (TAVI)/transcatheter aortic valve replacement (TAVR). J Cardiovasc Comput Tomogr. 2012;6(6):366–80.
44. Piazza N, et al. Anatomy of the aortic valvar complex and its implications for transcatheter implantation of the aortic valve. Circ Cardiovasc Interv. 2008;1(1):74–81.
45. Ng AC, et al. Comparison of aortic root dimensions and geometries before and after transcatheter aortic valve implantation by 2- and 3-dimensional transesophageal echocardiography and multislice computed tomography. Circ Cardiovasc Imaging. 2010;3(1):94–102.
46. Schmidkonz C, et al. Interobserver variability of CT angiography for evaluation of aortic annulus dimensions prior to transcatheter aortic valve implantation (TAVI). Eur J Radiol. 2014;83(9):1672–8.
47. Willson AB, et al. 3-dimensional aortic annular assessment by multidetector computed tomography predicts moderate or severe paravalvular regurgitation after transcatheter aortic valve replacement: a multicenter retrospective analysis. J Am Coll Cardiol. 2012;59(14):1287–94.
48. Jilaihawi H, et al. Cross-sectional computed tomographic assessment improves accuracy of aortic annular sizing for transcatheter aortic valve replacement and reduces the incidence of paravalvular aortic regurgitation. J Am Coll Cardiol. 2012;59(14):1275–86.
49. Binder RK, et al. The impact of integration of a multidetector computed tomography annulus area sizing algorithm on outcomes of transcatheter aortic valve replacement: a prospective, multicenter, controlled trial. J Am Coll Cardiol. 2013;62(5):431–8.
50. Kasel AM, et al. Standardized imaging for aortic annular sizing: implications for transcatheter valve selection. JACC Cardiovasc Imaging. 2013;6(2):249–62.
51. Gurvitch R, et al. Aortic annulus diameter determination by multidetector computed tomography: reproducibility, applicability, and implications for transcatheter aortic valve implantation. JACC Cardiovasc Interv. 2011;4(11):1235–45.
52. Koos R, et al. Association of aortic valve calcification severity with the degree of aortic regurgitation after transcatheter aortic valve implantation. Int J Cardiol. 2011;150(2):142–5.
53. John D, et al. Correlation of device landing zone calcification and acute procedural success in patients undergoing transcatheter aortic valve implantations with the self-expanding CoreValve prosthesis. JACC Cardiovasc Interv. 2010;3(2):233–43.
54. Ewe SH, et al. Location and severity of aortic valve calcium and implications for aortic regurgitation after transcatheter aortic valve implantation. Am J Cardiol. 2011;108(10):1470–7.
55. Binder RK, et al. Prediction of optimal deployment projection for transcatheter aortic valve replacement: angiographic 3-dimensional reconstruction of the aortic root versus multidetector computed tomography. Circ Cardiovasc Interv. 2012;5(2):247–52.
56. Gurvitch R, et al. Multislice computed tomography for prediction of optimal angiographic deployment projections during transcatheter aortic valve implantation. JACC Cardiovasc Interv. 2010;3(11):1157–65.
57. Arnold M, et al. A method to determine suitable fluoroscopic projections for transcatheter aortic valve implantation by computed tomography. J Cardiovasc Comput Tomogr. 2012;6(6):422–8.
58. Krishnaswamy A, et al. Predicting vascular complications during transfemoral transcatheter aortic valve replacement using computed tomography: a novel area-based index. Catheter Cardiovasc Interv. 2014;84(5):844–51.
59. Toggweiler S, et al. Percutaneous aortic valve replacement: vascular outcomes with a fully percutaneous procedure. J Am Coll Cardiol. 2012;59(2):113–8.
60. Hayashida K, et al. Transfemoral aortic valve implantation new criteria to predict vascular complications. JACC Cardiovasc Interv. 2011;4(8):851–8.
61. Theriault-Lauzier P, et al. Fluoroscopic anatomy of left-sided heart structures for transcatheter interventions: insight from multislice computed tomography. JACC Cardiovasc Interv. 2014;7(9):947–57.
62. Kasel AM, et al. Fluoroscopy-guided aortic root imaging for TAVR: "follow the right cusp" rule. JACC Cardiovasc Imaging. 2013;6(2):274–5.
63. Dvir D, et al. Transcatheter aortic valve implantation in failed bioprosthetic surgical valves. JAMA. 2014;312(2):162–70.
64. Gurvitch R, et al. Transcatheter valve-in-valve implantation for failed surgical bioprosthetic valves. J Am Coll Cardiol. 2011;58(21):2196–209.
65. Bapat V, et al. A guide to fluoroscopic identification and design of bioprosthetic valves: a reference for valve-in-valve procedure. Catheter Cardiovasc Interv. 2013;81(5):853–61.
66. Bapat VN, et al. Fluoroscopic guide to an ideal implant position for Sapien XT and CoreValve during a valve-in-valve procedure. JACC Cardiovasc Interv. 2013;6(11):1186–94.
67. Poon KK, et al. Impact of optimising fluoroscopic implant angles on paravalvular regurgitation in transcatheter aortic valve replacements – utility of three-dimensional rotational angiography. EuroIntervention. 2012;8(5):538–45.
68. Samim M, et al. Three-dimensional aortic root reconstruction derived from rotational angiography for transcatheter balloon-expandable aortic valve implantation guidance. Int J Cardiol. 2014;176(3):1318–20.
69. Samim M, et al. Automated 3D analysis of preprocedural MDCT to predict annulus plane angulation and C-arm positioning: benefit on procedural outcome in patients referred for TAVR. JACC Cardiovasc Imaging. 2013;6(2):238–48.

70. Lehmkuhl LH, et al. Comparison of aortic root measurements in patients undergoing transapical aortic valve implantation (TA-AVI) using three-dimensional rotational angiography (3D-RA) and multislice computed tomography (MSCT): differences and variability. Int J Cardiovasc Imaging. 2013;29(2):417–24.
71. Incani A, et al. Normal functioning of a constrained CoreValve with DynaCT imaging demonstrating incomplete stent frame expansion. Int J Cardiol. 2013; 163(1):e9–10.
72. Schultz CJ, et al. Rotational angiography with motion compensation: first-in-man use for the 3D evaluation of transcatheter valve prostheses. EuroIntervention. 2014.
73. Crowhurst JA, et al. Using DynaCT for the assessment of ilio-femoral arterial calibre, calcification and tortuosity index in patients selected for trans-catheter aortic valve replacement. Int J Cardiovasc Imaging. 2013;29(7):1537–45.
74. Sellers RD, et al. Left retrograde cardioangiography in acquired cardiac disease: technic, indications and interpretations in 700 cases. Am J Cardiol. 1964;14: 437–47.
75. Shibayama K, et al. Effect of transcatheter aortic valve replacement on the mitral valve apparatus and mitral regurgitation: real-time three-dimensional transesophageal echocardiography study. Circ Cardiovasc Imaging. 2014;7(2):344–51.
76. Smith LA, et al. Real-time three-dimensional transesophageal echocardiography adds value to transcatheter aortic valve implantation. J Am Soc Echocardiogr. 2013;26(4):359–69.
77. Willson AB, et al. Structural integrity of balloon-expandable stents after transcatheter aortic valve replacement: assessment by multidetector computed tomography. JACC Cardiovasc Interv. 2012;5(5): 525–32.
78. Binder RK, et al. Impact of post-implant SAPIEN XT geometry and position on conduction disturbances, hemodynamic performance, and paravalvular regurgitation. JACC Cardiovasc Interv. 2013;6(5):462–8.
79. Meredith Am IT, et al. Transcatheter aortic valve replacement for severe symptomatic aortic stenosis using a repositionable valve system: 30-day primary endpoint results from the REPRISE II study. J Am Coll Cardiol. 2014;64(13):1339–48.
80. Sinning JM, et al. CoreValve degeneration with severe transvalvular aortic regurgitation treated with valve-in-valve implantation. JACC Cardiovasc Interv. 2014;7(7):e71–2.
81. Genereux P, et al. Paravalvular leak after transcatheter aortic valve replacement: the new Achilles' heel? A comprehensive review of the literature. J Am Coll Cardiol. 2013;61(11):1125–36.
82. Grube E, et al. Percutaneous implantation of the CoreValve self-expanding valve prosthesis in high-risk patients with aortic valve disease: the Siegburg first-in-man study. Circulation. 2006;114(15): 1616–24.
83. Bleiziffer S, et al. Results of percutaneous and transapical transcatheter aortic valve implantation performed by a surgical team. Eur J Cardiothorac Surg. 2009;35(4):615–20; discussion 620–1.
84. Ussia GP, et al. Transcatheter aortic valve implantation: 3-year outcomes of self-expanding CoreValve prosthesis. Eur Heart J. 2012;33(8):969–76.
85. Gurvitch R, et al. Transcatheter aortic valve implantation: durability of clinical and hemodynamic outcomes beyond 3 years in a large patient cohort. Circulation. 2010;122(13):1319–27.
86. Kodali SK, et al. Two-year outcomes after transcatheter or surgical aortic-valve replacement. N Engl J Med. 2012;366(18):1686–95.
87. Abdel-Wahab M, et al. Predictors of 1-year mortality in patients with aortic regurgitation after transcatheter aortic valve implantation: an analysis from the multicentre German TAVI registry. Heart. 2014;100(16): 1250–6.
88. Abdel-Wahab M, et al. Aortic regurgitation after transcatheter aortic valve implantation with balloon- and self-expandable prostheses: a pooled analysis from a 2-center experience. JACC Cardiovasc Interv. 2014;7(3):284–92.
89. Kodali S, et al. Paravalvular regurgitation after transcatheter aortic valve replacement with the Edwards Sapien valve in the PARTNER trial: characterizing patients and impact on outcomes. Eur Heart J. 2015; 36(7):449–56.
90. Leon MB, et al. Standardized endpoint definitions for transcatheter aortic valve implantation clinical trials: a consensus report from the valve academic research consortium. J Am Coll Cardiol. 2011;57(3):253–69.
91. Kappetein AP, et al. Updated standardized endpoint definitions for transcatheter aortic valve implantation: the valve academic research consortium-2 consensus document. J Am Coll Cardiol. 2012;60(15):1438–54.
92. Ribeiro HB, et al. Cardiac magnetic resonance versus transthoracic echocardiography for the assessment and quantification of aortic regurgitation in patients undergoing transcatheter aortic valve implantation. Heart. 2014;100:1924.
93. Yared K, et al. Impact of aortic regurgitation after transcatheter aortic valve implantation: results from the REVIVAL trial. JACC Cardiovasc Imaging. 2012;5(5):469–77.
94. Feldman T, et al. Low profile vascular plugs for paravalvular leaks after TAVR. Catheter Cardiovasc Interv. 2014;83(2):280–8.
95. Luu J, et al. Percutaneous closure of paravalvular leak after transcatheter aortic valve replacement. JACC Cardiovasc Interv. 2013;6(2):e6–8.
96. Whisenant B, et al. Device closure of paravalvular defects following transcatheter aortic valve replacement with the Edwards Sapien valve. Catheter Cardiovasc Interv. 2013;81(5):901–5.
97. Saireddy R, et al. Immediate closure of paravalvular leak after transcatheter aortic valve implantation. Heart Lung Circ. 2014;23:e251.

Transcatheter Aortic Valve Replacement

15

George S. Hanzel

Abstract

Aortic stenosis is a common disease with a prevalence of approximately 5 % in elderly patients. The population of people in the United States older than 65 is expected to increase from 40 million in 2010 to nearly 80 million by 2050. With this demographic shift, the burden of valvular heart disease will increase as well. Surgical aortic valve replacement (SAVR) has long been the standard of care for the treatment of severe aortic stenosis. Multiple studies however, have documented that nearly 40 % of elderly patients with severe symptomatic aortic stenosis do not undergo surgery; mainly because of advanced age and comorbidities. This unmet clinical need was the impetus for the development of transcatheter aortic valve replacement (TAVR). Since Cribier treated the first patient in 2002, great strides have been made in the technology and TAVR has become the standard of care for appropriately selected inoperable patients and it is an alternative to surgery for high-risk patients.

Keywords

Transcatheter aortic valve replacement (TAVR) • TAVR outcomes • TAVR complications • Valve-in-valve replacement • Bicuspid aortic valve • Pure aortic regurgitation

Introduction

Aortic stenosis is a common disease with a prevalence of approximately 5 % in elderly patients [1]. The population of people in the United States older than 65 is expected to increase from 40 million in 2010 to nearly 80 million by 2050 [2]. With this demographic shift, the burden of valvular heart disease will

G.S. Hanzel, MD
Department of Cardiovascular Medicine,
Beaumont Health, Oakland University/William
Beaumont School of Medicine, Royal Oak, MI, USA
e-mail: ghanzel@beaumont.edu

A.E. Abbas (ed.), *Aortic Stenosis: Case-Based Diagnosis and Therapy*,
DOI 10.1007/978-1-4471-5242-2_15

increase as well. Surgical aortic valve replacement (SAVR) has long been the standard of care for the treatment of severe aortic stenosis. Multiple studies however, have documented that nearly 40 % of elderly patients with severe symptomatic aortic stenosis do not undergo surgery; mainly because of advanced age and comorbidities [3–8]. This unmet clinical need was the impetus for the development of transcatheter aortic valve replacement (TAVR). Since Cribier treated the first patient in 2002 [9], great strides have been made in the technology and TAVR has become the standard of care for appropriately selected inoperable patients and it is an alternative to surgery for high-risk patients.

Commercially Approved Transcatheter Heart Valves in the United States

The Edwards Sapien XT (Edwards Lifesciences Inc., Irvine, California) and the Medtronic CoreValve (Medtronic Inc., Minneapolis, Minnesota) transcatheter heart valves (THV) are the two currently commercially available THVs in the United States (Figs. 15.1 and 15.2). The Edwards Sapien XT THV, an iteration of the original Edwards Sapien THV, is a balloon expandable prosthesis with a cobalt chromium stent frame and bovine pericardial leaflets. The Edwards Sapien XT can be implanted via the

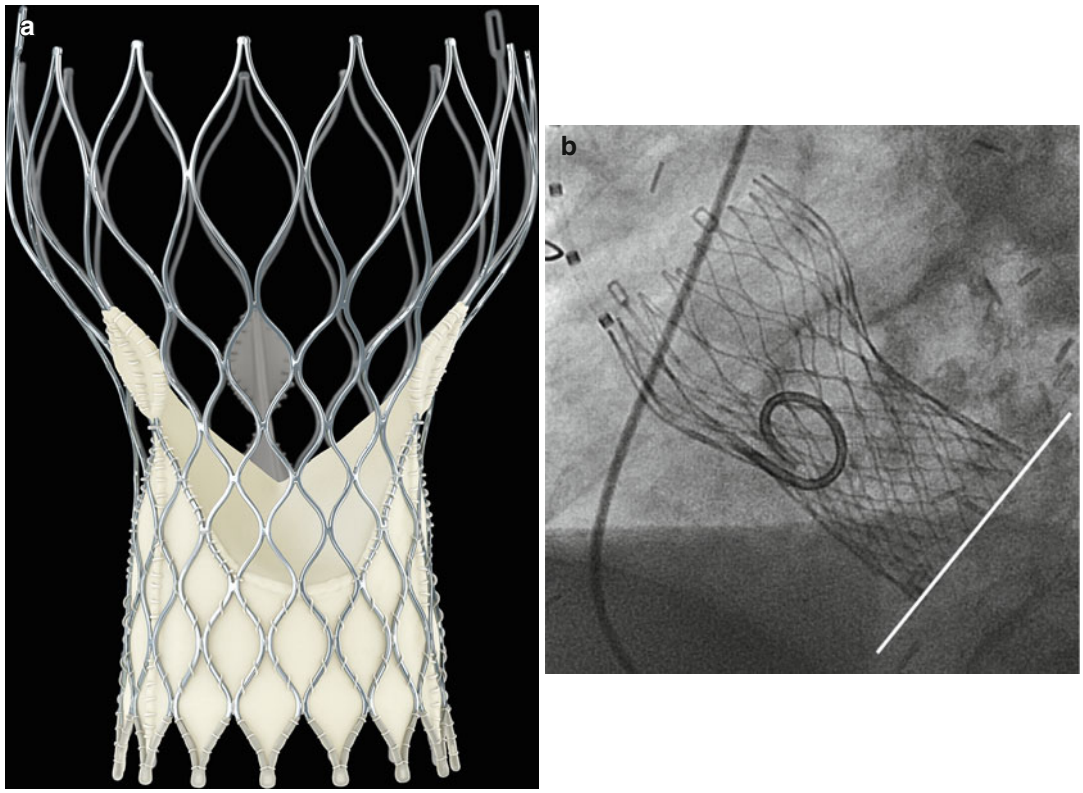

Fig. 15.1 Medtronic core valve, prosthesis diagram and under fluoroscopy in place (**a**, **b**) and (**a** copyright 2015 Medtronic, Inc.)

transfemoral approach with either a 16-French, 18-French, or 20-French expandable sheaths for the 23 mm, 26 mm, or 29 mm Sapiens XT, respectively. Alternate access routes include transaortic, transapical, and caval-aortic approaches [10]. The Medtronic CoreValve THV has a self-expanding nitinol frame and porcine pericardial leaflets. The CoreValve anchors both in the annulus as well as the proximal ascending aorta. The CoreValve can be implanted via an 18-French sheath in the femoral artery or subclavian artery. Additionally, CoreValve can be implanted via caval-aortic access or transaortic access.

Clinical Outcomes

The PARTNER (Placement of Transcatheter Aortic Valves) and CoreValve trials are the landmark randomized trials that established TAVR as a transformative technology for the treatment of aortic stenosis in high-risk and inoperable patients [11–14]. The PARTNER trial was the first randomized study to evaluate TAVR and it utilized the Edwards Sapien balloon expandable THV. It was a two-arm trial in which patients who were high risk for SAVR were randomized to TAVR vs SAVR and patients who were deemed inoperable were randomized to TAVR vs medical therapy. The CoreValve trial was also a two-armed trial which evaluated the Medtronic CoreValve self-expanding THV. High risk patients were randomized to SAVR vs TAVR and all inoperable patients were treated with CoreValve.

Survival

The PARTNER 1B trial randomized 358 inoperable patients to TAVR with Edwards Sapien THV versus medical therapy [11]. The 30 day mortality rate was 6.4 % compared with a

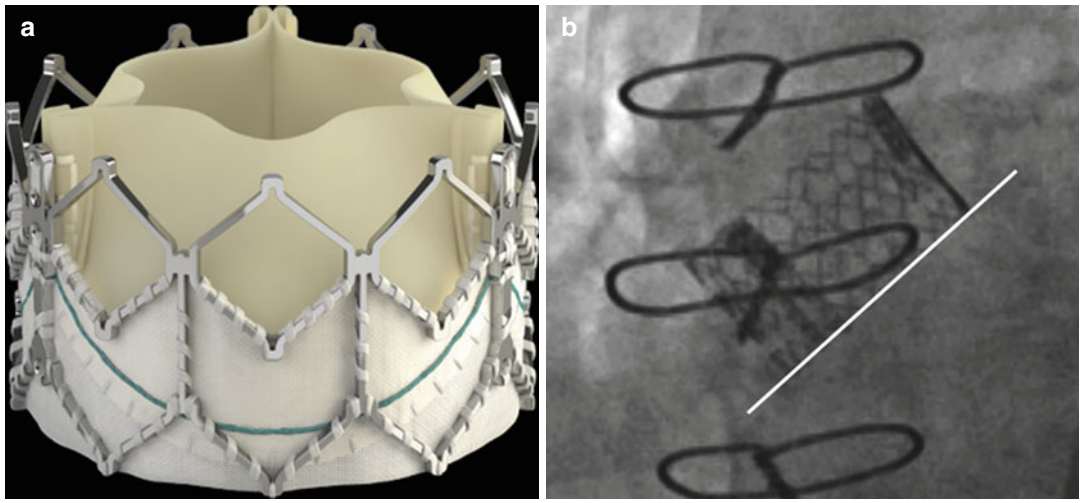

Fig. 15.2 Edwards Sapien XT valve prosthesis diagram and under fluoroscopy in place (**a**, **b**) (**a** courtesy of Edwards Lifesciences, Irvine, CA. Edwards, Edwards Lifesciences, Edwards SAPIEN, Edwards SAPIEN XT, SAPIEN, and SAPIEN XT are trademarks of Edwards Lifesciences Corporation)

Society of Thoracic Surgery (STS) predicted rate of mortality of 11.6 % for surgery. At 1 year the all-cause mortality rate, the primary endpoint of the trail, was 30.7 % for TAVR versus 50.7 % for medical therapy ($p < 0.0001$) with a number needed to treat (NNT) of 4.0 to save one life. By 3 years the mortality rate was 54.1 % vs 80.9 % ($p < 0.0001$) with NNT of 3.7 (Fig. 15.3) [15, 16]. This profound reduction in mortality led to the approval for the Edwards Sapien THV in inoperable patient in November 2011.

In the PARTNER 1A trial 699 high-risk patients were randomized to TAVR vs SAVR [12]. The mean STS score was nearly 12 % and TAVR could be performed via the transfemoral or transapical approach. The 30 day mortality rate was 3.4 % for TAVR vs 6.5 % for SAVR, $p = 0.07$. At 1 year the all-cause mortality rate, the primary endpoint of the trail, was 24.2 % vs 26.8 % for TAVR and SAVR, respectively, $p = 0.44$ (Fig. 15.4). By 3 years the mortality rate was 44.2 % vs 44.8 % (p=NS) [17, 18]. This suggests that TAVR is noninferior to SAVR in

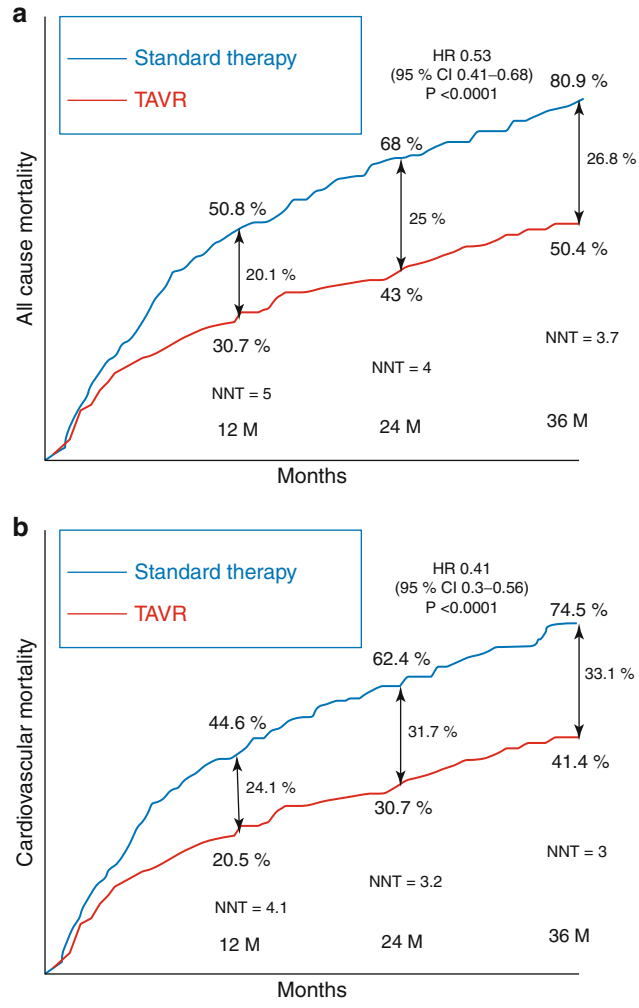

Fig. 15.3 PARTNER 1B: 3-year survival. Long-term outcomes of inoperable patients with aortic stenosis randomized to either transcatheter aortic valve replacement (*TAVR*) with Edwards Sapien valve or standard therapy revealing TAVR is superior to medical treatment in inoperable patients (**a**) reflects all cause mortality, (**b**) reflects cardiovascular mortality

high-risk patients. Interestingly, in an as treated analysis the 30 day mortality rate was 3.7 % for transfemoral TAVR, 8.7 % for transapical TAVR, and 8.2 % for SAVR. It is not clear to what extent the increased mortality seen in the transapical group was attributable to the procedure itself versus the selection of higher risk patients (i.e., severe peripheral arterial disease). However, this raises the question as to whether TAVR outcomes can continue to improve as sheath profile size decreases and more patients are treated via the transfemoral route. The Edwards Sapien valve was approved as an alternative to surgery for high-risk patients in October 2011.

In the inoperable arm of the US CoreValve trial 489 patients were treated with the CoreValve THV [13]. Patients were included in the trial if it was estimated that they had a 50 % risk of mortality or irreversible morbidity at 30 days with SAVR. The primary endpoint was the composite of all-cause mortality and stroke at 1 year compared with an objective performance goal. At 1 year all-cause mortality and stroke was 26.0 % compared with an objective performance goal of 43.0 % ($p<0.0001$) (Fig. 15.5). The 30 day and 1 year morality rates were 8.4 % and 24.3 %, respectively. This trial confirms the findings of PARTNER 1B: TAVR is superior to medical therapy in inoperable patients.

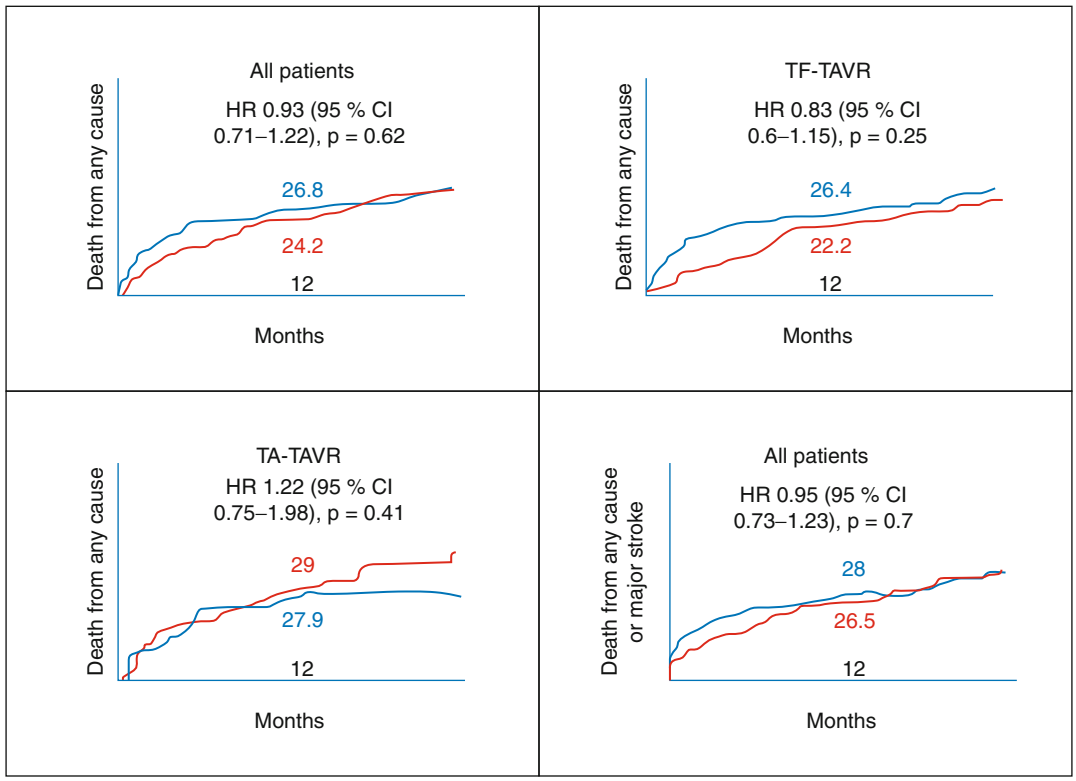

Fig. 15.4 (PARTNER 1A: 1-year outcomes. Transcatheter (*TAVR*) with Edwards Sapien valve versus surgical aortic-valve replacement (*SAVR*) in high-risk patients revealing that TAVR was non-inferior to SAVR in this cohort

In the high-risk arm of the US CoreValve trial the 795 patients were randomized to TAVR vs SAVR [14]. The primary endpoint was all-cause mortality at 1 year and the mean STS score was 7.3 %. The 30 day mortality rates were 3.3 % vs 4.5 % for TAVR and SAVR, respectively (p=0.43). The 1 year mortality rates were 14.2 % vs 19.1 % for TAVR vs SAVR, respectively (p<0.001) (Fig. 15.6). These findings of superiority of TAVR vs SAVR suggest that for high-risk patients TAVR may offer a survival advantage over conventional SAVR. Additional studies are needed to confirm these findings.

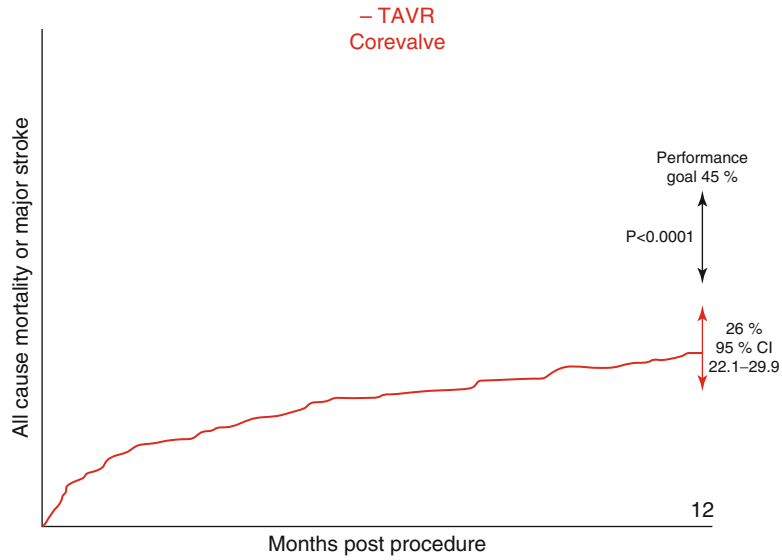

Fig. 15.5 Core valve extreme risk: all cause mortality and stroke. Transcatheter aortic valve replacement (*TAVR*) using a self-expanding Core Valve in patients with severe aortic stenosis at extreme risk for surgery revealing the outcomes were superior to the performance goal and confirming PARTNER 1B results

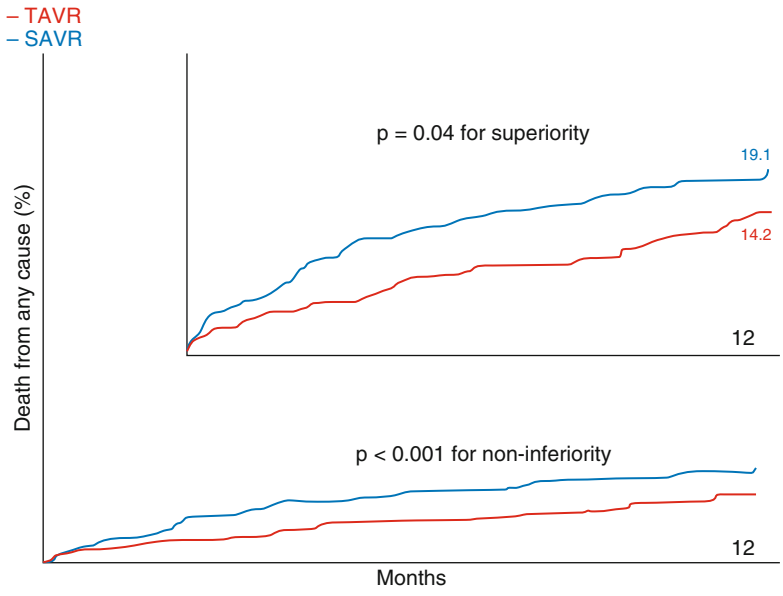

Fig. 15.6 Core valve high-risk cohort: all cause death at 1 year. Transcatheter aortic-valve replacement (TAVR) with a self-expanding Core Valve versus surgical aortic valve replacement (SAVR) in high-risk patients. Rate of death was non-inferior with TAVR versus SAVR and at 1 year a test for superiority demonstrated that TAVR was superior to SAVR. The inset shows same data with enlarged Y-axis

Functional Outcomes

TAVR with both the Sapien THV and CoreValve THV significantly improves functional capacity whether measured by New York Heart Association (NYHA) functional class, 6 min walk test or Kansas City Cardiomyopathy Quality of Life Questionnaire (KCCQ). In PARTNER 1B, >90 % of patients had NYHA class three-fourth symptoms at baseline. By 1 year less than 20 % of TAVR patients had NYHA class three-fourth symptoms compared with 60 % of medically treated patients [11]. At 1 year there was a 24.5 point improvement in KCCQ score (a 20 point change is considered a large improvement) in TAVR patients compared with no significant change in medically treated patients [19]. In CoreValve extreme risk, >90 % of patients had NYHA class three-fourth symptoms at baseline compared with <10 % of survivors at 1 year [13]. In PARTNER 1A and the CoreValve high-risk trial there was a similar improvement in NYHA class and KCQ scores in both the TAVR and SAVR arms. [12, 14, 20] The PARTNER trial also evaluated 6 min walk test. In PARTNER 1B, the TAVR arm had a significant increase in walk distance compared with medical therapy while in PARTNER 1A the TAVR and SAVR arms witnessed identical improvements in walk distance. Repeat hospitalization was evaluated in PARTNER 1B. At 2 years repeat hospitalization was decreased from 72.5 % in the medically treated arm to 35.5 % in the TAVR arm, HR 0.41 (95 % CI, 0.20–0.58) [16]. This has important implications for not just quality of like but also healthcare costs. By whichever metric is analyzed, TAVR confers significant improvements in functional outcomes and quality of life.

Valve Function and Durability

Sapien THV and CoreValve THV both have excellent valve performance. This has been demonstrated in multiple registries as well as the landmark clinical trials. The mean gradients and effective orifice area are even slightly superior to surgically implanted valves (PARTNER 1A: mean gradient 10.2 ± 4.3 mmHg vs 11.5 ± 5.4 mmHg, $p = 0.008$ and effective orifice area 1.6 ± 0.5 cm^2 vs 1.4 ± 0.5 cm^2, $p = 0.002$ for Sapien vs surgical valve, respectively; CoreValve: mean gradient 9.09 ± 3.49 mmHg vs 12.40 ± 7.38 mmHg, $p < 0.001$, and effective orifice area 1.91 ± 0.51 cm^2 vs 1.57 ± 0.49 cm^2, $p < 0.001$ for CoreValve vs surgical valve, respectively) [12, 13]. The durability of THVs is not well characterized since there is only intermediate-term follow-up of well-designed studies. Nonetheless, there appears to be excellent valve function at 5-year follow-up for the Sapien THV and 2-year follow-up for the CoreValve. Longer term follow-up will more completely define valve durability.

Complications

Neurological Events

Stroke is a devastating complication of both TAVR and SAVR. The etiology of periprocedural stroke is primarily atheroembolism from the aortic arch and the aortic valve. The incidence of silent embolic events assessed by diffusion weighted magnetic resonance imaging (MRI) is extremely high, nearly 85 % with TAVR and 75 % with SAVR, and similar between the transfemoral and transapical approaches [21–23]. Surprisingly, and contrary to the atrial fibrillation literature, silent cerebral infarcts in TAVR patients does not seem to affect intermediate term neurological and cognitive outcomes. Transcranial Doppler has been used to evaluate the timing of embolic events during TAVR. These transcranial Doppler studies have detected high-intensity transient signals (HITS) throughout all stages of the procedure: wire manipulation across the aortic arch and valve, valve implantation, and post-dilation [24, 25].

Fortunately the clinical stroke rate is significantly lower than could be expected from MRI studies. However, in many studies there seems to be a higher stroke risk associated with TAVR compared with SAVR. The PARTNER and CoreValve trials had rigorous neurological assessment and shed important light on the risk of stroke in TAVR. In the PARTNER 1A trial the

30 day total stroke rate was 4.6 % vs 2.4 % (p = 0.12) and the major stroke rate was 3.8 % vs 2.1 % (p = 0.20) for TVAR and SAVR, respectively. Although not statistically significant, the trend towards higher stroke rates with TAVR is concerning. By 2 years there was no difference in stroke. In the CoreValve trial the 30 day rate of total stroke was 4.9 % vs 6.2 % (p = 0.46) and the rate of major stroke was 3.9 % vs 3.1 % (p = 0.55) for TAVR and SAVR, respectively [12]. At 1 year there were, numerically, more strokes in the surgical arm. Approximately, half of all strokes are early, by 48 h. The remainder of strokes occur from day 2 through 30 [26, 27]. Early strokes are likely due to embolization of valvular calcification and aortic atheroma. Late stroke risk may be due to atrial fibrillation and atherosclerotic burden. Although the stroke risk is justified based on the dramatic reduction in mortality in inoperable patients, it is imperative to reduce the stroke risk if TAVR is to be performed in lower risk patients. Anecdotally it appears that stroke risk is decreasing with smaller profile devices [19]. Additionally, embolic protection devices may reduce the early stroke risk following TAVR. Lastly, refinement and optimization of anticoagulation strategy is also of critical importance to the reduction of stroke risk.

Access Site Complications and Bleeding

Major vascular access site complications and major bleeding are the most frequent complications of TAVR and are associated with a twofold increase in mortality [28]. In PARTNER 1 larger bore sheaths, 22-French and 24-French, were required leading to high access complication rates. These complications included dissection in 63 %, perforation in 31 %, hematoma in 22 %, and retroperitoneal bleed in 10 %. Predictors of vascular complications include significant tortuosity, moderate to severe calcification, and small arterial diameter (sheath to artery ratio of >1.1:1).

In PARTNER 1A and 1B the risk of access site complications was 11.0 % and 16.2 % and major bleeding rates were 9.3 % and 16.8 % [29]. In PARTNER 2 the risk of both access site complications and bleeding were both significantly reduce (11.3 % and 7.8 % respectively) with reduction in sheath size (16F, 18F and 20F for 23 mm, 26 mm and 29 mm Sapein XT, respectively) [30]. In the high risk CoreValve trial, which required 18-French sheath, the rates of access site complications were 5.9 % vs 1.9 % (p = 0.003) for TAVR and SAVR, respectively. The risk of bleeding was 28.1 % vs 35.4 % (p = 0.05) for TAVR and SAVR respectively [14]. Both the reduction in sheath size and well as improved patient selection, guided by CTA, are responsible for the reduction in these complications. Additionally, operators have become more adept at treating access site complications. With further reduction in sheath size and use of expandable sheaths it is anticipated that these risks will continue to decrease [31, 32].

Paravalvular Aortic Regurgitation

Significant paravalvular aortic regurgitation is a rare finding after SAVR however it is relatively common after TAVR [33]. Intuitively this makes sense, as the native valve is not resected there can be malapposition of the prosthesis with the annulus, particularly at the commissures. Additional causes of paravalvular aortic regurgitation include undersizing of the valve prosthesis and either high or low deployment of the THV [34]. Preliminary studies suggested that the CoreValve device may be associated with higher rates of paravalvular aortic regurgitation [35]. However, the US CoreValve trial demonstrated lower rates of paravalvular aortic regurgitation that seemed to decrease with time, possibly due to continued expansion of the nitinol frame. The risk of mild, moderate, and severe aortic regurgitation is 52 % and 41.5 %, 12 % and 10.9 %, and 1 % and 0.5 % for Sapien and CoreValve, respectively [11, 13]. Aortic regurgitation, even of mild degree, seems to be associated with worse outcomes, both in terms of functional recovery and survival [17]. In PARTNER 1A the mortality rates were 26.3 %, 33.4 %, and 50.7 % for none to trace, mild, and moderate or severe aortic regurgitation, respectively. Optimal THV sizing

(with judicious oversizing protocols), guided by CTA, significantly reduced the risk of paravalvular aortic regurgitation [36–41]. The assessment of paravalvular aortic regurgitation severity can be challenging as there are no validated echocardiographic parameters. Thus, it is often necessary to integrate echocardiography, aortography, and hemodynamics to determine aortic regurgitation severity [42–44]. If significant aortic regurgitation is seen after valve implant then redilation, or even implantation of a second THV, should be considered. New THV designs with fabric cuffs at the inflow portion of the valve, such as the Edwards Sapien 3 and Boston Scientific Lotus THVs will likely further decrease the risk of paravalvular aortic regurgitation and improve clinical outcomes.

Conduction Disturbances and Atrial Fibrillation

The bundle of His lays on the left ventricular septum immediately distal to the membranous septum. The proximity of the conduction system to the aortic annulus and the possibility of collateral damage during valve intervention is the basis for the development of left bundle branch block (LBBB) and complete heart block [45–47]. LBBB develops in 25–35 % of TAVR patients [48–51]. Interestingly, nearly 50 % of new LBBBs resolve by 1 year and it does not seem that pre- or post-procedural LBBB predicts the need for a permanent pacemaker. Patients who develop LBBB do not realize the same increase in left ventricular systolic function as do patients who do not develop a LBBB. There are mixed results regarding survival in patients who develop a new LBBB but most data would suggest that it does not impact long-term survival [48–51].

Complete heart block is seen in approximately 5 % of patients who undergo SAVR. Similarly, Edwards Sapien THV is associated with an approximately 5 % risk for heart block requiring permanent pacemaker implantation [11, 12]. The permanent pacemaker requirement is higher for Medtronic CoreValve THV, approximately 20–25 % [13, 14, 50]. The increased rate of complete heart block is likely due to lower implant in the left ventricular outflow tract and continued expansion of the nitinol frame. Preliminary data suggests that the Boston Scientific Lotus THV is also associated with higher risk of complete heart block (28 %) [52]. Risk factors for complete heart block requiring pacemaker implantation include baseline first degree AV block, left anterior fascicular block, and right bundle branch block and intra-procedural complete heart block [53]. Pacemaker requirement is associated with lack of improvement in left ventricular systolic function following TAVR but there does not appear to be an increase in mortality [54–56].

Atrial fibrillation is common after surgical aortic valve replacement and has been reported to have an incidence of up to 10–60 % [57, 58]. In surgical patients post-operative atrial fibrillation is associated with prolonged hospital stay, stroke, and mortality. The risk of atrial fibrillation is much lower, but still important, after TAVR. In the PARTNER and CoreValve trials the rate of new onset atrial fibrillation ranged from 12 to 15 % [12, 14].A Canadian registry suggests a higher rate of new onset atrial fibrillation after TAVR (31.9 % overall, 16 % for transfemoral and 38 % for transapical approaches, $p=0.47$) [57]. In this study, new onset atrial fibrillation significantly increases the risk for stroke at 1 year (13.6 % for new onset atrial fibrillation vs 3.8 % for no atrial fibrillation). Another study suggests a graded risk for the development of atrial fibrillation depending upon the approach used (SAVR = 60 %, transapical TAVR = 53 %, transaortic TAVR = 33 %, and transfemoral TAVR 14 %) [58]. Most of this difference is presumed to be related to pericardial access although patient characteristics may play a role as well. Additional studies will be required to determine the new onset atrial fibrillation rates as more and more patients are treated via the transfemoral approach.

Acute Kidney Injury

Many patients with aortic stenosis also have chronic kidney disease and are at risk for developing acute kidney injury following TAVR or SAVR. The causes of acute kidney injury include

contrast nephropathy, hypoperfusion, bleeding, atheroembolism [59]. The risk of acute kidney injury following TAVR ranges from 5.0 to 15.0 % and the risk of renal replacement therapy is approximately 1 % [11–14]. In a meta-analysis of over 16,000 patients, acute kidney injury was the third most common complication of TRV, after heart block and vascular access complications, occurring in 4.9 % of patients [50]. Acute kidney injury is a strong predictor of poor outcomes following TAVR and strategies to minimize acute kidney injury (such as hydration, contrast reduction strategies, bleeding avoidance strategies, and avoidance of nephrotoxic agents) are of utmost importance to optimize outcomes [59].

Annular Rupture

Annular rupture is a rare but devastating, and frequently fatal, complication of TAVR. It is thought to have an incidence of <1 % but is associated with a 50 % mortality rate. With balloon expandable THVs the three predictors of rupture are moderate to severe sub-annular calcification, area oversizing of the THV by >20 %, and post-dilation [60]. Pre-procedural CT imaging is critical to mitigate the risk of rupture [36–41]. Optimal THV size selection is essential to avoid significant oversizing to reduce the risk of rupture. Perhaps in the setting of severe sub-annular calcification some devices may offer specific advantages. For instance, with the Sapien 3 or Lotus THVs oversizing may be minimized due to the fabric cuff or adaptive seal. Alternatively, self-expanding devices such as CoreValve or Protico may be advantageous.

Coronary Occlusion

The risk of coronary occlusion is <1 % but associated with a 35–50 % mortality rate. Occlusion results from the displacement of bulky, calcified native leaflets that covers the coronary ostia and is rarely related to the stent frame of fabric cuff covering the coronaries. Risk factors for coronary occlusion include low coronary height (especially <10 mm from the annulus), bulky native leaflets, narrow sinus of Valsalva, and high THV implant [61]. Pre-procedural CT imaging may help predict patients who may be at risk for coronary occlusion. Rarely a patient with low coronary ostia and small sinus of Valsalva dimensions could be excluded from TAVR. In patients thought to be at higher risk for coronary occlusion it may be prudent to place a coronary guidewire, and even a balloon, in the coronary artery at the time of TAVR.

Patient Selection

There are numerous anatomical factors, specifically annulus size, access site, and prediction of complications, that are critical to assess when planning TAVR. In general CT imaging has become the accepted modality to make these assessments [36–41]. However, transesophageal echocardiography and magnetic resonance imaging have been evaluated and may be useful in select situations, such as patients with advanced chronic kidney disease [62].

Valve selection and sizing are based on annular area and perimeter (for Sapien XT and CoreValve, respectively), sinus of Valsalva dimensions, and diameter of the sinotubular junction. CT assessment of iliofemoral size, calcification, and tortuosity is useful in selecting access route. Noncalcified or minimally calcified vessels are frequently compliant and accommodate sheaths minimally larger than their nominal size. For instance, a noncalcified vessel may accommodate a sheath 1–2 mm larger. However, heavily calcified vessels may not accommodate sheaths of the same size. Experience is required to integrate vessel size, calcification, and tortuosity permitting optimal patient selection for the femoral approach. Fortunately with the lower profile of the current generation of THVs and expandable sheaths the vast majority of patients can be treated via the transfemoral approach. In the rare patient who requires an alternate access route, CT imaging can assess subclavian size and calcification as well as aortic calcification and distance from proposed aortic entry point to the annulus.

The patients treated in the PARTNER and CoreValve trials were of advanced age, had multiple comorbidities and were often frail. Although TAVR dramatically extends survival the 1 year mortality for PARTNER A, PARTNER B, CoreValve high risk, and CoreValve extreme risk was 24.3 %, 30.7 %, 14.2 %, and 26.0 %, respectively [11–14]. In fact, in PARTNER B at 6 months approximately 40 % of patients had either died or had not realized improvement in quality of life [63]. These findings highlight the importance of appropriate patient selection. Therefore, beyond the technical feasibility of performing TAVR, it is critical to select patients who will likely benefit in terms of survival and functional recovery and avoid those patient in which any procedure may be futile. Although it is difficult to turn down an individual patient based on any single comorbidity it is important to consider burden of comorbidities (particularly O_2 dependent COPD, severe left ventricular systolic dysfunction with low gradient, severe mitral regurgitation, advanced chronic kidney disease, malignancy, and neurological disorders such as dementia, advanced Parkinson's disease, or debilitating stroke) and frailty (conventionally measured by 5 m walk test, grip strength, albumin, and Katz activities of daily living scale) [64–72]. The assistance of geriatric medicine is often helpful in evaluating these patients and determining which patients likely will benefit from TAVR and who might not. Hopefully in the future TAVR specific risk score will be developed to help predict benefit and futility.

New Devices

Next generation THV device designs have been developed to address TAVR complications and improve ease of use (Fig. 15.7). In particular, some of the newer THVs are designed to minimize paravalvular arotic regurgitation which is associated with increased mortality and has been described as the "Achilles Heel" of TAVR. Some THVs can be recaptured, repositioned, and even fully retrieved to ensure optimal implant position in every case. The Sapien 3 (Edwards Lifesciences

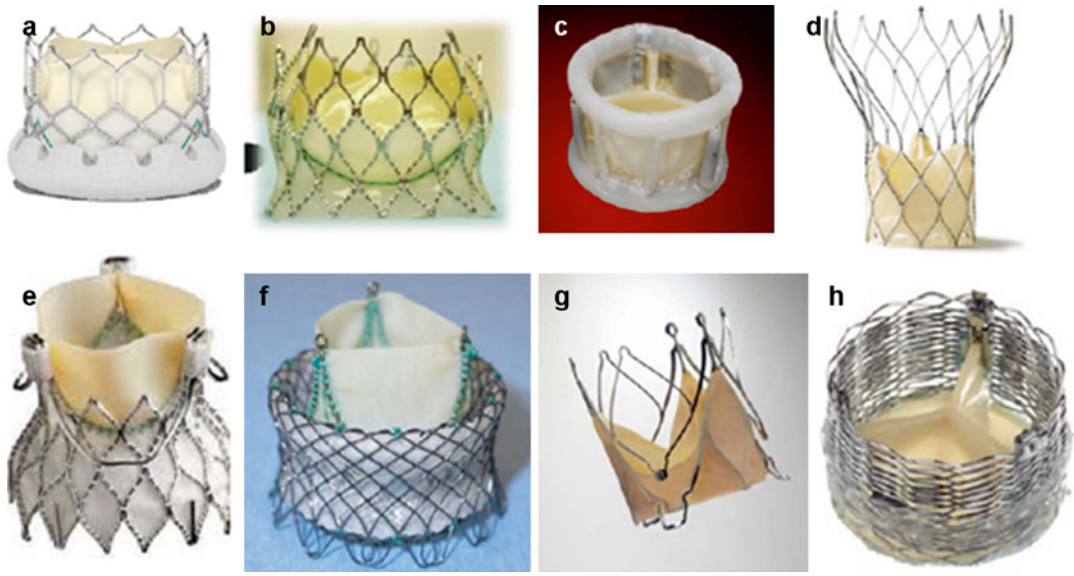

Fig. 15.7 Next generation transcatheter heart valve designs (**a**) SAPIEN 3, (Edwards Lifesciences, Irvine, California), (**b**) CENTRA, (Edwards Lifesciences), (**c**): Direct Flow Medical, (Direct Flow Medical, Santa Rosa, California), (**d**) Portico, (St. Jude Medical, St. Paul, Minnesota), (**e**) Engager, (Medtronic, Minneapolis, Minnesota), (**f**) Heart Leaflet, Heart Leaflet Technologies, Maple Grove, Minnesota), (**g**) JenaValve, (JenaValve Technology, Germany), (**h**) Sadra Lotus Medical (Boston Scientific Scimed Inc., Maple Grove, Minnesota) (From Genereaux et al. [90] with permission)

Inc., Irvine, California) THV has a fabric cuff at the inflow segment of the stent frame designed to reduce paravalvular aortic regurgitation and the 14 French expandable sheath will hopefully reduce vascular complications [73, 74]. In the first multicenter prospective registry of 150 patients with an STS risk score of 7.4 % the 30 day event rates were: death 2.1 %, moderate aortic regurgitation 3.5 %, severe aortic regurgitation 0 %, access site complications 4.2 %, stroke 2.7 %, and new pacemaker requirement 13.3 % [74]. These promising results suggest that Sapien 3 attains its intended goal of a significant reduction in paravalvular aortic regurgitation and access site complications. However, there seems to be a trade-off for greater heart block requiring pacemaker implantation from the fabric cuff impinging on the conduction system. The CoreValve Evolut R (Medtronic, Minneapolis, Minnesota) and PORTICO THVs have self-expanding stent frames that are fully recapturable, repositionable, and retrievable [75]. Unlike all other THVs the Direct Flow THV (Direct Flow Medical, Santa Rosa, California) has a non-metallic frame [76]. Dacron polyester rings in the aortic and ventricular position are inflatable and deflatable to allow precise positioning and reduce paravalvular aortic regurgitation. A multicenter study of 75 patients demonstrated a high procedural success rate, low paravalvular aortic regurgitation (1.4 % moderate, 0 % severe), and a pacemaker rate of 17 % [76]. Larger studies are required to confirm these promising results. The Lotus THV (Boston Scientific Corporation, Marlborough, Massachusetts) combines features of Sapien 3 as well as CoreValve Evolut R and PORTICO [52]. It is constructed from bovine pericardial leaflets and a nitinol frame. Rather than a self-expanding nitinol frame, during deployment the single nitinol element is shortened resulting in radial expansion. It is recapturable, repositionable, and retrievable and there is an adaptive seal on the inflow segment of the nitinol frame. In the 120 patient REPRISE II trial (Repositionable Percutaneous Replacement of Stenotic Aortic Valve Through Implantation of Lotus Valve System) there was a 100 % procedural success rate, 1.9 % of patients with moderate or severe paravalvular aortic regurgitation, and a 28.6 % new pacemaker rate. This preliminary data suggests that Sapien 3 and Lotus THVs dramatically reduce paravalvular aortic regurgitation but at a cost of a higher rate of pacemaker implantation [52, 74]. Whether this is confirmed in future trials and how this affects long-term outcomes will be important subject of additional studies. Whether repositionable THVs improve outcomes or conversely increase atheroembolic events will also need to be evaluated in clinical trials.

Adjunctive devices may also help minimize major risks related to TAVR. Embolic protection devices such as Claret Medical Sentinel Cerebral Protection System (Claret Medical, Santa Rosa, California) and Embrella (Edwards Lifesciences Inc., Irvine, California) are currently being studied to determine whether they reduce the incidence of new stroke following TAVR (Fig. 15.8).

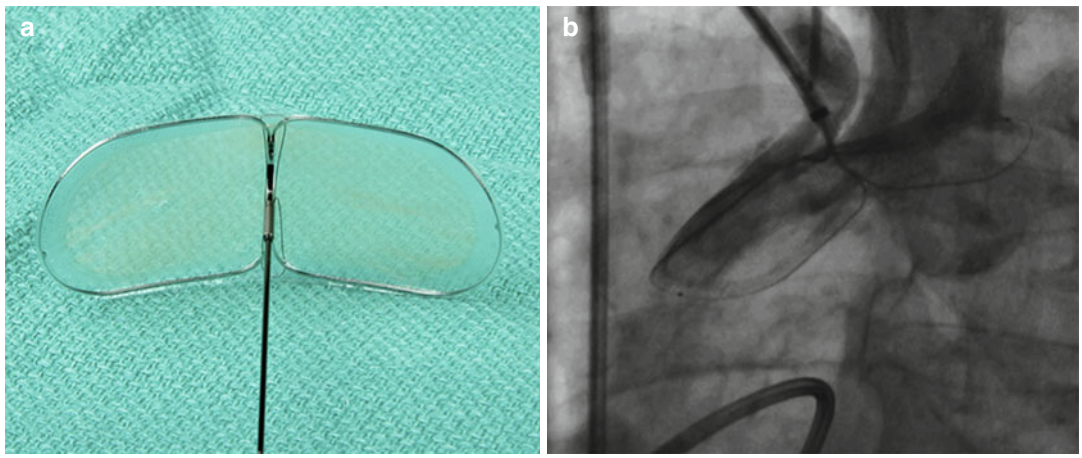

Fig. 15.8 Edwards Lifesciences embrella embolic protection device (**a**). The device in place under angiographic guidance, (**b**) (From Rodes-Cabau et al. [78] with permission)

Intuitively, embolic protection devices should reduce stroke rate. However, the current data is sparse and mixed. The recently presented CLEAN TAVI study (Claret Embolic Protection and TAVI) randomized 100 patients to TAVR with embolic protection versus TAVR alone. Diffusion weighted MRI at 7 days demonstrated a significant reduction the median number of new lesions (3 vs 7) and median lesion volume (101 mm^3 vs 292 mm^3) in patients treated with embolic protection [77]. However, in the small PROTAVI-C Pilot Study the Embrella did not reduce embolic events [78]. Diffusion weighted MRI was performed at 7 days in 36 patients treated with Embrella embolic protection and 6 control patients. There was no difference in median number of new lesions (7.5 with Embrella vs 4.0 for control) or median lesion volume (305 mm^3 with Embrella vs 180 mm^3 for control). Much more work is required to determine whether embolic protection devices truly reduce stroke rates.

New Patient Populations

TAVR is expanding into new anatomical subsets such as valve-in-valve replacement, bicuspid aortic valve, and pure aortic regurgitation. TAVR is an attractive treatment alternative for degenerated bioprosthetic valves. The circular, rigid, radiopaque ring provides a discrete landmark to aid in optimal THV positioning, nearly eliminates the concern for paravalvular aortic regurgitation, and mitigates against the risk of annular rupture and conduction disturbances [79–81]. The risk of coronary occlusion may be greater in patients with narrow sinuses of Valsalva and coronary ostia below bioprosthetic valve post. Additionally, patients with small bioprosthetic valves (less than 21 mm) may have unacceptably high gradients. The Valve-In-Valve International Data Registry (VIVID) which included 459 patients there was a 5 % rate of moderate or greater arotic regurgitation, a mean gradient of 16.1 mmHg, and a 1 year survival of 83.2 % [82]. Interestingly patients with degenerated bioprosthetic due to aortic regurgitation had better outcomes than patients with bioprosthetic aortic stenosis. PARTNER and CoreValve registries are being conducted to validate these promising results.

Unlike aortic stenosis, a regurgitant aortic valve does not typically have thickened leaflets and a calcified annulus to anchor to during deployment. As such, the risk of embolization and migration may be higher. Although specifically designed to address aortic stenosis, Edwards Sapien and Medtronic CoreValve have been used to treat pure aortic regurgitation in a limited number of patients [83]. It has been shown that these devices requires significant oversizing and there is a higher need for a second THV. Recently, two small case series employing Symetis ACURATE TA (Symetis, Ecublens, Switzerland) and JenaValve (JenaValve Technology, Munich, Germany) have demonstrated very high procedural success rates [84, 85]. Further studies of these THVs as well as other platforms such as the Helio system (Edwards Lifesciences) are required to define the role of TAVR in aortic regurgitation [86].

There has been concern that bicuspid valves may not be ideally treated by TAVR due to the elliptical orifice, highly asymmetric calcification, and frequently associated aortic root enlargement. This could lead to inadequate apposition of the THV to the commissures resulting in significant paravalvular aortic regurgitation. As a consequence, bicuspid aortic valves were excluded from the major clinical trials. Several case series suggest that TAVR is feasible for bicuspid valve disease [87, 88]. However, there is a greater risk for moderate or greater paravalvular aortic regurgitation, 28.4 % in one study [89]. For TAVR to have a role bicuspid disease the rates of aortic regurgitation must be improved whether by better patient selection and valve sizing by CT or new device iterations to specifically address the anatomical challenges of bicuspid valves.

Currently TAVR is approved in the United States only for high-risk and inoperable patients. Most patients who undergo surgical aortic valve replacement are low risk and only approximately 25 % of these patients have an STS risk score of ≥4 %. The PARTNER S3i (Sapien 3) and SURTAVI (CoreValve) trials are studying intermediate patients with an STS risk score of 4–8 %. These studies will define the role of TAVR in this relatively large population of patients.

Conclusions

TAVR has become the standard of care for high risk and inoperable patients with severe aortic stenosis owing to its dramatic improvement in patient survival and quality of life. However, many serious complications have come to light as TAVR has been rigorously studied over the last decade. Additionally, many of the initial patients treated were either too frail or had too many comorbidities to gain any significant improvement in survival or quality of life. With improved device design attributes and improved patient selection, based on imaging and clinical factors, the frequency of these complications are decreasing and patient outcomes are improving. As patient outcomes continue to improve, and if valve durability is proven, TAVR will likely gain expanded indications to treat ever larger populations of patients.

References

1. Nkomo VT, Gardin JM, Skelton TN, et al. Burden of valvular heart diseases: a population-based study. Lancet. 2006;368:1005–12.
2. Census. Gov – 2010 US Census Report.
3. Bouma BJ, Van Den Brink RB, Van Der Meulen JH, et al. To operate or not on elderly patients with aortic stenosis: the decision and its consequences. Heart. 1999;82:143–8.
4. Pellikka PA, Sarano ME, Nishimura RA, et al. Outcome of 622 adults with asymptomatic, hemodynamically significant aortic stenosis during prolonged follow-up. Circulation. 2005;111:3290–5.
5. Charlson E, Legedza AT, Hamel MB. Decision-making and outcomes in severe symptomatic aortic stenosis. J Heart Valve Dis. 2006;15:312–21.
6. Varadarajan P, Kapoor N, Banscal RC, Pai RG. Clinical profile and natural history of 453 nonsurgically managed patients with severe aortic stenosis. Ann Thorac Surg. 2006;82:2111–5.
7. Jan F, Andreev M, Mori N, Janosik B, Sagar K. Unoperated patients with severe symptomatic aortic stenosis. Circulation. 2009;120:S753.
8. Bach DS, Siao D, Girard SE, et al. Evaluation of patients with severe symptomatic aortic stenosis who do not undergo aortic valve replacement: the potential role of subjectively overestimated operative risk. Circ Cardiovasc Qual Outcomes. 2009;2:533–9.
9. Cribier A, Eltchaninoff H, Basha, et al. Percutaneous transcatheter implantation of an aortic valve prosthesis for calcific aortic stenosis: first human case description. Circulation. 2002;106:3006–8.
10. Greenbaum AB, O'Neill WW, Paone G, et al. Caval-Aortic access to allow transcatheter aortic valve replacement in otherwise ineligible patients. J Am Coll Cardiol. 2014;63:295–2804.
11. Leon MB, Smith CR, Mack M, PARTNER Trial Investigators, et al. Transcatheter aortic-valve implantation for aortic stenosis in patients who cannot undergo surgery. N Engl J Med. 2011;364:2187–98.
12. Smith CR, Leon MB, Mack MJ, PARTNER Trial Investigators, et al. Transcatheter versus surgical aortic-valve replacement in high-risk patients. N Engl J Med. 2011;364:2187–98.
13. Popma JJ, Adams DH, Reardon MJ, et al. Transcatheter aortic valve replacement using a self-expanding bioprosthesis in patients with severe aortic stenosis at extreme risk for surgery. J Am Coll Cardiol. 2014;63:1972–81.
14. Adams DH, Popma JJ, Reardon MJ, et al. Transcatheter aortic-valve replacement with a self-expanding prosthesis. N Engl J Med. 2014;370:1790–8.
15. Kapadia SR, Tuzcu EM, Makkar RR. Long-term outcomes of inoperable patients with aortic stenosis randomized to transcatheter aortic valve replacement or standard therapy. Circulation. 2014;130:1483–92.
16. Makkar RR, Fontana GP, Jilaihawi H, Partner Trial Investigators, et al. Transcatheter aortic-valve replacement for inoperable severe aortic stenosis. N Engl J Med. 2012;366:1696–704.
17. Kodali SK, Williams MR, Smith CR, PARTNER Trial Investigators, et al. Two-year outcomes after transcatheter or surgical aortic-valve replacement. N Engl J Med. 2012;366:1686–95.
18. Thourani V. PARTNER 1A 3 year outcomes. San Francisco: ACC; 2013.
19. Reynolds MR, Magnuson EA, Lei Y, Placement of Aortic Transcatheter Valves (PARTNER) Investigators, et al. Health-related quality of life after transcatheter aortic valve replacement in inoperable patients with severe aortic stenosis. Circulation. 2011;124:1964–72.
20. Reynolds MR, Magnuson EA, Wang K, PARTNER Trial Investigators, et al. Health-related quality of life after transcatheter or surgical aortic valve replacement in high-risk patients with severe aortic stenosis: results from PARTNER (Placement of AoRTic TraNscathetER valve) trial (Cohort A). J Am Coll Cardiol. 2012;60:548–58.
21. Kahlert P, Knipp SC, Schlamann M, et al. Silent and apparent cerebral ischemia after percutaneous transfemoral aortic valve implantation: a diffusion weighted magnetic resonance imaging study. Circulation. 2010;121:870–8.
22. Fairbairn TA, Mather AN, Bijisterveld P, et al. Diffusion-weighted MRI determined cerebral embolic infarction following transcatheter aortic valve implantation: assessment of predictive factors and relationship to subsequent health status. Heart. 2012;98:18–23.
23. Ghanem A, Müller A, Nahle CP, et al. Risk and fate of cerebral embolism after transcatheter aortic valve implantation: a prospective pilot study with diffusion-

weighted magnetic resonance imaging. J Am Coll Cardiol. 2010;55:1427–32.
24. Erdoes G, Basciani R, Huber C, et al. Transcranial Doppler detected cerebral embolic load during transcatheter aortic valve implantation. Eur J Cardiothorac Surg. 2012;41:778–83.
25. Kahlert P, Al-Rashid F, Döttger P, et al. Cerebral embolization during transcatheter aortic valve implantation: a transcranial Doppler study. Circulation. 2012;126:1245–55.
26. Nombela-Franco L, Webb JG, de Jaegere PP, et al. Timing, predictive factors, and prognostic value of cerebrovascular events in a large cohort of patients undergoing transcatheter aortic valve implantation. Circulation. 2012;126:3041–53.
27. Nuis RJ, Van Miehem NM, Schultz CJ, et al. Frequency and causes of stroke during or after transcatheter aortic valve implantation. Am J Cardiol. 2012;109:1637–43.
28. Van Mieghem NM, Tchetche D, Chieffo A, et al. Incidence, predictors, and implications of access site complications with transfemoral transcatheter aortic valve implantation. Am J Cardiol. 2012;110:1361–7.
29. Généreux P, Webb JG, Svensson LG, et al. Vascular complications after transcatheter aortic valve replacement. Insights from the PARTNER (Placement of AoRTic TraNscathetER valve) trial. J Am Coll Cardiol. 2012;60:1043–52.
30. Leon MB. PARTNER II trial. San Francisco: ACC; 2013.
31. Stortecky S, Wenaweser P, Diehm N, et al. Percutaneous management of vascular complications in patients undergoing transcatheter aortic valve implantation. J Am Coll Cardiovasc Interv. 2012;5:515–24.
32. Toggweiler S, Leipsic J, Binder RK, et al. Management of vascular access in transcatheter aortic valve replacement. Part 1: basic anatomy, imaging, sheaths, wires, and access routes. J Am Coll Cardiol Interv. 2013;6:643–53.
33. Généreux P, Head SJ, Van Mieghem NM, et al. Clinical outcomes after transcatheter aortic valve replacement using valve academic research consortium definitions. A weighted meta-analysis of 3,519 patients from 16 studies. J Am Coll Cardiol. 2012;59:2317–26.
34. Lerakis S, Hayek SS, Douglas PS. Paravalvular aortic leak after transcatheter aortic valve replacement. Current knowledge. Circulation. 2013;127:397–407.
35. Moat NE, Ludman P, de Belder MA, et al. Long term outcomes after transcatheter aortic valve implantation in high risk patients with severe aortic stenosis: the UK TAVI registry. J Am Coll Cardiol. 2011;58:2130–8.
36. Jilaihawi H, Doctor N, Kashif M, et al. Aortic annular sizing for transcatheter aortic valve replacement using cross-sectional 3-dimensional transesophageal echocardiography. J Am Coll Cardiol. 2013;61:908–16.
37. Jilaihawi H, Kashif M, Fontana G, et al. Cross-sectional computed tomographic assessment improves accuracy of aortic annular sizing for transcatheter aortic valve replacement and reduces the incidence of pavalvular aortic regurgitation. J Am Coll Cardiol. 2012;59:1275–86.
38. Bloomfield GS, Gillam LD, Hahn RT, et al. A practical guide to multimodality imaging of transcatheter aortic valve replacement. J Am Coll Cardiovasc Imaging. 2012;5:441–55.
39. Delgado V, Kapadia S, Schalij MJ, et al. Transcatheter aortic valve implantation: implications of multimodality imaging in patient selection, procedural guidance, and outcomes. Heart. 2012;98:743–54.
40. Kempfert J, Van Linden A, Lehmkuhl L, et al. Aortic annulus sizing: echocardiographic versus computed tomography derived measurements in comparison with direct surgical sizing. Eur J Cardiothorac Surg. 2012;42:627–33.
41. Messika-Zeitoun D, Serfaty JM, Brochet E, et al. Multimodal assessment of the aortic annulus diameter: implications for transcatheter aortic valve implantation. J Am Coll Cardiol. 2010;55:186–94.
42. Leon MB, Piazza N, Nikolsky E, et al. Standardized endpoint definitions for transcatheter aortic valve implantation clinical trials: a consensus report from the Valve Academic Research Consortium. J Am Coll Cardiol. 2011;57:253–69.
43. Généreux P, Head SJ, Van Mieghem NM, et al. Updated standardized endpoint definitions for transcatheter aortic valve implantation: the Valve Academic Research Consortium-2 consensus document. J Am Coll Cardiol. 2012;60:1438–54.
44. Sinning JM, Hammerstingl C, Vasa-Nicotera M, et al. Aortic regurgitation index defines severity of periprosthetic regurgitation and predicts outcome in patients after transcatheter aortic valve implantation. J Am Coll Cardiol. 2012;59:1134–41.
45. van der Boon RM, Nuis RJ, Van Mieghem NM, et al. New conduction abnormalities after TAVI-frequency and causes. Nat Rev Cardiol. 2012;9:454–63.
46. Khawaja MZ, Rajani R, Cook A, et al. Permanent pacemaker insertion after CoreValve transcatheter aortic valve implantation. Incidence and contributing factors (the UK CoreValve Collaborative). Circulation. 2011;123:951–60.
47. Laynez A, Ben-Dor I, Barbash IM, et al. Frequency of conduction disturbances after Edward SAPIEN percutaneous valve implantation. Am J Cardiol. 2012;110:1164–8.
48. Urena M, Mok M, Serra V, et al. Predictive factors and long-term clinical consequences of persistent left bundle branch block following transcatheter aortic valve implantation with a balloon-expandable valve. J Am Coll Cardiol. 2012;60:1743–52.
49. Houthuizen P, Van Garsse LA, Poels TT, et al. Left bundle-branch block induced by transcatheter aortic valve implantation increases risk of death. Circulation. 2012;126:720–8.
50. Khatri PJ, Webb JG, Rodes-Cabau J, et al. Adverse effects associated with transcatheter aortic valve implantation: a meta-analysis of contemporary studies. Ann Intern Med. 2013;158(1):35–46.
51. Franzoni I, Latib A, Maisano F, et al. Comparison of incidence and predictors of left bundle branch block

after transcatheter aortic valve implantation using the CoreValve versus the Edwards Valve. Am J Cardiol. 2013;112:554–9.
52. Meredith IT, Walters DL, Dumonteil N, et al. Transcatheter aortic valve replacement for severe symptomatic aortic stenosis using a repositionable valve system. 30-day primary endpoint results from the REPRISE II Study. J Am Coll Cardiol. 2014;64:1339–48.
53. Siontis GCM, Jüni P, Pilgrim T, et al. Predictors of permanent pacemaker implantation in patients with severe aortic stenosis undergoing TAVR. J Am Coll Cardiol. 2014;64:129–40.
54. Erkapic D, De Rosa S, Kelava A, et al. Risk for permanent pacemaker after transcatheter aortic valve implantation: a comprehensive analysis of the literature. J Cardiovasc Electrophysiol. 2012;23:391–7.
55. Hoffmann R, Herpertz R, Lotfipour S, et al. Impact of a new conduction defect after transcatheter aortic valve implantation on left ventricular function. J Am Coll Cardiovasc Interv. 2012;5:1257–63.
56. Buellesfeld L, Stortecky S, Hetg D, et al. Impact of permanent pacemaker implantation on clinical outcome among patients undergoing transcatheter aortic valve implantation. J Am Coll Cardiol. 2012;60:493–501.
57. Amat-Santos IJ, Rodés-Cabau J, Urena M, et al. Incidence, predictive factors, and prognostic value of new-onset atrial fibrillation following transcatheter aortic valve implantation. J Am Coll Cardiol. 2012;59:178–88.
58. Tanawuttiwat T, O'Neill BD, Cohen MG, et al. New-onset atrial fibrillation after aortic valve replacement: comparison of transfemoral, transapical, transaortic, and surgical approaches. J Am Coll Cardiol. 2014;63:1510–9.
59. Généreux P, Kodali SK, Green P, et al. Incidence and effect of acute kidney injury after transcatheter aortic valve replacement using the new valve academic research consortium criteria. Am J Cardiol. 2013;111:100–5.
60. Barbant M, Tae-Hyun Y, Rodes-Cabau J, et al. Anatomical and procedural features associated with aortic root rupture during balloon-expandable transcatheter aortic valve replacement. Circulation. 2013;128:244–53.
61. Ribeiro HB, Nombela-Franco L, Urena M, et al. Coronary obstruction following transcatheter aortic valve implantation: a systematic review. J Am Coll Cardiovasc Interv. 2013;6:452.
62. Jilaihaui A, Doctor N, Kashi FM, et al. Aortic annular sizing for transcatheter aortic valve replacement using cross-sectional 3-dimensional transesophageal echocardiography. J Am Coll Cardiol. 2013;61:908–16.
63. Arnold SV, Spertus JA, Lei Y, et al. How to define poor outcome after TAVR: conceptual framework and empirical observations from PARTNER trial. Circ Cardiovasc Qual Outcomes. 2013;6:591–7.
64. Green P, Woglom AE, Genereux P, et al. The impact of frailty status on survival after transcatheter aortic valve replacement in older adults with severe aortic stenosis; a single-center experience. J Am Coll Cardiovasc Interv. 2012;5:974–81.
65. Stortecky S, Schoenenberger AW, Moser A, et al. Evaluation of multidimensional geriatric assessment as a predictor of mortality and cardiovascular evens after transcatheter aortic valve implantation. J Am Coll Cardiovasc Interv. 2012;5:489–96.
66. Clavel MA, Webb JG, Rodés-Cabau J, et al. Comparison between transcatheter and surgical prosthetic valve implantation in patients with severe aortic stenosis and reduced left ventricular ejection fraction. Circulation. 2010;122:1928–36.
67. Svensson LG, Blackstone EH, Rajeswaran J, et al. Comprehensive analysis of mortality among patients undergoing TAVR. Results of the PARTNER Trial. J Am Coll Cardiol. 2014;64:158–68.
68. Lauten A, Figulla HR, Möllmann, et al. TAVI for low-flow, low-gradient severe aortic stenosis with preserved or reduced ejection fraction: a subgroup analysis from the German Aortic Valve Registry (GARY). EuroIntervention. 2014;10:850–9.
69. Amabile N, Agostini H, Gilard M, et al. Impact of low preprocedural transvalvular gradient on cardiovascular mortality following TAVI: an analysis from FRANCE 2 registry. EuroIntervention. 2014;10:842–9.
70. Puls M, Sobisiak B, Bleckmann A, et al. Impact of frailty on short- and long-term morbidity and mortality after transcatheter aortic valve implantation: risk assessment by Katz Index of activities of daily living. EuroIntervention. 2014;10:609–19.
71. Duir D, Waksman R, Barbash IM, et al. Outcomes of patients with chronic lung disease and severe aortic stenosis treated with transcatheter versus surgical aortic valve replacement or standard therapy. J Am Coll Cardiol. 2014;03:269–79.
72. Mok M, Nombela-Franco L, Dumont E, et al. Chronic obstructive pulmonary disease in patients undergoing transcatheter aortic valve implantation: insights on clinical outcomes, prognostic markers, and functional status changes. J Am Coll Cardiol Intv. 2013;6(10):1072–84.
73. Binder RK, Rodés-Cabau J, Wood DA, et al. Transcatheter aortic valve replacement with the SAPIEN 3. A new balloon-expandable transcatheter heart valve. J Am Coll Cardiol Intv. 2013;6:293–300.
74. Webb J, Gerosa G, Lefèvre T, et al. Multicenter evaluation of a next-generation balloon-expandable transcatheter aortic valve. J Am Coll Cardiol. 2014;64:2235–43.
75. Willson AB, Rodes-Caban J, Wood DA, et al. Transcatheter aortic valve replacement with the St. Jude medical Portico valve. J Am Coll Cardiol. 2012;60:581–6.
76. Schofer J, Colombo A, DeMarco F, Klugmann S, et al. Prespective multicenter evaluation of the direct flow medical transcatheter aortic valve. J Am Coll Cardiol. 2014;63:763–8.
77. Linke A. CLEAN-TAVI, TCT 2014, Washington, DC.
78. Rodés-Cabau J, Kahlert P, Neumann F-J, et al. Feasibility and exploratory efficacy evaluation of the embrella embolic deflector system for the prevention of cerebral emboli in patients undergoing transcatheter aortic valve replacement. J Am Coll Cardiol Intv. 2014;7:1146–55.
79. Piazza N, Bleiziffer S, Brockmann G, et al. Transcatheter aortic valve implantation for failing sur-

gical aortic bioprosthetic valve. From concept to clinical application and evaluation (Part 1). J Am Coll Cardiovasc Interv. 2011;4:721–32.
80. Piazza N, Bleiziffer S, Brockmann G, et al. Transcatheter aortic valve implantation for failing surgical aortic bioprosthetic valve. From concept to clinical application and evaluation (Part 2). J Am Coll Cardiovasc Interv. 2011;4:733–42.
81. Dvir D, Webb J, Brecker S, et al. Transcatheter aortic valve replacement for degenerative bioprosthetic surgical valves: results from the global valve-in-valve registry. Circulation. 2012;126:2335–44.
82. Dvir D, Webb JG, Bleiziffer S, et al. Transcatheter aortic valve implantation in failed bioprosthetic surgical valve. JAMA. 2014;312(2):162–70.
83. Roy DA, Schaefer U, Guetta V, et al. Transcatheter aortic valve implantation for pure severe native aortic valve regurgitation. J Am Coll Cardiol. 2013;61:1577–84.
84. Wendt D, Kahlert P, Pasa S, et al. Transapical transcatheter aortic valve for severe aortic regurgitation. J Am Coll Cardiol Intv. 2014;7:1159–67.
85. Seiffert M, Bader R, Kappert U, et al. Initial German experience with transapical implantation of a second-generation transcatheter heart valve for the treatment of aortic regurgitation. J Am Coll Cardiol Intv. 2014;7:1168–74.
86. Barbanti M, Ye J, Pasupati S, et al. The Helio transcatheter aortic dock for patients with aortic regurgitation. Eurointervention. 2013;9(Suppl):S91–4.
87. Chiam PT, Chao VT, Tan SY, et al. Percutaneous transcatheter heart valve implantation in a bicuspid aortic valve. J Am Coll Cardiovasc Interv. 2010;3:559–61.
88. Kochman J, Huczek Z, Scislo P, et al. Comparison of one- and 12-month outcomes of transcatheter aortic valve replacement in patients with severely stenotic bicuspid versus tricuspid aortic valves (results from a multicenter registry). Am J Cardiol. 2014;114:757–62.
89. Mylotte D, Lefevre T, Søndergaard L, et al. Transcatheter aortic valve replacement in bicuspid aortic valve disease. J Am Coll Cardiol. 2014;64:2330–9.
90. Genereaux P, Head SJ, Hahn R, et al. Paravalvular leak after transcatheter aortic valve replacement the new Achilles' heel? A comprehensive review of the literature. J Am Coll Cardiol. 2013;61(11):1125–36.

Index

A.E. Abbas (ed.), *Aortic Stenosis: Case-Based Diagnosis and Therapy*,
DOI 10.1007/978-1-4471-5242-2